

Dominic W. S. Wong

Mechanism and Theory in Food Chemistry

Second Edition

 Springer

Mechanism and Theory in Food Chemistry, Second Edition

Dominic W.S. Wong

Mechanism and Theory in Food Chemistry, Second Edition

 Springer

Dominic W.S. Wong
Western Regional Research Center
Albany
California
USA

ISBN 978-3-319-50765-1 ISBN 978-3-319-50766-8 (eBook)
<https://doi.org/10.1007/978-3-319-50766-8>

Library of Congress Control Number: 2017954280

© Springer International Publishing AG 2018

This work is subject to copyright. All rights are reserved by the Publisher, whether the whole or part of the material is concerned, specifically the rights of translation, reprinting, reuse of illustrations, recitation, broadcasting, reproduction on microfilms or in any other physical way, and transmission or information storage and retrieval, electronic adaptation, computer software, or by similar or dissimilar methodology now known or hereafter developed.

The use of general descriptive names, registered names, trademarks, service marks, etc. in this publication does not imply, even in the absence of a specific statement, that such names are exempt from the relevant protective laws and regulations and therefore free for general use.

The publisher, the authors and the editors are safe to assume that the advice and information in this book are believed to be true and accurate at the date of publication. Neither the publisher nor the authors or the editors give a warranty, express or implied, with respect to the material contained herein or for any errors or omissions that may have been made. The publisher remains neutral with regard to jurisdictional claims in published maps and institutional affiliations.

Printed on acid-free paper

This Springer imprint is published by Springer Nature
The registered company is Springer International Publishing AG
The registered company address is: Gewerbestrasse 11, 6330 Cham, Switzerland

To: Benjamin and Theodore

Preface to the Second Edition

The first edition of this book was written with the intention to provide an in-depth treatment of food chemistry focusing on the reaction mechanism and theory. In the preparation of this new edition, I had the following aims in mind: first, to update the chemistry and references; second, to add new topics and rewrite topics of emerging importance; third, to better explain some of the chemistry concepts in the text.

Food chemistry builds upon a knowledge base of all major branches of chemistry applied specifically to food and food systems. The complexity of food is manifested in its chemical beauty. For every aspect of food, the “what,” “how,” and “why” are always best expressed in the language of chemical equations, reactions, and mechanisms, with chemical structures as the building block. Much of the confusion about food would not occur if the attention focuses more on the reactions, interactions, and transformations at the chemical and molecular level.

I have found deep satisfaction in the rewriting of this book. It has been a humble experience to learn the remarkable effort and dedication of numerous scientists contributing to the advancement in food chemistry. My sincere appreciation goes to all the authors whose publications and materials are referenced in this book. I should thank also the publishers for giving permissions to use the copyrighted materials listed in the text. Special thanks are due to the editorial staff of Springer for the very helpful arrangement and assistance in developing this new edition.

Dominic W. S. Wong

Albany, CA, USA

Preface to the First Edition

The primary objective of this book is to focus on the reaction mechanism and theory essential to understanding the many chemical processes occurred in food and food systems. Too often, food chemistry courses tend to be descriptive and require mere memorization of unrelated chemical structures. It is the author's firm belief that an adequate comprehension of the principles of food chemistry is based on a thorough knowledge of the reaction mechanisms and theories under a coherent theme.

For every phenomenon or change observed in food or food systems, there is a corresponding chemical equation or model. Most of the presentations in this book are found in reaction mechanisms explained by equations and figures.

This book is organized in ten chapters: (1) Lipids, (2) Proteins, (3) Carbohydrates, (4) Colorants, (5) Enzymes, (6) Flavors, (7) Sweeteners, (8) Natural Toxicants, (9) Additives, and (10) Vitamins. The first three chapters constitute the foundation of food chemistry and hence require a broad coverage. Other chapters are slightly more selective in the presentation of the materials. The references at the end of each chapter is by no means encyclopedic, but provide a guide to those who would like to obtain more information on a particular area discussed in the text. Selected references are included mainly for certain topics the author finds interesting and deserving further reading.

There are three appendices: (1) General kinetics of olefin autoxidation, (2) Singlet oxygen, and (3) Where do the radicals come from? These were written to cover certain chemical principles that students are normally expected or assumed to, but rarely actually understand. The latter two are especially important, since they contain information basic to the numerous chemical reactions often discussed in food systems.

I am grateful to Professors Robert E. Feeney and John R. Whitaker (University of California, Davis) for their comments, criticisms, encouragement, and help in the preparation of this book. I would also like to thank Professors Donald R. Babin (Creighton University), Benito O. de Lumen (University of California, Berkeley), Dr. Ram T. Shet, Mr. Wayne M. Camirand (Western Regional Research Center, USDA), for their valuable comments and suggestions. The librarians, Julia F. Cooksey, Carol M. Nybro-Stevens, and Rena Schonbrun, have always been helpful during my two-year stay at WRRC. Finally, my deep admiration and sincere appreciation go to all scientists for their contributions to the many progresses in the field of food chemistry, without which this book could not have been written.

Dominic W. S. Wong

Ithaca, NY, USA

Contents

1	Lipids	1
1.1	Fatty Acids and Triacylglycerols	3
1.2	Lipid Oxidation	6
1.2.1	Autoxidation.....	6
1.2.2	Primary Products of Autoxidation.....	7
1.2.3	The Stereochemistry of Product Hydroperoxides in Autoxidation.....	9
1.2.4	The Role of Metal Ions in Lipid Autoxidation.....	10
1.3	Photosensitized Oxidation	11
1.4	Secondary Products from Hydroperoxides	13
1.5	Thermal and Oxidative Thermal Reactions	16
1.5.1	Thermal Reactions.....	17
1.5.2	Oxidative Thermal Reactions.....	20
1.6	Radiolysis of Lipids	22
1.7	Polymorphism of Triglycerides	24
1.7.1	Structures of Polymorphic Crystals.....	24
1.7.2	Crystal Habit of Fat.....	27
1.8	Plasticity of Fat	28
1.9	Hydrogenation	29
1.9.1	Mechanism.....	30
1.9.2	<i>Cis-Trans</i> Isomerization.....	30
1.9.3	Selectivity.....	31
1.10	Interesterification	32
1.10.1	Mechanism.....	32
1.11	Emulsions	34
1.11.1	Surface Tension and Surface Area.....	34
1.11.2	Formation of Emulsion.....	34
1.11.3	Breakdown of Emulsions.....	35
1.12	Emulsifiers	37
1.12.1	Monoglycerides.....	37
1.12.2	Monoglyceride Derivatives.....	38
1.12.3	Ester Derivatives of Alcohols (Nonglycerol).....	39
1.12.4	Lecithin.....	40
1.12.5	Hydrophilic/Lipophilic Balance.....	42
1.13	Molecular Arrangement of Emulsifier Molecules at the Interface: Mesomorphic Behavior	42
1.14	Functions of Emulsifiers in Stabilization	44
1.14.1	Electric Double Layer.....	44
1.14.2	Adsorption at Interface.....	45
1.14.3	Formation of Liquid-Crystalline Mesophase.....	46
1.14.4	Complexation with Starch.....	46
1.14.5	Emulsifier Interaction with Proteins.....	47
1.14.6	Control of Fat Crystallization.....	47
1.15	Antioxidants	47
1.15.1	Reaction Mechanism.....	48
	References	51

2	Proteins	55
2.1	Protein Structure	56
2.1.1	The Role of Water	59
2.1.2	Change of Conformation.....	61
2.2	Protein-Stabilized Emulsification and Foaming	65
2.3	Gel Formation	67
2.4	Chemical Reactions	68
2.4.1	Alkali Degradation.....	68
2.4.2	Heat-Induced Formation of Isopeptides	70
2.4.3	Radiolysis.....	71
2.4.4	Photolysis	75
2.4.5	Photosensitized Oxidation.....	76
2.4.6	Chemical Oxidation.....	77
2.4.7	Reaction with Carbonyl Compounds	78
2.4.8	Reaction with Products from Lipid Oxidation	78
2.5	Organized Protein Systems	80
2.5.1	Meat Proteins	80
2.5.2	Water-Holding Capacity.....	88
2.5.3	Milk Proteins	91
2.5.4	Wheat Proteins	97
2.5.5	Soybean Proteins	106
2.5.6	Collagen.....	113
	References	119
3	Carbohydrates	123
3.1	Glycosidic Linkage	125
3.2	Action of Alkali on Monosaccharides	127
3.2.1	Aldose-Ketose Rearrangement	127
3.2.2	Formation of Saccharinic Acid	128
3.2.3	Fragmentation	129
3.3	Action of Acid on Monosaccharides	130
3.3.1	Formation of Anhydro Sugars.....	130
3.3.2	Formation of Furan Derivatives.....	130
3.4	Nonenzymatic Browning (Maillard Reaction)	132
3.4.1	Chemistry of the Reaction	135
3.4.2	Secondary Reactions	139
3.5	Complexes of Sugars with Metal Ions	141
3.5.1	In Neutral Solution	141
3.5.2	In Alkaline Solution	142
3.6	Hydrocolloids	143
3.7	Starch	143
3.7.1	Chemical Structure of Starch	143
3.7.2	Gelatinization and Retrogradation.....	146
3.7.3	Chemical Modification of Starch.....	147
3.7.4	Starch Structure and Digestibility	148
3.8	Alginate	149
3.8.1	Chemical Structure of Alginate	149
3.8.2	Gelling	149

3.9	Pectin	151
3.9.1	Chemical Structure of Pectin.....	151
3.9.2	Classification of Pectin	151
3.9.3	Gelling	152
3.10	Cellulose	153
3.10.1	Chemical Structure of Cellulose	153
3.10.2	Gelling	153
3.11	β-Glucan	156
3.12	Hemicellulose	159
3.12.1	Dietary Fiber	160
3.13	Xanthan Gum	161
3.13.1	Chemical Structure of Xanthan Gum.....	161
3.13.2	Gelling	162
3.14	Guar Gum	162
3.15	Carrageenan	163
3.15.1	Chemical Structure of Carrageenan.....	163
3.15.2	Gelling	165
3.15.3	Interaction with Proteins.....	165
3.15.4	Synergism with Locust Bean Gum.....	166
	References	167
4	Colorants	169
4.1	Light Absorption	171
4.2	Conjugation	173
4.3	Substituent Effects	175
4.4	Carotenoids	176
4.4.1	Isomerization.....	178
4.4.2	Autoxidation.....	179
4.4.3	Thermal Degradation	179
4.4.4	Photochemical Reactions.....	180
4.4.5	Carotenoids as Color Additives	180
4.4.6	Carotenoproteins and Bathochromic Shift.....	181
4.5	Annatto	182
4.6	Anthocyanins	183
4.6.1	Effect of pH on the Color of Anthocyanins	184
4.6.2	Thermal Degradation of Anthocyanidins.....	186
4.6.3	Decoloration by Sulfur Dioxide	186
4.6.4	Self-Association and Copigmentation	186
4.6.5	Condensation.....	188
4.6.6	Oxidation	189
4.7	Betanain	189
4.8	Caramel	191
4.9	Dyes and Lakes	192
4.10	Coordination Chemistry	194
4.11	Metalloporphyrin: Electronic Structure	197
4.12	Myoglobin	200
4.12.1	Molecular Structure	200
4.12.2	The Heme Iron	202

4.12.3	The Role of Globin	205
4.12.4	Oxygenation of Myoglobin.....	205
4.12.5	Autoxidation of Oxymyoglobin.....	206
4.12.6	Absorption Spectra	208
4.12.7	Myoglobin and Lipid Oxidation	211
4.13	Chlorophyll	212
4.13.1	The Magnesium-Ligand Coordination	213
4.13.2	Dimers and Oligomers	213
4.13.3	Chlorophyll Derivatives.....	214
4.13.4	Oxidation and Reduction	216
	References	216
5	Enzymes	219
5.1	Papain	223
5.1.1	The Active-Site Region	224
5.1.2	The Ionization of the Essential Groups	225
5.1.3	Reaction Mechanism	226
5.1.4	Action on Meat Fractions	226
5.2	Lipoxygenase	227
5.2.1	Soybean Lipoxygenase-1	227
5.2.2	Regiospecificity and Stereospecificity	228
5.2.3	The Iron in Lipoxygenase	229
5.2.4	The Aerobic Reaction Mechanism	230
5.2.5	The Anaerobic Reaction Mechanism	230
5.2.6	The Fate of Hydroperoxide	231
5.2.7	Co-oxidation.....	232
5.3	Polyphenol Oxidase	233
5.3.1	Enzyme Characteristics	233
5.3.2	Reaction Mechanism	234
5.3.3	Secondary Reaction Products.....	236
5.4	Glucose Oxidase	237
5.4.1	Enzyme Characteristics	237
5.4.2	Reaction Mechanism	238
5.4.3	Industrial Uses	239
5.5	Amylases	240
5.5.1	Enzyme Characteristics	240
5.5.2	Reaction Mechanism	241
5.5.3	Action Pattern	242
5.5.4	The Multimolecular Process	244
5.5.5	Subsites of Amylases	244
5.5.6	Industrial Uses	244
5.6	Pectic Enzymes	245
5.6.1	Pectinesterases.....	246
5.6.2	Polygalacturonases	247
5.6.3	Pectate Lyases.....	249
5.6.4	Industrial Importance.....	250

5.7	Lipolytic Enzymes	251
5.7.1	Pancreatic Lipases.....	251
5.7.2	The Role of Colipase.....	252
5.7.3	Mechanism of Catalysis.....	253
5.7.4	Specificity.....	254
5.7.5	The Acyl Transfer Reaction.....	255
5.8	Xylose Isomerase	256
5.8.1	Protein Structure.....	256
5.8.2	Metal Cations.....	257
5.8.3	Reaction Mechanism.....	258
	References	259
6	Flavors	263
6.1	The Sensation of Taste	265
6.2	The Mechanism of Taste Sensations	266
6.3	Glutamate and Umami Receptor	267
6.4	Taste Enhancers	268
6.5	Odor: The Stereochemical Theory for Olfaction	269
6.6	Character-Impact Compounds	271
6.7	Odorant Receptors: Molecular Mechanism of Odor Recognition	271
6.8	The Origin of Flavor	272
6.8.1	Biosynthesis.....	272
6.8.2	Chemical Reactions During Processing.....	276
6.9	Beverage Flavor	280
6.9.1	Tea.....	280
6.9.2	Beer.....	283
6.9.3	Coffee.....	285
6.10	Spice Flavor	287
6.10.1	Garlic and Onion.....	287
6.10.2	Black Pepper.....	290
6.10.3	Hot Pepper.....	292
6.10.4	Ginger.....	293
6.10.5	Peppermint.....	293
6.10.6	Cinnamon.....	294
6.11	Fruits and Vegetables	294
6.11.1	Fruit Flavor.....	294
6.11.2	Vegetables.....	298
6.12	Meat Flavor	302
6.12.1	Simulated Meat Flavors.....	305
6.13	Microencapsulation of Flavors	305
	References	306
7	Sweeteners	309
7.1	The Tripartite Theory of Sweetness	310
7.2	Sweet Taste Receptors	312
7.3	Amino Acids and Dipeptides	313
7.3.1	Aspartame.....	313
7.3.2	Neotame.....	316

7.4	The Aminosulfonates	316
7.5	Dihydrochalcone	317
7.6	Glycyrrhizin	319
7.7	Stevioside	320
7.8	Sugar Alcohol	321
7.9	Corn Sweeteners	322
7.10	Sweet Proteins	323
	References	325
8	Natural Toxicants	327
8.1	Cyanogenic Glycosides	329
8.1.1	Chemical Structure.....	329
8.1.2	Mechanism of Toxicity.....	330
8.2	Glycoalkaloids	330
8.2.1	Chemical Structure.....	330
8.2.2	Mechanism of Toxicity.....	331
8.3	Glucosinolates	332
8.3.1	Chemical Structure.....	332
8.3.2	Mechanism of Toxicity.....	333
8.4	Methylxanthines	335
8.4.1	Metabolic Pathway.....	335
8.4.2	Mechanism of Toxicity.....	337
8.5	Amino Acids, Peptides, and Proteins	338
8.5.1	Nonprotein Amino Acids.....	338
8.5.2	Mechanism of Toxicity.....	338
8.5.3	Toxic Peptides	340
8.5.4	Proteins: Botulinum Neurotoxins.....	341
8.6	Amines	343
8.6.1	Metabolism.....	345
8.7	Mycotoxins	345
8.7.1	Chemical Structure.....	345
8.7.2	Mechanism of Toxicity.....	346
8.8	Polycyclic Aromatic Hydrocarbons	348
8.8.1	Chemical Structures.....	348
8.8.2	Mechanism of Toxicity.....	349
8.9	Heterocyclic Amines	349
8.9.1	Mutagenicity.....	351
8.9.2	Mechanism of Toxicity.....	351
8.10	Nitrosamines	352
8.10.1	The General Chemistry of <i>N</i> -Nitrosation.....	352
8.10.2	Inhibition of Nitrosation.....	353
8.10.3	Nitrosamines in Cured Meat.....	354
8.10.4	In Vivo Nitrosation.....	355
8.10.5	Chemical Reactions of Nitrosamine.....	356
8.10.6	Metabolic Mechanism.....	357
	References	358

9	Additives	361
9.1	Phosphates	362
9.1.1	Chemical Structure.....	362
9.1.2	Sequestering.....	365
9.1.3	Water Holding Capacity.....	366
9.1.4	Stabilizing Emulsion.....	367
9.1.5	Leavening.....	367
9.2	Citric Acid	368
9.2.1	Acidification.....	368
9.2.2	Buffering.....	368
9.2.3	Flavor Enhancing.....	369
9.2.4	Sequestering.....	369
9.2.5	Phosphoric Acid and Others.....	371
9.3	Antimicrobial Short-Chain Acid Derivatives	371
9.3.1	Mechanism of Inhibition.....	372
9.4	Sulfite	372
9.4.1	Chemical Equilibrium of the Oxospecies.....	373
9.4.2	Inhibition of Nonenzymatic Browning.....	373
9.4.3	Inhibition of Enzymatic Browning.....	374
9.4.4	Antimicrobial Action.....	374
9.4.5	Reaction with Pyrimidines.....	374
9.4.6	Transamination.....	375
9.4.7	Free-Radical Reactions.....	376
9.4.8	Mutagenicity.....	378
9.4.9	Metabolic Pathway.....	379
	References	379
10	Vitamins	381
10.1	Vitamin A	383
10.1.1	Biological Function.....	384
10.1.2	Action of Dilute Acid.....	385
10.1.3	Photochemical Reactions.....	386
10.2	Thiamin (Vitamin B₁)	387
10.2.1	Biochemical Mechanism.....	387
10.2.2	Action of Alkali and Acid.....	388
10.2.3	Oxidation and Reduction.....	389
10.2.4	Reaction with Bisulfite.....	390
10.2.5	Photolysis.....	391
10.3	Riboflavin (Vitamin B₂)	391
10.3.1	Biochemical Mechanism.....	393
10.3.2	Alkaline Degradation.....	394
10.3.3	Reaction with Sulfite.....	394
10.3.4	Photochemical Reaction.....	395
10.3.5	Flavin-Sensitized Reactions.....	396
10.4	Pyridoxol, Pyridoxal, and Pyridoxamine (Vitamin B₆)	397
10.4.1	Biochemical Mechanism.....	397

10.5 Folic Acid (Vitamin B₉)	399
10.5.1 Biological Functions.....	401
10.5.2 Degradation of Folates.....	401
10.6 Vitamin B₁₂	404
10.6.1 Biochemical Mechanism.....	405
10.6.2 Photolytic Degradation.....	405
10.6.3 Oxidation.....	406
10.7 Biotin (Vitamin B₇)	406
10.7.1 Biochemical Mechanism.....	407
10.8 Niacin (Vitamin B₃)	408
10.8.1 Biochemical Mechanism.....	408
10.9 Vitamin C	409
10.9.1 Biochemical Mechanism.....	409
10.9.2 Biological Functions.....	410
10.9.3 Loss of Vitamin C.....	412
10.9.4 Uses of Vitamin C.....	414
10.10 Vitamin D	415
10.10.1 The Chemical Structures.....	415
10.10.2 Biological Functions.....	416
10.10.3 Side Reactions of Irradiation.....	417
10.10.4 Thermal Reaction.....	418
10.11 Vitamin E	419
10.11.1 Thermal Decomposition.....	420
10.11.2 Chemical Oxidation.....	420
10.11.3 Free Radical Reactions.....	421
10.11.4 Quenching of Singlet Oxygen.....	423
References	424

Supplementary Information

Appendix 1: General Kinetics of Olefin Autoxidation.....	428
Appendix 2: Singlet Oxygen.....	431
A2.1 Photosensitized Oxygenation.....	432
A2.2 Physical and Chemical Quenching.....	432
Appendix 3: Where Do the Radicals Come From?.....	434
A3.1 Photolysis.....	434
A3.2 Photodissociation.....	435
A3.3 Photosensitized Reaction.....	435
A3.4 Radiolysis.....	435
A3.5 Molecular Homolytic Decomposition.....	436
A3.6 The Fenton Reaction.....	437
A3.7 Enzyme-Catalyzed Reactions.....	437
A3.8 Reduction Potentials.....	438
Appendix 4: Flavonoids.....	439
Index.....	441

Lipids

- 1.1 Fatty Acids and Triacylglycerols – 3**
- 1.2 Lipid Oxidation – 6**
 - 1.2.1 Autoxidation – 6
 - 1.2.2 Primary Products of Autoxidation – 7
 - 1.2.3 The Stereochemistry of Product Hydroperoxides in Autoxidation – 9
 - 1.2.4 The Role of Metal Ions in Lipid Autoxidation – 10
- 1.3 Photosensitized Oxidation – 11**
- 1.4 Secondary Products from Hydroperoxides – 13**
- 1.5 Thermal and Oxidative Thermal Reactions – 16**
 - 1.5.1 Thermal Reactions – 17
 - 1.5.2 Oxidative Thermal Reactions – 20
- 1.6 Radiolysis of Lipids – 22**
- 1.7 Polymorphism of Triglycerides – 24**
 - 1.7.1 Structures of Polymorphic Crystals – 24
 - 1.7.2 Crystal Habit of Fat – 27
- 1.8 Plasticity of Fat – 28**
- 1.9 Hydrogenation – 29**
 - 1.9.1 Mechanism – 30
 - 1.9.2 *Cis-Trans* Isomerization – 30
 - 1.9.3 Selectivity – 31
- 1.10 Interesterification – 32**
 - 1.10.1 Mechanism – 32

1.11 Emulsions – 34

- 1.11.1 Surface Tension and Surface Area – 34
- 1.11.2 Formation of Emulsion – 34
- 1.11.3 Breakdown of Emulsions – 35

1.12 Emulsifiers – 37

- 1.12.1 Monoglycerides – 37
- 1.12.2 Monoglyceride Derivatives – 38
- 1.12.3 Ester Derivatives of Alcohols (Nonglycerol) – 39
- 1.12.4 Lecithin – 40
- 1.12.5 Hydrophilic/Lipophilic Balance – 42

1.13 Molecular Arrangement of Emulsifier Molecules at the Interface: Mesomorphic Behavior – 42

1.14 Functions of Emulsifiers in Stabilization – 44

- 1.14.1 Electric Double Layer – 44
- 1.14.2 Adsorption at Interface – 45
- 1.14.3 Formation of Liquid-Crystalline Mesophase – 46
- 1.14.4 Complexation with Starch – 46
- 1.14.5 Emulsifier Interaction with Proteins – 47
- 1.14.6 Control of Fat Crystallization – 47

1.15 Antioxidants – 47

- 1.15.1 Reaction Mechanism – 48

References – 51

Dietary lipids supply approximately 35–40% of the total calories taken by an average adult and exhibit the most efficient energy conversion, yielding nine calories per gram, twice as many calories supplied by carbohydrates or proteins. The large consumption of fats and oils necessitates a thorough understanding of the basic chemistry involved in the various changes, both under natural conditions and during food processing.

Lipid oxidation has been one of the most extensively studied areas in food science and will remain so, since it is related to the production of numerous desirable and undesirable breakdown products and involved in many side reactions associated with other food constituents. The chemistry is complicated by the fact that these reactions are initiated, inhibited, or altered by many factors, including metals, enzymes, antioxidants, light, pH, and temperature.

The physical chemistry of lipids is another area of great interest to food chemists. The polymorphic property and crystal habit of acylglycerols are of great importance in the formulation of fat and oil products, such as margarine, ice cream, and mayonnaise. Knowledge on the formation and breakdown of emulsions is required for the effective application of emulsifiers in many food-processing systems.

The chemistry of lipids and the mechanisms and reactions occurred in processing, including degradations via oxidation, thermal and radiolytic reactions, hydrogenation, interesterification, and polymorphic changes, are presented. A considerable portion of the discussion is devoted to the theory and applied chemistry of emulsions in food systems.

1.1 Fatty Acids and Triacylglycerols

Commercial oils and fats of plant and animal origins consist exclusively of triacylglycerols (TAG), with the chemical structure of trihydric alcohol glycerol esterified with fatty acids. The common fatty acids in edible oils and their systematic names are presented in **Table 1.1**. Most fatty acids have a straight chain of an even number of carbons, commonly classified into short chain (2–6 carbons), medium chain (8–10), and long chain (12–24). Depending on the absence or presence of double bonds, fatty acids are referred to as saturated and unsaturated, respectively. The latter may be monounsaturated (monoenic, containing one double bond) or polyunsaturated (polyenoic, containing two or more double bonds). The double bonds are all in the *cis* configuration. Some fatty acids may contain functional groups, such as hydroxy- or keto- groups. The carbon atoms in the fatty acid chain are numbered from the carboxyl end. If the fatty acid is unsaturated, the double bond position is counted from the carboxyl end. For example, linoleic acid is 18:2 (indicating 18 carbons with two double bonds) or *cis,cis*-9,12-octadecadienoic acid (indicating the double bonds at the C9 and C12 positions counting from the carboxyl end). In another naming system, the double bonds are counted from the methyl end, denoted by ωx (omega ω representing the methyl terminal carbon and x = the position of the first double bond from the methyl end) or $n-x$ (n = total number of carbon). For example, linoleic acid using this system is named 18:2($\omega 6$) or ($n-6$), indicating 18 carbons, two double bonds, the first double bond at C6 counting from the terminal methyl group. Occasionally, the delta (Δ) system is used. Linoleic acid in this case is represented by 18:2 Δ 9,12, indicating 18 carbons, two double bonds at positions C9 and C12.

In the TAG structure, when the two primary hydroxyl groups of the glycerol moiety are esterified with different fatty acids as in most edible fats and oils, the molecule becomes asymmetric. In order to designate the configuration of a TAG molecule, the IUPAC-IUB

■ **Table 1.1** Common fatty acids of vegetable and animal origin

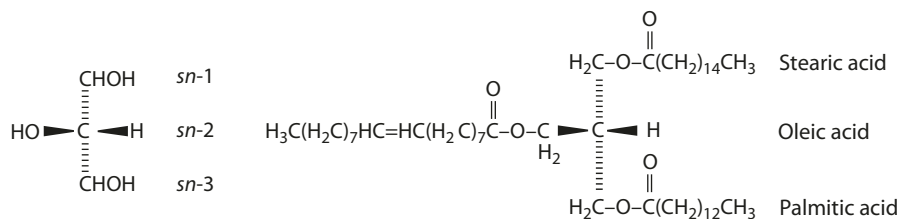
linoleic acid
cis,cis-9,12-octadecadienoic acid
 18:2 (n-6)
 18:2 (ω6)

	Chain length	Common name	Systemic name
Saturated	10:0	Capric acid	Decanoic
	12:0	Lauric acid	Dodecanoic
	14:0	Myristic acid	Tetradecanoic
	16:0	Palmitic acid	Hexadecanoic
	18:0	Stearic acid	Octadecanoic
	20:0	Arachidic acid	Eicosanoic
	22:0	Behenic acid	Docosanoic
Mono-unsaturated	16:1 (n-7)	Palmitoleic acid	<i>cis</i> -9-Hexadecenoic
	18:1 (n-9)	Oleic acid	<i>cis</i> -9-Octadecenoic
	22:1 (n-9)	Erucic acid	<i>cis</i> -10-Docosenoic
Di-unsaturated	18:2 (n-6)	Linoleic acid	<i>cis,cis</i> -9,12-Octadecadienoic
Tri-unsaturated	18:3 (n-6)	γ-linolenic acid	<i>cis,cis,cis</i> -6,9,12-Octadecatrienoic acid
	18:3 (n-3)	α-linolenic acid	<i>cis,cis,cis</i> -9,12,15-Octadecatrienoic acid
	20:4 (n-6)	Arachidonic	5,8,11,14-Eicosatetraenoic acid (all <i>cis</i>)
	20:5 (n-3)	EPA	5,8,11,14,17-Eicosapentaenoic acid (all <i>cis</i>)
	20:6 (n-3)	DHA	4,7,10,13,16,19-Docosahexaenoic (all <i>cis</i>)

The notation represents the number of carbon atoms and of double bonds (separated by a colon), e.g., 16:0 for palmitic acid, 18:1 for oleic. The position of the double bond is indicated by «n-x» (number of carbon atoms in the fatty acid chain minus the carbon number where the double bond counting from the methyl end group carbon). All the double bonds are of the *cis* configuration. The linolenic acid 18:3 (n-3) sometimes called α-linolenic acid, distinguishable from its isomers, γ-linolenic acid (*cis,cis,cis*-6,9,12-octadecatrienoic acid, 18:3 (n-6))

Commission on Biochemical Nomenclature has recommended the stereospecific numbering (*sn*) system [23]. (The prefix «*sn*» stands for «stereospecifically numbered.») In the Fischer projection of L-glycerol derivatives (■ Fig. 1.1), the secondary OH group on the carbon atom (in the mid position) is shown to the left, then the primary (end) carbons on

1.1 · Fatty Acids and Triacylglycerols



■ **Fig. 1.1** Stereospecific numbering of glycerol and *sn*-glycerol-1-stearate-2-oleate-3-palmitate (*sn*-SOP)

■ **Table 1.2** Fatty acid and triacylglycerol compositions of common oils and fats

Fatty acids	Corn	Soy-bean	Sun-flower	Olive	Pea-nut	Canola	Palm	Cotton-seed	Cocoa butter ^a	Lard
16:0	10.4	10.4	6.2	10.7	11.2	3.9	44.0	24.4	25.5	20.7
18:0	2.0	3.7	4.8	3.7	3.3	1.9	4.5	2.2	36.5	10.9
18:1	26.9	21.1	19.8	76.2	38.7	64.1	39.2	17.2	35.0	39.1
18:2(n-6)	58.5	55.7	67.0	6.8	37.9	18.7	10.1	55.0	2.0	19.6
18:3(n-3)	0.9	7.6	0.1	0.7	0.1	9.2	0.4	0.3	1.0	1.2
Major TAGs	LLL	LLL	LLL	OOO	OOL	OOO	POP	PLL	POS	SPO
	LLO	LLO	OLL	OOP	POL	LOO	POO	POL	SOS	OPL
	LLP	LLP	LOO	OLO	OLL	OOLn	POL	LLL	POP	OPO

From Sebedio et al. [47], Small [50]

P = 16:0 (palmitic acid), S = 18:0 (stearic acid), O = 18:1 (oleic acid), L = 18:2 (linoleic acid), Ln = 18:3 (linolenic acid)

^aFrom Wille and Lutton [61]

the top and the bottom are designated as *sn*-1 and *sn*-3, respectively, and the mid position carbon becomes *sn*-2. For example, the triacylglycerol in the figure is described as *sn*-glycerol-1-stearate-2-oleate-3-palmitate or *sn*-SOP or simply SOP with the understanding that the *sn* system is used.

Oils and fats do not exist as a single molecular species of triacylglycerol, but as mixtures of TAG species (■ Table 1.2). Soybean oil consists of 15 species of TAGs, with LLL, OLL, and PLL being more abundant. Sunflower oil contains 17 species, with the more abundant OLL, LLL, and OOL. Most of the data for lipid contents of oils and fats are reported as the total fatty acid composition in the TAG mixture as a whole. This type of information is useful in telling which major fatty acids present in a particular oil or fat. However, it does not tell the distribution of the fatty acids among the positions of the glycerol moiety in the TAG molecule. Stereospecific distribution has significant implication on the chemistry, biochemistry, and metabolism of the lipid, as described in later sections.

1.2 Lipid Oxidation

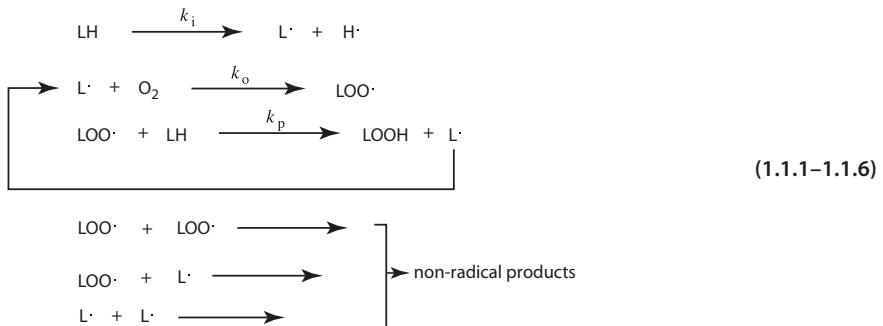
Lipid oxidation in foods is associated with the reaction with molecular oxygen, involving two types of mechanisms: (a) autoxidation and (b) photosensitized oxidation.

1.2.1 Autoxidation

Autoxidation is a free-radical chain reaction involving the following steps (Eq. 1.1) [17,18,41,42,54,57].

1. Initiation: Homolytic abstraction of hydrogen from an unsaturated lipid molecule (LH) to form a carbon-centered alkyl radical (L·) in the presence of an initiator.
2. Propagation: The alkyl radical reacts with O₂ to form a peroxy radical (LOO·) which reacts with another molecule of LH to form a hydroperoxide (LOOH). The alkyl radical thus formed can in turn react with O₂ to form more peroxy radicals. Hence, autoxidation is a radical chain reaction.
3. Termination: The chain reaction can be terminated by the formation of nonradical products.

The steady-state rate for autoxidation is expressed as oxygen [O₂] consumption or hydroperoxide [LOOH] formation with respect to time, as expressed in Eq. 1.2. (Refer to Appendix 1 for the complete kinetic rate equation.)



$$- \frac{d[\text{O}_2]}{dt} = \frac{d[\text{LOOH}]}{dt} = \left(\frac{R_i}{k_t} \right)^{1/2} k_p [\text{LH}] \quad (1.2)$$

oxygen consumption hydroperoxide formation

The initiation step involves the homolytic breakage of a C–H bond in the presence of an initiator (light, heat, metal ions). This step of hydrogen abstraction is rate-determining and hence selective for the C–H bond with the lowest dissociation energy. In all cases, the removal of H atom therefore depends on the stability of the carbon radical generated in the process. For linoleate, stability was imposed by a pentadiene system by delocalization over the five carbons. For oleate, the radical generated is the less stable allyl radical. The bond dissociation energy of an allylic hydrogen is about 10 kcal/mol greater than that of a bisallylic hydrogen. The C–H bond at the bisallylic position C11 of linoleate is 78–80 kcal/mol. As a result, autoxidation of monoenes, such as oleate, can only be activated at high temperatures, whereas that of dienes and trienes, such as linoleate and linolenate, occurs readily at room temperature. The reaction rate increases with the degree of unsaturation. Linoleate is oxidized ten times faster than oleate, linolenate 20–30 times faster. In autoxidation, the time period during which there is little or no detectable peroxide formation is the induction period.

Under normal oxygen pressure, the alkyl radical (L·) reacts rapidly with oxygen to form the peroxy radical (LOO·) (Eq. 1.1.2). This reaction is fast with near diffusion-controlled rate (k_o of $\sim 10^9 \text{ M}^{-1} \text{ s}^{-1}$ for linoleate). Consequently, most of the free radicals are in the form of the peroxy radical, which is the principal chain-carrying species under most circumstances.

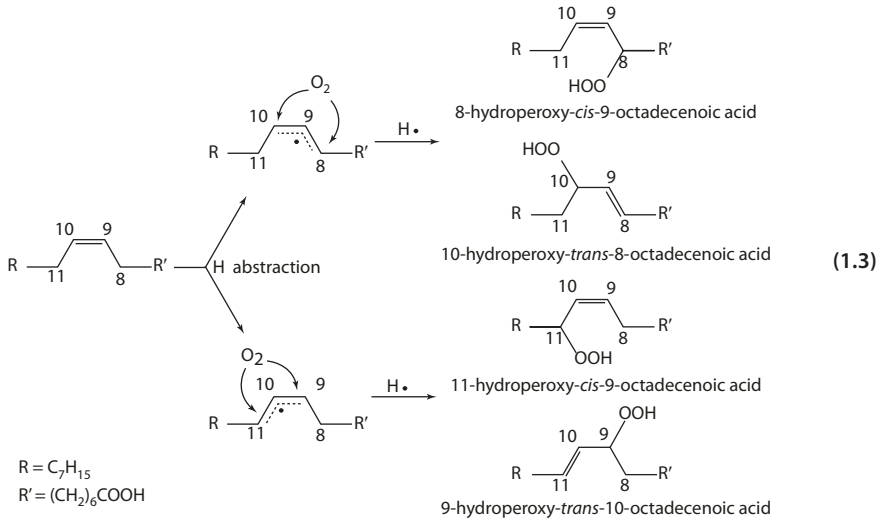
The propagation step (Eq. 1.1.3) is the transfer of a hydrogen atom from LH (or other suitable organic substrates) to the chain-carrying peroxy radical, yielding a hydroperoxide (LOOH) and an alkyl radical (L·). This reaction is relatively slow compared with the others in the chain reaction. The peroxy radical is quite stable and not very reactive. The rate constant k_p for peroxy radical (LOO·) reacting with LH (Eq. 1.1.3) is about $1 \text{ M}^{-1} \text{ s}^{-1}$ for LH = oleate and $60 \text{ M}^{-1} \text{ s}^{-1}$ for LH = linoleate. At room temperature, only linoleate and the higher polyunsaturated fatty acids are targets for H abstraction by peroxy radicals.

The major termination takes place via reaction 1.1.4 by combinations of peroxy radicals and/or alkyl radicals to form nonradical products. The reaction rate constant k_t is 1×10^5 to $10^7 \text{ M}^{-1} \text{ s}^{-1}$ (for linoleate).

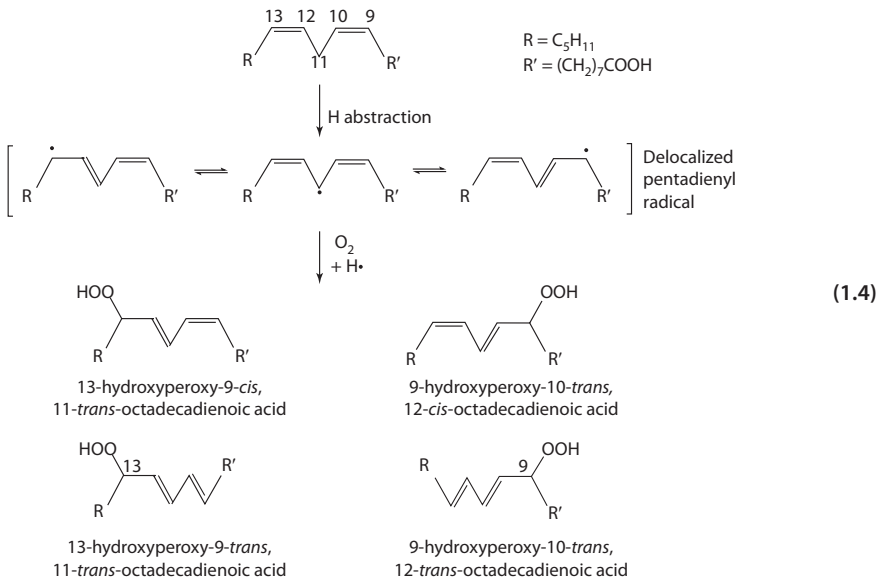
With increase in temperature such as in frying oil, the solubility of O_2 decreases. At oxygen-limiting condition, the initiation reaction (before the step of O_2 addition) in the formation of alkyl radicals becomes important. Many thermal decomposition reactions may occur. (Refer to section «[Thermal and Oxidative Thermal Reactions](#)».)

1.2.2 Primary Products of Autoxidation

For oleate, H abstraction occurs at the *cis*-double bond C9–C10. For C9–H abstraction, the radical product is stabilized by the allylic radical delocalized among C8–C9–C10. For C10–H abstraction, the resulting alkyl radical structure is stabilized by the allylic radical delocalized among C9–C10–C11 (Eq. 1.3). Thus, four hydroperoxides with mixtures of *cis* and *trans* isomers are formed: 8-OOH-*cis*- $\Delta 9,10$, 11-OOH-*cis*- $\Delta 9,10$, 9-OOH-*trans*- $\Delta 10,11$, and 10-OOH-*trans*- $\Delta 8,9$.



For linoleate, H abstraction occurs at C11, since the C–H bond at the bisallylic position is the weakest bond in the molecule. The resulting radical structure is stabilized by a delocalized pentadiene. Addition of oxygen takes place at C9 and C13, producing predominantly the 9- and 13-hydroperoxides, since stability of the conjugated diene system favors the oxygen attack at the end positions (Eq. 1.4). Also, the 9- and 13-hydroperoxides assume *trans*, *cis* configurations. Experimentally, hydroperoxides with *trans*, *trans* configurations are shown to exist in considerable proportion [17]. Likewise, autoxidation of linolenate results in the formation of the 9-, 12-, 13-, and 16-hydroperoxides (Table 1.3).



■ **Table 1.3** Product distribution of autoxidized oleate, linoleate, and linolenate

Distribution of hydroperoxides (%)						
	8-OOH	9-OOH	10-OOH	12-OOH	13-OOH	16-OOH
Oleate	27	23	23	27		
Linoleate		50			50	
Linolenate		30		12	12	46

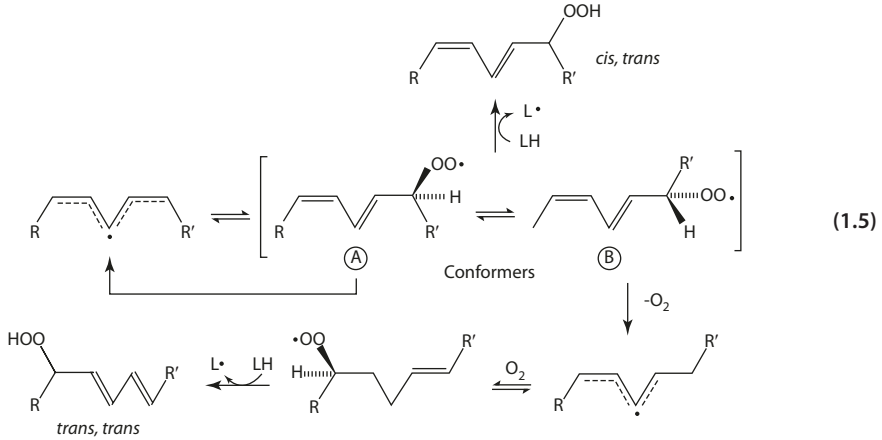
From Frankel [17]

1.2.3 The Stereochemistry of Product Hydroperoxides in Autoxidation

The classical mechanism of autoxidation does not adequately establish the controlling factor for the stereochemical course of the reaction. Experimentally, in the autoxidation of linoleic acid, four hydroperoxides (13-hydroperoxy-9-*cis*,11-*trans*-octadecadienoic; 13-hydroxyperoxy-9-*trans*,11-*trans*-octadecadienoic; 9-hydroxyperoxy-10-*trans*,12-*cis*-octadecadienoic; and 9-hydroperoxy-10-*trans*,12-*trans*-octadecadienoic) are formed. These four major stereoisomers comprise about 97% of the product mixture. To account for the stereochemistry of the products, a mechanism has been postulated in which the peroxy radical exists in two conformers (A and B), undergoing competitive pathways (Eq. 1.5) [41, 42].

1. H abstraction: The linoleate peroxy radical exists in two conformations. Each conformer can abstract H to give the *cis*, *trans* hydroperoxides.
2. β fragmentation (oxygen readdition mechanism): Both peroxy radical conformers can undergo β fragmentation (scission of the C–O bond). Fragmentation of conformer A leads to the initial *cis* peroxy radical. However, fragmentation of conformer B leads to the formation of a *trans*, *trans* pentadienyl radical, which can then repeat the autoxidation process to form a *trans*, *trans* product.

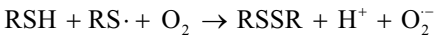
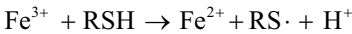
High temperature favors the scission pathway and decreases the *trans*, *cis* to *trans*, *trans* ratio. At high concentration of linoleate, the reaction is directed toward the *trans*, *cis* hydroperoxides, since the pathway involving transfer of hydrogen becomes competitive. Linolenate autoxidation undergoes a similar mechanism, except that there are three independent pathways: hydrogen abstraction, C–O scission, and cyclization.



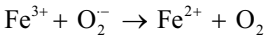
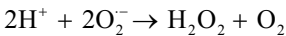
1.2.4 The Role of Metal Ions in Lipid Autoxidation

The autoxidation of lipids can be catalyzed by metal ions, in the presence of thiols or other common reducing agents in biological systems, such as ascorbate, NADH, and FADH₂, in both microsomal and model systems. In the case of thiols, Fe³⁺ reacts with the reductant to produce the thiyl radical, which catalyzes the reduction of O₂ to superoxide anion. The latter dismutates to H₂O₂ or undergoes a one-electron reduction of Fe³⁺ to Fe²⁺ (Eq. 1.6). In the Fenton reaction between Fe³⁺ and H₂O₂, hydroxyl radical (·OH) is produced, which is a strong oxidant and has been suggested to be an active initiator of lipid peroxidation.

Autoxidation



Reaction of Superoxide Anion

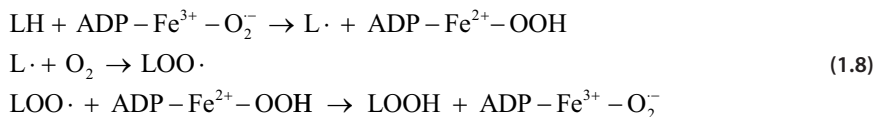
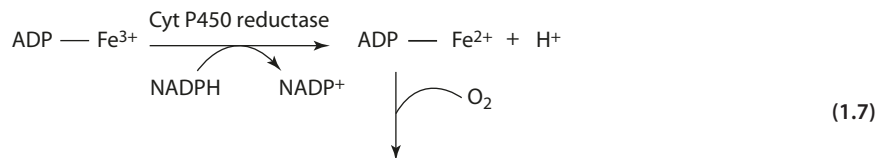


(1.6)

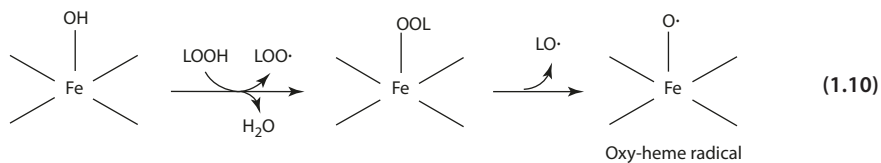
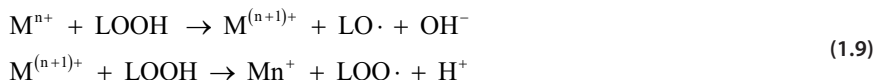
Fenton Reaction



In *in vivo* systems, metal ions, however, do not exist freely, but are often bound to ligands such as ATP and DNA as well as metalloproteins. The above reactions, therefore, may occur via a chelated ion, ADP-Fe²⁺ [7, 13, 63]. For example, in NADPH-induced microsomal peroxidation, cytochrome P-450 reductase catalyzes the formation of a chelated perferryl iron [Fe(V)] [7, 13] (Eq. 1.7). The initiation of peroxidation then proceeds via the reaction between the perferryl ion and polyunsaturated fatty acids (Eq. 1.8).



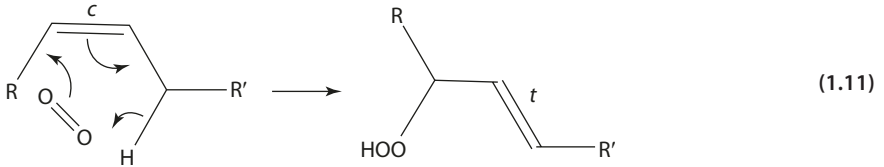
The above discussion describes the role of metal ions in the initiation of lipid oxidation in biological systems. However, metal ions are often involved in the propagation step as well, by catalyzing homolytic decomposition of lipid hydroperoxides to yield alkoxy or peroxy radicals, which in turn, initiate lipid oxidation (Eq. 1.9). In muscle tissues, both heme and nonheme irons are implicated as oxidants. It is generally believed that MbFe(III) or the hypervalent iron Fe(IV) is the heme protein species responsible for the initiation of lipid oxidation in meat. Peroxidation catalyzed by heme compounds consists of abstraction of the allylic hydrogen of the polyunsaturated fatty with the formation of the peroxy radical. The latter can then abstract a H· radical from another molecule of unsaturated fatty acid to start a new cycle (Eq. 1.10) [52]. (Refer to «Myoglobin and Lipid Oxidation» in Chap. 4.)



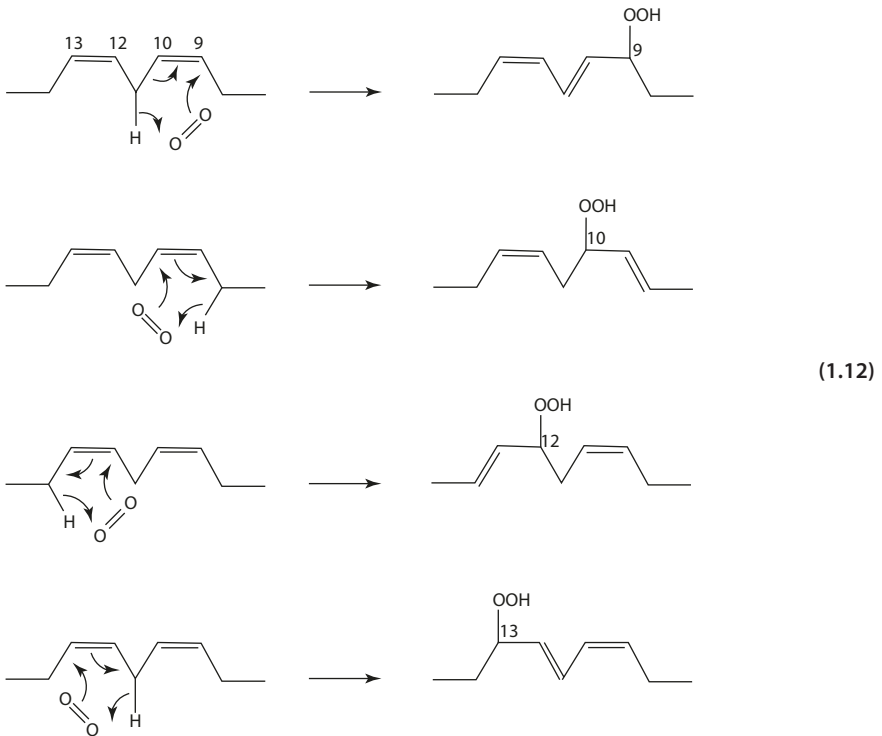
1.3 Photosensitized Oxidation

A different route of lipid oxidation involves singlet oxygen ($^1\text{O}_2^*$) addition to the olefin molecule via the «ene» reaction in the presence of a suitable sensitizer, such as chlorophyll or flavins (Eq. 1.11) [21]. The dioxygen molecule is added to the olefinic (double bond) carbon with a subsequent shift in the position of the double bond. The reaction (1) involves

no free radicals, (2) results in changes from *cis* to *trans* configuration of the double bond, (3) is independent of oxygen pressure, (4) shows no measurable induction period, and (5) is inhibited by singlet oxygen quenchers, such as β -carotene and tocopherols but is unaffected by antioxidants. (Refer to Appendix 2.)



The mechanism of photosensitized oxidation therefore takes a different stereochemical course than the free-radical autoxidation. In photosensitized oxidation, the hydroperoxides are formed at each of the unsaturated carbons. Photosensitized oxidation of linoleate, as presented in Eq. 1.12, yields 9-, 10-, 12-, and 13-hydroperoxides (Table 1.4).



■ **Table 1.4** Product distribution of photosensitized oxidation of oleate, linoleate, and linolenate

Distribution of hydroperoxides (%)						
	9-OOH	10-OOH	12-OOH	13-OOH	15-OOH	16-OOH
Oleate	50	50				
Linoleate	31	18	18	33		
Linolenate	21	13	13	14	13	25

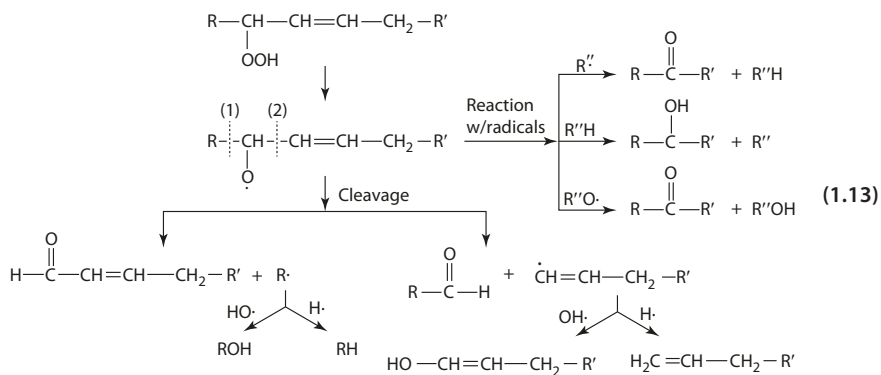
From Frankel [17]

1.4 Secondary Products from Hydroperoxides

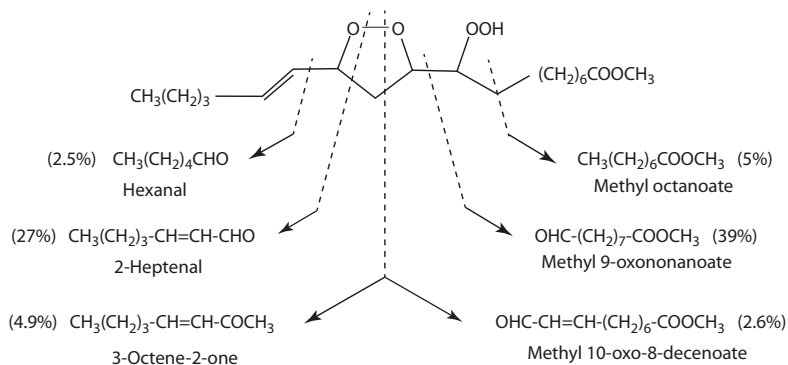
■ Decomposition Products of Hydroperoxides

The hydroperoxides formed in lipid oxidation are unstable at high temperature or in the presence of metal ions and decompose to form alkoxy radicals. The energy for breaking the O–O bond in LOOH is ~44 kcal/mole.

The alkoxy radical (1) undergoes C–C bond cleavage on either side of the alkoxy group, (2) reacts with other radicals, (3) gains or loses a H atom to form hydroxy or keto acids. These reactions account for many of the aldehydes, ketones, alcohols, and short-chain hydrocarbons, responsible for oxidized flavors. The general reaction scheme is presented in Eq. 1.13.



The decomposition of 8-OOH in oxidized oleate is presented in Eq. 1.14. The scission products consist of octanol, 1-decene, decenol, and decanal generated from the cleavage between C8 and C9 and heptane, heptanol, 2-undecenal from C7–C8 scission. Likewise, autoxidation of linoleate and linolenate produces well-defined chemicals, for example, 2,4-decadienal and 3-nonenal from 9-hydroperoxy-linoleate and hexanal and pentanal from 13-hydroperoxy-linoleate. The products are a complex multitude of volatile compounds, which contribute to rancidity, and nonvolatiles that also affect the flavor and chemical and physical quality of the oil.

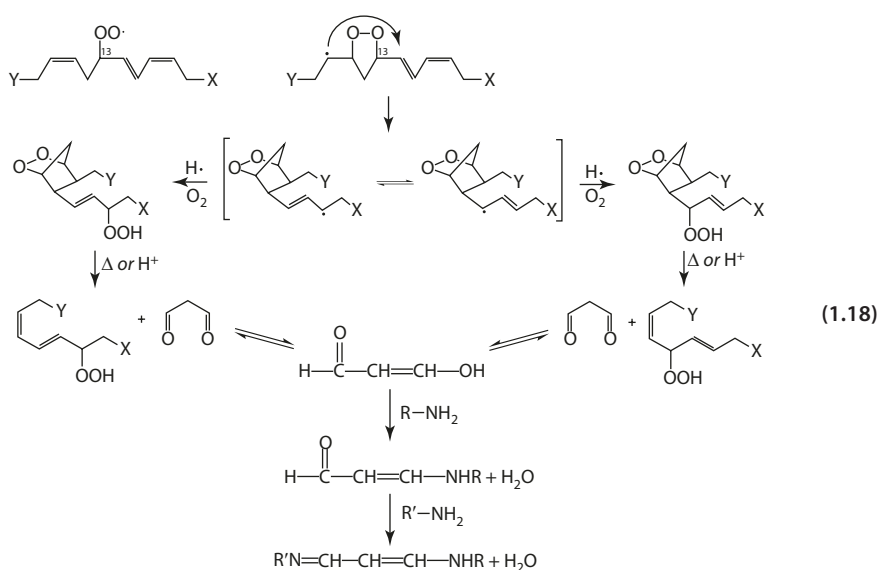


■ **Fig. 1.2** Thermal decomposition of methyl-9-hydroperoxy-10,12-epidioxy-*trans*-1,3-octadecenoate (From Frankel et al. [19])

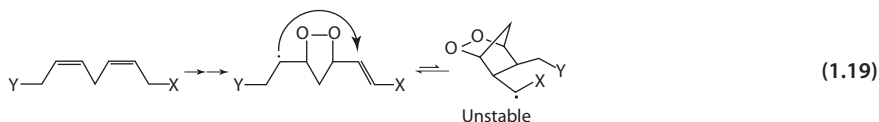
Hydroperoxy-cyclic peroxides undergo thermal decomposition mainly through C–C cleavage between the peroxide ring and the carbon with the hydroperoxide group (■ Fig. 1.2). Types of volatiles produced are similar to those of the corresponding mono-peroxides. Cleavage at the peroxide ring results in the formation of unsaturated aldehyde and aldehyde esters and, uniquely, unsaturated ketones [19].

■ ■ Formation of Malonaldehyde

In the case of linolenate hydroperoxide, 1,4-cyclization after the initial 1,3-cyclization yields a bicyclic peroxide, which is stabilized by an allylic radical (Eq. 1.18). Thermal degradation of the bicyclic peroxide gives malonaldehyde as one of the products [17]. Malonaldehyde is known to crosslink proteins, enzymes, and DNA and reacts with amino acids to form fluorescent products that absorb at 435 nm.



For linoleate, formation of the bicyclic peroxide will result in a nonallylic structure (Eq. 1.19), and therefore the yield of bicyclic peroxides in the diene system is much smaller.



1.5 Thermal and Oxidative Thermal Reactions

With increase in temperature such as in frying oil often reaching ≥ 180 °C, the solubility of O_2 decreases, oxygen availability is lower, and the rate of lipid oxidation becomes dependent on oxygen pressure. All these will affect the free-radical mechanism. The alkyl radicals formed in the initiation step (before the step of O_2 addition (Eq. 1.1.1) becomes more important.) The termination reactions involve mostly alkyl radicals (rather than the peroxy radicals $LOO\cdot$) (Eq. 1.1.3). Furthermore, the initial hydroperoxides formed in the propagation reaction (Eq. 1.1.2) rapidly decompose to form complex mixtures of products [9].

In addition to oxidation, thermal hydrolysis is another major reaction occurred in frying oil. Water released from the fried food acts as a nucleophile breaking the ester bonds between the fatty acids and the glycerol backbone in the triacylglyceride. Mono- and diacylglycerols, glycerols, and free fatty acids are formed, which undergo further reactions. The accumulation of free fatty acids is broadly used as an index to monitor the quality of the frying oil. The acid value should not exceed the 0.7–1.0% limit (on oil weight) for reusing the oil [20].

Thermal and oxidative thermal reactions lead to numerous volatile compounds that evaporate out of the oil, the main cause of favorable aroma or off-flavor in fried foods. (Refer to Chap. 6.) Formation of nonvolatile compounds would adsorb onto the food but more importantly change the physical and chemical characteristics of the oil. Deep frying leads to a decrease of the total unsaturation and an increase in free fatty acids, polar compounds, and polymerized materials. At the same time, changes in physical properties, such as increase in foaming, color, density, viscosity, and specific heat, occur in the process [4].

The degree to which an oil or fat may be heated without undue breakdown to volatile substances determines the temperature range within which it may be effectively used for cooking or frying. The temperature at which the oil begins to smoke is the smoke point, indication of appreciable decomposition (■ Table 1.5). Volatile products like acrolein (2-propenal) are evolved in sufficient quantity to become visible [46]. The smoke point value depends on the level of refinement of the oil, the presence of free fatty acids in the oil, as well as the TAG composition and distribution. Refined oils have smoke points higher than that of the corresponding unrefined oils.

■ **Table 1.5** Smoke point of refined oils

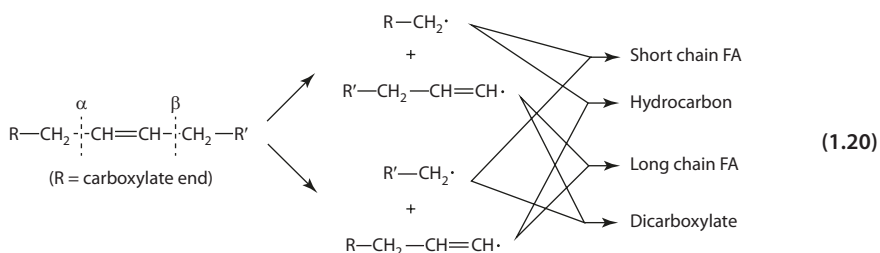
Name	Smoke point	Name	Smoke point
Corn	232	Soybean	238
Sunflower	232	Peanut	232
Safflower	266	Canola	204
Olive (extra light)	242	Coconut	232
Lard	188	Butter	177 range
Cottonseed	216	Palm	229
Sesame	210		

Unrefined oils = 160 °C or less for all

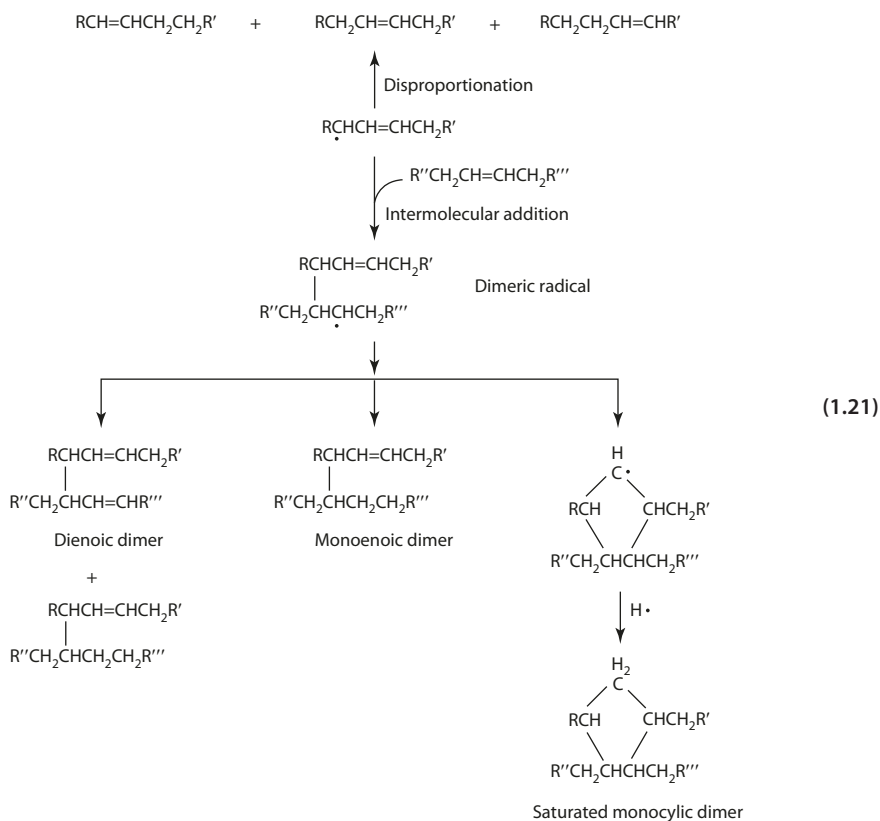
Olive oil promace = 238 °C, virgin = 199 °C, extra virgin = 191 °C

1.5.1 Thermal Reactions

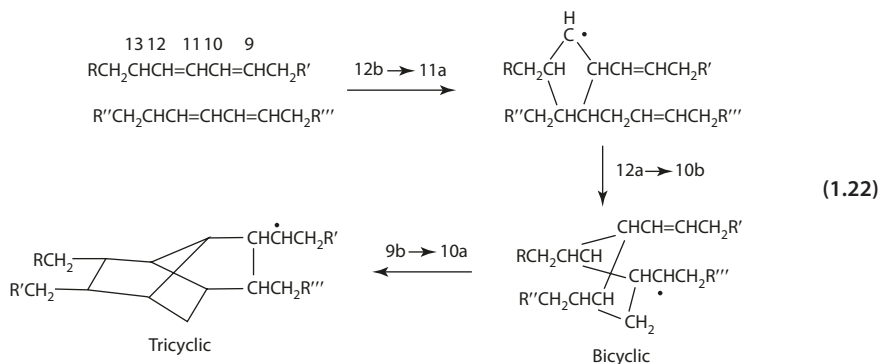
Under anaerobic conditions, a relatively high temperature (>200 °C) is required to decompose saturated triacylglycerols. Triacylglycerols break down to free fatty acids and glycerol. The former converts to a series of normal alkanes and alkenes, C_{2n-1} symmetric ketone, C_n oxopropyl ester, C_n propene and propanediol esters, and C_n diglyceride. The glycerol decomposes to acrolein and carbon dioxide [11].



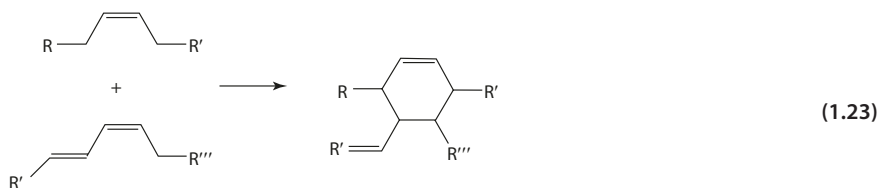
Thermal treatment of unsaturated lipids in the absence of oxygen produces predominantly dimers and cyclic compounds [15]. One major mechanism involves homolytic cleavage of the C–C bond α or β to the double bond, with the formation of radical fragments (Eq. 1.20). Direct combination of these radical fragments yields short- and long-chain fatty acids, straight-chain dicarboxylic acid, and hydrocarbon. The radical fragments may also abstract hydrogen from the fatty acid (e.g., oleate) to give allyl radicals, which undergo (1) disproportionation to monoenoic and dienoic acids or (2) intermolecular addition to the C–C double bond of another fatty acid chain to form a dimeric radical. The dimeric radical disproportionates to monoenoic and dienoic dimers, abstracts $\text{H}\cdot$ to form a dimer, or undergoes intramolecular addition to form a cyclic dimer (Eq. 1.21) [15].



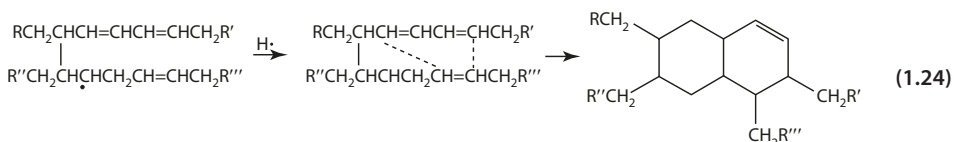
For linoleate, similar types of reactions are observed, but the products are complex mixtures of dimers – acyclic, bicyclic, and tricyclic of various unsaturation. The conjugated allyl radicals combine to form acyclic dimers or undergo intermolecular addition to form dimeric radicals. Since the dimeric radicals in this case contain conjugated double bonds, successive intramolecular addition may yield bicyclic and tricyclic dimers (Eq. 1.22).



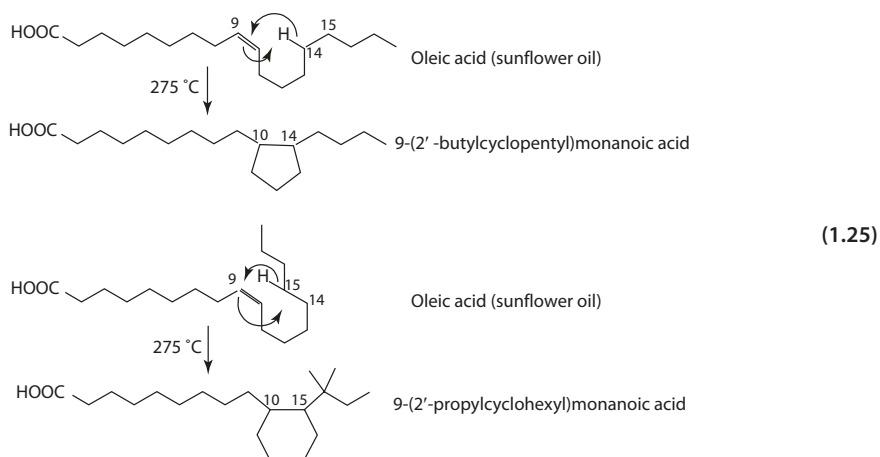
Dimerization to cyclic structures also occurs by the Diels-Alder reaction between the conjugated diene in linoleate, for example, and a double-bond dienophile in another molecule of the fatty acid (Eq. 1.23).



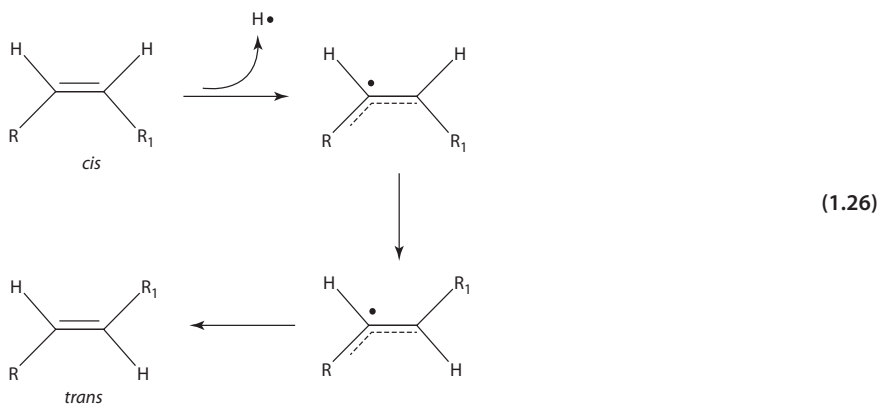
Bicyclic and tricyclic structures can be explained by a free-radical mechanism combined with an intramolecular Diels-Alder cyclization. Some acyclic dimers formed by the combination of free-radical fragments may contain conjugated dienes. The acyclic trienoic dimer, for example, can further undergo Diels-Alder reaction to a bicyclic compound (Eq. 1.24).



Cyclic fatty acid monomers containing five- and six-member rings are produced by direct internal cyclization of unsaturated fatty acids. In oleate, this involves cycloaddition at the vinylic carbon at C9 with ring closure assisted by [1,6]-prototropic migration of the allylic hydrogen at C5 to form a cyclopentyl monoenoic acid. In addition, cycloaddition at C10 with ring closure by [1,7]-prototropic migration of the allylic hydrogens at C15 will produce a cyclohexyl monoenoic acid [12] (Eq. 1.25).



Heat treatment, for example, at frying oil temperatures, increases isomerization of *cis* double bonds to the *trans* configuration in the triacylglycerol. In contrast to isomerization in the hydrogenation oil, the *trans*-fatty acids are formed without double bond migration. The mechanism involves the abstraction of the H atom from the double bond to form the radical L· in the *cis* form, followed by rotation of the bond, and interconversion to the *trans* configuration [55] (1.26). Heating reduces the energy barrier for the bond rotation and facilitates the isomerization process.



1.5.2 Oxidative Thermal Reactions

Oxidation of saturated fatty acids at high temperatures occurs with O₂ attack at the α, β, or γ carbon (positions from the ester carbonyl group) to form the respective alkoxy radicals [11]. Thermolytic cleavages between the α, β, or γ carbons of the radical species produce various short-chain hydrocarbons, carbonyls, and ketones (Fig. 1.3).

Oxidative thermal decomposition of unsaturated fatty acids generally leads to dimers, trimers, and tetramers with polar groups, often containing linkages of C–O–C and C–O–O–C in the molecules. The hydroperoxide formed from oxidative thermal treatment decomposes into oxyl and peroxy radicals which can (1) abstract a hydrogen atom from another fatty acid molecule, forming new radicals, or (2) be added to a C=C double bond of a fatty acid molecule to form radical dimers with ether or peroxide

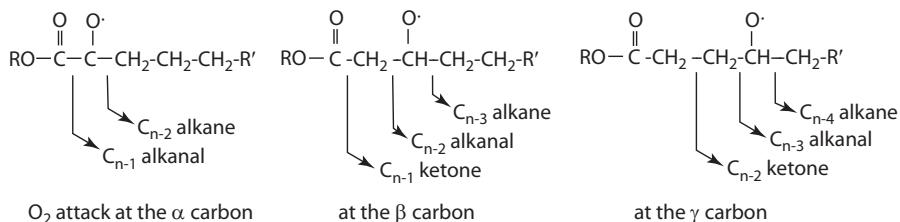
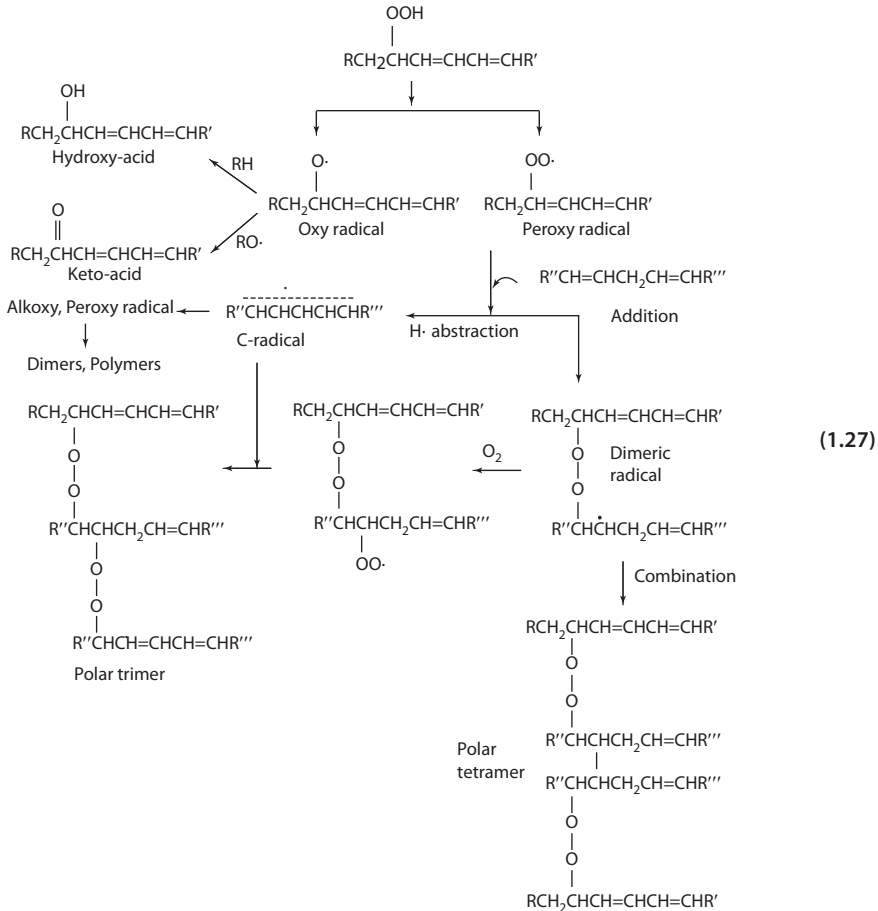


Fig. 1.3 Thermal cleavage of a α-, b β-, and c γ-oxidation products (From Crnjar et al. [11])

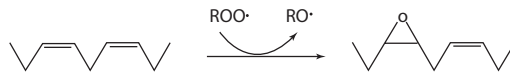
1.5 · Thermal and Oxidative Thermal Reactions

bridges (Eq. 1.27). The new radicals from either route may pick up a molecule of oxygen to form peroxy radical, which then undergoes a second addition or combination to form longer polymers.

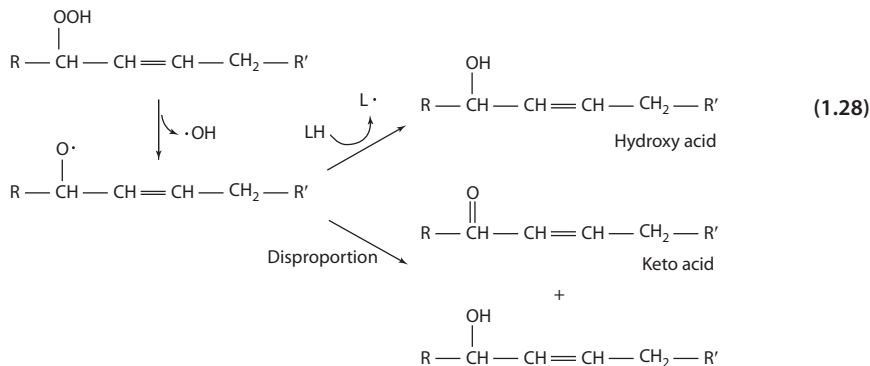


Considerable amount of the oxidized products in used frying oils are characterized by the presence of one or more oxygenated (epoxy, hydroxy, keto) functions. Epoxy acids are shown to form in high-temperature heating of oleic and linoleic acids. The reaction involves a direct attack by a hydroperoxyl radical on the vinylic carbons, leading to the formation of an oxirane ring [34] (Eq. 1.28). Two saturated epoxides, *cis*-9,10- and *trans*-9,10-epoxystearates, are produced from thermo-oxidation of oleate or triolein, while six epoxides, *cis*-9,10-, *trans*-9,10-, *cis*-12,13-, and *trans*-12,13-epoxyoleates are produced from linoleate or trilinolein. Hydroxy acids and keto acids are formed at lower levels. The alkoxy radical can abstract H atom from another lipid molecule to form a hydroxy acid. The alkoxy radical may also undergo disproportionation to yield a keto acid (Eq. 1.28). The amount of total polar compounds in used frying oils should not exceed 25% (on oil weight), which is the recommended limit for discarding the oil [20].

I. Epoxidation



II. Hydroxy and Keto functions



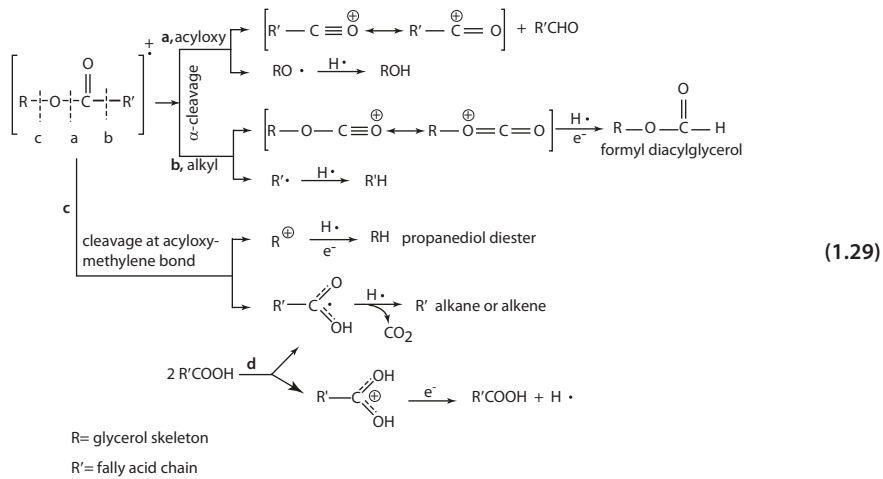
1.6 Radiolysis of Lipids

The radiation of interest in food preservation is ionization radiation, which involves the exposure of food to γ -rays, x-rays, or accelerated electron. The power limits are regulated not to exceed 5 MeV for γ - and x-rays and 10 MeV for electrons. The amount of ionizing energy absorbed by a material is the dose, measured in grays (Gy, equal to 1 joule per kg) or kilograys (kGy). For applications, the common source of ionizing energy is cobalt 60 γ -rays, produced by the decay of ${}_{27}\text{Co}^{60}$ to the stable ${}_{28}\text{Ni}^{60}$ emitting γ -rays in the process. Electrons are created in an electron beam linear accelerator by heating a wire filament in an evacuated tube. X-rays are produced by targeting accelerated electrons on a metal plate. The energy given up by the electrons during the interaction is converted to x-rays. Both γ - and x-rays are a form of electromagnetic energy of high frequency compared to lower-range microwave, infrared, visible light, and ultraviolet light in the spectrum. (See S-3.)

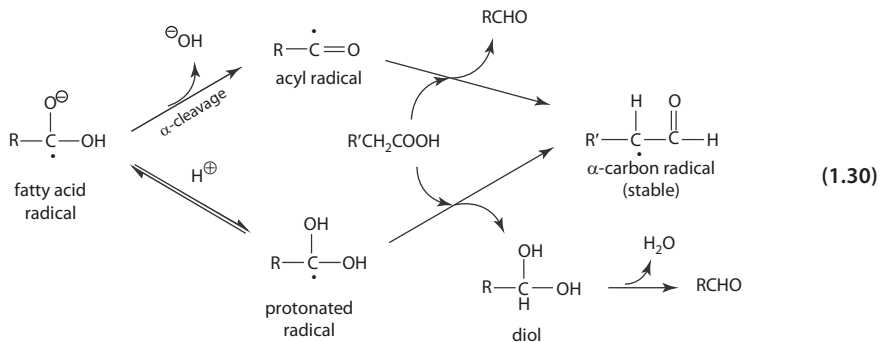
The general mechanism of radiolysis of lipids involves ionization. The removal of an electron from the olefin molecule results in an electron deficiency or «hole» localized in the carboxyl group or the double bond. The resulting molecular ion $[\text{R}-\text{CH}=\text{CH}-(\text{CH}_2)_7-\text{COOH}]^+$ undergoes the following types of reactions (Eq. 1.29) [36].

1. Fragmentation proceeds via α cleavage at the (1) acyloxy or (2) alkyl chain. The former reaction yields the acylium ion, RCO^+ , and the latter the fragment ion, $\text{R}-\text{O}-\text{C}\equiv\text{O}^+$. These cations, together with the corresponding radical fragments, can abstract hydrogen atoms to form various stable products. The radicals may also combine to form polymers.
2. Decarboxylation takes place if cleavage occurs at the acyloxy-methylene bond in triacylglycerols or if intermolecular transfer of $\text{H}\cdot$ occurs in fatty acids. The acyloxy radical forms rapidly and loses CO_2 to yield a primary alkyl radical that can abstract $\text{H}\cdot$ to form the alkane or alkene.

1.6 • Radiolysis of Lipids



Studies of γ -irradiated fatty acids or triacylglycerols at low temperatures by electron spin resonance indicate the formation of radical anions from electron capture by the carboxyl group [14]. The radical anion is protonated to form the protonated anion radical or decays by α cleavage to yield the acyl radical. The protonated radical and the acyl radical react with the parent fatty acid to generate the stable α -carbon radical (Eq. 1.30).



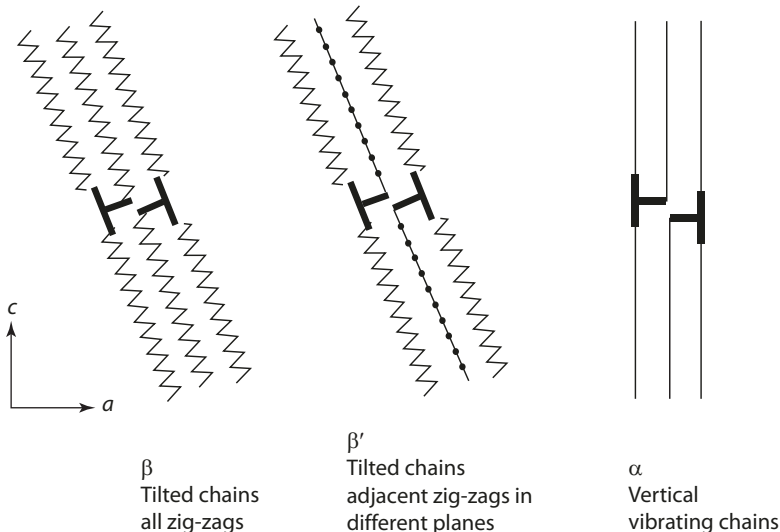
For triacylglycerols, electron addition occurs at either the 1' or 2' fatty acid chain [48]. The anion radical can be protonated or undergoes β cleavage to yield the free fatty acid and the propanediol diester radical. The radicals in turn abstract H \cdot from a parent triacylglycerol to produce aldehyde, glycerol and diacetate, and α -carbon radical (Eq. 1.31). The radicals in these reactions may enter into termination reactions by disproportionation or by combination to dimers.

hydrocarbon chain. The orientation of these periods determines the stability of the crystalline structure. There are three main types of packing arrangements that concern oil chemists.

1. Trichlic parallel (TII): All zigzag planes (a , b planes) are parallel.
2. Orthorhombic ($O\perp$): The planes are alternate.
3. Hexagonal (H): The planes are random with rotational freedom.

Triacylglycerols exhibit the same different types of packing arrangements. The triclinic, orthorhombic, and hexagonal packing types are designated β , β' , and α , respectively, and schematically represented in **Fig. 1.5**. The β form is associated with the triclinic subcell and has all the zigzag planes in parallel. The β' form is associated with the

a TAG crystals viewed along the b axis



b Cross-sectional view

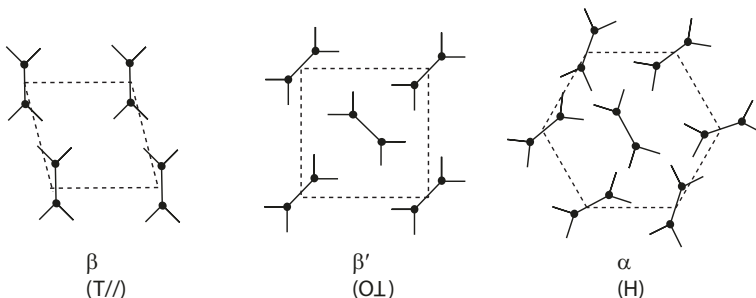


Fig. 1.5 Polymorphic crystals: **a** TAG crystals viewed along the b axis; **b** cross-sectional view (From Timms [53] with permission. Copyright 1984 Elsevier)

■ **Table 1.6** Stable polymorphs of selected triacylglycerols

Triglyceride	Melting pt. (°C)	Polymorph	Triglyceride	Melting pt. (°C)	Polymorph
LLL	46	β -2	PPO	35	β' -3
PPP	66	β -2	SSO	43.5	β' -3
SSS	73	β -2	PSO	40	β' -2
OOO	5	β -2	SPO	37	β' -3
PSS	65	β -2	PEP	54	β -2
SPS	68	β -2	SES	60	β -2
PSP	68	β' -2	PEE	40	β -2
POP	38	β -3	EPE	44.5	β -2
POS	38	β -3	POO	19	β' -3
SOS	44	β -3	OPO	21	β' -3

From Timms [53]

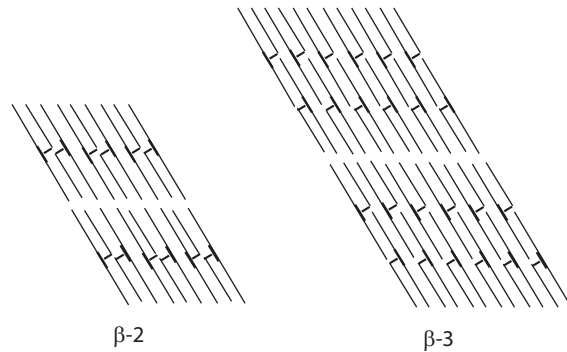
Major TAG in cocoa butter: SOS

orthorhombic subcell, with every chain having its zigzag plane perpendicular to the zigzag plane of its neighboring chain. The α form is associated with the hexagonal subcell and has the fatty acid chains perpendicular to the basal plane, oscillating with a high degree of molecular freedom [33].

Saturated monoacid TAGs, such as SSS, follow the standard $\alpha \rightleftharpoons \beta' \rightleftharpoons \beta$ transition to form stable β crystals. Saturated mixed-acid TAGs, like most fully hydrogenated TAGs consisting of predominantly palmitic (16:0) and stearic (18:0) acids, acquire β' or β properties (■ Table 1.6). For saturated/unsaturated mixed-acid TAGs, multiple β' and β forms (or subforms) may be observed. A well-known example is SOS, a major TAG present in cocoa butter, which shows 5 polymorphs: α , γ , β' , β_2 , and β_1 [43].

In the molecular arrangement, individual triacylglycerols assume a turning fork configuration. The central and one of the two fatty acid ester chains align along the same axis. The third remaining fatty acid chain parallels the central chain. The TAG molecules are stacked head to tail. Two pairing modes are possible, resulting in double-chain or triple-chain lengths. A double-chain length is formed when the acyl chains are of the same or very similar types. A triple-chain length is formed in the TAG where the fatty acids differ much in the chain length. The mode of pairing is indicated by adding -2 or -3 to the polymorphic symbols, for example, β -2, β' -3, etc. The chemical nature of the fatty acids in an individual TAG also affects the packing arrangement. For example, in monounsaturated TAGs such as 2-oleodistearin, the stereo requirement of the *cis*-double bond in the oleic acid causes the molecule to adopt a bent configuration packed in triple-chain length units [29]. Also, with the exception of the α form, β' and β crystals have the chains tilted at a certain angle to accommodate the branching structure. The schematic arrangement of TAG in the β -2 and β -3 polymorph packing arrangement of mixed glycerides in the β form is represented in ■ Fig. 1.6.

■ **Fig. 1.6** TAG in the β -2 and β -3 polymorphic arrangement (From Timms [53] with permission. Copyright 1984 Elsevier)



The head-to-tail stacked TAG molecules are assembled side by side laterally resulting in a long lamellar structure. The thickness of a lipid lamella depends on (1) the length of the fatty acid chains, (2) the pairing arrangement, and (3) the angle of tilt between the chain axes and the basal plane.

1.7.2 Crystal Habit of Fat

A TAG lamella has a scale of 30–60 Å. Several lamellae stack epitaxially forming a layered structure called nanoplatelet (nanocrystal) [1]. The average size of the nanoplatelet for tristearin (β polymorphic form) is $\sim 150 \times 60 \times 30$ nm. These platelet crystals aggregate to form spherulites of 0.25–200 μm . Fats that crystallize in the β form have large and coarse nanocrystals. Clumps of these crystals are responsible for grainy and sandy texture. α -Crystals are fragile platelets of ~ 5 μm in size. Fats with stable β' forms appear as tiny needles of ~ 1 μ length microscopically. These are typically of randomized fats, such as rearranged lard, tallow, and the hydrogenated cottonseed oils. The β' crystals can incorporate large amounts of tiny bubbles, providing a smooth, creamy texture to the oil product. For margarine and shortening, the desirable crystal form is β' .

The fatty acid composition of an acylglycerol molecule determines in part its crystal habit. Acylglycerols with uniform fatty acid composition tend to have β crystals. Fats containing mixed compositions tend to form β' crystals. For example, soybean oil contains less than 10% of palmitic acid. Upon increased hydrogenation, it is increasingly composed of predominantly tristearic acid, which can arrange in orderly fashion to form β crystals. Palm oil and the β' -type oil contain at least twice the amount of palmitic acid. Palm oil has 50% palmitic acid, and the hydrogenated product, a mixture of stearic and palmitic acid, tends to crystallize in the β' form. Interesterification usually converts a β' -type to a β -type fat.

The position of a particular fatty acid in the acylglycerol also affects the crystal habit. A mixed triacylglycerol such as 2-stearoyl dipalmitin generally shows great stability for the β' form, and the stable β form is difficult to obtain. On the other hand, 2-palmitoyl distearin exhibits a stable β form, and the β' form is seldom obtained. Lard is the most extensively studied in this aspect. Contrary to common vegetable oils, which tend to have saturated acids in the 1- or 1- and 3-positions, natural lard contains 60% palmitic acid in the 2-position. Interesterification changes the palmitic acid proportion in the 2-position, and the randomized lard crystallizes in the β' form instead of the β form for natural lard [33, 60].

■ **Table 1.7** Hydrogenated fats and crystal habits

β Type	β' Type
Soybean	Cottonseed
Safflower	Tallow
Sunflower	Butter oil
Peanut	Palm
Olive	Modified lard
Lard	Rapeseed
Corn	
Coconut	
Cocoa butter	
Sesame	

From Wiedermann [60]

Therefore, the process of hydrogenation and interesterification can be controlled to chemically modify the acylglycerols, producing fats and oils with different melting and crystal habits to fit the demands for a wide variety of food uses. In industrial processing, the polymorphic form of a fat or blend has significant practical meaning. ■ Table 1.7 lists some of the fully hydrogenated common fats in categories of their crystal habits [60].

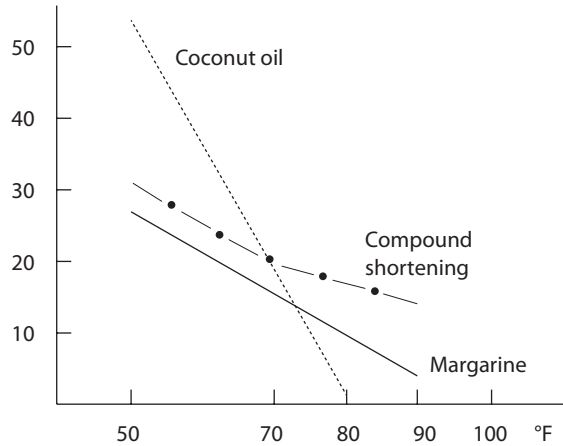
The important effect of fatty acid composition and the position of a particular fatty acid in the acylglycerol is well illustrated by cocoa butter [61]. Cocoa butter contains about 60% saturated fatty acids (stearic acid and palmitic acid) and 35% oleic acid (which is sandwiched in the 2-position of the triacylglycerol structure). This type and position arrangement result in what is known as Form V (beta) crystal in cocoa butter processing, contributing to the characteristic mouthfeel and texture in the chocolate and confectionery products. The Form V crystal melts around 34–38 °C, rendering solid chocolate at room temperature that readily melts inside the mouth. In recent years, cocoa butter alternatives have been formulated from triacylglycerol combinations developed from vegetable oils. Cocoa butter equivalents have ingredients originated from palm, shea, and sunflower. Cocoa butter substitutes contain high content of lauric acid from palm kernel and coconut.

1.8 Plasticity of Fat

The physical characteristics, such as spreadability, softness, and consistency, of commercial solidified edible fats (margarine, shortening, etc.) depend on the following: (1) amount of solids (acylglycerol crystals) present at a given temperature, (2) melting point of component acylglycerols in fat, and (3) polymorphic form (crystal habit) of the component acylglycerols.

A plastic fat can be visualized as a mass of interlocking crystals (solid phase) holding a liquid phase. For example, margarine contains water droplets within the fat crystal network. The plasticity of a fat depends on the proper proportion between the solid and the liquid phase. A right balance between the solid and liquid phase insures that the solids yield and flow when the external workforce applied exceeds the internal bonding forces of

Fig. 1.7 Solid-liquid ratio measurement of margarine, coconut oil, and shortening (From Wiedermann [60] with permission. Copyright 1978 Springer)



the solid mass. The fat regains the original consistency after the external force is lifted. The temperature range in which the fat retains this plastic characteristic (plasticity) is the plastic range. If the fat contains too few solid crystals, the fat will melt, and if the solid content is too high, the fat becomes brittle [24]. In practice, the percent solid fat is 10–30%.

Figure 1.7 shows the relative solid content of margarine as compared to coconut oil and shortening at various temperatures [60]. Margarine has 30% maximum solid at low temperature, making it less brittle (hence, high degree of softness) than coconut oil. Compared to shortening, it has a steeper slope at the higher temperature range (70–90 °C). The product therefore possesses a quicker melt in the mouth than shortening.

Fats consisting of largely a single class of acylglycerols usually have a very narrow plastic range. Coconut oil and butter oil, containing largely a single class of saturated glyceride, melt sharply. Fats made of a mixture of acylglycerols melt over a wider temperature range and usually have desirable plastic properties, since each component acylglycerol will melt at different temperatures.

1.9 Hydrogenation

Hydrogenation is used extensively in the oil industry to manipulate the chemistry and composition of fatty acids to produce various oil or fat stocks with specific functional characteristics. There are two main objectives in hydrogenation.

1. Vegetable oil typically contains considerable amount of unsaturated fatty acids. For use in cooking or frying, it is partially hydrogenated to improve oxidative stability by reducing unsaturation and hence the rate of oxidation. The rate of oxidation in fatty acids is correlated with the degree of unsaturation, as shown in Table 1.3. In most practices, it is preferable to convert polyenic acids to give triacylglycerol mixtures of C18:2 or C18:1, thereby increasing the stability of the product.
2. Hydrogenation is used to modify the physical characteristics, especially the melting range and crystallization behavior desirable for formulation of oil blends [22]. The process is particularly important in producing oil stocks for margarines, spreads, and shortenings. For example, margarine oil base stock contains hydrogenated oil blended with liquid oil to produce desirable solid fat content and functionality for the characteristic consistency and spreadability. The product solidifies at a low temperature, yet melts quickly at body temperature to yield the desirable mouthfeel.

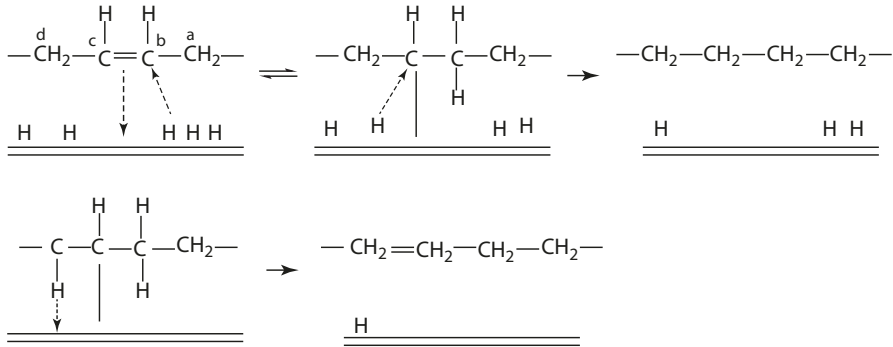


Fig. 1.8 Mechanism of hydrogenation (From Larsson [30])

1.9.1 Mechanism

The degree of hydrogenation is controlled by several factors, including hydrogen concentration, reaction temperature and time, and the catalyst. In industrial process, vegetable oils are subjected to partial hydrogenation at moderate temperatures (140–190 °C) and pressure (≤ 60 psi), using nickel as the catalyst. The chemistry aspect of hydrogenation may involve the following steps [30].

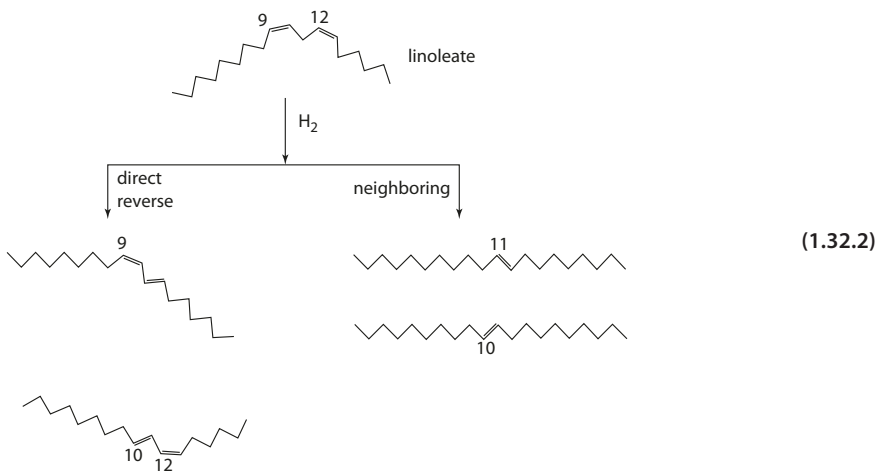
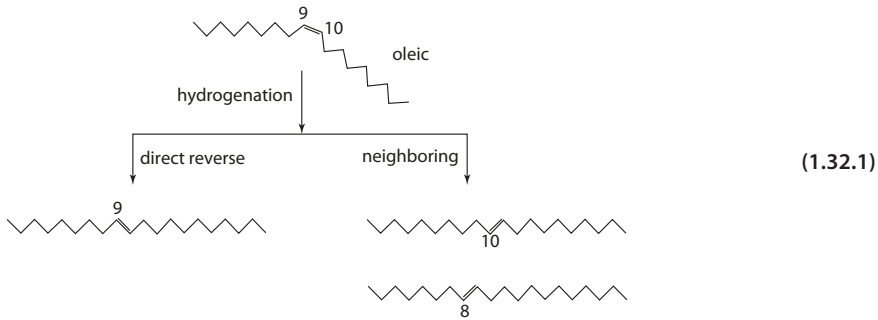
1. The double bond is adsorbed (π -bonding interaction) onto the surface of the metal catalyst (Fig. 1.8a).
2. A hydrogen atom from the metal surface is transferred to one of the carbons of the double bond, and the other carbon binds (σ -bonding) with the metal surface.
3. A second hydrogen transfer liberates the saturated product.

The first reaction step is reversible, with the hydrogen atom retained to the metal surface, and the molecule «desorbed». *Cis-trans* isomerization occurs with rotation around the C–C bond. A shift of the double bond position also occurs, if the reverse reaction proceeds at the neighboring methylene group of the double bond (Fig. 1.8b).

The changes in the degree of saturation and in the isomer configuration of the fatty acids resulting from hydrogenation have a profound effect not only on the increased stability but also on the melting properties and indirectly the crystal habits of the triacylglycerols.

1.9.2 *Cis-Trans* Isomerization

Changes in the isomeric configuration of individual fatty acid chains indirectly alter the spatial structure of the triacylglycerol molecule. This is evident by considering the isomerization of *cis*-C18:1 (Eq. 1.32.1) and *cis*-C18:2 (Eq. 1.32.2) [3].



The spatial arrangement of triacylglycerols of saturated fatty acids is quite different from those of unsaturated fatty acids. The unsaturated fatty acid bends at the *cis* double bond, so these molecules cannot fit closely together. Notice the similarity in spatial arrangement between oleic acid and *cis-trans* linoleic acid. A *trans* double bond has physical properties similar to those of a saturated bond: The *cis-trans* linoleic acid is similar to oleic acid rather than *cis-cis* linoleic acid. *Trans* oleate is fairly hard and has physical properties approaching those of stearate.

1.9.3 Selectivity

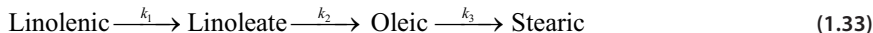
In order to produce products suitable for various purposes, hydrogenation must be selective and requires rigorous control of the reaction conditions [2]. ■ Table 1.8 summarizes the effects of different parameters, such as pressure, temperature, agitation, and catalyst load, on the rate of hydrogenation and the degree of isomerization.

■ **Table 1.8** Factors affecting selectivity in the hydrogenation process

Increasing	Selectivity ratio	Isomerization	Rate
Temperature	+	+	+
Pressure	–	–	+
Agitation	–	–	+
Catalyst	+	+	+

From Allen [2]

Selectivity is explained by assuming the following simplified picture of sequences of events in hydrogenation in Eq. 1.33. Linoleic acid selectivity is defined as a ratio of the hydrogenation rate constants of linoleic acid and oleic acid, that is, $S = k_2/k_3$. The higher the rate, the higher is the selectivity. If $S = 0$, all molecules react straight through to stearic acid. When $S = \infty$, no stearic acid is formed. Likewise, the linolenic acid selectivity is the ratio of the hydrogenation rate constants of linolenic acid and linoleic acid $S = k_1/k_2$. Hydrogenation of vegetable oil is carried out under selective conditions not only to minimize *cis-trans* isomerization but also to control the undesirable formation of saturated stearate because the high melting characteristic of tristearin produces a sandy or grainy taste to the product.



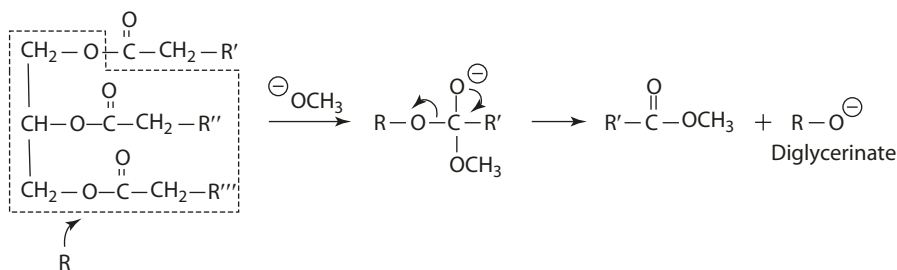
1.10 Interesterification

Oil or fat stocks are often directly blended in various combinations to formulate a wide range of products from liquid to plastic to sharp melting solid. Interesterification changes the distribution pattern of the fatty acids in the triacylglycerol molecule, producing fats and oils with desirable melting and crystallization characteristics. In practice, a catalyst, alkali metals, or their alkoxides are used (in the range of 0.2–0.4%). The reaction starts at low temperatures of 50–75 °C and is usually processed at ~100 °C.

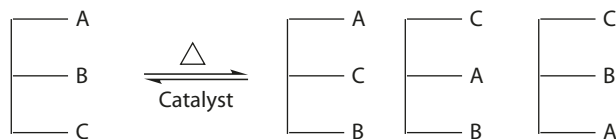
The migration of fatty acids within the same acylglycerol molecule is referred to as intraesterification. The random migration and replacement of fatty acids among acylglycerol molecules ultimately attain equilibrium with all possible combinations of fatty acids in acylglycerol structures. The random rearrangement of fatty acids among glyceride molecules is termed interesterification. Take, for example, the equilibrium mixture of intra- and interesterification of a triacylglycerol ABC that is shown in ■ Fig. 1.9. (For lipase-catalyzed interesterification, see Chap. 5.)

1.10.1 Mechanism

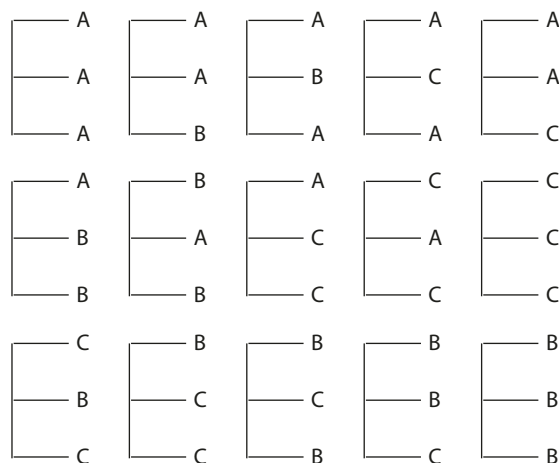
The reaction mechanism of interesterification involves nucleophilic substitution at the carbonyl carbon (Eq. 1.31) [51]. The diglycerinate generated reacts with another



Intraesterification



Interesterification



■ Fig. 1.9 Equilibrium triacylglycerol mixtures of intra- and interesterification

acylglycerol, forming a new triacylglycerol and regenerating another diglycerinate until an equilibrium mixture of all possible compositions of the fatty acids is obtained.

Due to health concerns, interesterification has been an alternative to hydrogenation for the similar results but with lower *trans* fatty acid levels [25, 56].

1. Substituting certain percentage of modified tropical oils such as palm oil for hydrogenated vegetable oils to produce a low-*trans* blend. Tropical oils contain high level of saturated fats and are oxidatively stable compared to common vegetable oils and do not require hydrogenation.

2. Blending a mixture of fully hydrogenated oil (high level of stearin, <1% TFAs) with unhydrogenated oil.
3. Blending fractionated palm oil with unhydrogenated vegetable oil to produce *trans*-free fat-phase component suitable for margarine and shortenings.

1.11 Emulsions

Emulsions are a mixture of two immiscible phases; one is the dispersed or discontinuous phase as droplets or liquid crystals; the other is the nondispersed, continuous phase. If the oil is dispersed as finite droplets in a solution of water (which is the continuous phase), the emulsion is termed as oil-in-water (o/w) type. When water is dispersed in oil, the emulsion is referred to as water-in-oil (w/o). The discussion here focuses on the o/w type of emulsion.

1.11.1 Surface Tension and Surface Area

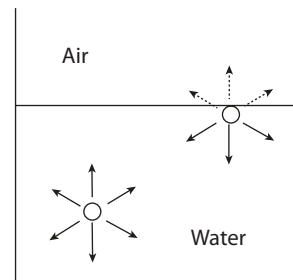
Surface tension arises from unbalanced intermolecular forces on the surface molecules. Consider an air/water system: A water molecule at the interface, quite different from the water molecule in the bulk of the solution, experiences an uneven effect of intermolecular forces (■ Fig. 1.10). The molecule tends to move into the bulk of the water solution, since a water molecule in the bulk solution has a lower potential energy than at the interface. This driving force for the water molecule at the interface to move into the bulk is referred to as surface tension. Another way of reasoning is to consider that energy is required to move a water molecule from the bulk solution to the surface. The energy is used to increase the surface area of the interface. For this reason, water droplets spontaneously assume a spherical form since a sphere has the smallest surface/volume ratio. The same reasoning can be applied to an o/w system. The oil molecules tend to stay in the oil phase. It requires work to disperse the oil molecules in a water solution.

1.11.2 Formation of Emulsion

The formation of an emulsion requires energy to form the dispersed droplets in the continuous phase. This energy is represented by Eq. 1.34, where γ = surface tension and σ = surface area.

$$dw = \gamma d\sigma \quad (1.34)$$

■ Fig. 1.10 Water molecule at interface



Obtaining a fine emulsion means reducing the size of the droplets and hence increasing the surface area. Hence, it takes more energy to maintain a finely dispersed emulsion, implying that the formation of an emulsion is thermodynamically unfavorable. However, if the γ term in Eq. 1.34 can be diminished, the energy required to produce a given emulsion is decreased. Lowering the surface tension at the interface enhances emulsification. One of the primary roles of surfactants is to lower the surface tension. A surfactant molecule possesses both a polar end which interacts with water molecules and a hydrophobic end which interacts with the oil phase. This subject will be discussed again in a later section.

1.11.3 Breakdown of Emulsions

Three processes contribute to the breakdown of emulsions [16, 39].

1. *Sedimentation*: Due to the density difference between the two phases, the droplets tend to rise or sediment through the continuous phase. This process is referred to as «creaming up» or «creaming down.»
2. *Disproportionation*: Droplets or bubbles tend to decrease their surface area to minimize the potential energy at the interface. This decrease in surface area is balanced by the rise in internal pressure (Eq. 1.35).

$$\Delta P = 4\gamma / r \quad (1.35)$$

where

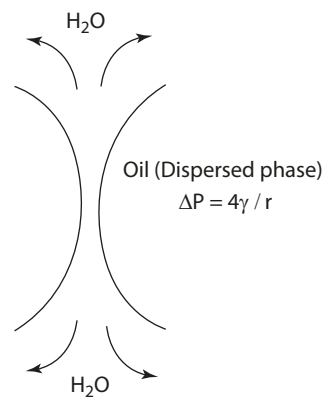
ΔP = pressure (inside) – pressure (outside).

γ = surface area

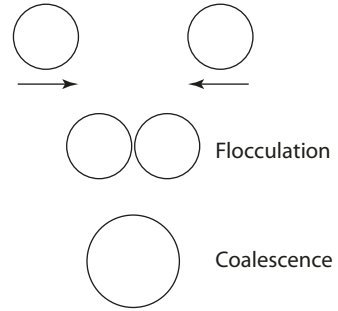
r = radius of the droplet

The Laplace equation (Eq. 1.35) suggests that the pressure increases inversely with the size of the droplet. At high dispersed-phase volume, the continuous phase forms the lamella in between the dispersed droplets. The pressure of the droplets causes thinning of the lamella (■ Fig. 1.11). The process is often viewed as «draining» of the water past the dispersed phase. The critical lamella thickness is reached at 50–150 Å. Diffusion starts from the small droplets to larger droplets or to the bulk phase.

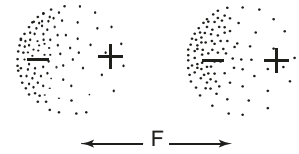
■ Fig. 1.11 Thinning of the lamella between dispersed droplets



■ Fig. 1.12 Schematic representation of flocculation and coalescence



■ Fig. 1.13 Van der Waals attraction between two adjacent atoms



3. *Flocculation and coalescence*: When two droplets in an emulsion (without surfactants present) come close to one another, they tend to flocculate and coalesce (■ Fig. 1.12). The process of flocculation and coalescence is dependent on the balance between two interactions: (1) Van der Waals attraction and (2) electrostatic repulsion between the droplets.

■ ■ Van der Waals Attraction

The attractive force is derived from the fluctuation in the electron density of a neutral atom. The uneven distribution of electron density momentarily creates a dipole, which induces the adjacent atoms into similar orientation (■ Fig. 1.13). This London energy varies inversely with the distance of separation between the atoms (Eq. 1.36).

$$F = -\beta / r^6 \text{ where } \beta = \text{constant, and } r = \text{distance in between} \quad (1.36)$$

The Van der Waals attractions are additive. The attractive potential between particles is equal to the summation of all attractions between every atom. The attractive potential increases with (1) increasing particle size and (2) decreasing distance between two particles.

■ ■ Electrostatic Repulsion

A particle with a uniformly charged surface can cause an uneven distribution of ions in the solution, forming an electric double layer at the surface. Ions with opposite charges (counterions) are found accumulated near the particle surface, with the concentration gradually decreasing with distance. Such distribution of counterions is described as ion atmosphere (■ Fig. 1.14a).

Consider two particles approaching one another. Their counterion atmospheres start to interfere, hence creating repulsion between the particles. The repulsion decreases exponentially with increasing distance of separation (■ Fig. 1.14b).

Fig. 1.14 Interactions in **a** ion and **b** counterion atmosphere

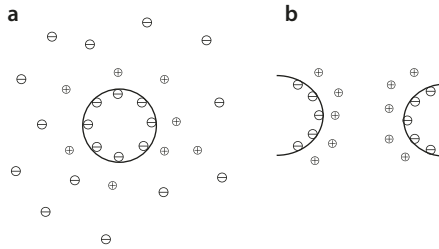
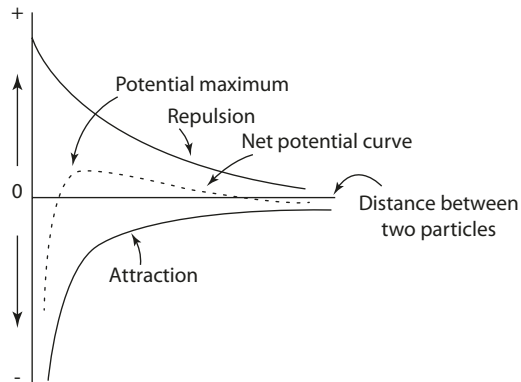


Fig. 1.15 Repulsion and attraction as a function of the distance between two particles (From Friberg [16] with permission. Copyright 1976 Taylor & Francis)



The stability of an emulsion, therefore, can be considered to depend on the balance between attraction and repulsion. **Figure 1.15** is a plot of the two potential energies as a function of the distance between two particles [16]. A very important difference between repulsion and attraction is their changes with respect to distance. The net potential is always attraction at long and short distance ranges. At certain intermediate ranges, repulsion may be greater than attraction, and a measure of stability may exist, depending on the magnitude of the net potential.

1.12 Emulsifiers

Food-grade emulsifiers are partial esters of fatty acids, polyols, and water-soluble organic acids. An emulsifier, therefore, consists of both hydrophilic and hydrophobic segments spatially separated in the same molecule. In food systems, their functions are:

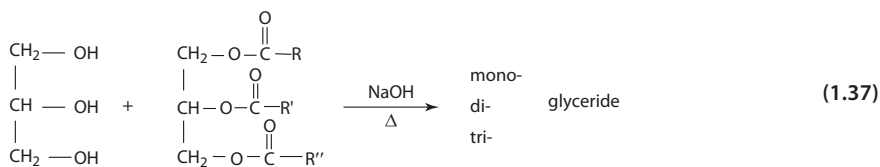
1. To promote stability of an emulsion by control of aggregation of fat globules
2. To slow the rate of staling in baked products by starch complexation
3. To use as dough strengthener/conditioner by interaction with gluten, to increase gas retention, improve texture, and increase loaf volume
4. To improve consistency of fat-based products by controlling fat crystallization

1.12.1 Monoglycerides

Monoglycerides are the most widely used emulsifier in food. Commercial monoglycerides are combinations of mono- and diglycerides, although monoglycerides are the main active emulsifier. Monoglyceride is prepared by the interesterification of

triglycerides with excess glycerol (Eq. 1.37) [58]. (The terms «monoglyceride» and «glyceride» are used here as these are trade names and also commonly used in food labeling.)

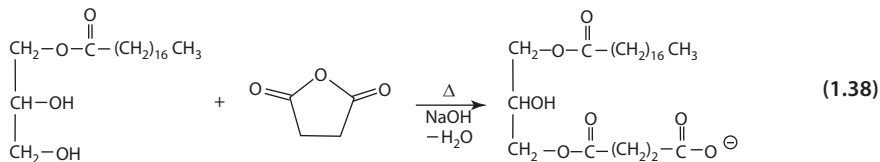
To obtain a high concentration of monoglycerides, the mixture is vacuum distilled to a product of >90% total monoglyceride. This product is termed distilled monoglyceride. The «soft» varieties, prepared from partially hydrogenated oils, are soft and plastic. The «hard» varieties, obtained from fully hydrogenated oil, are solid in powder form. Distilled «hard» monoglycerides are microdispersions in water as monoglyceride hydrates. Monoglycerides are nonionic and are used as dough softeners.



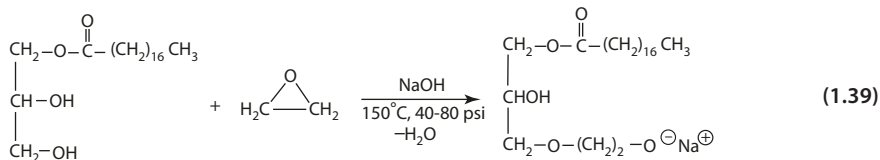
1.12.2 Monoglyceride Derivatives

The properties of a monoglyceride can be modified by introduction of functional groups ester linked to the glycerol backbone [58].

Succinylation of monoglycerides with succinic anhydride results in a product that is anionic. This alteration in the hydrophilic/lipophilic balance (HLB) of the molecule changes its degree of stability in water and also its functional properties. Succinylated monoglycerides function as both softeners and conditioners in baked products (Eq. 1.38).



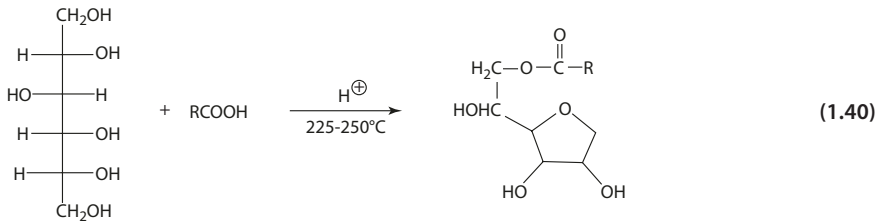
Similarly, ethoxylated monoglycerides are produced by reacting the monoglyceride with ethylene oxide (Eq. 1.39).



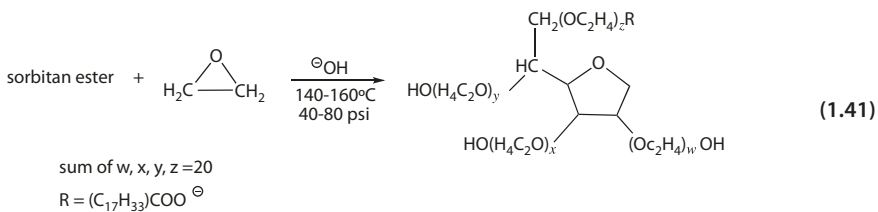
Diacetyl tartaric acid ester of monoglyceride is prepared by first reacting acetic anhydride and tartaric acid to form acetyl tartaric anhydride, which then reacts with monoglyceride. The product has increased HLB and water solubility.

1.12.3 Ester Derivatives of Alcohols (Nonglycerol)

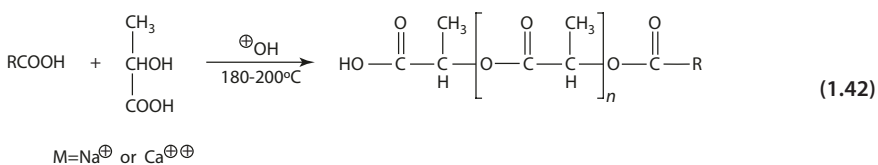
Sorbitan monostearate is the product of the reaction between sorbitol and fatty acid (Eq. 1.40). It is an antiblocking agent in confectionery products containing cocoa butter substitute and an emulsifier in cakes.



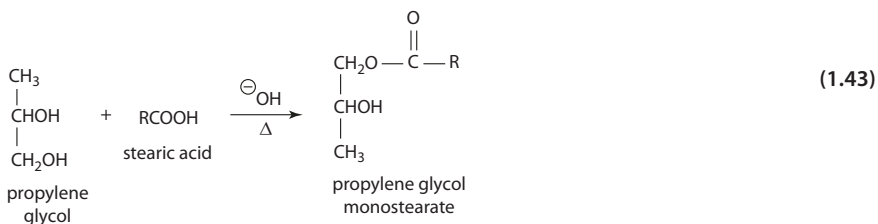
When the product is ethoxylated by reacting with ethylene oxide, the resulting product is polysorbate (Eq. 1.41), which is used as an emulsifying agent in cake and cake mixes and as a dough strengthener.



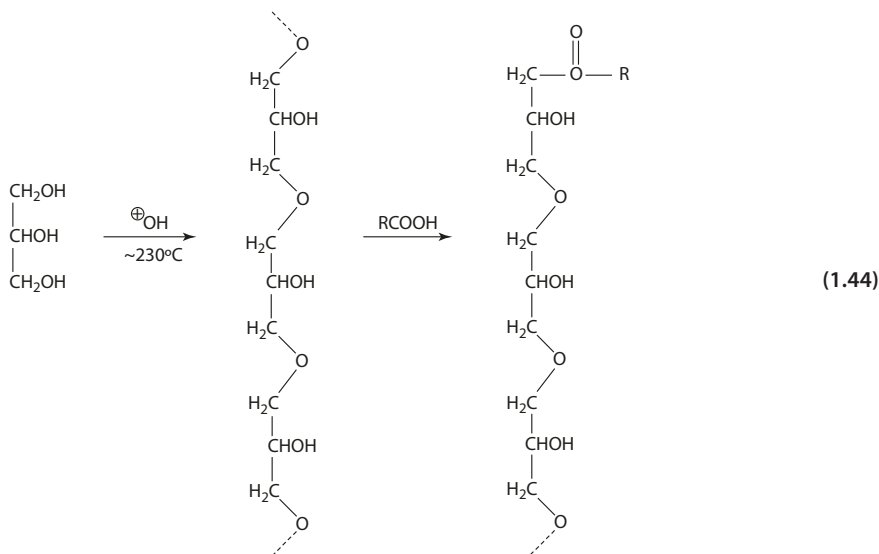
Stearoyl-2-lactylate, used as a dough softener and conditioner, is prepared by reacting stearic acid with lactic acid (Eq. 1.42).



Propylene glycol monostearate is produced by the esterification of propylene glycol with stearic acid (Eq. 1.43).



Polymerization of glycerol under alkaline conditions at high temperature produces polyglycerols. Condensation of the α -hydroxyl group forms an ether linkage, and the resulting polymer is linear. Direct esterification with fatty acid yields the ester of polyglycerol (Eq. 1.42) [35].



1.12.4 Lecithin

The name «lecithin» refers to a mixture of phospholipids including phosphatidylcholine (lecithin specifically), phosphatidylethanolamine (cephalin), phosphatidylinositol, and phosphatidylserine (■ Fig. 1.16), removed from the oil (predominantly from soybean in the United States) in the degumming process. Commercial crude lecithins contain small amounts of triacylglycerols, fatty acids, pigments, carbohydrates, and sterols. The amount of lecithin used in food formulations is in the range of 0.1–0.3% [59].

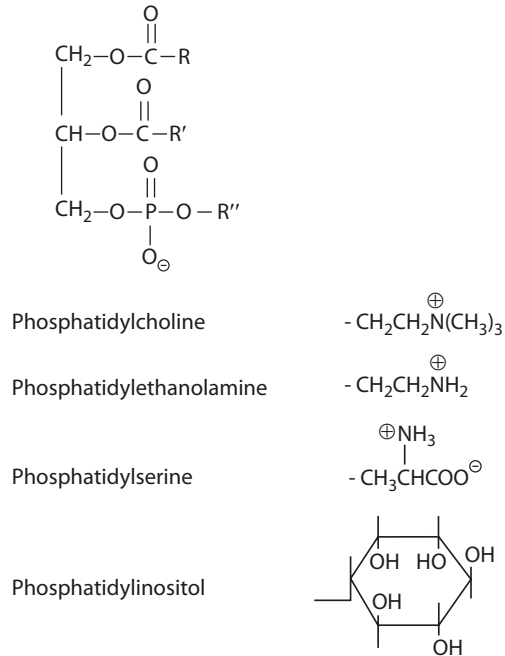
Saturated fatty acids are found primarily in the α position of phosphatidylcholine and the β position of phosphatidylethanolamine. The various phosphatides in lecithin have lipophilic and hydrophilic balance resulting in typical emulsifying properties.

Phosphatidylcholine (PC) and phosphatidylinositol (PI) have w/o emulsifying properties. A mixture of these phospholipids in lecithin results in both weak w/o and o/w emulsifying properties. Phosphatidylethanolamine (PE) flocculates and loses its emulsifying power in high concentrations of calcium and magnesium salts present in hard water. For more stable emulsions, lecithin is used in combination with other emulsifiers. In some cases, the lecithin is chemically or enzymatically modified to improve its emulsifying properties and to reduce its reactivity toward metal ions [8].

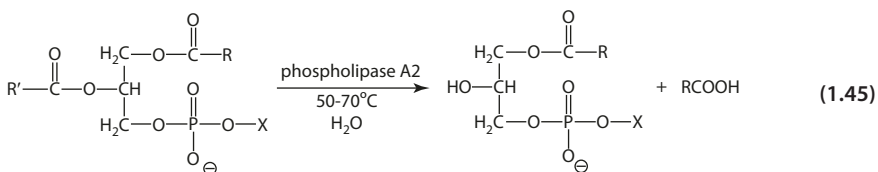
1. *Alcohol fractionation:* PC dissolves to a greater extent than PE in ethanol.

Fractionation of lecithin in 19% ethanol concentrates the PC in the product with the PC to PE ratio increased to 8:1. The product has improved o/w emulsifying property and is commonly used as an antispattering agent in margarine.

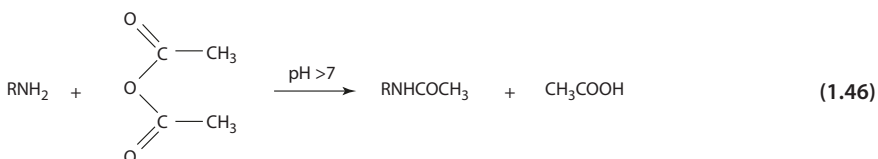
■ **Fig. 1.16** Composition of «lecithin» mixture (From van Nieuwenhuyzen [27])



2. *Hydrolysis*: Phospholipase A2 (used in industrial scale) specifically hydrolyzes the fatty acid at the 2-position of the phospholipids (Eq. 1.45). (Refer to Chap. 5 for details.) The modified product has improved o/w emulsifying properties. Chemical hydrolysis of phospholipid is less specific than the enzymatic reaction, and the reaction is difficult to control.



3. *Acetylation*: Reaction with acetic anhydride acetylates the primary amino group of PE (Eq. 1.46). The acetylated PE will not exist in zwitterion form. The modified lecithin has improved o/w emulsifying property.



Lecithin has been used extensively as emulsifier in a variety of food products. The following two specific examples illustrate its useful applications.

1. Antispattering in margarine: Margarine is a w/o emulsion, with 18% water (milk) dispersed in a continuous fat phase. Monoglyceride is often used to stabilize the w/o emulsion. In heating, the margarine melts, and the water coalesces into large droplets which evaporate vigorously, causing spattering of hot oil. Lecithin functions as nuclei for water droplets where slow evaporation is possible.
2. Dispersion of cocoa powder: Cocoa powder contains a film of cocoa butter on the surface and is not able to disperse in water or milk at low temperatures (melting point of cocoa butter $\sim 35^\circ\text{C}$). To enhance dispersion and wetting of the cocoa powder in aqueous solution, a thin spray of lecithin is deposited onto the cocoa powder. The lipophilic part of the phospholipid is incorporated in the cocoa butter, and the hydrophilic portion brings the powder into solution.

1.12.5 Hydrophilic/Lipophilic Balance

Both the chain length and the degree of unsaturation are important for functional properties. The emulsifiers described above may be classified according to their hydrophilic/lipophilic balance (HLB), which depends on the hydrophilicity of the polar group in relation to the lipophilicity of the fatty acid chain [27].

1. HLB = 3–9: monoglyceride, propylene glycol stearate, acetylated monoglyceride, ethoxylated, lactylated monoglyceride
2. HLB = 8–12: diacetylated tartaric acid ester, succinylated monoglyceride
3. HLB = 12–20: polysorbate, stearyl-2-lactylate, polyglycerol ester

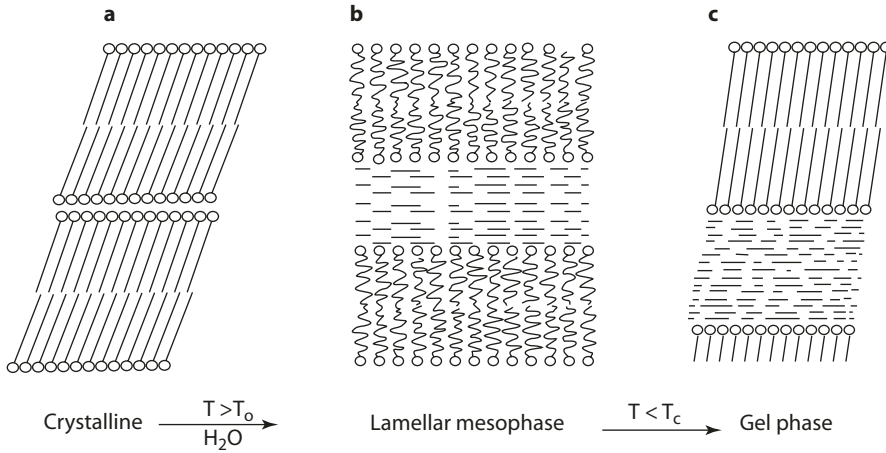
The HLB score may serve as indicators of the surface activity of the emulsifier, in its ability to reduce the interfacial tension and promote the emulsification of the two phases.

1.13 Molecular Arrangement of Emulsifier Molecules at the Interface: Mesomorphic Behavior

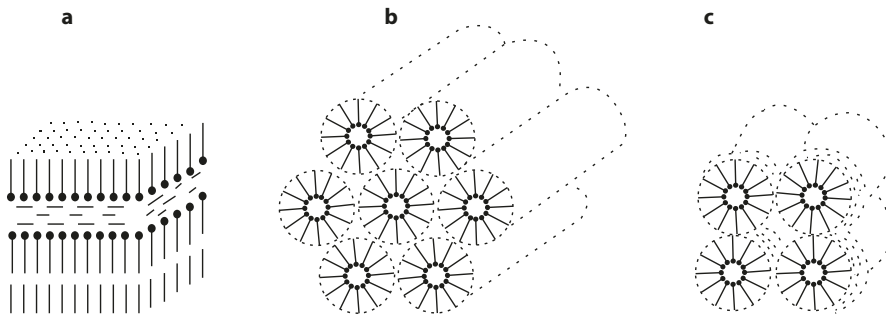
Emulsifiers adsorb in one or more layers at the interface and form various types of films depending on the packing conditions of the hydrocarbon chains. Many food emulsifiers including distilled monoglyceride, sorbitan, polyglycerol esters, and lecithin are known to form liquid-crystalline interfaces in an emulsion with various mesomorphic forms. When an emulsifier is dispersed in water and heated, the emulsifier crystal melts at a temperature, known as the Kraft point (T_c), before the true melting point is reached [28]. The hydrocarbon chain, held by relatively weak Van der Waal forces, melts at a lower temperature than the polar end group, which is hydrogen bonded, to assume a liquid crystalline structure with both liquid (melted chains) and crystal (polar end). A lamella mesophase is formed consisting of bimolecular lipid molecules separated by water. The chains are disordered, and the polar groups are oriented toward the water (■ Fig. 1.17).

On cooling of the lamellar mesophase, a gel is formed. The structure is still lamella, but the lipid chains are crystallized and are extended. The gel mesophase is a metastable state

1.13·MolecularArrangementofEmulsifierMoleculesattheInterface:MesomorphicBehavior



■ Fig. 1.17 Structural model of a crystalline state, b lamellar mesophase, and c gel state (From Krog [28] with permission. Copyright 1981 American Association of Cereal Chemists)



■ Fig. 1.18 Structural model of a lamellar, b hexagonal, and c cubic mesophase (From Krog [28] with permission. Copyright 1981 American Association of Cereal Chemists)

at the transition temperature between the solid crystal form and the liquid crystal (lamellar) form of the emulsifier.

Upon further heating, the lamellar mesophase breaks down to a viscous cubic or reversible hexagonal form (■ Fig. 1.18). Lamellar mesophase has bimolecular lipid layers alternating with water layers. Two types of hexagonal mesophases have been reported. Hexagonal I has the lipid molecules aggregated in cylinders with the polar groups oriented toward the outer water phase and the hydrocarbon chains filling the core. Hexagonal II exhibits the reverse arrangement, where the polar groups are oriented inward and the hydrocarbon chains radiate outward. The cubic phase consists of spherical aggregates with the polar groups facing the water and the hydrocarbon chains lining the exterior. ■ Table 1.6 lists the mesomorphic behavior of some emulsifiers in water [31]. Some of these emulsifiers produce different mesophases at different temperatures (■ Table 1.9).

■ **Table 1.9** Mesomorphic behavior of some emulsifiers in water

Emulsifier	Mesophase formation temperature °C	Types of mesophase
Saturated monoglyceride	55	lamellar $\xrightarrow{65^\circ\text{C}}$ cubic
Unsaturated monoglyceride	20	cubic $\xrightarrow{55^\circ\text{C}}$ hexagonal II
Sorbitan monostearate	55	Lamellar
Polyglycerol monostearate	60	Lamellar
Polysorbate	40	Hexagonal I or micelle
Sodium stearyl-2-laccrylate	45	Lamellar

From Lauridsen [31]

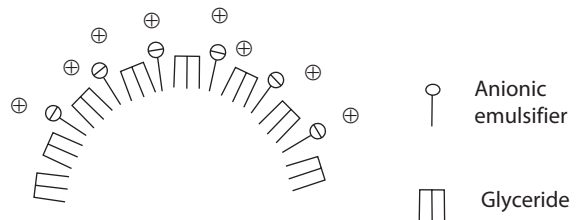
1.14 Functions of Emulsifiers in Stabilization

Once an emulsion is formed, the stabilizing action of an emulsifier on an existing emulsion can be ascribed to a variety of functions.

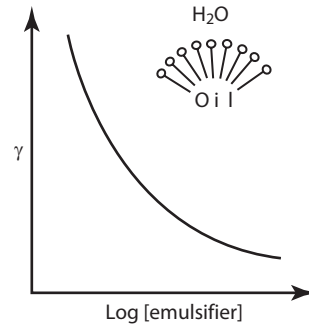
1.14.1 Electric Double Layer

As stated earlier, the process of flocculation and coalescence is governed by the net potential between the Van der Waals attraction and the repulsion between the double layer. In an o/w system without emulsifier, the emulsion is not stable, although an electric double layer is often present. The energy of repulsion is too small to overcome the attraction. The oil droplets tend to flocculate and coalesce. When ionic emulsifier is added to the system, it accumulates at the interface, causing an increase in the repulsion potential. ■ Figure 1.19 schematically shows the effect of an anionic emulsifier on the electric double layer. Stabilization through an electric double layer, however, is not observed in the case of non-ionic emulsifiers or in w/o emulsions that develop no electric double layer.

■ **Fig. 1.19** Schematic representation of electric double layer



■ Fig. 1.20 Reduction of surface tension by emulsifier

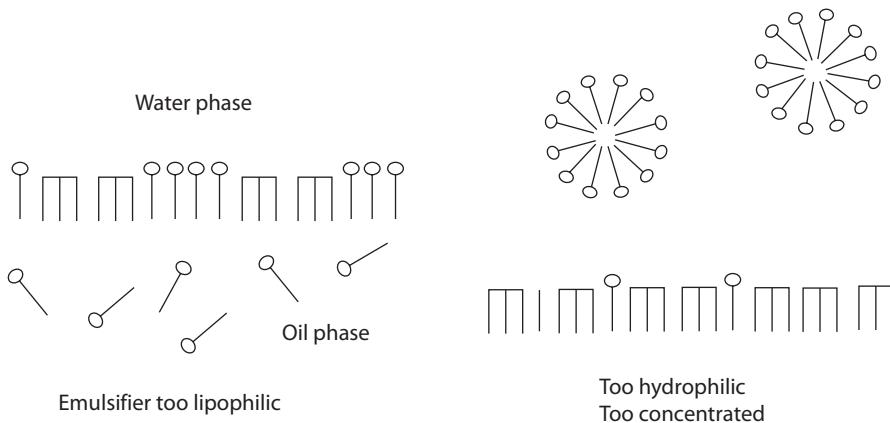


1.14.2 Adsorption at Interface

In an emulsion, emulsifier molecules orient themselves at the interface, and this adsorption leads to a reduction of the surface tension (■ Fig. 1.20). The adsorbed molecules form interfacial layers of various types, depending on the hydrophilic/lipophilic properties (HLB scores) of the emulsifier [27].

In *o/w* emulsions, if the emulsifier used is too lipophilic for the system, some molecules tend to partition between the interface and the oil phase, resulting in a loose, discontinuous film. Emulsifiers too hydrophilic for the system tend to form micelles in the water phase. High concentrations also favor the formation of micelles and in many cases, multi-layer films (■ Fig. 1.21).

Optimum stability is obtained when the emulsifier molecules form a densely packed layer at the interface, with the polar groups facing the water phase and the hydrocarbon chain interacting with the oil phase. The closely packed interfacial film of emulsifier molecules provides a steric barrier against coalescence.



■ Fig. 1.21 Orientation of emulsifier molecules at interface (From Krog [27])

■ **Table 1.10** Mesophases of emulsifiers at interfaces

Emulsifier	Mesophase formed by emulsifier into water (1:1)	Mesophase formed after introducing soybean oil
Glycerol monostearate	Lamellar	Hexagonal II
Sodium stearyl-2-lacrylate	Lamellar	Hexagonal II
Polysorbate 60	Hexagonal II	Lamellar

From Krog [26]

1.14.3 Formation of Liquid-Crystalline Mesophase

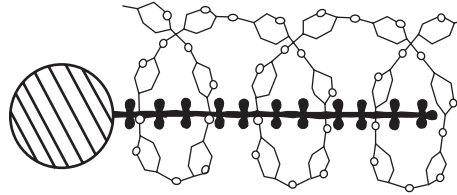
A special example of emulsifier adsorption at the interface is the formation of liquid-crystalline mesophase. The ordered layer of liquid-crystalline mesophase causes a considerable reduction of attractive forces between droplets. Furthermore, the mesophase is highly viscous (1000 times water alone), forming a steric barrier against coalescence between droplets. The formation of liquid crystalline layer requires a high emulsifier-to-oil concentration ratio of 1:20. The thickness of the film may vary from 100 to 300 nm. Lamellar mesophase is often found in o/w emulsions, while cubic and hexagonal II are present in w/o emulsions. Increase in the relative volume of the hydrocarbon region often causes a transformation of the mesophase. A few studied examples are listed in ■ Table 1.10 [26].

The presence of lamellar mesophase has been found at the surface of oil droplets in the o/w emulsion in salad dressings made with egg yolk lecithin. Liquid crystalline structures have also been shown to provide desirable conditions in bread making. Sodium stearyl-2-lactylate, ethoxylated monoglycerides, diacetyl tartaric acid esters of monoglycerides, and polysorbate are all able to form mesophases in water at dough mixing temperatures, forming associated lipid-water structures (28). Both lamellar and hexagonal liquid-crystalline mesophases exist in ternary systems of nonpolar and polar flour lipids and water.

1.14.4 Complexation with Starch

Staling of bread is related to the crystallization of amylose that is leached out of the starch granules during gelatinization. The function of emulsifier to retain softness and to decrease staling rate is mainly attributed to its complex formation with amylose. The linear chain of amylose coils up to form a helix with the emulsifier, analogous to that with iodine. In the complexation, the amylose assumes a helical form known as V-amylose. The C–H groups and the glycosidic oxygen atoms orient inward, forming a lipophilic core, with the hydrophilic OH groups pointing outward. The inside diameter of the hydrophilic core is 4.5–6.0 Å (■ Fig. 1.22) [6].

The hydrocarbon chain such as that of saturated monoglycerides fits in the core. Distilled, saturated monoglycerides are most effective as dough softeners and are used extensively for this purpose. The complex is insoluble in water and less likely to leach out from the starch granule during heat processing. When the amylose inside the granule is retained, association of the amylose is retained and retrogradation is reduced.



■ **Fig. 1.22** Schematic illustration of monostearin-amylose helical complex with the whole chain inside the helical space. The hydrocarbon chain is extended to give the approximate geometric relations three turns per chain. The hydrogen atoms of the monostearin are indicated (From Carlson et al. [6] with permission. Copyright 1979 John Wiley & Sons)

1.14.5 Emulsifier Interaction with Proteins

The anionic stearyl-2-lactylate or organic acid esters of monoglycerides, or nonionic hydrophilic polysorbates, function as dough strengtheners or conditioners through their interactions with the wheat flour gluten.

It is known that nonpolar lipids are often detrimental to the dough, and polar lipids, especially glycolipids, tend to improve the dough [10]. (Refer to wheat proteins, Chap. 2.) The final loaf volume depends on the ability of the dough to retain carbon dioxide in the structural network of the gluten in the early stages of baking, and the ordering of these structural networks during dough mixing is facilitated by the addition of lipids.

The emulsifier is bound to gluten by possibly both hydrophobic and hydrophilic interactions during dough mixing. During baking, the bonds are weakened (denaturation of the gluten) as temperature increases. The emulsifier molecules are translocated and bound to the gelatinized starch molecules, forming a protein-lipid-starch complex.

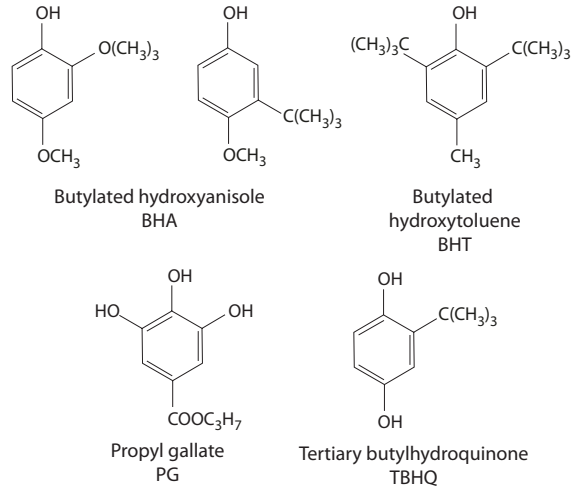
1.14.6 Control of Fat Crystallization

Sorbitan esters have the specific function of stabilizing the β' form of fats and prevent the transformation to β form. During the shelf life of chocolate, or chocolate coating, the β' crystals tend to change to the more stable β form, forming a gray film known as «bloom» on the surface. Similarly, polymorphic transformation during storage causes «sandiness» in margarine made from sunflower oil.

1.15 Antioxidants

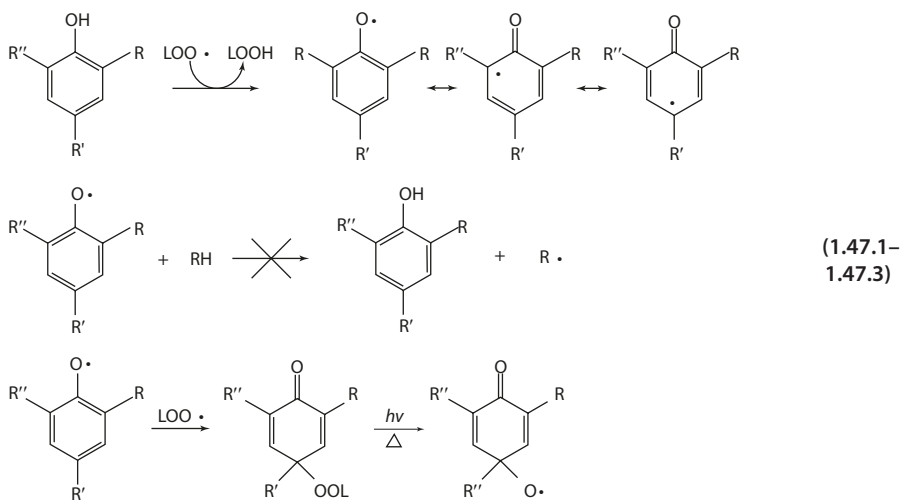
Since autoxidation of lipids involves the formation of free radicals, removal of the free radicals should terminate the chain reaction. The commonly used antioxidants are substituted phenolic compounds (■ Fig. 1.23). In addition, a large number of polyphenolic compounds in the flavonoid group are found in food plants that exhibit antioxidant activities. (Refer to Appendix 4 for flavonoids and Chap. 10 for vitamin A and E as antioxidants.)

Fig. 1.23 Phenolic antioxidants



1.15.1 Reaction Mechanism

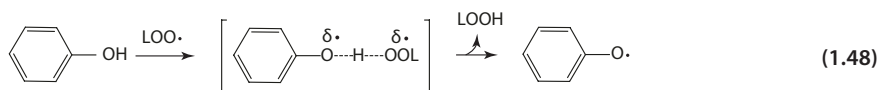
Antioxidants inhibit autoxidation of lipids by trapping peroxy radicals in two types of reactions. The antioxidant acts by transferring a H atom to the peroxy radical (Eq. 1.47.1). The resulting aryloxy radical of the antioxidant further reacts with a second peroxy radical by radical-radical coupling to yield a peroxide product, peroxydienone [5]. Aryloxy radicals are stable by resonance and relatively unreactive toward LH and O₂ and therefore incapable of initiating or propagating oxidation reactions (Eq. 1.47.2). However, the formation of peroxydienone can limit the effectiveness of the antioxidant at high temperature and exposure to UV light, since under these conditions new free radicals are generated (Eq. 1.47.3) [45].



The effectiveness of phenolic antioxidants depends on the resonance stabilization of the phenoxy radical. This is determined by the substituent on the aromatic ring and by

1.15 · Antioxidants

the size of the substituting group [44]. Substitution at the ortho- and para-positions increases the reactivity. Substitution at the meta-position is less effective. Electron-releasing groups reduce the energy of the transition state for the formation of the phenoxyl radical (Eq. 1.48). Bulky substituents create steric hindrance and provide further stability to the phenoxyl radical. However, steric hindrance also makes the antioxidant less accessible to the peroxy radical.



Since antioxidant acts as a H donor in the initial reaction (Eq. 1.47.1), autoxidation of lipids in the presence of phenolic antioxidant leads not only to the expected decreasing of autoxidative consumption of LH but also an alteration of the distribution of the products. In the two competitive pathways in Eq. 1.19, the conversion of initially formed peroxy radical to the *trans*, *cis* hydroperoxides is highly favorable. The ratio of *trans*, *cis* to *trans*, *trans* hydroperoxides is greatly increased, and the proportion of conjugated hydroperoxide to diperoxides is also expected to increase.

In the autoxidation of methyl linolenate, the proportion of 12- and 13-hydroperoxide to 9- and 15-hydroperoxides also shows significant increase (Table 1.11) [40]. Commercially used synthetic antioxidants generally have less effect compared to tocopherols. (For the antioxidation mechanism of tocopherol, refer to Chap. 10.)

Most antioxidants are added to finished products, but sometimes also used during processing. The tertiary alkyl group in BHA and BHT adds stability to the phenoxyl radi-

Table 1.11 Effect of antioxidants on autoxidation of methyl linolenate (100 h, 40 °C)

Antioxidant	Wt. added (X 10 ² µg/g)	Conjugated diene (µmol/g sample)	Molar proportion of product types		
			Total hydroperoxide	<i>c</i> , <i>t</i> Isomer	12,13-Isomer
Control	–	434	46	27	6
BHA	2	27	56	36	14
	50	35	73	61	26
	250	69	85	79	41
BHT	2	13	42	27	11
	50	7	51	32	13
	250	8	48	41	14
Control	–	490	49	27	7
α-Tocopherol	2	15	62	34	18
	50	83	88	82	39
	250	354	98	95	50

From Peers et al. [40]

cal and is responsible for the carry-through characteristics of these two antioxidants [49]. BHA and BHT retain much of their effectiveness in thermally processed foods (baked or fried temperatures). However, the bulky substituent creates steric hindrance and makes the antioxidant less reactive with peroxy radicals. For this reason, BHA and BHT are relatively weak antioxidants. They are often used together with other antioxidants (such as PG and TBHQ) for synergistic effects and to take advantage of their carry-through effect in baked and fried foods.

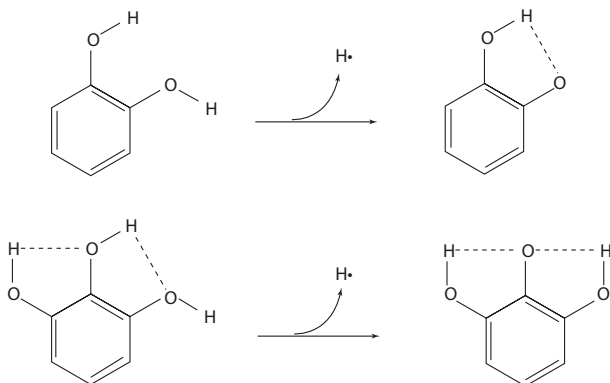
PG has relatively high antioxidant potency in oils, due to the three hydroxyl groups with no steric hindrance. However, PG forms a highly colored complex with iron. Furthermore, PG is heat sensitive, and much of its effectiveness as an antioxidant is lost at high temperatures. For this reason, formulations of PG also include chelating agents. Unlike other antioxidants, PG is water soluble. In water-fat systems, PG tends to leach from the fat into the water phase, causing a decrease in its antioxidant property. The use of high-alkyl gallate (e.g., octyl, dodecyl) serves to change the solubility. TBHQ is the more effective in that it shows no discoloration with metal and good stability in fats and oils.

Since the presence of metal accelerates the oxidation process, citric acid or ethylenediaminetetraacetic acid (EDTA) is often included in an antioxidant formulation as a chelating agent to complex or scavenge trace metals present in the food.

Many flavonoids of higher plants possess antioxidant activities and are often considered as natural antioxidants. (Refer to Appendix 4.) Flavonoid molecules inactivate free-radicals $R\cdot$ by transferring a hydrogen atom through homolytic dissociation of the O–H bond in the B ring. The flavonoid aryloxy radical ($ArO\cdot$) is a stable radical species characterized by extended conjugation and delocalization involving the aromatic rings rather than the presence of additional or particular substitutions [32, 62].



The presence of *o*-dihydroxyl groups in the B ring, such as in quercetin (3,5,7,3',4'-hydroxyl flavanol) is an important determinant for H-atom transfer. The catechol moiety imparts reducing property enhanced by intramolecular H-bonding, stabilizing the aryloxy radical, thus lowering the O–H bond dissociation energy (Eq. 1.49). The 3–OH group in combination with a C2–C3 double bond increases the activity. Some catechins have trihydroxy functions potentially providing the radical with two hydrogen bonds. For example, epigallocatechin gallate is one of the most active compounds in this group (Chap. 6). In both cases, the internal hydrogen bond in the B ring is the main stabilizing factor.



(1.49)

For some flavonoids, the antioxidant property can also be attributed to the ability of metal chelating. For example, quercetin has been shown to chelate via the oxygen atoms belonging to the 3–OH and 4–O and to the 5–OH and 4–O groups. Quite often flavonoids naturally exist as glycosides, and glycosylation generally makes the molecule less reactive toward free radicals and more water soluble. (Refer to Appendix 4.)

References

1. Acevedo NC, Peyronel F, Marangoni AG (2011) Nanoscale structure intercrystalline interactions in fat crystal networks. *Curr Opin Colloid Interface Sci* 16:374–383
2. Allen RR (1978) Principles and catalysts for hydrogenation of fats and oils. *J Am Oil Chem Soc* 55: 792–295
3. Beckmann HJ (1983) Hydrogenation practice. *J Am Oil Chem Soc* 60:282–290
4. Blumenthal MM, Stier RF (1991) Optimization of deep-fat frying operations. *Trends Food Sci Technol* 2:144–149
5. Burton GW, Ingold KU (1984) β -Carotene: an unusual type of lipid antioxidant. *Science* 224:569–573
6. Carlson T-G, Larsson K, Dinh-Nguyen N, Krog N (1979) A study of the amylose-mono-glyceride complex by ramen spectroscopy. *Stärke* 31:222–234
7. Cheng Z, Li Y (2007) What is responsible for the initiating chemistry of iron-mediated lipid peroxidation: an update. *Chem Rev* 107:748–766
8. Cherry JP, Gray MS (1981) A review of lecithin chemistry and glandless cottonseed as a potential commercial source. *J Am Oil Chem Soc* 58:903–913
9. Choe E, Min DB (2007) Chemistry of deep-fat frying oils. *J Food Sci* 72:R77–R86
10. Chung OK, Pomeranz Y, Finney KF (1978) Wheat flour lipids in breadmaking. *Cereal Chem* 55:598–618
11. Crnjar ED, Witchoot NWW (1981) Thermal oxidation of a series of saturated triacylglycerols. *J Agric Food Chem* 29:39–42
12. Destaillets F, Angers P (2005) On the mechanisms of cyclic and bicyclic fatty acid monomer formation in heated edible oils. *Eur J Lipid Sci Technol* 107:767–772
13. Ernster L, Nordenbrand K, Orrenius S (1982) Microsomal lipid peroxidation: mechanism and some biomedical implications. In: Yagi K (ed) *Lipid peroxides in biology and medicine*. Academic, New York
14. Faucitano A, Locatelli P, Perotti A, Faucitano MF (1972) γ -radiolysis of crystalline oleic acid. *J.C.S. Perkin II* 1972:1786–1791
15. Figge F (1971) Dimeric fatty acid [1-14C] methyl esters. I. Mechanism and products of thermal and oxidative-thermal reactions of unsaturated fatty acid esters – literature review. *Chem Phys Lipids* 6:164–182
16. Friberg S (1976) Emulsion stability. In: Friberg S (ed) *Food emulsions*. Marcel Dekker, New York
17. Frankel EN (1984) Lipid oxidation: mechanism, products and biological significance. *J Am Oil Chem Soc* 61:1908–1917
18. Frankel EN (1991) Recent advances in lipid oxidation. *J Sci Food Agric* 54:495–511
19. Frankel EN, Neff WE, Selke E, Weisleder D (1982) Photosensitized oxidation of methyl linoleate: secondary and volatile thermal decomposition products. *Lipids* 17:11–18
20. Gertz C (2000) Chemical and physical parameters as quality indicators of used frying oils. *Eur J Lipid Sci Technol* 102:566–572
21. Gunstone ED (1984) Reaction of oxygen and unsaturated fatty acids. *J Am Oil Chem Soc* 61:441–444
22. Haighton AJ (1976) Blending, chilling, and tempering of margarines and shortenings. *J Am Oil Chem Soc* 53:397–399
23. IUPAC-IUB Commission on Biochemical Nomenclature (1978) The nomenclature of lipids. *J Lipid Res* 19:114–128
24. Joyner NT (1953) The plasticizing of edible fats. *J Am Oil Chem Soc* 30:526–535
25. Korver O, Katan MB (2006) The elimination of trans fats from spreads: how science helped to turn an industry around. *Nutr Rev* 64:275–279
26. Krog N (1975) Interaction between water and surface active lipids in food systems. In: Duckworth RB (ed) *Water relations of foods*. Academic, New York
27. Krog N (1977) Functions of emulsifiers in food systems. *J Am Oil Chem Soc* 54:124–131

28. Krog N (1981) Theoretical aspects of surfactants in relation to their use in breadmaking. *Cereal Chem* 58:158–164
29. Larsson K (1972) Molecular arrangement in glycerides. *Fette-Seifen Anstrichmittel* 74(3):136–142
30. Larsson R (1983) Hydrogenation theory: some aspects. *J Am Oil Chem Soc* 60:275–281
31. Lauridsen JB (1976) Food emulsions: surface activity, edibility, manufacture, composition, and application. *J Am Oil Chem Soc* 53:400–407
32. Leopoldini M, Russo N, Toscano M (2011) The molecular basis of working mechanism of natural polyphenolic antioxidants. *Food Chem* 125:288–306
33. Lutton ES (1972) Lipid structures. *J Am Oil Chem Soc* 49:1–9
34. Marmesat S, Velasco J, Dobargaries MC (2008) Quantitative determination of epoxy acids, keto acids and hydroxy acids formed in fats and oils at frying temperatures. *J Chromatogr A* 1211:129–134
35. McIntyre RT (1979) Polyglycerol esters. *J Am Oil Chem Soc* 56:835A–840A
36. Nawar WW (1985) Thermal and radiolytic decomposition of lipids. In: Richardson T, Finley JW (eds) *Chemical changes in food during processing*. AVI, Westport
37. Neff WE, Frankel EN, Weisleder D (1981) High pressure liquid chromatography of autoxidized lipids: II. Hydroperoxycyclic peroxides and other secondary products from methyl linolenate. *Lipids* 16:439–448
38. Neff WE, Frankel EN, Weisleder D (1982) Photosensitized oxidation of methyl linolenate secondary products. *Lipids* 17:780–790
39. Overbeek TGT (1972) Colloid and surface chemistry part 2: lyophobic colloids. Massachusetts Institute of Technology, Cambridge
40. Peers KE, Coxon DT, Chen HWS (1984) Autoxidation of methyl linolenate: the effect of antioxidants on product distribution. *J Sci Food Agric* 35:813–817
41. Porter NA, Caldwell SE, Mills KA (1995) Mechanisms of free radical oxidation of unsaturated lipids. *Lipids* 30:277–290
42. Porter NA, Lehman LS, Weber BA, Smith KJ (1981) Unified mechanism for polyunsaturated fatty acid autoxidation. Competition of peroxy radical hydrogen atom abstraction, β -scission, and cyclization. *J Am Chem Soc* 103:6447–6455
43. Sato K, Ueno S, Yano J (1999) Molecular interactions and kinetic properties of fats. *Prog Lipid Res* 38:91–116
44. Scott G (1965) Atmospheric oxidation and antioxidants. Elsevier, London/New York
45. Scott G (1985) Antioxidants in vitro and vivo. *Chem Br* 21(7):648–653
46. Seaman VY, Bennett DH, Cahill TM (2009) Indoor acrolein emission and decay rates resulting from domestic cooking events. *Atmos Environ* 43:6199–6204
47. Sebedio JL, Grandgivard A (1989) Cyclic fatty acids: natural sources, formation during heat treatment, synthesis and biological properties. *Prog Lipid Res* 29:303–336
48. Sevilla CL, Swarts S, Sevilla MD (1983) An ESR study of radical intermediates formed by γ -radiolysis of tripalmitin and dipalmitoyl phosphatidylethanolamine. *J Am Oil Chem Soc* 55:950–957
49. Sherwin ER (1976) Antioxidants for vegetable oils. *J Am Oil Chem Soc* 53:430–436
50. Small DM (1991) The effects of glyceride structure on absorption and metabolism. *Annu Rev Nutr* 11:413–434
51. Sreenivasan B (1978) Interesterification of fats. *J Am Oil Chem Soc* 55:796–805
52. Tappel AL (1962) Heme compounds and lipoxidase as biocatalysts. In: Schutz HW, Day EA, Sinnhuber RO (eds) *Symposium on foods: lipids and their oxidation*. AVI, Westport
53. Timms RE (1984) Phase behavior of fats and their mixtures. *Prog Lipid Res* 23:1–38
54. Traynham JG (1986) A short guide to nomenclature of radicals, radical ions, iron-oxygen complexes and polycyclic aromatic hydrocarbons. *Adv Free Radical Biol Med* 2:191–209
55. Tsuzuki W (2010) Cis-trans isomerization of carbon double bonds in monounsaturated triacylglycerols via generation of free radicals. *Chem Phys Lipids* 163:741–745
56. Uprichard JE, Zeelenberg MJ, Huizinga H, Verschuren PM, Trautwein EA (2005) Modern fat technology: what is the potential for heart health? *Proc Nutr Soc* 64:379–386
57. Uri N (1961) Physico-chemical aspects of autoxidation. In: Lundberg WO (ed) *Autoxidation and antioxidants*, vol 1. Interscience Publishers, New York/London
58. Van Haften JL (1979) Fat-based food emulsifiers. *J Am Oil Chem Soc* 56:831A–835A
59. Van Nieuwenhuizen W (1976) Lecithin production and properties. *J Am Oil Chem Soc* 53:425–427

References

60. Wiedermann LH (1978) Margarine and margarine oil, formulation and control. *J Am Oil Chem Soc* 55:823–829
61. Wille RL, Lutton ES (1966) Polymorphism of cocoa butter. *J Am Oil Chem Soc* 43:491–496
62. Wright JS, Johnson ER, DiLabio GA (2001) Predicting the activity of phenolic antioxidants: theoretical method, analysis of substituent effects, and application to major families of antioxidants. *J Am Chem Soc* 123:1173–1183
63. Yin H, Xu L, Porter NA (2011) Free radical lipid peroxidation: mechanisms and analysis. *Chem Rev* 111:5944–5972

Proteins

2.1 Protein Structure – 56

- 2.1.1 The Role of Water – 59
- 2.1.2 Change of Conformation – 61

2.2 Protein-Stabilized Emulsification and Foaming – 65

2.3 Gel Formation – 67

2.4 Chemical Reactions – 68

- 2.4.1 Alkali Degradation – 68
- 2.4.2 Heat-Induced Formation of Isopeptides – 70
- 2.4.3 Radiolysis – 71
- 2.4.4 Photolysis – 75
- 2.4.5 Photosensitized Oxidation – 76
- 2.4.6 Chemical Oxidation – 77
- 2.4.7 Reaction with Carbonyl Compounds – 78
- 2.4.8 Reaction with Products from Lipid Oxidation – 78

2.5 Organized Protein Systems – 80

- 2.5.1 Meat Proteins – 80
- 2.5.2 Water-Holding Capacity – 88
- 2.5.3 Milk Proteins – 91
- 2.5.4 Wheat Proteins – 97
- 2.5.5 Soybean Proteins – 106
- 2.5.6 Collagen – 113

References – 119

There is a constant and increasing demand for high-quality protein foods for an ever-growing world population. Food scientists are interested not only in the chemical principles underlying protein structures and mechanisms but applications of the knowledge in exploring the unique characteristics of proteins that are relevant in complex food systems. The basic chemistry is always related to the functionality of the protein. Thus, the chemistry of muscle contraction is related to rigor mortis and the postmortem tenderness of meat. The chemical structure of collagen and the unfolding and refolding of the helical chains help to explain the formation of gelatin gel. The understanding of protein chemistry would provide new ideas that challenge food scientists and technologists to improve existing and formulate new food products.

The chemical changes of proteins during food processing and storage are an area that requires unique attention. Chemical or enzymatic modifications occur, intentionally or unintentionally, to an extent greater than generally realized and impart desirable as well as unwanted effects. Not only the functional properties are affected, but the nutritional quality of the food product is altered. One typical example is the use of alkaline treatment in food processing and its implication in protein degradation. On the other hand, modifying food proteins often has the advantage of enhancing functional properties that are necessary for food processing and production.

In this chapter the basic chemistry of proteins is covered, with particular attention given to the reactions and mechanisms that are of importance in food processing. Organized protein systems, such as meat, wheat, soybean, and milk proteins, are discussed with emphasis on their structures and functionality.

2.1 Protein Structure

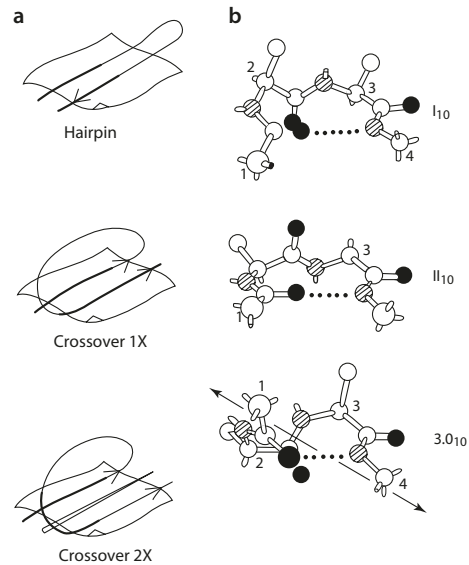
The primary structure of proteins consists of polypeptide chains of a repeating backbone of peptide bonds and various side chains of the amino acids. The peptide bond ($-\text{CO}-\text{NH}-$) is *trans*-planar due to its partial double-bond character resulting from resonance between the oxygen and the nitrogen. There are two free rotations about the $\text{C}_\alpha-\text{N}$ bond axis and the $\text{C}_\alpha-\text{C}$ axis designated by torsional angles ϕ and ψ , respectively. The polypeptide chain folds into an α helix or β -pleated sheet to assume a secondary structure.

In the α helix, the CO group of each amino acid residue is hydrogen bonded to the NH group of the amino acid residue four units apart. The neighboring amino acid residues are 1.5 Å apart with a rotation of 100° , resulting in 3.6 amino acid residues per turn. This stable helix type is denoted as $3.6_{13}r$, where 13 is the number of atoms between the hydrogen bond and r denotes right-handed. The backbone phi (ϕ) and psi (ψ) dihedral angles of this type of α -helices are -57.8 and -47.0 , respectively.

The other type of secondary structure is the β sheet, formed by hydrogen bonding between the amine and carboxyl groups across strands (polypeptide chains), instead of within a strand (as in α helices). The amino acids have their side chains more extended, with 3.5 Å between adjacent residues. The side groups of the amino acids are above and below the β sheet. The polypeptide chains align in the same direction (parallel) or in opposite directions to each other (antiparallel). The backbone connections between the β strands in a β sheet are classified into two categories [75] (■ Fig. 2.1a).

1. Hairpin connection—the chain reenters the sheet at the same end it left from.
2. Crossover connection—the chain loops around to reenter the sheet on the opposite end from where it left.

Fig. 2.1 **a** Hairpin and crossover connections in β sheet and **b** type I_{10} , II_{10} , 3.0_{10} helix conformation (From Birktoft and Blow [8] with permission. Copyright 1972 Elsevier)



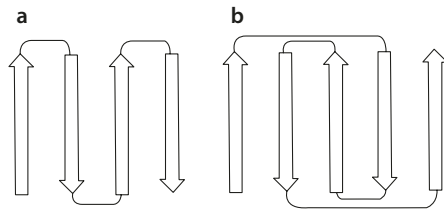
The reentry of the β strand may be the immediate neighboring strand or separated by one or more strands. β sheets are commonly right-handed twisted (when viewed along the direction of the polypeptide chains). The twist confers a lower free energy than straight or left-handed twist. The backbone connections involve reverse turns (also called β turns), where the polypeptide chain folds back upon itself by forming a hydrogen bond between the CO group to the NH group in the third residue back along the chain. A total of four amino acids are included in the formation of turns. In many globular proteins, about one-third of the amino acid residues are found in turns. Amino acid residues, such as proline, asparagine, and glycine, occur in high frequency in these reverse turns. There are three types of turns, characterized by the dihedral angles of the second and third amino acid residues ($\varphi_2, \psi_2, \varphi_3, \psi_3$) [8] (■ Fig. 2.1b).

- Type I_{10} : $-60^\circ, -30^\circ; -90^\circ, 0^\circ$
- Type II_{10} : $-60^\circ, 120^\circ; 80^\circ, 0^\circ$
- Type 3.0_{10} : $-60^\circ, -30^\circ; -60^\circ, -30^\circ$

Certain folding patterns are commonly found in proteins, involving a number of secondary structure elements, but not yet comprising the complete tertiary structure. These assemblies are known as supersecondary structures. The 4- α -helical arrangement is common to a number of proteins. It is organized as sequentially connected four α helices packed together in an antiparallel pattern at angles of about 18° . The stability of the structure is the result of helix-dipole interaction. Another structural arrangement is coiled-coil α helix, where two α helices are wound together, resulting in a left-handed superhelix. The most common arrangement is β - α - β , where two parallel β sheets are connected by an α helix. In antiparallel sheets, the structure may wrap around in barrels. The topology assumes the β -meander (+1, +1, +1 as in papain), or Greek key pattern (-3, +1, +1, -3, or +3, -1, -1, as in chymotrypsin) [76] (■ Fig. 2.2).

Many proteins can be considered as layered structures of α helices and β sheets and classified into four categories: $\alpha\alpha$ (mainly α helix, e.g., myohemerythrin, myogen,

Fig. 2.2 a β -meander and b Greek key pattern



myoglobin), $\beta\beta$ (mainly β sheet, e.g., superoxide dismutase, chymotrypsin), $\alpha+\beta$ (α helix and β strand, but not mixed, e.g., papain, insulin, lysozyme), α/β (mixed, mostly alternating α helix and β strand, e.g., carboxypeptidase A, alcohol dehydrogenase, triose phosphate isomerase) [51].

Almost all globular proteins consist of locally compact globular regions, which are potentially independent and geometrically separate units with specific functions, such as binding sites. These regions are generally known as domains. The active site of a protein molecule is usually found at the interface between domains.

The polypeptide chain and, in fact, the protein molecule are stabilized by many interactions, including electrostatic interactions, hydrogen bonds, and hydrophobic forces (Fig. 2.3), providing a unique spatial arrangement and orientation of the side chain groups and their special functional properties.

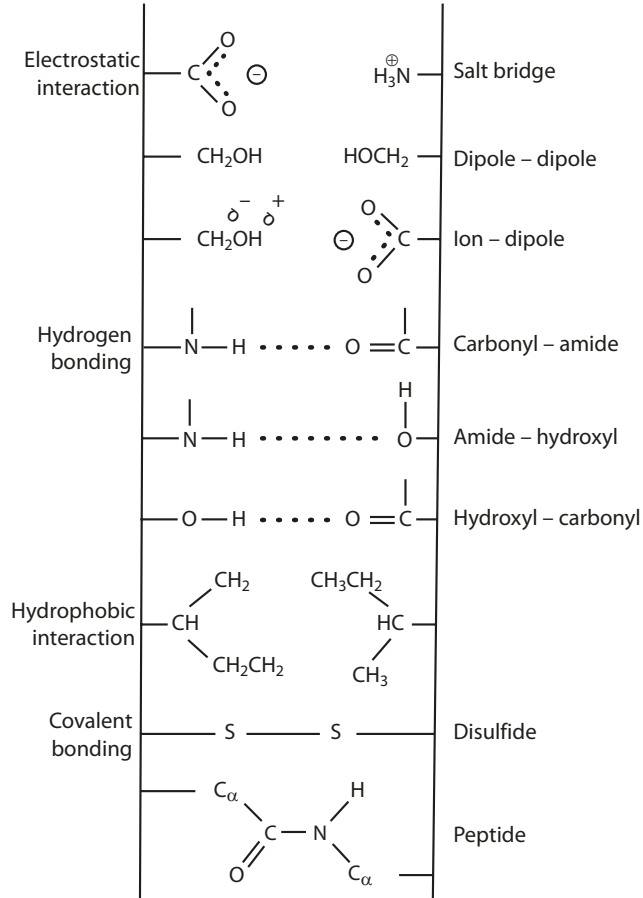
Electrostatic interactions that occur between charged side chains are governed by Coulomb's law (Eq. 2.5) and depend on the dielectric constant of the medium. Interaction between ion pairs may be attractive or repulsive; about one-third of the ion pairs found in proteins may involve repulsive interactions. The common amino acid residues involved in forming ion pairs are Arg, Asp, Glu, Lys, and His. A salt bridge formed between Lys and Asp has a binding energy of -5 kcal/mol. However, ion pair interactions between amino acid residues are not as significant in protein folding as are the ion-dipole interactions between the charge groups and water molecules. Uncharged but polar side chains also participate in electrostatic interactions due to their partial charges expressed as dipole moments. The interaction of dipoles has electrostatic repulsion or attraction depending on the orientation and the extent of polarizability due to induction by neighboring molecules. Dipole-dipole interactions yield energies of 0.1 – 0.2 kcal/mol.

Hydrogen bonding has an intermediate energy between electrostatic interaction and covalent bonding. The energy of a carbonyl-amide hydrogen bond is about -3 kcal/mol. Depending on the type of hydrogen bond, the bond distance between the donor and acceptor atom is about 2.8 – 3.0 Å. All hydrogen bonds are linear to assume the lowest potential energy.

Hydrophobic interaction constitutes a major stability force in proteins. The interactions are due to unfavorable changes in water entropy when the nonpolar side chains are exposed to the aqueous medium. The details are to be discussed in relation to the role of water in proteins.

Besides the noncovalent forces described above, disulfide bonds provide further stabilization to many proteins. Disulfide bonds often create intrachain loops. The -Cys-Cys- sequence in some proteins links segments of polypeptide chains in close proximity as in the case of wheat germ agglutinin and human serum albumin. The 17 disulfide bonds in human serum albumin align the protein molecule in a series of nine loops of repeated triplets of different sizes. Disulfides may also participate in enzyme catalysis, as in the example of the flavoenzyme glutathione reductase. The active center of the enzyme consists of two redox systems: FAD and the disulfide between Cys46 and Cys41 that function in the transfer of reduction equivalent from NADPH to glutathione GSSG.

■ Fig. 2.3 Types of bonding stabilizing protein structure



2.1.1 The Role of Water

Aside from the covalent and monovalent interactions, the stability of protein conformation is greatly affected by the solvent. Proteins contain both hydrophilic and hydrophobic side chains. In an aqueous environment, the hydrophobic groups tend to move away from the water phase and aggregate in the interior core of the protein molecule. If the hydrophobic side chains are unfolded and exposed to the aqueous phase, as in the case when a protein is denatured, the process is accompanied by a large negative entropy ($\Delta S^\ddagger < 0$) which causes the corresponding free energy to be positive ($T\Delta S^\ddagger > \Delta H^\ddagger$) (Eq. 2.1). Therefore, this process of hydrophobic hydration is thermodynamically unfavorable. Some of the calculated thermodynamic parameters of transferring hydrophobic amino acid side chains from a hydrophobic environment to water is presented in ■ Table 2.1 [17]. The hydrophobicity is linearly correlated with the surface area of the nonpolar side chain, and it follows that hydrophobicity is additive in that the hydrophobicity of a molecule is the summation of that of its constituent residues.

$$\Delta G = \Delta H - T\Delta S \quad (2.1)$$

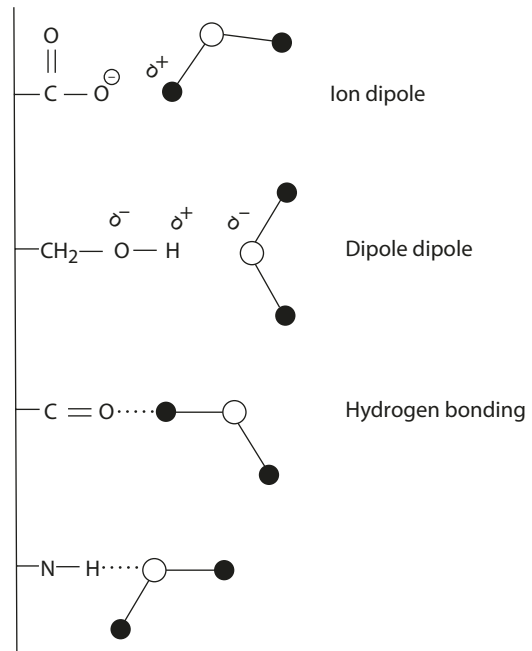
Table 2.1 Calculated thermodynamic parameters of transfer of amino acid side chains from a hydrocarbon medium to water at 25 °C

Amino acid side chain	ΔG^\ddagger (KJ/mol. 25°C)	ΔH^\ddagger (KJ/mol)	ΔS^\ddagger (J/mol-degree)
Alanine	+5.5	-6.3	-39.5
Valine	+8.0	-9.2	-57.5
Leucine	+8.0	-10.1	-60.1
Phenylalanine	+7.6	-4.2	-39.9

From England [17]

The water located inside the protein molecule is isolated from the surrounding water and also plays an important role in stabilizing the conformation of the protein molecule. Three types of water molecules are found within a protein molecule. (1) Water molecules trapped inside the protein help fill the empty crevices in side chain packing. (2) Partially ordered water with an altered freezing point is produced by interaction with protein side chain groups. This layer of water molecules covers about one-third of the protein surface. (3) Tightly bound water molecules from the first coordination layer with substantially lower energy than the bulk water. In addition to these "structural" waters, the surface of the protein molecule is also solvated by layers of "interfacial" water. The monolayer that covers the immediate surface shows decreased mobility and structural changes. The water molecules are oriented by their own polarity and by the polar groups on the surface of the protein molecule. The "structural" and "interfacial" waters are included under the category of "bound" water, in contrast to the "bulk" water in the system. Interactions between water and protein molecules involve ion-dipole, dipole-dipole, and hydrogen bonding as illustrated in [Fig. 2.4](#).

Fig. 2.4 Interactions between water and protein molecules



2.1.2 Change of Conformation

The structural conformation of proteins can be altered by heat, salt, pH, organic solvent, and denaturing agent such as guanidium salt. Two types of changes can occur. (1) Chain-chain interaction (among side chain groups in the polypeptide) resulting in association, aggregation, flocculation, coagulation, and precipitation. (2) Chain-solvent interaction (between solvent molecules and side-chain groups) resulting in solubilization, dissociation, swelling, and denaturation.

■ ■ Heat

The process of folding and unfolding of a protein is represented by Eq. 2.2, and the equilibrium constant is related to the change in enthalpy.

$$\begin{aligned} \text{Native} &\rightleftharpoons \text{Denatured} \\ K &= \frac{\text{Denatured}}{\text{Native}} = e^{(-\Delta H^\circ + T\Delta S^\circ)/RT} \end{aligned} \quad (2.2)$$

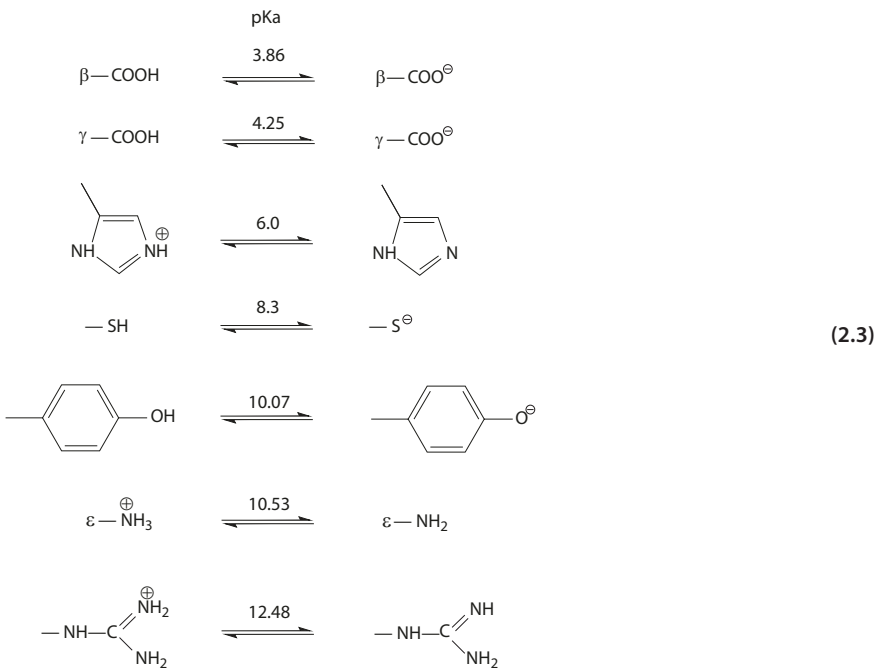
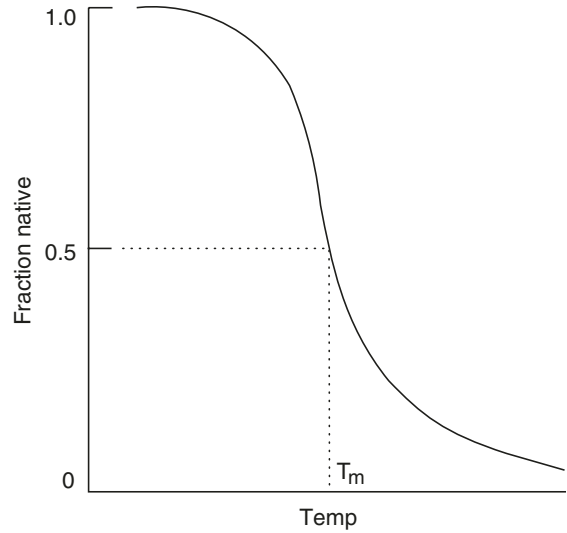
For most proteins, the unfolding enthalpy, ΔH° , is in the range of 50–150 kcal/mol and $\Delta G^\circ < 20$ kcal/mol (■ Table 2.2) [69]. Heating provides energy to break the noncovalent interactions that stabilize the native structure. The process usually occurs in a narrow temperature range. T_m is the melting temperature at which [native] = [denatured] (■ Fig. 2.5). The sharp transition from the native to the denatured state is indicative of "cooperativity". The many noncovalent interactions "cooperate" by breaking together. It is difficult for a single residue to initiate bond breaking. However, once the initial breaking starts, breaking at adjacent sites occurs more readily and so does the third site neighboring it. Thus, the observed ΔH° and ΔS° would be the sum of all the combinations from individual bond breaking, so that the exponential term in Eq. 2.2 exhibits a large change for a small change in temperature.

■ Table 2.2 Enthalpy for unfolding of various proteins

Protein	ΔH° (kcal mole ⁻¹)
Ribonuclease	96
Lysozyme	88
Cytochrome c	50
Metmyoglobin	68

From Privalov and Khechinashvili [69]

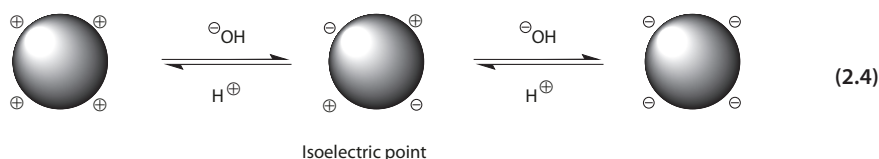
■ Fig. 2.5 Thermal denaturation of macromolecules of the cooperative type



■ pH

Protonation at low pH increases the cationic properties of the protein, while alkaline pH increases the anionic species. Using the amino acid lysine as an example, half of the ϵ -amino groups are protonated at pH 10.5. Increasing the pH will shift the equilibrium to the formation of $\epsilon\text{-NH}_2$ in lysine, and decreasing pH will favor protonation of the amino group to $\epsilon\text{-NH}_3^+$. The pK_a values for the various amino acid side chains are listed in Eq. 2.3.

The change in pH, therefore, changes the distribution of cationic, anionic, and non-ionic polar sites on the protein molecule, which in turn affects water-protein and protein-protein interactions. At the isoelectric point, the protein molecule has a net charge of zero (Eq. 2.4). The protein exhibits the maximum amount of electrostatic interaction between the charged groups, and the protein molecule becomes shrunken. The charged groups are least available for interaction with water molecules, and the amount of bound water is decreased to a minimum. The protein molecule, therefore, exhibits minimal hydration, swelling, and solubility. Above the isoelectric point, the protein has a net negative charge, and in the acid range, a net positive charge. The like-charge side chains repel each other, and at extreme pH ranges, the protein tends to unfold.



■ ■ Organic Solvents

The force between two charged sites in a protein molecule is described by the Coulomb's law (Eq. 2.5). If Q_1 and Q_2 are of like sign, the force is positive, indicating repulsion. Likewise, if they are of opposite sign, the force is negative, indicating attraction.

$$F = \frac{Q_1 Q_2}{\epsilon r^2} \quad \begin{array}{l} Q = \text{Charges } \oplus \text{ or } \ominus \\ \epsilon = \text{Dielectric constant of medium} \\ r = \text{Distance between sites} \end{array} \quad (2.5)$$

Organic solvents usually have dielectric constants lower than water (■ Table 2.3). Therefore, adding organic solvents lowers the dielectric constant and thereby increases the force of attraction between opposite charges in the protein molecule, causing them to come close enough to aggregate and precipitate.

■ ■ Salts

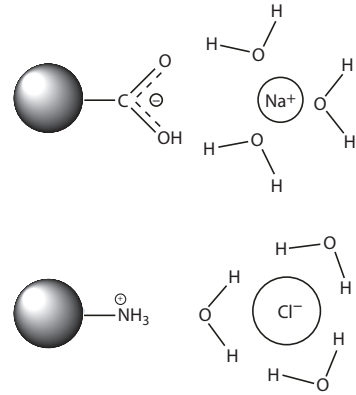
For most proteins, low salt concentrations (ionic strength <0.1–0.15) tend to increase the solubility of the protein molecule. The "salting-in" process is the result of the salt effect on electrostatic interaction. At high concentrations, salt decreases the solubility of the protein molecule. The "salting-out" process is the result of the salt effect on the hydrophobic interaction.

The salt effect is represented by Eq. 2.6 [59]. At low salt concentrations, $\Delta G_{e.s.}$ is positive, which accounts for the "salting-in" effect. Salt ions interact with the countercharges

■ Table 2.3 Dielectric constants of selected solvents

Solvent	Dielectric constant (25°C, 1 atm)
Benzene	22.7
Methanol	32.6
Ethanol	24.3
Water	78.5

■ Fig. 2.6 Salt ion interaction with protein



on the protein (■ Fig. 2.6), decrease the potential energy for ion-ion interactions, and increase the solubility of the protein.

$$\ln \frac{w}{w_0} = \frac{\Delta G_{e.s.} + \Delta G_{cav}}{RT} + \text{constant} \quad (2.6)$$

w = weight of protein soluble in 1 liter of salt solution

w_0 = weight of protein soluble in 1 liter of water

$\Delta G_{e.s.}$ = free energy change of electrostatic interactions when the protein goes into salt solution

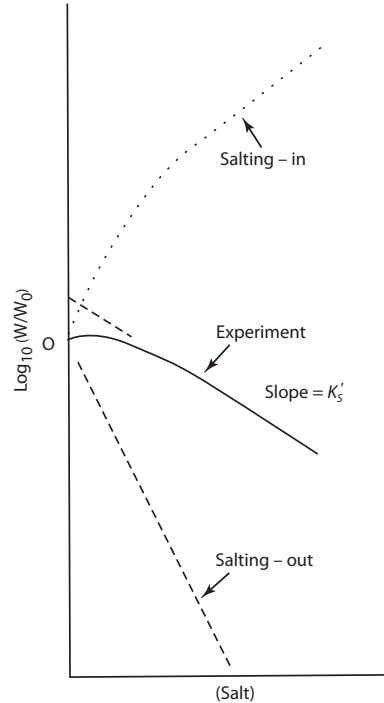
ΔG_{cav} = free energy required for formation of a cavity in the solvent to accommodate hydrophobic groups expected on surface

However, $\Delta G_{e.s.}$ increases nonlinearly with salt concentration. With increasing salt concentration, eventually all the charged groups are shielded, and the protein is effectively a neutral dipole molecule. The hydrophobic term (ΔG_{cav}) in the equation becomes dominant, and $\Delta G_{cav} = -\Omega\sigma m$, where Ω is related to the hydrophobic area and σm is the surface tension of the salt solution. For most simple salts, σm is positive (increases the surface tension of water). This means that ΔG_{cav} is always increasingly negative and hence W/W_0 (the solubility) is decreased.

Some proteins do not follow the process predicted by the equation and exhibit "salting-out" before salting-in. The salting-out effect of ions on hydrophobic interactions can occur at relatively low salt concentration, especially in proteins that tend to associate in salt solutions. In general, it is the salt effect on the charge profiles of the electrostatic and hydrophobic forces that determines the solubility behavior of a protein molecule.

If the solubility is plotted against salt concentration (expressed as ionic strength), the electrostatic and hydrophobic effects counteract each other. Normalization of these two effects results in a curve with intercept β' and slope K_s' (■ Fig. 2.7). Protein solubility at high salt concentration, therefore, can be expressed by Eq. 2.7 [59]. The β' term is dependent on the type of protein, pH, and temperature, whereas the K_s' term is affected by the nature of the salt.

■ **Fig. 2.7** Plot of solubility (log) against salt concentration (molal) for hemoglobin in ammonium sulfate (From Melander and Horváth [59])



$$\log S = \beta' - K'_s \mu \quad (2.7)$$

where

S = solubility

β' = hypothetical solubility at zero ionic strength

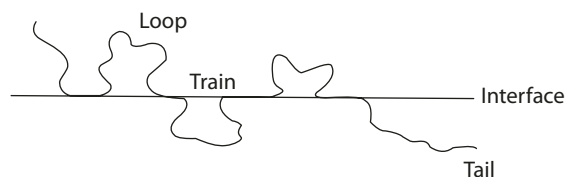
K'_s = salting-out constant

μ = ionic strength

2.2 Protein-Stabilized Emulsification and Foaming

Protein molecules contain both hydrophilic and hydrophobic groups and, as expected, may act like a surface-active substance. The protein molecule adsorbs at the interface of the emulsion system, denatures, and unfolds with trains of amino acids along the interface and with loops and tails protruding into either phase (■ Fig. 2.8). The orientation of the loops and tails depends on the hydrophobicity and hydrophilicity of the amino acid side chains [10].

■ **Fig. 2.8** Protein conformation at interface



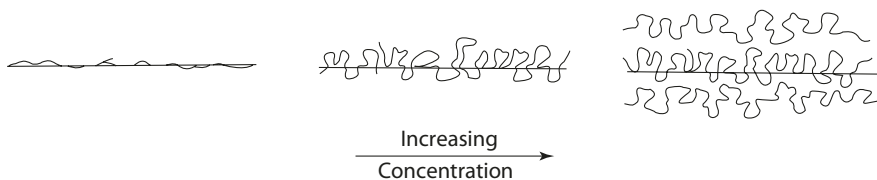
Formation of loops and tails is favored with increasing concentration of the protein. At low concentration, most polypeptides have their amino acid backbone lying along the interface with few loops and tails. As the concentration increases, the polypeptides are more closely packed, and hence more loops and tails are formed. Finally, the looped conformation creates enough electrostatic repulsion and steric hindrance that further protein adsorption becomes energetically unfavorable. The protein concentration at the interface is at the saturated level, and more concentrated solutions give rise to multilayer adsorption (■ Fig. 2.9).

In colloidal system such as a protein solution, foam formation occurs when air is mechanically incorporated. A monolayer film of surface-denatured protein is adsorbed at the air-water interface of the colloidal solution similar to that discussed in an emulsion system. When air is mechanically incorporated into the protein solution (e.g., shaking the solution or, in practical application, whipping egg white), cells are formed with air surrounded by the protein film at the air-water interface (■ Fig. 2.10).

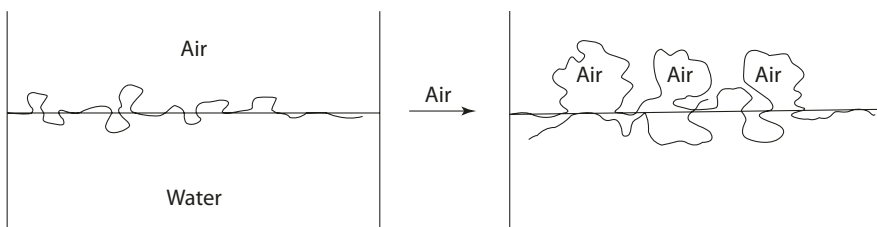
Adsorption of surface-denatured protein continues to occur at the interface to replace the coagulated regions of the film around the air cells. When bubbles come in close contact, drainage occurs from the aqueous lamella formed between the bubbles and finally causes rupture of the film (■ Fig. 2.11). The adsorbed protein film at the interface provides stability against coalescence by:

1. Reinforcing the repulsive forces: the charged groups in the protein create, between the air cells, a relatively dense electric double layer that helps prevent thinning of the lamella.
2. Forming a steric barrier: the rigidity of the protein film helps stabilizing against coalescence of the cells and disruption of the lamella.
3. Increasing viscosity: increasing viscosity in the aqueous solution in the lamella tends to act against drainage.

It should be expected that the molecular structure and hence the parameters that affect the unfolded state of the protein (e.g., pH, ionic strength, temperature) all playing important roles in the stability properties of the protein film. Proteins that have a flexible structure, such as β -casein, are easily surface denatured. Highly structural globular proteins, such as

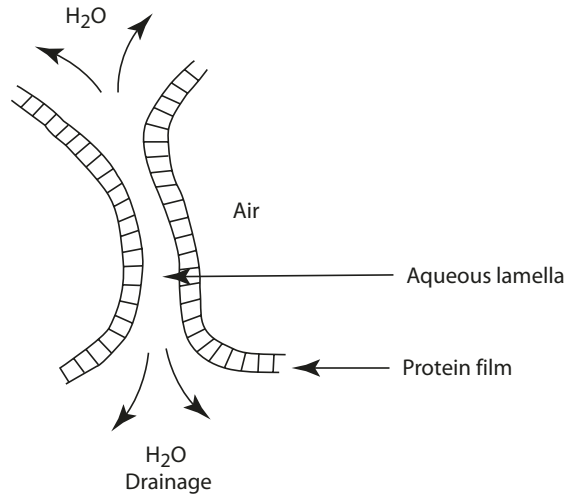


■ Fig. 2.9 Protein conformation at interface with increasing concentration



■ Fig. 2.10 Foam formation at air-water interface

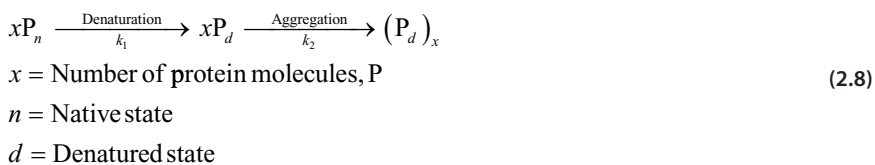
■ Fig. 2.11 Drainage from aqueous lamella



lysozyme, are difficult to surface denature. The degree of unfolding at the interface affects the rheology of the film. Thus, a β -casein film is liquid-like and provides good stability in emulsion. A lysozyme film tends to be rigid and more resistant to deformation. A more denatured protein is a more extended molecule and hence enables the development of better structure and network for film formation [67].

2.3 Gel Formation

Protein gelation is an aggregation of denatured molecules with a certain degree of order, resulting in the formation of a continuous network. The mechanism for the formation of protein gel is represented by Eq. 2.8.



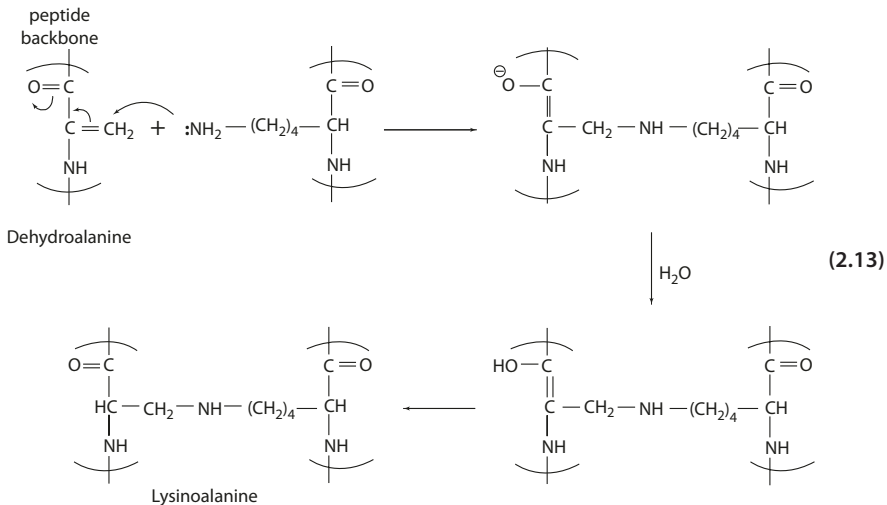
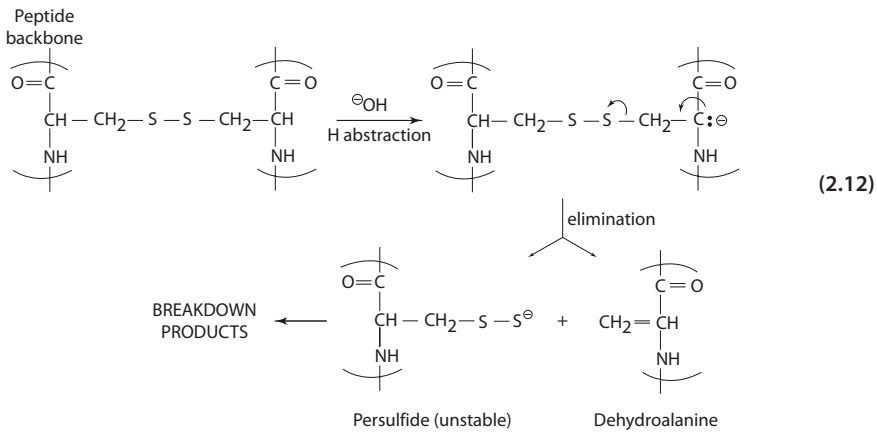
The first step in gel formation is denaturation of the protein, and the second step is an aggregation process. If k_2 is faster than k_1 , a coarse network of protein molecules is formed. The gel is opaque with large interstices that exhibit syneresis. If k_2 is sufficiently slow, the resulting gel becomes finer, less opaque, and elastic. If the second step is irreversible (i.e., the gel melts upon heating), the intermediate state (xP_n) is a progel. The formation of a progel is accompanied by increased viscosity and "sets" to form the gel. This gel type is called "thermoset" or "reversible" to separate it from the thermoplastic or irreversible gels [85]. Gelatin is an example of a thermally reversible gel, whereas milk gel is irreversible.

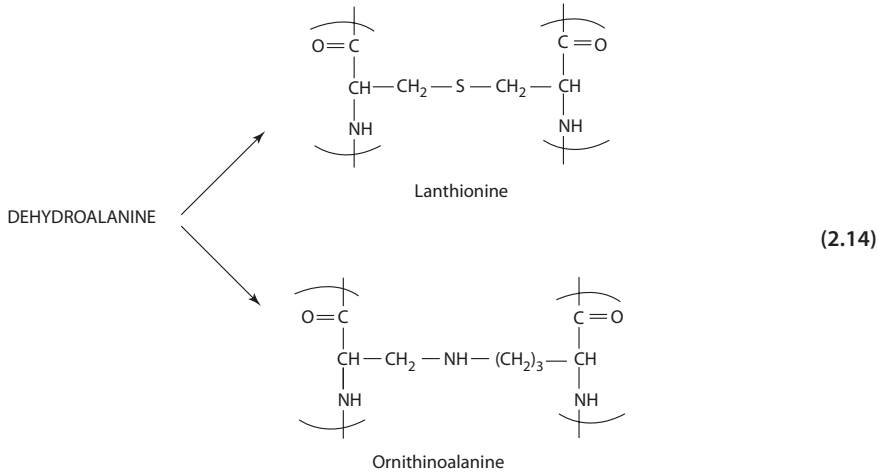
The kind and nature of intra- or intercrosslinks in the gel network are crucial to the gel characteristic. Both covalent and noncovalent bonds are involved. Noncovalent bondings may include hydrogen bonding and hydrophobic interaction, and covalent bondings include disulfide crosslinks. Disulfide crosslinks help in bridging and ordering of the gel network, while noncovalent bondings help in stabilizing and strengthening the gel structure.

■ ■ β-Elimination

The α -hydrogen of an amino acid residue is easily abstracted by hydroxide ion. In protein-bound cysteine, the resulting products are the persulfide and dehydroalanine (Eq. 2.12). Phosphoseryl and phosphothreonyl residues also undergo similar reactions, as does cysteine.

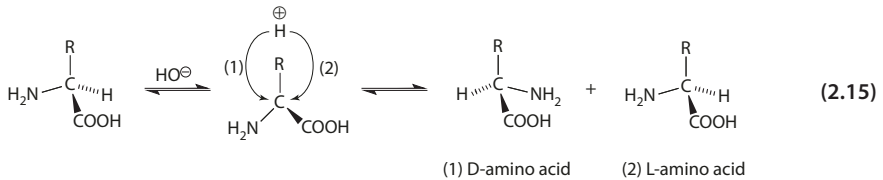
Nucleophilic side groups such as the ϵ -NH₂ group of lysine can then react with dehydroalanine (which is an α,β -unsaturated compound) to form lysinoalanine (Eq. 2.13). Similarly, dehydroalanine reacts with a cysteinyl residue to form lanthionine, ornithine to form ornithinoalanine, and NH₃ to form β -aminoalanine (Eq. 2.14). These addition products lead to new crosslinkings in the protein and render the essential amino acids unavailable. Lysinoalanine has been extensively studied for its physiological and toxicological effects.





■ ■ Racemization

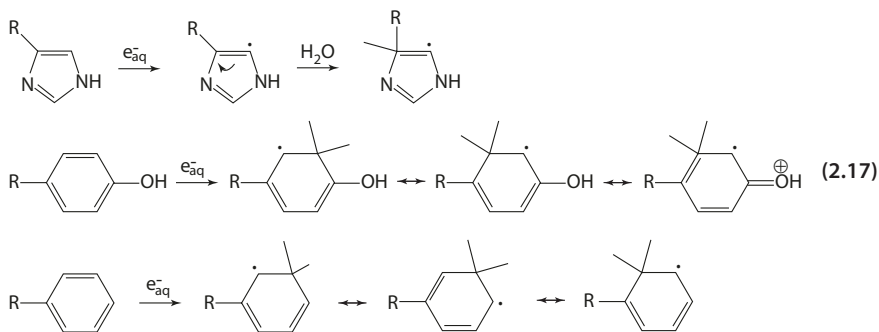
Alkali-treated proteins contain D-amino acid residues due to racemization (Eq. 2.15). Amino acid residues in proteins are more susceptible to α -hydrogen abstraction, and hence racemization, than free amino acids. Free amino acids racemize about ten times slower than bound residues [52]. The D-enantiomers are not available for utilization in the synthesis of proteins. Furthermore, since enzymes are usually stereospecific, substrates with D-amino acids may bind to enzymes to form unreactive intermediates.



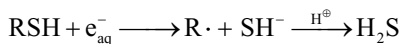
2.4.2 Heat-Induced Formation of Isopeptides

Mild heating causes changes in the tertiary structure of proteins, which in turn influences the physical as well as the chemical properties and alters the functional properties of the proteins that are of significance in food processing.

The nutritional value of the protein is reduced when under prolonged (>10 h) high-temperature (>100 °C) heating, due to crosslinking reactions between the ϵ -amino group of lysine with the carboxyl group of aspartic or glutamic acids (■ Fig. 2.12) and the amide group of glutamine and asparagine [42].

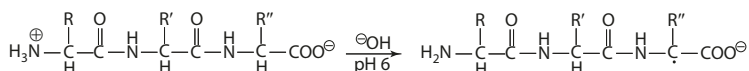
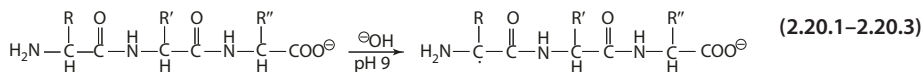
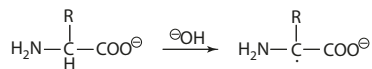


Sulfur-containing amino acids are the most reactive with cysteine and cystine reacting with e_{aq}^- near diffusion-controlled rates. Electron addition to the disulfide forms the radical anion intermediate, which decomposes unimolecularly to the radical (Eq. 2.18). For cysteine (and most other thiols), the reaction is dissociative electron capture, and the products are the radicals and anions (Eq. 2.19.1). The amino radicals undergo "repair" by hydrogen transfer from another molecule (Eqs. 2.19.2, 2.19.3) [99].



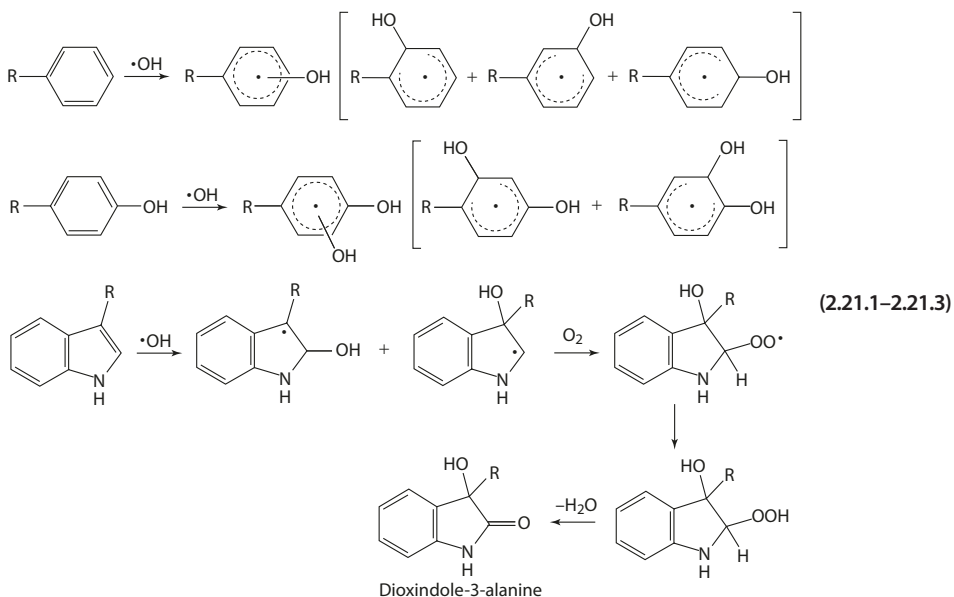
■ Hydroxyl Radical

Hydroxyl radical ($\cdot\text{OH}$) reacts with amino acids by (1) hydrogen abstraction and/or (2) addition. Most aliphatic amino acids have the α -hydrogen abstracted under basic pH (Eq. 2.20.1). In acidic solution, protonation of NH_2 groups decreases the acidity of the α -hydrogen, and abstraction occurs farther from the amino group (Eqs. 2.20.2, 2.20.3). The same is true for aliphatic peptides [71].



Unsaturated compounds are extremely reactive toward $\cdot\text{OH}$ radical. With aromatic amino acids, $\cdot\text{OH}$ reacts by addition to the π system, forming substituted cyclohexadienyl radicals (Eqs. 2.21.1-2.21.2). The rate constant is in the order of 10^9 - $10^{10} \text{ M}^{-1}\text{S}^{-1}$ and

greatly affected by the substituent effect on the electron density in the π ring. Abstraction of H \cdot and the formation of a phenyl radical are comparatively negligible. For tryptophan, addition is at the nitrogen ring, and under aerobic conditions, the radical has been shown to undergo oxygen addition and hydrogen abstraction to form dioxindole-3-alanine (Eq. 2.21.3).

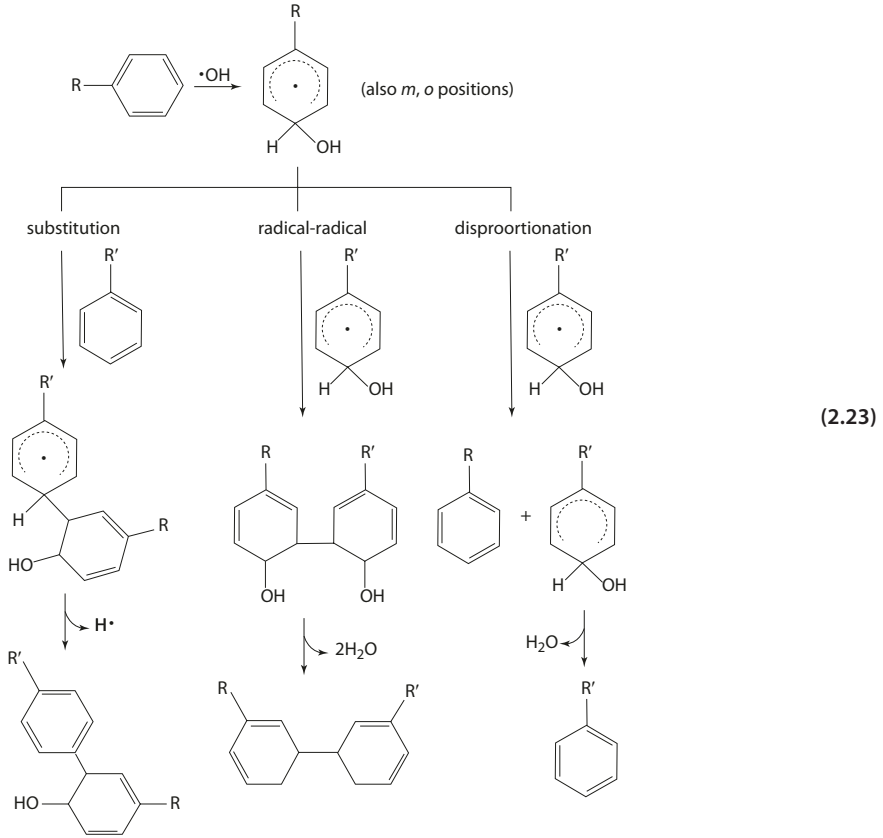


All sulfur-containing amino acids, like the aromatic, react with $\cdot\text{OH}$ at diffusion-controlled rates. For cysteine, hydrogen abstraction occurs at the thiol group (Eq. 2.22.1). For cystine, $\cdot\text{OH}$ adds to the $-\text{S}-\text{S}-$, and the product undergoes cleavage at the C–S or S–S bond (Eqs. 2.22.2 and 2.22.3).



■ Hydroxycyclohexadienyl Radical

The hydroxycyclohexadienyl radicals formed by the addition of $\cdot\text{OH}$ may undergo various reactions. Disproportionation yields hydroxy phenol and hydroxycyclohexadiene. The radicals may crosslink by radical-radical binding or substitution-type reaction [44, 102] (Eq. 2.23). Thiyl radicals likewise also react with aromatic compounds via substitution [103].



Radiation-induced crosslinks have been shown to occur between DNA and protein, both in vivo and in vitro. Radiation-generated $\cdot\text{OH}$ radicals in aqueous solutions of thymine and phenylalanine induce crosslinking between the hydroxycyclohexadienyl radical and the thymine at the C5 position (Fig. 2.13). Crosslinking between phenylalanine and thymine is favored over self-crosslinking among the same radical species [14].

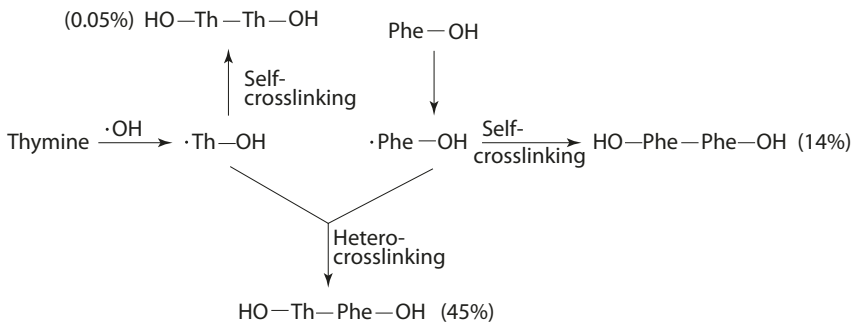


Fig. 2.13 Radiation-induced crosslinking DNA and protein

2.4.4 Photolysis [82]

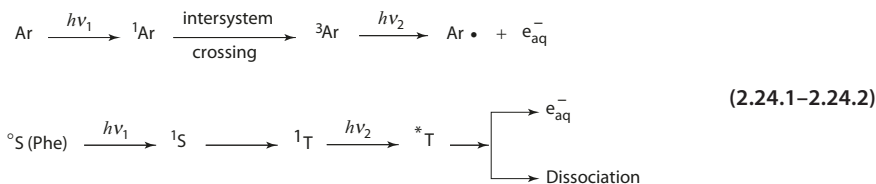
For aliphatic amino acids, absorption of light energy results in excitation, followed by hydrogen abstraction and deamination. Side chain abstraction of $-\text{CH}_3$, $-\text{OH}$, and $-\text{NH}_2$ groups occurs under prolonged UV exposure.

For the aromatic amino acids, the primary photochemical reaction is ionization to hydrated electrons and radicals, involving possibly the triplet excited state, via a biphotonic process (Eq. 2.24.1). For example, the photoionization of phenylalanine is represented by Eq. 2.24.2 [7]. The photoejected e_{aq}^- then reacts with other molecules similar to those discussed on radiation. These secondary reactions account mostly for the role of aromatic amino acids in photosensitized reactions. The major degradative reaction, however, comes from disruption of the ring structure, forming aliphatic amino acids.

Histidine \rightarrow aspartic acid, glutamic acid, γ -hydroxyglutamic, and citrulline.

Phenylalanine \rightarrow tyrosine, serine, alanine, asparagine, ammonia, mono- or dihydroxyphenylalanine (dopa).

Tyrosine \rightarrow aspartic acid, glycine, alanine, serine, asparagine, acetic acid, *p*-hydroxyphenyl lactic acid, tyramine, dopa.

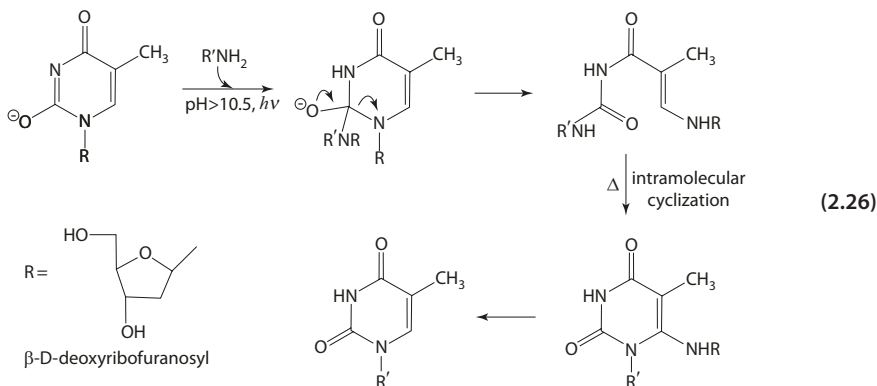


For sulfur amino acids, light absorption leads to excitation of the molecule, which then undergoes cleavage at the $-\text{S}-\text{S}-$ or $-\text{C}-\text{S}-$ bond (Eq. 2.25). Photolytic cleavage of the disulfide leads to further reactions: (1) radical-radical recombination to give back the disulfide, (2) deamination, (3) thiol-disulfide exchange, and (4) oxidation to various acids. Subsequent degradation products include pyruvic acid, ammonia, cysteic acid, sulfinic acid, sulfenic acid, alanine, serine, glycine, trisulfide, and tetrasulfide.



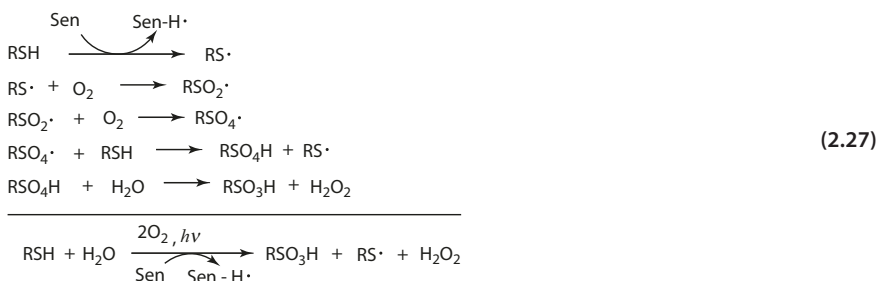
■ ■ Crosslinking

A number of proteins have been demonstrated to crosslink DNA. Lysine is the most sensitive among the amino acids in this respect, and its reaction with thymine has been well established. The reaction occurs only at alkaline pH 8–12, where the thymine exists as a monoanion. The first step of photoreaction is a nucleophilic attack of the ϵ - or α -amino group at C2 of the excited anion of thymine (singlet). Subsequent ring opening and protonation yields a stable conjugated adduct (Eq. 2.26) [78]. Intramolecular cyclization followed by β -elimination, when heated in aqueous solution, gives the cyclic conjugate. Other amino acids also react, but at a lower rate and more alkaline pH range (>11).



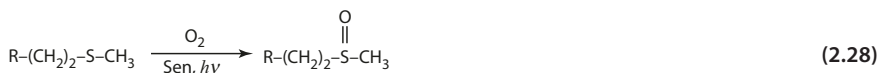
2.4.5 Photosensitized Oxidation

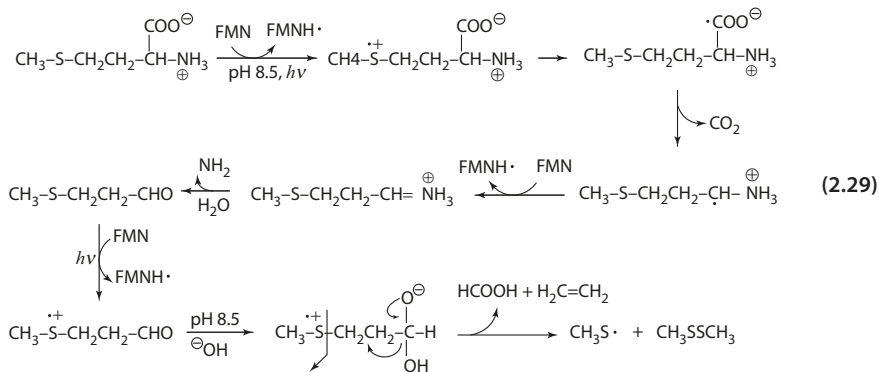
Photosensitized oxidation is more specific than photolysis. Both type I and type II reactions can occur. Cysteine, methionine, histidine, tryptophan, and tyrosine residues in proteins are oxidized in the presence of a suitable sensitizer. (Refer to Appendix 3 for photosensitized type I and type II reactions.)



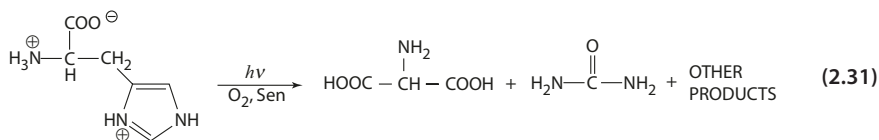
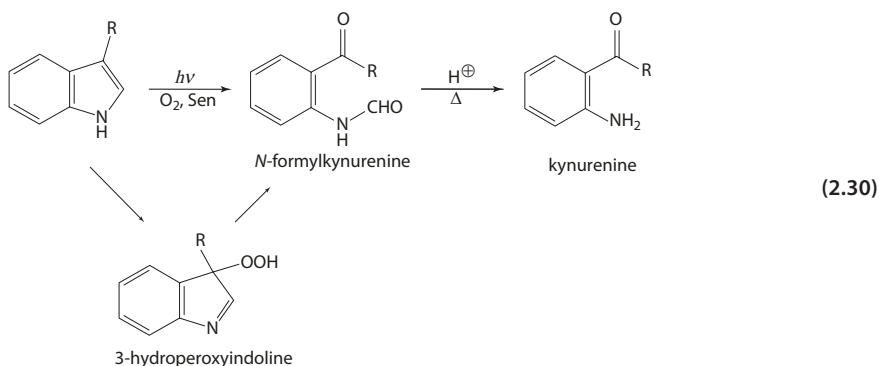
Cysteine is oxidized to cysteic acid by the type I reaction, involving H \cdot subtraction by the triplet sensitizer from the thiol group (Eq. 2.27) [27]. The thiyl radical is further oxidized to cysteic acid or recombines to give cystine.

Methionine is oxidized to methionine sulfoxide via the type II reaction (Eq. 2.28). In the presence of flavin sensitizer, methionine is converted to methional. The reaction involves electron transfer from the sulfur atom to the photoactivated FMN*, followed by intramolecular migration of the electron, deamination, and decarboxylation. At alkaline pH of 8.5 and above, methional is decomposed to ethylene, methyl disulfide, and formic acid (Eq. 2.29) [105].



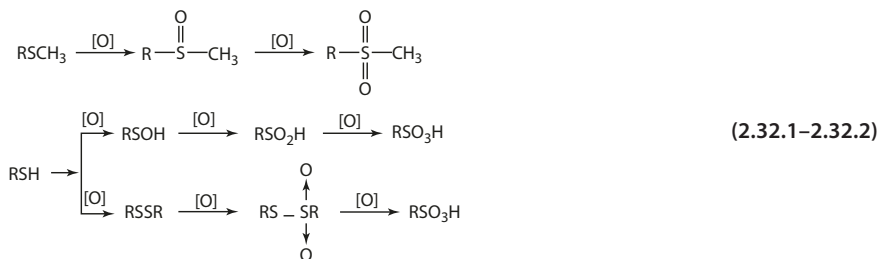


With aromatic amino acids, photooxidation proceeds via the type II reaction, with subsequent degradation and disruption of the ring structure. The pathway of photosensitized oxygenation involves complicated reactions of intermediates of hydroperoxides (Eqs. 2.30 and 2.31) [77].



2.4.6 Chemical Oxidation

Oxidizing agents such as H_2O_2 oxidize (1) methionine to methionine sulfoxide and methionine sulfone (Eq. 2.32.1), and (2) cysteine to cysteic acid (Eq. 2.32.2). The rate of oxidation of cysteine decreases at low pH, whereas the oxidation of methionine increases at low pH.



Hydrogen peroxide can further react with organic acids to form acylperoxides (e.g., performic acid from formic) which are extremely potent oxidants and less selective than H_2O_2 . Acylperoxides oxidize tryptophan to formylkynurenine and other products. Tyrosine, serine, and threonine are also destroyed.

2.4.7 Reaction with Carbonyl Compounds

Reducing sugars, carbonyl compounds from the Maillard reaction, and short- and long-chain aldehydes and ketones from lipid oxidation form Schiff-base adducts with the lysyl ϵ -amino group in proteins (► Chap. 1). Bifunctional aldehydes, such as malonaldehyde may cause intra- or intermolecular crosslinking.

2.4.8 Reaction with Products from Lipid Oxidation

The hydroperoxides formed during lipid oxidation can interact and cause changes in the structural and functional properties of proteins/amino acids. Susceptibility of proteins to lipid oxidation damage depends on the following factors [83]:

1. Accessibility of reactive amino acids on the surface of the protein molecule
2. Hydrophobic interaction or hydrogen bonding between lipid molecules and the protein surface, which results in: (a) bringing the reactants to proximity and (b) exposing the buried amino acid side chain for reaction
3. Presence of radical initiators in the system

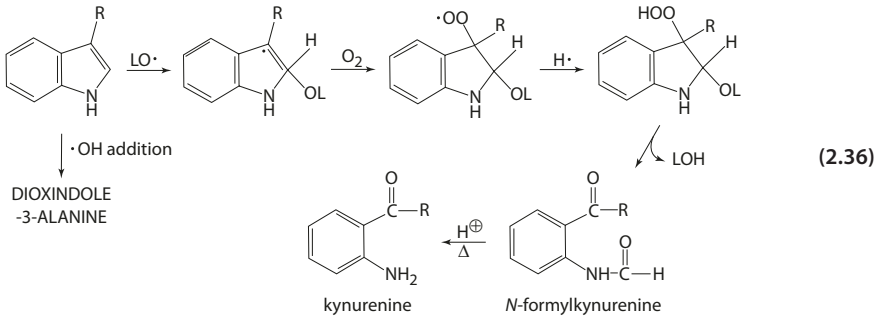
The following scheme depicts, in general, the mechanisms of oxidizing lipids on proteins, which include (1) formation of protein radicals (Eq. 2.33.1), (2) crosslinking of the radicals with lipids (Eq. 2.33.2), and (3) protein-lipid polymerization (Eq. 2.33.3) [86].

Formation of protein radical

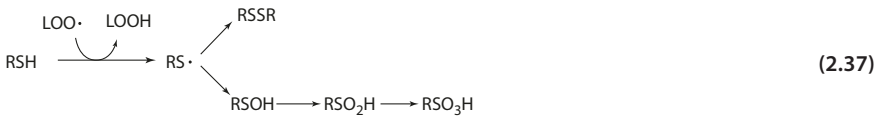


Lipid crosslinked to protein





For cysteine, the products include alanine, H₂S, cysteic acid, and cystine (Eq. 2.37).



2.5 Organized Protein Systems

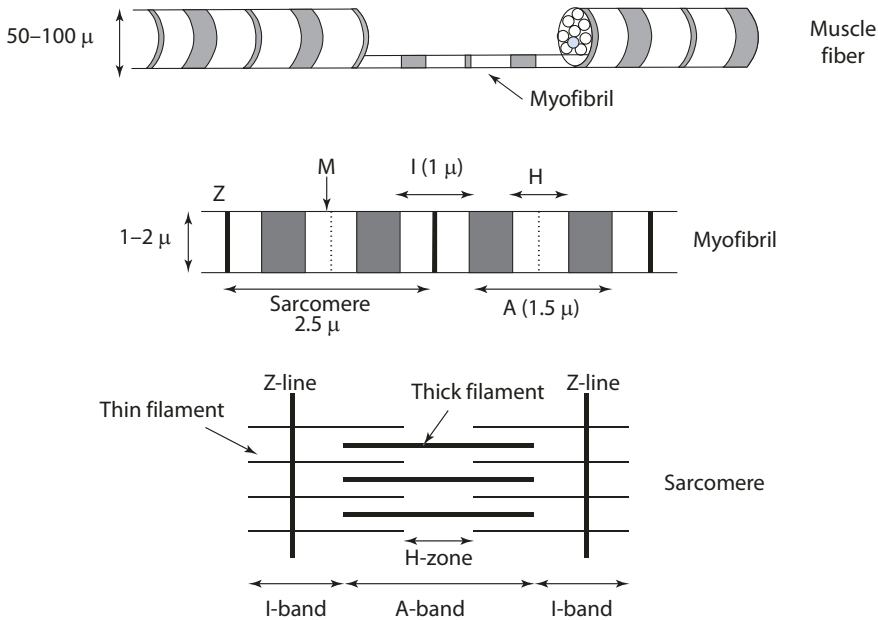
2.5.1 Meat Proteins

Macroscopic Structure of Muscle

The muscle organ is made up of parallelly arranged bundles of muscle fibers (50–100 μ in diameter) separated by sheaths of connective tissue. A muscle fiber is composed of specialized cells formed by the fusion of many separate cells, with a two-layered cell membrane (sarcolemma), the invagination of which forms a network of transverse tubules ("T" system), and a fine longitudinal network of sarcoplasmic reticulum which serves as a reservoir for calcium ions. This membrane system is responsible for the sequestering and the releasing of calcium.

The sarcoplasm (which is the cell's cytoplasm) is filled with myofibrils 1–2 μ in diameter extending the entire length of the cell. Under light microscopy, the myofibril appears striated, consisting of dark bands (A-band) and light bands (I-band) (Fig. 2.14). (1) The A-band comprises thick filaments of myosin and proteins that bind the myosins. In the middle of the A band is the dark M-line, where neighboring thick filaments are transversely connected by the binding actions of M-protein and myomesin. (2) The I-band comprises thin actin filaments and proteins that bind the actins. In the middle of the I-band is the Z-line or disc. The segment between two Z-discs, termed the sarcomere (2.5 μm long), is the basic contractile unit of the myofibril.

The thin and thick filaments are held in the right positions and geometry in the muscle cell in order to function. There are hundreds of proteins forming the cytoskeleton of the muscle cell to provide strength for various attachments and flexibility to accommodate the changes and movement during contraction. Each thick filament is connected longitudinally to the Z-disc via the giant elastic protein titin (3 × 10⁶ Da, 400–700 nm). The N-terminal ends of titin from adjacent sarcomeres, overlap in the Z-line, span the I- and A-bands, and their C-terminal ends overlap in the M-line along the thick filament. Six



■ Fig. 2.14 Structural organization of skeletal muscle

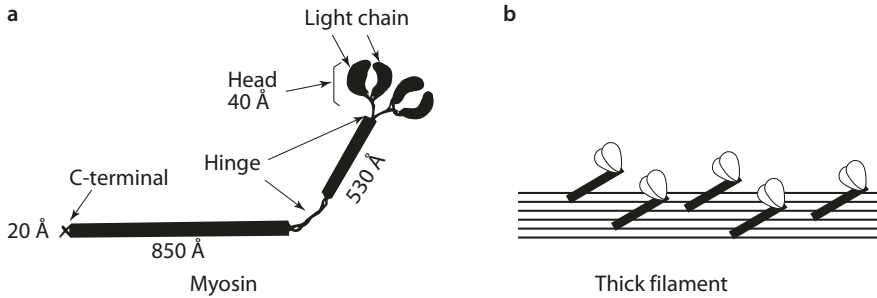
molecules of titin associate with each half of a thick filament. The segment of titin spanning the Z-disc functions as the key contributor to sarcomere integrity. The titin portion in the I-band acts as a molecular spring. In addition to titin, thick filament-associated proteins wrap around the proximal portions of each half thick filaments.

Each thin filament in the I-band is linked through the Z-disc to the four closest thin filaments in the adjacent sarcomeres. The Z-disc therefore functions to anchor both the thin and thick filaments during contraction. In addition to titin, an array of Z-disc proteins have been identified with various functions, for example, (1) α -actinin (scaffold protein crosslinking actin and titin to the Z-disc), (2) nebulin (a giant actin-binding protein, 800 kDa), and (3) desmin (55 kDa, 10 nm "intermediate" filament laterally linking the Z-discs between myofibrils as part of the cytoskeletal network) [11].

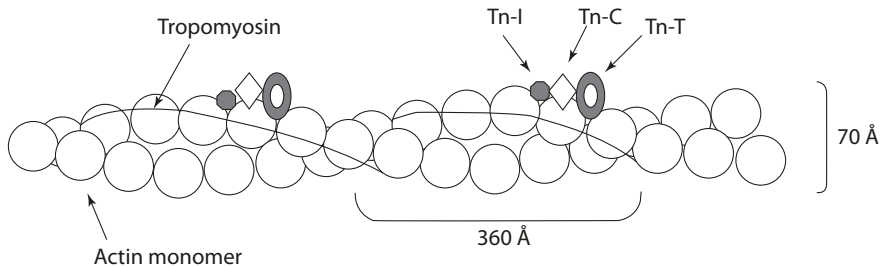
To effectively transmit force, the contractile cytoskeleton described above must be tethered to the sarcolemma, the cellular membrane that envelops the myofibrils. This membrane is rich in extracellular protein matrix acting to transduce the contractile force from the Z-line to the basement membrane, where the force is transmitted laterally to the muscle termini. In addition, the protein matrix provides adhesion anchoring Z-line and M-line to the basement membrane for structural stability and linkages.

The Muscle Proteins

The molecular structure of myofibrils consists of thick and thin filaments. The thick filament is 1200 Å long and 150 Å in diameter. It contains largely the protein myosin, which is composed of six polypeptide chains: two identical heavy chains (200 kDa) and two pairs of light chains (two 20 kDa regulatory light chains and two 16 kDa essential light chains). The two α -helical heavy chains coil around each other to form a rodlike tail domain. At the N-terminal end, each heavy chain coils by itself and complexes with one molecule of each



■ Fig. 2.15 Molecular structure of **a** myosin arranged into **b** thick filament



■ Fig. 2.16 Molecular structure of thin filament

type of light chains to form a double-headed globular head (■ Fig. 2.15a). The tail segment and the head are joined by a flexible hinge region. The regulatory light chains have active function in muscle contraction, whereas the essential light chains are involved in structural stability of the myosin head. The rodlike segments of myosin molecules are packed together forming the thick filament proper of the sarcomere with the heads projected along the thick filaments (■ Fig. 2.15b).

The thin filament is made up of three major proteins (■ Fig. 2.16): one structural (actin) and two regulatory proteins (tropomyosin and troponin):

1. Actin: the monomer of actin is a globular protein called G-actin. G-actins are arranged in a twisted double-strand, bead-like chain known as F-actin (filamentous actin).
2. Tropomyosin: these are long, thin proteins that aggregate end to end along the groove of F-actin, with one protein molecule covering seven actin monomers. The function is to stabilize and stiffen the actin filament.
3. Troponin: this protein is associated with tropomyosin in a one-to-one ratio. Troponin is a protein consisting of three separated subunits:
 - Troponin C (calcium-binding protein)
 - Troponin I (inhibitory protein)
 - Troponin T (tropomyosin-binding protein)

The Myosin Protein Structure

The myosin protein can be conveniently separated into the proteolytic fragment SI which comprises the first 800 amino acid residues of the heavy chain together with the two light chains. This is the morphological crossbridge and contains all the enzymatic activity and function of the parent myosin.

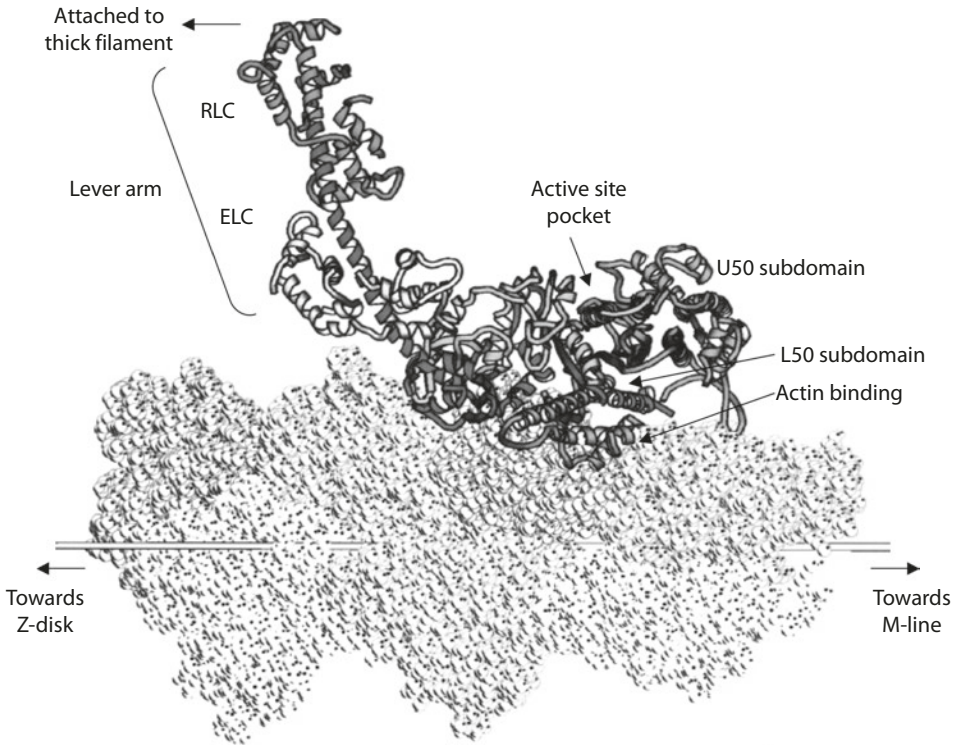


Fig. 2.17 A ribbon representation of myosin (motor domain) structure attached to actin (From Raymond and Holden [73] with permission. Copyright 1994 Elsevier. PDB 1b7t)

The head region (also known as the catalytic or motor domain) has a pear-shaped structure consisting of four subdomains: (1) N-terminal subdomain, (2) upper 50 kD subdomain (U50), (3) lower 50 kD subdomain (L50), and (4) converter subdomain (Fig. 2.17). A prominent feature of the myosin motor domain is a large cleft (also called 50 kD cleft) enclosed by the U50 and L50 subdomains. The central seven-stranded β sheets and associated loops in the U50 subdomain and the N-terminal subdomain form the transducer element that plays a critical role in moving the cleft in opening and closing configurations. The C-terminal segment of the proteolytic fragment SI contains the extended rod domain (about 1100 amino acids) that forms a long parallel α -helical coil-coil structure. The rod domains of neighboring myosins interact and pack together to form the thick filament proper [72, 73].

The nucleotide-binding (ATPase) site is located at the apex of the 50 kD cleft in the U50 subdomain bordered with the N-terminal domain. The P loop (in the N-terminal subdomain) and the switch I segment (in the U50 subdomain) are involved in the binding of ATP and the release of Mg.ADP in the hydrolysis. Situated close to the ATP binding site is the switch II connector (between U50 and L50 subdomains), which controls the exit of the phosphate P_i during the contraction cycle.

The actin-binding site is located at the tip (outer end) of the cleft. This site involves a number of flexible loops in both U50 and L50 subdomains. When the 50 K cleft is closed, these loops are positioned to provide a large contact surface for charge and hydrophobic interactions with actin for tight binding.

Several flexible elements undergo conformational changes, facilitating the catalytic events in the molecular mechanism of muscle contraction:

1. The turning of the converter domain
2. The kink formation in the relay helix
3. The movement of switch I and switch II (SW1, SW2) segments
4. The positioning of the P loop
5. The twist of the central β sheet

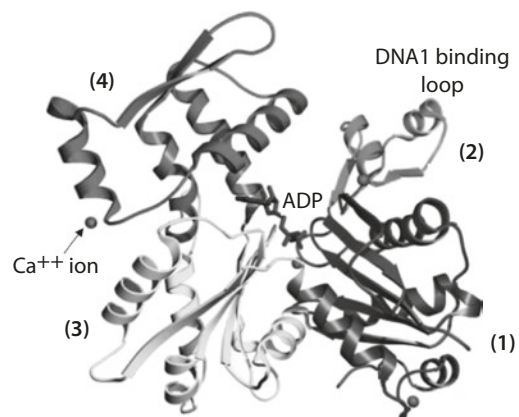
The head region is extended at the C-terminal direction to form an α -helical tail, known as the "neck" domain, more commonly called the "level arm." This domain is composed of two IQ motifs typically of 25 amphiphilic residues with an α -helical structure. It has a consensus sequence of [I,L,V]QxxxRGxxx[R,K], which provide the binding site for the light chains, contributing to the structural stability of the arm.

Joining the head region and the lever arm is a small compact domain called the converter. This domain is asymmetrically connected to the rest of the motor domain by the relay helix (in the L50 subdomain). The converter domain acts as a socket for the lever arm and rotates by $\sim 60^\circ$ during force generation with respect to the body of the crossbridge. Therefore, conformational rearrangements (as in ATP binding and catalysis, formation of the actin binding interface) in the motor domain are effectively transmitted and amplified through the rotational movement in the converter domain to the swinging motion of the lever arm. The swinging action amounts to a change in the position at the end of the arm for a distance (a step size) of about 10 nm. The cleft in the head is closed on strong binding to actin. The U50 subdomain moves to close the actin-binding cleft and open the nucleotide-binding pocket.

The Actin Protein Structure

The components of thin filament include (1) actin, consisting of monomeric or globular G-actin and filamentous or F-actin, (2) tropomyosin, and (3) troponin. The actin monomer is a globular protein of 42 kDa (375 amino acids), consisting of four domains: two large domains known as 1 and 3 in one half, and two small domains 2 and 4 in the other half of the molecule [90]. Both the N- and C-termini are in domain 1 (■ Fig. 2.18). The polypeptide chain starting from domain 1, goes into domain 2, back to domain 1, across to domain 3,

■ **Fig. 2.18** A ribbon representation of the structure actin in the ADP state (From Otterbein et al. [62] with permission. Copyright 2001 American Association for the Advancement of Science. PDB 1J6z)



then to domain 4, through domain 3, and across to domain 1. The primary binding site for the myosin head is in domain 1. Between the two halves of the molecule is the binding site for ATP or ADP with a calcium ion bound to the phosphates [62].

The globular or G-actin polymerizes into F-actin that resembles twisted double strands of bead-like strings. In the F-actin, the G-actins are oriented with domains 3 and 4 on the inside, where neighboring monomers interact with each other. The structure of F-actin can be described in terms of a 13/6 helix with 13 actin monomers per six turns and a repeat of 360 Å. The actin helix morphologically appears as two right-handed steep helices, which twine around each other [37].

Tropomyosin consists of two 32.8 kDa chains folded into a parallel coiled-coil α -helical structure, labeling seven actin monomers in the F-actin. End-to-end binding of tropomyosins produces a continuous strand along the groove of the actin helix for their cooperative action. Each helical repeat of the thin filament also contains along each strand a troponin protein complex, comprising troponin TnC (which reversibly binds to Ca^{2+}), TnT (which binds to tropomyosin), and TI (which inhibits contraction).

What are the mechanistic actions of troponin and tropomyosin? The formation of the activated actin-myosin complex is regulated by low concentrations of Ca^{2+} . The muscle is in a relaxed state in the presence of 10^{-7} M Ca^{2+} or less and fully contracted by 10^{-5} M Ca^{2+} . A nerve impulse transmitted to a muscle cell causes the cell membrane to depolarize. The depolarization of the membrane system causes a release of calcium from the sarcoplasmic reticulum tubules into the sarcoplasm. The binding of calcium to troponin G induces a conformational change in the troponin-protein complex. This interaction pulls the tropomyosin toward the groove of the F-actin, allowing the binding of the actin monomers (G-actin) to the activated myosin. Removal of calcium allows the troponin to return to its original conformation and the tropomyosin to a position sterically blocking the actin from binding. Thus, Ca^{2+} functions to control the "on" and "off" states of the actin filament via conformational changes of the troponin complex.

Conversion of Chemical Energy to Mechanical Work: The Fate of ATP

The following sequence of steps occurs in muscle contraction during which ATP is utilized to generate work (■ Fig. 2.17, 2.19) [12, 26, 36]:

1. The rigor (rigor-like) state [AM]

Starting from the *rigor-like* state, the myosin and actin are strongly bound by interactions at the actin/myosin interface forming the actomyosin crossbridge (AM).

In the rigor state, the 50 kD cleft is in closed position, the U50 subdomain β sheet is in a twisted (strained) conformation, and the relay helix assumes a kink configuration.

2. The post-rigor state [AM + ATP \rightarrow AM•ATP \rightarrow A + M•ATP]

In the first step of the muscle contraction cycle, an ATP molecule binds onto the myosin head (i.e., the nucleotide-binding/active site) of the actomyosin (AM) to form AM•ATP. Binding of ATP induces conformational changes of the nucleotide-binding site. The movement of the motifs/loops (SW1, SW2, P-loop) forming the binding pocket results in the opening of the 50 kD cleft, leading to the disruption of the actin-myosin interface, and weakening of the binding affinity of myosin for actin.

The actomyosin complex dissociates to form the *post-rigor* state ($M \cdot ATP$). As a result, the β sheet is untwisted and the relay helix is straightened.

2

3. The pre-rigor state (or pre-powerstroke state) [$M \cdot ATP \rightarrow M \cdot ADP \cdot Pi$]

Hydrolysis of ATP (Mg^{++} ATPase activity) occurs rapidly leading to the formation of a stable myosin product. The cleaved Pi remains tightly bound in the myosin active site as $M \cdot ADP \cdot Pi$, which is known as the *pre-rigor* state, also known as the pre-powerstroke state. The conformational change in the enclosed binding of $M \cdot ADP \cdot Pi$ triggers the closing of the 50 kD cleft and positions the myosin to interact forming stereo-specific binding with actin. The tight binding interactions at the myosin-actin interface leads to a series of conformational changes (known as "repriming") of the myosin motor (in preparation for the powerstroke event). (1) The whole of L50 subdomain rotates toward the U50 subdomain and forces the central β sheet to twist (a strained state). (2) This change causes the relay helix to assume a kink configuration. (3) The kink leads to a rotation of the converter domain through 60° and thus relieves and straightens the relay helix. The U50 β sheet is also known as the "transducer," because it acts as a processor in muscle motor contraction. In short, strong binding puts the β sheet under strain (twisted) and moves the converter in a 60° rotation, in building up the force for contraction.

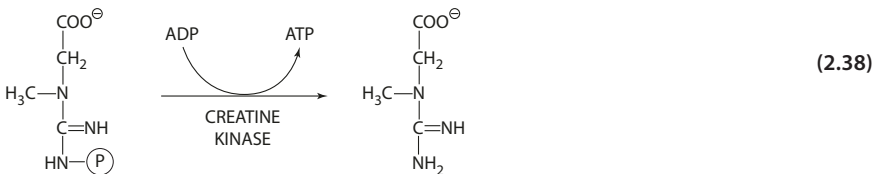
4. The powerstroke [$A + M \cdot ADP \cdot Pi \rightarrow AM \cdot ADP + Pi$ (released) $\rightarrow AM + ADP$ (released)]

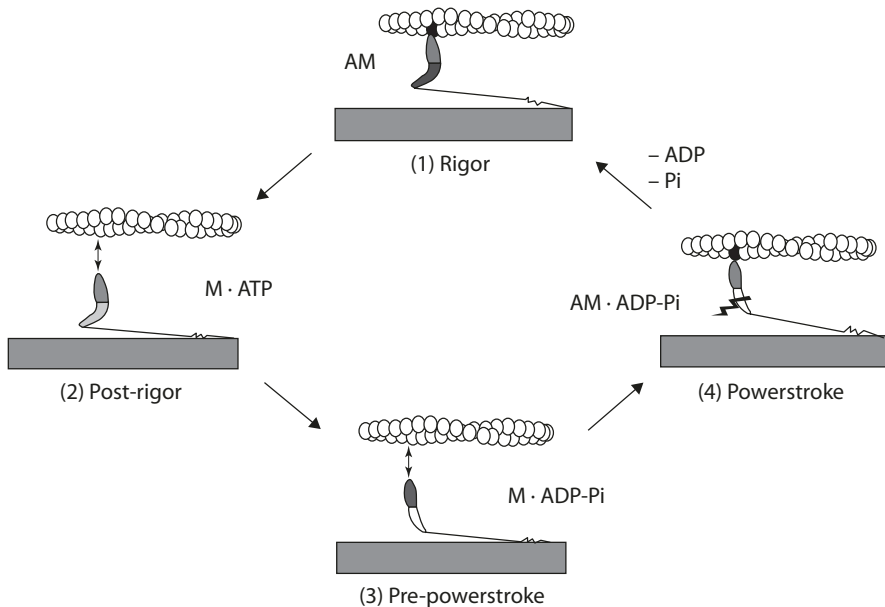
The actin-myosin tight binding interaction causes movement of the loops in the nucleotide-binding site, destabilizes Pi binding, and allows the escape of the γ -phosphate. The loss of Pi is associated with relieving the strain in the U50 β sheet and the 60° rotation of the converter and final swing of the lever arm (powerstroke). The lever arm movement slides the myosin along the actin filament with single steps of ~ 5 nm. Relieving the strain in the myosin motor triggers structural rearrangement of the nucleotide-binding site to loosen the ADP. The rate of ADP release defines how fast a muscle contracts. Thus the working stroke is coupled to the release of Pi from the $A \cdot M \cdot ADP \cdot Pi$ complex and the subsequent release of ADP. The AM (rigor-like) state is regenerated at the end of the powerstroke and is poised for starting a new cycle (■ Fig. 2.19).

Rigor Mortis

Muscle contraction requires ATP, which can come from three potential routes:

1. Regular pathways: these include glycolysis, amino acid metabolism, fatty acid oxidation, and oxidative phosphorylation.
2. Short-duration supply: muscle cells store phosphocreatine for the transfer of a phosphate to ADP to form ATP (Eq. 2.38).





■ **Fig. 2.19** Schematic representation of mechanical and biochemical stress in muscle contraction (From Geeves and Holmes [26] with permission. Copyright 2005 Elsevier)

3. Immediate supply: conversion of ADP to ATP is catalyzed by adenylate kinase (Eq. 2.39).



Immediately after the animal is sacrificed, oxygen becomes unavailable, and the aerobic pathway of producing ATP is stopped. The supply of phosphocreatine is rapidly depleted. The major anaerobic pathway (glycolysis) becomes the remaining source of ATP. However, the conversion of glycogen or glucose to lactic acid with the production of ATP is self-limiting under these conditions, since the buildup of lactic acid causes a drop in pH that is inhibitory to the enzymes involved in glycolysis.

The rapid depletion of ATP is also related to the breakdown in the regulatory system that controls the Ca^{2+} level. The calcium concentration builds up in the sarcoplasm, induces the contraction of the muscle fibers, and consumes the ATP supply. Since there is no ATP to effect the dissociation of the actin-myosin complex (AM in ■ Fig. 2.19), the muscle loses its natural extensibility due to shortening of the sarcomere. The contraction or shortening involves a decreased length of the I-band and the H-zone, whereas the A-band in the sarcomere remains relatively unchanged. The state at which the postmortem changes occur is known as rigor mortis. In the sense of the chemical process, rigor mortis is defined as the time where there is no available ATP for the release of myosin from the actomyosin complex.

The Ultimate pH

The accumulation of lactic acid lowers the pH of the muscle, and eventually the muscle reaches an ultimate pH that is critical to postmortem changes. The pH in beef muscle generally decreases from 7.0 upon slaughter to 5.5–5.8, when rigor mortis sets in. The typical decline in pH is about 18–40 h for beef (faster for pork about 6–12 h). The ultimate pH value is critical for color development of the meat. Both the rate and extent of the pH drop are important factors affecting the quality of the meat. Beef muscle with a low ultimate pH has a bright red color, whereas a high ultimate pH gives a blueish purple color. The latter is often referred to as "dark-cutting" beef. This is due to formation of metmyoglobin, because the mitochondria on the meat surface are not inactivated and compete with myoglobin for oxygen. (See ► Chap. 4., section on "Myoglobin.")

A sharp rapid decrease in pH may cause the denaturation of proteins if the carcass temperature is still high. Denaturation of muscle proteins leads to both a decrease in the water-holding capacity and an adverse effect on the texture. Denatured proteins do not bind water well, partly responsible for exudative conditions which refer to leaking of fluid from the meat tissue. Denaturation also causes the collapse of the protein structure and a change in the reflection of light, resulting in paleness of the meat. This so-called pale-soft-exudative condition due to rapid pH drop is found relatively more common in pork muscle.

It should also be noted that rapid cooling of the carcass causes a sharp decline in temperature ($<15\text{ }^{\circ}\text{C}$) before the onset of rigor (i.e., while the carcass still in the early pre-rigor state and the $\text{pH} \geq 6.0$). The sarcoplasmic tubular system of the pre-rigor muscle is stimulated to release calcium ions, leading to "cold shortening" and toughening of the meat. In a similar situation, if the meat is frozen at pre-rigor and thawed, contraction occurs with the sudden release of calcium, leading to extensive shortening, release of fluids, and severe toughening.

2.5.2 Water-Holding Capacity

Lean muscle contains about 75% water, 20% proteins, plus variable amounts of lipids and carbohydrates, and small amounts of soluble organic and inorganic components. In the muscle cell, water is found within the myofibril, between myofibrils, and between myofibrils and the base membrane (sarcolemma). Minimum water-holding capacity is observed around pH 5.0. Water-binding capacity of fresh meat describes the ability to retain inherent water, often interpreted as drip loss. Drip contains significant amount of proteins on average of 110 mg per ml of fluid, mostly water-soluble sarcoplasmic proteins, including glycolytic enzymes and myoglobin.

In connection to water-binding capacity, three types of water are described:

1. Bound water—mostly bound to proteins and cannot be easily removed.
2. Entrapped water—held by steric (space) effect and by attraction to the bound water, does not flow freely in the tissue, and can be removed by drying and frozen to form ice.
3. Free water—flows from tissue mostly by capillary forces between the liquid and the surrounding matrix.

The water most affected by the changes in muscle-to-meat conversion is the entrapped (or immobilized) water. During the conversion of muscle to meat, this population of water molecules can be mobilized due to changes of the cell structure and its components [40, 66]:

1. As muscle goes into rigor, the thick and thin filaments are tightly bound. Longitudinal shortening of the sarcomere reduces the intracellular volume, expelling the water into extramyofibrillar compartment. Studies have found correlation between postmortem extramyofibrillar volume and drip loss.
2. Shrinkage of myofibrils during rigor mortis is transmitted to the whole muscle cell and thus reduces the volume of the muscle cell itself. (The myofibrils are linked to each other and to the cell membrane sarcolemma via several intermediate filament proteins, such as desmin, filamins, and titin.)
3. At the ultimate pH of 5.5–5.8, the major proteins in myofibrils (such as myosin with pI of 5.4) are near their isoelectric point with net charge of zero. The proteins are more packed, reducing the space available to hold water.
4. Rapid pH decline while the carcass is still warm may cause denaturation of proteins. Short-term stress in animals can accelerate their metabolism causing a more rapid pH decline. Genetic factors influence basal metabolism as well.
5. Other factors affecting water binding characteristics include muscle types, slaughter age, animal growth rate, preslaughter handling, and chilling effect.
6. Meat processing, such as addition of salts or phosphates, causes an increase in water-holding capacity and swelling. (Refer to ► Chap. 9, phosphates.)

Postmortem Tenderness

Water-holding capacity may associate with juiciness and tenderness of the meat. However, meat tenderness is mostly related to enzymatic degradation of myofibrillar proteins, particularly the Z-disc proteins. After the muscle tissue goes into rigor mortis, there is a gradual decrease in the toughness upon postmortem storage. During this period (first 72–96 h) of increasing tenderness, the following changes are evident:

1. Disintegration of the Z-disk and slow loss of the M-line
2. Change of actin-myosin complex
3. Gradual degradation of troponin T [29]

It is generally agreed that proteolysis is responsible for meat tenderness postmortem and during aging of the meat. Muscle proteases can be classified into three groups: (1) the alkaline proteases, (2) the acidic proteases, and (3) the neutral proteases. It is unlikely that the alkaline proteases would have a major role in postmortem tenderization due to the fact that these enzymes have their optimum activity at pH ranges not found in the postmortem condition.

Among the acidic proteases, the lysosomal cathepsins have received much attention. These proteases are either exopeptidases (the cathepsins A, C, and H) or endopeptidases (B, D, and L). Both cathepsins B and D degrade myosin and actin to fragments of various sizes, with the latter being more active. Cathepsins B and D have their optimum pH at pH 5.2 and 4.0, respectively. Cathepsins L and H have ten and five times more activity than cathepsin B in the degradation of myosin. Cathepsin L also cleaves actin, α -actinin, troponin-T, and troponin-I, but the optimum pH is 4.2, lower than normally found in meat.

The calcium-dependent proteinase family, the calpains, has been extensively studied and implicated as the major enzyme causing postmortem tenderization. Calpains are

non-lysosomal cysteine proteases consisting of at least three isoforms in skeletal muscles, with calpain I (μ -calpain) found mostly in myofibrils and calpain II (m-calpain) in the cytosol. These isoforms require Ca^{2+} to be active. μ -Calpain and m-calpain are heterodimers of 80 and 28 kDa, respectively. μ -Calpain has been demonstrated at postmortem conditions (pH 5.6, 4 °C, 100 mM CaCl_2) to degrade rapidly the Z-disk and M-line (titin, nebulin, desmin) and also the protein troponin T [41]. The enzyme has an unusual specificity, in that it will not act on myosin, actin, α -actinin, and troponin, under most conditions.

Other proteolytic enzymes may also be involved. For example, the proteases involved in cell apoptosis and enzymes present in proteasomal complexes have been investigated with implication in postmortem degradation [47]. β -Glucuronidase and β -galactosidase have been associated with the breakdown of proteoglycans in connective tissues. The degradation of collagen by collagenase has also been implicated as one of the processes involved in postmortem aging.

Meat Emulsion

The formation of meat emulsion consists of two phases: mechanical comminution and a subsequent heating process. During comminution, the muscle and fatty tissues are reduced to microparticles. The myofibrillar proteins are released, allowing water binding and higher degree of swelling. The fat is dispersed as fine droplets within the heterogeneous aqueous phase. Initial melting is accomplished by the heat generated by comminution (~18 °C). Adsorption of protein molecules at these newly formed oil-water interfaces results in the formation of protein films surrounding the oil droplets.

Heating causes the protein molecules to denature and aggregate into a gel network. Between fat droplets, the formation of a layer of protein gel matrix sets a steric barrier against coalescence. Simultaneously, the water molecules are held in the interstices by various protein-water interactions, now including capillary actions between surfaces in the network that physically holds the water molecules in solution or suspension. The result is a three-dimensional network of protein gel that physically and chemically stabilizes dispersed fat droplets and water molecules.

Not all muscle proteins exhibit the same degree of stabilizing effect in a meat emulsion. Muscle cell proteins can be classified into three fractions: the salt-soluble myofibrillar proteins (50–55%), the water-soluble sarcoplasmic proteins (30–35%), and the connective tissue proteins (10–15%). It is the salt-soluble proteins that are chiefly involved in the formation of a gel network in a meat emulsion. Among the myofibrillar proteins, myosin and actomyosin produce the most stabilized emulsion [33] (Table 2.4).

Table 2.4 Stability of emulsion of salt-soluble proteins

Protein	pH	Ionic strength	Stability of emulsion (days)
Myosin	8.0	0.35	>4 weeks
Sarcoplasmic	7.0	0.35	12 h
Actin-myosin	6.7	0.35	>3 weeks
Actin	7.2	0.35	<36 h

From Hegarty et al. [33]

■ **Table 2.5** Heat-induced changes of muscle proteins

Temperature (°C)	Protein	Action
30–35	Tropomyosin	Dissociates from actin backbone
38	F-actin	Helical strands dissociate into single chains
40–45	Myosin	
	Head	Some conformational change
	Hinge	Helix to coil conformational change
45–50	Actin-myosin	Complex dissociates
50–55	Myosin	
	"Tail"	Helix to coil conformational change
>70	G-actin	Major conformational change

From Ziegler & Acton [109]

The Role of Myosin in Gelation

Denaturation of muscle proteins involves a series of transition temperatures (T_m) corresponding to heat-induced conformational changes of many individual protein molecules in the muscle fiber. ■ Table 2.5 lists the events that occur during heat treatment [109].

Two transition temperatures ($T_m = 43\text{ °C}$, 55 °C) are critical for the formation of gels, implying two types of conformational changes in heat-induced gelation. Studies suggest myosin is the major protein in the myofibrils that is involved in the process of gelation. The myosin heads start to aggregate upon heating at a relatively low temperature, while the rod segments unfold with increasing temperature. The aggregation of the heads involves disulfide exchange and possibly intermolecular association of side chains [80]. The head-to-head aggregation provides a junction zone linking the myosin rods to form a gel network, in a way very similar to the polysaccharide gels.

The gel network is further stabilized by noncovalent bonding among the binding sites made available by the unfolding of the myosin protein. The presence of actin enhances the gel formability of myosin. Under the optimum conditions for gel formation (0.6 M salt, pH 6.0, and 65 °C), a myosin/actin ratio of 1.5–2.0 has been shown to substantially augment the rigidity of the gel.

2.5.3 Milk Proteins

Cow's milk contains 3.9% fat, 3.3% protein, 5.0% lactose, and 0.7% minerals. Milk proteins are classified into two major fractions: the caseins and the whey proteins. Caseins are the phosphoproteins precipitated from raw skim milk at pH 4.6 and 20 °C . The casein fraction comprises ~80% of the total protein content of milk. The principal proteins in this group are the α_{s1} -, α_{s2} -, β -, and κ -caseins (in a ratio of 4:1:3.5:1.5 in cow's milk). These four families of caseins are identified according to homology of their primary structures. Proteins that do not precipitate at the pH 4.0–5.0 range are whey proteins. The term whey proteins also refer to proteins that remain in solution after coagulation of the caseins due

to rennet treatment in cheese manufacturing. Whey proteins constitute about 0.5% (w/w) of milk and include β -lactoglobulin, α -lactalbumin, serum albumin, lactoferrin, and immunoglobulins [20].

2

α_{s1} -Caseins

α_{s1} -Caseins constitute up to 40% of the total casein fraction in bovine milk. The α_{s1} -casein is a 23 kDa protein, consisting of 199 amino acid residues, with eight phosphoserine residues distributed between residues 43–79. This same segment also contains 12 carboxyl residues, forming the hydrophilic region (acidic peptide segment) of the protein. Five genetic variants are found in the α_{s1} -casein family, differing in the degree of phosphorylation. The phosphate groups bind calcium ion, and the α_{s1} -casein tends to precipitate in the presence of calcium. The rest of the polypeptide chain has a high percentage of nonpolar residues, is hydrophobic, and exhibits strong association in the formation of micelles. There is very little discernible secondary structure due to the 8.5% proline residues uniformly distributed in the molecule (except in the highly charged region). However, the protein is not a complete random coil. The hydrophobic region with nonpolar residues form the interior and the acidic (charged) segment tend pointing outward on the surface.

α_{s2} -Caseins

α_{s2} -Caseins constitute up to 10% of the casein fraction. The α_{s2} -casein molecule consists of a single polypeptide of 25 kDa, consisting of 207 amino acid residues. Four genetic variants exist in this family of caseins due to the extent of phosphorylation. The protein has two internal cysteine residues (like κ -caseins), which form predominantly intramolecular disulfide bonds. α_{s2} -Casein is the most hydrophilic among all the caseins, consisting of three clusters of anionic groups (phosphoserine and glutamyl residues). As a result, the association behavior of the protein molecule is very dependent on the ionic strength, and the protein is very sensitive to precipitation by low levels of Ca^{2+} concentration. α_{s2} -Caseins have a low proline content, in contrast to its high number of phosphoserine residues.

β -Casein

β -Caseins constitute 30–35% of the total caseins. The protein molecule is a single polypeptide chain of 24 kDa, consisting of 209 amino acid residues. The five phosphoserine residues and seven carboxylates are clustered near the N-terminal acidic segment (residues 1–43), while the C-terminal half (136–209) is highly hydrophobic. This concentration of hydrophilic and hydrophobic regions at the terminal ends results in the β -casein being more surfactant-like than the α_{s1} -casein. β -Casein associates at a slower rate than the α -caseins, and it is not as readily precipitated by calcium compared to α_{s1} -casein. Seven genetic variants are known in this family.

κ -Casein

κ -Caseins constitute about 15% of the total caseins. The monomer is 19 kDa, which forms polymers via disulfide bonds in size ranging from 60 to 600 kDa. The κ -casein monomer has only one phosphate residue but has 0–5 carbohydrate (trisaccharide) chains. The monomer contains 169 amino acid residues, with a hydrophobic N-terminal segment (1–105) and a hydrophilic C-terminal segment (106–169) known as para- κ -casein and macropeptide, respectively. Para- κ -casein possesses no carbohydrates, whereas the macropeptide is glycosylated at Thr residues with mixed chains of *N*-acetylneuraminic acid,

galactose, and galactosamine. This uneven distribution of carbohydrates, combined with a high content of aspartic acid and glutamic acid, results in an acidic and highly soluble C-terminal segment of the κ -casein monomer. The κ -casein is the least sensitive to calcium ion precipitation. Its main function is to stabilize the α -caseins against calcium precipitation in the casein micelle. Seven genetic variants are known to exist in this casein family.

Casein Micelle

Caseins exist in large spherical colloidal micelles with calcium phosphate. Casein micelles are highly hydrated consisting of 4 g water per g protein, with 15% of the water bound to the proteins, and the remaining water being simply occluded within the colloidal particle. Casein micelles comprise 93% (w/w) caseins and range in size of 50–200 nm with a particle weight from 10^7 to 3×10^{10} . The remaining 7% comprises inorganic calcium (3%), phosphate (3%), and small amounts of magnesium, sodium, potassium, and citrate [84]. The calcium and phosphate play an important role in maintaining the integrity of the casein micelles and are commonly referred to as colloidal calcium phosphate. Various models have been proposed to describe the molecular architecture of casein micelles, which can be grouped into two categories: the submicelle model and the nanocluster model.

The Submicelle Model. In this model, a casein micelle is assembled from submicelles with a particle weight of $3\text{--}6 \times 10^5$ and a diameter of 10–20 nm, containing mixed casein molecules. The variations in the size, composition, and particle weight of submicelles are determined by factors such as concentration of individual casein type, pH, ionic strength, and temperature. Submicelles comprise a mixture of α_{s1} -, α_{s2} -, β -, and κ -caseins, with the hydrophobic regions of the casein molecules oriented inward and the hydrophilic regions of the caseins located on the surface. Hence the core of the submicelle is hydrophobic and the surface is hydrophilic. Furthermore, the κ -caseins undergo self-association and are restricted to one area of the surface. Therefore, on the surface of the submicelle, there are carbohydrate-rich (macropeptide portion) areas of the κ -caseins and phosphate-rich (phosphoserine residues) areas of the other caseins (α_s and β). The phosphate groups on the surface interact with calcium to form calcium-phosphate bridges. Therefore, in the presence of calcium, part of the surface of the submicelle is available for hydrophobic interaction. In building up a micelle, the hydrophilic interactions among submicelle surfaces tend to align the entering submicelles with the hydrophilic areas oriented outward. Consequently, the resulting micelle must have a highly hydrophilic surface, rich in κ -casein. The size of the micelle is dictated by the relative concentration of κ -casein in the submicelle [89].

A modification of the above model has been suggested in that the binding of submicelles is facilitated by electrostatic interaction via colloidal calcium phosphate rather than hydrophobic bonds. The binding takes place between the negatively charged phosphoserine residues of the caseins and colloidal calcium phosphates in the form of $\text{Ca}_9(\text{PO}_4)_6$ clusters positively charged with the adsorption of two calcium ions. Since κ -casein is almost phosphate-free, binding occurs only among the α - and β -caseins. Submicelles with a low κ -casein content or with no κ -casein are buried in the interior of the micelles. Micellar growth stops when the micelle surface is covered predominantly with κ -casein [86] (■ Fig. 2.20).

■ ■ The Nanocluster Model

In this model (■ Fig. 2.21), a casein micelle is not formed by assembling submicelles. Instead, the colloidal calcium phosphate is present in the form of amorphous

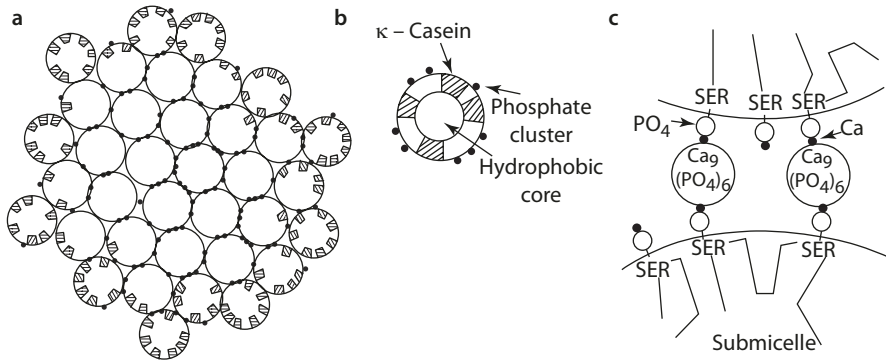


Fig. 2.20 Schematic representation of **a** a casein micelle composed of submicelles, **b** a submicelle, and **c** two submicelles bound via $\text{Ca}_9(\text{PO}_4)_6$. (From Schmidt [86] with permission. Copyright 1982 Elsevier)

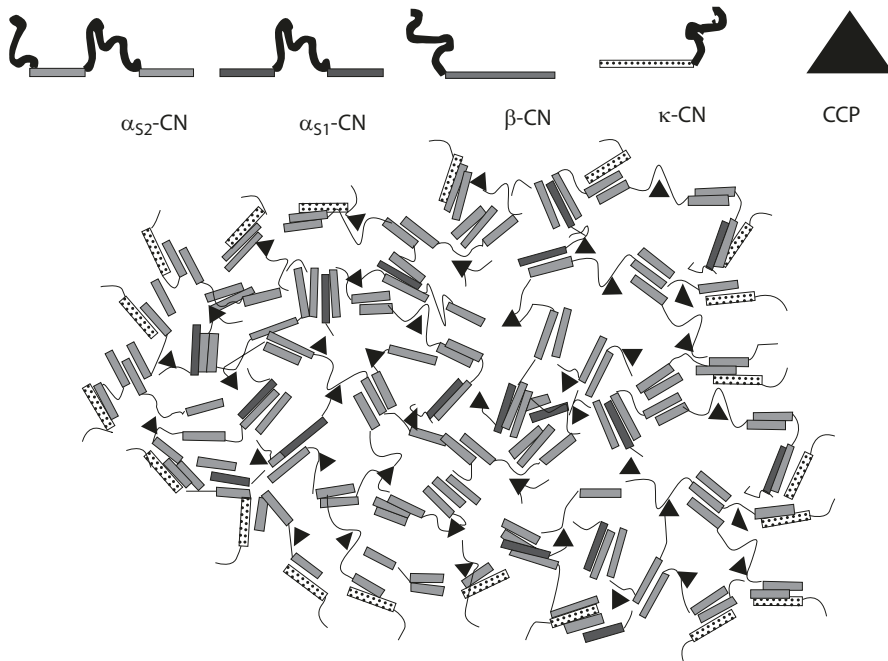


Fig. 2.21 Assembly of the micelle by crosslinking of individual caseins through hydrophobic regions of the caseins and bridging involving colloidal calcium phosphate. Rectangular bars and black lines represent hydrophobic segments and hydrophilic segments of the casein molecules, respectively (From Horne [39] and Lucey [55] with permission. Copyright 1998, 2002 Elsevier)

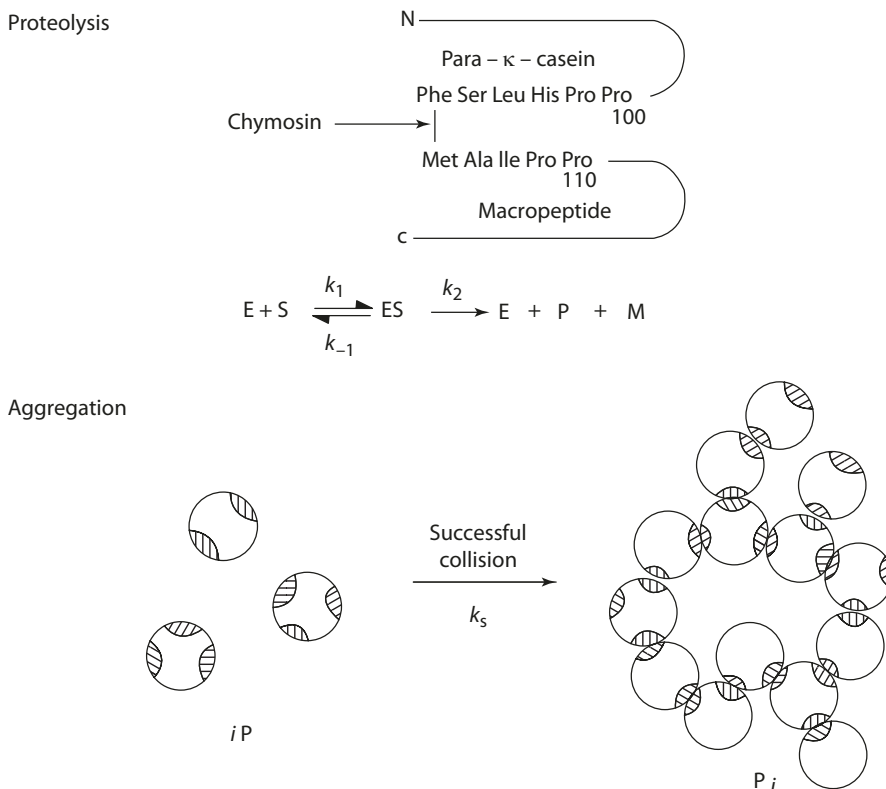
nanometer-sized clusters throughout the matrix of the casein micelle. These calcium phosphate nanoclusters are stabilized by interactions with the serine phosphate groups of the casein molecules (mostly α_s and β) to form aggregates holding the micelle together [38]. The nanocluster model has been further modified to include interactions of caseins through their hydrophobic regions, in addition to the bridging action by calcium phosphate nanoclusters [39, 58]. The formation of micelle is therefore considered to involve

two types of binding: (1) specific phosphoserine-mediated interactions with calcium phosphate nanoclusters and (2) protein hydrophobic interactions. Unlike α - and β -caseins, κ -casein molecules consisting of only one phosphoserine residue do not form clusters of phosphoserine residues and have one type of binding (hydrophobic). While α - and β -caseins have dual binding functionality, κ -casein acts as a terminator in micelle formation, mostly covering the surface of the micelle.

Milk Coagulation

The coagulation of milk by chymosin includes two steps (■ Fig. 2.22):

1. Proteolysis of κ -casein: Chymosin hydrolyzes the peptide bond at Phe₁₀₅-Met₁₀₆ of κ -casein, to form a highly acidic macropeptide and a basic and hydrophobic para- κ -casein, resulting in a reduction in half of the hydrophilicity of the micelle surface. The reaction follows the Michaelis-Menten mechanism. The release of hydrophilic macropeptide reduces the surface charges and hence the surface potential that creates the barrier for the micelles to come close. (Refer to ► Chap. 1, ■ Fig. 1.15.) Consequently, there is an increase in hydrophobic interaction, which provides a major force in coagulation. Proteolysis also destroys the stabilizing action of κ -casein, particularly its resistance to precipitation in the presence of calcium ion. The other caseins in the micelle, which are calcium sensitive, are now susceptible to calcium precipitation. Therefore, in a milk



■ Fig. 2.22 Coagulation of milk involves **a** proteolysis and **b** aggregation (From Payens [65]; Daigleish [13])

system, the action of chymosin is followed by formation of coagulum in the presence of calcium. Proteolysis of κ -casein changes the functionality of the entire protein system.

2. Aggregation: The reaction is a bimolecular process. There is a lag phase between the addition of chymosin to the milk and observable coagulation. This lag period is about 60% of the clotting time. In the lag period, coagulation will not occur as the concentration of the para- κ -casein produced by the enzymatic hydrolysis is low. It has been suggested that a critical degree of proteolysis (~80%) must be completed before aggregation occurs [13].

The rate of aggregation does not follow a single diffusion-controlled mechanism. The bimolecular rate constant (k_s) is lower than the equation $k_s = 4\kappa T / 3\eta$ predicts, where k = Boltzmann's constant, T = absolute temperature, and η = viscosity of the dispersing medium. The micelles that are sufficiently close may not interact, because the micelle surface is heterogeneous in reactivity. The para- κ -casein micelles need the surface reactive sites oriented close to each other to register a successful collision. The reactivity of the micelle surface is largely related to the extent of proteolysis. Upon the completion of proteolysis, the micelles are almost completely denuded, and the contribution of the steric factor to the coagulation process is decreased, accompanied by an increase in k_s . The introduction of this steric factor offers an explanation for the slow coagulation process in milk, and also the fact that clotting of chymosin-treated micelles almost always forms a porous gel rather than a precipitate [65].

Heat Stability of Milk

The characteristic heat stability of milk is important in dairy processing, for example, the production of condensed or evaporated milk. The colloidal structure of casein micelles constitutes a very stable system [24, 88]. Typical milk is stable to a temperature of 140 °C for 20 min. The heat coagulation time (usually determined at 130–140 °C) of milk is known to be very much pH dependent. Two types of stability curves are evident. Type A milk shows a stability maximum of pH 6.7 and a minimum at pH 6.9. Type B milk has increasing stability with increasing pH, with no maximum or minimum. The shape of the stability curves is related primarily to the interaction between the whey protein, the β -lactoglobulin, and the micelles, particularly the κ -casein. The variation and balance of calcium, magnesium, phosphates, and lactose in the milk may also have effect on the stability curve.

■ ■ Characteristics of β -Lactoglobulin

The whey protein, β -lactoglobulin, is a globular protein of 18 kDa, consisting of 162 amino acids (which varies slightly for different genetic variants). The secondary structure of β -lactoglobulin is 15%, 51%, 17%, and 17% α helix, β sheet, β turn, and aperiodic structure, respectively. The antiparallel β sheet is formed by nine β strands wrapped around to assume a flattened cone shape. There are two disulfide bonds (66–160, 106–119) and a free Cys121 buried at the sheet-helix (β strand 115–124 and α helix 129–143) interface [63]. The protein is remarkably acid stable, resisting denaturation at pH 2. In physiological conditions, native β -lactoglobulin exists as a dimer resulting from the association of the monomer at the respective α -helical segments (129–143) through hydrophobic interactions. Dimerization therefore serves to protect the sulfhydryl group from being reactive. As the pH and temperature increase, the protein undergoes reversible conformational change, which exposes the polypeptide segment containing the Cys121.

When heated above 70 °C, the denaturation temperature, and at pH 7.0, β -lactoglobulin polymerizes and aggregates in the absence of other proteins [100]. Two reactions can be identified in the process. The primary reaction that occurs at temperatures above 65 °C involves the formation of intermolecular disulfide bonds, either by sulfhydryl-disulfide interchange or by sulfhydryl oxidation. The secondary reaction takes place after the initiation of the first reaction, yielding high-molecular aggregates. In this reaction, disulfide bonds are not involved and the process is nonspecific. The aggregates show different electrophoretic mobility and higher particle weight than products from the primary reaction. Polymerization also occurs at low temperatures at alkaline pH (>8.5), involving similar disulfide interchange reactions, although the possibility of base-catalyzed hydrolysis of the disulfide bonds may not be excluded.

■ Interactions with κ -Casein

At temperatures above 60 °C and pH 6.5, the β -lactoglobulin starts to unfold and associates with the κ -caseins on the surface of the micelles, likely involving sulfhydryl-disulfide exchange. The complexation between β -lactoglobulin and κ -casein alters the steric and electrostatic interactions of the surface, providing a greater stability to the micelle. The whey-protein-coated micelles have been shown to increase in the size and the zeta potential, are more stable to heat, and are less sensitive to calcium, ethanol, and chymosin actions. This increase in stability reflects as the maximum in the stability-pH curve.

At a higher pH, the κ -casein dissociates from the micelles together with the whey protein as small soluble aggregates. Some α_s - and β -caseins are also liberated. The dissociation may be attributed to the increase in electrostatic repulsion on the surface of the micelles with increasing pH. This may also be the result of heat-induced precipitation of the calcium phosphate at the higher pH. The micelles depleted of κ -casein are sensitive to calcium coagulation, reflected as the minimum in the stability-pH profile.

2.5.4 Wheat Proteins

Wheat proteins are fractionated according to their solubility into albumins (soluble in water), globulins (soluble in 10% NaCl, insoluble in water), gliadins (soluble in 70–90% alcohol), and glutenins (insoluble in water or alcohol, but soluble in acid or alkali).

Commercial gluten is the water-insoluble protein fraction separated from wheat flour. The freshly extracted wet gluten, known as gum gluten, yields a cream-colored powder of high protein content (75–80%) upon drying. The product contains largely the storage proteins, gliadins and glutenins, small amount of albumins, other non-storage proteins, 5–10% lipids, and 10–15% carbohydrates. Gliadins and glutenins comprise about 50–60% and 40–50% of the gluten proteins, respectively.

Gliadins

The composition of gliadins varies in wheat varieties. Heterogeneity occurs in both the composition and in the sequence of the amino acids [70]. All gliadins are monomeric consisting of exceptionally high contents (38–56%) of glutamic acid (mostly as glutamine), proline (15–30%), and phenylalanine, but are low in basic acids, lysine, arginine, and histidine (■ Table 2.6) [46]. Based on the electrophoretic mobility, four groups of gliadins can be distinguished, α -, β -, γ -, ω -gliadins (in the order of decreasing mobility), all in the range of 32–42 kDa, except ω -gliadins in the range of 74 kDa. Based on amino

■ **Table 2.6** Amino acid composition of whole gliadin and glutenin (Ponca)

Amino acid	Gliadin	Glutenin
	(Amino acid residues/100,000 g)	
Asp	20	23
Thr	18	26
Ser	38	50
Glu	317	278
Pro	148	114
Gly	25	78
Ala	25	34
Cys	10	10
Val	43	41
Met	12	12
Ile	37	28
Leu	62	57
Tyr	16	25
Phe	38	27
Trp	5	8
Lys	5	13
His	15	13
Arg	15	20
Amide	301	340

From Kasada et al. [46]

acid sequences and compositions, α - and β -gliadins share more similarities than the other types and are often grouped together as α -type gliadins or as α/β gliadins.

The structures of α -, β -, and γ -gliadins contain 30–35% α helix and 10–20% β sheet, while ω -gliadins contain β turns but no β sheet or α helix [94]. All gliadin types consist of a central domain with repeated proline- and glutamine-rich penta- and heptapeptides and nonrepetitive N- and C-termini. The α -, β -, and γ -gliadins contain an even number of 6–8 Cys residues in the C-terminal half, all involved in and stabilized by the formation of intramolecular disulfide bonds [93]. In contrast, ω -gliadins do not have sulfur-containing amino acids and are stabilized by strong hydrophobic interactions. All gliadin types assume the shape of prolate ellipsoids of ~3.2 nm diameter with an extended conformation [93]. Gliadins take part in the development of gluten network during mixing through non-covalent interactions with glutenin and other components. These globular proteins contribute to dough resistance to extension by forming a viscous matrix within the

glutenin polymer network, playing a "space-filling" role. (See the following section on "Glutenins.") Dough resistance is a description of dough strength by measuring the maximum force in B.U (Brabender unit) reached as a cylindrical piece of dough is stretched before breaking. The measurement is performed using an extensograph. The resistance increases as the dough mix is more vicious.

Glutenins

After the extraction of albumin and globulin from the flour with dilute salt solution, and of gliadins with 70% ethanol, the remaining residue is extracted with acid (usually acetic acid) to obtain the glutenins. The insoluble residue left behind, which accounts for more than 30% of the total proteins, is known as residue protein or acetic acid-insoluble glutenin. The acetic-acid-insoluble glutenin can be dissolved by reduction and the action of detergent such as SDS (sodium dodecyl sulfate).

Glutenins are large complex molecules of about 15 subunits, with molecular weights reaching into the millions. The subunits (monomeric) of glutenin (which is polymeric) can be classified into 4 groups according to electrophoretic mobility in SDS-PAGE after reduction of the S—S bonds:

The A-type (between 80 and 120 kDa) corresponds to HMW-GS.

The B-type (between 42 and 51 kDa) corresponds to LMW-GS.

There are two additional C- and D-type LMW-GS, which are minor fractions related to gliadins: The C-type subunits are modified α/β - and γ -gliadin (monomeric) which may have been incorporated into the glutenin polymer because of mutations in the number and/or position of Cys residues. Likewise, the D-type subunits are modified ω -gliadins formed by gene mutation, resulting in the presence of a single Cys residue that allow intermolecular disulfide bond formation in the glutenin macropolymer. The C- and D-type proteins are gliadin-like in a biochemical point of view. However, these proteins are considered glutenin components and are generally accepted as LMW-GS.

Glutenins consisting of only LMW subunits are known as low-molecular-weight glutenin, high-molecular-weight gliadin, or aggregated gliadin, which has also been obtained from the purification of gliadin fractions. The high-molecular-weight glutenins contain HMW and LMW subunits crosslinked by intermolecular disulfide bonds. Hydrogen bonding and especially hydrophobic interactions play an important role in the association of the subunits.

Whereas hydrated gliadin fractions are viscous, glutenin fractions exhibit high elasticity and extensibility as major factors contributing to dough strength. The amount of HMW-GS is positively correlated with dough strength. Elasticity is measured by the breath of the curve at its peak in a farinogram, which represents the force in B.U. required to turn two mixing arms in a mixing chamber with dough at an adjusted hydration. Extensibility shows how much the dough is able to stretch/extend without breaking. This is measured in millimeter, the base length of the curve in an extensograph, from the starting point of stretch to the breaking point of the dough.

■ ■ HMW-GS [28, 43]

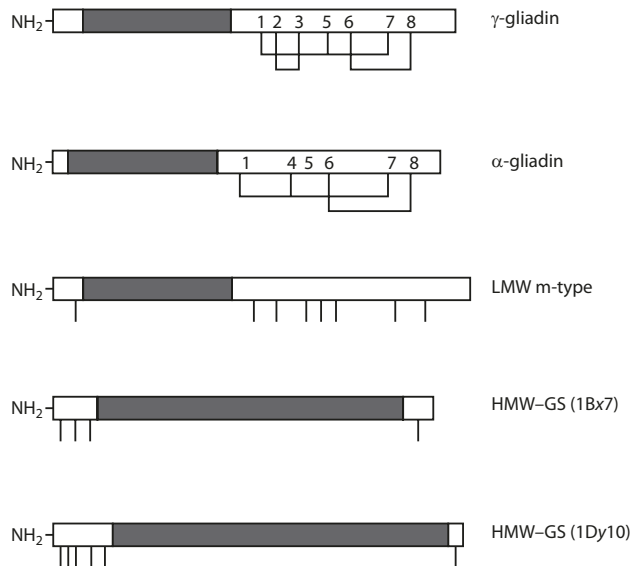
These subunits represent a minor component (5–10%) of the gluten total proteins. However, it has been well established that dough properties are strongly influenced by HMW-GS as the major determinant of gluten elasticity through the formation of glutenin macropolymers. Each wheat genotype contains three to five HMW-GS of both x- and y-types. The x-type subunits, compared to the y-type, have a slower electrophoretic

mobility on SDS-PAGE and higher molecular mass (83–88 kDa and 67–74 kDa, respectively), because of a longer repeated structure in the repetitive central domain of the polypeptide. All HMW-GS molecules have a general structure of a repetitive central domain with interspersed repeats of hexa- and nona-peptide motifs rich in glutamine, proline, and glycine. The repetitive sequences form β reverse turns that are organized into a β spiral structure. The central domain varying in length of 420–700 residues is flanked by nonrepetitive N- and C-termini, which contain most of the cysteine residues present in HMW-GS. The N-terminal domain varies in length from 81 to 104 residues. The C-terminal domain always comprises 42 amino acid residues. Both N- and C-terminal domains are globular with one or more helices.

The x-type has four Cys: three in the N-terminal domain and one in the C-terminal domain. The y-type has seven Cys: five in the N-domain, one within the central domain, and one close to the C-terminus. The number of intra- and intermolecular disulfide bonds varies in individual subunits depending on the distribution and position of the active sulfhydryl groups, as well as conformation of the subunit molecule (■ Fig. 2.23).

A note about wheat genome and sequence nomenclature: Bread wheat is a hexaploid consisting of three diploid genomes (AA, BB, and DD) derived from three different wild-type species. Each genome consists of seven pairs of chromosomes resulting in a total of 21 pairs. Each chromosome pair is designated by a number (i.e., 1–7), which is followed by a letter (A, B, or D) referring to the individual genome. The HMW subunits of glutenin are coded by genes *Glu-A1*, *Glu-B1*, and *Glu-D1* at three genetically unlinked loci present in the long arms of the group 1 (1A, 1B, and 1D) chromosomes. Each locus consists of two genes encoding subunits of x-type and y-type that differ in their properties. Each locus also exhibits allelic variations (mutations in the genes) that are responsible for differences in the subunit proteins among wheat varieties. The subunit proteins are numbered in order of increasing mobility on SDS-PAGE. For example, subunit 1Dx5 represents chromosome group 1 of D genome, x-type, and electrophoretic mobility of 5 on SDS-PAGE. Theoretically bread wheat contains potentially six HMW-GS: 1Ax, 1Ay, 1Bx, 1By, 1Dx, and 1Dy.

■ Fig. 2.23 Location of cysteine residues in gliadins and glutenins (From Lindsay and Skerritt [53] with permission. Copyright 2006 American Chemical Society)



However, some of the genes are silenced, resulting in the presence of only three (1Bx, 1Dx, 1Dy) to five (1Ax, 1Bx, 1By, 1Dx, 1Dy) subunits. In some cases, individual or allelic pairs of subunits have been scored in relation to bread-making quality. For example, the *Glu-1D*-encoded HMW-GS allelic pair Dx5 + Dy10 is associated with greater dough strength; the pair Dx2 + Dy12 is associated with weaker dough.

The loci *Gli-A1*, *Gli-B1* and *Gli-D1* located on the short arms of the group 1 chromosomes (1A, 1B, 1D) carry genes encoding for ω -gliadins, γ -gliadins, and LMW-GS. The loci *Gli-A2*, *Gli-B2*, and *Gli-D2* near the end of the short arms of the group 6 chromosomes (6A, 6B, 6D) code for α - and β -gliadins.

■ ■ LMW-GS [16]

The amount of LMW-GS is about 5–6 times more abundant than HMW-GS. LMW-GS plays an important role in dough resistance and extensibility. Each wheat genotype contains 7–16 different LMS-GS, which are highly heterogeneous.

The B-type subunits include most of the typical and abundant LMW-GS. The general structure consists of a central repetitive domain rich in β turns. Flanking on each side are nonrepetitive domains rich in Cys residues: a single Cys located in the N-terminal domain and seven Cys residues found in the long and highly conserved C-terminal domain. Six of the Cys residues in the C domain form three intramolecular disulfide bonds with the seventh Cys residue left unpaired (■ Fig. 2.23). The remaining free Cys in the C domain and the lone Cys residue in the N-terminal domain have been shown to involve in interchain disulfide bonding with other LMW-GS or with HMW-GS molecule.

In contrast, the C-type subunits contain either seven or nine Cys residues, one more than that in the α/β and γ -gliadins, resulting in an unpaired Cys capable of intermolecular disulfide formation. The D-type (gliadin-like LMW-GS) subunits contain a single Cys (likely by mutation of the ω -gliadin) in the entire molecule and can only form intermolecular bonding.

■ ■ Chain Extender and Chain Terminator

The number and distribution of Cys residues in the primary structures separate the glutenin subunit into two categories according to their functions in building the glutenin macropolymer [92]: (1) Chain extenders are subunits with two or more Cys residues available for interchain disulfide bond formation (such as HMW-GS, B-type LMW-GS), enhancing glutenin polymer formation, and (2) chain terminators are subunits with only one Cys residue available for intermolecular bonds (such as C- and D-type LMW-GS), leading to the termination of the growth of the glutenin polymer. Chain extenders promote the formation of strong dough, whereas chain terminator in general negatively affects the quality of gluten/dough.

It should note that chain extenders that contain two available Cys residues for interchain disulfide bonds would link the subunits into linear polymers only. Those that consist of three or more free Cys for interchain disulfide bonds would lead to branching of the glutenin polymer. It is generally agreed that the ability to branching and thus the formation of large network contributes strength to the dough. Examples are provided for the intrinsic contribution of some glutenin subunits in ■ Fig. 2.24 [45].

The following types of interchain disulfide bonds have been identified experimentally: (1) one interchain disulfide bond within the N-terminal domain of an x-type subunit, (2) interchain disulfide bonds connected in parallel between adjacent Cys residues in the N

	Dx5	>	Dx2	>	Dy10	=	Dy12	>	Bx7	>	LMW-GS (LMW-s, LMS-m)
No. InterMol. crosslinks	5		4		3		3		2		2
AAs in repeat domain	690		680		481		492		647		200–150
Polymer type	Branched		Branched		Branched		Branched		Linear		Linear
											

Fig. 2.24 Hierarchical arrangement of HMW and LMW-GS in relation to their proposed intrinsic contributions to dough strength (From Kasada [45])

termini of two γ -type subunits, (3) disulfide bond linking x -type and γ -type subunits in a head-to-tail mode, and (4) interchain bond between a γ -type subunit and a LMW glutenin subunit.

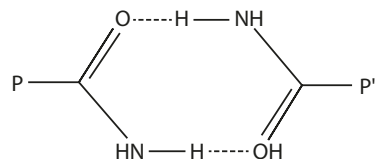
Glutenin Polymer Models and Gluten

■ Molecular Arrangement of Glutenin Polymer

It is generally recognized that the number and distribution of disulfide bonds and the properties and interactions of the repetitive domains of HMW-GS play a key role in providing and affecting dough strength and elasticity [54].

1. The building block of glutenin consists of subunits linked by intermolecular (interchain) disulfide bonds. The bonding primarily involves the HMW-GS x - and γ -type in various combinations. The typical (B-type) LMW-GS may also form interchain disulfides, however to a lesser extent, while the chain terminators, C- and D-type LMW-GS, would limit the growth and size of the glutenin network. It should also note the importance of some HMW subunits that consist of three or more free Cys residues for interchain disulfide bonds to form branched polymer as described in the previous section. It is generally agreed that it is the ability to branch and thus form large network that contributes strength to the dough.
2. Noncovalent interactions such as hydrogen bonds and hydrophobic interaction play a significant role in maintaining the glutenin structure. The large number of amide side chains (glutamines) and the high proportion of nonpolar amino acid residues (prolines, glycine) in the repetitive domains of the subunits support the significant contribution of these secondary interactions (Fig. 2.25). In this regard, the length of the repeating sequence domain is a determining factor for the arrangement of the glutenin polymer.

Fig. 2.25 Hydrogen bonding between two glutamines of adjacent gluten chains



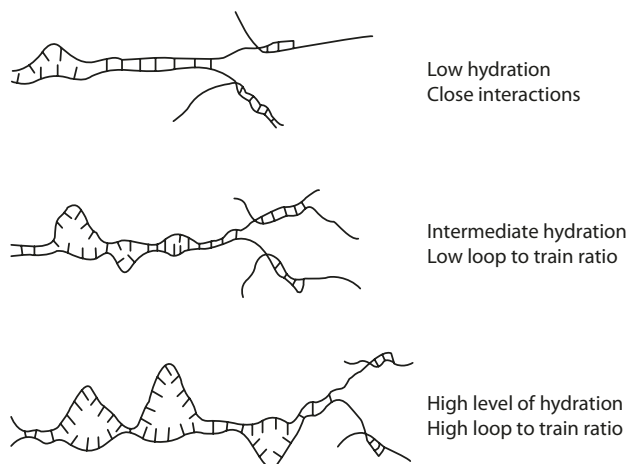
■ ■ The "Loop and Train" Model

These observations have led to the "loop and train" model to describe the elastic properties of gluten based on the molecular architecture of glutenin [5, 6, 87]. In this model the backbone structure of glutenin polymer is held together by interchain disulfide bonds formed between HMW subunits. Neighboring chains in the network form extensive noncovalent interaction involving the large number of glutamine residues mostly in the repetitive domain. Interchain protein-protein hydrogen bonding between the amide side chains of glutamine residues results in the formation of train segments in the network. When the glutenin is in a hydrated state (as water is added in a dough), the structure will consist of considerable amount of hydrogen bonds between water and glutamine, forming regions of loop segments, at the expense of train formation (■ Fig. 2.26).

In the train region, protein-protein intermolecular interactions between the repetitive domains of neighboring chains results in the alignment of the β turns to form structures that resemble interchain β sheet. However, as hydration increases with added water, loop regions are formed with extended β turns that are mobile and more random conformation. Gluten elasticity is envisioned as the glutenin network stretched by deformation of the loops first and then the trains. Resistance to stretching in the glutenin network is dependent on the loop/train ratio, since the energy required to deform the loops will be less than that required to "unzip" the trains. As more force is applied in repeated stretching, further extension of the glutenin network will give rise to closer alignment of the HMW subunits with the formation of more train segments (protein-protein interaction). Breaking and remaking of disulfide bonds (disulfide exchange reaction) under extension also result in the formation of the network with closer alignment of the subunits to form protein-protein interactions. Therefore, the combined action of deformation by stretching as well as disulfide exchange reactions would favor the formation of train regions (β sheets) at the expense of loop regions (β turns).

When the applied (stretching) force is lifted, recovery of the original dimensions occurs as a result of returning to the equilibrium of loops and trains. The relaxation time depends on the loop/train ratio in the extended network. Low loop/train ratio will require longer relaxation time to resume the initial state, and the process may not be entirely complete. During dough mixing (energy input), the progressive stretching and alignment of

■ Fig. 2.26 The "loop and train" model and the effect of hydration (From Belton [5] with permission. Copyright 1999 Elsevier)



the gluten network result in a transition from predominantly β turn (loop) to β sheet (train) structures. Eventually a threshold of loop/train ratio is reached that is resistant to further deformation. This phenomenon in dough development is known as strain hardening. Mixing beyond this point (high enough input) results in the disruption of the β sheet structure in the train regions and a stage in dough mixing called strain thinning.

■ ■ The Glutenin Macroparticles in Dough Development [15, 31]

This model describes the formation of the gluten network and interactions in the microscopic and macroscopic levels that correlate to the rheology behavior. Dough development is considered to involve aggregation of polymeric glutenin (with the basic molecular structure described above) via entanglement stabilized by hydrogen bonding and additional disulfide bridges to form particles. These particles called glutenin macropolymer (GMP) exist in a gluten fraction which is experimentally unextractable and insoluble in SDS or acetic acid. In flour, GMP isolates are spherical with a size of about 0.1–100 μm . In dough mixing, the spherical shape is lost, resulting from disruption (disentanglement) of the particles from the flour. During dough resting that follows mixing, glutenin polymers from disrupted particles reassemble and interact at many more contact points with more entanglement to form highly aggregated GMP network throughout the gluten. The aggregation is predominantly influenced by the process conditions, such as mixing intensity, time, energy input, and temperature.

Transformation of Flour into Dough

A gluten complex can be visualized as a composition of the various flour proteins bound by covalent bonding and noncovalent interactions. At the microscopic level, the HMW glutenins form networks with fibrillar extension, whereas LMW-GS form clusters often at the branch point of the HMW-GS backbone [53]. Gliadins are randomly distributed as individual particles, filling spaces within the glutenin network [96]. Maximum resistance and extensibility of dough and gluten are strongly determined by both the amount of glutenin subunits and by the ratio of gliadin to glutenin subunits.

Wheat flour contains about 12% protein (~80% gluten), 70% starch (amylose:amylopectin = 1:3), and 1–1.5% lipid. Wheat flour lipids can be classified into free (extractable by petroleum ether) and bound (extractable with water-saturated n-butanol). In general, polar lipids, such as glycolipids and phospholipids, make up 70–75% of the total flour lipids. In dough mixing, flour components are integrated into the gluten network, forming a matrix of starch-protein-lipid complex. A dough may also contain various additives to improve its baking quality making the composition even more complicated.

Dough proteins For gluten proteins, major chemical changes occur through the reduction of disulfide bonds during the mixing of dough, and reoxidation during the resting period. Disulfide breakage and reformation occur primarily within the high-molecular-weight crosslinked glutenins. The intramolecular disulfide bonds in the gliadins are generally not accessible to the reaction. The initiation of reduction in dough mixing may be due to (1) thio-disulfide exchange and/or (2) possible formation of free radicals or superoxide anions, which mediates the reduction of certain metalloproteins and in turn the reduction of disulfides. Disulfide reduction physically loosens the gluten and facilitates better interactions with the lipids, starch, and other additives (e.g., emulsifiers, fortified soy beans), via noncovalent interactions to form a continuous network of starch-protein-lipid complex.

Dough starch Both mixing and resting doughs show starch particles more or less embedded in the protein matrix. Starch granules are dispersed in the continuous network of hydrated gluten by interfacial interactions and adhesion with the proteins. The system is compared to the general behavior of particle-filled polymers. Starch functions in bread dough to act as fillers in the gluten network; to absorb, swell, and hold the water; and to provide a continuous supply of sugars (by α -amylase action in the flour) for fermentation. During baking, the starch granules gelatinize, contributing to the characteristic structure and texture of the bread. Baking quality is related to the granule size distribution, temperature of gelatinization, viscosity of the gel, and swelling property.

Dough lipids Wheat flour lipids constitute only a minor component of total flour components, but have a significant effect on the quality in terms of loaf volume and crumb grain of the bread through the stabilization of gas cells. Flour lipids are mostly polar lipids, comprised predominantly of galactolipids (monogalactosyldiacylglycerols (MGDG) and digalactosyldiacylglycerols (DGDG)), phospholipids (phosphatidylcholine, PC), and, to a lesser amount, lysophosphatidylcholine (LPC) [21]. Nonpolar lipids are composed largely of triacylglycerols. In the dough, the flour lipids become bound to or trapped within the gluten-starch network, mostly associated with the proteins. During the making of dough (adding water and mixing), the polar lipids form a continuous film in the gluten-starch matrix. This lipid layer provides stabilization during incorporation and expansion of gas cells and prevents coalescence and disproportionation of gas cells when they come in close contact with each other during late proving and early baking stages [91]. Polar lipids have stabilizing effects, while nonpolar lipids tend to destabilize gas cell structures.

Addition of surfactants These ingredients are often added at 0.3–1.0% as dough strengtheners (that interact with gluten) and crumb softeners (antistaling, antifirming) that form complexes with gelatinized starch in dough making. Examples of strengtheners are derivatives of diacylglycerols, such as diacetyltartaric acid ester of mono- and diglycerides (DATEM), succinylated monoglyceride, polysorbate fatty acid ester, sorbitan monostearate, and sodium and calcium stearoyl lactylate (SSL, CSL). Monoacylglycerols and diacylglycerols are typical examples of crumb softeners. Saturated monoacylglycerols are known to have a better softening property than the unsaturated ones. These additives augment and enhance the functional role of the flour lipids.

In the dough, surfactants, similar to the polar lipids in the flour, interact more with gluten proteins and less with starch. Surfactant absorption causes the proteins to associate and increases the elastic behavior of the dough. The additive also stabilizes the mixed protein-lipid interface lining the gas cells either by modulating the surface tension or indirectly changing the protein-starch matrix to a more continuous and homogeneous system. It may also form a liquid-crystalline lamellae structure, which stabilizes the thin film covering the gluten-air interface developed when the gas cells are expanding rapidly in the dough. The fine crumb grain obtained by the addition of surfactants to bread making can be attributed to increased air incorporation during dough mixing and formation of smaller gas cells.

During baking, the bonds between the gluten proteins and the surfactant lipids weaken due to the denaturation of the proteins. As the dough temperature increases and the starch gelatinizes, the lipid molecules form strong complexes with starch [68]. (Refer to ► Chap. 3 for complexation of emulsifiers with amylose.) The antistaling and antifirming function of surfactants depends largely on how well the additive is dispersed in the dough before starch gelatinization occurs.

Addition of Shortenings Bread making often requires the addition of 0.5–1% shortening or hardened vegetable fat (mostly MAG, DAG, TAG). The major effect of added solid fats to the bread dough is to increase loaf volume. The dough exhibits more tolerance to higher strain. Contrary to the surfactants, little of the shortening becomes bound to the dough proteins during mixing. Free rather than bound fat solids are important to the final quality of the bread. Fats in smaller β' crystals is more effective than other polymorphic forms.

There are a number of hypotheses to explain the effect of shortening in dough [4, 64, 91, 97]. (1) The effectiveness of shortening is related to facilitating uniform distribution of the dough components, resulting in a smooth and even dispersion of gluten and starch granules in the dough. This arrangement enables the dough to readily form a continuous and expandable gas-retaining structure for air cell development. (2) The fat crystals adsorbed at the air-water interface stabilize and preserve the continuous gas-retaining structure during expansion. During dough mixing, the fat forms an ordered structure as a liquid-crystalline lamellae. This may act as a second stabilizing mechanism providing gluten-starch matrix with greater expandability and air retention during baking. (3) The fat may melt during mixing and early baking stage to seal off the pores and passages in the gluten network so that the escape of carbon dioxide is retarded during the expansion of the dough. (4) There is also indication that the transition temperature for the induction period during which there is no loss of carbon dioxide is raised by the presence of shortening. As a result, there is a delay in the release of carbon dioxide in the early stage of baking.

Addition of enzymes Two enzymes present in wheat flour are significant in baking technology. Both of these will be discussed in ► Chap. 5. Amylases catalyze the degradation of starch to fermentable sugars, which are essential for the formation of carbon dioxide. The addition of enzyme-active soy flour in dough often results in an increase in dough relaxation time and improvement of the gluten proteins and mixing tolerance [23]. The enzyme lipoxygenase in the soy flour catalyzes the formation of radicals ($\text{LOO}\cdot$) from unsaturated free lipid substrates in dough, which, in turn, causes both lipid-protein and protein-protein crosslinks.

2.5.5 Soybean Proteins

Soybean [*Glycine max* L. Merr.] is a legume crop native to Asia, now grown worldwide (35% in the United States). This is a value crop for its oil-rich and proteinaceous seeds. About half of the production in the United States is used in domestic oil processing. The defatted flakes after mechanical crushing and extraction of the soybean seed are ground into soybean meal serving primarily as a high-quality protein source in animal feed. It is also used for production of vegetable protein, soy concentrate, and isolate as food ingredients in meat products, soup bases, baked goods, and others. Soybean (seed) has been the major protein source in traditional Asian foods, such as soymilk, tofu, soy sauce, soy paste, tempeh, and miso, just to name a few.

Soybean proteins constitute about 40% of the dry weight of the seed and are present as storage proteins in the subcellular structures called protein bodies located in the cotyledon. About 90% of these proteins are extractable by dilute salt solution and have been shown to contain four fractions of globulins: 2S, 7S, 11S, and 15S by ultracentrifugation. The two major proteins, glycinin and β -conglycinin, corresponding to the 11S and the 7S fractions, respectively, make up about 70–80% of the total seed proteins.

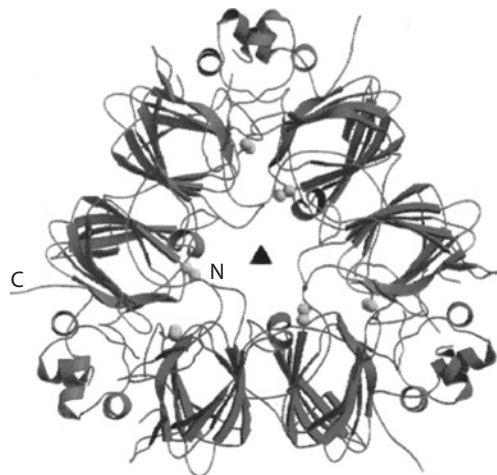
Structure of Glycinin

Glycinin accounts for 40% of the total seed proteins and plays an important role in the functional properties of soybean foods. Glycinin extracted from seeds has a hexameric structure of 360–380 kDa. Each subunit is composed of an acidic polypeptide (35 kD, pI 4.75–5.40) covalently linked to a basic polypeptide (20 kD, pI 8.0–8.5) by a disulfide bond. Six acidic polypeptides (A1a, A1b, A2, A3, A4, and A5) and five basic polypeptides (B1a, B1b, B2, B3, and B4) combine nonrandomly to form five major subunits. The subunits have been characterized and classified into two groups according to their amino acid sequences: Group I (A1aB1b, A2B1a, A1bB2) and Group II (A5A4B3, A3B4). These five subunits are also called glycinin G1, G2, G3, G4, and G5, respectively. In the subunit nomenclature, "A" designates acidic polypeptide, "B" designates basic polypeptide, and the numbers and lower case letters refer to the peak order of the denatured polypeptide in ion-exchange chromatographic separation. Genetic variations of glycinin subunits are found among cultivated and wild-type soybean species. The structural heterogeneity of the subunit is due mainly to the hypervariable regions, which are at the C-terminus of the acidic polypeptide. Group I subunits are relatively uniform in size (~58 kD), are rich in Met, and exhibit ~80% sequence identity within the group. Group II subunits also exhibit high sequence homology within the group (~80%), but contain less Met, and are larger in size (62–65 kD). Sequence homology between Groups I and II is 60–70%.

■ ■ Hexameric Structure

The crystal structure of glycinin A3B4 homo-hexamers (i.e., glycinin composed of six single A3B4 subunits purified from mutant soybean cultivar) has been determined [1, 2]. The hexamer is formed by face-to-face stacking of two trimers. The constituent subunits in the trimer are arranged around a threefold symmetry axis with dimensions of 97 Å × 95 Å × 40 Å. The core of each subunit contains (1) 27 strands and 7 helices folded into two jelly-roll β-barrel domains and (2) two extended helix domains (■ Fig. 2.27). The core structure consists of two highly similar N-terminal and C-terminal domains. Each domain consists of β barrel and extended helix arranged in a pseudo-dyad symmetry. The binding between two trimers involves hydrophobic interaction, hydrogen bonding, and electrostatic attraction.

■ Fig. 2.27 A ribbon representation of proglycinin trimer. The threefold axis runs perpendicular to the paper, indicated by a filled triangle (From Adachi et al. [1] with permission. Copyright 2001 Elsevier. PDB 1FXZ)



Structure of β -Conglycinin

β -Conglycinin (7S) accounts for about 30% of the total seed proteins. The native protein has a trimer structure composed of three kinds of subunits α (67 kDa), α' (71 kDa), and β (50 kDa). Various hetero- and homotrimers are found in soybean seeds due to random combinations of these subunits. The α and α' subunits contain core regions and extension regions, whereas the β subunit consists of only the core region. The core regions of the three subunits exhibit high homology of 90%, 76%, and 76% between α and α' , α and β , and α' and β , respectively. The α , α' , and β subunits are glycosylated at specific Asn sites, 199 and 455 for α , 215 and 471 for α' , and 328 for β , respectively. This is in contrast to the glycinin subunits, which are non-glycosylated, and devoid of disulfide bonds.

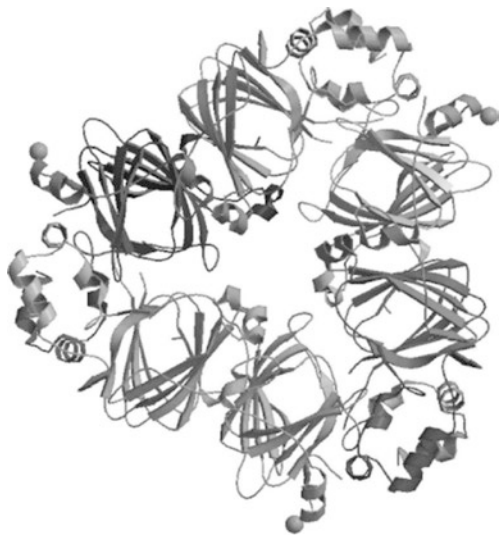
■ ■ Trimer Structure

The crystal structure of a β homotrimer (i.e., all subunits are β) has been determined [56]. It has a dimension of $96 \text{ \AA} \times 96 \text{ \AA} \times 44 \text{ \AA}$. The monomer (i.e., the β subunit in the trimer) consists of a core domain of β barrels and a loop domain of several α helices (■ Fig. 2.28). The loop domain protrudes from either side of the monomer as a pair of hooks. The association between the domains and between the monomers involves mostly hydrophobic interaction.

Effect of pH and Ionic Strength on Physicochemical Characteristics

Heat denaturation, gel formation, and resulting gel structure of soy proteins have been extensively studied using conditions of pH 7.6 and ionic strength of 0.5, where the soy proteins are known to be soluble. However, the large effect of pH and ionic strength on the physicochemical changes of soy proteins and gel structures should not be overlooked. Conditions more representative for food systems are ranged at pH 3–7 and ionic strength of 0.02–0.2. In the context of the discussion below, pH range of 3–5 is denoted as "low" and $\text{pH} \geq 7$ as "high" and ionic strength of 0.5 as "high" and 0.02–0.2 as "low."

■ Fig. 2.28 A ribbon representation of β -conglycinin homotrimer (From Maruyama et al. [56] with permission. Copyright (2001) John Wiley & Sons. PDB 1UIK)



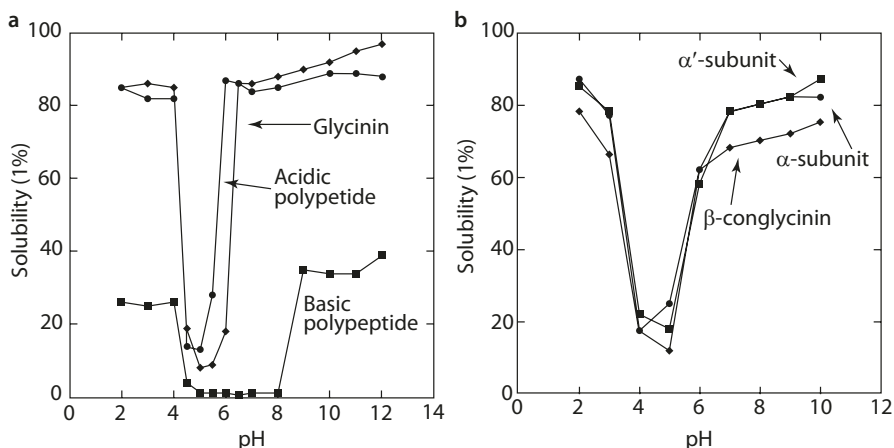
The effect of pH is related to the influence on the net charge of a protein. The protein carries net positive charge at pH below its isoelectric point, and net negative charge above its pH, and exhibits minimum solubility at its pI (isoelectric precipitation). The effect of salt on proteins involves two mechanisms:

1. Electrostatic shielding effect: At high ionic strength, the charges on the protein are shielded, with the result that the repulsive forces are no longer able to counteract the attractive forces responsible for holding the subunits together. This imbalance leads to suppression of dissociation and decrease in solubility.
2. Ion-specific effect on hydrophobic interactions: The presence of salt stabilizes the quaternary structure and suppresses denaturation. The denaturation temperature of the protein is raised, and the amount of dissociation products is lowered by increasing salt concentration.

■ ■ Effect of pH on Glycinin

Glycinin subunits (acidic-S-S-basic) are amphipathic molecules, consistent with the fact that the acidic polypeptides are on the exterior surface, and the hydrophobic core consists mostly the basic polypeptides. Acidic polypeptide is hydrophilic with limited hydrophobic associations. Its solubility is very much pH dependent as affected predominantly by electrostatic interactions. Acidic polypeptide has a pI value of 4.75–5.40 with sharp minimal solubility (isoelectric precipitation) at pH 5.0 similar to that of native glycinin (pI = 5.4–6.4) [60]. At pH values ≤ 4.4 or ≥ 6.0 , the acidic polypeptide experiences increased electrostatic repulsion and increased solubility (■ Fig. 2.29).

In contrast to the acidic polypeptide, the basic polypeptide is hydrophobic and considerably insoluble. Basic polypeptide contains much less acidic amino acids (Asp, Glu), more basic residues (Lys, Arg, His), and high content of hydrophobic residues (Ala, Ile, Leu, Phe, Val). Hydrophobic interaction becomes the predominant force of association. Basic polypeptide has a pI of 8.0–8.5, but is known to be insoluble in a wide pH range (4.5–8.0), suggesting limited effect of electrostatic interaction.



■ Fig. 2.29 pH solubility profile of a glycinin and subunit polypeptides and b β -conglycinin and subunits at 0.1% protein in water, without salt or heat (From Mo et al. [60] and Zheng et al. [108] with permission. Copyright 1999, 2009 Elsevier)

■ ■ Effect of Salt on Glycinin

The surface of the glycinin 11S complex is predominantly exposed with acidic polypeptides under the typical conditions as already described above. At the ionic strength of 0.2, the basic polypeptides in the interior of the glycinin molecule shift more to the exterior partially replacing the acidic polypeptides on the surface. This altered arrangement of the location of the two types of polypeptides influences the solubility profile of glycinin [50]. At low ionic strength, the pH of minimum solubility (precipitation) of the glycinin molecule is shifted to a higher value toward the pI value of the basic polypeptides.

■ ■ Effect of pH and Salt on Glycinin

At low pH and low ionic strength, the 11S hexamer dissociates to 7S trimers and smaller components. Dissociation is caused by electrostatic repulsion due to an increase in positive charges on the subunits, resulting in irreversible structural changes [101]. High ionic strength suppresses acid-induced dissociation, due to shielding of the electrostatic charges. At the molecular level, dissociation is correlated to changes in the structure at the secondary and less extent at the tertiary folding level. At high pH, thermal treatment causes disruption of the disulfide bond and the noncovalent interactions between the acidic and the basic polypeptides, resulting in extensive rearrangement of the structure.

Thermal denaturation of glycinin at acidic low pH range tends to form larger aggregates due to acid precipitation, producing coarse gels with greater stiffness and turbid appearance. Relatively less aggregates and fine-stranded gels are formed at high pH and decreasing ionic strength, because of the higher solubility of the glycinin protein [95]. The acidic polypeptides are found mostly in the soluble fraction after heat treatment, whereas the basic polypeptides are found in the precipitate (due to their low solubility). Breaking the S-S bond is not observed to occur at lower pH conditions. Disulfide bridges may involve and promote protein-protein aggregation. The topology of the free SH residues that may affect disulfide exchange reaction is also related to the heat-induced gel-forming property of the protein [95].

■ ■ Effect of pH and Salt on Conglycinin

The β -conglycinin α and α' subunits containing both core region and extension region are amphipathic molecules [57]. In contrast, the β subunit has a core region only and in comparison with the α and α' subunits has a higher content of hydrophobic amino acids and a lower content of carbohydrates.

All three subunits of β -conglycinin have acidic pI values (4.0–5.0 for α , 4.0–5.0 for α' , and 4.0–6.0 for β), and the native β -conglycinin exhibits isoelectric precipitation at pH range of 4.0–6.0 [108]. The thermal stability of individual subunits differ in the order of β (91 °C) > α' (83 °C) > α (79 °C) and for the core region (with the extension deleted), α' core (83 °C) > α core (77 °C). At the subunit level, it is the core region that determines the thermal stability.

β -Conglycinin is soluble in a wide pH range at ionic strength of 0.5 (without heating). The extension region, being hydrophilic, together with the glycan moiety, contributes to the high solubility of the subunit structures as well as the β -conglycinin during heating [57]. In the absence of salt, heating at high pH causes dissociation of β -conglycinin into its constituent subunits arising from electrostatic repulsion. (The subunits of β -conglycinin possess net negative charges at high pH.) In the presence of salt (>0.01 ionic strength), electrostatic shielding effect of the salt promotes hydrophobic interactions to form soluble

aggregates [104]. On continued heating, the soluble aggregates associate randomly to form soluble macroaggregates which results in gel formation.

Heat Treatment and Gel Formation

Heat treatment is the oldest method used in soy food production, for two important purposes. Depending on the cultivar, soybean contains varying amounts of protease inhibitors (about 6% of the soybean protein). The best characterized are the Bowman-Birk trypsin-chymotrypsin inhibitor and the Kunitz trypsin inhibitor. These inhibitors inhibit pancreatic enzymes, reduce digestibility of proteins, and cause pancreatic hypertrophy and hyperplasia in some animals. Heat treatment is commonly used to reduce protease inhibitor activity to eliminate their adverse effect in nutrition.

The second purpose is for technological reasons. Heat treatment of soy proteins causes dissociation of the quaternary structures, denatures the subunits, and promotes aggregation of the polypeptides via electrostatic, hydrophobic, hydrogen bonding, and disulfide exchange interactions. Typical food applications involve heating $\approx 10\%$ total soy protein extracts at temperature $> 95^\circ\text{C}$ to form stable gels and/or textured products. Proper gel formation involves a complex process of several steps [35, 61, 74]. (Refer also to the section on "Gel Formation.")

1. Denaturation is a prerequisite for the onset of gelation. The heating process is to unfold the protein structure. The soy proteins dissociate into their respective subunits. Glycinin has a more compact structure stabilized by disulfide bonds and shows a higher melting temperature ($\sim 90^\circ\text{C}$) compared to β -conglycinin ($\sim 70^\circ\text{C}$). Glycinin is more heat stable than β -conglycinin under the same pH and ionic strength. Denaturation temperatures of both proteins are higher at higher pH. The same effect occurs with higher ionic strength.
2. Formation of aggregates occurs following protein unfolding as heating continues. Exposed amino acid functional groups participate in various interactions, leading to irreversible protein-protein aggregation and loss of solubility.
3. A continuous rearrangement of the gel network involves dissociation, reassociation, and condensation of protein aggregates, resulting in denser and stiffer structure.
4. Upon cooling, the gel stiffens due to decreased mobility of the proteins. The process is thermoreversible.

In general, the gel formed by (pure) glycinin is turbid, in contrast to the transparent gel from β -conglycinin when heated under typical pH and ionic strength conditions. Glycinin gels have a higher tensile strength, corresponding to higher degree of hardness. It has a higher water-holding capacity than 7S gels and can expand more on heating [79]. β -Conglycinin and glycinin show different thermal aggregation behaviors. For β -conglycinin, the extent of aggregation and the growth in the size of the aggregates tend to be limited. Heat-denatured subunits dissociate and reassociate with hydrophobic interactions to form aggregates. Once after the hydrophobic sites are covered, electrostatic repulsion becomes the predominant force (due to the N-linked glycans and extension regions on the surface) preventing further association in building larger aggregates. In contrast, glycinin aggregation exhibits continuous growth in size due to more hydrophobic sites available, particularly from the basic polypeptides. Rapid growth and condensation of the aggregates lead to insoluble macroaggregates. Glycinin aggregation exhibits larger particle size distributions in heated soymilk (pH ~ 7) than β -conglycinin aggregates.

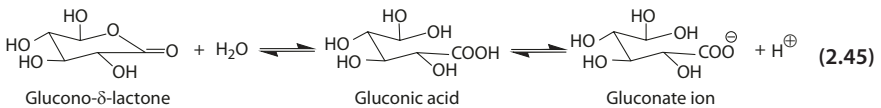
In a mixed system, at low pH, gelation starts at the denaturation temperature of the β -conglycinin protein. At this pH (and at low ionic strength), the 11S glycinin dissociates

to the 7S form, leading to a lower denaturation temperature more like that of β -conglycinin. At high pH, gelation starts above the denaturation temperature of the glycinin protein. Soy protein isolate gels formed on heating at high pH are less stiff, correlating with a higher amount of soluble proteins. Increase of β -conglycinin in a mixed system causes a decrease in the extent of protein aggregation during heating [30]. The aggregates are smaller, less dense, more soluble, and more flexible. Studies using different soybean varieties containing different ratios of 11S to 7S proteins support this conclusion.

Mechanism of Tofu Making

Tofu (bean curd) is made by coagulating the protein aggregates in heated soymilk with calcium or magnesium salts (sulfate, chloride) or by acidification using glucono- δ -lactone (GDL) [30, 49]. The total solid content of soymilk is about 6%. Silken tofu (made without removing the whey) has 5% protein, and regular tofu (made by removing the whey by filtering and pressing the coagulated solid) contains about 6.8% protein. The pH of soymilk is ~ 7 which is above the pI values of 7S (4.5–5.0), and 11S (6.3–7.0), and the globulins are therefore mostly negatively charged. About half of the protein content in soymilk consists of aggregates of particle size 40–100 nm, which are formed by unfolding, dissociation, and reassociation of soy proteins (subunits) in the soymilk during heating. Higher glycinin content in the soybean corresponds to higher particle content in soymilk and increased hardness of the tofu.

The type and the amount (concentration) of the coagulant affect the nature of the product. In general, CaSO_4 and GDL give a curd of finer and more uniform texture than the other salts. Coagulation by calcium is faster than using GDL, and high concentration of calcium may cause syneresis, particularly in soymilk containing high ratio of glycinin to β -conglycinin. The primary effect of a coagulant involves shielding and neutralization of the negative charges of the protein aggregates. Shielding is accomplished by interacting with the protons released in the dissociation of gluconic acid from hydrolysis of GDL (Eq. 2.45), or with the calcium cation in the case of using calcium salt. The neutralization effect leads to a decrease in electrostatic repulsion. Hydrophobic interaction becomes predominant leading to further coagulation of the aggregates, resulting in condensation, rapid growth in size, and curd formation.



In addition to neutralization, calcium cation can form bridges between adjacent charged groups of neighboring polypeptides, thus further enhance condensation of the aggregates. The addition of calcium salt does not change the pH of soymilk. Soybean curd formed by calcium coagulation has a pH ~ 7.2 same as that of soymilk. In contrast, GDL produces a gel of pH ~ 4 due to dissociated gluconic acid [48]. The decrease in pH further promotes acid precipitation, since the minimum solubility of soy proteins correlates to their respective pI values, which are mostly in the acidic range.

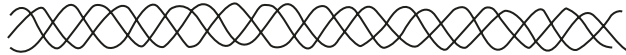
The mechanism of tofu formation is much more complex than just described. Soymilk is a hydrocolloid suspension of about 3.8% protein, 2.9% carbohydrate, and 2% fat, plus small amount of other components, such as phytic acid, minerals, vitamins, isoflavones, saponins, and others. During tofu processing, proteins and oils are concentrated (about 12% and 6%, respectively), carbohydrates constitute $\sim 3\%$, and phytic acid is mostly retained (~ 100 mg per g). Tofu is a protein network enclosing considerable amount of lipid droplets. Phytic acid in

soymilk has the effect of softening the tofu gel. Taking into account the presence of considerable amount of non-proteinaceous components, many physical and chemical interactions can potentially occur in tofu processing which need to be considered as well.

2.5.6 Collagen

Collagen is the fibrous protein that contributes to the unique physiological functions of connective tissue in the skin, tendons, bones, cartilages, etc. The structural unit of collagen is tropocollagen. It is a rod-shaped protein (15 Å diameter, 3000 Å length) consisting of three polypeptide units (called α chains) intertwined to form a triple helical structure. Each α chain coils in a left-handed helix with three residues per turn, and the three chains are twisted right-handed to form the triple helix (■ Fig. 2.30).

■ Fig. 2.30 Triple helical structure of collagen



Triple Helix

The α chains contain about 1,000 amino acid residues and vary in amino acid composition. These variations in the α chains constitute at least four major types of collagen (■ Table 2.7). More than one collagen type is usually present in a particular tissue.

Amino Acid Composition

The amino acid composition of collagen as a whole is unique in that it is exceptionally high in glycine (33%), proline (12%), and alanine (11%), plus two amino acids that are not commonly present in many other proteins, hydroxyproline (12%) and hydroxylysine (1%) (■ Table 2.8) [22].

Hydroxylysine usually has a carbohydrate residue (glucose or galactose) attached. The amino acid sequence indicates that most of the polypeptide chain consists of glycine-led triplets of the following distribution, where I = imino acid residue (proline or hydroxyproline) and X = other amino acid residues (■ Table 2.9). The segments of the polypeptide chain consisting of repeating triplets with imino acid residues are the nonpolar regions, and the segments containing Gly–X–X triples are mostly polar.

■ Table 2.7 Collagens and their distribution

Type	Triple helix	Distribution
I	Two identical $\alpha 1(I)$ chain + one $\alpha 2$ chain	Skin, tendon, bone
II	Three $\alpha 1(II)$ chains	Intervertebral disc, cartilage
III	Three $\alpha 1(III)$ chains	Cardiovascular vessel, uterus
IV	Three $\alpha 1(IV)$ chains	Basement membrane, kidney glomeruli, lens capsule

From Eyre [18]

Table 2.8 Amino acid composition of collagen from rat-tail tendon and its component α chains

Amino acid	Whole collagen	$\alpha 1$ Chain	$\alpha 2$ Chain
	(Amino acid/100 residues)		
Ala	10.7	11.0	10.3
Arg	5.0	4.9	5.1
Asp (+ Apn)	4.5	4.7	4.4
Glu (+ Gln)	7.1	7.4	6.8
Gly	33.1	32.9	33.5
His	0.4	0.2	0.7
Hydroxylysine	0.7	0.5	1.0
Hydroxyprolinea	9.4	9.7	8.6
Ile	1.0	0.6	1.5
Leu	2.4	1.8	3.1
Lys	2.7	3.0	2.1
Met	0.8	0.9	0.7
Phe	1.2	1.2	1.1
Pro	12.2	12.9	11.5
Ser	4.3	4.1	4.3
Thr	2.0	2.0	2.0
Tyr	0.4	0.4	0.4
Val	2.3	1.9	3.0
Gly	33.1	32.9	33.5
Pro + Hyp	21.6	22.6	20.1
Other	45.3	44.5	46.4

From Fraser and MacRae [22]

Table 2.9 Glycine-led triplets

Triplet	Proportion
Gly–X–X	0.44
Gly–X–I	0.20
Gly–I–X	0.27
Gly–I–I	0.09

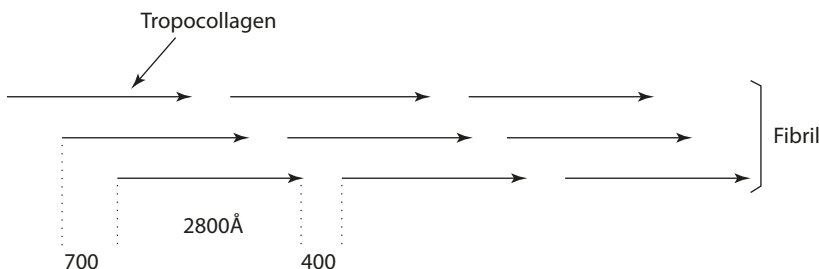
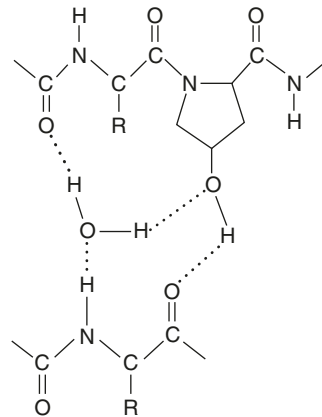
Crosslinking

Each of the three polypeptide chains in the tropocollagen unit forms its own helix, held together by hydrogen bonding between the NH groups of glycine residues in one chain with the CO group on the other chain. The pyrrolidine rings of proline and hydroxyproline impose restrictions on the conformation of the polypeptide chain and help to strengthen the triple helix. The hydroxyl group of the hydroxyproline plays a part in the stability of the helix by interchain hydrogen bonding via a bridging water molecule as well as direct hydrogen bonding to a carbonyl group (■ Fig. 2.31) [3].

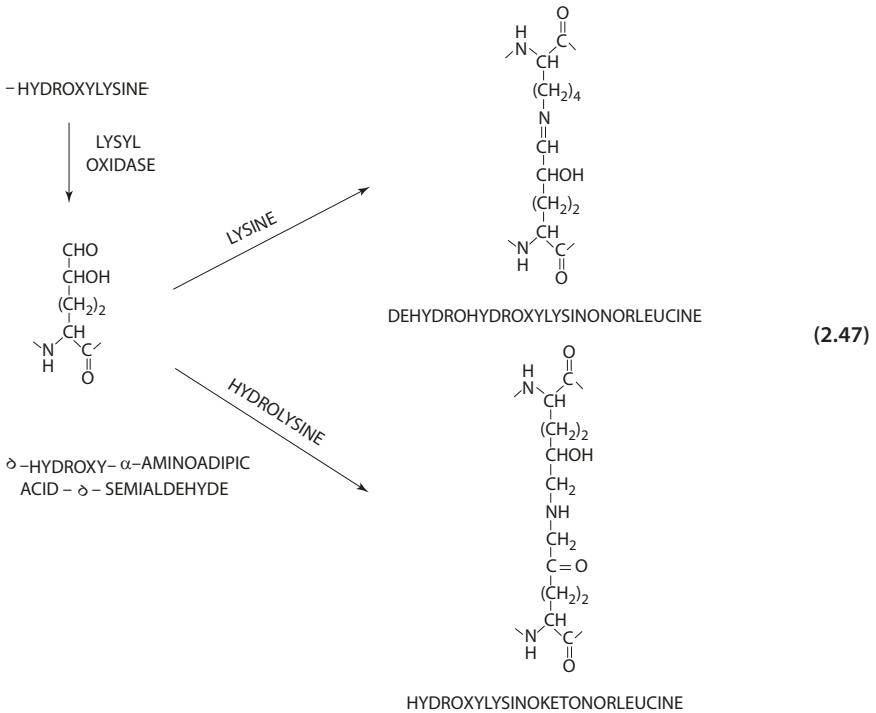
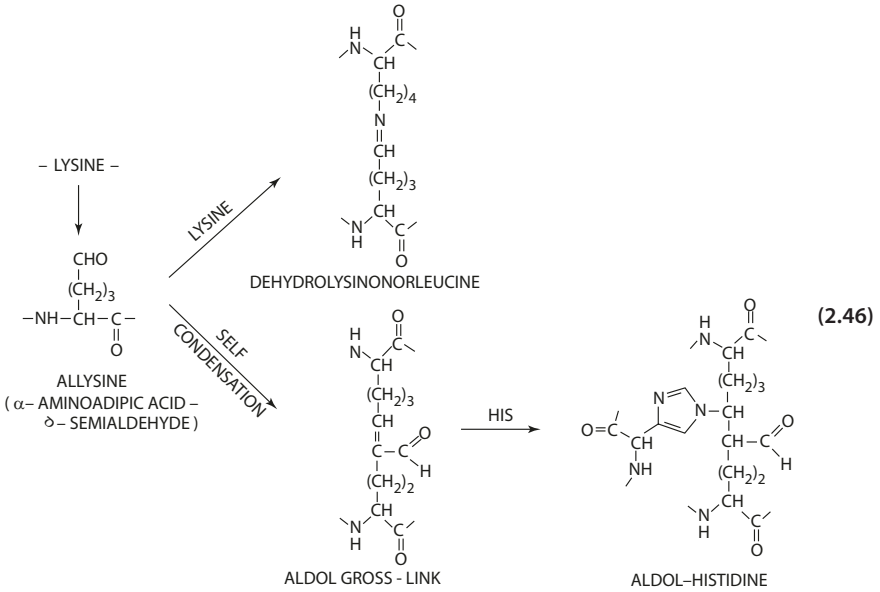
The arrangement of tropocollagen to form collagen fibrils is determined by the region of basic and acidic amino acids in the polypeptide chain. Each tropocollagen stacks over the other by one-fourth of its length (■ Fig. 2.32).

The polypeptide chains of the tropocollagens are covalently crosslinked involving side chains of lysine, hydroxylysine, and histidine. The reaction originates from the oxidative deamination of lysine or hydroxylysine by lysyl oxidase to form the aldehyde, allysine, or hydroxyallysine. The aldehydes can then condense with lysine or with each other or with histidine. Some typical crosslinking reactions are outlined in two schemes, one based on allysine (Eq. 2.46) and the other on hydroxyallysine (Eq. 2.47). Most of these crosslinks are glycosylated, because the hydroxyallysine residues are usually glycosylated.

■ Fig. 2.31 Interchain bridging by hydroxyproline

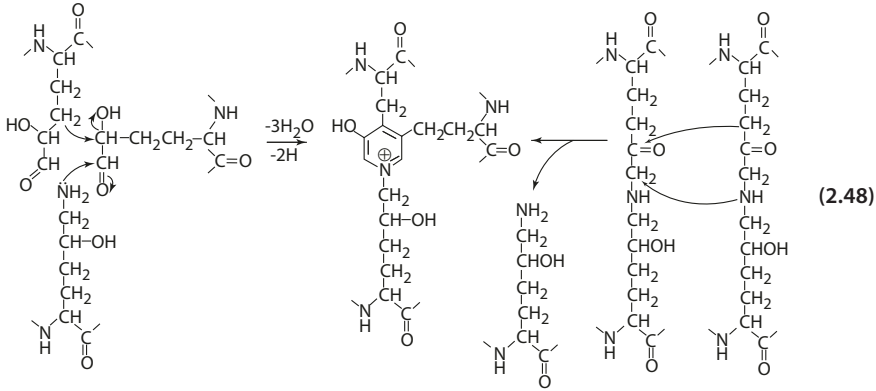


■ Fig. 2.32 Arrangement of tropocollagen



The crosslinks derived from aldol condensation or Schiff-base reactions are reducible and gradually replaced by nonreducible crosslinks during maturation of the connective tissue. A nonreducible crosslink, pyridinoline, is formed by the condensation

of one hydroxylysine and two hydroxyallysines or by the interaction of two residues of hydroxylysine-5-ketonorleucine (Eq. 2.48) [25]. The latter pathway involves an initial aldol addition followed by a nucleophilic displacement reaction. It is the type of nonreducible crosslinks occurring in collagen that causes the tough texture of meat from aged animals.



From Collagen to Gelatin

The common source of collagen includes pigskin, cattle hides, and bones. In the United States, pigskin is the chief raw material for edible gelatin production.

The raw material has to be pretreated by (1) soaking at ambient temperature (15–20 °C) with 2–5% lime suspension for 8–12 weeks before neutralization, or (2) soaking in dilute mineral acid solution (<5%, pH 3.5–4.5) at ambient temperature for 24–48 h before washing.

The gelatin is then extracted at neutral or weakly acidic pH at a temperature range of 50–60 °C. The alkali process is used extensively for processing cattle hide and skin, while the acid process is mostly utilized for pigskin. The gelatin obtained by the acid process is described as type A. Alkali-processed gelatin is referred to as type B.

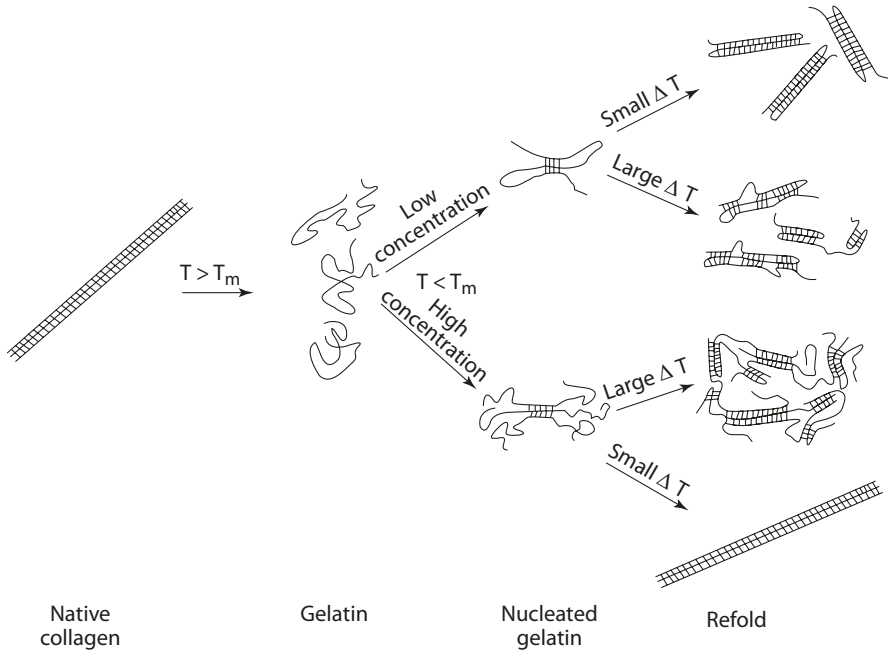
Pretreatment depolymerizes the collagen by breaking down the inter- and intramolecular crosslinkages. Acid process is less effective, but the raw material, pigskin, commonly used in this process consists of less mature collagen and hence has a lower degree of crosslinking. Lime treatment also hydrolyzes asparagine and glutamine, and the isoelectric point of alkali-processed gelatin is in the range of pH 5, in contrast to the pI of ~9 for acid-processed gelatin.

Extraction at high temperature continues the breaking of crosslinkages, but most importantly serves to break down the hydrogen bonds which are the key stabilizing factors in collagen structure. The gelatin extract is then subjected to clarification, filtration, evaporation, sterilization, and drying to a powdered product.

■ The Mechanism of Gelation

The thermal stability of collagen is related to the content of imino acids (proline and hydroxyproline). The higher the imino acid content, the more stable the helices. Collagen denatures at temperatures above 40 °C to a mixture of random-coil single, double, and triple strands. Upon controlled cooling below the melting temperature, T_m reformation of the helices occurs.

The energy barrier for refolding is about 4 KJ/mol. The initial refolding is rapid and involves the –gly–I–I– regions of the polypeptide chain, forming a single turn of a left-handed helix. This "nucleation" along the polypeptide chain is structurally stabilized by



■ **Fig. 2.33** Concentration- and temperature-dependent pathways for helix formation in α chains derived from collagen (From Harrington and Venkateswara [32] with permission. Copyright 1970 American Chemical Society)

water bridging. The "nucleated polypeptide then (1) folds back into loops, with the nucleated regions aligned to form triple strands, and (2) has its nucleated region aligned with that of the other nucleated polypeptide chain (■ Fig. 2.33) [32]. At high enough concentrations, interchain alignment becomes possible, and association of polypeptide chains to form triple helical collagen molecules can occur.

In both cases, since the nucleated regions are aligned, the remainder of the chain (or chains) starts renaturation, the rate of which depends on the cooling temperature. Rapid cooling with large ΔT would cause rapid renaturation, resulting in areas of unavailable for the formation of helical structures. Renatured collagen with various degrees of imperfection is obtained.

The setting of gelatin solution corresponds to the reformation of disordered gelatin molecules to the collagen structure. However, commercial gelatin is heterogeneous in structure and composition, due to the processing conditions and the source of raw material. Gelatin may contain polypeptide chains ranging from 30 to 300 kDa. Amino acid compositions differ; alkali-processed gelatin contains more free carboxyl groups, for example. Therefore, in a gelatin solution, the process of reformation is limited. Various processes contribute to the formation of a gelatin gel network. Nucleation involving imino-rich sections provides junction zones for the gel network. Upon further cooling, additional ordering is achieved by intra- and interchain association. At certain regions, recoiling and refolding give rise to reformation of the collagen structure, which provides reinforcement and hence rigidity of the gel. The resulting gel is essentially an open network through chain association with imino-rich junctions and reinforced by regions of reformed collagen helices.

References

1. Adachi M, Takenaka Y, Gidamis AB, Mikami B, Utsumi S (2001) Crystal structure of soybean proglycinin A1aB1b homotrimer. *J Mol Biol* 305:291–305
2. Adachi M, Kanamori J, Masuda T, Yagasaki K, Kitamura K, Mikami B, Utsumi S (2003) Crystal structure of soybean 11S globulin: glycinin A3B4 homohexamer. *Proc Natl Acad Sci U S A* 100:7395–7400
3. Asghar A, Henrickson RL (1982) Chemical, biochemical, functional, and nutritional characteristics of collagen in food systems. *Adv Food Res* 28:231–372
4. Bell BM, Daniels DGH, Fisher N (1977) Physical aspects of the improvement of dough by fat. *Food Chem* 2:57–70
5. Belton PS (1999) On the elasticity of wheat gluten. *J Cereal Sci* 29:103–107
6. Belton PS (2005) New approaches to study the molecular basis of the mechanical properties of gluten. *J Cereal Sci* 41:203–211
7. Bent DV, Hayon E (1975) Excited state chemistry of aromatic amino acids and related peptides. II. Phenylalanine. *J Am Chem Soc* 97:2606–2611
8. Birktoft JJ, Blow DM (1972) Structure of crystalline α -chymotrypsin. *J Mol Biol* 68:187–240
9. Braams R (1966) Rate constants of hydrated electron reactions with amino acids. *Radiat Res* 27:319–329
10. Cherry JP, MeWatter KH (1981) Whippability and aeration. In: Cherry JP (ed) Protein functionality in foods. ACS symposium series, vol 147. American Chemical Society, Washington, D.C.
11. Clark KA, McElhinny AS, Beckerle MC, Gregorio CC (2002) Striated muscle cytoarchitecture: an intricate web of form and function. *Annu Rev Cell Dev Biol* 18:637–706
12. Cooke R (2004) The sliding filament model: 1972–2004. *J Gen Physiol* 123:643–656
13. Daigleish DG (1979) Proteolysis and aggregation of casein micelles treated with immobilized or soluble chymosin. *J Dairy Res* 46:653–661
14. Dizdaroglu M, Simic MG (1985) Radiation-induced crosslinks between thymine and phenylalanine. *Int J Radiat Biol* 47:63–69
15. Don C, Lichtendonk WJ, Plijter JJ, Hamer RJ (2003) Understanding the link between GMP and dough from glutenin particles in flour towards developed dough. *J Cereal Sci* 38:157–165
16. D'Ovidio R, Masci S (2004) The low-molecular-weight subunits of wheat gluten. *J Cereal Sci* 39:321–339
17. England D (1975) Protein hydration – its role in stabilizing the helix conformation of the protein. In: Duckworth RB (ed) Water relations of foods. Academic, New York
18. Eyre DR (1980) Collagen: molecular diversity in the body's protein scaffold. *Science* 207:1315–1322
19. Faraggi M, Bettelheim A (1977) The reaction of the hydrated electron with amino acids, peptides, and proteins in aqueous solution III. Histidyl peptides. *Radiat Res* 71:311–324
20. Farrell HM Jr, Jimenez-Flores R, Bleck GT, Brown EM, Butler JE, Creamer LK, Hicks CL, Hollar CM, Ng-Kwai-Hang KF, Swaisgood JE (2004) Nomenclature of the proteins of cow's milk – Sixth Edition. *J Dairy Sci* 87:1641–1674
21. Finnie SM, Jeannotte R, Faubron JM (2009) Quantitative characterization of polar lipids from wheat whole meal, flour, and starch. *Cereal Chem* 86:637–645
22. Frazer DB, MacRae TP (1973) Conformation in fibrous proteins and related synthetic polypeptides. Academic, New York, p 347
23. Frazier PJ, Brimblecombe FA, Daniels NWR, Eggitt PWR (1977) The effect of lipoxigenase action on the mechanical development of doughs from fat-extracted and reconstituted wheat flour. *J Sci Food Agric* 28:247–254
24. Fox PF, Hoynes MCT (1975) Heat stability of milk: influence of colloidal calcium phosphate and β -lactoglobulin. *J Dairy Res* 42:427–435
25. Fujimoto D, Moriguchi L, Ishida T, Hayashi H (1978) The structure of pyridinoline, a collagen crosslink. *Biochem Biophys Res Commun* 84:52–57
26. Geeves MA, Holmes KC (2005) The molecular mechanism of muscle contraction. *Adv Protein Chem* 71:161–194
27. Gennari G, Gauzzo G, Jori G (1974) Further studies on the crystal-crystal-violet-sensitized photooxidation of cysteine to cysteic acid. *Photochem Photobiol* 20:497–500
28. Gianibelli MC, Larroque OR, MacRitchie F, Wrigley CW (2001) Biochemical, genetic, and molecular characterization of wheat glutenin and its component subunits. *Cereal Chem* 78:635–646

29. Goll DE, Otsuka Y, Nagainis PA, Shannon JD, Sathe SK, Muguruma M (1983) Role of muscle proteinases in maintenance of muscle integrity and mass. *J Food Biochem* 7:137–177
30. Guo S-T, Ono T (2005) The role of composition and content of protein particles in soymilk on tofu curdling by glucono- δ -lactone or calcium sulfate. *J Food Sci* 70:C252–C262
31. Hamer RJ, van Vliet T (2000) Understanding the structure and properties of gluten: an overview. In: Shewry PR, Tatham AS (eds) *Wheat Gluten proceedings of the 7th international workshop, Gluten 2000*. Royal Society of Chemistry 2000, pp 125–131
32. Harrington WF, Venkateswara R (1970) Collagen structure in solution. I. Kinetics of helix regeneration in single-chain gels. *Biochemistry* 9:3714–3724
33. Hegarty GR, Bratzler LJ, Pearson AM (1963) Studies on the emulsifying properties of some intracellular beef muscle proteins. *J Food Sci* 28:663–668
34. Hermansson AM (1979) Aggregation and denaturation involved in gel formation. In: Pour-El A (ed) *Functionality and protein structure*. ACS symposium series, vol 92. American Chemical Society, Washington, D.C.
35. Hermansson AM (1986) Soy protein gelation. *J Am Oil Chem Soc* 63:658–666
36. Hibberd MG (1986) Relationships between chemical and mechanical events during muscular contraction. *Ann Rev Biophys Chem* 15:119–161
37. Holmes KC, Popp D, Gebhard W, Kabsch W (1990) Atomic model of the actin filament. *Nature* 347:44–49
38. Holt C, Wahlgren NM, Drakenerg T (1996) Ability of a β -casein phosphopeptide to modulate the precipitation of calcium phosphate by forming amorphous dicalcium phosphate nanoclusters. *Biochem J* 314:1035–1039
39. Horne DS (1998) Casein interactions: casting light on the black boxes, the structure in dairy products. *Int Dairy J* 8:171–177
40. Huff-Lonergan E, Lonergan SM (2005) Mechanisms of water-holding capacity of meat: the role of postmortem biochemical and structural changes. *Meat Sci* 71:194–204
41. Huff-Lonergan E, Mitsuhashi T, Beekman DD, Parrish FC, Dennis GO, Robson RM (1996) Proteolysis of specific muscle structural proteins by μ -calpain at low pH and temperature is similar to degradation in postmortem bovine muscle. *J Am Sci* 74:993–1008
42. Hurrell RF, Carpenter KJ (1976) Mechanisms of heat damage in proteins. 7. The significance of lysine-containing isopeptides and of lanthionine in heated proteins. *Br J Nutr* 35:383–395
43. Johansson E, Malik AH, Hussain A, Rasheed F, Newson WR, Plivelic T, Hedenqvist MS, Gallstedt M, Kuktaite R (2013) Wheat gluten polymer structures: the impact of genotype, environment, and processing on their functionality in various applications. *Cereal Chem* 90:367–376
44. Karam LR, Dizdaroglu M, Simic MG (1984) OH radical-induced products of tyrosine peptides. *Int J Radiat Biol* 46:715–724
45. Kasarda DD (1999) Glutenin polymers: the in vitro to in vivo transition. *Cereal Foods World* 44:566–571
46. Kasada DD, Bernardin JE, Nimmo CC (1976) Wheat proteins. *Adv Cereal Sci Technol* 1:158–236
47. Kemp CM, Sensky PL, Bardsley RG, Buttery PJ, Parr T (2010) Tenderness – an enzymatic view. *Meat Sci* 84:248–256
48. Kohyama K, Nishinari K (1993) Rheological studies on the gelation process of soybeans 7S and 11S proteins in the presence of glucono- δ -lactone. *J Agric Food Chem* 41:8–14
49. Kohyama K, Sano Y, Doi E (1995) Rheological characteristics and gelation mechanism of tofu (soybean curd). *J Agric Food Chem* 43:1808–1812
50. Lakemond CMM, de Jongh HHJ, Hessing M, Gruppen H, Voragen AGJ (2000) Soy glycinin: influence of pH and ionic strength on solubility and molecular structure at ambient temperatures. *J Agric Food Chem* 48:1985–1990
51. Levitt M, Chothia C (1976) Structural patterns in globular proteins. *Nature* 261:552–538
52. Liardon R, Ledermann S (1986) Racemization kinetics of free and protein-bound amino acids under moderate alkaline treatment. *J Agric Food Chem* 34:557–565
53. Lindsay MP, Skerritt JH (1999) The glutenin macropolymer of wheat flour doughs: structure-function perspectives. *Trends Food Sci Technol* 10:247–253
54. Lindsay MP, Tamas L, Appels R, Skerritt JH (2000) Direct evidence that the number and location of cysteine residues affect glutenin polymer structure. *J Cereal Sci* 31:321–333
55. Lucey JA (2002) Formation and physical properties of milk protein gels. *J Dairy Sci* 85:281–294

References

56. Maruyama N, Adachi M, Takahashi K, Yagasaki K, Kohno M, Takenaka Y, Okuda E, Nakagawa S, Mikami B, Utsumi S (2001) Crystal structures of recombinant and native soybean β -conglycinin β homotrimers. *Eur J Biochem* 268:3595–3604
57. Maruyama N, Salleh MRM, Takanashi K, Yagasaki K, Goto H, Hontami N, Nakagawa S, Utsumi S (2002) The effect of the N-linked glycans on structural features and physicochemical functions of soybean β -conglycinin homotrimers. *JAOCS* 79:139–144
58. McMahon DJ, Oommen BS (2008) Supramolecular structure of the casein micelle. *J Dairy Sci* 91:1709–1721
59. Melander W, Horvath C (1977) Salt effects on hydrophobic interaction in precipitation and chromatography of proteins: an interpretation of the lyotropic series. *Arch Biochem Biophys* 183:200–215
60. Mo X, Zhong Z, Wang D, Sun X (2006) Soybean glycinin subunits: characterization of physicochemical and adhesion properties. *J Agric Food Chem* 54:7589–7593
61. Morr CV (1990) Current status of soy protein functionality in food systems. *JAOCS* 67:265–271
62. Otterbein LR, Graceffa P, Dominguez R (2001) The crystal structure of uncomplexed actin in the ADP state. *Science* 293:708–711
63. Papiz MZ, Sawyer L, Eliopoulos EE, North ACT, Findley JBC, Siraprasadarao R, Jone TA, Newcomer ME, Kraulis PJ (1986) The structure of β -lactoglobulin and its similarity to plasma retinol-binding protein. *Nature* 324:383–385
64. Pareyt B, Finnie SM, Putreys JA, Delcour JA (2011) Lipids in bread making: sources, interactions, and impact on bread quality. *J Cereal Sci* 54:266–279
65. Payens TAJ (1979) Casein micelles: the colloid-chemical approach. *J Dairy Res* 46:291–306
66. Pearce KL, Rosenvold K, Andersen HJ, Hopkins DL (2011) Water distribution and mobility in meat during the conversion of muscle to meat and aging and the impacts on fresh meat quality attributes – a review. *Meat Sci* 89:111–124
67. Philips MC (1981) Protein conformation at liquid interfaces and its role in stabilizing emulsions and foams. *Food Technol* 35(1):50–57
68. Pomeranz Y, Chung OK (1978) Interaction of lipids with proteins and carbohydrates in breadmaking. *J Am Oil Chem Soc* 55:285–289
69. Privalov PL, Khechinashvili NN (1974) A thermodynamic approach to the problems of stabilization of globular protein structure: a calorimetric study. *J Mol Biol* 86:665–684
70. Qi PF, Wei YM, Yue YW, Yan ZH, Zheng YL (2006) Biochemical and molecular characterization of gliadins. *Mol Biol* 40:713–723
71. Rao PS, Hayon E (1975) Reaction of hydroxyl radicals with oligopeptides in aqueous solutions. A pulse radiolysis study. *J Phys Chem* 79:109–115
72. Rayment I, Rypniewski WR, Schmidt-Base K, Smith R, Tomchick DR, Benning MW, Winkelmann DA, Wesenberg G, Holden HM (1993) Three-dimensional structure of myosin subfragment-1: a molecular motor. *Science* 261:50–58
73. Rayment I, Holden HM (1994) The three-dimensional structure of a molecular motor. *TIBS* 19:129–134
74. Renkema JMS, van Vliet T (2002) Heat-induced gel formation by soy proteins at neutral pH. *J Agric Food Chem* 50:1569–1573
75. Richardson JS (1976) Handedness of crossover connections in β sheets. *Proc Natl Acad Sci U S A* 73:2619–2623
76. Richardson JS (1977) β -Sheet topology and the relatedness of proteins. *Nature* 268:495–500
77. Saito I, Matsuura T (1977) Peroxidic intermediates in photosensitized oxygenation of tryptophan derivatives. *Acc Chem Res* 10:346–352
78. Saito I, Matsuura T (1985) Chemical aspects of UV-induced cross-linking of proteins to nucleic acid. Photoreaction with lysine and tryptophan. *Acc Chem Res* 18:134–141
79. Saio K, Watanabe T (1978) Differences in functional properties of 7S and 11S soybean proteins. *J. Texture Stud* 9:135–157
80. Samejima KJ, Ishioroshi M, Yasui T (1981) Relative roles of the head and tail portions of the molecule in heat-induced gelation of myosin. *J Food Sci* 46:1412–1418
81. Schaich KM (1980) Free radical initiation in proteins and amino acids by ionizing and ultraviolet. *CRC Crit Rev Food Sci Nutr* 13:89–129
82. Schaich KM (1980) Free radical initiation in proteins and amino acids by ionizing and ultraviolet radiations and lipid oxidation – part II: ultraviolet radiation and photolysis. *CRC Crit Rev Food Sci Nutr* 13:131–159

83. Schaich KM (1980) Free radical initiation in protein and amino acids by ionizing and ultraviolet radiation and lipid oxidation – part III: free radical transfer from oxidizing lipids. *CRC Crit Rev Food Sci Nutr* 13:189–244
84. Schmidt DG (1980) Colloidal aspects of casein. *Neth Milk Dairy J* 34:42–
85. Schmidt DG (1981) Gelation and coagulation. In: Cherry JP (ed) *Protein functionality in foods*. ACS symposium series, vol 147. American Chemical Society, Washington, D.C.
86. Schmidt DG (1982) Association of caseins and casein micelle structure. In: Fox PF (ed) *Developments in dairy chemistry*. Applied Science Publishers, Ltd., London/New York
87. Shewry PR, Popineau Y, Lafandra D, Belton P (2001) Wheat glutenin subunits and dough elasticity: findings of the EUROWHEAT project. *Trends Food Sci Technol* 11:433–441
88. Singh H (2004) Heat stability of milk. *Int J Dairy Technol* 57:111–119
89. Slattey CW, Evard R (1973) A model for the formation and structure of casein micelles from subunits of variable composition. *Biochim Biophys Acta* 317:529–538
90. Squire JM, Al-Khayat HA, Knup C, Luther PK (2005) Molecular architecture in muscle contractile assemblies. *Adv Protein Chem* 71:17–87
91. Sroan BS, Bean SR, MacRitche F (2009) Mechanism of gas cell stabilization in bread making. I. The primary gluten-starch matrix. *J Cereal Sci* 49:32–40
92. Tamas L, Gras PW, Solomon RG, Morell MK, Appels R, Bekes F (2002) Chain extension and termination as a function of cysteine content and the length of the central repetitive domain in storage proteins. *J Cereal Sci* 36:313–325
93. Tatham AS, Shewry PR (1985) The conformation of wheat gluten proteins. The secondary structures and thermal stabilities of α , β , and γ -gliadins. *J Cereal Sci* 3:103–113
94. Thomson NH, Miles MJ, Popineau Y, Harris J, Shewry P, Tatham AS (1999) Small angle X-ray scattering of wheat seed storage proteins α -, γ - and ω -gliadins and the high molecular weight (HMW) subunits of glutenin. *Biochim Biophys Acta Protein Struct Mol Enzymol* 1430:359–366
95. Utsumi S, Maruyama N, Satoh R, Adachi M (2002) Structure–function relationships of soybean proteins revealed by using recombinant systems. *Enzyme Microb Technol* 30:284–288
96. Wall JS (1979) The role of wheat proteins in determining baking quality. In: Laidman DL, Jones RGW (eds) *Recent advances in the biochemistry of cereals*. Academic, New York
97. Watanabe A, Yokomizo K, Eliasson A-C (2003) Effect of physical states of nonpolar lipids in rheology, ultracentrifugation, and microstructure of wheat flour dough. *Cereal Chem* 80:281–284
98. Whitaker JR, Feeney RE (1983) Chemical and physical modification of proteins by the hydroxide ion. *CRC Crit Rev Food Sci Nutr* 19:173–212
99. Wikenning VG, Lai M, Arends M, Armstrong DA (1968) The cobalt-60 γ -radiolysis of cysteine in deaerated aqueous solutions at pH values between 5 and 6. *J Phys Chem* 72:185–190
100. de Wit JN (2009) Thermal behavior of bovine b-lactoglobulin at temperatures up to 150 °C, a review. *Trends Food Sci Technol* 20:27–34
101. Wolf WJ, Rackis JJ, Smith AK, Sasame HA, Babcock GE (1958) Behavior of the 11S protein of soybeans in acid solutions. I. Effects of pH, ionic strength and time in ultracentrifugal and optical rotatory properties. *J Am Chem Soc* 80:5730–5735
102. Yamamoto O (1972) Radiation-induced binding of methionine with serum albumin, tryptophan or phenylalanine in aqueous solution. *Int J Radiat Phys Chem* 4:335–345
103. Yamamoto O (1975) Radiation-induced binding of OH-substituted aromatic amino acids, tyrosine and dopa, mutually and with albumin in aqueous solution. *Radiat Res* 61:251–260
104. Yamauchi F, Yamagishi T, Iwabuchi S (1991) Molecular understanding of heat-induced phenomena of soybean protein. *Food Rev Intl* 7:283–322
105. Yang SF, Ku HS, Pratt HK (1967) Photochemical production of ethylene from methionine and its analogues in the presence of flavin mononucleotide. *J Biol Chem* 242:5274–5280
106. Yong SH, Karel M (1978) Reaction of histidine with methyl linoleate: characterization of the histidine degradation products. *J Am Oil Chem Soc* 55:352–357
107. Yong SH, Lau S, Hsieh Y, Karel M (1980) Degradation products of L-tryptophan reacted with peroxidizing methyl linoleate. In: Simic MG, Karel M (eds) *Autoxidation in food and biological systems*. Phenum Press, New York
108. Zheng H-G, Yang X-Q, Ahmad I, Min W, Zhu J-H, Yuan D-B (2009) Soybean β -conglycinin constituent subunits: solubility and amino acid composition. *Food Res Int* 42:998–1003
109. Ziegler GR, Acton JC (1984) Mechanisms of gas formation by proteins of muscle tissue. *Food Technol* 38(5):77–82

Carbohydrates

3.1 Glycosidic Linkage – 125

3.2 Action of Alkali on Monosaccharides – 127

3.2.1 Aldose-Ketose Rearrangement – 127

3.2.2 Formation of Saccharinic Acid – 128

3.2.3 Fragmentation – 129

3.3 Action of Acid on Monosaccharides – 130

3.3.1 Formation of Anhydro Sugars – 130

3.3.2 Formation of Furan Derivatives – 130

3.4 Nonenzymatic Browning (Maillard Reaction) – 132

3.4.1 Chemistry of the Reaction – 135

3.4.2 Secondary Reactions – 139

3.5 Complexes of Sugars with Metal Ions – 141

3.5.1 In Neutral Solution – 141

3.5.2 In Alkaline Solution – 142

3.6 Hydrocolloids – 143

3.7 Starch – 143

3.7.1 Chemical Structure of Starch – 143

3.7.2 Gelatinization and Retrogradation – 146

3.7.3 Chemical Modification of Starch – 147

3.7.4 Starch Structure and Digestibility – 148

3.8 Alginate – 149

3.8.1 Chemical Structure of Alginate – 149

3.8.2 Gelling – 149

3.9 Pectin – 151

3.9.1 Chemical Structure of Pectin – 151

3.9.2 Classification of Pectin – 151

3.9.3 Gelling – 152

3.10 Cellulose – 153

3.10.1 Chemical Structure of Cellulose – 153

3.10.2 Gelling – 153

3.11 β -Glucan – 156

3.12 Hemicellulose – 159

3.12.1 Dietary Fiber – 160

3.13 Xanthan Gum – 161

3.13.1 Chemical Structure of Xanthan Gum – 161

3.13.2 Gelling – 162

3.14 Guar Gum – 162

3.15 Carrageenan – 163

3.15.1 Chemical Structure of Carrageenan – 163

3.15.2 Gelling – 165

3.15.3 Interaction with Proteins – 165

3.15.4 Synergism with Locust Bean Gum – 166

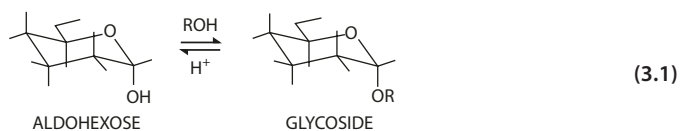
References – 167

Studies of the chemistry of monosaccharides and oligosaccharides have largely focused on the degradations of these carbohydrates and subsequent rearrangements and reactions. The many flavor and color compounds in food are the results of these changes and the various interactions among the breakdown products and with other food components in the system. Among the many reaction mechanisms involved, the Maillard reaction remains the most important and extensively studied. The basic chemistry of these reactions is discussed here, and many more secondary reactions are covered in ► Chap. 6.

Polysaccharides are important due to their physical and chemical characteristics in solution. The study of flow properties and gelling mechanisms of a particular food polysaccharide requires an understanding of the orientation of its molecular structure in crystal and in solution. Quite often, gelling of polysaccharide molecules requires complexation with metal ions, with the degree and the nature of the substituents play a significant role. A number of polysaccharides important for food uses are presented, with particular emphasis on the relationship between molecular arrangement and gelling characteristic.

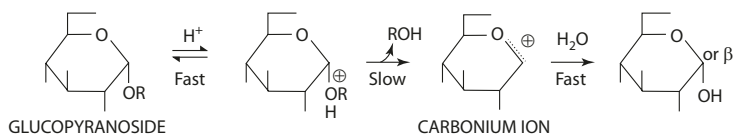
3.1 Glycosidic Linkage

Many carbohydrates are found in nature linked to phenolic compounds as glycosides. The monosaccharide and the glycoside in Eq. 3.1 are hemiacetal and acetal, respectively. Glycosides are fairly stable in aqueous alkali solution but hydrolyzed when heated in aqueous acid.

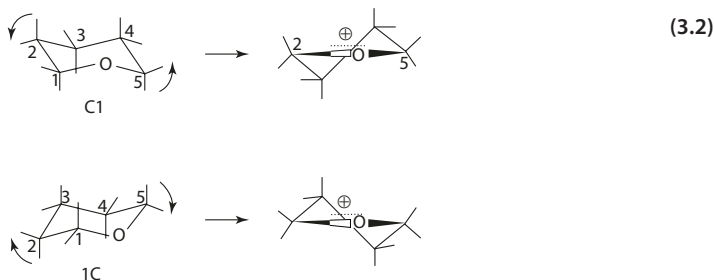


Acid hydrolysis proceeds via a carbonium ion intermediate with the exocyclic oxygen atom being protonated, followed by the C1–O bond cleavage, as shown in Eq. 3.2 for the hydrolysis of D-glucopyranoside. The carbonium ion is stabilized by conjugation with the ring oxygen atom, under which conditions the molecule assumes a half-chair conformation.

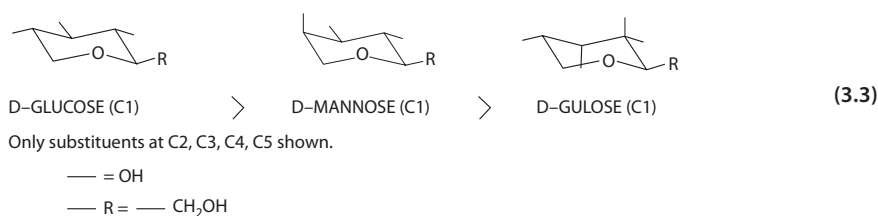
The conversion of the chair form to the half-chair conformation, and hence the stability of the glycoside to acid depends on the steric interaction of the substituents. The formation of the half-chair form, in which the –C1(OH, Me)–O– bridge is planar, requires rotation about the C2–C3 and C4–C5 bonds as illustrated in Eq. 3.2 for both the C1 and 1C conformers. Therefore, bulky substituents at these positions tend to increase steric hindrance to the rotation. Deoxyglycosides such as 2- and 3-deoxyglycosides are more labile to acid hydrolysis compared with the corresponding normal glycosides.



3



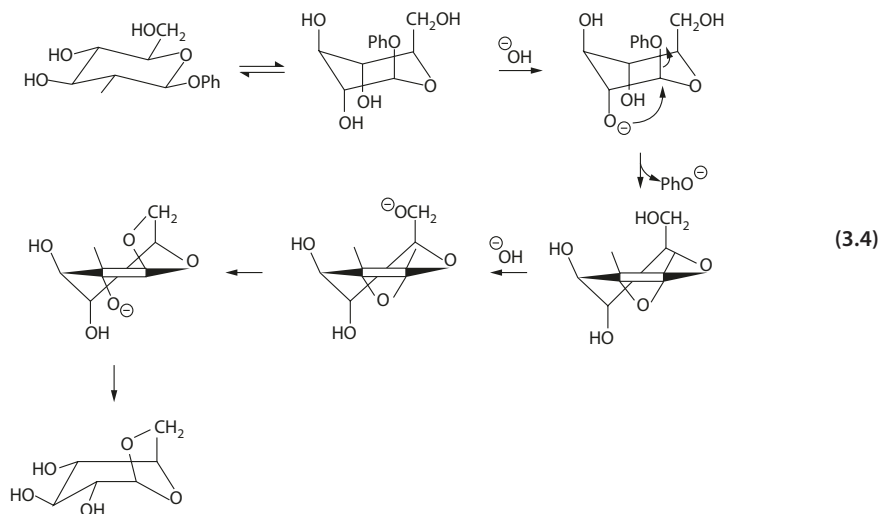
The conversion of the chair to the half-chair form is also assisted by the changes of the C2 and C5 axial substituents away from the C4 and C3 axial substituents, respectively. Therefore, in their C1 conformation, the order of stability for methylpyranosides will be glucose (no axial OH) > mannose (one axial OH) > gulose (two axial OH) (Eq. 3.3) and similarly for methyl pentopyranosides, xylose > arabinose > lyxose.



Base-catalyzed hydrolysis of glycosides occurs only under extreme conditions with highly concentrated hydroxide and at high temperatures. For example, experiments have been done using 10% NaOH and heating at 170 °C for the hydrolysis of methylpyranosides. *Trans*-1,2-glycosides are suggested to undergo hydrolysis via intermediate 1,2-anhydro formation by inversion. The 1,2-anhydro sugar reacts by a second inversion with the C6 alkoxide ion to form the 1,6-anhydride (Eq. 3.4) [9].

Alkyl glycosides are very resistant to alkaline degradation, but aryl glycosides, especially with electron-withdrawing substituents, are found to react readily. *Trans*-1,2-glycosides generally react faster than the *cis* isomers, since formation of the 1,2-anhydride intermediate involves a *trans* configuration for the nucleophilic attack of the C2 alkoxide at C1. From Eq. 3.4, it is also conceivable that hydrolysis may proceed via a bimolecular nucleophilic substitution in which a backside attack of the hydroxide ion displaces the phenoxide [9]. The monosaccharides resulting from acid or alkaline hydrolysis enter into further degradation by a number of pathways.

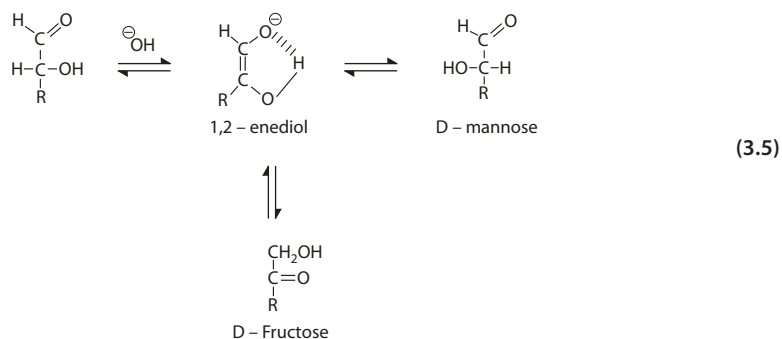
3.2 · Action of Alkali on Monosaccharides



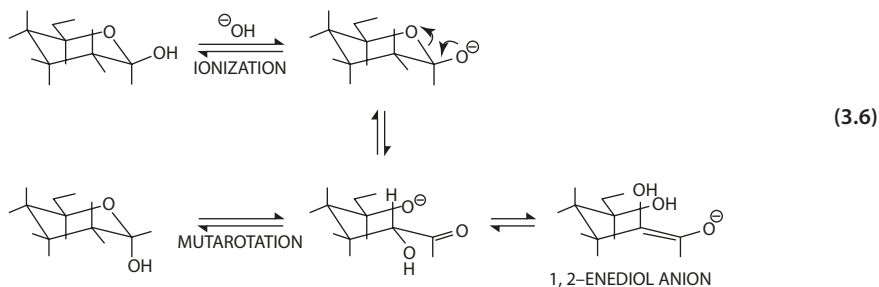
3.2 Action of Alkali on Monosaccharides

3.2.1 Aldose-Ketose Rearrangement

In the presence of dilute base, D-glucose enolizes to form a mixture of anomers of D-glucose, D-fructose, and D-mannose. The interconversion proceeds via a 1,2-enediol intermediate in a rearrangement known as the Lobry de Bruyn-Alberda-van Ekenstein reaction (Eq. 3.5).

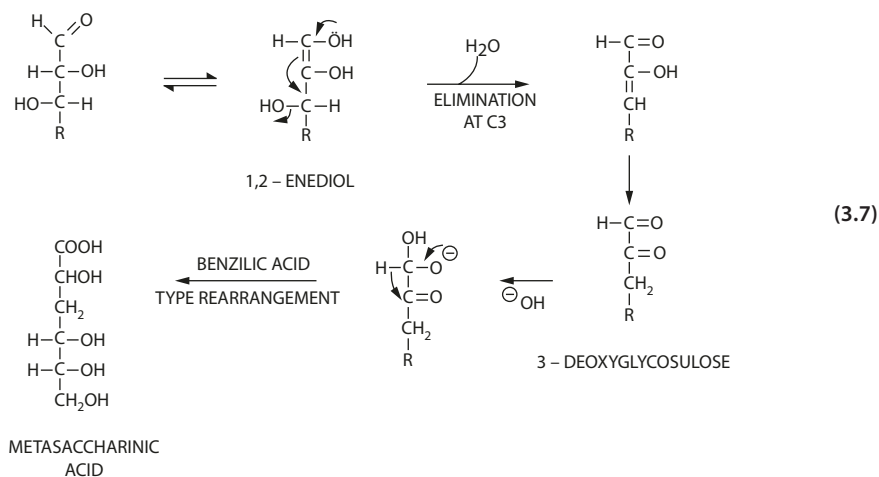


The formation of 1,2-enediol in alkaline solution is considered to involve the ionization of the C1–OH, followed by enolization via a pseudo-cyclic intermediate which allows an intramolecular proton shift from C2 to the C5 oxygen (Eq. 3.6) [14]. The resulting enediol anion rearranges in the reverse process of enolization to form the isomer.



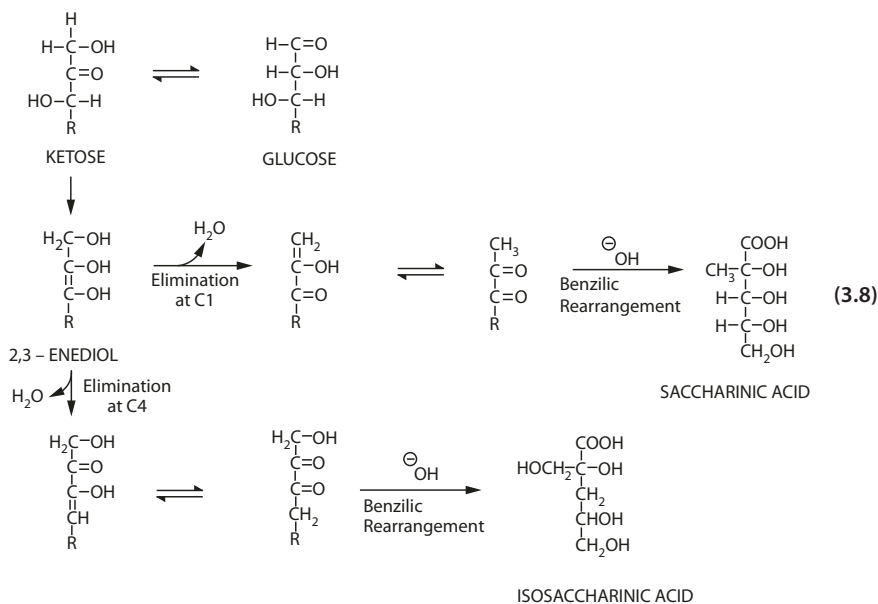
3.2.2 Formation of Saccharinic Acid

In a strong alkaline solution, the 1,2-enediol undergoes elimination at C3 to yield 3-deoxyglycosulose, which undergoes a benzilic acid-type rearrangement to metasaccharinic acid. For simplification, glucose is the aldohexose used in the reaction scheme (Eq. 3.7). Formation of the 2,3-enediol, which then undergoes similar reaction sequences, leads to the formation of saccharinic and isosaccharinic acids (Eq. 3.8) [18]. For saccharinic acid, elimination occurs at C1, whereas elimination at C4 of the 2,3-enediol, followed by benzilic rearrangement, yields the isosaccharinic acid.



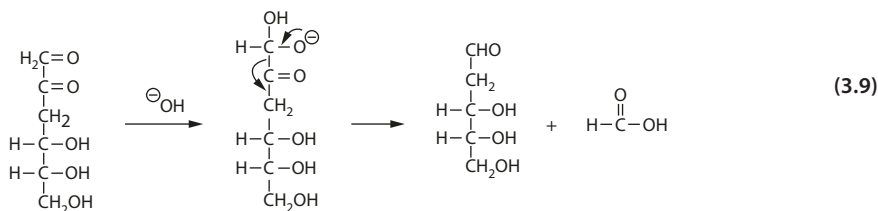
METASACCHARINIC
ACID

3.2 · Action of Alkali on Monosaccharides

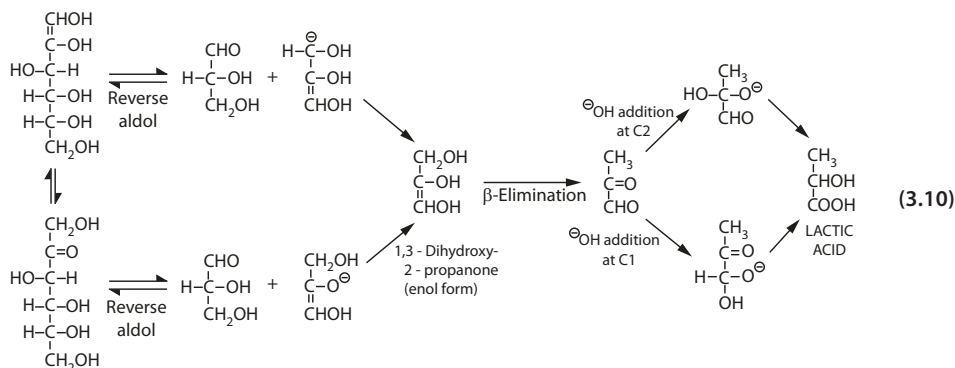


3.2.3 Fragmentation

1. Dicarbonyl compounds such as deoxyglycosulose in Eq. 3.7 undergo cleavage at C1–C2 leading to the formation of an acid and an aldehyde (Eq. 3.9).



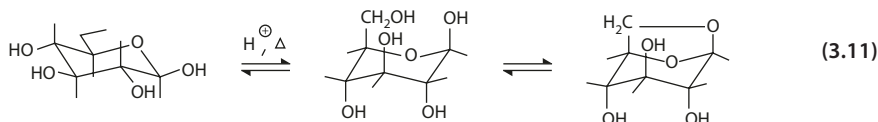
2. Cleavage of the 1,2-enediol at C3–C4 via a reverse aldol reaction results in the formation of two trioses. One of the trioses, 1,3-dihydroxy-2-propanone, undergoes benzilic rearrangement to lactic acid. Addition of hydroxide ion to C1 results in a hydride transfer, whereas addition to C2 involves a methyl shift (Eq. 3.10). The reverse aldol reaction can also occur via ketose formation, yielding the same product.
3. The aldehyde fragments formed in the above two reactions readily undergo cross-aldol condensation, yielding new polyhydroxy compounds [38].



3.3 Action of Acid on Monosaccharides

3.3.1 Formation of Anhydro Sugars

In dilute acid solution, aldohexoses form anhydro sugars with the loss of a water molecule, the common product being 1,6-anhydro sugars (Eq. 3.11). Note that for β -D-glucopyranose, in order for the C1–OH and C6–OH to be in the axial position, the other hydroxyl groups will also be in axial positions, which constitute the unstable conformation due to steric interaction. In contrast, with D-altrose, D-gulose, and D-idose, the molecule assumes a more stable conformation when the C1–OH and C6–OH are oriented axially. This conformation factor affects the proportion of 1,6-anhydro products found in a particular sugar solution, as indicated in Table 3.1.



3.3.2 Formation of Furan Derivatives

When a monosaccharide is heated in a strong acidic solution, dehydration occurs, resulting in the formation of furfural compounds [1, 18]:

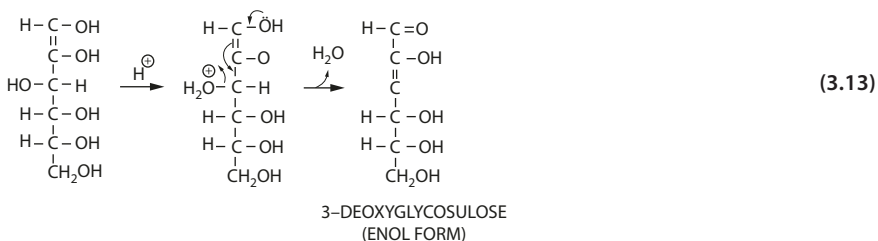
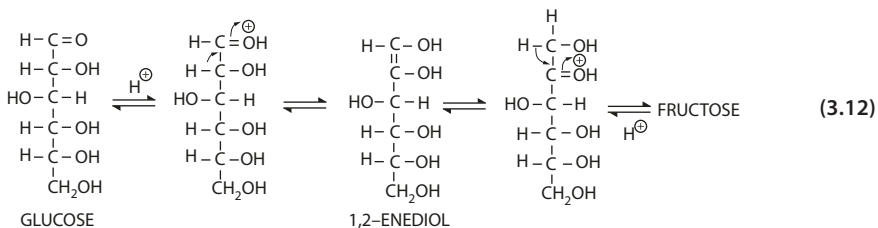
1. The first step is protonation of the carbonyl oxygen, followed by 1,2-enolization to form 1,2-enediol (Eq. 3.12). (Glucose is the aldohexose used in the scheme.) The 1,2-enolization is the rate-determining step. The enediol is formed from both aldose and ketose, since it is the common intermediate in the aldose-ketose rearrangement (Eq. 3.5).

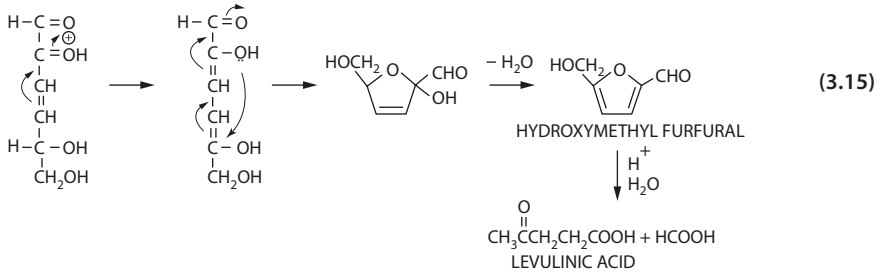
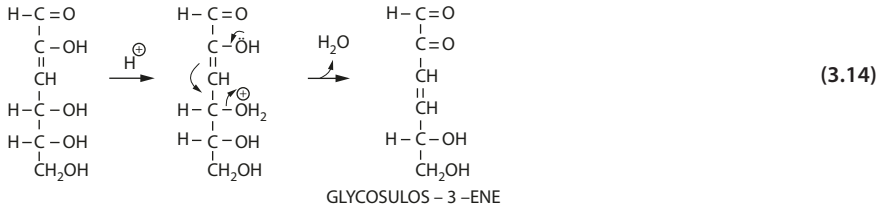
■ **Table 3.1** Percentage of 1,6-anhydro sugars in equilibrium mixture

Sugar solution (0.25–0.50%, 0.25M H ₂ SO ₄ , 100 °C)	% 1,6-anhydrohexose
D-Glucose	0.2
D-Mannose	0.8
D-Altrose	65.5
D-Gulose	65.0
D-Idose	86.0

From Cerny and Stanek [11]

- Elimination at C3, assisted by protonation of the hydroxyl group at C3 and nucleophilic addition at C1, leads to the formation of the enol form of 3-deoxyglycosulose (Eq. 3.13). This elimination step involves an allylic shift or oxotropic rearrangement.
- Elimination at C4, assisted by protonation of the oxygen at C4 and nucleophilic addition at C2, yields the 3,4-unsaturated glycosulose (glycosulos-3-ene) (Eq. 3.14). Unlike the reaction in alkaline solution, the 3-deoxyglycosulose intermediate is not formed [17].
- Protonation of the carbonyl group at C2, followed by enolization, extends the conjugated unsaturated system. Cyclodehydration involving C5 and C2 oxygen yields the furfural (Eq. 3.15).

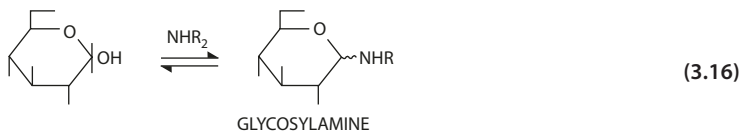




3.4 Nonenzymatic Browning (Maillard Reaction)

The Maillard reaction is one of the most important reactions occurred in food. The reaction is critical in the production of the many flavor and color compounds in processed food products, both desirable and undesirable (▶ Chap. 6). Reduction of nutritional quality and possible generation of toxic and mutagenic compounds, via the Maillard reaction, are causes for concern (▶ Chap. 8). The Maillard reaction comprises a series of reactions, with the following generally recognized steps [1, 25, 31]:

1. Formation of glycosylamine via a Schiff-base formation between the carbonyl group of a reducing sugar and the amino group of amine. This first reaction step is reversible. Formation of the glycosylamine is favored with low water content (Eq. 3.16). (Glucose is the aldohexose used in the reaction schemes.) In foods, it is essentially the monosaccharides, glucose, fructose, and the disaccharides, maltose and lactose, that react with protein amino acids, such as the primary amino groups of lysine side chains.

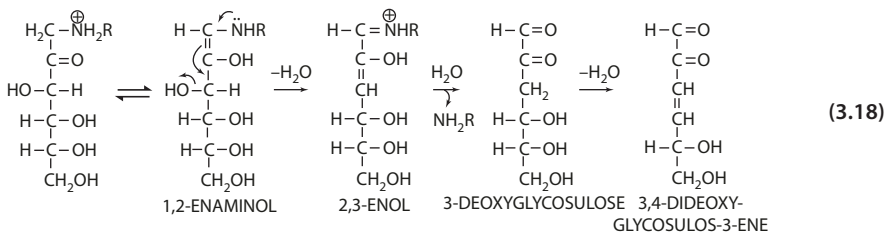
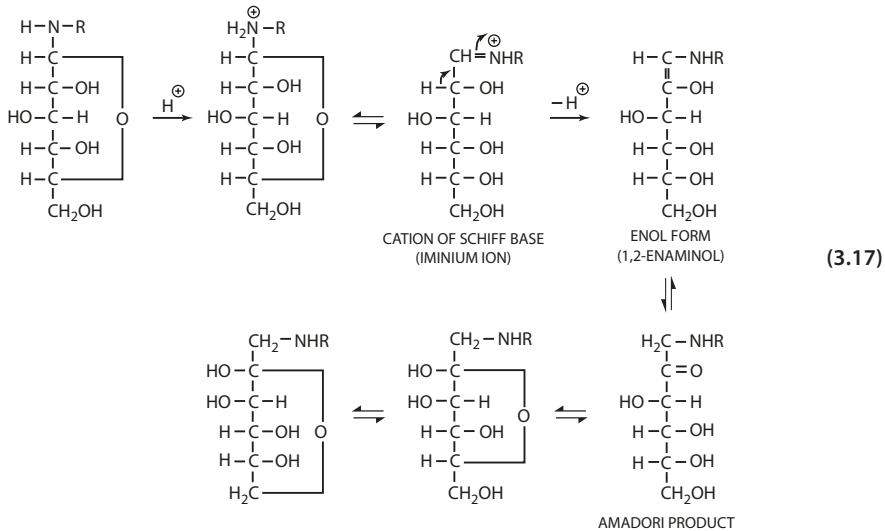


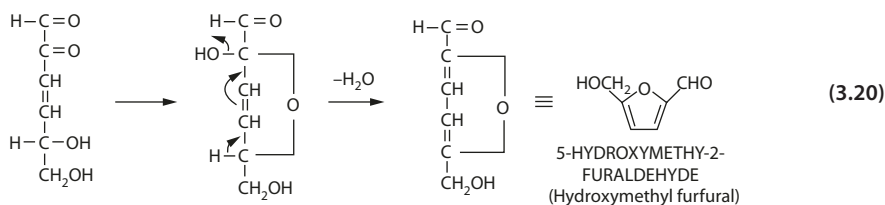
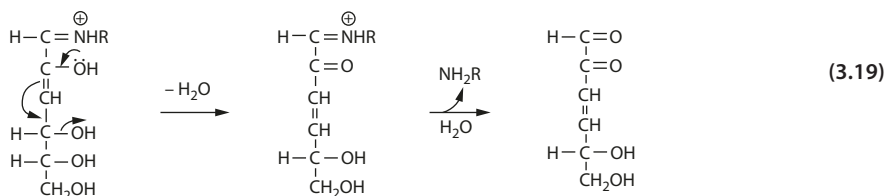
2. Amadori rearrangement in which the glycosylamine is transformed to the ketos-amine. The nitrogen of the glycosylamine accepts a proton to form the amine salt, which is in equilibrium with the cation of the Schiff base (iminium ion). Rearrangement of the latter gives the enol form (1,2-enaminol), which then tautomerizes

3.4 · Nonenzymatic Browning (Maillard Reaction)

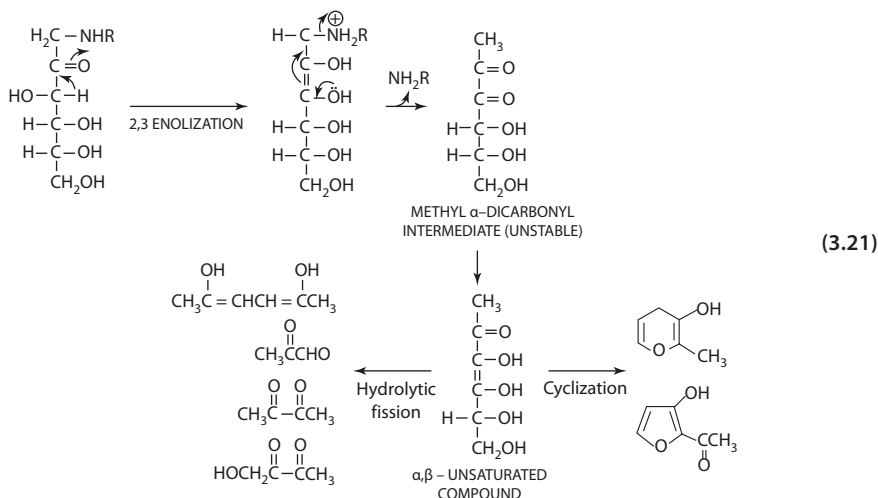
to yield the keto form of the Amadori compound (1-amino-1-deoxy-2-ketose) (Eq. 3.17). The tautomerization to the keto form is driven by the formation of the cyclic structure [24]. The mechanism of Amadori rearrangement is catalyzed by a weak acid, and in the reaction involving amino acids, the carboxyl group of the amino acid may act as the catalyst by furnishing the necessary proton.

- Under acidic conditions, the Amadori compound exists in its salt form. The presence of the positively charged amino group assists in shifting the equilibrium to the enol form, which undergoes elimination of the hydroxyl group from C3 to yield the 2,3-enol. The 2,3-enol is readily hydrolyzed at the C1 Schiff base to the glycosulose. Further elimination of the hydroxyl group at C4 yields an unsaturated glycosulos-3-ene (Eq. 3.18).
- Alternatively, elimination at C4 before hydrolysis of the Schiff base also gives the glycosulos-3-ene. Once the hydroxyl group has been eliminated at C3, the course of reaction is not affected by the removal of the amino group (Eq. 3.19).
- The glycosulos-3-ene, which is an unsaturated dicarbonyl compound, undergoes cyclodehydration to form furaldehyde (Eq. 3.20).





6. In the above pathway, the 3-deoxyglycosulose is formed from the 1,2-enaminol resulting by 1,2-enolization. Another pathway is also possible involving irreversible 2,3-enolization of the Amadori compound by β -elimination of the C1 amino group to form a methyl α -dicarbonyl intermediate. Rapid enolization of the unstable intermediate yields the α,β -unsaturated carbonyl compound, which may form reductones and carbonyl products via hydrolytic fission or *O*-heterocyclic compounds by cyclization (Eq. 3.21).



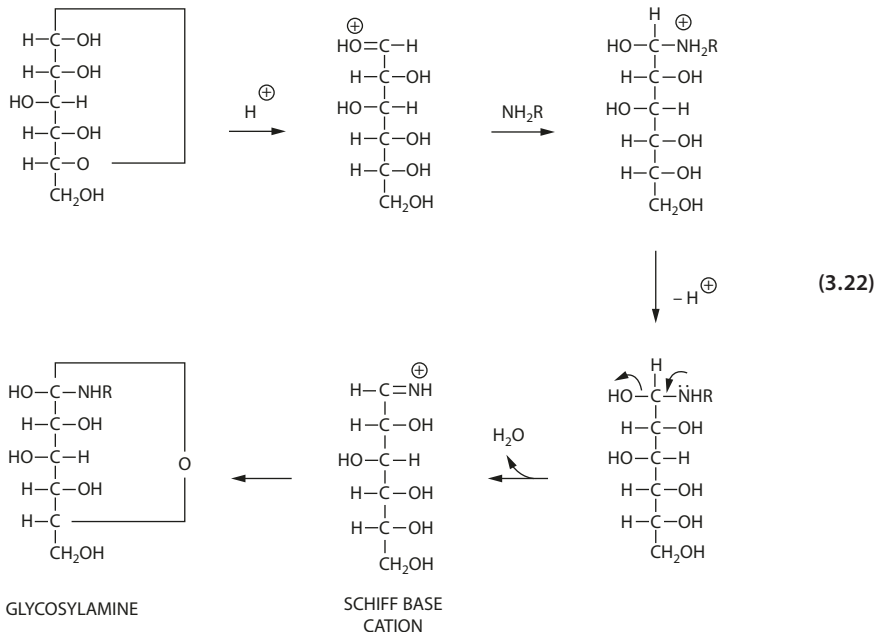
Factors affecting the Maillard reaction are pH, time, temperature, and types of reactants. The rate increases with increasing temperature. The reaction rate roughly doubles with 10 °C increase in temperature. A typical temperature range of 110–170 °C is suited

3.4 · Nonenzymatic Browning (Maillard Reaction)

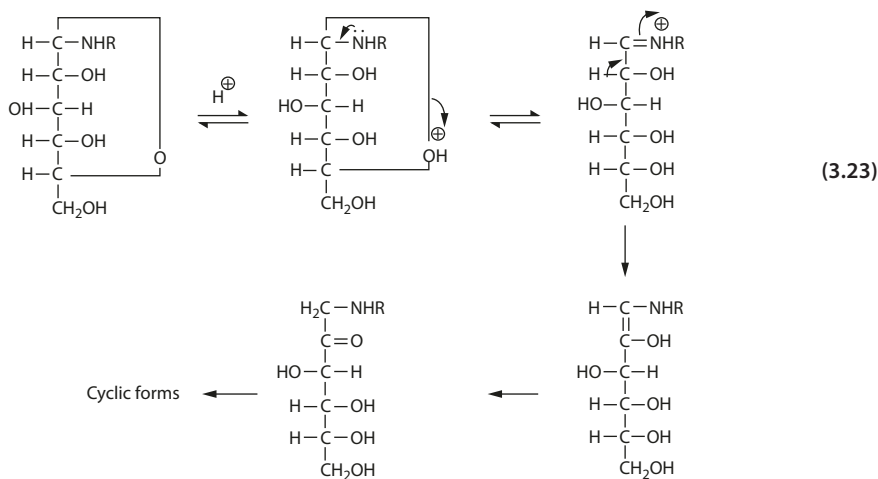
for Maillard product formation. The formation of products (Amadori compound, melanoid, and the Strecker degradation products) proceeds in increasing order of heating temperature. In the Maillard reaction, a pH range of ≥ 7 is often needed for product formation. As the pH goes acidic, protonation of the reactive amino group would render it less nucleophilic (Eq. 3.16). Water activity is important; optimal condition is in the range of 0.6. Simple reducing sugars react faster than oligosaccharides and complex sugars, and likewise with amines. The effect of these reaction conditions may be utilized as the basis to control nonenzymatic browning. Removal of the reactants should also work. An example is the removal of glucose by enzymatically converting it to gluconic acid with the use of glucose oxidase. This technology is employed for preventing dried egg products from browning and the formation of off-flavor due to high heat and dehydration.

3.4.1 Chemistry of the Reaction

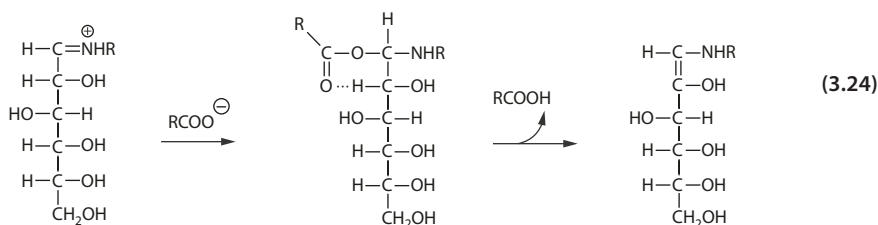
The formation of glycosylamine involves the addition of the amine to the acyclic aldehyde or the cation generated from the sugar by mutarotation. Most ketoses and hexoses exist in less than 0.05% as the open aldehydic form, the stability of which depends on the conformational orientation of the hydroxyl groups. The formation of acyclic cation $[R-CH=OH]^+$ by general acid catalysis enhances the reactivity of the carbonyl function. Nucleophilic attack of the amine at C1, followed by the elimination of the hydroxyl ion, results in forming the iminium ion of glycosylamine (Eq. 3.22) [27].



In the Amadori rearrangement outlined in Eq. 3.17, the initial step involves *N*-protonation. The mechanism has also been interpreted to involve the addition of the proton to the ring oxygen rather than the nitrogen atom, since the ammonium ion is stable and quite unreactive. Enolization of the resulting immonium ion by elimination of the hydrogen atom at C2 yields the enol form, 1,2-enaminol. Tautomerization of the enolic glycosylamine leads to the same end product, 1-amino-1-deoxy-2-ketose (Eq. 3.23).



The mechanism of Amadori rearrangement is dependent on the *N*-substituent of the amino component. The formation of the iminium ion is favored by strongly basic amines. However, the following enolization step by the elimination of the hydrogen atom at C2 is facilitated by a weakly basic amino component. In reactions involving amino acids, the enolization reaction is assisted by the carboxyl group. Condensation of the iminium ion with the carboxylate anion, followed by intramolecular decomposition, leads to the formation of the glycosylamine (Eq. 3.24).



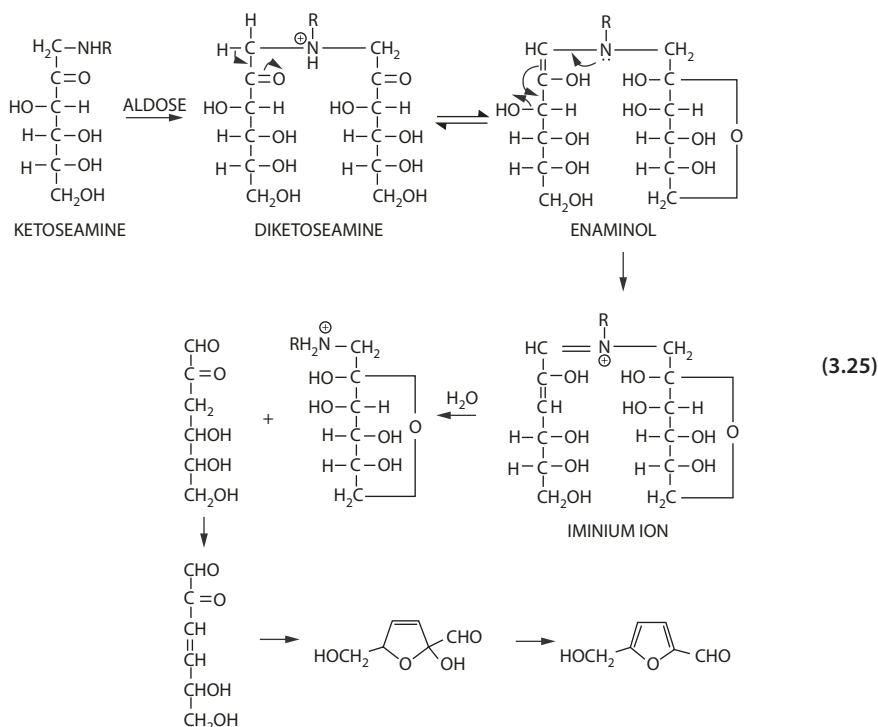
The Amadori rearrangement via 1,2-enolization (as presented in Eq. 3.17) is the dominant pathway under acidic conditions. In this pathway, the Amadori compound has the nitrogen protonated, and 1,2-enolization is assisted by the positively charged nitrogen acting as an electron sink. However, under weakly alkaline conditions, and

3.4 · Nonenzymatic Browning (Maillard Reaction)

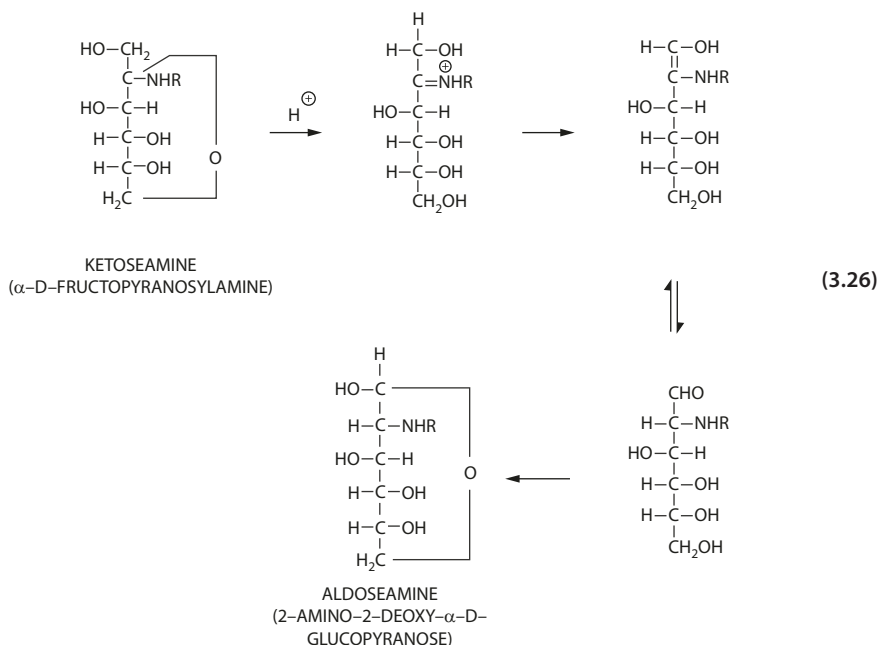
with a strongly basic secondary amino component, the 2,3-enolizatin pathway is favored. In the free-base form, as present in an alkaline condition, the Amadori compound has the electron density at C1 increased by the amino nitrogen that is unfavorable to 1,2-enolization, and this effect is further enhanced when the amino component is strongly basic.

However, the elimination step following the enolization exhibits the opposite enhancing effect. For the 1,2-enolization pathway, the elimination at C3 is accelerated by having the amino nitrogen in the free-base form, whereas the elimination step in the 2,3-enolization pathway is facilitated by a protonated nitrogen. Hence, degradation via 1,2-enolization occurs under conditions where the weakly basic amine is present in approximately equal proportions of the salt and the free-base forms. Similarly, the degradation involving 2,3-enolization occurs at optimum conditions in the presence of strong basic amine salts with excess amine [1].

The discussion thus far has focused on the monosubstituted amines. It is also possible that the ketosamine, once formed, can react with another aldose molecule. The resulting diketosamine undergoes rearrangement, and subsequent elimination to 3-deoxyglycosulose, which on dehydration, yields the glycosulos-3-ene. Cyclization and further dehydration of the latter yield the furfural (Eq. 3.25) [8]. This reaction pathway is probably more important in systems with high ratio of sugar-to-nitrogen substrates and at low pH conditions.



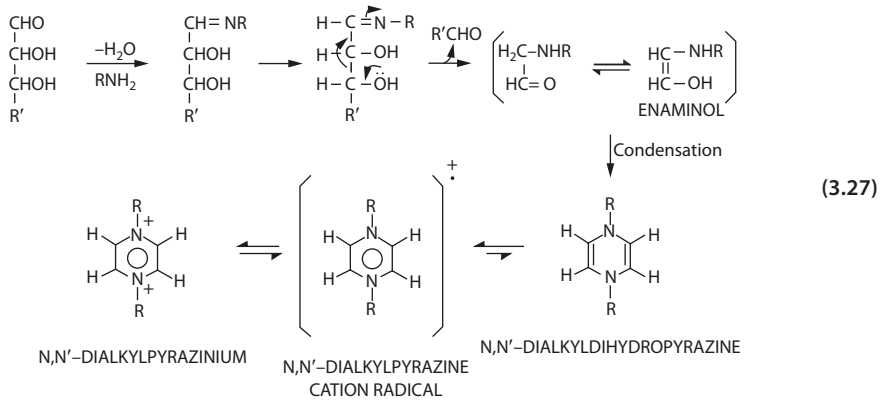
The Amadori rearrangement explains the conversion of an aldosylamine to a ketosamine. However, the reverse pathway in which a ketosamine is rearranged to yield the corresponding aldosamine also occurs in a similar mechanism, known as Heyns rearrangement, in the conversion of D-fructosylamine to 2-amino-2-deoxy-D-glucose (Eq. 3.26).



As suggested in Eq. 3.15, acid-catalyzed 1,2-enolization in the absence of amines also leads to the formation of furfurals. But the condensation of amino compounds allows enolization and elimination to occur near neutral pH and at low temperature, conditions commonly found in food systems. Furthermore, the degradation pathway of 2,3-enolization generates products such as C-methyl aldehydes, keto-aldehydes, ketols, and reductones that are important to flavor development.

Another pathway has been suggested involving sugar fragmentation and free-radical formation prior to the Amadori rearrangement [39]. The free radical develops rapidly at an early stage and decreases, while the formation of the Amadori compound and 3-deoxyglycosulose remains increasing. Carbonyl compound with enediol groups and amino compounds with primary amino groups are most effective in the formation of free radicals. Free-radical formation occurs at neutral pH, increases with pH, and disappears above pH 11. It has been shown that the radical is *N,N*-disubstituted pyrazine cation radical formed by dimerization of a two-carbon enaminal product from fragmentation of the glycosylamine. The mechanism, as shown in Eq. 3.27, involves (1) a reversible aldol reaction of the glycosylamine to yield the 2-carbon enaminal, glycoaldehyde alkylimine, and (2) condensation of the latter to form the unstable dialkyldihydropyrazine, which is

readily oxidized to the dialkylpyrazinium product via the cation radical intermediate. It has been shown that the dialkylpyrazinium product is likely an active intermediate for polymerization in browning.



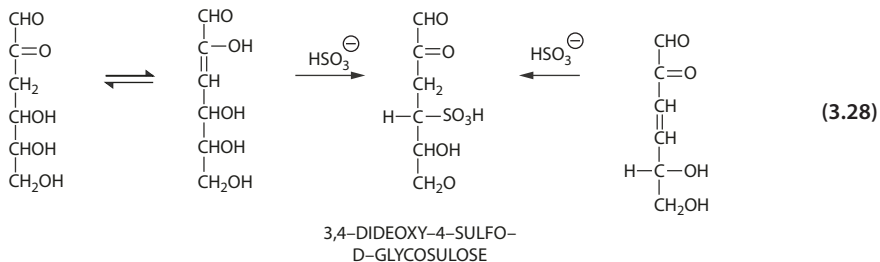
3.4.2 Secondary Reactions

Both degradation pathways via 1,2- or 2,3-enolization provide dicarbonyl compounds that are the key intermediate for subsequent reactions and degradations that are of significance in changing the characteristic attributes in food systems. (Refer to ► Chap. 6 for more discussion on secondary reactions.)

■ Reaction with Sulfite and Bisulfite

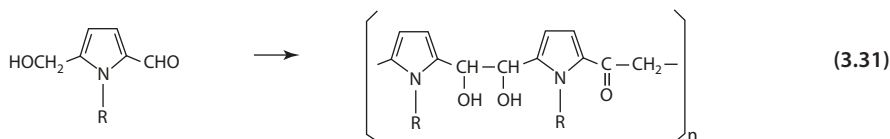
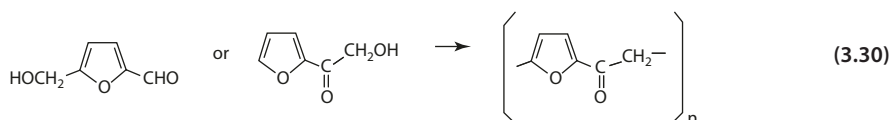
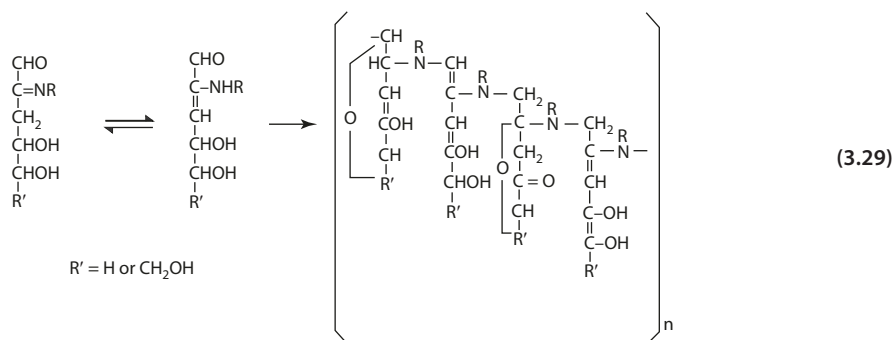
Sulfur dioxide has been used to inhibit the Maillard reaction occurred in food. Inhibition of nonenzymatic browning reaction involves the reaction between browning intermediates such as α,β -unsaturated carbonyls with sulfite to form stable sulfonate products.

At pH 6 or above, the 3-deoxyglycosulose in its enol form may have the C4 hydroxyl group replaced by sulfite ion, with possible inversion at C4 (Eq. 3.28). The α,β -unsaturated ketone, such as glycosulos-3-ene, reacts with sulfite by addition, and the same product, 3,4-dideoxy-4-sulfo-D-glycosulose, has been isolated and identified [1].



■ ■ Formation of Melanoidins

Melanoidin is a heterogeneous mixture produced by various combinations of polymerizing reactions. The Maillard reaction generates highly reactive intermediates, such as unsaturated carbonyls, α -dicarbonyls, furaldehydes, furans, pyrroles, furanones, and their derivatives. These low molecular weight substances rapidly interact with each other. A range of complex reactions may occur, including condensation, dehydration, cyclization, rearrangement, and isomerization, ultimately leading to the formation of brown polymers and copolymers. Various structures of melanoidin have been proposed based on model system studies. One proposal suggests the composition of repeating units of Schiff base formed between 3-deoxyglycosulose and its enamine as shown in Eq. 3.29 [30]. It has also been suggested that furans (Eq. 3.30) and pyrroles (Eq. 3.31), through polycondensation reactions, can form melanoidins of repeating units. The polymer structure consists of ether bonds and reductone systems. Another model has proposed that the low molecular substances may cross-link amino groups (protein amino acid side chains) to produce melanoidins.

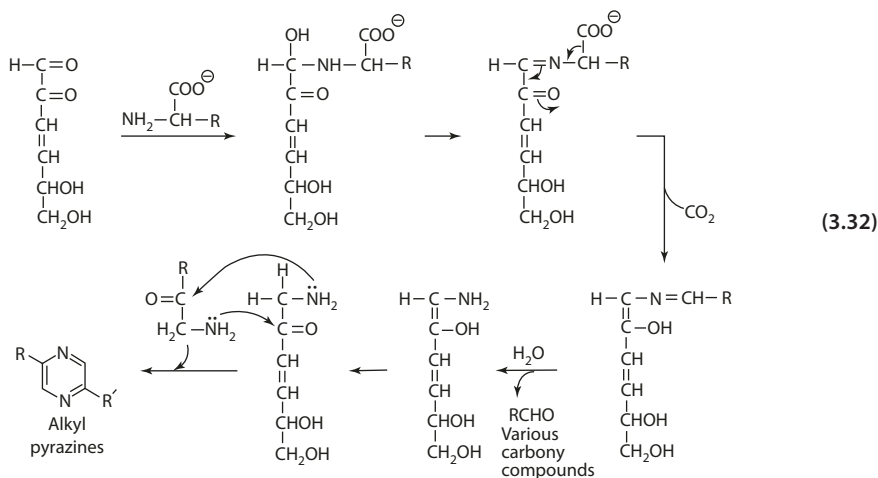


■ ■ The Strecker Degradation

The dicarbonyl compounds from the Maillard reaction react by forming Schiff base with the α -amino group of an amino acid. The enol form is an α -amino acid that decarboxylates readily to yield the enaminol. The enaminol undergoes self-condensation to a brown polymer or hydrolysis to the amine and the aldehyde, with the latter corresponding to the original amino acid with one less carbon (Eq. 3.32) [25]. The aldehydes derived from the Strecker degradation constitute many of the important flavor compounds in food systems.

3.5 · Complexes of Sugars with Metal Ions

It is mostly the amino acid that contributes to the odor quality of the product. The Strecker degradation has been implicated in the formation of acrylamide in heated foods containing high amount of asparagine. The α -amino group of asparagine reacts with a carbonyl source such as sugar to form a Schiff base [57]. Under high heat ($>100\text{ }^\circ\text{C}$), the Schiff base decarboxylates and (1) decomposes to form acrylamide or (2) further hydrolyzes to form 3-aminopropinamide that degrades to acrylamide.



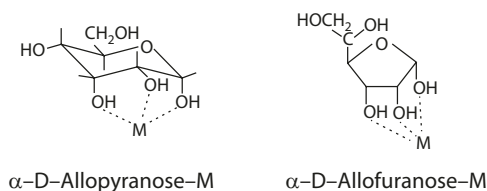
3.5 Complexes of Sugars with Metal Ions

3.5.1 In Neutral Solution

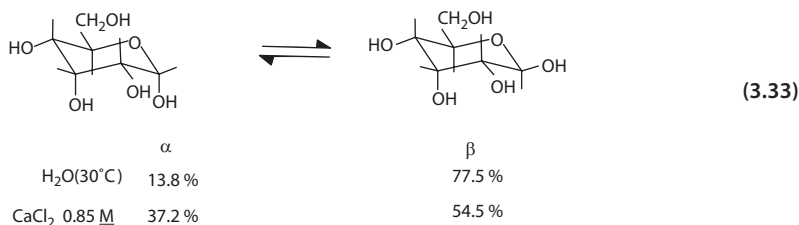
Sugar molecules containing axial-equatorial-axial hydroxyl groups in a six-member ring or a *cis,cis* sequence in a five-member ring form complexes with metal cations (■ Fig. 3.1). Only cations with an ionic radius $>0.8\text{ \AA}$ form complexes readily. Alkaline earth metals such as Ca^{2+} and Ba^{2+} usually form strong complexes. Univalent cations form only weak complexes.

Cis-inositol, with three axial-equatorial-axial sequences, possesses four sites for metal complexing, and subsequently the inositol-metal complex is very stable [2]. Reducing sugars, as a hemiacetal, is readily hydrolyzed by water, and the α - and β -anomers are interconverted via mutarotation to an equilibrium mixture. If either anomer is combined with metal cation to form stable complexes, the equilibrium is shifted in favor of that anomeric

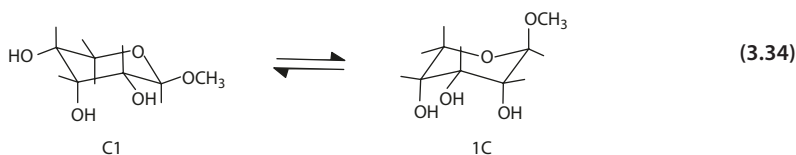
■ Fig. 3.1 Complexation of allopentopyranose and allopentofuranose with metal



form. For example, the α -anomer of allopuranose contains the axial-equatorial-axial hydroxyl groups at C1, C2, and C3. Addition of CaCl_2 increases the percent proportion of the α -anomer as indicated in Eq. 3.33.



Similar reasoning can be applied to the equilibrium shift in favor of the conformation that complexes with metal ions. In the equilibrium mixture of α -D-ribofuranoside, only the 1C configuration has the axial-equatorial-axial sequence to complex metal ions (Eq. 3.34). Addition of CaCl_2 shifts the equilibrium in favor of the 1C form.

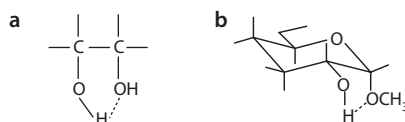


3.5.2 In Alkaline Solution

In alkaline pH, the sugar molecule readily loses protons to form alcoholates with metal hydroxides and oxides (■ Fig. 3.2a) [48]. Both alkaline metal and alkali-earth metal alcoholates can be prepared.

Polyhydroxy compounds are comparatively more acidic than monohydric alcohols. Dissociation constants for carbohydrates usually are in the range of 10^{-12} to 10^{-14} while ethanol about 10^{-16} . The higher acidity of carbohydrate is due to the inductive effect of neighboring substituents and intramolecular hydrogen bonding. Electron-withdrawing substituents tend to cause the neighboring hydroxyl group to be more acidic. For example, in a methyl- α -pyranoside, the hydroxyl group at C2 is more acidic. Hydrogen bonding between neighboring hydroxyl groups helps to stabilize the oxygen anion (■ Fig. 3.2b).

■ Fig. 3.2 Alcoholate a general structure and b methyl- α -pyranoside



3.6 Hydrocolloids

Hydrocolloids (gums) are a heterogeneous group of polymers, mostly polysaccharides characterized by their properties of forming viscous solutions/dispersions and even gels under some conditions. They provide texture, body, and mouthfeel to the food and may also impart freeze-thaw stability and control syneresis during storage of the food. Hydrocolloids are frequently classified as thickeners and gelling agents based on their food applications. Hydrocolloids that are used as thickening agents in food include starch, modified starch, xanthan gum, cellulose derivatives, guar gum, locust bean gum, gum arabic, and Konjac mannan. Hydrocolloid gelling agents include modified starch, agar, carrageenan, pectin, alginate, and cellulose derivatives. Gums form colloidal dispersion rather than true solutions. To obtain good dispersion (rapid separation of the powder particles when added to the aqueous phase), vigorous mixing is important. Alternatively, the powder can be dispersed in oil or in a water-miscible solvent, such as alcohol or propylene glycol. Once the particles have been dispersed, hydration can occur, sometimes with heating as in starch granules. Gelation usually involves the formation of junction zones and three-dimensional network, by cooling heated solutions or adding ions to induce cross-linking as in low-methoxy pectin.

3.7 Starch

3.7.1 Chemical Structure of Starch

Starch contains two polysaccharide fractions: amylose and amylopectin. Amylose typically makes up about 20–30% and much less in waxy starches. High amylose starch (amylostarch) can contain up to 70% amylose. Waxy starch contains $\geq 90\%$ amylopectin. Amylose is a linear chain of 10^5 to 10^6 Da, consisting of up to 4000 glucosyl residues connected by α -1,4-glucosidic linkages. The linear chain contains 2 to 8 α -1,6 branch points carrying side chains from 4 to 100 glucose units in length. Amylopectin is a much larger molecule compared to amylose, with a molecular mass of 10^7 to 10^9 Da and a DP (degree of polymerization) of 9500 to 16,000 glucose units. The molecule consists of a branched polymer of 95% α -1,4- and 5% α -1,6-linkages (■ Fig. 3.3).

Amylopectin has a cluster type structure with the branching points collected together toward the reducing end (■ Fig. 3.4) [40, 46]. The structure contains three types of chains: (1) A chains only connect to one other chain by α -1,6-linkages; (2) B chains connect to one other chain and also substituted by one or more other chains; and (3) a single C chain carries the sole reducing end group of the molecule. The distribution of chain length is classified into three groups: short chains of DP 14–18 (composed of outer A chains and inner B chains), longer chains of DP 45–55 (composed inner B chains), and a few very long B chains of DP > 60.

■ ■ Starch Granules

All starches are biosynthesized as granules containing densely packed amylose and amylopectins with relatively little water. Starch granules have diameters of 0.1 to 100 μm depending on the botanical origin and come in different shapes. Shapes may

Fig. 3.3 Amylose and amylopectin

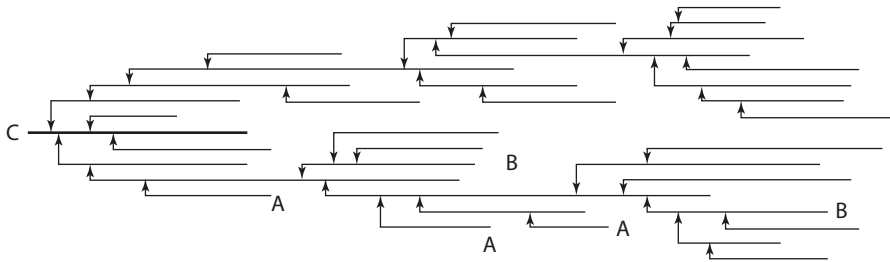
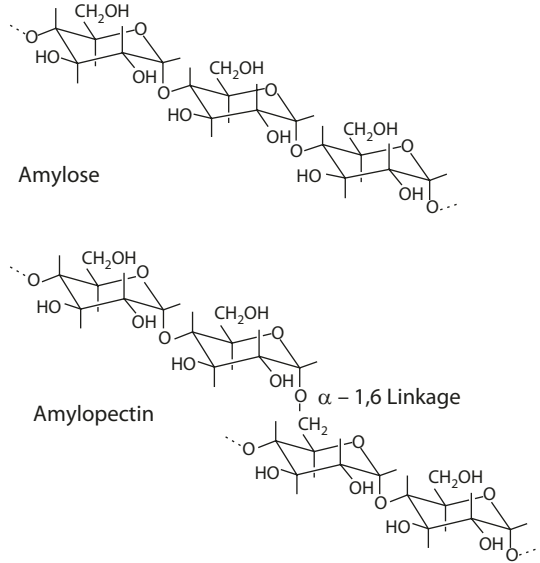
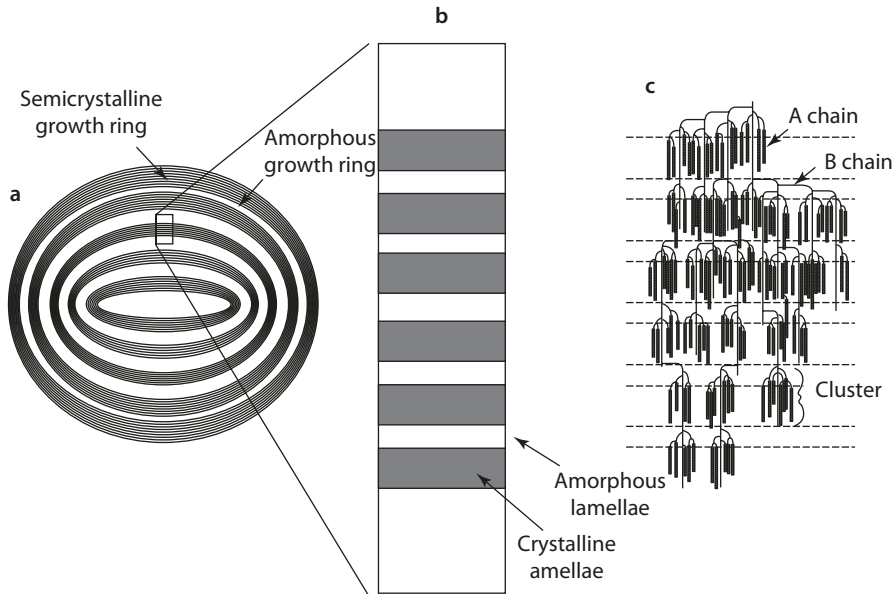


Fig. 3.4 The cluster model of amylopectin (From Manners [40] with permission. Copyright 1989 Elsevier)

assume spherical, polyhedral, or lenticular, and sizes decrease from potato ($<110 \mu\text{m}$) to wheat ($<30 \mu\text{m}$), corn ($<25 \mu\text{m}$), and rice ($<20 \mu\text{m}$). Starch granules contain amorphous (disordered single-chain) and crystalline (ordered double-helix) regions. The crystalline structure of different starches may vary in the packing order, leading to the existence of polymorphic forms, A (in cereal starch, e.g., corn, wheat, rice), B (in tuber starch, e.g., potato), and C (a mixture form as in tapioca) based on X-ray diffraction patterns. Both A and B types contain ordered arrays of double helices of similar conformations but differ in packing density of the double helices. A-type has a close-packed arrangement, whereas B-type adopts a more open arrangement containing more water [19].



■ **Fig. 3.5** Schematic diagram of starch granule. **a** A single granule consisting of concentric rings of alternating amorphous and semicrystalline layers. **b** Expanded view of the internal structure. **c** Cluster structure of amylopectin within semicrystalline growth ring (From Jenkins and Donald [28] with permission. Copyright 1995 Elsevier)

At the molecular level, the crystalline region is composed of amylopectin with double-helix formation of the outer branches. The amorphous region includes the branching points of amylopectin along with some neighboring portion of the chains (■ Fig. 3.5) [20]. Amylose molecules are located in this region as randomly interspersed radial chains, although a small amount may be trapped in the crystalline region as well. Interaction between amylose and amylopectin may cause a decrease in crystallinity. The crystalline and the amorphous regions form alternate lamellae, resulting in a multilayer structure, generally described as growth rings. X-ray diffraction shows a periodicity of 9–10 μm corresponding to the thickness of a single layer of combined amorphous and crystalline lamellae.

■ ■ Starch in Solution

In aqueous solution, the configuration of amylose largely exists as a random coil, with a very small amount of left-handed pseudohelical backbone. Amylopectin molecules assume a randomly branched structure. In the presence of complexing agents, such as fatty acids, the amylose assumes a helical structure, known as V-amylose [10, 45]. The methylene groups line the inner surface of the helix, creating a hydrophobic environment for complexing with the fatty acid molecule. The hydrophilic carboxyl group of the fatty acids locates outside the amylose V-helix. Helices with six, seven, or eight glucose units per turn (8 \AA) can exist (Refer to ► Chap. 1, ■ Fig. 1.23).

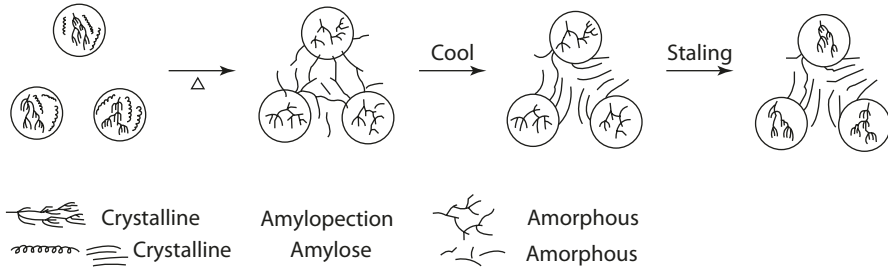


Fig. 3.6 Changes in a starch granule during heating and cooling (From Kulp [33] with permission. Copyright 1981 Taylor & Francis)

3.7.2 Gelatinization and Retrogradation

A characteristic feature of starches is their lack of cold-water solubility. For practical application, starch is dispersed in cold water and then hydrated by heating. Heating provides sufficient energy to disrupt the association of the starch chains. The granule starts to hydrate and swell, loses its birefringence, and imparts viscosity to the solution (■ Fig. 3.6) [33]. Starch is the most widely used food thickener and gelling agent.

Upon heating, the linear-chain amylose diffuses out of the swollen granules, forming the continuous phase outside the granules. The swollen granules are enriched in amylopectin losing its crystallinity. The resulting starch essentially consists of gelatinized, swollen, porous granules (mostly amylopectin) embedded within a solubilized amylose matrix [22].

Upon cooling and storage, the physical state of gelatinized starch gradually changes from an initially amorphous state to a more ordered crystalline state, and this re-formation of double helical and crystalline structure is called retrogradation. However, features such as lamella structure, growth rings, etc. in the original starch granular are not recovered. Retrogradation involves changes in both the solubilized amylose and the amylopectin in the gelatinized starch granule, each playing different roles in the process:

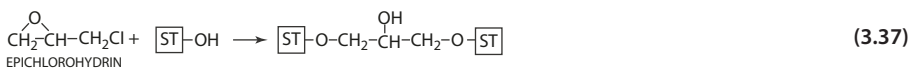
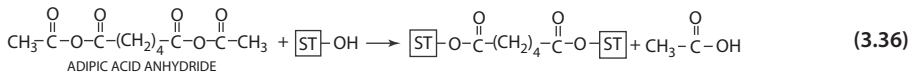
1. On cooling of the gelatinized starch, the flexible chains of amylose molecules interact by interchain association resulting in opaque gel network. In concentrated amylose solution (5–10%), realignment is rapid and disordered, and association of the molecules occurs at limited location, with water entrapped in the interstices. These changes attributed to the amylose fraction occur and are complete within 24 h. The process involving amylose is generally known to be short-term development. Amylose gel is thermally irreversible. The melting temperature is above 100 °C.
2. The amylopectin in the swollen granule recrystallizes resulting in long-term rheological and structural changes of the starch gel. Usually the B-type pattern is found. The increase in crystallinity is slow and continues for weeks. The process is thermally reversible and the crystallites melt below 100 °C. Compared to amylose, amylopectin has shorter chain segments and high number of branching contributing to lower stability. Recrystallization of amylopectin within the gelatinized granule is the primary cause of the staling of bread during storage. Optimal temperature for amylopectin crystallization is close to refrigeration temperature.

Starch-degrading enzymes, such as α -amylases, are often used for (1) maintaining the level of sugar for yeast fermenting and (2) maintaining and prolonging the softness of bread. In the latter case, the added amylases hydrolyze and reduce the chain length of the outer branches of amylopectin. Shorter chains would in turn have less ability to form double helices or recrystallize. Further, the crystallization process is thermally reversible, which explains why it is possible to refresh staled bread by oven heating. The amylopectin crystallites melt, and the bread regains softness to some extent. Emulsifiers are used in bread making, due to the ability to complex with amylose and the long outer branches in amylopectin. The effect is to prevent chain association in the formation of crystallites.

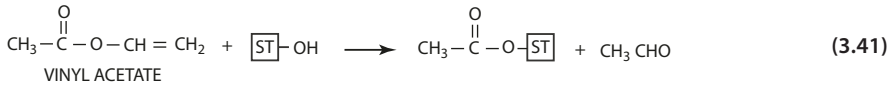
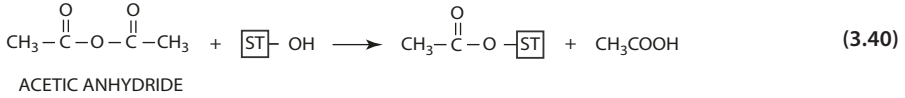
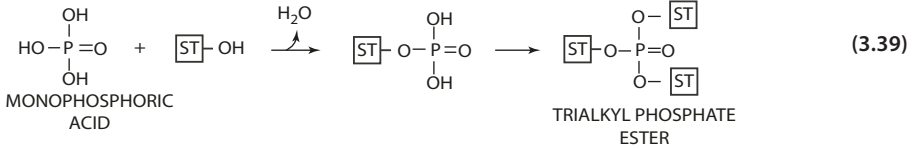
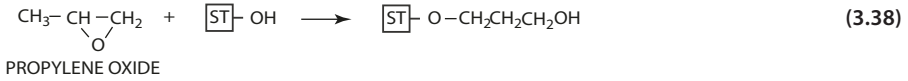
3.7.3 Chemical Modification of Starch

The rheological characteristic of starch can be changed by chemically modifying the functional groups in the starch molecule [37]:

1. **Cross-linking:** It involves the reaction between the hydroxyl groups with di- and polyfunctional reagents. Phosphorus oxychloride (Eq. 3.35), adipic acid anhydride (Eq. 3.36), and epichlorohydrin (Eq. 3.37) are used to form ester linkages with the hydroxyl group. The cross-linked starch exhibits more resistance to acid hydrolysis, increased shear resistance, greater heat tolerance, and higher temperature requirement for hydration of the granules. The modified starch is used in acid food products.



2. **Substitution with stabilizing functional groups:** Substituted starch is utilized in frozen or refrigerated food products. The reaction involves the addition of monofunctional groups, such as hydroxylpropyl (Eq. 3.38), phosphate (Eq. 3.39), and acetyl (Eqs. 3.40 and 3.41). Attachment of these functional groups interferes with the association of the amylose molecules by hydrogen bonding and allows the starch to remain hydrated, clear, and stable. The modified starch has reduced temperature required for hydration, increased viscosity in solution, reduced syneresis, and increased stability to freezing and freeze-thaw.
3. **Cleavage:** Acid hydrolysis is used to produce limited, random cleaving of the starch molecules to obtain a modified starch with less viscosity, low-temperature hydration, low resistance to heat, and greater retention of gel structure. Oxidative cleavage with sodium hypochlorite produces modified starch with excellent flow properties that will not cake during processing.

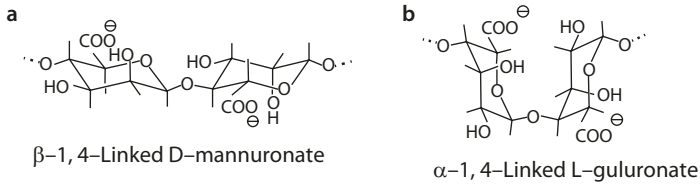


3.7.4 Starch Structure and Digestibility

According to the digestibility (based on the action of amylase enzymes and the rate and extent of digestion in vitro and in vivo), starch is classified into three types [15]:

1. Rapidly digestible starch (RDS): This type of starch is rapidly (within 20 min) converted to glucose by enzymatic digestion. Examples are freshly cooked starchy foods (rice, potato, bread, legumes).
2. Slowly digestible starch (SDS): This type of starch is slowly converted to glucose (within 20–120 min) by enzymatic digestion. Examples include unrefined starch from cereals, legumes, roots, and tubers and foods made from these starches with processing control in preserving the integrity of the starch crystalline structure. The loss of SDS content in cereal foods correlates with the extent of starch gelatinization (destruction of the crystalline structure), which is in turn affected by hydrothermic parameters (temperature, moisture, time, pressure, etc.) in the processing.
3. Resistant starch (RS) is defined as a type of starch that is not hydrolyzed by enzymatic actions in the small intestine within 120 min. Digestion of the starch may or may not occur in the colon. RS is further classified into three subtypes:
 - A. RS type 1: This type of starch resists digestion because it is physically inaccessible due to its entrapment within whole or partly milled grains or seeds. Intact cell wall materials form a physical barrier and also inhibit swelling and dispersion of starch. Examples include brown rice and whole grain bread.
 - B. RS type 2: This type of starch resists to digestion because of the effect of structural conformation. B- and C-type crystallites tend to be more resistant to digestion. Examples are raw potato, banana starch, and high amylose cornstarch.
 - C. RS type 3: This category consists mainly of retrograded starch. Cooked and cooled potatoes, bread, and cornflakes are typical examples.

In addition, chemically modified starch, such as esterification, cross-linking, is less susceptible to enzymatic digestion.



■ Fig. 3.7 a D-mannuronate and b L-guluronate residues

3.8 Alginate

3.8.1 Chemical Structure of Alginate

Alginates are extracted from a number of brown seaweeds (Class Phaeophyceae, species *Fucus serratus*, *Ascophyllum nodosum*, *Laminaria digitata*, *Laminaria cloustonii*, *Ecklonia maxima*, and *Macrocystis pyrifera*).

Alginic acid is a linear polymer of 1,4-linked β -D-mannuronic acid and α -L-guluronic acid (■ Fig. 3.7). Commercial alginates have a degree of polymerization in the range of 100 to 1000.

Alginic acid is insoluble in water. Salts (alginates) of alkali metals (e.g., sodium, potassium) are soluble and salts of di- and trivalent metals (e.g., calcium) are insoluble. In practice, the seaweed is acidified to remove undesirable impurities, and the alginic acid is then neutralized to a soluble salt for extraction [36].

The D-mannuronate residues and the L-guluronate residues are arranged in the following sequences:

1. Mannuronic acid block: -M-M-M-M-M-
2. Guluronic acid block: -G-G-G-G-G-
3. Alternating block: -M-G-M-G-M-

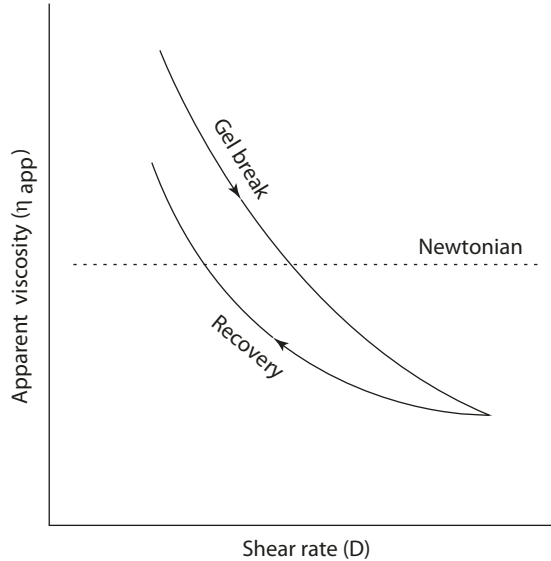
Each block type contains about 20 residues. The homogeneous block types (1 and 2) are comparatively more resistant to hydrolysis than the alternating block type.

3.8.2 Gelling

Alginate solution gels quickly with calcium ions. In order to produce a uniform gel structure, soluble calcium salts are not suitable. Instead, slightly soluble calcium salts such as calcium citrate, calcium tartrate, or dicalcium phosphate dihydrate are used. Calcium salts that are insoluble in neutral solution (e.g., calcium carbonate, dicalcium phosphate anhydrous), but become soluble with increasing acidity, are also used. In this case, the pH of the system can be controlled by using glucono- δ -lactone (which hydrolyzes slowly in solution to gluconic acid). (Refer to Eq. 2.40.) Gels can also form by controlling diffusion of soluble calcium salts through the alginate solution. This last method is used primarily in the production of fabricated foods.

At low concentrations of calcium (less than 35% of the sodium replaced in a 1% sodium alginate solution), the alginate solution is thixotropic, breaking down to a liquid on agitation and reverting back to a thick solution or weak gel on standing. The apparent viscosity decreases with increasing shear rate and also is related to the duration of the

Fig. 3.8 Viscosity versus shear rate for thixotropic flow

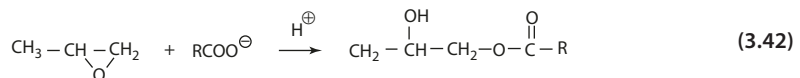


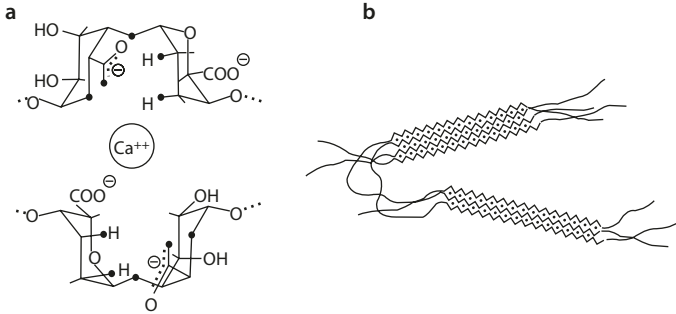
shear. With the same shear rate, the apparent viscosity decreases with time. The resulting plot of apparent viscosity against shear rate shows a hysteresis loop: deformation where the thinning and thickening do not coincide (Fig. 3.8).

Alginate gels are not thermally reversible. The mechanism of gelation has been shown to be the interaction between calcium ions and polyguluronate blocks. Polymannuronic acid exists as a flat ribbonlike chain with the sugar units in the C1 chair form equatorially 1,4-linked. However, polyguluronic acid has sugar units in the 1C chair form, diaxially 1,4-linked to form chairs of a rodlike conformation favorable for the binding of calcium ions. The polyguluronate is shown to form chains of twofold symmetry, which allows four-oxygen coordination involving C6–O, C5–O, C2–O, and C3–O (Fig. 3.9a). The association between polyguluronic acid and calcium ions provides junctions cross-linking the alginate polymers into a three-dimensional network. This arrangement has been termed the “eggbox” model (Fig. 3.9b) [23, 47].

Alginate has found wide applications as a gelling agent in the production of fabricated foods, such as artificial cherries, gelled confectionary powder with dairy desserts, and fabricated onion rings. It is also used as a thickener for sauces and condiments, sausages, and bakery fillings, as a stabilizer for the cream to prevent ice crystal formation, and for whipped cream and toppings, yogurt, and milk drinks. The concentration of alginate used in food gel ranges from 0.5% to 1.5%.

At low pH, alginate is converted to alginic acid, which becomes increasingly insoluble and finally precipitates. For the alginate to be used as a stabilizer in acid foods, the carboxylic groups are esterified partially with propylene oxide to form propylene/glycol alginate esters (Eq. 3.42).





■ **Fig. 3.9** a Interaction of polyguluronate with Ca^{++} to form an “eggbox”; b the “eggbox” model (From Rees and Welsh [47] with permission. Copyright 1977 John Wiley & Sons)

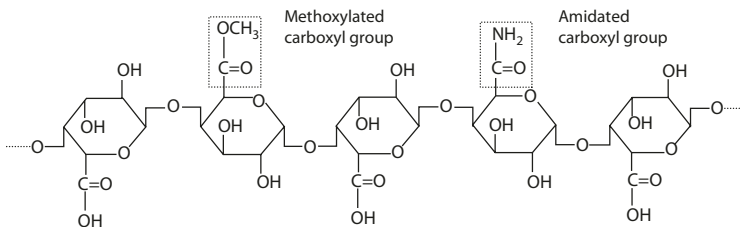
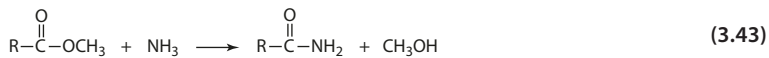
3.9 Pectin

3.9.1 Chemical Structure of Pectin

Commercial pectin is obtained from apple pomace and citrus fruits pulp. The native pectin (protopectin) in the pulp is made soluble during extraction with hot, acidic solution. Pectin is a polysaccharide of 30–100 kDa with 150–500 galacturonic acid units and the carboxyl groups partially esterified with methoxy groups (■ Fig. 3.10). The backbone chain also contains residues of L-rhamnose and is branched with side chains composed mainly of β -D-galactopyranose and α -L-arabinofuranose.

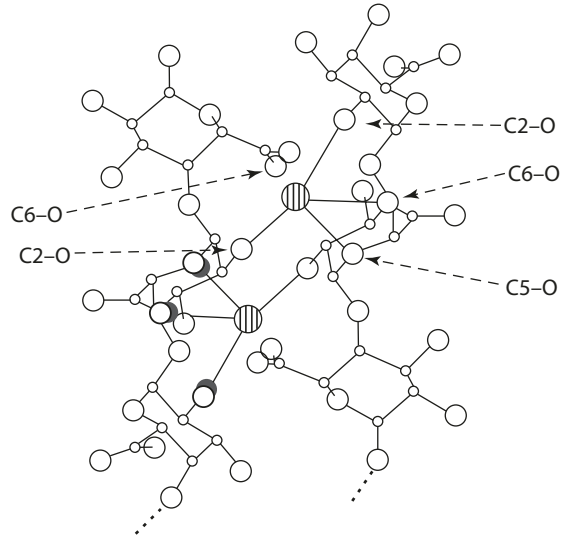
3.9.2 Classification of Pectin

The percentage of galacturonic acid units esterified is called the degree of esterification (DE). Amidation occurs when ammonia is used to de-esterify pectin containing a high percentage of methoxy groups (Eq. 3.43).



■ **Fig. 3.10** Structure of pectin

■ **Fig. 3.11** The calcium pectate unit cell (From Walkinshaw and Arnott [54] with permission. Copyright 1981 Elsevier)



3.10 Cellulose

3.10.1 Chemical Structure of Cellulose

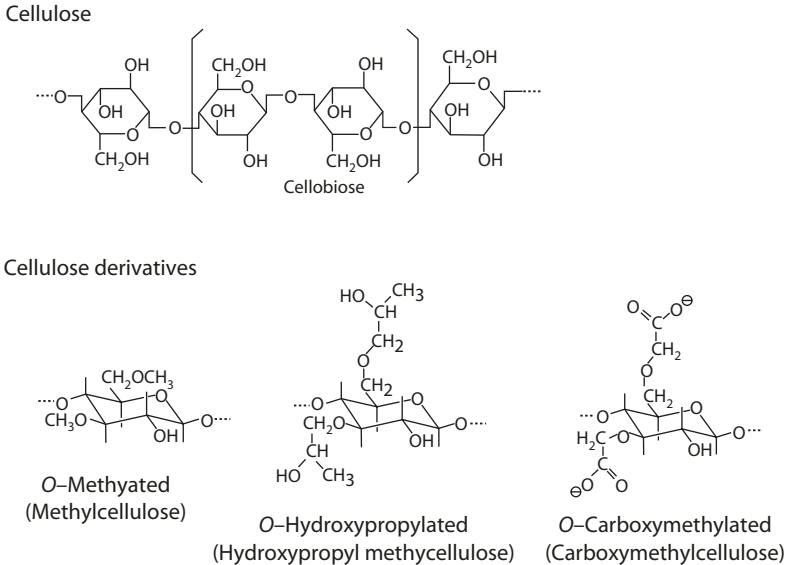
Cellulose is the structural material of plant cell walls. Chemically, it is a polysaccharide chain of repeating cellobiose units (consisting of two glucose units linked by β -1,4-linkage) (■ Fig. 3.12a). The hydroxyl groups may be substituted with methyl, hydroxylpropylmethyl, or carboxymethyl groups (■ Fig. 3.12b).

3.10.2 Gelling

The gelling characteristics depend largely on (1) degree of polymerization (DP), usually in the range $>100,000$, and (2) degree of substitution (DS). The maximum theoretical degree of substitution is 3.0 when all the hydroxyl groups are derivatized. Usually the ether substituents are unevenly distributed, with some segments of the polysaccharide chain more densely substituted. As the DP increases, the viscosity of the solution increases. The degree of substitution may increase or decrease the viscosity depending on the nature of the substituents.

■ ■ Methylcellulose [47]

O-Methylated cellulose is stable over a wide pH range of 3.0–11.0. It exhibits an unusual property of thermal gelation. It gels when heated and melts upon cooling. The gelling temperature ranges from 50 to 70 °C for most methylcellulose products, forming heat set



■ Fig. 3.12 Structure of a cellulose and b cellulose derivatives

gels [42]. This is in contrast to the common gelling characteristics of other polysaccharides, such as carrageenan, agarose, and galan, which form cold set gels.

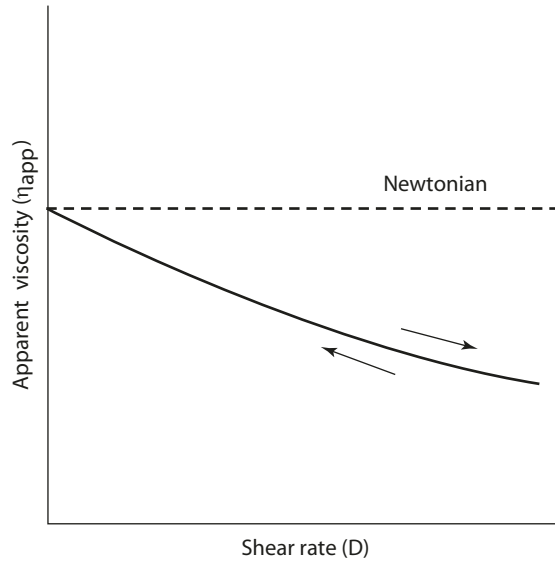
The phenomenon of thermal gelation can be explained in terms of the structural effect of the polysaccharide molecules in water. In solution, the polysaccharide molecules are hydrated, but the molecules contain some segments that are more densely substituted than the others and are less water soluble. An increase in temperature weakens the hydrogen bonds maintained by water molecules and facilitates phase separation of the less polar segments. The relatively nonpolar densely substituted segments are excluded from the liquid phase to form clusters analogous to lipid micelles, while the less densely substituted segments remain in solution, cross-linking the clusters of less polar segments into an extended network.

Formation of clusters of less polar segments depends on the degree of hydrophobicity along the chain, and not the cooperative binding of the chains through electrostatic interactions among substituted groups or with cations as described in the cross-linking of other gel types. Methylcellulose with its slight affinity for fat molecules (less hydrophilic than most other hydrocolloids), combined with its gelling property, forms a good coating for fried foods. Methylcellulose (and hydropropyl methylcellulose to a lesser degree) is utilized to reduce oil absorption/uptake in deep-fried foods [53].

■ Hydroxypropyl Methylcellulose [32]

O-Hydroxypropylated cellulose gels when heated and precipitates at high temperatures. During the substitution reaction, the hydroxypropyl groups are not attached to the hydroxyls of the glucose residues, but some may condense with each other to form propylene glycol side chains. These hydrophobic side chains are capable of forming clusters in a way similar to the O-methylated segments, reinforcing cross-linking and end up with a tighter network.

■ **Fig. 3.13** Viscosity versus shear rate for pseudoplastic flow



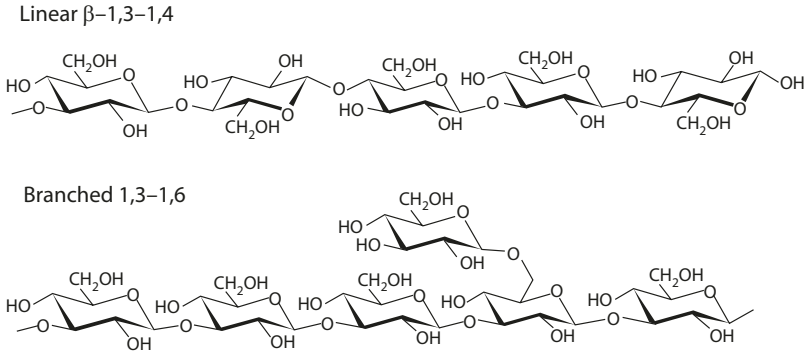
■ ■ Carboxymethyl Cellulose [3]

Carboxymethylated cellulose (CMC, cellulose gum) has properties quite different from the two derivatives described above. Here, the substituent contains a hydrophilic carboxyl group, which tends to make the polysaccharide more soluble in water. In general, all carboxymethyl cellulose solutions (and in fact, many polysaccharide solutions) are pseudoplastic, in which the apparent viscosity decreases with increasing shear rate and is independent of the duration of the shear (■ Fig. 3.13). When the shear stress is removed, it instantly reverts to its original viscous state.

The viscosity of the cellulose gum solution decreases with high temperature and increases with acidic pH. High temperature, especially long periods of heating, degrades the cellulose. Under acidic pH, the less soluble carboxylic acid predominates and the viscosity increases. Carboxymethyl cellulose solutions exhibit maximum stability at a pH of 7–9.

The polysaccharide chain is dispersed in solution in a loose network. Maximum viscosity is obtained when the polysaccharide chains dissolve in water while partially retaining the loose network. Increasing the degree of substitution makes the cellulose more hydrophilic and therefore more dissolving. It finally reaches a point when the polysaccharide network is completely disaggregated and the viscosity drops.

Gels can be produced by the addition of trivalent metal salts, such as aluminum acetate, to the cellulose gum solution. The polysaccharide molecules are cross-linked by the metal ions between the carboxymethyl groups. The gel texture depends on the concentration of the gum, the ratio of metal ions to carboxylate anions, pH, and degree of polymerization. High concentration, low DP, and high DS yield more elastic gels. High concentration of metal ions gives brittle gels. High temperature and low pH tend to increase the solubility of aluminum acetate and speed up its release into the solution and hence the rate of gel formation.



■ Fig. 3.14 Structure of two common β -glucans

3.11 β -Glucan

β -Glucan refers to a common structure composed of a polymeric linear chain of β -(1,3)- and/or β -(1,4)-D-glucopyranosyl units, along with side-chain branches of varying lengths. Thus, cellulose is also called a β -(1,4)-glucan. Various structural forms are found in bacteria, algae, fungi, and plants, including linear (1,3), linear (1,3;1,4), side-chain branched (1,4;1,6), cyclic (1,2), and others (■ Fig. 3.14). Common names have been assigned to some of these β -glucans. For example, curdlan refers to bacteria linear (1,3) β -glucan, and laminarin refers to side-chain branched (1,3;1,6) β -glucan from algae *Laminaria* spp. [5]. The type of β -glucan of great interest to food scientists is the linear (1,3;1,4) β -glucan present in the cell wall of the endosperm and the aleurone layer of barley, oats, wheat, sorghum, and other cereals (■ Table 3.2). Whole grain oat contains 2–8% and oat bran from 6% to 12% β -glucan. Products of β -glucan with much higher concentrations can be obtained in industrial processing, giving greater flexibility in food formulation.

Cereal (1,3;1,4) β -glucans consist of block arrangements of two or three adjacent 1,4-linked units (cellotriose and cellotetraose blocks) separated by a single 1,3-linked unit (■ Fig. 3.15). The distribution of these blocks is random. About 10% of the glucan polymer contains longer cellulosic sequences of 5 to 14 β -D-glucosyl residues. The (1,3) linkages cause interruption of the conformational chain structure of the polymer, forming a molecule highly soluble and flexible [34]. The ratio of cellotriosyl to cellotetraosyl blocks provides a fingerprint of a particular grain: 2:1 for oats, 3:1 for barley, and 4:1 for wheat.

The molecular size of cereal β -glucans varies considerably because of varietal and environmental (growth) factors as well as methods of analysis (extraction, purification, separation, detection). Oat, barley, and rye in the range of $65\text{--}3100 \times 10^3$, $31\text{--}2700 \times 10^3$, and $21\text{--}1100 \times 10^3$ kDa, respectively, have been reported [34]. Oat and barley β -glucans average of 1.3 million kDa. β -Glucan can easily be depolymerized by enzymatic or chemical hydrolysis during food processing.

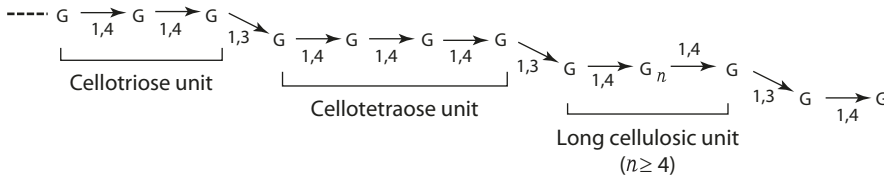
β -Glucan has the ability to form very viscous solution at low concentrations due to its high molecular weight and high solubility critical. High viscosity at low concentrations leads to large liquid volumes, and β -glucan exists as random coils in aqueous media,

■ **Table 3.2** Comparative composition of cell walls of some cereal grains

Cereal	Origin of cell wall	Component ^a		
		Cellulose	β -Glucan	Heteroxylan
Wheat	Aleurone	2	29	65
	Starchy endosperm	4	20	70
Barley	Aleurone	2	26	71
	Starchy endosperm	2	75	20
Rice	Starchy endosperm	28	20	27

From Stone [50]

^aPercent by weight

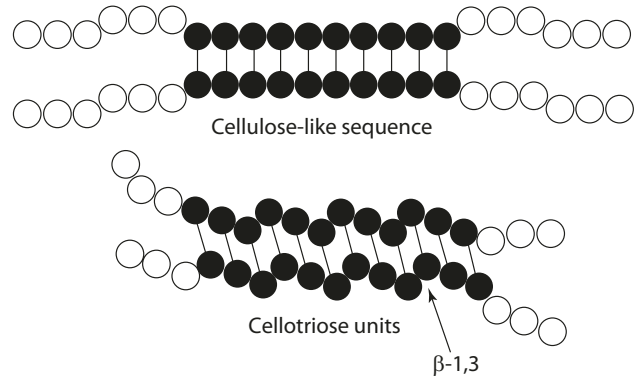


■ **Fig. 3.15** Block arrangement of cereal (1,3;1,4) β -glucan (From Lazaridou and Biliaderis [34] with permission. Copyright 2007 Elsevier)

typical of non-interacting polysaccharides. This is due to irregularly spaced (1,3) linkages interrupting the β -glucan polymer, resulting in high flexibility and high solubility in water. However, not all cell wall β -glucan polymers are soluble. The polydispersity of β -glucan has been demonstrated relating to the presence and abundance of longer blocks of adjacent (1,4) linkages in the β -glucan structure. The interactions between β -glucan and other cell wall polysaccharides also have impacts on the solubility. Processing, isolation, extraction, and fractionation of β -glucan are known to cause depolymerization, resulting in modified rheological behavior and structural changes.

The flow behavior of β -glucan solution is particularly sensitive to the concentration. A β -glucan solution below 0.2% (for oat) is essentially Newtonian, but becomes non-Newtonian, shear-thinning, or pseudoplastic as the concentration increases. Above a minimum shear rate, the apparent viscosity declines with increasing shear rate. Cereal β -glucans have been shown to form gels under isothermal conditions of 5–45 °C and at high polymer concentration of 4–12% w/v. Gelation involves interchain cellulose-like associations through the formation of intermolecular hydrogen bonds between the long β -1,4-linked segments (cellulose-like) in the β -glucan chains [49, 56]. An alternative model suggests that several cellotriosyl blocks occurred consecutively in the polymeric chains associate to form aggregated networks (■ Fig. 3.16) [7, 52]. X-ray diffraction patterns of lichenan and barley β -glucans suggest sequences of three consecutive cellotriosyl blocks may form stable antiparallel complexes [52].

Fig. 3.16 Chain interactions in (1,3;1,4) β -glucan for gelling (From Bohn & Kulieke [7] with permission. Copyright 1999 Elsevier)



The use of β -glucans as functional food ingredient is based on their rheological properties of high viscosity in dilute concentration. β -Glucans are suitable alternatives as non-caloric thickening and stabilizing agents in beverages, sauces, salad dressings, and ice creams. It may serve as replacement of traditional beverage thickeners such as gum arabic, pectin, xanthan gum, and carboxymethyl cellulose. β -Glucans are useful fat substitutes in dairy products, for example, in the manufacture of low-fat ice cream and low-fat cheese.

A health claim that β -glucan soluble fiber from either whole oats or barley or a combination of whole oats and barley at a level of 3 g or more per day may reduce cholesterol and lower risk of coronary heart diseases has been approved by the US Food and Drug Administration. One or more of the whole oat or barley foods should contain at least 0.75 g of soluble fiber per reference amount customarily consumed of that food product [16]. The whole oat and barley sources include:

1. Oat bran is produced by grinding oat groats or rolled oats and separating oat flour into fractions. Oat bran fraction contains at least 5.5% dry wt. basis of β -glucan soluble fiber and a total dietary fiber content of 16%.
2. Rolled oat (oatmeal) is produced from dehulled, oat groats by steaming, cutting, rolling, and flaking. It provides at least 4% of β -glucan soluble fiber and total dietary fiber content of at least 10%.
3. Whole oat flour is produced from dehulled oat groats by steaming and grinding. It provides at least 4% of β -glucan soluble fiber and a total dietary fiber of at least 10%.
4. Oatrim is the soluble fraction of α -amylase treated oat bran or whole oat flour. It provides up to 10% β -glucan soluble fiber.
5. Whole grain barley and dry milled barley grain: Dehulled whole grain barley provides at least 4% β -glucan soluble fiber. Dry milled barley products include barley bran, barley flakes, barley grits, pearl barley, barley flour, barley meal, and sieved barley meal, produced by dry milling techniques of dehulled barley grain. These products contain at least 4% of β -glucan soluble fiber and at least 8% of total dietary fiber.

6. Barley betafiber is partially hydrolyzed β -glucan obtained in the ethanol precipitated soluble fraction of cellulase and α -amylase-hydrolyzed whole grain barley. It provides at least 70% β -glucan soluble fiber.

3.12 Hemicellulose

Hemicellulose is found together with cellulose, lignin, and pectin in plant cell walls. The name hemicellulose is designated for cell wall polysaccharides extractable by aqueous alkali after delignification, and its composition varies with the plant source.

Unlike cellulose, which has a degree of polymerization (DP) in the range of 6000 to 10,000, hemicellulose is commonly composed of 50–100 units. Most hemicelluloses are heteropolysaccharides containing two to four different types of sugar residues and can be classified based on the backbone chains into (1) xylans, (2) mannans, and (3) galactans [55].

The most interesting hemicelluloses are the arabinoxylans. Cold-water extraction of wheat flour and subsequent fractionations of the extract result in a product commonly called water-soluble pentosans (a term for any plant polysaccharides that yield pentoses upon acid hydrolysis). Pentosans are known to exhibit high water binding and gel formation properties as important functional attributes in dough development and bread baking. One major polysaccharide component of the water-soluble pentosan is arabinoxylans.

The chemical structure of arabinoxylan is a xylan backbone of β -1,4-linked xylose, with single α -L-arabinofuranosyl side groups attached randomly to the C2 or C3 position (■ Fig. 3.17). Other side groups include ferulic acid, acetic acid, and methyl glucuronic acid. The α -L-arabinose side groups prevent the association and precipitation of the arabinoxylan polymer. Removal of the side chains causes precipitation. One of the unique properties of pentosans is their ability to form gels via cross-linking under oxidative conditions (e.g., H_2O_2 -peroxidase present in flour). The ability of “oxidative gelation” is due to the small amount of ferulic acid present in the arabinoxylan (■ Fig. 3.18a). The ferulic acid residues self-cross-link in part responsible for the formation of the three-dimensional network (■ Fig. 3.18b) [43]. Ferulic acids may also cross-link with tyrosine residues in proteins involving aromatic rings (■ Fig. 3.18c). Another possible reaction involves 1,4-addition of the α,β -unsaturated bond of the ferulic acid as indicated in ■ Fig. 3.18d [26]. These types of cross-linking are believed to be the cause of increase in viscosity and possibly gelling in flour suspension. In dough, the cross-linked network retains water in the interstices. About 23% of the water is associated with the pentosan fraction. Since pentosans do not coagulate or retrograde, they tend to decrease the rate of staling in bread. Other properties such as crumb characteristics, bread volume, and elasticity are also improved [12].

3

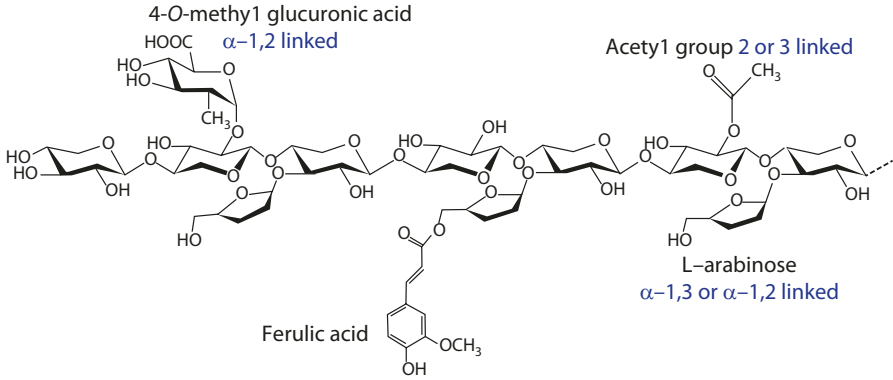


Fig. 3.17 Structure of glucuronoarabinoxylan

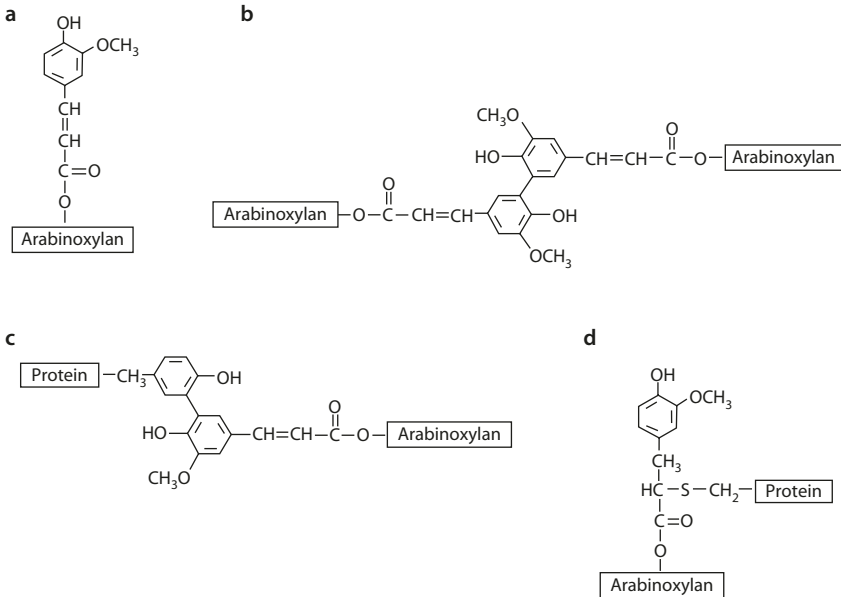


Fig. 3.18 a Ferulic acid, b self-cross-linked, c cross-linked with tyrosine, and d cross-linked with thiol

3.12.1 Dietary Fiber

The codex definition of dietary fiber means carbohydrate polymers with ten or more monomeric units, which are not hydrolyzed by endogenous enzymes in the small intestine and belong to the following categories:

1. Edible carbohydrate polymers naturally occurring in the food as consumed
2. Carbohydrate polymers, which have been obtained from food raw material by physical, enzymatic, or chemical means and which have been shown to have a physiological effect of benefit to health as demonstrated by generally accepted scientific evidence to competent authorities

- Synthetic carbohydrate polymers which have been shown to possess a physiological effect of benefit to health as demonstrated by generally accepted scientific evidence to competent authorities [29]

Practically, all plant cell wall polymers can be included in these categories. Resistant starch in general may also be considered a form of dietary fiber.

In terms of functionality and nutritional descriptions, it may still be useful to classify fibers into soluble and insoluble in aqueous systems. Insoluble fibers include cellulose, hemicellulose, and lignin present in plant cell wall. Food sources of insoluble fibers include whole grains, brans, and nuts. These fibers come from the remnants of plant cell walls. These cell wall polysaccharides have pseudocrystalline structures held by hydrogen bonds and are therefore insoluble in gastrointestinal fluid and poorly fermented by gut microbes. Soluble fibers are found primarily in the space between the cell walls called the middle lamella. These fibers include β -glucan, pectin, gum, and some hemicellulose, which are noncrystalline and hydrophilic, forming viscous colloidal suspension (sols) or gels in aqueous solution. Food sources of soluble fibers include oats and oatmeal, legumes, barley, fruits, and vegetables. Soluble fiber can be extensively fermented by gut microflora.

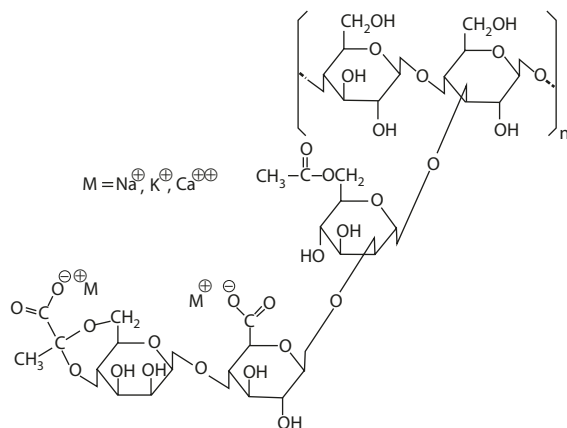
3.13 Xanthan Gum

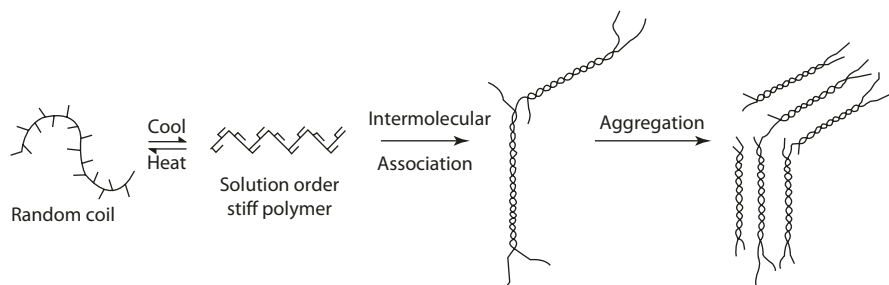
3.13.1 Chemical Structure of Xanthan Gum

Xanthan gum is produced by aerobic fermentation of *Xanthomonas campestris* culture in a medium of carbohydrates and nutrients. The gum is precipitated with isopropanol, dried and milled.

The polymer backbone consists of 1,4-linked β -D-glucose, which is similar to cellulose in this respect. A trisaccharide side chain composed of one glucuronic acid and two mannose units branches from the 3-position of alternate glucose units. About half of the terminal D-mannose residues contain a pyruvic acid residue linked via the keto group to the 4- and 6-positions (■ Fig. 3.19).

■ Fig. 3.19 Structure of xanthan gum





■ Fig. 3.20 Gelling mechanism of xanthan gum

3.13.2 Gelling

In solution, the trisaccharide side chain aligns with the backbone, forming a stiff polymer that is stable to a temperature in excess of 100 °C before transforming into the coil form. The stiff chains can also exist as a double-helix or multiple-stranded assembly through intramolecular associations forming a network of entangled, stiff, rod-shaped polymers (■ Fig. 3.20) [6, 51].

Metal ions or low concentrations of electrolyte enhance the stability of the structure by reducing the electrostatic repulsion between the carboxyl groups. The stable helical conformation is resistant to temperature denaturation and accounts for the properties of (1) uniform viscosity over a temperature range of –18 to 80 °C, (2) exceptional stability to changes in pH from 1 to 11, and (3) compatibility with high salt concentration. The trisaccharide side chains tend to protect the glycosidic linkage on the backbone against hydrolytic cleavage chemically or enzymatically, making the structure exceptionally stable.

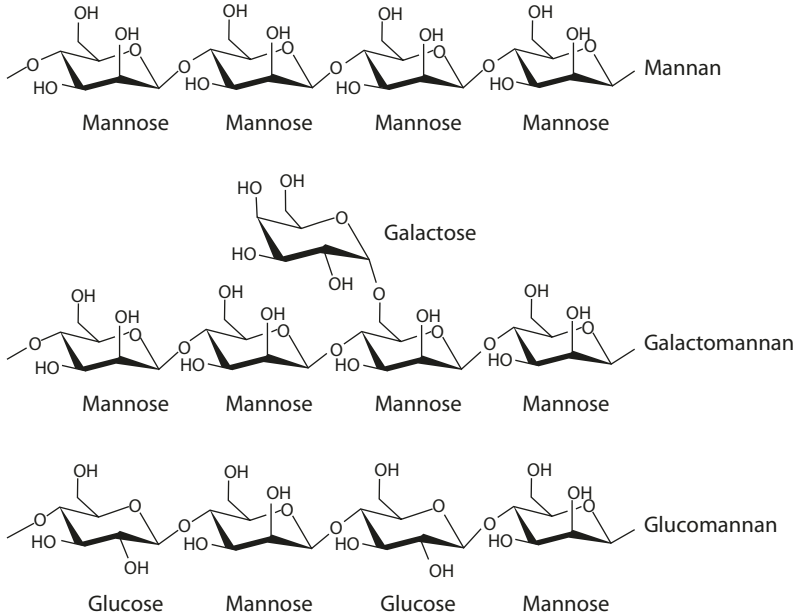
Xanthan gum solution exhibits a high degree of pseudoplastic flow over a broad shear rate and concentration range. Shear thinning and recovery are instantaneous. This unique flow property is attributed to the stiffness of the native conformation of the xanthan polymer and to the aggregation of these polymers into multi-stranded zones that allow a rapid re-formation after shear dissipation.

Xanthan is often used synergistically with galactomannans such as locust bean gum to form a viscous solution and at high concentrations (0.5% xanthan gum of total gum), a cohesive thermoreversible gel. The mechanism is similar to that between carrageenan and locust bean gum as described in the following section. The unbranched segment of the galactomannan complexes with the helical strands, resulting in a three-dimensional network with water trapped in the interstices.

3.14 Guar Gum

Guar gum is a widely used food thickener. It is extracted from seeds (endosperm) of *Cyamopsis tetragonoloba*, an annual legume plant, and, like locust bean gum, is a galactomannan (■ Fig. 3.21), consisting of mannose backbone with single-unit galactose side groups randomly distributed (linear chain of 1,4-β-D-mannopyranosyl units with 1,6-linked α-D-galactopyranosyl residues as side groups) [41]. Guar gum consists of molecules of about 10,000 residues, with mannose to galactose ratio of 1.6:1 to 1.8:1. The molecule typically ranges from 1 to 2 million kDa. The degree of solubility depends on the

3.15 · Carrageenan



■ Fig. 3.21 Mannan, galactomannan, and glucomannan

amount of galactose side groups. Guar gum hydrates rapidly in cold water, in contrast to locust bean gum, which requires heating. Guar gum can bind up to 100 times its own weight in water, about 8 times that of cornstarch. Guan gum in aqueous solution shows pseudoplastic (shear-thinning) behavior of decreasing viscosity with increasing shear rate similar to many high molecular weight polymers. In food application, it is used at concentrations of less than 1%. At higher concentration, the solution exhibits a thixotropic rheological behavior. Guan gum is useful as thickening agent to control the texture and flow of sauces, gravy, and dressings and in firming and gelling of processed meat products and preventing syneresis in bakery goods.

Guar gum is not very acid stable. It is often mixed with other hydrocolloids such as xanthan gum or gum arabic to alleviate the problem and to extend the functional properties. Galactomannans have a unique functional feature of interacting with xanthan gum. This interaction involves association between the xanthan molecule and the unsubstituted (smooth) region of the mannan backbone of the galactomannan. Guar gum acts synergistically with xanthan gum in increasing viscosity. Gum arabic is one of the most important exudate gums widely used in beverage emulsion. It can form solutions of concentrations up to 50%, a feature that allows the gum to be used in confectionery products to provide texture and control sugar crystallization.

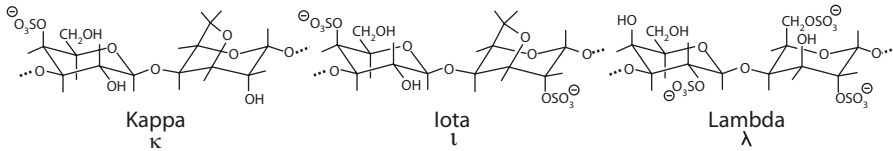
3.15 Carrageenan

3.15.1 Chemical Structure of Carrageenan

Carrageenan is isolated from a number of closely related species of red seaweed (Class Rhodophyceae; *Chondrus*, *Eucheuma*, and *Gigartina* species) by hot alkali

extraction. Carrageenan is a polysaccharide chain consisting of galactose units and 3,6-anhydrogalactose, both sulfated and nonsulfated, joined by alternating α -1,3 and β -1,4 glycosidic linkages. The number and the location of the sulfate groups contribute to the gelling characteristics of carrageenan. Accordingly, there are three types of carrageenan, κ , ι , and λ (■ Fig. 3.22). Some of their properties are listed in ■ Table 3.3 [4].

3

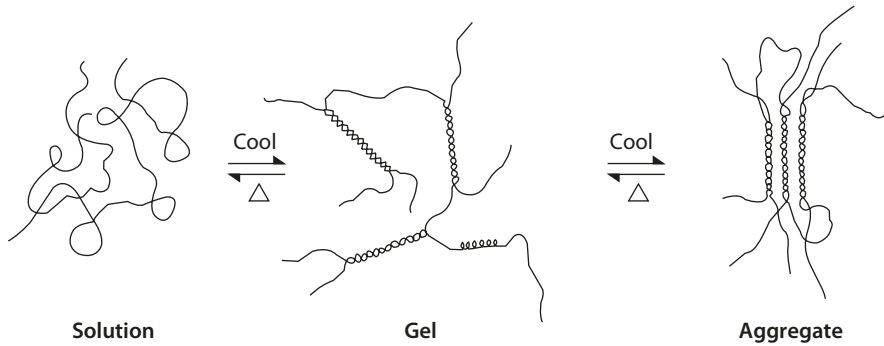


■ Fig. 3.22 Kappa, iota, and lambda carrageenan

■ Table 3.3 Structures and functional properties of carrageenan

Kappa (κ)	Iota (ι)	Lambda (λ)
<i>Repeating unit</i>		
Galactose-4-sulfate-3, 6-anhydrogalactose	Galactose-4-sulfate-3, 6-anhydrogalactose-2-sulfate	Galactose-2-sulfate-galactose-2,6-disulfate
<i>Degree of esterification</i>		
25% ester sulfate	32% ester sulfate	35% ester sulfate
34% 3,6-AG	30% 3,6-AG	Small amount
<i>Ion for gelling</i>		
K^+	Ca^{2+}	No gel
<i>Texture</i>		
Strong, rigid, opaque	Elastic, clear	No gel
<i>Syneresis</i>		
+	–	–
<i>Freeze-thaw stability</i>		
–	+	+
<i>Acid stability</i>		
+	+	+
<i>Shear stability</i>		
–	+	–

Marine Colloids, Introductory Bulletin A-1 [4]



■ Fig. 3.23 Gelling mechanism of carrageenan

3.15.2 Gelling

The three forms of carrageenan differ structurally in terms of their respective 3,6-anhydrogalactose and ester sulfate contents. The anhydrogalactose units are required for gelation, and the degree of sulfation controls the gel texture and characteristics. The κ and ι forms contain 3,6-anhydrogalactose for gel formation. The λ form does not form gels and is used as a thickener. The function of the sulfate anions is to keep the carrageenan in solution. Transformation of the polysaccharide chains from random coil to helices is favored with decreasing sulfate content. Therefore, the less sulfated κ -carrageenan forms gel that is opaque. With higher percentages of ester sulfate, the ι -carrageenan tends to stay in solution as a random coil, and the gel is clear and elastic and does not aggregate.

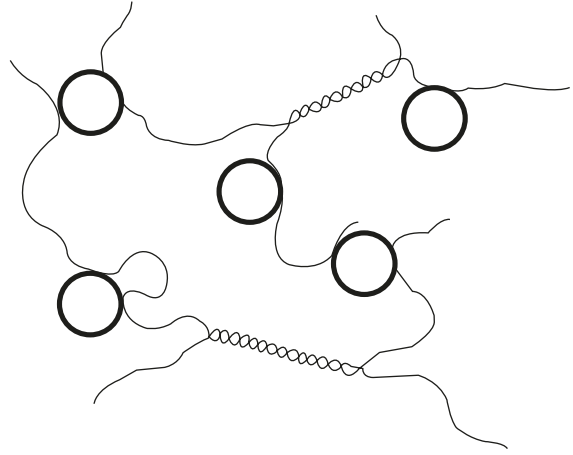
Both κ - and ι -Carrageenans form thermally reversible gels with frameworks that are cross-linked by double helices. In solution, the polysaccharide chains are dispersed randomly. On cooling, gelation occurs when sufficient helices provide cross-linking junctions to build a continuous network (■ Fig. 3.23) [21]. As more helices continue to form, they start to associate into aggregates and the gel turns opaque. Finally, enough aggregation will cause contraction of the network with subsequent exclusion of the liquid from the interstices, and the gel becomes brittle.

The helices are held by specific hydrogen bonding between the O–2 and O–6 of the galactose residues in different strands of the same double helix, and every unsubstituted hydroxyl group is then hydrogen bonded within the double helix, making the conformation very stable. Sulfate residues located on the outside reinforce the backbone of the helices. Association of the chain, and stacking of helices to form junctions, is reinforced by the electrostatic attraction between cations (K^+ in κ carrageenan, Ca^{2+} for elastic ι -gel) and the sulfate anions. The gelling of carrageenan can be regulated by adjustment of the cation concentration. Addition of cations increases the gelling temperature.

3.15.3 Interaction with Proteins

Carrageenan has the ability to interact and form stable complexes with milk proteins through electrostatic interaction between the sulfate anions with the many positive charges on the surface of casein micelles [35].

Fig. 3.24 Interactions between κ -carrageenan and κ -casein in gelling



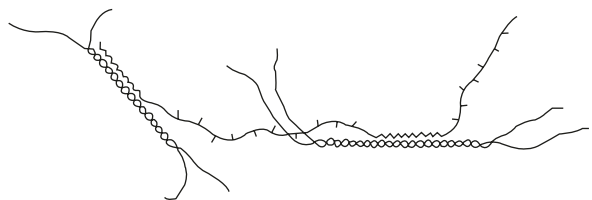
At neutral pH, κ -casein has an extensive region of positively charged amino acid residue (between residues 20 and 115). Since κ -casein is the only milk protein to interact with carrageenan, it is suggested that this region is responsible for the electrostatic interaction. The interaction of a carrageenan molecule with a micelle leaves the unadsorbed segments of the polysaccharide chain free in solution, in the form of loops and tails. The free segments then associate to form the gel network (Fig. 3.24).

The milk protein-carrageenan interaction serves to reinforce the double helices that normally occur in aqueous systems, increasing the gel strength tenfold. Carrageenan has found wide use in dairy products, whipped cream, pie filling with milk, imitation milk, coffee creamer, etc. The concentration is usually in the range of 0.1–0.5%. Dilute concentration (0.01–0.04%) of κ -carrageenan and milk protein forms a weak thixotropic gel. This special property is utilized to suspend cocoa in making chocolate milk.

3.15.4 Synergism with Locust Bean Gum

Locust bean gum and κ -carrageenan interact to increase gel strength, making the gel more elastic and resistant to syneresis. Locust bean gum consists of a backbone chain of mannose residues with side chains composed of essentially galactose units. The unbranched region of the backbone assumes a ribbonlike conformation stabilized by the carrageenan helices (Fig. 3.25). The branched regions (with galactose side chains) cannot bind but have the following functions: (1) they serve to connecting the cross-linked junctions in the network; (2) because they are randomly dispersed, they confer elasticity to the gel; and (3) because they cannot associate, the gel network resists aggregation and syneresis [13].

Fig. 3.25 Synergistic interaction between κ -carrageenan and locust bean gum



References

1. Anet EFLJ (1964) 3-Deoxyglycosuloses (3-deoxyglycosones) and the degradation of carbohydrates. *Adv Carbohydr Chem* 19:181–218
2. Angal SJ (1980) Sugar-cation complexes – structure and applications. *Chem Soc Rev* 9:415–428
3. Anonymous (1984) Cellulose gum: sodium carboxymethyl cellulose, chemical and physical properties. Hercules Incorporated, Wilmington
4. Anonymous (1984) Marine colloids, introductory bulletin A-1. FMC Corporation, Philadelphia
5. Barsanti L, Passarelli V, Evangelista V, Frassanito M, Gualtieri P (2011) Chemistry, physico-chemistry and applications linked to biological activities of β -glucans. *Nat Prod Rep* 28:457–466
6. Betz DA (1979) Xanthan gum, a biosynthetic polysaccharide for the food industry. *Food Technol Aust* 31:11–16
7. Bohm N, Kulicke W-M (1999) Rheological studies of barley (1->3)(1->4)- β -glucan in concentrated solution: mechanistic and kinetic investigation of the gel formation. *Carbohydr Res* 315:302–211
8. Burton HS, McWeeny DJ (1964) Non-enzymatic browning: routes to the production of melanoidins from aldoses and amino-compounds. *Chem Ind* 14:462–463
9. Capon B, Overend WG (1960) Constitution and physicochemical properties of carbohydrates. *Adv Carbohydr Chem* 15:11–51
10. Carlson LG, Larsson K, Dinh-Nguyen N, Krog KA (1979) A study of amylose-mono-glyceride complex by ramen spectroscopy. *Starch/Stärke* 31:222–224
11. Cerny M, Stanek J Jr (1977) 1,6-Anhydro derivatives of aldohexoses. *Adv Carbohydr Chem Biochem* 34:24–177
12. Courtin CM, Delcour JA (2002) Arabinoxylans and endoxylanases in wheat flour bread-making. *J Cereal Chem* 35:225–243
13. Dea ICM (1979) Interactions of ordered polysaccharide structure-synergism and freeze-thaw phenomena. In: Blanshard JMV, Mitchell JR (eds) *Polysaccharides in food*. Butterworths, London
14. de Wit G, Kieboom APG, van Bekkum H (1979) Enolization and isomerization of monosaccharides in aqueous alkaline solution. *Carbohydr Res* 74:157–175
15. Englyst HN, Kingman SM, Cummings JH (1992) Classification and measurement of nutritionally important starch fractions. *Eur J Clin Nutr* 46:S33–S50
16. FDA 2015. CFR-code of federal regulations title 21 (21CFR101.81)
17. Feather MS, Harris JF (1970) On the mechanism of conversion of hexoses into 5-(hydroxymethyl)-2-furaldehyde and metasaccharinic acid. *Carbohydr Res* 15:304–309
18. Feather MS, Harris JF (1973) Dehydration reactions of carbohydrates. *Adv Carbohydr Chem Biochem*:161–224
19. Gidley MJ, Bociek SM (1985) Molecular organization in starches: a ^{13}C CP/MAS NMR study. *J Am Chem Soc* 107:7040–7044
20. Gilbert RG, Witt T, Hasjun J (2013) What is being learned about starch properties from multiple-level characterization. *Cereal Chem* 90:312–325
21. Glicksman M (1979) Gelling hydrocolloids in food product applications. In: Blanshard JMV, Mitchell JR (eds) *Polysaccharides in foods*. Butterworths, London
22. Gudmundsson M (1994) Retrogradation of starch and the role of its components. *Thermochim Acta* 246:329–341
23. Grant GT, Morris ER, Rees DA, Smith PJC, Thorn D (1973) Biological interactions between polysaccharides and divalent cations: the egg-box model. *FEBS Lett* 32:195–198
24. Hodge JE (1955) The Amadori rearrangement. *Adv Carbohydr Chem* 10:169–205
25. Hodge JE (1967) Origin of flavor in foods – non-enzymatic browning reactions. In: Schultz HW, Day EA, Libbey LM (eds) *The chemistry and physiology of flavors*. AVI, Westport
26. Hosney RS (1984) Functional properties of pentosans in baked foods. *Food Technol* 38(1):114–116
27. Isbell HS, Frush HI (1958) Mutarotation, hydrolysis and rearrangement reactions of glycosylamine. *J Org Chem* 23:1309–1319
28. Jenkins PJ, Donald AM (1995) The influence of amylose on starch granule structure. *Int J Biol Macromol* 17:315–321
29. Jones JM (2013) Dietary fiber future directions: integrating new definitions and findings to inform nutrition research and communication. *Adv Nutr* 4:8–15
30. Kato H, Tsuchida H (1981) Estimation of melanoidin structure by pyrolysis and oxidation. *Prog Food Nutr Sci* 5:147–156

31. Kort MJ (1970) Reactions of free sugars with aqueous ammonia. *Adv Carbohydr Chem Biochem* 25:311–349
32. Klug ED (1970) Hydroxypropylcellulose. *Food Technol* 24(1):51–54
33. Kulp K, Ponte JC Jr (1981) Staling of white pan bread: fundamental causes. *CRC Crit Rev Food Sci Technol* 15:1–48
34. Lararidou A, Biliaderis CG (2007) Molecular aspects of cereal β -glucan functionality: physical properties, technological applications and physiological effects. *J Cereal Sci* 46:101–108
35. Ledward DA (1979) Protein-polysaccharide interactions. In: Blanshard JMV, Mitchell JR (eds) *Polysaccharides in food*. Butterworths, London
36. Littlecott GW (1982) Food gels – the role of alginates. *Food Technol Aust* 34:412–418
37. Luallen TE (1985) Starch as a functional ingredient. *Food Technol* 39(1):59–63
38. Mizuno T, Weiss AH (1974) Synthesis and utilization of formose sugars. *Adv Carbohydr Chem Biochem* 29:173–227
39. Namiki M, Hayashi T (1983) A new mechanism of the Maillard reaction involving sugar fragmentation and free radical formation. In: Walter GR, Feather MS (eds) *The Maillard reaction in foods and nutrition*. ACS symposium series, vol 215. American Chemical Society, Washington, D.C.
40. Manners DJ (1989) Recent developments in our understanding of amylopectin structure. *Carbohydr Polym* 11:87–112
41. Mudgil D, Barak S, Khatkar BS (2014) Guar gum: processing, properties and food applications – a review. *J Food Technol* 5:409–418
42. Nishinari K (2000) Sol-gel transition of biopolymer dispersions. *Macromol Symp* 159:205–214
43. Neukom H (1976) Chemistry and properties of the non-starchy polysaccharides (NSP) of wheat flour. *Lebensm Wiss u-Technol* 9:143–148
44. Oakenfull D, Scott A (1984) Hydrophobic interaction in the gelation of high methoxy pectins. *J Food Sci* 49:1093–1098
45. Obiro WC, Ray SS, Emmambux MN (2012) V-amylose structural characteristics, methods of preparation, significance, and potential applications. *Food Rev Intl* 28:412–438
46. Osaka ZN (1978) Studies on starch granules. *Starch/Stärke*:105–111
47. Rees DA, Welsh EJ (1977) Secondary and tertiary structure of polysaccharides in solutions and gels. *Agnew Chem Int Engl* 16:214–224
48. Rendleman JA Jr (1973) Ionization of carbohydrates in the presence of metal hydroxides and oxides. In: Isbell HS (ed) *Carbohydrates in solution*. Advances in chemistry series, vol 117. American Chemical Society, Washington, D.C.
49. Ryu J-H, Lee S, You S, Shim J-H, Yoo S-H (2012) Effects of barley and oat β -glucan structures on their rheological and thermal characteristics. *Carbohydr Polym* 89:1238–1243
50. Stone B (2005) Cell walls of cereal grains. 55th Australian cereal chemistry conference, Charles Sturt University, NSW Australia
51. Symes KC (1980) The relationship between the covalent structure of the Xanthomonas polysaccharide (xanthan) and its function as a thickening, suspending and gelling agent. *Food Chem* 6:63–76
52. Tvaroska I, Ogawa K, Deslandes Y, Marchessault RH (1983) Crystalline conformation and structure of lichenan and barley β -glucan. *Can J Chem* 61:1608–1616
53. Varela P, Fiszman SM (2011) Hydrocolloids in fried foods. A review. *Food Hydrocoll* 25:1801–1812
54. Walkinshaw MD, Arnott S (1981) Conformations and interactions of pectins II. Models for junction zones in pectinic acid and calcium pectate gels. *J Mol Biol* 153:1075–1085
55. Whistler RL, Richards EL (1970) Hemicelluloses. In: Pigman W, Horton D (eds) *The carbohydrates chemistry and biochemistry*, 2nd edn. Academic, New York
56. Woodward JR, Fincher GB, Stone BA (1983) Water-soluble (1 \rightarrow 3), (1 \rightarrow 4)- β -D-glucans from barley (*Hordeum vulgare*) endosperm. II. Fine structure. *Carbohydr Polymers* 3:207–225
57. Zyzak DV, Sanders RA, Stojanovic M, Tallmadge DH, Eberhart L, Ewald DK, Gruber DC, Morsch TR, Strothers MA, Rizzi GP, Villagran MD (2003) Acrylamide formation mechanism in heated foods. *J Agric Food Chem* 51:4782–4787

Colorants

- 4.1 **Light Absorption – 171**
- 4.2 **Conjugation – 173**
- 4.3 **Substituent Effects – 175**
- 4.4 **Carotenoids – 176**
 - 4.4.1 Isomerization – 178
 - 4.4.2 Autoxidation – 179
 - 4.4.3 Thermal Degradation – 179
 - 4.4.4 Photochemical Reactions – 180
 - 4.4.5 Carotenoids as Color Additives – 180
 - 4.4.6 Carotenoproteins and Bathochromic Shift – 181
- 4.5 **Annatto – 182**
- 4.6 **Anthocyanins – 183**
 - 4.6.1 Effect of pH on the Color of Anthocyanins – 184
 - 4.6.2 Thermal Degradation of Anthocyanidins – 186
 - 4.6.3 Decoloration by Sulfur Dioxide – 186
 - 4.6.4 Self-Association and Copigmentation – 186
 - 4.6.5 Condensation – 188
 - 4.6.6 Oxidation – 189
- 4.7 **Betanain – 189**
- 4.8 **Caramel – 191**
- 4.9 **Dyes and Lakes – 192**
- 4.10 **Coordination Chemistry – 194**
- 4.11 **Metalloporphyrin: Electronic Structure – 197**

4.12 Myoglobin – 200

- 4.12.1 Molecular Structure – 200
- 4.12.2 The Heme Iron – 202
- 4.12.3 The Role of Globin – 205
- 4.12.4 Oxygenation of Myoglobin – 205
- 4.12.5 Autoxidation of Oxymyoglobin – 206
- 4.12.6 Absorption Spectra – 208
- 4.12.7 Myoglobin and Lipid Oxidation – 211

4.13 Chlorophyll – 212

- 4.13.1 The Magnesium-Ligand Coordination – 213
- 4.13.2 Dimers and Oligomers – 213
- 4.13.3 Chlorophyll Derivatives – 214
- 4.13.4 Oxidation and Reduction – 216

References – 216

Color compounds constitute a unique class in that they are structurally diverse, and the chemical and physical properties are extremely complex. For many color compounds, their chromophoretic properties can only be adequately explained by referring to their molecular orbital structures.

Based on theoretical consideration, color compounds can be classified into two groups: one has chromophores with conjugated systems, and the other has metal-coordinated porphyrins. The former group includes carotenoids, anthocyanins, betanains, caramel, dyes, and lakes. The latter consists of myoglobins, chlorophylls, and their derivatives.

From the standpoint of applications, an understanding of the basic chemistry of these compounds would provide useful information for the development and formulation of color additives. It is also important for food processing, in retaining the natural color, or eliminating undesirable color changes in the food products.

4.1 Light Absorption

The quantum light energy is related to the wavelength (λ) and frequency (ν) by Eq. 4.1, where h = Planck's constant and c = speed of light in a vacuum. A molecule absorbs a quantum of light if the energy of the quantum is equal to the energy of transition: $E(\text{light}) = E(\text{excited}) - E(\text{ground})$.

$$\varepsilon = hc / \lambda = h\nu \quad (4.1)$$

A number of molecular transitions can occur depending on the wavelength. The present discussion will be limited to the visible region where the molecule is electronically excited. The electrons may undergo several types of transitions of different energies, schematically presented in Fig. 4.1. Not all of the transitions are equally probable: Some are forbidden transitions. Experimentally, transition are measured by the molar extinction coefficient (Eq. 4.2)

$$\log(I_o / I) = \varepsilon cl \quad (4.2)$$

where I_o = intensity of incident light

I = intensity of light transmitted

ε = molar concentration of solute

l = length of pathway through solution

The position and intensity of an absorption band is affected by factors like substituent group and conjugation, as well as the conformation of the molecule. The effects may be hypsochromic, bathochromic, hypochromic, or hyperchromic (Fig. 4.2).

Fig. 4.1 Electronic energy transitions

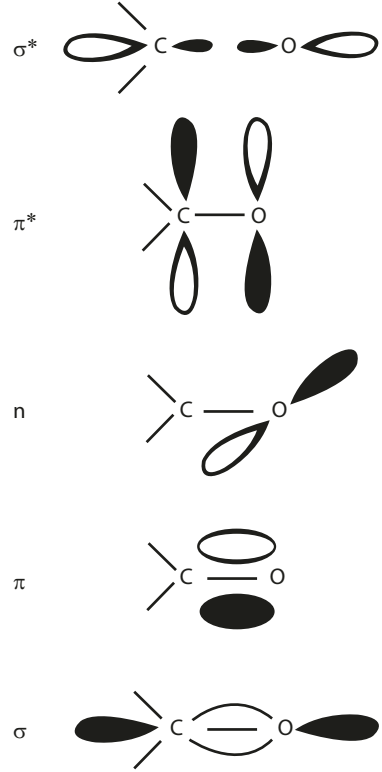
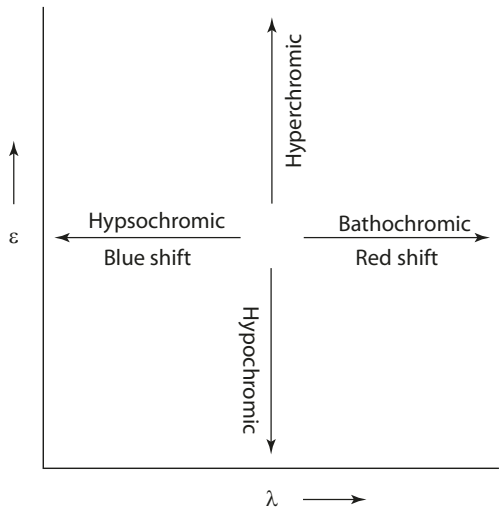


Fig. 4.2 Types of effect on position and intensity of absorption



4.2 Conjugation

The effect of conjugation on transition energy can be visualized by considering the π molecular orbitals of 1,3-butadiene as an example (■ Fig. 4.3). The total π -electron energy = $2(\alpha + 1.62\beta) + 2(\alpha + 0.62\beta) = 4\alpha + 4.48\beta$

If the orbitals are localized in the 1,3-butadiene, the total π -electron energy will be equal to $4(\alpha + \beta)$. The energy of delocalization, therefore, is $(4\alpha + 4.48\beta) - (4\alpha + 4\beta)$, which equals 9 kcal/mol ($\beta = 19$ kcal/mol) (■ Fig. 4.4).

The higher the degree of conjugation, the lower energy it will require for the π to π^* transition from the highest occupied molecular orbital (HOMO) to the lowest unoccupied molecular orbital (LUMO). Increased conjugation in the molecule shifts the absorption maximum to a higher wavelength (red shift).

A simple set of rules (Fieser-Kuhn rules) has been used for estimating the λ_{\max} and hence the ϵ_{\max} for long-chain polyenes like β -carotene. Thus, λ_{\max} (in hexane) = $114 + 5M + n(48.0 - 1.7n) - 16.5R_{\text{endo}} - 10R_{\text{exo}}$, and ϵ_{\max} (in hexane) = $1.74 \times 10^4 n$,

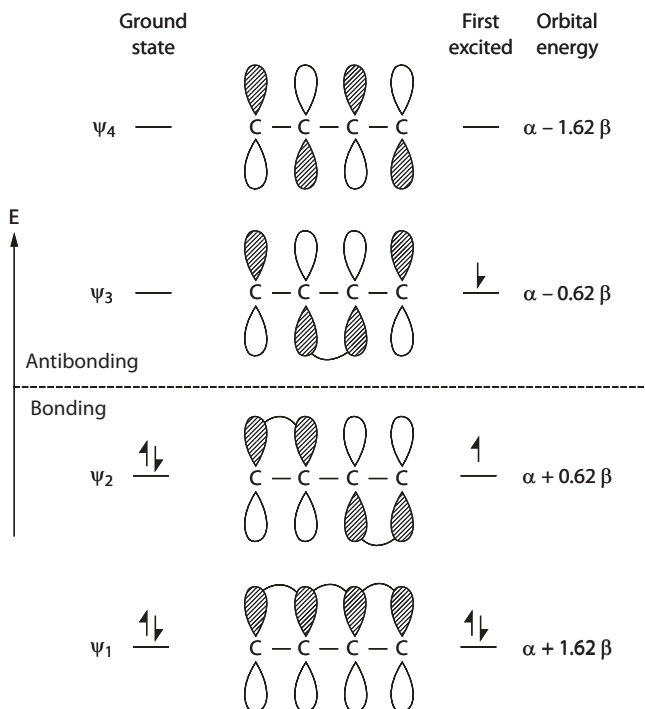
where M = number of alkyl substituents

n = number of conjugated double bonds

R_{endo} = number of rings with endocyclic double bonds

R_{exo} = number of rings with exocyclic double bonds

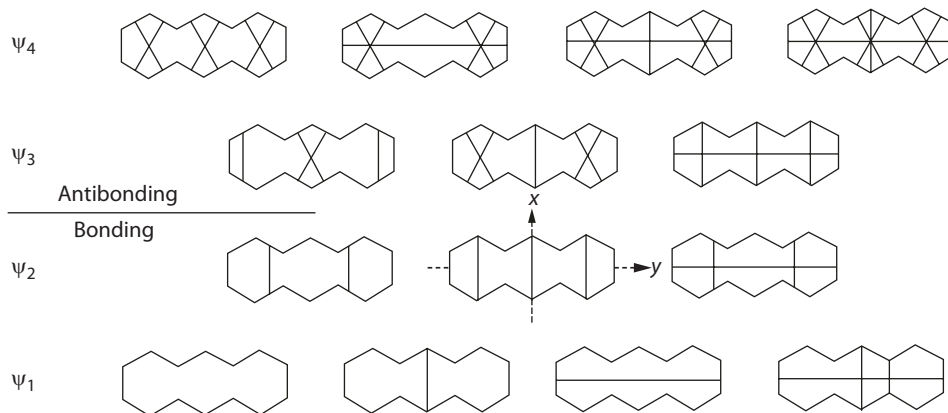
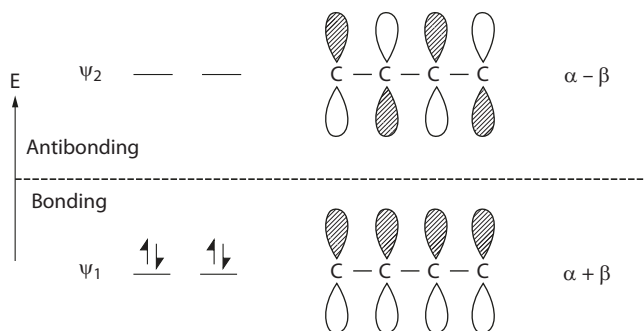
■ Fig. 4.3 Configuration of π electrons and orbital energy in ground state and first excited state



For β -carotene, $\lambda_{\max} = 452$ nm in hexane, and the calculated $\lambda_{\max} = 114 + (5 \times 10) + 11(48.0 - 1.7 \times 11) - (16.5 \times 2) - (10 \times 0) = 453$ nm. The same red shift effect of increasing conjugation is observed in polynuclear aromatic compounds. However, in these asymmetric compounds, the nodal planes intersect along either the x or y axis, producing different energy level orbitals. Transitions along the x or y direction give separate distinct absorption bands [41]. Take for example, the molecular orbitals of anthracene; the π to π^* transition along the x and y directions results in absorption bands at λ_{\max} 250 and 370, respectively (■ Fig. 4.5).

4

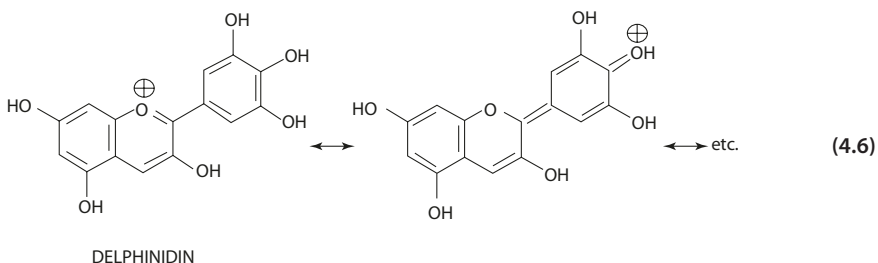
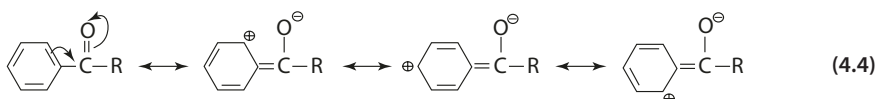
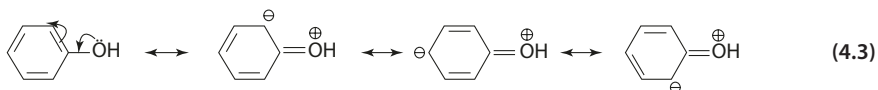
■ Fig. 4.4 Configuration of π electrons and energy in localized orbitals



■ Fig. 4.5 The molecular orbitals of anthracene (From Bowen [4] with permission. Copyright 1950 Royal Society of Chemistry)

4.3 Substituent Effects

Substituent groups with lone pairs of electrons tend to increase π conjugation through resonance (Eq. 4.3). Similar resonance structures can be written for $-\text{OR}$ ($\text{R} = \text{CH}_3, \text{C}_2\text{H}_5$), $-\text{X}$ (Br, Cl), $-\text{NH}_2$ (or $-\text{NRH}$), etc. Electron-withdrawing groups, such as $-\text{COR}$, $-\text{CN}$, $-\text{COOH}$, $-\text{CHO}$, $-\text{NO}_2$, $-\text{COOR}$, $-\text{SO}_3\text{H}$, are also capable of π configuration (Eq. 4.4).



In the above examples (Eqs. 4.3 and 4.4), the conjugated π systems are benzenoid rings, which constitute the absorbing chromophore. Substituents that cause a red shift in the λ_{max} and increase the ϵ are called auxochrome. As expected, disubstitution also shows the effect of extended π conjugation. Para-substitution with both π -electron donor and acceptor groups is particularly effective in enhancing a bathochromic shift and increasing absorption intensity due to resonance stability (Eq. 4.5). With the substituent effect in mind, it is then not so hard to understand that the anthocyanins with the structural formula in Eq. 4.6 are intensely colored. For simple reference, the relationship between the absorption wavelength and the observed color (transmitted light) is illustrated in [Fig. 4.6](#).

Fig. 4.6 Visible absorption spectrum

Frequency cm ⁻¹	Wavelength nm	Spectral color (absorbed light)	Color of compound (transmitted light)
25,000	400	Purple	Yellow
		Blue	Orange
20,000	500	Green	Red
		Yellow	Purple
15,000	600	Orange	Blue
		Red	Green
	700		

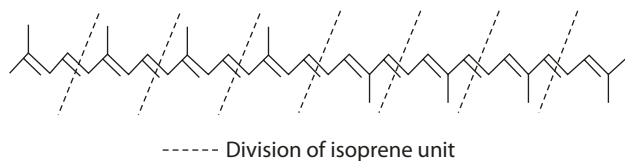
4.4 Carotenoids

Carotenoids represent one of the most widespread classes of naturally occurring pigments in higher plants. The basic carbon skeleton of carotenoid consists of repeating isoprene units (Fig. 4.7).

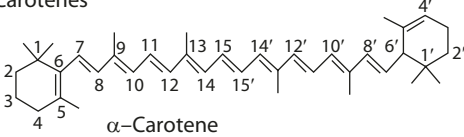
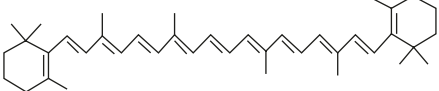
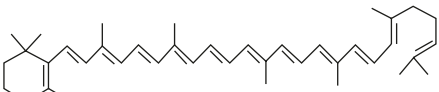
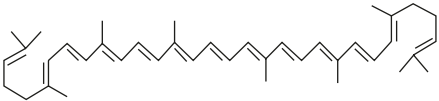
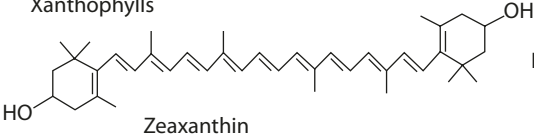
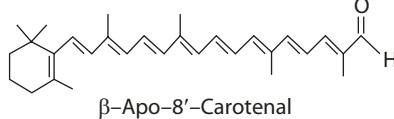
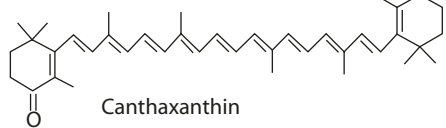
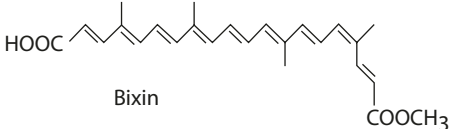
There are more than 300 individual carotenoids, and they can be classified into two general groups: (1) carotene: carotenoid hydrocarbons, (2) xanthophylls (or oxycarotenoids): oxygen-containing derivatives (Fig. 4.8) [3].

Carotenoids are often considered to be plant constituents; however, they also widely occur in animal products, mainly in meat, eggs, fish, and crustaceans. As animals are unable to synthesize carotenoids *de novo*, they consume the carotenoids from the diet. The carotenoids imparting color to animal products are primarily xanthophylls (notably astaxanthin, canthaxanthin, and lutein) (Fig. 4.9). A yolk's yellow color is due to the

Fig. 4.7 Repeating isoprene units



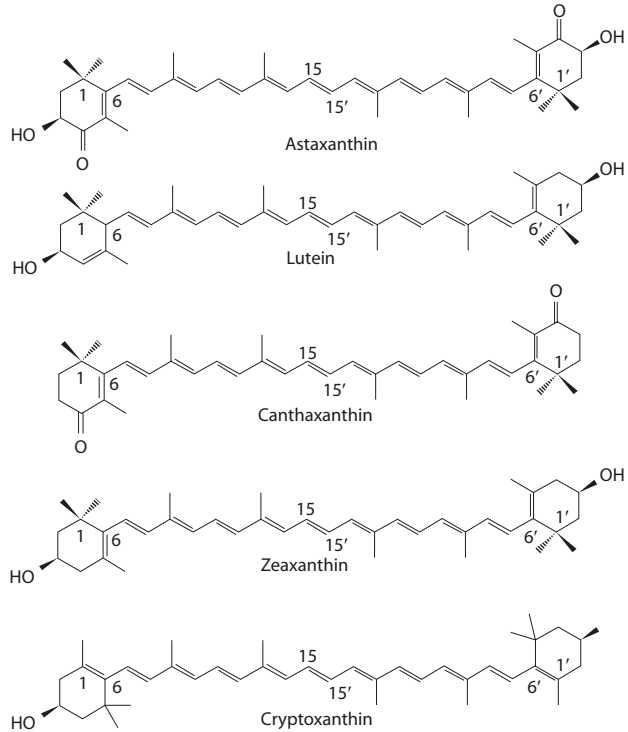
4.4- Carotenoids

Carotenoids	Vitamin A activity	Occurrence
 <p>α-Carotene</p>	50 – 54	Carrot, squash, tomato, peach, orange, most fruits and vegetables,
 <p>β-Carotene</p>	100	"
 <p>γ-Carotene</p>	42 – 50	"
 <p>Lycopene</p>	Inactive	Tomato, carrot, pink citrus fruits apricot watermelon, green pepper.
Xanthophylls		
 <p>Zeaxanthin</p>	Inactive	Spinach, corn, green pepper,
 <p>β-Apo-8'-Carotenal</p>	72	Citrous fruits, alfalfa meal, green plants.
 <p>Canthaxanthin</p>	Inactive	Mushroom, trout, crustaceans, brine shrimp, hydra, algae, microorganisms
 <p>Bixin</p>	Inactive	Annatto seed

■ Fig. 4.8 Structure, activity, and occurrence of some selected carotenoids (Bauernfeind [3])

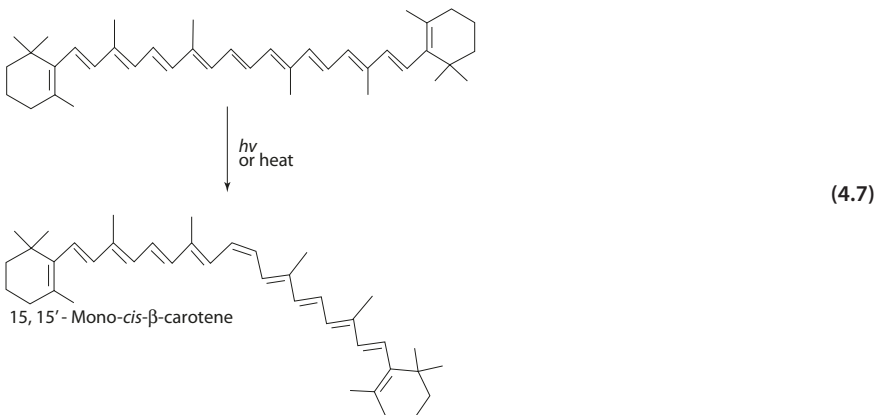
xanthophyll-containing diet of the hen, mainly lutein, zeaxanthin, and cryptoxanthin. However, brown egg shell comes from the pigment protoporphyrin, a breakdown product of hemoglobin, deposited on the outer layer during its formation in the oviduct. Chicken eggs of other shell colors are also known to exist. The red-pink color of fish, notably salmon and trout, is due to the feeding of krill and phytoplankton in the food chain rich in xanthophylls. In often cases, mixed formulations of xanthophylls are added in animal feeds for poultry farming and for aquaculture [5].

Fig. 4.9 Xanthophylls found in animal products



4.4.1 Isomerization

Naturally occurring carotenoids exist in the all-*trans* form. When carotenoids are exposed to light, strong acid, or high heat (e.g., canning at 121 °C), isomerization occurs resulting in a mixture of stereoisomers. One example is the isomerization of β -carotene to 15,15'-mono-*cis*- β -carotene (Eq. 4.7) [52].



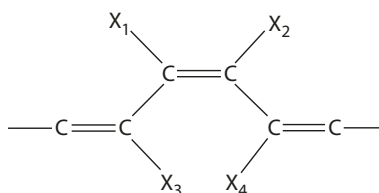
4.4 Carotenoids

Theoretically, the number of possible stereoisomers for β -carotene is 272. However, there are only 20 possible unhindered stereoisomers of β -carotene (all-*trans*, 3 mono-*cis*, 6 di-*cis*, 5 tri-*cis*, 3 tetra-*cis*, and 1 penta-*cis*) and only 12 are actually observed (mostly mono-*cis* and di-*cis*) [24]. A *cis* double bond in a carotenoid polyene chain will encounter steric hindrance depending on the orientation of the CH_3 group (■ Fig. 4.10).

If it happens that X_3 or X_4 are methyl groups, *trans-cis* isomerization becomes unfavorable. Another restriction factor on *trans-cis* rearrangement is the fact that the probability of a given configuration decreases with increasing number of *cis* double bonds. The equilibrium ratio of mono-*cis*/all-*trans* is 1/10, while that of tetra-*cis*/all-*trans* is 1/1000.

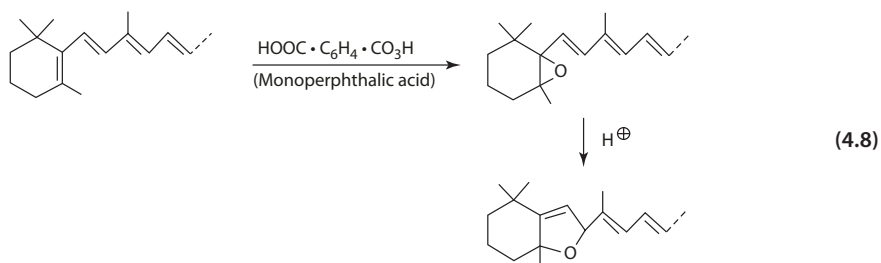
The *cis*-isomers absorb light at shorter wavelengths and exhibit lower extinction coefficients than the parent all-*trans* carotenoids, and the *cis* peak appears in the near-ultraviolet region at 320–380 nm. In addition to the λ_{max} , *cis*-isomers exhibit decreased color intensity and lower melting point.

■ Fig. 4.10 Effect of orientation of methyl substitutions on *trans-cis* isomerization



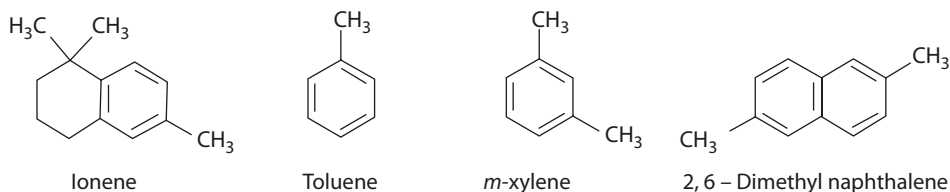
4.4.2 Autoxidation

Controlled chemical oxidation of carotenoids gives various mono- or di-epoxy derivatives [25, 52]. In the presence of acid, the 5,6-epoxide is isomerized to 5,8-furanoxide, reducing the length of conjugation (Eq. 4.8). The 5,6-epoxide is found in potatoes, red pepper, paprika, and orange peel. Epoxide isomerization also occurs in canned fruit juice, causing appreciable loss of color. Further degradation of the epoxy compounds produce short chain carbonyls, carbon dioxide, and carboxylic acids.



4.4.3 Thermal Degradation

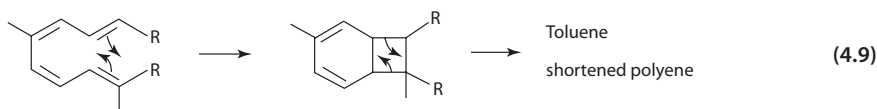
Carotenoids and many long-chain conjugated polyenes, when heated at a sufficiently high temperature (~ 190 °C), form degradation products of ionene, toluene, *m*-xylene, and 2,6-dimethylnaphthalene (■ Fig. 4.11). The mechanism consists of cyclization and



■ Fig. 4.11 Degradation products from thermal degradation of β -carotene

4

elimination reactions, involving a four-membered ring intermediate. Rearrangement of the eight-electron system results in the formation of toluene and the corresponding shortened polyene (Eq. 4.9) [37].



4.4.4 Photochemical Reactions

A. *Quenching of Triplet Sensitizers:* Carotenoids participate in triplet energy transfer with other photosensitizers. One of the most studied systems is the quenching of triplet chlorophyll by carotenoids. The quenching reaction explains the protective role of carotenoids against photobleaching of chlorophylls (Eq. 4.10).

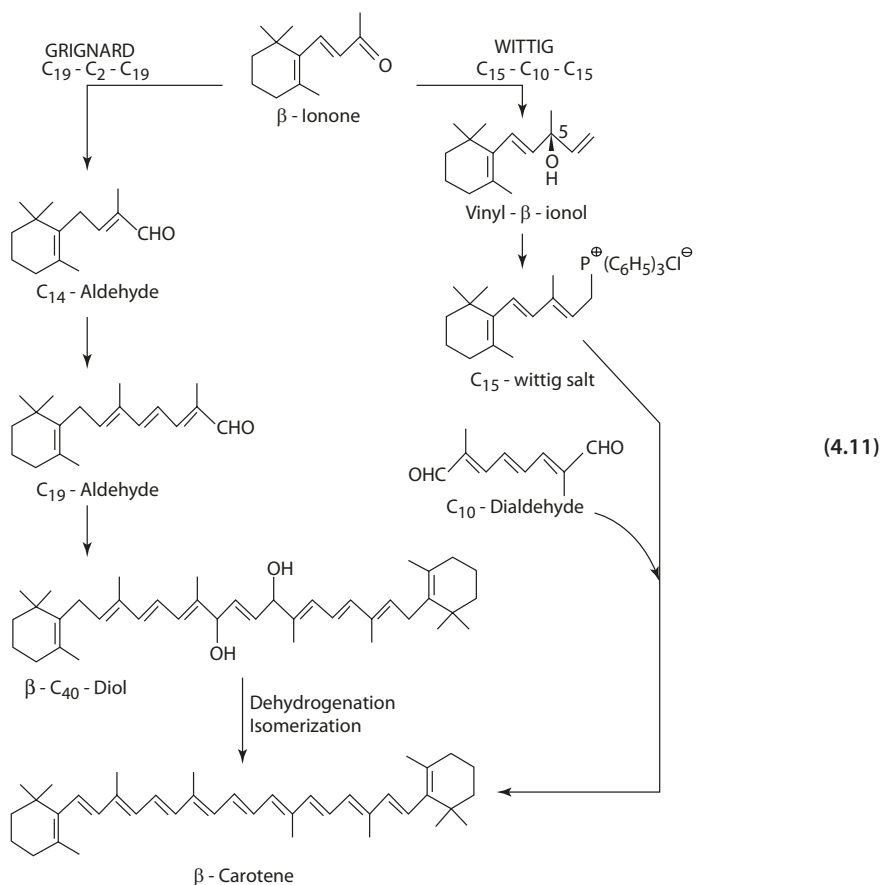


B. *Quenching of Singlet Oxygen* [10]. β -Carotene has been shown to quench singlet oxygen to the triplet (ground) state by electronic energy transfer. The quenching rate is close to that expected for diffusion-controlled reaction (refer to ► Chap. 10, vitamins A and E, and also Appendix 2).

4.4.5 Carotenoids as Color Additives

Three naturally occurring carotenoids are color additives. These are the β -carotene (orange-red), β -apo-8'-carotenal (red), and canthaxanthin (purplish red). All three can be synthesized from β -ionene [20]. The two important steps involved in the chemical synthesis are the Grignard and Wittig reactions. In the Grignard reaction, two β -C19-aldehydes are condensed with acetylene to form a C40 compound. In the Wittig reaction, two C15 Wittig salts condense with the C10 dialdehyde (Eq. 4.11).

4.4 Carotenoids



β -Apo-8'-carotenal and canthaxanthin are synthesized by similar processes. All these color additives are available in two main forms. (1) The oil-soluble form: These are suspensions of the color compounds in a modified vegetable oil carrier, usually partially hydrogenated cottonseed or soybean oils, fractionated triacylglycerols, and monoacylglycerols. Antioxidants such as BHA, BHT, or α -tocopherol are incorporated to provide stability of the product. (2) The water-dispersible forms: The color additives are dissolved in oil which is emulsified into an aqueous matrix before drying. Various matrices are employed, for example, gelatin/sucrose/modified food starch, and gum/acacia/dextrin.

4.4.6 Carotenoproteins and Bathochromic Shift

In nature, carotenoids often form carotenoprotein complexes, whose apparent function is that of protective coloration. A well-studied example is found in crustaceans, such as lobsters, and likewise crabs and prawns. The lobster body (epidermis and exoskeleton) color is associated with the carotenoid astaxanthin taken up from the diet and stabilized by

noncovalent binding with a carotenoprotein. The native protein (α -crustacyanin) is a high molecular weight multimeric molecule which is composed of eight dimeric subunits called β -crustacyanin. Each dimeric subunit (40 kD) is associated with two astaxanthin molecules. The protein chains (in the dimer) assume an open-ended barrel with eight β strands. In the dimeric subunit, the two astaxanthin molecules are close together in parallel, with one end deep in the barrel of each protein subunit and the other end in a surface depression in the opposite subunit [6].

The binding of astaxanthin to α -crustacyanin causes a bathochromic shift in the emission spectrum of astaxanthin (unbound λ_{\max} 472 nm, red color) to that of the carotenoprotein (λ_{\max} 632, slate-blue color). The mechanism of bathochromic shift is the result of several perturbations of the carotenoid. (1) In the bound complex, the β -ionone rings become coplanar with the polyene chain, thus extending the conjugation in the molecule. (2) The astaxanthin forms hydrogen bonds with the His residues in the protein, facilitating protonation and polarization of the C4 keto groups. (3) These protein-induced changes cause an increase in the delocalization in the electronic ground state, resulting in a reduced energy gap between ground and excited states of the astaxanthin molecule [6, 15]. Heat denaturation of the crustacyanin (as in cooking) results in the characteristic color change of the shell from blue to red.

4.5 Annatto

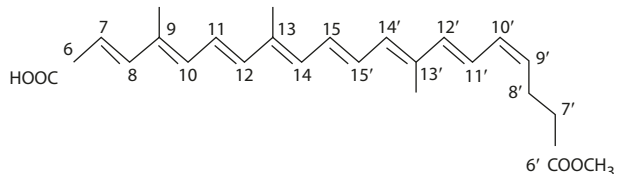
Annatto is the pigmented extract found in the pericarp of the fruit of *Bixa orellana* L., a large shrub of 2–5 m high, native to tropical America. The orange pigment in the annatto is a carotenoid, *cis*-bixin-(9'-*cis*-6,6'-diapocarotene-6,6'-dioate) [32] (■ Fig. 4.12). The *cis*-bixin is insoluble in oil. Heat treatment used in extraction converts the *cis*-bixin to *trans*-bixin, which is red and oil soluble.

Oil-soluble annatto is produced by mechanically abrading (a process known as «raspeeling») the pericarp immersed in heated vegetable oil (70 °C). Commercial annatto contains 0.2–0.25% bixin. Alternatively, the pigment is extracted by using suitable solvents, such as acetone. The solvent is removed to prepare a high-strength bixin powder. The powder is then suspended into oil to produce 3.5–5.2% bixin.

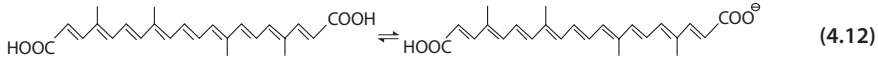
Water-soluble annatto is prepared by abrading the pericarp of annatto seed in aqueous alkali at 70 °C. The product is a salt of norbixin (both *cis* and *trans*) (Eq. 4.12).

Norbixin is orange, and being a dicarboxylic acid, is not soluble in water. However, the salt formed in alkaline media is readily soluble in water. Most food products have pH in

■ Fig. 4.12 *cis*-Bixin



the acid range. When a solution of norbixin salt is added, the pigment is dispersed into the food system and turns insoluble due to the lowering of the pH. This unique characteristic of norbixin enables the preparation of uniformly colored food products that will not leach color. For this reason, norbixin is valuable for use in breakfast cereals where leaching of color into milk is undesirable.

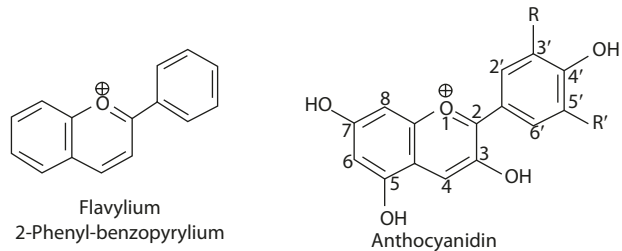


4.6 Anthocyanins

Anthocyanins are the water-soluble pigments responsible for the brilliant orange red through deep purple colors in flowers and fruits. Anthocyanins are glycosides of anthocyanidins. Anthocyanidins are thus the aglycones of the glycoside anthocyanins. The basic structure of anthocyanidin is a flavylium (2-phenyl-benzopyrylium). Some of the common anthocyanidins in fruits and vegetables are listed in Fig. 4.13.

In nature, anthocyanidins always occur as glycosides, most often 3-monoglycosides and sometimes 2,5-diglycosides. Various monosaccharides (glucose, galactose, rhamnose, arabinose), disaccharides, and trisaccharides may glycosylate the same group of anthocyanidins. In some cases, the sugar is acylated with *p*-coumaric, caffeic, or ferulic acids. In grapes, the major aglycone is malvidin, hence the anthocyanin is malvidin 3-monoglucoside with the 3-position glycosylated with glucose and the 3' and 5' hydroxyls methylated (Fig. 4.14). Also shown in Fig. 4.14 is the chemical structure of the major anthocyanin in egg plant, delphinidin-3-[4-(*p*-coumaroyl)-L-rhamnosyl (1,6) glucosideo]-5-glucoside [49].

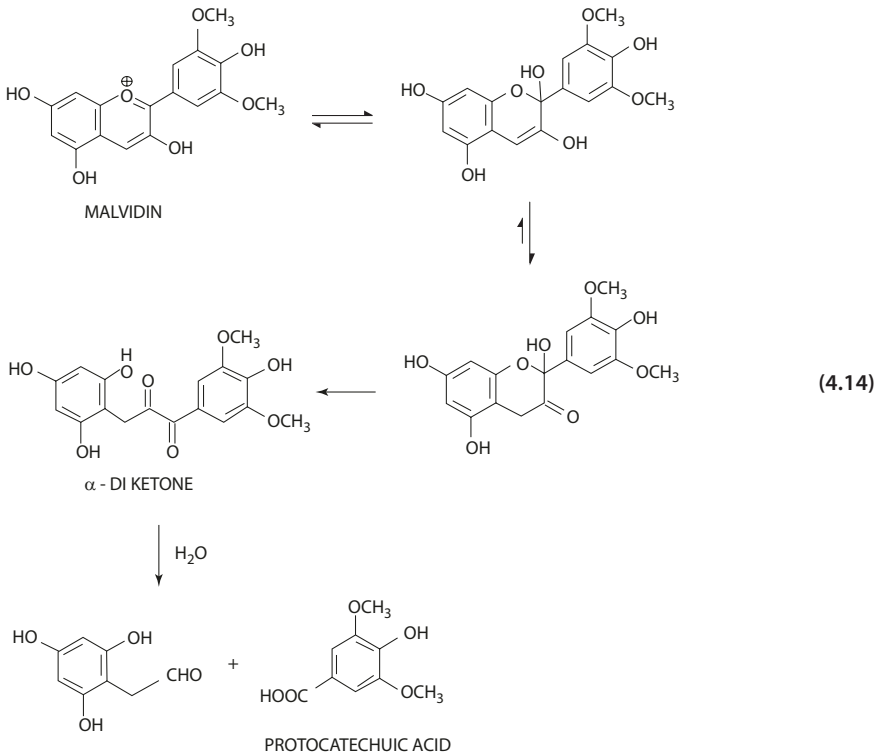
Fig. 4.13 Some common anthocyanidins



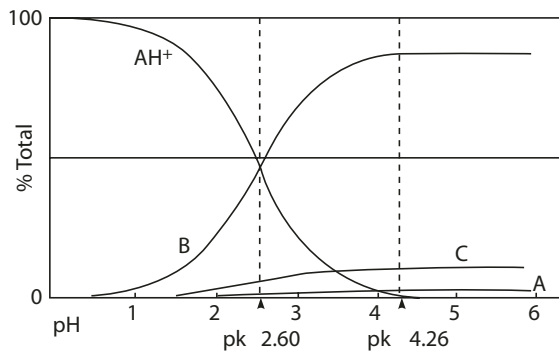
	R	R'	λ_{max} CH ₃ OH/HCl 0.01%	Occurrence
Pelargonidin	H	H	520	Strawberry
Cyanidin	OH	H	535	Apple
Peonidin	OCH ₃	H	532	Peony
Delphinidin	OH	OH	546	Delphinium
Petunidin	OCH ₃	OH	543	Petunia
Malvidin	OCH ₃	OCH ₃	542	Grapes

The proton transfer reaction of A to AH^+ is very fast (microseconds) and has a pK_a of 4.25. The percentage of the quinoidal base (A) is very small in the equilibrium mixture at any pH (■ Fig. 4.15). In very acidic solution (pH 0.5), the red AH^+ is the only species in solution. As the pH increases, the concentration and color of the anthocyanin decreases as AH^+ may (1) deprotonate to the blue quinoidal or (2) tautomerize to the chalcone. The pK_a values for B/AH^+ and A/AH^+ are 2.60 and 4.25, respectively. As the percentage of quinoidal base in the total is very small at any pH, there is very little color in anthocyanin when the pH is increased beyond pH 4 [46].

Anthocyanidins are less stable than the anthocyanins. The instability is due to the lack of substituents at position 3, and the chalcone is an unstable α -diketone which is readily hydrolyzed irreversibly to yield protocatechuic acid (Eq. 4.14).

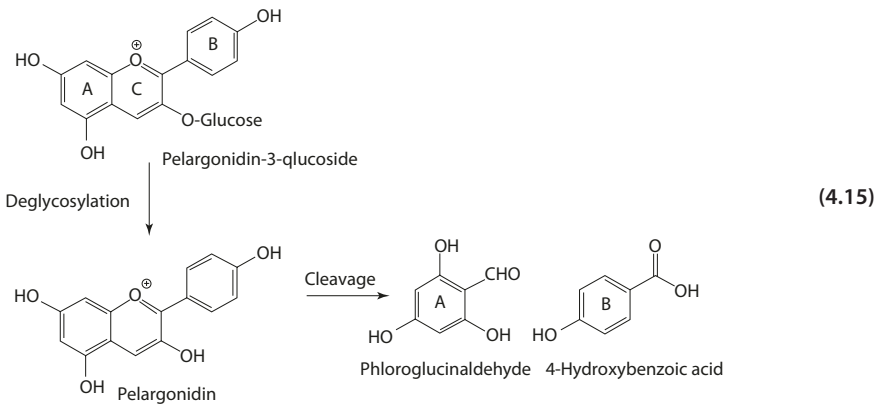


■ Fig. 4.15 Structural transformation and distribution with pH (malvidin 3-glucoside; 25 °C). AH^+ = red cation, B = colorless carbinol base, C = colorless chalcone, A = blue quinoidal base (From Timberlake [46] with permission. Copyright 1980 Elsevier)



4.6.2 Thermal Degradation of Anthocyanidins

Thermal processing affects degradation of anthocyanidins, and the rate of degradation increases with rising temperatures. The first step of thermal degradation (96 °C, pH 3.5) involves opening of the pyrylium ring and formation of the chalcone glycoside. The latter is cleaved to the chalcone, which is unstable and rapidly degrades to phenolic acid and aldehyde. In the case of cyanidin-3-glucoside, which is the major anthocyanin in blackberry, raspberry, sweet cherries, black currant, blood orange, and others, the product would be protocatechuic acid and phloroglucinaldehyde. In the case of pelargonidin (major anthocyanin in strawberry), the product would be 4-hydroxybenzoic acid and phloroglucinaldehyde (Eq. 4.15) [30, 34].



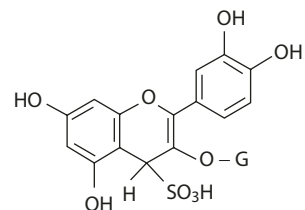
4.6.3 Decoloration by Sulfur Dioxide

Sulfur dioxide adds to the 4-position of the anthocyanin to form a bisulfite addition compound [47] (■ Fig. 4.16). The addition does not occur at the 2-position, and the reaction is reversible. Anthocyanins with the 4-position blocked by methyl or phenyl groups are unaffected by SO₂ and show increased stability to light in the presence of ascorbic acid or traces of iron.

4.6.4 Self-Association and Copigmentation

Plant tissues have pH values typically in the range of 3.5–5.5. How can the anthocyanins retain the vivid color without being transformed to the colorless forms as in

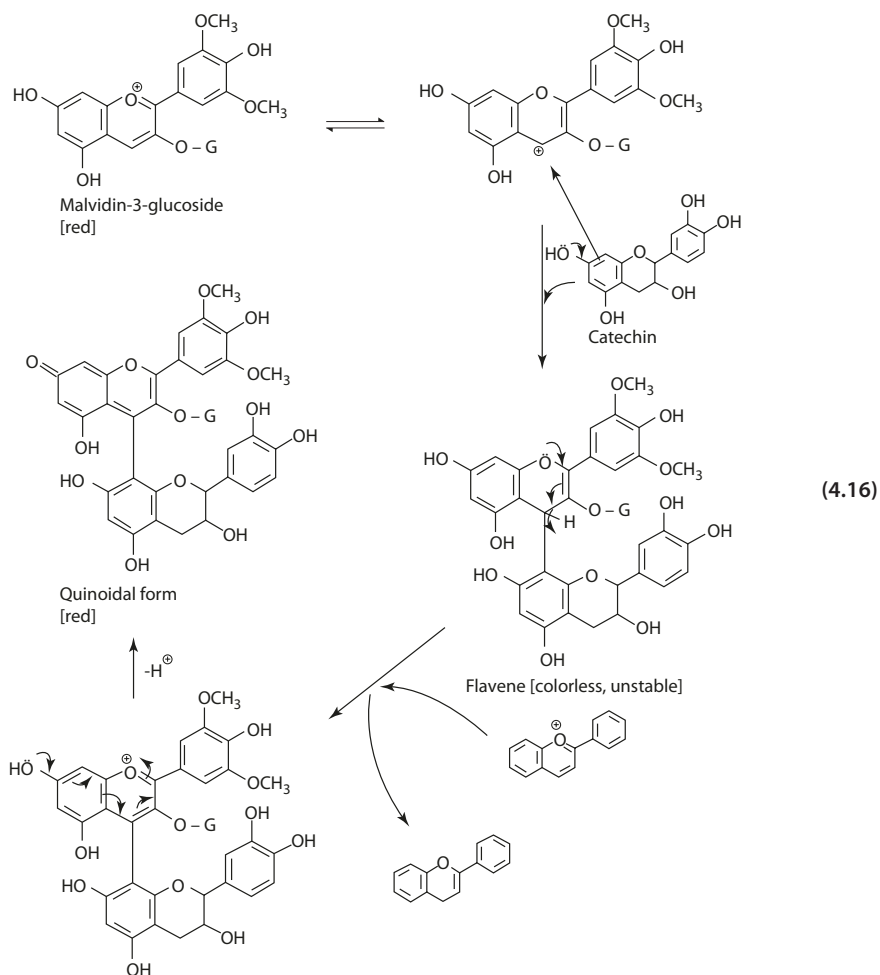
■ Fig. 4.16 Bisulfite addition product of anthocyanin



4.6 Anthocyanins

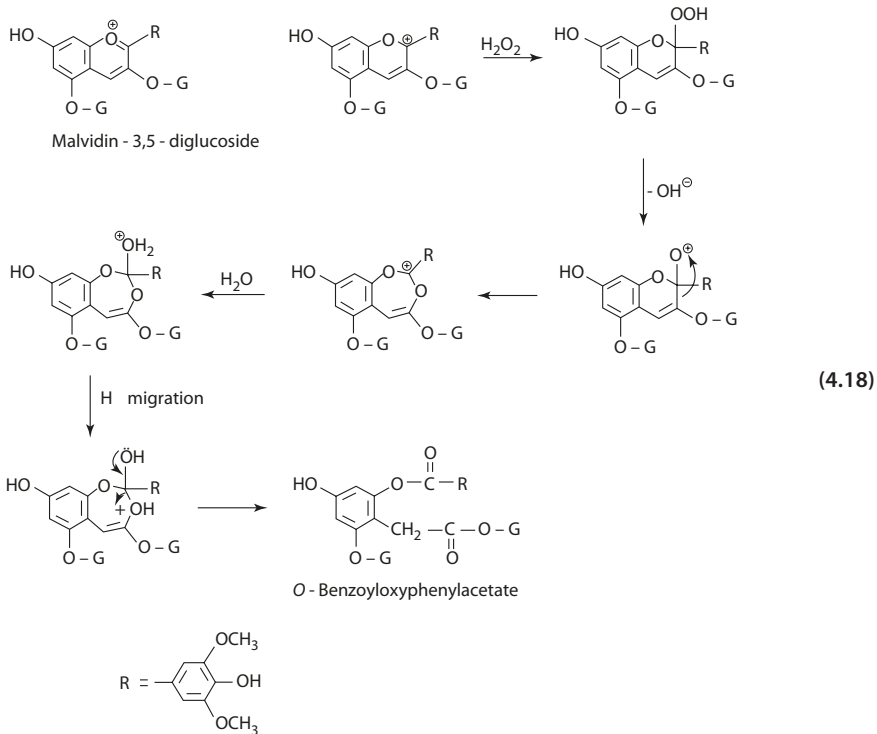
solution? Anthocyanins have been shown to self-associate to form helical stacks through hydrophobic attraction and hydrogen bonding between the flavylium nuclei. Stacking effectively shelters the chromophores behind the sugar groups from the hydration reaction [16].

Another protective mechanism is copigmentation through hydrogen bonding of the phenolic groups between anthocyanin and flavone molecules. The flavone molecules are interleaved between anthocyanin molecules to form alternate stacking. Addition of flavonols, aurones, tannins, and polypeptides also has been shown to stabilize anthocyanins. In some anthocyanins, the acylating groups, like caffeic acid, are tucked between and under the stacked flavylium nuclei. Copigmentation usually causes bathochromic shifts in the visible λ_{\max} and a large increase in intensity. The increased stability and the spectral shift is due to the interaction between anthocyanin and copigment forming a π - π complex. Copigmentation is believed to be the main mechanism of stabilization. It provides protection from nucleophilic attack of the flavylium ion and from other species such as peroxides and sulfur dioxide.



4.6.6 Oxidation

Hydrogen peroxide oxidizes 3-substituted anthocyanins (e.g., malvidin-3,5-diglucoside) to benzoyloxyphenylacetic acid esters of the malvone type. The reaction follows a Bayer-Villiger type oxidation. After the nucleophilic attack of the H_2O at C2, the hydrogen atom migrates to the adjacent oxygen resulting in the cleavage between C2 and C3. The esters formed are readily hydrolyzed to various breakdown products (Eq. 4.18) [18].



4.7 Betanain

Betanain is classified into betaxanthins (yellow) and betacyanins (red-violet), which occur abundantly in red beet (commercial source), pokeberry, and other plants. Betanain occurs naturally in the salt form, which is water soluble [43]. The general structure of betanain consists of the basic structure betalamic acid conjugated with a chromophore. The chromophore is a protonated 1,7-diazaheptamethin system forming a conjugated resonance structure (■ Fig. 4.17).

In betaxanthins, the chromophore contains amino acid or amine cationic conjugates. The R or R' does not extend the conjugation system (■ Fig. 4.17), and this group of betanins are yellow with λ_{max} near 480 nm. An example of betaxanthin is indicaxanthin (■ Fig. 4.18) isolated from cactus fruit (*Opuntia ficus-indica*).

Fig. 4.17 Betanain: resonance of conjugated cation

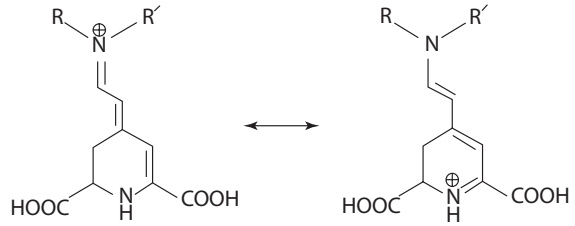
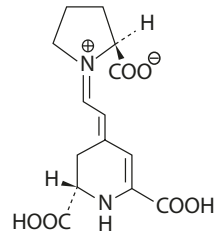
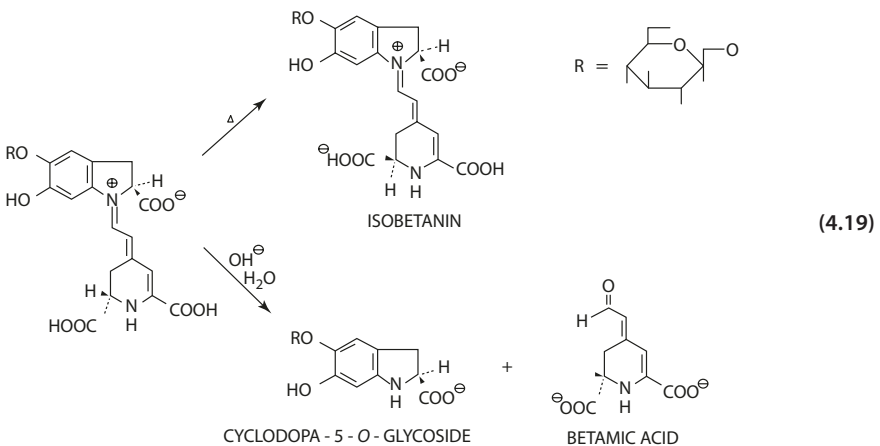


Fig. 4.18 Indicaxanthin



In betacyanins, the conjugation is extended by an aromatic substituent, and the chromophore shows a bathochromic shift to 540 nm. In betacyanins, various substituents are found conjugated to the cyclodopa hydroxyl group, including sugar monomers, such as glucose, apiose, and acid functions, such as malonic, caffeic, and ferulic acids.

The most extensively studied betacyanin is betanin found in red beet (*Beta vulgaris*). Betanin readily isomerizes to isobetanin upon heating [36]. In alkaline medium, hydrolysis yields cyclodopa-5-O-glycoside and betamic acid (Eq. 4.19).



During thermal processing of canned beets, loss of color occurs. However, a partial regeneration of the red color has been observed and known for years in the industry. The mechanism likely involves hydrolysis of the Schiff base and, in the reverse reaction, condensation of the amino group of cyclodopa-5-*O*-glycoside and the aldehyde of the betamic acid.

4.8 Caramel

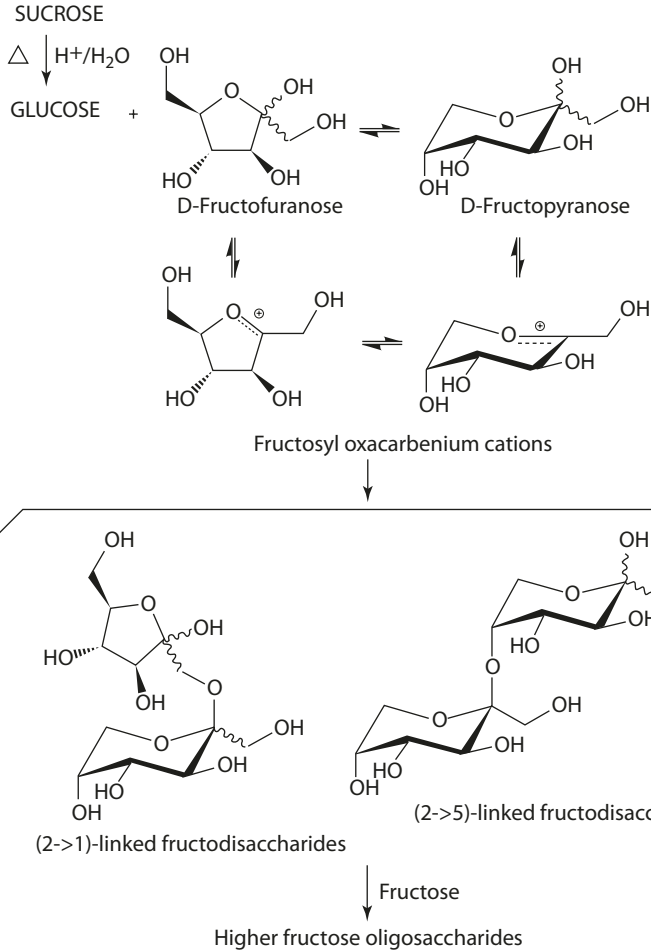
Caramel is the amorphous, dark brown product resulting from controlled heat treatment of food grade carbohydrates, usually corn syrup with 75% dextrose content. Acids, alkalis, or salts are added in small amounts to increase the caramelization rate and to obtain the desirable characteristics for various food uses. Caramel is widely used for coloring and flavoring of foods and beverages, and also plays an important role in nonenzymatic browning (Refer to ► Chap. 3: Carbohydrates).

The initial chemical change in caramelization is the high-temperature isomerization of glucose to fructose through the Lobry de Bruyn-Alberda van Eckenstein aldose ketose rearrangement (Eq. 4.20). The early stage of decomposition of sugar is characterized by the formation of volatile aroma compounds, such as furans (nutty), diacetyl (butterscotch-like), and maltol (toasty). Within the nonvolatile fraction, one of the major and well-defined products is fructose dianhydride, which is formed by dimerization of D-fructose with the loss of two water molecules and generation of two reciprocal glycosidic linkages [44]. Higher molecular oligomers and polymers are found in caramelization, but the exact chemical structure and the reaction pathways are not defined. The chemistry in the formation of caramel likely involves glycosidic bond and ring cleavages of the sugars, combined with condensation, dehydration, hydration, and disproportionation reactions. [13].

Caramel is considered to be a complex polymeric mixture of indefinite compositions, and has been traditionally classified into three groups:

Caramelan	$C_{24}H_{36}O_{18}$
Caramelen	$C_{38}H_{50}O_{25}$
Caramelin	$C_{125}H_{188}O_{80}$

The net charge of caramel is critical to the choice of applications for a particular food product [29]. Caramel in aqueous solution can be positively or negatively charged depending on the manufacturing process and the pH of the medium. A positively charged caramel can interact with other negatively charged molecules in the food system causing precipitation. Caramel for soft drinks and beverages is required to carry strong negative charges. For bakery products, beer, and gravies, the caramel mixture should carry positive charges. A variety of caramels is available to match particular requirements. The «acid-proof» caramel is compatible with phosphoric acid and used in soft drinks. Baker's caramel is made for breads, biscuits, and other baked goods. Powdered caramel is for cake mixes and species.



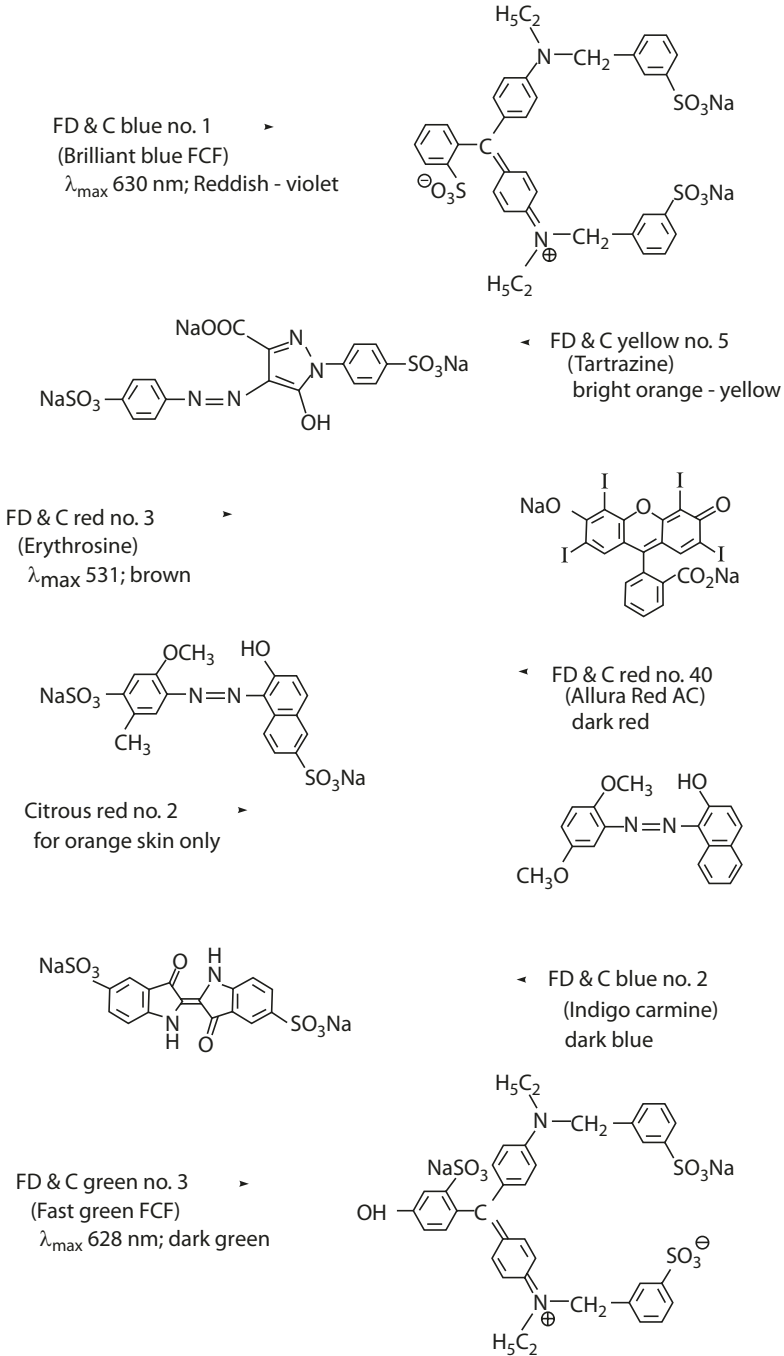
(4.20)

4.9 Dyes and Lakes

Color additives are classified in two categories [26].

1. Uncertified color additives are natural colors that may be obtained from natural sources or synthetic duplicates of the natural colors. Many of the uncertified color additives have already been discussed above and include the chlorophyll derivatives described in later sections.
2. Certified color additives are synthetic colors that do not occur in nature. These are the dyes and lakes which include some important and useful food colorants. Compared to natural colors, the certified color additives have (a) higher tinctorial (coloring) strength, (b) higher stability, and (c) uniform standardization of hue and color strength.

The dyes are available in liquid, powder, dispersion, and paste forms. A list of the certified color dyes is presented in [Fig. 4.19](#). Structurally, all these dyes are extensively conjugated and several of them are azo compounds. The azo dyes are susceptible to reduction by reducing agents, resulting in color fading.



■ Fig. 4.19 Chemical structure of color dyes

Lakes are common names for the aluminum salts of FD&C color dyes. These are formed by the precipitation and adsorption of a water-soluble dye on an insoluble base or substrate, alumina hydrate, $\text{Al}(\text{OH})_3$. The alumina hydrate base is very insoluble in water, so the products are insoluble forms of dye, hence, a pigment. Lakes, therefore, are basically dyes modified for application in nonaqueous systems. Icings, fillings, frostings, confectionary coatings, and gum products are some of the examples. Lakes typically 5 μ in particle size are applied to foods by dispersion, and are stable in the pH range of 4.0–9.0 with very little leaching.

4

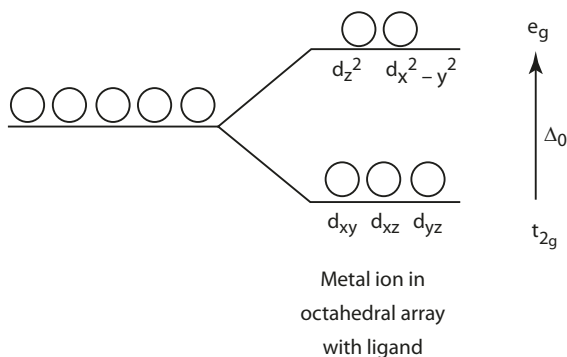
4.10 Coordination Chemistry

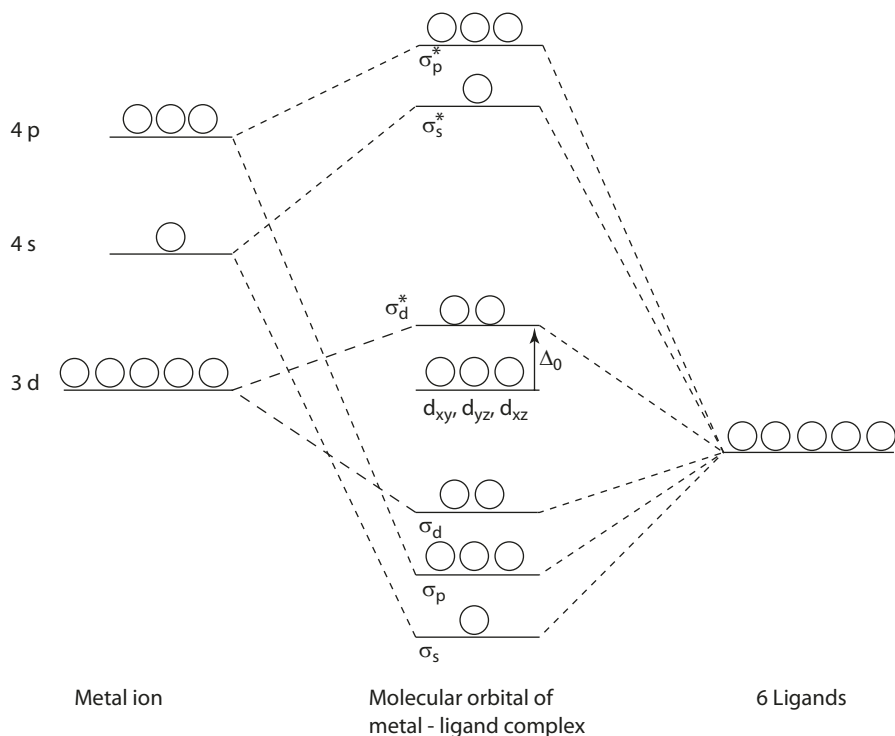
Thus far, the discussion has focused on colored compounds that are chiefly conjugated polyenes. There is another unique class of compounds that are highly colored – the metalloporphyrins. In order to understand the chemistry and chromophoretic properties of metalloporphyrins, a brief presentation of coordination chemistry is appropriate here [7].

A simple approach will be to consider what would happen to the five d orbitals of a transition metal (Fe, Co, etc.) when it is placed in an octahedral array of six ligands along the three Cartesian coordinate systems of the d orbitals. Here, the ligands are treated as point negative charges. The $d_{z^2-y^2}$ and the d_{z^2} orbitals have each of their lobes of electron density pointing towards the ligand, while the d_{xy} , d_{xz} , and d_{yz} orbitals have each of their lobes directed between the ligands. The $d_{x^2-y^2}$ and d_{z^2} orbitals thus experience a higher electrostatic potential energy compared to the d_{xy} , d_{xz} , and d_{yz} orbitals. The net result is that the five d orbitals are split into two energy levels (t_{2g} and e_g) (■ Fig. 4.20).

Taking into account the orbitals of the ligands bonding to the metal ion, the qualitative molecular orbital (MO) energy-level diagram for an octahedral complex between a metal ion and the six ligands that do not possess π orbitals is presented in ■ Fig. 4.21. The d_{xy} , d_{xz} , and d_{yz} orbitals of the metal ion are nonbonding, since they have the wrong symmetry for binding with the ligands. The energy level therefore remains the same. The d_{z^2} and $d_{x^2-y^2}$ can overlap with the ligand orbitals forming the σ_d^* and σ_d bonds. The nonbonding and the lowest antibonding levels are analogous to the t_{2g} and e_g in the point model discussed above. Most ligands, however, have π orbitals which also interact with the nonbonding orbitals, d_{xy} , d_{xz} , and d_{yz} .

■ Fig. 4.20 Energy-level diagram for the five d orbitals of a metal ion in an octahedral field





■ **Fig. 4.21** Molecular orbital energy-level diagram for octahedral coordination between a metal ion and six ligands

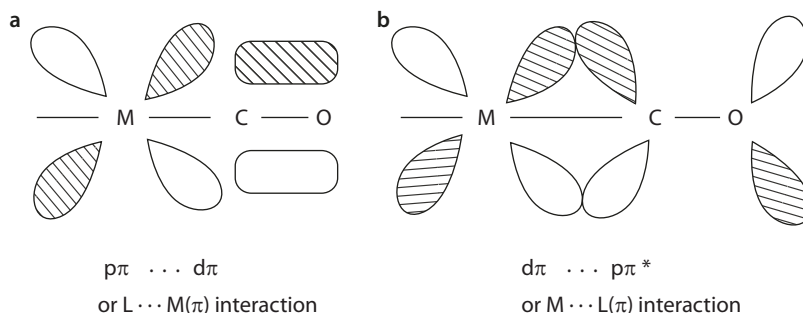
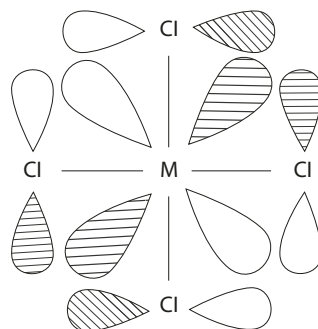
The ligand π orbitals may be simple $p\pi$ orbitals or molecular orbitals of a polyatomic ligand (e.g., O_2 , CO, NO). The interaction of d_{xy} , d_{xz} , and d_{yz} orbitals of the metal ion with the π orbitals of the ligands affects the magnitude of the splitting energy, Δ_0 , negatively or positively. Ligands with π orbital symmetry that destabilize the metal t_{2g} orbitals tend to cause the Δ_0 value to decrease. Likewise, ligands that stabilize the metal t_{2g} orbitals tend to increase the splitting energy Δ_0 .

For a simple $p\pi$ system of a single atom (e.g., Cl^-) overlapping with $d\pi$ orbitals of the metal ion, the lone-pair electrons in the π orbitals of the Cl^- repel the electrons in the d_{xy} , d_{yz} , and d_{xz} orbitals. Such ligand-to-metal interaction, $p\pi-d\pi$ or $L-M(\pi)$, is illustrated in ■ Fig. 4.22. In this case, the energy of the t_{2g} level is increased, and Δ_0 is decreased. Such ligands (including Cl^- , Br^- , and OH^-) are called weak-field ligands.

The effect of π interaction via polyatomic ligands is more complicated. Consider the π and π^* orbitals of the ligand CO. The π -bonding orbital destabilizes the t_{2g} orbitals of the metal ion by $L-M(\pi)$ interactions similar to the Cl^- example discussed above. The antibonding π^* orbital also interacts with the metal $d\pi$ orbitals in a $M-L(\pi)$ interaction (■ Fig. 4.23).

In the π -bonding orbital of the ligand, most of the electron density stays in the CO π bond. However, the π^* antibonding orbital of the ligand is unfilled. Therefore, overlapping of the empty π^* orbital with the metal $d\pi$ orbital results in the delocalization of the electrons from the metal to the ligand. The interaction is therefore often called π back

■ Fig. 4.22 Interactions between $p\pi$ orbital of Cl^- with $d\pi$ orbital of metal



■ Fig. 4.23 Interactions between **a** $p\pi$ orbital and **b** $p\pi^*$ orbital of polyatomic ligand and $d\pi$ orbital of metal

■ Table 4.1 L-M Transitions

Ligand	Metal (d Orbital)
π	$\pi^* (t_{2g}^*)$
π	$\sigma^* (e_g)$
σ	$\pi^* (t_{2g}^*)$
σ	$\sigma^* (e_g)$

bonding, indicating the donation of a π electron from the metal ion to the ligand. Delocalization of electron density stabilizes and lowers the energy of the t_{2g} orbitals of the metal ion, resulting in increased Δ_o . Ligands such as CO , O_2 , and NO that increase the splitting energy, Δ_o this way, are known as strong-field ligands.

In light absorption, two types of electron transitions are possible:

1. $d-d$ Transition: If ν is equal to Δ_o/h , the metal-ligand can transfer the light energy to energy of excitation of electrons from t_{2g} to the e_g metal ion centered orbital.
2. Charge-transfer transition: This is the excitation of electrons from the molecular orbital centered in the ligand to the metal ion centered orbital. These L-M transitions are listed in ■ Table 4.1. The process requires higher energy than the $d-d$ transition, and the resulting spectrum lies in the range of shorter wavelengths (less than 400 nm) [7].

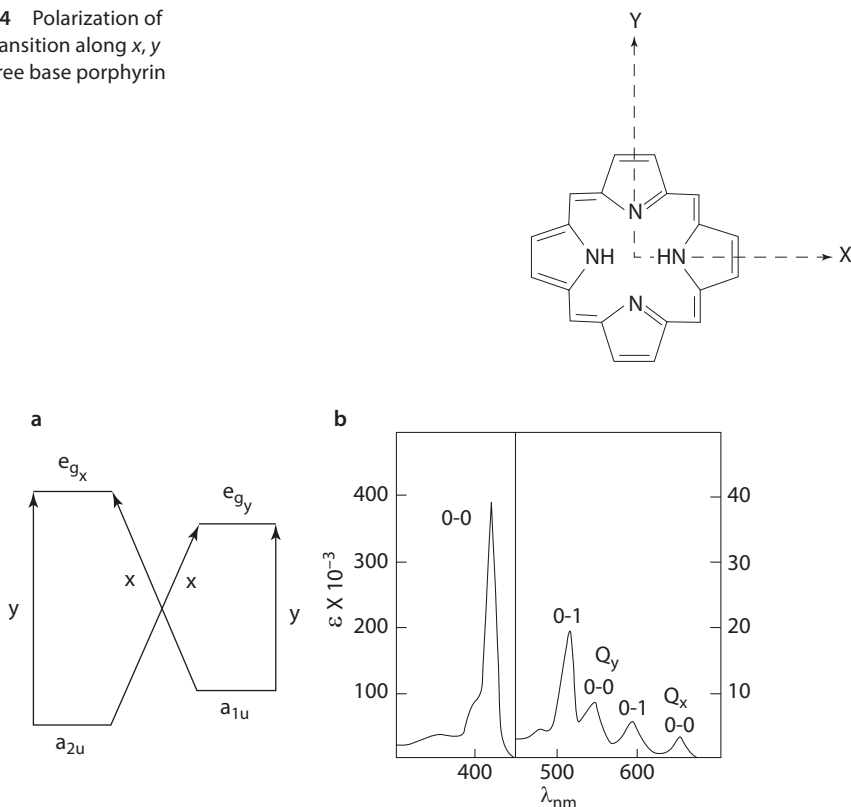
4.11 Metalloporphyrin: Electronic Structure

In metalloporphyrins, the situation is complicated by the fact that the porphyrin that complexes with metal ion through the four nitrogen atoms possesses 18 π electrons in an 18-atom ring [1, 14]. It is no surprise that all porphyrins are highly colored due to the conjugated π -electron system (π - π^* transition). All free-base porphyrins show similar four-banded visible spectra of moderate intensity between 500 and 660 nm and a strong band at 400 nm. The visible and UV bands are labeled Q and B, respectively. The UV band is also known as the Soret band. The highest filled π orbital of a porphyrin has a_{1a} and a_{2u} symmetry and the lowest unfilled orbitals are of e_g symmetry, according to MO calculations which are beyond the scope of this book. The excited states correspond to the π - π^* transition of one of the four electrons from the highest occupied molecular orbital (HOMO) to the lowest unoccupied molecular orbital (LUMO).

In a free-base porphyrin, the π - π^* transition is polarized along the x, y axes (■ Fig. 4.24). The π -electron conjugation is shown, where the lone-pair electrons in the two imino nitrogens do not enter the π system.

Polarization of the π - π^* transition results in the splitting of Q_o into Q_x and Q_y bands (■ Fig. 4.25a, b). Further vibrational coupling between these transitions with the Soret bands gives rise to two more visible bands designated as vibronic overtones (Q_v). The

■ Fig. 4.24 Polarization of the π - π^* transition along x, y axes of a free base porphyrin



■ Fig. 4.25 a Energy splitting of the π - π^* transition, and b absorption spectrum of a free-base porphyrin (From Gouterman [13] with permission. Copyright 1961 Elsevier)

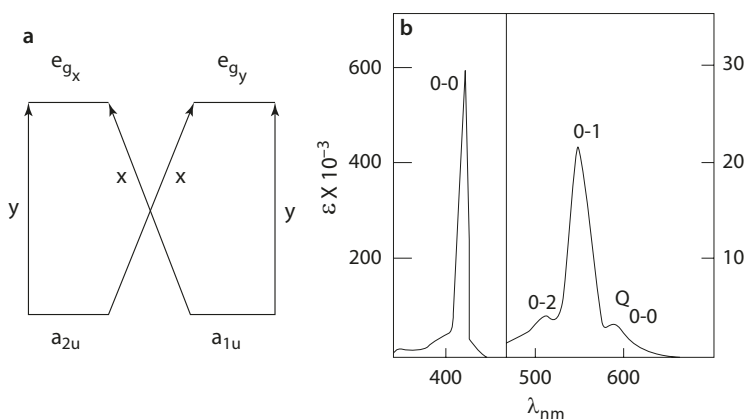
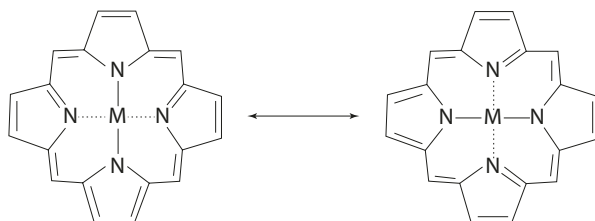
intensity of the Q_x and Q_y bands is sensitive to substituents, while the intensity of the overtones is less affected.

In the metal-porphyrin complex, the molecule assumes a D_{4h} (full square) symmetry, partly due to the resonance of the complex (■ Fig. 4.26). Transitions in the x and y directions are equivalent. The two LUMOs (e_g) are strictly degenerate, and the HOMOs (a_{1u} , a_{2u}) are almost degenerate (■ Fig. 4.27a, b). The π - π^* transition results in a single Q_o band plus the vibronic overtone Q_v . (The Q_o and Q_v bands are also known as α and β bands in some literature.) The differences in symmetry, orbital energy, and absorption spectra between the free-base porphyrin and metalloporphyrin are summarized in ■ Table 4.2.

In a metal-porphyrin complex, the main effect of the metal on the transitions is the conjugation of the metal $p\pi$ orbital with the porphyrin π orbital having a_{2u} symmetry (■ Fig. 4.28). The interactions either raise or lower the orbital energy and consequently shift the absorption spectrum.

The porphyrin π -metal transfer occurs in the transitions from the HOMO of the porphyrin (a_{2u} , a_{1u} , a'_{2u} , b_{2u} symmetry) to the metal e_g orbitals (d_{z^2} , $d_{x^2-y^2}$). The d - d transitions are affected since the splitting of the d -orbital symmetry is altered. The splitting of the d orbitals of the metal ion (due to the porphyrin) exhibits additional loss of degeneracy

■ Fig. 4.26 Resonance of metal-porphyrin complex



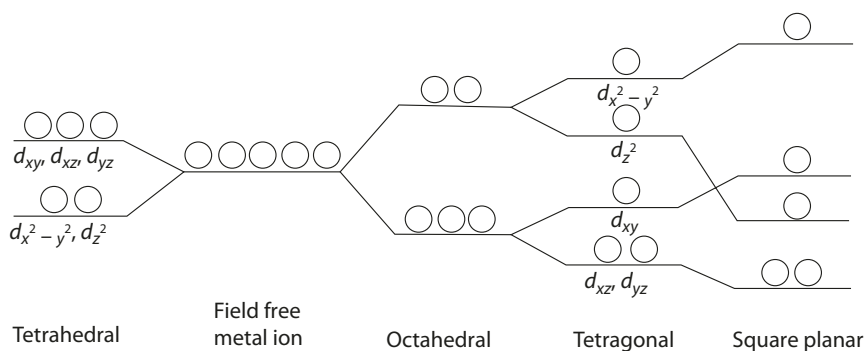
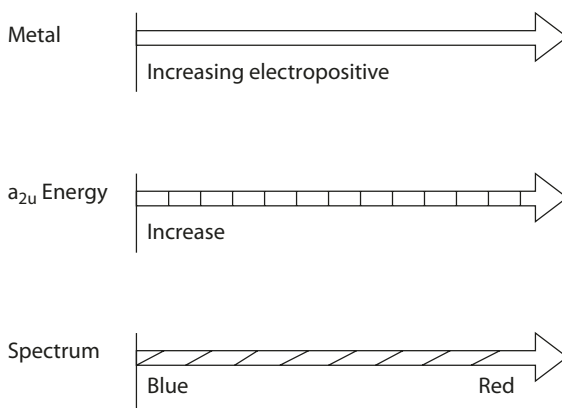
■ Fig. 4.27 a Energy splitting of π - π^* transition, and b absorption spectrum of a metal porphyrin (From Gouterman [14] with permission. Copyright 1961 Elsevier)

4.11· Metalloporphyrin: Electronic Structure

■ **Table 4.2** Comparison of orbital energy and spectrum between free-base porphyrin and metalloporphyrins

	Orbital energy		Visible bands	
	HOMO	LUMO	Q	Overtone
Free-base porphyrin $x \neq y$ (polarized) D_{2h} (rectangular)	$e_{g_x} > e_{g_y}$	$a_{1u} > a_{2u}$	$2(Q_x, Q_y)$	$2Q_v$
Metalloporphyrin $x = y$ (equivalent) D_{4h} (full square)	$e_{g_x} = e_{g_y}$	$a_{1u} \approx a_{2u}$	$1(Q_o)$	$1Q_v$

■ **Fig. 4.28** Metal effect on the transition energy of the porphyrin π orbital



■ **Fig. 4.29** Energy-level diagram of some common coordinations

from the theoretical predicted octahedral symmetry. In myoglobin, the octahedral symmetry is distorted to assume tetragonal or square planar symmetry (■ Fig. 4.29). The visible spectra of myoglobin and their derivatives are shown in ■ Fig. 4.30 [11, 21, 27], which will be discussed further in the following sections.

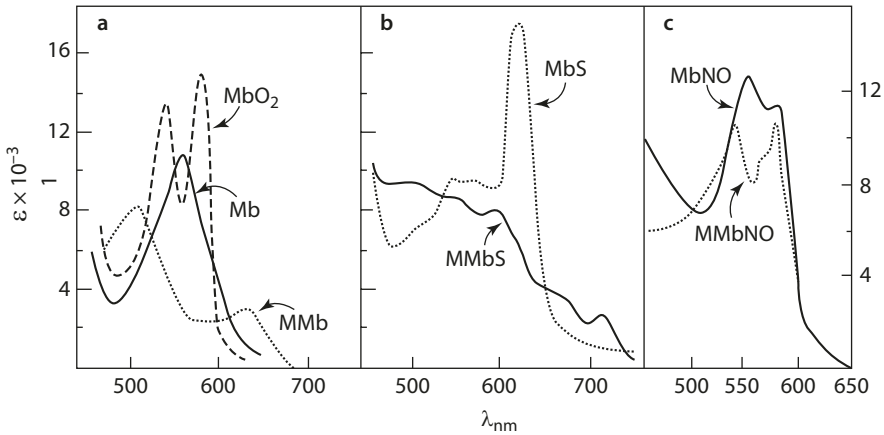


Fig. 4.30 Spectra of **a** deoxymyoglobin, oxymyoglobin, and metmyoglobin; **b** sulfmyoglobin and met-sulfmyoglobin; (From Nicholis [27] with permission. Copyright 1961 The Biochemical Society and Portland Press Ltd.); and **c** nitrosylmyoglobin and nitrosylmetmyoglobin (From Fox and Thompson [11] with permission. Copyright 1963 American Chemical Society)

4.12 Myoglobin

Myoglobin is the main pigment in meat, and the structural form, including the prosthetic group, of this protein in meat and processed meat determines the color of the product.

4.12.1 Molecular Structure

Myoglobin is a single polypeptide of 153 amino acid residues, consisting of a protein moiety (globin) and a prosthetic group (heme) [8]. The 18 kDa globular protein is folded with eight major α -helical segments (referred to as A, B, C, D, E, F, G, and H) and nonhelical segments in between. The folding is such that the prosthetic heme is buried in a hydrophobic cleft. The heme is an iron-porphyrin complex with the iron covalently linked to His residue F8 (proximal His), and is closely associated with a second His residue E7 (distal His) (■ Figs. 4.31 and 4.32).

Porphyrins are derivatives of the parent structure porphyrin, which consists of four pyrrole rings joined by methine ($-\text{CH}=\text{}$) bridges. The porphyrin of heme consists of methyl, ethenyl, and propionyl side chains. This particular porphyrin derivative is classified as protoporphyrin IX (■ Fig. 4.33).

4.12· Myoglobin

Fig. 4.31 α -Carbon diagram of myoglobin molecule. α -Helical regions are given letter-number labels, and nonhelical regions are designated by letter-letter-number symbols. Heme group framework with side groups identified by: *M* methyl, *V* vinyl, *P* propionic acid. Five member rings at F8 and E7 represent His residues associated with heme group (From Dickerson [8] with permission. Copyright 1964 Elsevier)

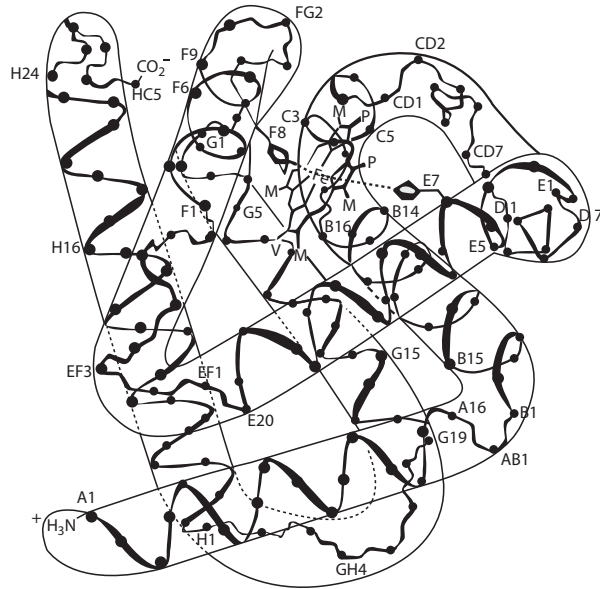
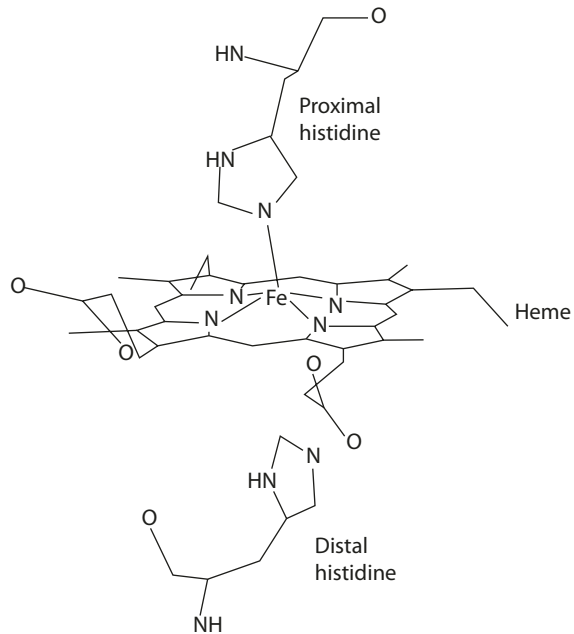


Fig. 4.32 Heme in myoglobin



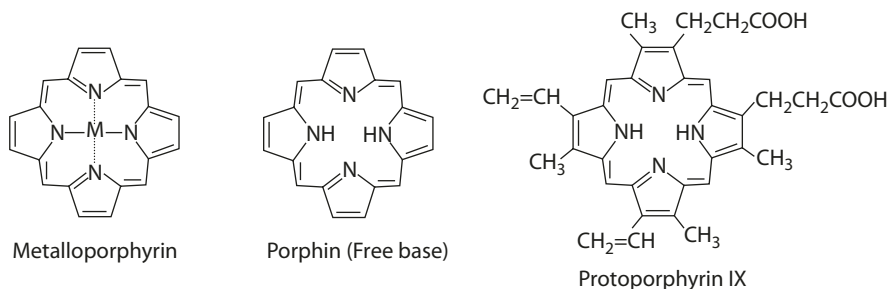


Fig. 4.33 Porphyrin compounds

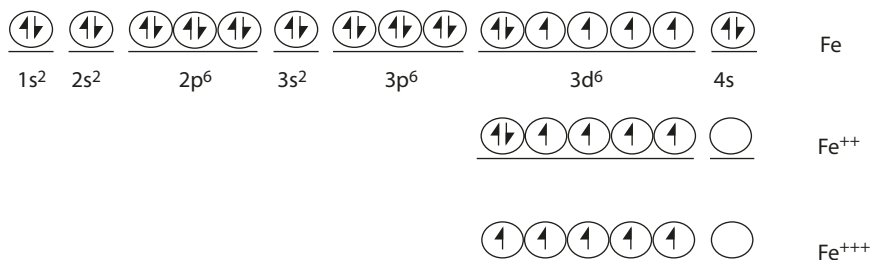


Fig. 4.34 Electronic configuration of iron

4.12.2 The Heme Iron

Deoxymyoglobin (Mb, also represented as Mb(II) to emphasize the iron state) contains heme iron in the +2 state with only five ligands (without bound oxygen). When the myoglobin has oxygen bound reversibly, it is referred to as oxymyoglobin (MbO₂, also represented as Mb(II)O₂). Other neutral ligands such as CO and NO can also bind to the sixth coordination position. The Fe(II) is readily oxidized to Fe(III) state to give ferrimyoglobin (FMb, Mb(III), or FMb(III), also known as metmyoglobin represented as MetMb or MetMb(III).

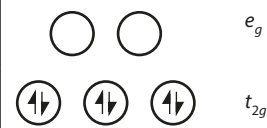
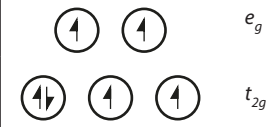
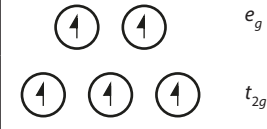
The electronic configurations are shown in Fig. 4.34. The Fe atom can be oxidized to the ferrous ion (Fe²⁺) or the electronically more stable ferric ion (Fe³⁺) by losing two and three electrons, respectively [12].

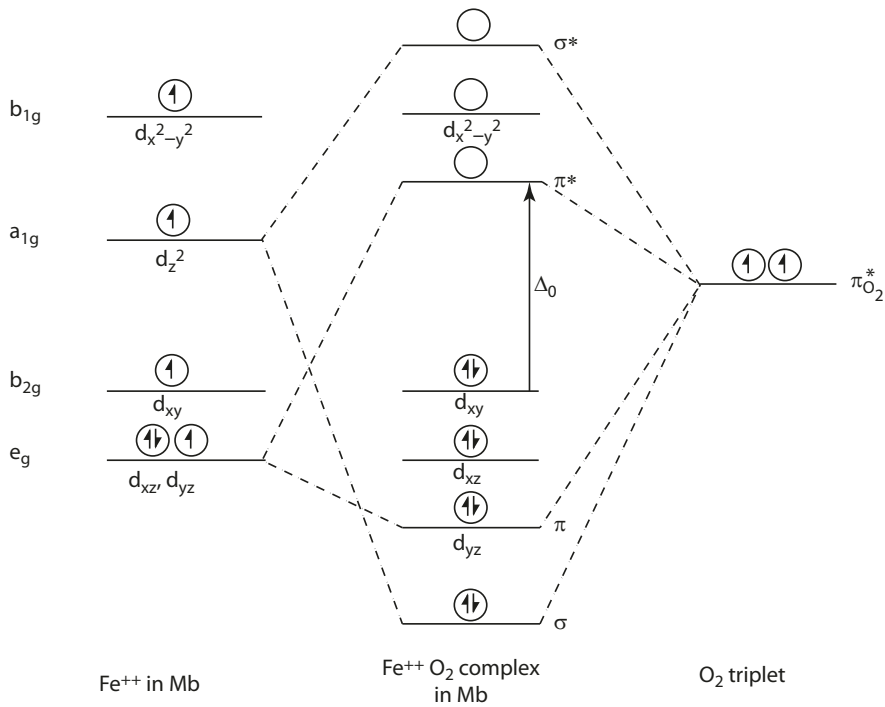
For an Fe atom coordinated with ligands, the 3d orbitals split into two energy levels. (The octahedral is distorted in metalloporphyrin, but for simplicity, a perfect octahedral symmetry is assumed.) The way that the d electrons fill the t_{2g} and e_g orbitals depends on the nature of the ligands. Three electronic configurations are of interest in the present discussion (Table 4.3).

In the heme complex, the coordination positions are directed to the four porphyrin nitrogens, and in the fifth and the sixth positions to His F8 and O₂ (or H₂O), respectively. Deoxymyoglobin has only five ligands (four porphyrin nitrogens and axial coordinated His F8 nitrogen), and binds O₂ readily to form the low-spin, diamagnetic oxymyoglobin. The molecular orbital scheme is presented in Fig. 4.35.

4.12· Myoglobin

■ **Table 4.3** Electronic configuration of the heme iron

1. Oxymyoglobin low spin, ferrous $S = 0$ diamagnetic	
2. Deoxymyoglobin high spin, ferrous $S = 2$ Paramagnetic	
3. Ferrimyoglobin high spin, ferric $S = 5/2$	



■ **Fig. 4.35** Molecular orbital energy-level diagram of $Fe^{2+}-O_2$ complex in oxymyoglobin

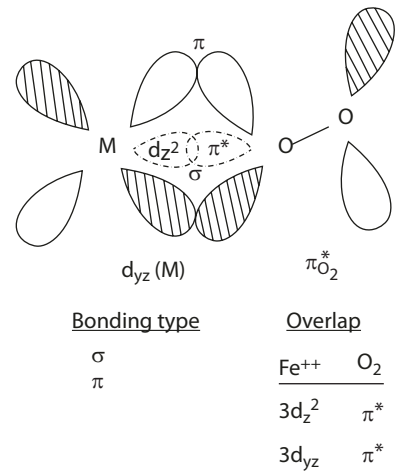
A σ bond is formed by the overlap of the $3d_z$ orbital of the Fe with π^* of O_2 , and a π bond is formed by the overlap of the $3d_{yz}$ orbital of the Fe^{2+} with the other π^* of the O_2 (■ Fig. 4.36).

The $Fe^{2+}-O_2$ complex in oxyhemoglobin is at a lower energy level than the dioxygen on the Fe^{2+} . The $Fe^{2+}-O_2$ complex is generally regarded to have the characteristic at least as if it were a ferric-superoxide adduct $Fe^{3+}-O_2^-$. The oxygen binds in the end-on orientation to give a 135° bend.

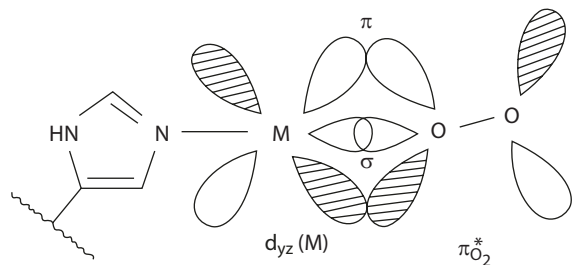
The dioxygen is hydrogen bonded to the distal His imidazole. The proximal His imidazole nitrogen is hydrogen bonded to adjacent amino acid side groups in the globin, thereby increasing its basicity. This increase in electron density strengthens the back-bonding in which the iron donates the $d\pi$ electron back to the π^* orbital of O_2 . Since O_2 is a weak σ electron donor, the σ and π bondings provide stability of the complex (■ Fig. 4.37).

The bonding of O_2 to the heme Fe is reversible. In physiological conditions, equilibrium exists between free oxygen and oxygen bound to the heme iron (■ Fig. 4.38) [31].

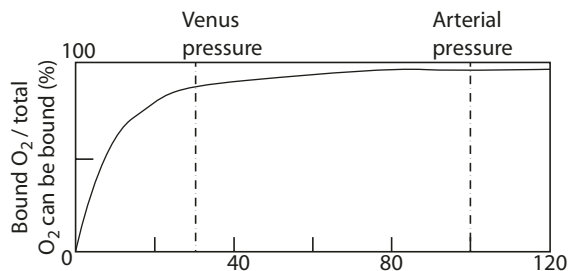
■ Fig. 4.36 Overlap of $d\pi$ orbital of Fe^{2+} and π^* orbital of O_2



■ Fig. 4.37 Back-bonding assisted by histidine



■ Fig. 4.38 Partial pressure (mm Hg) of oxygen over solution in equilibrium (Perutz [31])



4.12.3 The Role of Globin

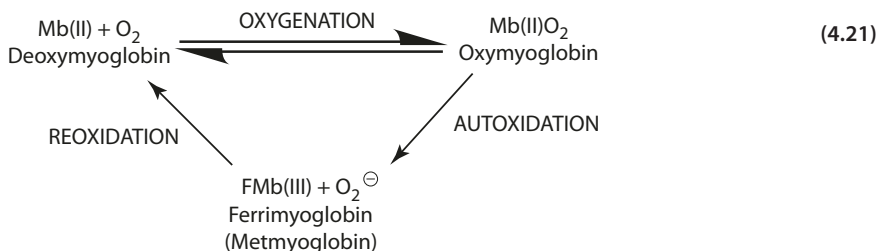
The protein globin functions to stabilize the steric and electronic configuration of the iron heme through more than 60 hydrophobic interactions and hydrogen bonds. Changes in the protein conformation inevitably influence the ligand binding property of the heme. Similarly, binding of a ligand is expected to induce conformational changes of the globin. Transition from deoxy- to oxymyoglobin is associated with movement of the iron and the proximal His into the porphyrin plane, as to enhance π and σ overlap with the iron and dioxygen. The proximal His nitrogen plays a primary role in the synergistic π and σ binding within the $\text{Fe}^{2+}-\text{O}_2$ complex by feeding electron density that enables the back-bonding of electrons from the iron to the π^* orbital of the oxygen as already noted.

The hydrophobic pocket creates a low dielectric environment that is unfavorable for ionic ligands (e.g., CN^- , OH^-). The closely packed amino acid side chains in the pocket also restrict the accessibility of large ligands, and restrict the size and orientation of the ligand bound to the myoglobin. Only small ligands (O_2 , CO , NO) can bind to the heme iron. The heme iron, being embedded inside the protein molecules and in a hydrophobic environment, is protected from autoxidation. It is spatially isolated from close contact with another heme iron oxidizing to form a dioxygen-bridged di-iron complex (porphyrin- $\text{Fe}^{2+}-\text{O}_2-\text{Fe}^{2+}$ -porphyrin). If the globin is heat-denatured (as in cooking), the free heme would undergo rapid autoxidation.

Structural studies of myoglobin reveal that the distal His E7 resembles a gate with open and closed conformation controlling the entrance of ligands to the active site on the distal side of the heme group [51]. At neutral pH, the closed conformation is dominant. At low pH, the His E7 gate is in its open conformation resulting from protonation and increased solvent exposure of the imidazolium cation. The dependency of myoglobin autoxidation on pH is discussed in section 4.12.5 "The Autoxidation of Oxymyoglobin".

4.12.4 Oxygenation of Myoglobin

It is in the ferrous form that myoglobin, Mb(II), binds molecular oxygen reversibly as the primary physiological function (Eq. 4.21). The oxygen dissociation constant K_d is 1.15×10^{-6} M calculated from $k_f = 1.64 \times 10^7 \text{ s}^{-1} \text{ M}^{-1}$ and $k_r = 19 \text{ s}^{-1}$ (sperm whale, pH 7.0, 25 °C) [40].



4.12.5 Autoxidation of Oxymyoglobin

Oxymyoglobin is known to undergo slow oxidation to ferrimyoglobin (Eq. 4.22). Under air-saturated conditions, the primary step for the autoxidation reaction is first order with respect to the unoxidized Mb(II)O₂, with $k_{\text{ob}} = 8 \times 10^{-3} \text{ h}^{-1}$ (sperm whale, pH 7.0, 25 °C) [40]. The rate is different from protein to protein depending on the source.

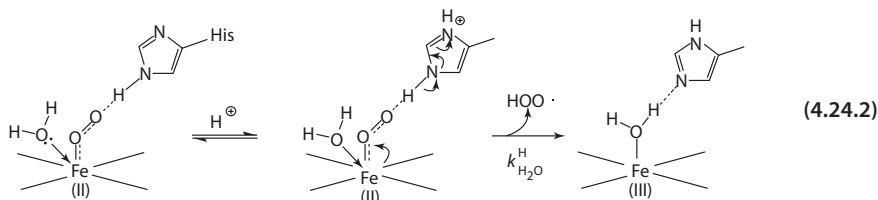
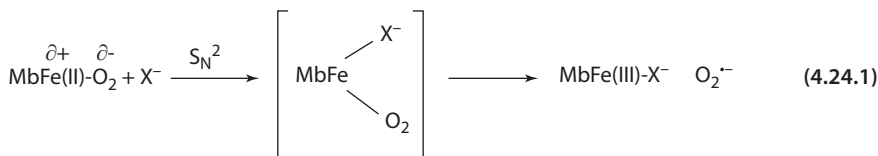
Several factors affect the rate of myoglobin autoxidation: (1) The rate increases markedly with increasing H⁺ concentration (lowering pH). The pH effect is attributed to the promotion of proton-assisted catalysis (see below). (2) The rate is also markedly affected by temperature, with increased rate at higher temperatures. (3) The rate is dependent on the partial pressure of oxygen, proceeding maximally at the half-saturating oxygen ($p\text{O}_2$ of 1–2 torr) pressure where Mb(II) and Mb(II)O₂ are equal in concentration.



In the autoxidation of Mb(II)O₂ to FMb(III), the simple one-electron transfer process in which Fe²⁺ is oxidized to Fe³⁺, and O₂ is reduced to the superoxide anion (O₂^{·-}) (Eq. 4.23), cannot occur, because ΔG of the reaction is +30.8 kcal/mol.

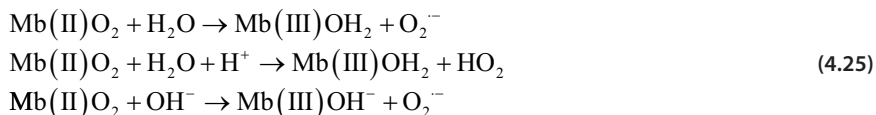


Instead, myoglobin autoxidation proceeds via a S_N2 nucleophilic displacement of O₂^{·-} from Mb(II)O₂ by a water molecule or a hydroxide ion entering the heme pocket from the surrounding solvent, followed by the conversion of the Fe²⁺ to the ferric form [40]. The reaction involves the formation of an intermediate with a partial positive center on the Fe(II) (Eq. 4.24.1) [35].



The reductive displacement of the bound dioxygen as O₂^{·-} by H₂O is greatly enhanced by a proton-assisted catalysis (Eq. 4.24.2) by a factor of $5 \times 10^7 \text{ mol}^{-1}$ [39]. The distal His

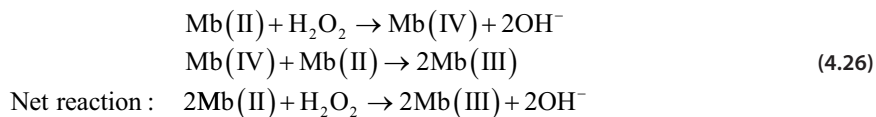
E7 promotes the protonation of the bound oxygen, acting via its imidazole ring in a charge-relay mechanism. Polarized dioxygen facilitates a charge transfer from Fe(II) to O₂ produced by a water molecule (H₂O) or hydroxide ion (OH⁻) entering the heme pocket from the surrounding solvent. This leads to a favorable displacement of O₂^{·-} as hydroperoxyl radical (HOO·), which with a pK_a of 4.8 dissociates rapidly to the superoxide anion (O₂^{·-}). The stability of Mb(II)O₂ is therefore highly dependent on pH, with optimal rate in the acidic range, and the autoxidation [Mb(II)O₂ to Fmb(III)] can be represented by three types of displacement equations (Eq. 4.25).



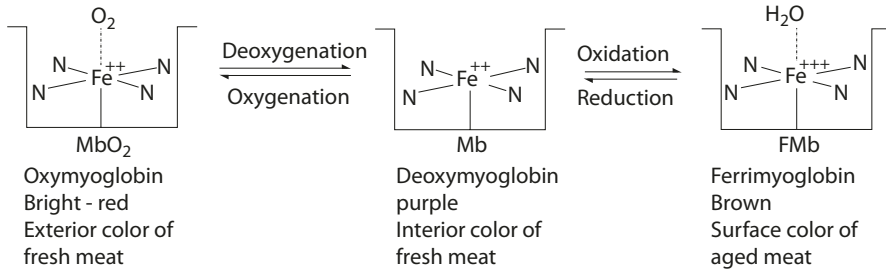
The ferrimyoglobin produced in the autoxidation of Mb(II)O₂ has the heme iron in the Fe(III) state, and a H₂O molecule in the sixth ligand. Mb(III) is brown and responsible for the discoloration of meat under normal storage conditions.

■ ■ The Role of Hydrogen Peroxide

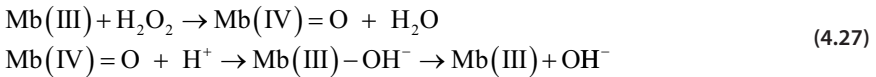
The superoxide anion formed in the autoxidation reaction (from either normal or proton-assisted autoxidation) converts (dismutates) with high rates to H₂O₂ (according to 2O⁻ + 2H⁺ → H₂O₂ + O₂). The product H₂O₂ is a potent oxidant. H₂O₂ oxidizes the oxy and deoxy species, Mb(II)O₂ and Mb(II), to Mb(III) through the intermediate ferryl-iron forms, [Mb(IV)=O] and [Mb(IV)], respectively. Since the preferred target of H₂O₂ is the deoxy species, about 10 times that of the MbO₂, the reaction is favored at decreasing O₂ pressure (i.e., condition in which the equilibrium of oxygenation is shifted towards the deoxy species). Under air-saturated conditions (pO₂ = 150 Torr), the oxy form is predominant, and only ~0.5% exists in the deoxy form, in the equilibrium Mb(II)O₂ = Mb(II). At low pO₂ < 1 Torr, almost half of the Mb(III) formation comes from the oxidation of Mb(II) with H₂O₂ (Eq. 4.26). As Mb(II) is oxidized by H₂O₂ to form Mb(III), the equilibrium is shifted and more deoxy species are formed for further oxidation to the Met form. A good supply of oxygen is a good defense against the oxidation of myoglobin [50].



H₂O₂ has also been shown to rapidly oxidize Mb(III) resulting in its decomposition. Oxidation of Mb(III) proceeds via two electron oxidation, producing an intermediate species, the ferrylmyoglobin form [Mb(IV)=O] (Eq. 4.27) [9]. One equivalent at the iron center forms the oxyferryl complex Fe(IV)=O, and one is located at the globin as a protein-centered radical. Ferrylmyoglobin is slowly reduced back to Mb(III) at physiological pH, but with an increasing rate at decreasing pH. This autoreduction reaction involves protonation of the ferrylmyoglobin, followed by abstraction of an electron from the porphyrin or the globin protein [33].



■ Fig. 4.39 Interconversion of Mb(II), Mb(II)O₂, and FMB(III)



■ ■ Reduction of Ferrimyoglobin

Reduction of Mb(III) to Mb(II) has been shown to occur enzymatically. Metmyoglobin reductase has been purified from beef heart and dolphin muscle. Nonspecific reducing systems, including ascorbate, NADPH, and flavins, also can reduce Mb(III) to the deoxy ferrous species. The reduction of the Met form by the reductase enzyme and the nonspecific reducing agents is the basis for the recycling and continuity of the physiological function of myoglobin *in vivo*. The Mb(II) (the active form which binds oxygen) to Mb(III) (the inactive form) content in various muscle tissues is commonly found in a ratio of 60:40%.

In fresh meat, reducing substances endogenous to the tissue reduce ferrimyoglobin to deoxymyoglobin, which is then oxygenated to oxymyoglobin if oxygen is present as in the case of the surface layer of fresh meat. In the interior, the deoxy form is the predominant species and the meat color is thus purple. Schematically, the interconversion of Mb(II), Mb(II)O₂, and Mb(III) can be represented in ■ Fig. 4.39.

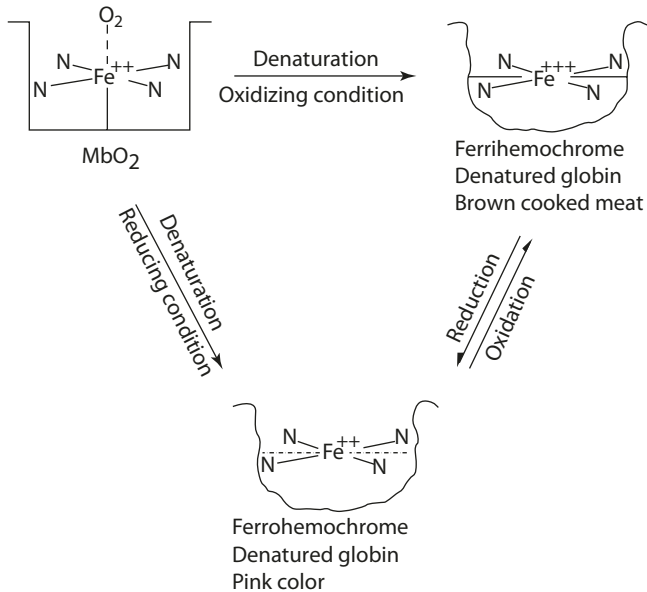
4.12.6 Absorption Spectra

A comparison of the visible spectra among Mb(II), Mb(II)O₂, and FMB(III) shows that the spectrum of Mb(II)O₂ is characterized by a typical porphyrin $\pi-\pi^*$ transition with two bands, while Mb(II) exhibits a single broad band and Mb(III) a diffuse band with four peaks from 500 to 650 nm (■ Fig. 4.30).

Strong ligands such as O₂ increase Δ_o , and the $d-d$ transition is close to the energies of the porphyrin $\pi-\pi^*$ transition. Consequently, the $d-d$ transition bands are masked by the porphyrin bands.

In the high-spin ferric complex, the weak-field ligands, such as OH or H₂O in Mb(III), tend to increase the e_g orbital energy, which increases the mixing of porphyrin π and iron d orbitals. There is 35–45% mixing of porphyrin π orbitals with the iron e_g orbitals. Charge transfer transition from the porphyrin π orbitals (a_{2u} , a_{1u} , a'_{2u} , b_{2u}) to the iron e_g orbitals accounts for the multiple peaks that appear in the spectrum.

4.12· Myoglobin



■ Fig. 4.40 Formation of hemochromes

■ Hemochromes

In cooked meat, both myoglobin and ferrimyoglobin are converted to ferro- and ferrihemochromes which can exchange ligands within the globin (■ Fig. 4.40). Amino acid side chains, including imidazole and carboxyl groups, may coordinate to the heme iron in hemochromes. Ferrohemochrome has a visible spectrum similar to oxymyoglobin, but it can be oxidized to ferrihemochrome, resulting in browning and color fading.

■ Sulfmetmyoglobin

Processing and storage conditions that cause changes in the structure of the native porphyrin affect the electronic configuration of the heme. Hydrogen peroxide oxidizes the porphyrin to form a green polypyrrole compound, cholemyoglobin. Hydrogen sulfide reduces the porphyrin of myoglobin, resulting in the formation of sulfmyoglobin and sulfmetmyoglobin with absorption maxima at 617, and 595 and 715, respectively [27, 28]. The formation of sulfmetmyoglobin increases with low pH, and involves H₂S reacting with the ferrylmyoglobin, Mb(IV)=O. These reactions cause undesirable color changes (usually green) in fresh meat and cured meat.

Green pigment is also found to occur during heat processing of some dark meat muscle fish such as tuna. The pigment is formed when myoglobin reacts with trimethylamine oxide (TMAO) in the presence of a reducing substance, for example, cysteine. Heat denaturation unfolds the Mb(III) protein to facilitate the formation of disulfide bonds with cysteine under mild oxidizing conditions by TMAO. TMAO is an osmolyte commonly found in tissues of marine fish derived from the trimethylammonium group of choline.

The chlorine may be degraded by bacteria in the gut of the fish to trimethylamine (TMA, the characteristic fishy odor), which is then enzymatically (trimethylamine oxygenase) oxidized to TMAO [38].

■ ■ Nitrosylmyoglobin

In cured meat, the 6-position ligand of myoglobin is nitric oxide (NO). Nitric oxide binds to both ferrimyoglobin Fe^{3+} and deoxymyoglobin Fe^{2+} . The product in both cases is nitrosylmyoglobin (MbNO), which is low-spin ($s = 1/2$) and paramagnetic.

The molecular orbital of NO has a single electron in the π^*2p orbital. In the nitrosylferromyoglobin, the complex contains σ bonding between NO π^* and the iron d_{z^2} orbitals. The binding in the complex is stabilized via d_{yz} to $p\pi$ back bonding. The MbNO is red, with the visible spectrum similar to Mb(II)O_2 . The Fe^{2+}NO complex is bent at a bond angle of $108\text{--}110^\circ$. Nitrosylmyoglobin is unstable due to the slow photodissociation of the nitric oxide from the Fe^{2+}NO complex, involving excitation of electrons from the porphyrin π electron cloud and hence the withdrawal of π -electron density from the iron to the porphyrin [45]. This tends to weaken the bond between Fe^{2+} and NO, leaving the Fe susceptible to oxidation. However, cured meat color is stabilized when the protein is denatured to ferrohemochrome. Meat denaturation (or acidic pH) of the protein labilizes the His F8 ligand to substitution with a second NO ligand, resulting in the formation of a stable diamagnetic complex, $\text{Fe}^{2+}(\text{NO})_2$, known as dinitroferrohemochrome.

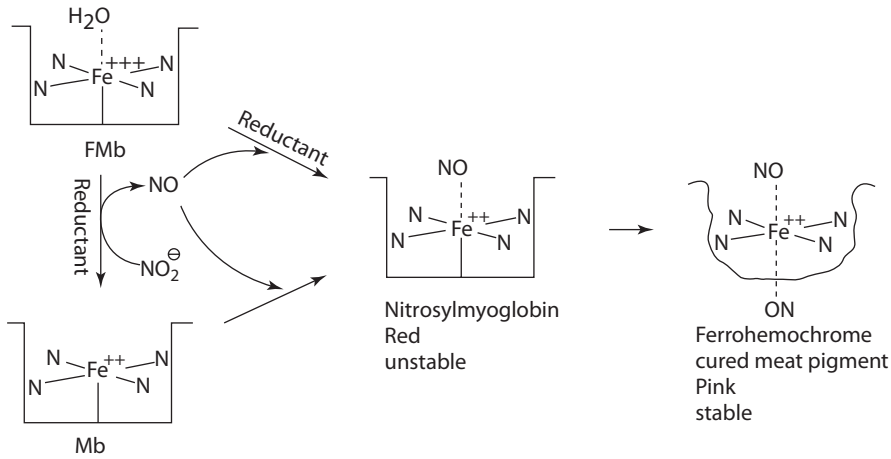
What is the source of nitric oxide (NO) in cured meat? The chemistry of this is related to the reduction-oxidation of nitrogen compounds, which can be represented by the Latimer reduction potential as follows.

Oxidation state	+5	+3	+2	+1	0	-3
	NO_3^- (nitrate)	NO_2^- (nitrite)	NO (nitric oxide)	N_2O (nitrous oxide)	N_2	NH_4^+
E° (in acidic solution)	+0.94	+0.99	+1.59	+1.77	+0.27	
E° (in basic solution)	+0.01	-0.46	+0.76	+0.94	-0.74	

Disproportionation occurs if E° to the right of the intermediate is greater than the E° to the left. Thus, in acid solution, nitrite (NO_2^-) exists as nitrous acid (HNO_2), which is unstable with respect to NO and NO_3^- . For the reaction $3\text{HNO}_2 \rightarrow \text{NO}_3^- + \text{H}^+ + 2\text{NO} + \text{H}_2\text{O}$; ΔE° is positive and $\Delta G (= -nFE^\circ)$ is negative. In basic solution, NO_2^- is stable with respect to disproportionation to NO and NO_3^- .

In cured meat, the reduction of nitrite (NO_2^-) to nitric oxide (NO) is mostly catalyzed by the presence of a reductant. Reductants such as ascorbate, sulfhydryl compounds, and NADH-flavins can reduce (1) NO_2^- to NO, or (2) Fe^{3+} to Fe^{2+} (in myoglobin), which can in turn reduce NO_2^- to NO. The scheme in ■ Fig. 4.41 summarizes the transformation of myoglobin derivatives during the curing of meat.

4.12· Myoglobin



■ Fig. 4.41 Transformation of myoglobin derivatives in meat curing

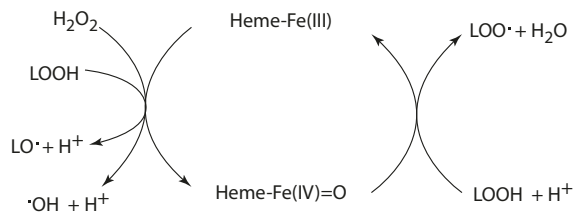
4.12.7 Myoglobin and Lipid Oxidation

Lipid oxidation is known to cause meat discoloration. Primary products, such as alkyl, alkoxy and peroxy radicals, and peroxides are reactive. Secondary lipid oxidation products such as α - and β -aldehydes decrease the redox stability of oxymyoglobin, by covalent modification (via histidine residues) of the protein. In general, fish meat contains a high concentration of polysaturated fatty acids and more susceptible to oxidation. Likewise, nonruminants contain relatively more unsaturated fats than ruminants. Dark muscle fish contains relatively high concentration of myoglobin and iron. Ground meat has more mixing of reactive compounds, more oxygen incorporated, and increased surface area.

All myoglobin forms, Mb(II)O₂, Mb(II), and FMb(II), have been shown to initiate lipid oxidation. The actual process of myoglobin oxidation is a catalyst of lipid oxidation with H₂O₂ a major factor [2]. Autoxidation of myoglobins Mb(II) and Mb(II)O₂ to FMb(III) produces superoxide anion O₂^{•-}, which spontaneously dismutates to form hydrogen peroxide H₂O₂ (according to $2\text{O}_2^{\bullet-} + 2\text{H}^+ \rightarrow \text{H}_2\text{O}_2 + \text{O}_2$). The H₂O₂ oxidation of FMb(III) in the formation of ferrylmyoglobin [Mb(IV)=O] provides a strong prooxidant that initiates and enhances lipid peroxidation in a wide pH range.

The dissociation of both heme from myoglobin and iron from the heme may also cause an increase in lipid oxidation (■ Fig. 4.42). Heme affinity and heme loss rate have shown a great effect on lipid oxidation. Denaturation and unfolding of the globin expose the heme iron to the environment, causing heme-iron catalyzed peroxidation.

■ Fig. 4.42 Heme-iron catalyzed one-electron transfer and lipid oxidation



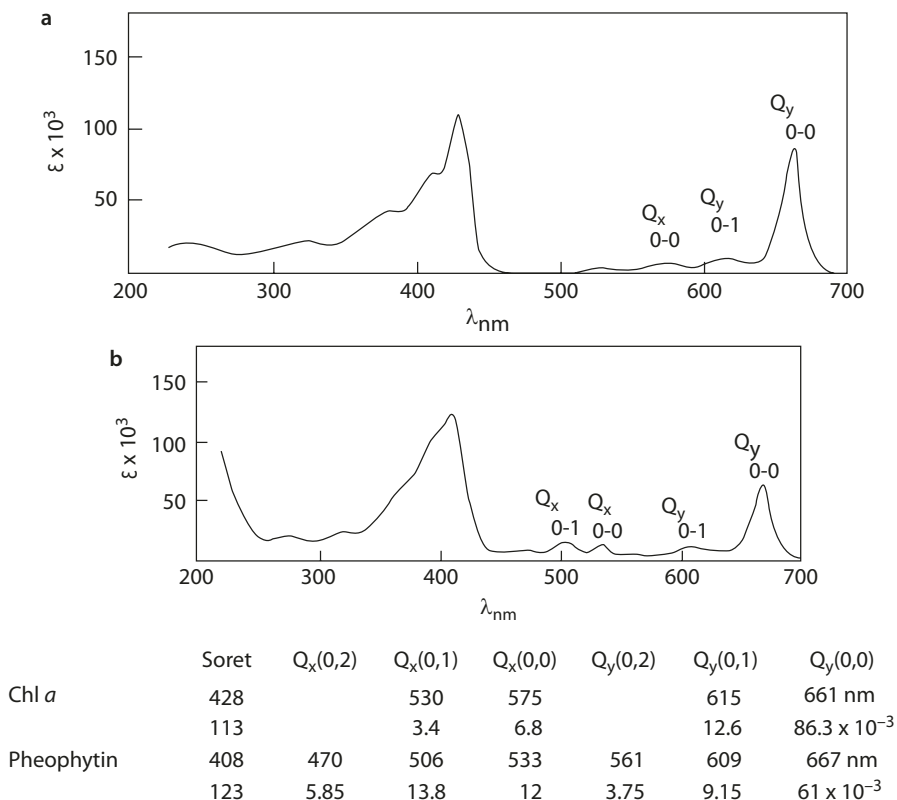
4.13.1 The Magnesium-Ligand Coordination

Since the chlorophyll contains an alicyclic ring with carbonyl substituents, the orbitals do not have square symmetry as in metalloporphyrins. The Q bands are split into x - and y -polarized transitions (Q_x , Q_y) [17] (■ Fig. 4.44).

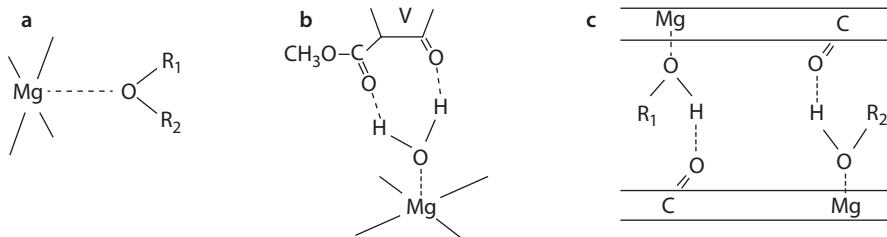
Unlike myoglobins, hemoglobins, catalases, and peroxidases, which are all complexes of transition metal ions, the chlorophylls are complexed with the alkali earth metal Mg^{++} (electronic configuration $1s^2 2s^2 2p^6 3s^2$). Magnesium with a coordination number of 4 as present in the chlorophyll structure is coordinately unsaturated. At least one of the axial positions must be coordinated with an electron donor ligand.

4.13.2 Dimers and Oligomers

Solvent molecules usually act as electron donor ligands. For example, diethyl ether, acetone, and tetrahydrofuran are nucleophiles with one donor site. The interaction between these molecules and Mg results in monosolvated chlorophyll (with pentacoordinated Mg) [23] (■ Fig. 4.45a).

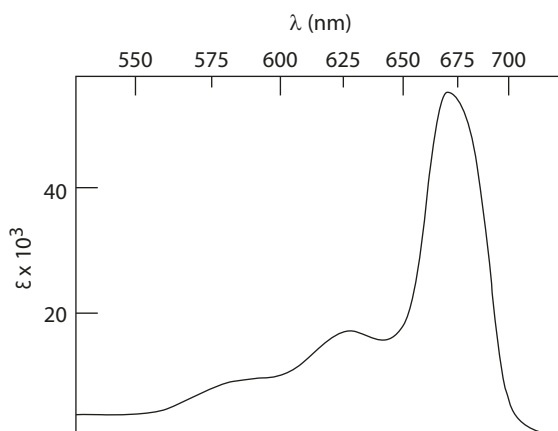


■ Fig. 4.44 Absorption spectrum of a chlorophyll *a* in ether, and b pheophytin *a* in ether. From Houssier and Saver [17] with permission. Copyright 1970 American Chemical Society



■ Fig. 4.45 Crosslinking of chlorophyll via: **a** monofunctional nucleophile, **b–c** dinucleophile (Katz et al. [22])

■ Fig. 4.46 Visible absorption spectrum of chlorophyll *a* dimer in carbon tetrachloride solution (Katz et al. [22])



Bifunctional nucleophiles such as H_2O and CH_3OH act as an electron donor and also can form hydrogen bond. These $\text{R}'\text{--O--H}$ ligands can bridge Chl molecules, forming oligomeric adducts. The chlorophyll molecule is bridged by one H_2O molecule coordinated to Mg and hydrogen-bonded to the two carboxyl oxygens in ring V of another chlorophyll molecule (■ Fig. 4.45b). In another arrangement, the chlorophyll molecule (Chl *a*) is held by two $\text{R}'\text{--O--H}$ ligands coordinated through its oxygen to the Mg of one Chl *a* and hydrogen-bonded to the keto C=O function of the other Chl *a* molecule (■ Fig. 4.45c) [22].

Chlorophyll, being an electron acceptor, also can act as an electron donor. The keto C=O at ring V in the chlorophyll molecule can interact with the Mg atom of another chlorophyll, resulting in the formation of dimers and oligomers. The formation of these aggregates occurs mostly in nonpolar solvents, in which there is little competition for the donor role from other nucleophilic ligands.

The visible spectrum of Chl *a* dimer has many overlaps in the Q_x , Q_y transitions, with the latter red-shifted to 675 nm (■ Fig. 4.46). In fact, all 5- and 6-coordinated Mg complexes have the visible spectrum red-shifted.

4.13.3 Chlorophyll Derivatives

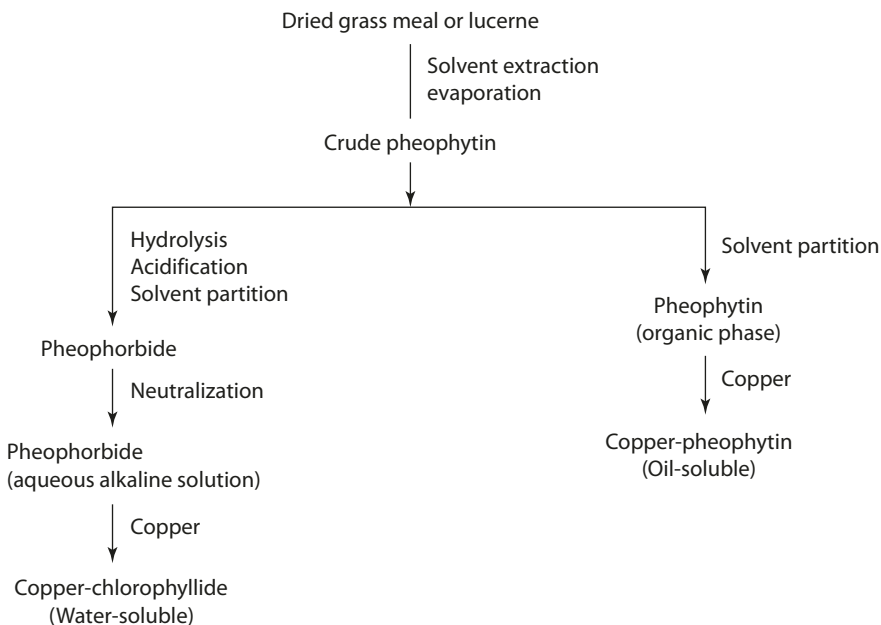
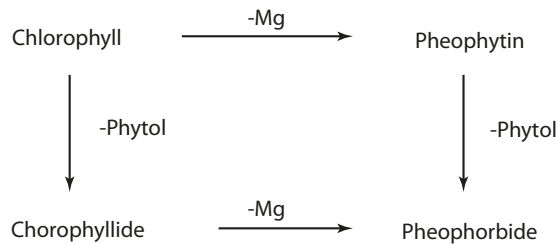
The Mg atom of chlorophyll is readily replaced by weak acids or Cu^{2+} , Ni^{2+} , Co^{2+} , Fe^{2+} , and Zn^{2+} . The free-base chlorophyll obtained in weak acid is pheophytin (gray-brown color).

The visible spectrum of pheophytin shows four bands, Q_x , Q_y , and two overtones. The high-intensity Q transition is shifted to a lower wavelength (■ Fig. 4.44b).

Removal of the phytol chain from the chlorophyll yields the chlorophyllide [19]. The hydrolytic reaction is catalyzed by dilute alkali or by the enzyme chlorophyllase normally present in green plants. Chlorophyllides are water soluble and green-colored, and have the same spectral properties as the chlorophyll. Chlorophyllide with the Mg removed yields the corresponding pheophorbides, which have the same color and spectral properties as those of the pheophytins (■ Fig. 4.47). The conversion of chlorophyll to pheophytin and pheophorbide is the common cause for the loss of the green color in heat-processed green vegetables.

Copper complexes of pheophytin and chlorophyllide are very stable, and the copper ion cannot be removed by acid. Chl *a* and Chl *b*, copper-pheophytin, and copper-chlorophyllide are permitted food colors in restricted applications. The commercial production of these color pigments is shown in the scheme in ■ Fig. 4.48. The product should not contain more than 200 ppm free ionizable copper.

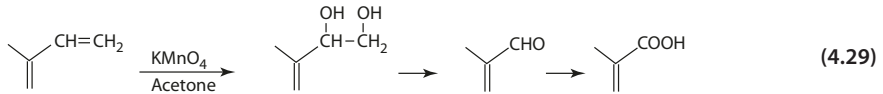
■ Fig. 4.47 Formation of chlorophyll derivatives



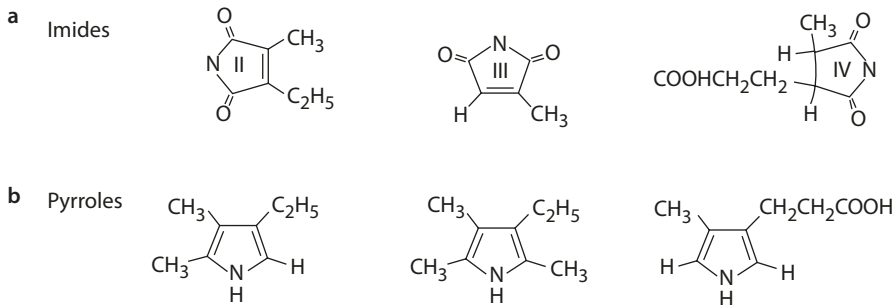
■ Fig. 4.48 Copper-pheophytin and chlorophyllide production (From Humphrey [19])

4.13.4 Oxidation and Reduction

The vinyl group of chlorophylls *a* and *b* can be oxidized by KMnO_4 to glycol, formyl, and carboxylic and substituents. In Chl *a*, the 3-position CHO is also oxidized (Eq. 4.29).



Chromic acid (20% H_2SO_4 , 1 h, -10°C) oxidizes the chlorophylls to imides (■ Fig. 4.49a). Exhaustive reduction (100 $^\circ\text{C}$, 2 h, $\text{HI}/\text{PH}_4\text{I}/\text{CH}_3\text{COOH}$) of chlorophyll gives a mixture of pyrroles (■ Fig. 4.49b).



■ Fig. 4.49 Products of **a** oxidation, and **b** reduction of chlorophyll

References

- Adar F (1978) Electronic absorption spectra of hemes and hemoproteins. In: Dolphin D (ed) The porphyrins. Physical chemistry, part A, vol III. Academic, New York
- Baron CP, Andersen HJ (2002) Myoglobin-induced lipid oxidation. A review. *J Agric Food Chem* 50:3887–3897
- Bauernfeind JC (1972) Carotenoid, vitamin A precursors and analogs in foods and feeds. *J Agric Food Chem* 20:456–473
- Bowen EJ (1950) Light absorption and photochemistry. *Q Rev Chem Soc* 4:236–250
- Breithaupt DE (2007) Modern application of xanthophylls in animal feeding – a review. *Trends Food Sci Technol* 18:501–506
- Cianci M, Rizkallah PJ, Olczak A, Raftery J, Chayen NE, Zagalsky PF, Helliwell JR (2002) The molecular basis of the coloration mechanism in lobster shell: β -crustacyanin at 3.2-Å resolution. *Proc Natl Acad Sci* 99:9795–9800
- Cotton FA, Wilkinson G (1980) Inorganic chemistry. Wiley, New York
- Dickerson RE (1964) X-ray analysis and protein structure. In: Neurath H (ed) The proteins, vol 2, 2nd edn. Academic, New York
- Egawa T, Shimada H, Ishimural Y (2000) Formation of compound I in the reaction of native myoglobins with hydrogen peroxide. *J Biol Chem* 275:34858–34866
- Foote CS, Chang YC, Denny RW (1970) Chemistry of singlet oxygen XI. *Cis-trans* isomerization of carotenoids by singlet oxygen and a probable quenching mechanism. *J Am Chem Soc* 92:5218–5219
- Fox JB Jr, Thomson JS (1963) Formation of bovine nitrosylmyoglobin I. pH 4.5–6.5. *Biochemistry* 2:465–470

References

12. Giddings GG (1977) The basis of color in muscle foods. *CRC Crit Rev Food Sci Technol* 9(1):81–114
13. Golon A, Kuhnert N (2012) Unraveling the chemical composition of caramel. *J Agric Food Chem* 60:3266–3274
14. Gouterman M (1961) Spectra of porphyrins. *J Mol Spectrosc* 6:138–163
15. Helliwell JR (2010) The structural chemistry and structural biology of colouration in marine crustacea. *Crystallogr Rev* 16(3):231–242
16. Hoshino T, Matsumoto U, Goto T (1981) Self-association of some anthocyanins in neutral aqueous solution. *Phytochemistry* 20:1971–1976
17. Houssier C, Sauer K (1970) Circular dichroism and magnetic circular dichroism of the chlorophyll and photochlorophyll pigments. *J Am Chem Soc* 92:779–791
18. Hrazdina G, Franzese AJ (1974) Oxidation products of acylated anthocyanins under acidic and neutral conditions. *Phytochemistry* 13:231–234
19. Humphrey AM (1980) Chlorophyll. *Food Chem* 5:57–67
20. Isler O (1979) History and industrial application of carotenoids and vitamin A. *Pure Appl Chem* 51:447–462
21. James BR (1978) Interaction of dioxygen with metalloporphyrins. In: Dolphin D (ed) *The porphyrins. Physical chemistry, part C, vol V*. Academic, New York
22. Katz JJ, Norris JR, Shipman LL (1977) Models for reaction center and antenna chlorophyll. *Brookhaven Symp Biol* 28:16–55
23. Katz JJ, Shipman LL, Cotton TM, Janson TR (1978) Chlorophyll aggregation. Coordination interaction in chlorophyll monomers, dimers, and oligomers. In: Dolphin D (ed) *The porphyrins. Physical chemistry, part C, vol V*. Academic, New York
24. Land DG (1962) Stability of plant pigments. In: Hawthorn J, Leitch JM (eds) *Recent advances in food science, proceeding, vol II*. Butterworths, London
25. Mordi RC, Walton JC (1993) Oxidative degradation of β -carotene and β -apo-8'-carotenal. *Tetrahedron* 49:911–928
26. Newsome RL (1986) Food colors. *Food Technol* 40(7):49–56
27. Nicholis P (1961) The formation and properties of sulphmyoglobin and sulphcatalase. *Biochem J* 81:374–383
28. Nicol DJ, Shaw MK, Ledward DA (1970) Hydrogen sulfide production by bacteria and sulfmyoglobin formation in prepared chilled beef. *Appl Microbiol* 19:937–939
29. North RS (1973) Caramel- the versatile colouring. *Flavor Industry* 4:337–338
30. Patras A, Brunion NP, O'Donnell C, Tiwari BK (2010) Effect of thermal processing on anthocyanin stability in foods; mechanisms and kinetics of degradation. *Trends Food Sci Technol* 21:3–11
31. Perutz MF (1978) Hemoglobin structure and respiratory transport. *Sci Am* 239:92–125
32. Preston HD, Rickard MD (1980) Extraction and chemistry of annatto. *Food Chem* 5:47–56
33. Reeder B, Wilson M (2001) The effects of pH on the mechanism of hydrogen peroxide and lipid hydroperoxide consumption by myoglobin: a role for the protonated ferryl species. *Free Radic Biol Med* 30:1311–1318
34. Sadilova E, Carle R, Stintzing FC (2007) Thermal degradation of anthocyananins and its impact on color and in vitro antioxidant capacity. *Mol Nutr Food Res* 51:1461–1471
35. Satoh Y, Shikama K (1981) Autoxidation of oxymyoglobin: a nucleophilic displacement mechanism. *J Biol Chem* 256:10272–10275
36. Schwartz SJ, von Elbe JH (1983) Identification of betanin degradation products. *Z Lebensm Unters Forsch* 176:448–453
37. Schweiter M, Englett G, Rigassi N, Vetter W (1969) Physical organic methods in carotenoid research. *Pure Appl Chem* 20:365–420
38. Seibel BA, Walsh PJ (2002) Trimethylamine oxide accumulation in marine animals: relationship to acylglycerol storage. *J Exp Biol* 205:297–306
39. Shikama K (1988) Stability properties of dioxygen iron(II) porphyrins: an overview from simple complexes to myoglobin. *Coord Chem Rev* 83:73–91
40. Shikama K (2006) Nature of the FeO₂ bonding in myoglobin and hemoglobin: a new molecular paradigm. *Prog Biophys Mol Biol* 91:83–162
41. Sinsheimer RL (1955) Ultraviolet absorption spectra. In: Hollaender A (ed) *Radiation biology. Ultraviolet and related radiations, vol II*. McGraw Hill, New York
42. Somers TC (1971) The polymeric nature of wine pigments. *Phytochemistry* 10:2175–2186

43. Stintzing FC, Carle R (2007) Betalains – emerging prospects for food Scientists. *Trends Food Sci Technol* 18:514–525
44. Suarez-Pereira E, Rubio CM, Pilard S, Mellet CO, Fernandez JMG (2010) Di-D-fructose dianhydride-enriched products by acid ion-exchange resin-promoted caramelization of D-fructose: chemical analyses. *J Agric Food Chem* 58:1777–1787
45. Tarladgis BG (1962) Interpretation of the spectra of meat pigment. II. Cured meats. The mechanism of colour fading. *J Sci Food Agric* 13:485–491
46. Timberlake CF (1980) Anthocyanins – occurrence, extraction and chemistry. *Food Chem* 5:69–80
47. Timberlake CF, Bridle P (1968) Flavylium salts resistant to sulfur dioxide. *Chem Ind* 1968:1489
48. Timberlake CF, Bridle P (1976) Interactions between anthocyanins, phenolic compounds, and acetaldehyde and their significance in red wines. *Am J Enol Vitic* 27:97–105
49. Watanabe S, Sakamura S, Obata Y (1966) The structures of acylated anthocyanins in eggplant and Perilla and the position of acylation. *Agric Biol Chem* 30:420–422
50. Wazawa T, Matsuoka A, Tajima G-i, Sugawara Y, Nakamura K-I (1992) Hydrogen peroxide plays a key role in the oxidation reaction of myoglobin by molecular oxygen. *Biophys J* 63:544–550
51. Yang F, Phillips GN (1996) Crystal structures of CO-, deoxy- and met-myoglobins at various pH values. *J Mol Biol* 256:762–774
52. Zechmeister L (1962) *Cis-trans isomeric carotenoids, vitamins A and arylpolyenes*. Academic, New York

Enzymes

5.1 Papain – 223

- 5.1.1 The Active-Site Region – 224
- 5.1.2 The Ionization of the Essential Groups – 225
- 5.1.3 Reaction Mechanism – 226
- 5.1.4 Action on Meat Fractions – 226

5.2 Lipoxygenase – 227

- 5.2.1 Soybean Lipoxygenase-1 – 227
- 5.2.2 Regiospecificity and Stereospecificity – 228
- 5.2.3 The Iron in Lipoxygenase – 229
- 5.2.4 The Aerobic Reaction Mechanism – 230
- 5.2.5 The Anaerobic Reaction Mechanism – 230
- 5.2.6 The Fate of Hydroperoxide – 231
- 5.2.7 Co-oxidation – 232

5.3 Polyphenol Oxidase – 233

- 5.3.1 Enzyme Characteristics – 233
- 5.3.2 Reaction Mechanism – 234
- 5.3.3 Secondary Reaction Products – 236

5.4 Glucose Oxidase – 237

- 5.4.1 Enzyme Characteristics – 237
- 5.4.2 Reaction Mechanism – 238
- 5.4.3 Industrial Uses – 239

5.5 Amylases – 240

- 5.5.1 Enzyme Characteristics – 240
- 5.5.2 Reaction Mechanism – 241
- 5.5.3 Action Pattern – 242
- 5.5.4 The Multimolecular Process – 244
- 5.5.5 Subsites of Amylases – 244
- 5.5.6 Industrial Uses – 244

5.6 Pectic Enzymes – 245

- 5.6.1 Pectinesterases – 246
- 5.6.2 Polygalacturonases – 247
- 5.6.3 Pectate Lyases – 249
- 5.6.4 Industrial Importance – 250

5.7 Lipolytic Enzymes – 251

- 5.7.1 Pancreatic Lipases – 251
- 5.7.2 The Role of Colipase – 252
- 5.7.3 Mechanism of Catalysis – 253
- 5.7.4 Specificity – 254
- 5.7.5 The Acyl Transfer Reaction – 255

5.8 Xylose Isomerase – 256

- 5.8.1 Protein Structure – 256
- 5.8.2 Metal Cations – 257
- 5.8.3 Reaction Mechanism – 258

References – 259

The study of enzymes is a subject of special importance to food science in two aspects. Enzymes are known to cause numerous changes, desirable or undesirable, on the chemical and physical attributes in a food system. Some notable examples include the many flavor compounds generated by the action of lipoxygenases on unsaturated lipids, the change of color caused by polyphenol oxidase, and the softening of texture in ripening fruits by pectic enzymes. A thorough understanding of the mechanism of catalysis and regulation of these enzymes is essential to the effective control of the changes during processing and storage.

Furthermore, the knowledge learned from these basic studies has led to the development of innovative technology in food processing and production. The introduction of immobilized glucose isomerase by the corn syrup industry for the production of high-fructose corn syrup provides a well-known example. The list of enzymes used in food processing includes amylases, cellulases, pectic enzymes, glucose oxidase, lipase, papain, chymosin, and others as presented in [Table 5.1](#) [54, 75].

Table 5.1 Some uses of enzymes in food and food processing

EC No.	Systematic name ^a	Common names
<i>Oxidoreductases</i>		
1.1.3.4	β -D-Glucose:O ₂ 1-oxidoreductase	Glucose oxidase
1.11.1.6	H ₂ O ₂ :H ₂ O ₂ oxidoreductase	Catalase
1.13.11.12	Linoleate:O ₂ 13-oxidoreductase	Lipoxygenase
1.14.18.1	o-Diphenol:O ₂ oxidoreductase	Polyphenol oxidase, tyrosinase
<i>Transferases</i>		
2.4.1.19	1,4- α -D-Glucan:1, 4- α -D-(1,4- α -D-glucano)-transferase, cyclizing	Cyclodextrinase
<i>Hydrolases</i>		
3.1.1.3	Triacylglycerol acylhydrolase	Lipase
3.1.1.11	Pectin pectylhydrolase	Pectinesterase
3.2.1.1	1,4- α -D-Glucan glucanohydrolase	α -Amylase, diastase
3.2.1.2	1,4- α -D-Glucan maltohydrolase	β -Amylase
3.2.1.3	1,4- α -D-Glucan glucohydrolase	Glucoamylase, amyloglucosidase
3.2.1.4	1,4-(1,3;1,4)- β -D-Glucan 4-glucanohydrolase	Endo-1,4- β -glucanase, cellulase
3.2.1.8	1,4- β -D-Xylan xylanohydrolase	Endo-1,4- β -xylanase, xylanase
3.2.1.15	Poly-(1,4- α -D-galacturonide)-glycanohydrolase	Endopolygalacturonase, polygalacturonase
3.2.1.17	Mucopeptide N-acetylmuramoylhydrolase	Lysozyme, muramidase
3.2.1.20	α -D-Glucoside glucohydrolase	Maltase, α -glucosidase

(continued)

■ **Table 5.1** (continued)

EC No.	Systematic name ^a	Common names
3.2.1.21	β-D-glucoside glucohydrolase	β-Glucosidase, cellobiase
3.2.1.23	β-D-Galactoside galactohydrolase	β-D-Galactosidase, lactase
3.2.1.25	β-D-Mannoside mannohydrolase	Mannanase
3.2.1.91	1,4-β-D-Glucan cellobiohydrolase	Cellobiohydrolase, exoglucanase, cellobiosidase, exocellulase
3.4.21.1	Chymotrypsin	–
3.4.21.4	Trypsin	–
3.4.21.14	Subtilisin	–
3.4.22.2	Papain	–
3.4.22.3	Ficin	–
3.4.22.4	Bromelain	–
3.4.23.4	Chymosin	Rennet, chymase
3.4.23.6	Microbial aspartic proteinases	Acid proteinase, aspartic proteinase
3.4.24.4	Microbial metalloproteases	Thermolysin
<i>Lyases</i>		
4.2.99.3	Polygalacturonic lyase	Pectate lyase
<i>Isomerases</i>		
5.3.1.5	D-Xylose ketol-isomerase	Xylose isomerase, glucose isomerase

From Fariza and Johnson [54]; Uhlig [75]

^aIUBMB enzyme nomenclature [49]

Enzymes are classified into six main groups: (1) oxidoreductases catalyzing oxidation-reduction reactions, (2) transferases catalyzing group transfer reactions, (3) hydrolases catalyzing hydrolytic reactions, (4) lyases catalyzing elimination reactions in which a double bond is formed, (5) isomerases catalyzing isomerization reactions, and (6) ligases catalyzing reactions in which two molecules are joined at the expense of an energy source (ATP). In this chapter, several selected groups of enzymes of importance in food science are covered, with emphasis on the mechanism of catalysis to provide an overview of the chemical principles of enzymatic reactions. ■ Table 5.2 lists some of their commercial applications.

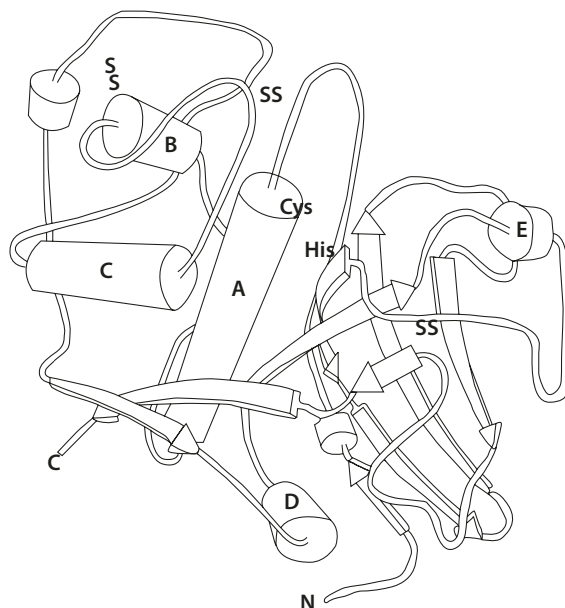
■ **Table 5.2** Applications of some selected food enzymes

<i>Papain</i>
Used for tenderizing meat
Production of protein hydrolysates (soy sauce, tamari sauce, dehydrated soups, gravy powders, processed meats)
Softening and increase in extensibility of doughs. Improvement in texture and loaf volume of baked goods
Preventing haze formation during chill-proofing of beer
<i>Lipoxygenase</i>
Development of off-flavors in a variety of foods
<i>Polyphenol oxidase</i>
Development of browning during ripening, fermenting, and/or aging of wine, tea, cocoa.
<i>Glucose oxidase</i> (in combination with catalase):
Desugaring of egg prior to spray drying to prevent Maillard reaction
Deoxygenation of beverages to prevent oxidation
<i>Amylases</i>
Production of syrups and sugars – conversion of starches to low molecular dextrans
Increase in maltose content for dough fermentation. Improvement of bread quality
<i>Pectic enzymes</i>
Clarification of juices by breaking down pectin
Increase in efficiency and yield in juice processing
Reducing haze formation or gelling in wine making
<i>Lipase</i>
Development and enhancement of flavors in cheese manufacturing
Modification of triacylglycerols in production of margarine and oil products
<i>Xylose isomerase</i>
Production of sweeteners and syrups

5.1 Papain

The proteolytic enzyme papain (EC 3.4.22.2) is found in the latex and in the fruit of *Carica papaya*. The crude latex (which also contains peptidase A and chymopapain) is used to prevent "chill hazes" in beer and also commonly used as meat tenderizer.

Fig. 5.1 Polypeptide chain folding in papain. Domain L consists of helices *A*, *B*, and *C*. Domain R is a double β sheet with helices *D* and *E* at opposite ends. The catalytic Cys and His residues are indicated (From Baker and Drenth [3] with permission. Copyright 1987 John Wiley & Sons)

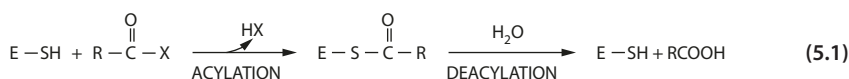


5.1.1 The Active-Site Region

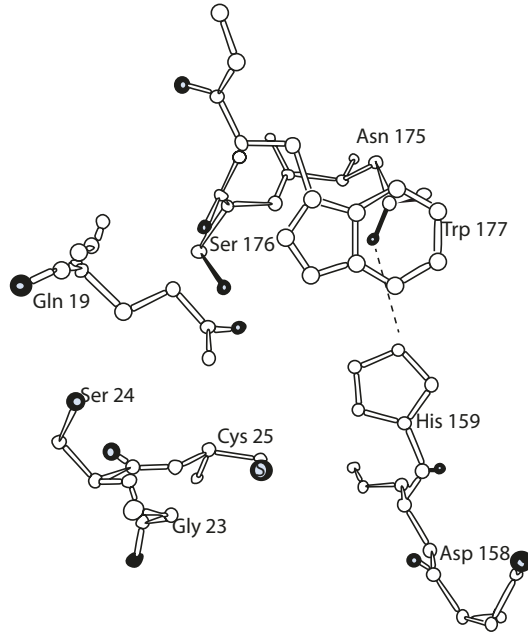
Papain is a sulfhydryl proteinase, consisting of a single polypeptide chain of 23 kDa with 212 amino acid residues [17]. The molecule is an ellipsoid of $50\text{\AA} \times 37\text{\AA} \times 37\text{\AA}$ in dimension, folded into two domains. The L domain consists of three α helices *A*, *B*, and *C*, forming a central core of hydrophobic residues. The R domain is a twisted antiparallel β sheet forming a barrel with a large hydrophobic core (Fig. 5.1). The N- and C-terminal end segments (from the L and R domains, respectively) connect the two domains by cross folding.

Between the two domains lies a deep cleft, where the active site is situated. The essential Cys25 in the left domain is in close proximity to the imidazole of His159 in the opposite wall of the cleft. The His residue is embedded in a hydrophobic region and hydrogen-bonded to Asn175 (Fig. 5.2).

The enzyme catalyzes the hydrolysis of amide, ester, and thioester substrates. The reaction is a two-step process: (1) acylation with the formation of an acylenzyme intermediate; and (2) deacylation, which is the hydrolysis of the intermediate (Eq. 5.1).



■ **Fig. 5.2** The active-site region of papain near the essential SH group (From Drenth et al. [17] with permission. Copyright 1971 Elsevier)



5.1.2 The Ionization of the Essential Groups

The kinetics of hydrolysis by papain of several substrates suggests that acylation has a bell-shaped pH rate profile with pK_a values of 3.0–4.0 and 8.0–8.5. Deacylation of the acylenzyme intermediate, however, shows a sigmoidal pH rate profile with a pK_a of approximately 4.0. The ionization groups are attributed to Cys25 and His159.

The exceptionally low pK_a (3.0–4.0) of Cys25 and the shifting of the pK_a from 8.5 to 4.0 for His159 are the result of the interactive ionization of these two groups, as evidenced by NMR and fluorescenc titration studies [43]. The pK_a of the thiol group changes from 7.6 to 3.3 on protonation of the histidine. Similarly, the pK_a of the histidine shifts from 8.5 to 4.3 when the thiol group is protonated (Eq. 5.2).

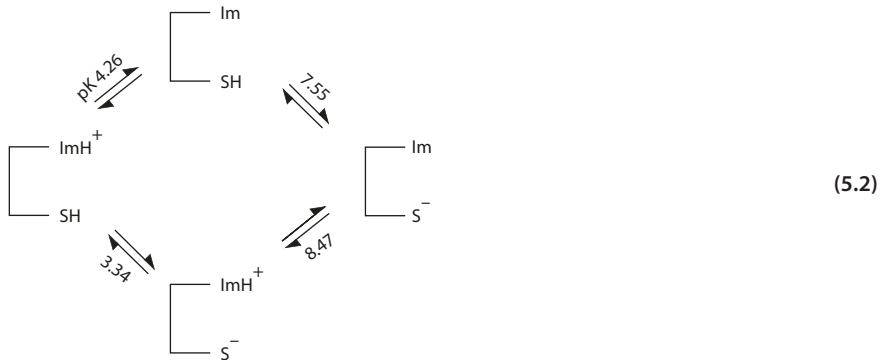
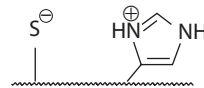


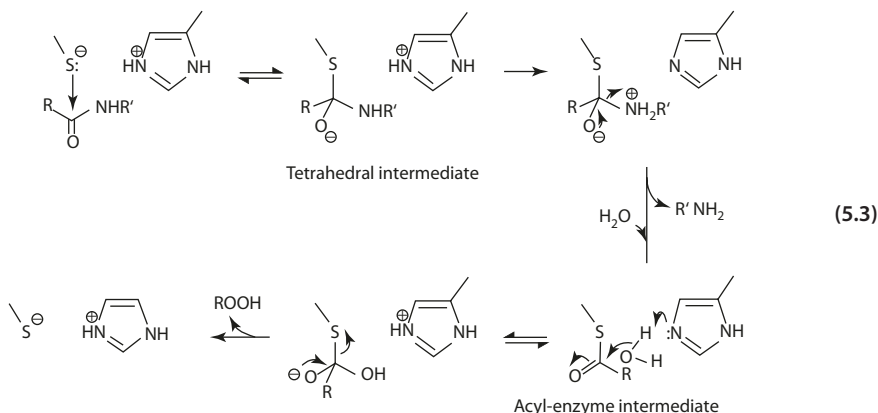
Fig. 5.3 The imidazolium-thiolate ion pair



5.1.3 Reaction Mechanism

Therefore, at physiological pH, the imidazole with a pK_a of 8.5 will remain protonated, while the thiol group with its pK_a shifted from 7.6 to 3.3 is deprotonated. The values of these pK_a 's, together with other studies, suggest that Cys25 and His159 may exist as an imidazolium-thiolate ion pair (Fig. 5.3) [56].

The active form of the enzyme thus has the thiolate anion acting as a strong nucleophile to form a tetrahedral intermediate with the carbonyl carbon of the substrate (Eq. 5.3). Formation of the tetrahedral intermediate blocks the thiol group, causing the pK_a of the His159 imidazole to decrease from 8.5 to 4.0. This increase in the acidity of the imidazolium cation facilitates the proton transfer from the imidazole to the leaving group and the formation of the acyl-enzyme intermediate [70]. It is also conceivable that a concerted attack of the ion pair would also result in the formation of the tetrahedral intermediate [43]. Deacylation occurs through general base catalysis assisted by the imidazole (Eq. 5.3), although intramolecular nucleophilic catalysis by the imidazole has also been suggested [27].



5.1.4 Action on Meat Fractions

Besides papain, other sulfhydryl proteinases, such as ficin (from figs) and bromelain (pineapple), are also used to increase the tenderness of meat. These enzymes are shown to solubilize various fractions of meat muscle to different degrees (Table 5.3) [36].

The degree of hydrolysis of meat fractions varies with individual enzymes. Papain and ficin show the strongest activity on the salt-soluble fraction, while the other enzymes hydrolyze the insoluble fractions more efficiently. Antemortem injection of papain indicates that 12–19% of the injected enzyme is found in the muscle.

■ **Table 5.3** Percent of meat fractions solubilized by enzyme treatment

Enzyme	Meat fractions		
	Water soluble	Salt soluble	Insoluble
Papain	25	60	15
Ficin	9	54	37
Bromelain	16	33	51
Collagenase	13	26	61
Trypsin	19	38	43

From Kang and Rice [36]

■ **Table 5.4** Characteristics of lipoxygenases from soybean and pea

	Soybean		Pea	
	LOX-1	LOX-2	LOX-1	LOX-2
MW	98,500	98,500	95,000	95,000
pH optimum	9.0	6.5	7.0	6.0
pI	5.5–5.7	5.8–6.2	6.25	5.82
9/13 00H at pH optimum	10:90	50:50	50:50	—
Carotenoid cooxidation activity	Low	Low	High	Low

From Gallard and Chan [20] and Yoon and Klein [89]

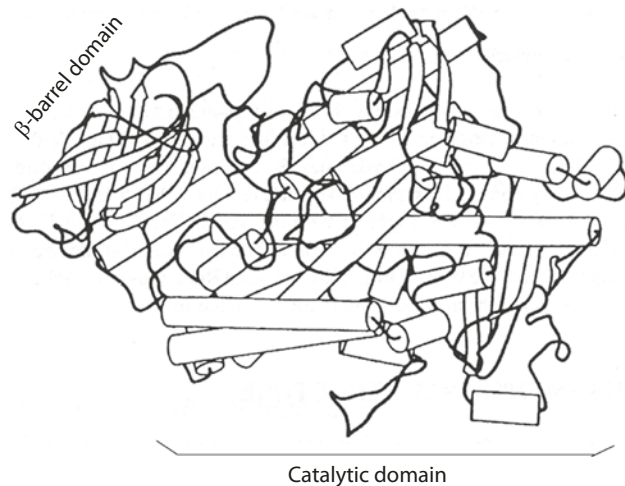
5.2 Lipoxygenase

Lipoxygenase (linoleate:oxygen oxidoreductase, EC 1.13.11.12) is a dioxygenase that catalyzes the oxygenation of polyunsaturated fatty acids containing a *cis,cis*-1,4-pentadiene system to hydroperoxides. The enzyme exists in multiple forms, three in soybean, wheat and peas, and two in corn. Lipoxygenases from different sources, as well as their isozymes, may differ in substrate specificity, pH optimum, and activity, as indicated in ■ Table 5.4 [20, 89].

5.2.1 Soybean Lipoxygenase-1

The present information regarding lipoxygenases comes mostly from studies on lipoxygenase-I (LOX-1), the isozyme first isolated and crystallized from soybean. The LOX-1 enzyme has a molecular mass of 94 kDa, containing one atom of nonheme iron per molecule of the protein. Soybean LOX-1 has a pH optimum of 9.0, although for most lipoxygenases the pH range is 5.5–7.0.

Fig. 5.4 Ribbon diagram of soybean lipoxygenase-1 (From Boyington et al. [4] with permission. Copyright 1993 The Biochemical Society and Portland Press Ltd.)



Soybean LOX-1 consists of a single polypeptide chain of 839 amino acid residues that folds into a two-domain structure: (1) a small N-terminal β -barrel domain of 146 residues, and (2) a large mostly helical catalytic domain of 693 residues [4, 5]. The N domain is involved in membrane binding, and not essential for the catalytic activity. The C-terminal domain harbors the nonheme iron in octahedral coordination with five amino acid residues (3 His, 1 Asn and a C-terminal Ile) and a water molecule. Two sides of the iron center face large internal cavities that connect to the exterior of the molecule. A conical hydrophobic channel (cavity I) forms a passage for the movement of molecular oxygen from outside to the iron site. A second hydrophobic channel (cavity II) intersects with cavity I in proximity of the nonheme iron, forming a substrate-binding pocket (■ Fig. 5.4).

5.2.2 Regiospecificity and Stereospecificity

Lipoxygenases oxygenate polyunsaturated fatty acids with a *cis,cis*-1,4-pentadiene system. The ω 6 carbon must be a double bond, and the carboxyl group must be unhindered for the enzyme to act. Substrates containing double bonds at the ω 6 and ω 9 positions (such as in linoleic acid) are usually oxidized at high rates. (Refer to ► Chap. 1 for fatty acid nomenclature.)

The orientation of the pentadiene system on the enzyme is considered to be planar, and the hydrogen abstraction at the ω 8 (■ Fig. 5.5) occurs either above or below the plane, $H(L_s)$ or $H(D_r)$ [18]. Oxygen enters from the opposite side of the plane from which the hydrogen is abstracted, at positions ω 6 or ω 10. Corn germ lipoxygenase at an optimum pH of 6.6 oxidizes linoleic acid to primarily 9- D_s -hydroperoxy-10-*trans*,12-*cis*-octadecanienoic acid: abstraction of $H(D_r)$, followed by O_2 attack above the plane at the ω 10 position. Lipoxygenase-1 from soybean, at an optimum pH of 9.0, converts linoleic acid predominantly to 13- L_s -hydroperoxy-9-*cis*,11-*trans*-octadecadienoic acid: abstraction of $H(L_s)$ followed by O_2 addition to the ω 6 position from below the plane.

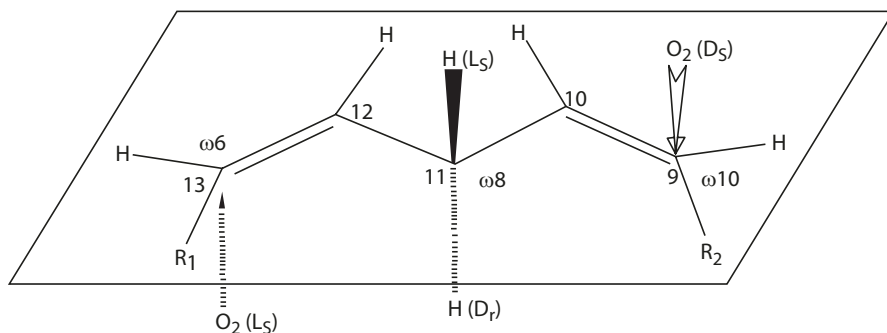


Fig. 5.5 Oxygenation of linoleic acid by lipoxygenase. The pentadiene is planar. The hydrogen at $\omega 8$, $H(L_s)$ and $H(D_s)$ are above and below the plane, respectively. The oxygen approaches from above and below. $R_1 = \text{CH}_3(\text{CH}_2)_4-$, $R_2 = \text{COOH}-(\text{CH}_2)_7-$. The symbols L and D refer to Fischer convention; R and S refer to Cahn, Ingold, and Prelog convention (Egmond et al. [18])

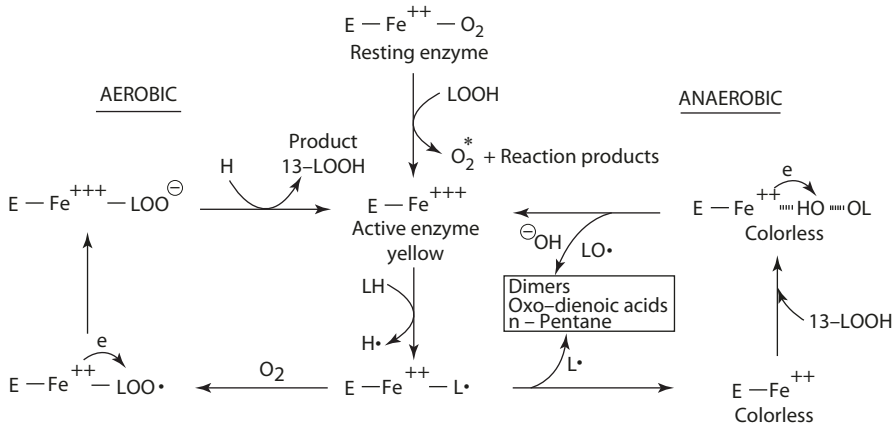
In the oxidation of arachidonic acid (all-*cis*-5,8,11,14-eicosatetraenoic acid) by soybean LOX-1, the product of the first oxygenation is 15- L_s -hydroperoxy-5-*cis*,8-*cis*,11-*cis*,13-*trans*-eicosatetraenoic acid. The second oxygenation produces the 8- D_s ,15- L_s -dihydroperoxy-5-*cis*,9-*trans*,11-*cis*,13-*trans*- and 5- D_s ,15- L_s -dihydroperoxy-6-*trans*,8-*cis*,11-*cis*,13-*trans*-eicosatetraenoic acids [77].

The conventional nomenclature system classifies lipoxygenases according to their positional specificity of fatty acid oxygenation against linoleic acid (for plant enzymes) or arachidonic acid (for animal enzymes). With linoleic acid as the substrate, molecular oxygen may be introduced at C9 or C13, which leads to the formation of 9-hydroperoxy- and 13-hydroperoxy-derivatives. Hence, the lipoxygenases are named 9-LOX and 13-LOX, respectively. Using this system, corn germ lipoxygenase described above is a 9-LOX and soybean LOX-1 is a 13-LOX.

5.2.3 The Iron in Lipoxygenase

Lipoxygenase-1 in its resting form is colorless and EPR silent [68]. The iron is high-spin Fe(II) ($S = 4/2$, paramagnetic) with one of the ligands being dioxygen. The iron atom is coordinated to amino acid residues of the polypeptide chain.

The ferrous form is converted, by the addition of an equal molar concentration of 13-hydroperoxy-octadecadienoic acid, to a yellow ferric enzyme with an EPR signal indicating high-spin Fe(III) ($S = 5/2$). Excess hydroperoxide results in an unstable purple complex between the ferric enzyme and 13-LOOH, which reverts to the activated yellow form with concomitant conversion of the hydroperoxy to a hydroxyepoxy product [12]. In the case of 13-hydroperoxy-linoleate, the product of conversion is 11-hydroxy-12:13-epoxy-9-*cis*-octadecenoic acid. The yellow and purple forms differ in symmetry, the former having largely axial ligands and the latter rhombic symmetry.



■ Fig. 5.6 The aerobic and anaerobic reaction mechanisms of soybean lipoxygenase-1 (deGroot et al. [16])

5.2.4 The Aerobic Reaction Mechanism

The reaction scheme for soybean lipoxygenase 1 is outlined in ■ Fig. 5.6 [16].

1. The native resting enzyme (E-Fe²⁺-O₂) is activated to the active form (E-Fe³⁺). The period for the resting enzyme to react with the substrate linoleic acid can be abolished by the addition of its own product, 13-*L*_s-hydroperoxide. A one-electron transfer occurs from the iron to the oxygen, which is released as superoxide anion or excited oxygen.
2. The active enzyme (E-Fe³⁺) catalyzes the stereospecific abstraction of hydrogen from the substrate, with it reduced to the enzyme radical complex (E-Fe²⁺-L•). The abstraction of hydrogen is the rate-limiting step in the overall reaction.
3. Oxygen then combines stereospecifically with the enzyme free radical followed by a one-electron transfer from the iron to the peroxy radical to form the enzyme peroxy-anion (E-Fe³⁺•LOO⁻).
4. Protonation of the peroxy-anion releases the hydroperoxide and regenerates the active enzyme (E-Fe³⁺).

The above mechanism is referred to as the aerobic cycle in which the product is hydroperoxide. However, under anaerobic conditions, reaction products other than hydroperoxides are formed, including oxo acids, pentane, and dimers.

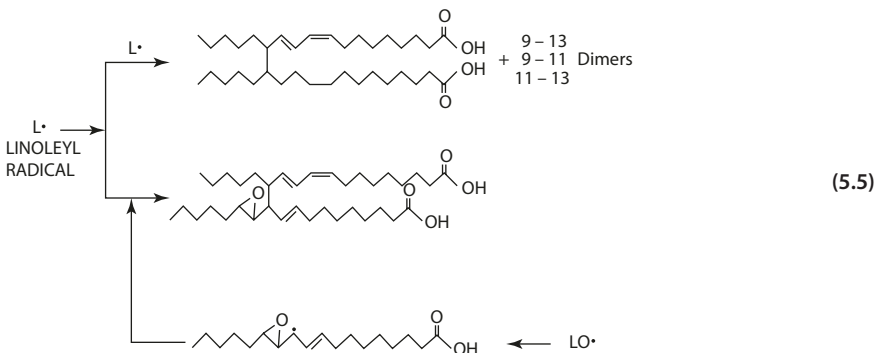
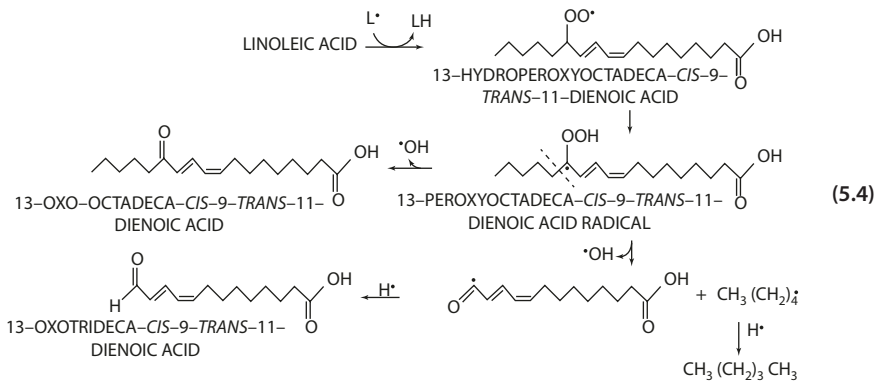
5.2.5 The Anaerobic Reaction Mechanism

Two systems can lead to the formation of products other than hydroperoxides: (1) system containing linoleic acid and the preformed substrate (13-*L*_s-hydroperoxy-9-*cis*,11-*cis*-octadecanienoic acid) in the absence of oxygen, and (2) system with oxygen in limiting concentration and the substrate linoleic acid in excess. In the latter system, there is a lag period during which hydroperoxide is formed, and the oxygen is depleted before the reaction starts [16, 23, 24, 79].

The anaerobic reaction proceeds according to the following scheme (Eq. 5.4), where linoleic acid and 13-hydroperoxy-linoleic acid are converted by LOX-1 in coupled reactions. The ferric enzyme is reduced by linoleic acid, and the ferrous enzyme is oxidized by the 13-LOOH, leading to the formation of oxodienoic acids (■ Fig. 5.6).

5.2 · Lipoxygenase

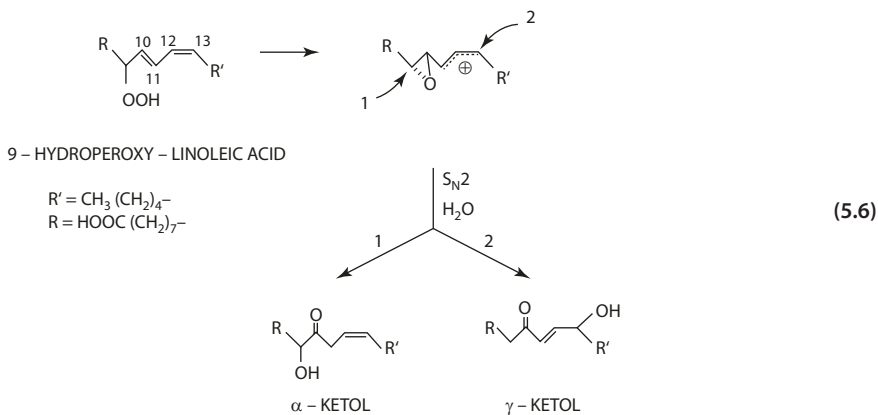
1. The enzyme radical complex ($E-Fe^{2+}-L\cdot$) dissociates to yield the free enzyme in the ferrous state ($E-Fe^{2+}$) and the fatty acid radical ($L\cdot$).
2. The enzyme in the ferrous state ($E-Fe^{2+}$) is oxidized to the active form ($E-Fe^{3+}$) by the product hydroperoxide (13-LOOH), with the formation of alkoxy radical ($LO\cdot$) and hydroxide ion (OH^-).
3. Reaction of fatty acid radicals ($L\cdot$ and $LO\cdot$) and fatty acids (LH) results in the formation of oxodienoic acids and dimeric fatty acids. Oxodienoic acids are formed from the rearrangement and decomposition of hydroperoxide via the fatty acid radicals (Eq. 5.4). Nonoxygenated dimeric fatty acids are derived from the combination of two $L\cdot$ radicals. Dimers containing oxygen originate from reactions between $LO\cdot$ and $L\cdot$ (Eq. 5.5).



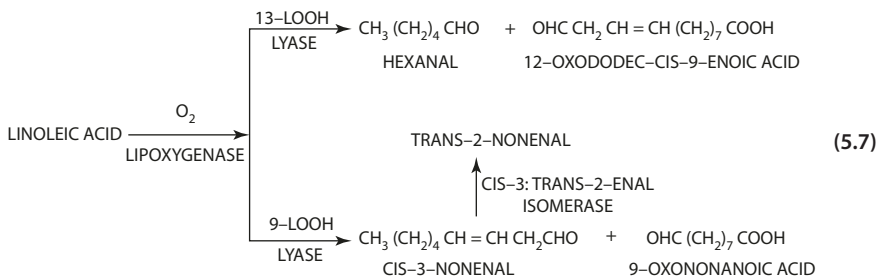
5.2.6 The Fate of Hydroperoxide

The hydroperoxides do not accumulate in the cell tissues but undergo further enzymatic rearrangement or breakdown to secondary products. Hydroperoxide isomerase catalyzes the conversion of hydroperoxide to α -keto fatty acid. One of the oxygen atoms from the hydroperoxide is transferred to the vicinal olefinic carbon, and incorporated into the oxo group. The mechanism for the action of linoleic acid hydroperoxide isomerase on 9-hydroperoxy-linoleic acid may involve an epoxy-cation intermediate. Nucleophilic substitution at the C9 or C13 carbon and hydride shift from C10 to C11 or C9 yield the

10-oxo-9-hydroxy-12-*cis*-octadecenoic acid (α -ketol) and 10-oxo-13-hydroxy-11-*trans*-octadecenoic acid (γ -ketol), respectively (Eq. 5.6). The configuration at C9 is inverted from D_s to L_r [22, 80].

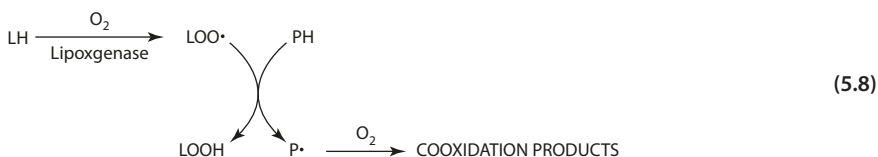


Hydroperoxide lyase, the enzyme that catalyzes the reaction leading to the formation of volatile compounds with characteristic odors in plants, has been found in cucumber, tomato fruits, and others. The enzyme cleaves hydroperoxide to oxoacids and carbonyls. The enzymatic sequences for the formation of carbonyl fragments from linoleic acid in cucumber fruits is outlined in Eq. 5.7 [21]. *Trans*-2-nonenal is a major flavor compound of cucumber. The other two aldehydes, hexenals and nonadienals, originate from linolenic acid via similar pathways.



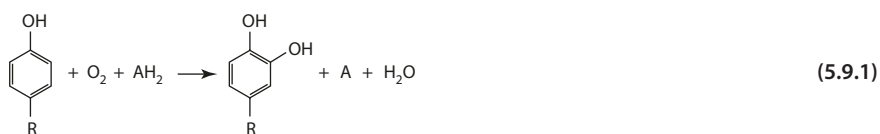
5.2.7 Co-oxidation

The ability of lipoxygenase to bleach pigments has been applied to bread making by adding soybean flour to wheat flour. The oxidative destruction of pigments (e.g., carotenoids, chlorophyll) during lipid oxidation is a free-radical mediated reaction [66]. The reactive species are $\text{LOO}\cdot$ and $\text{L}\cdot$ radicals (Eq. 5.8).



5.3 Polyphenol Oxidase

Polyphenol oxidase is a copper-containing enzyme that acts on two general types of substrates: (1) a monooxygenase in the *o*-hydroxylation of monophenols to *o*-dihydroxyphenols (dihydroxyphenylalanine: oxygen oxidoreductase, EC 1.14.18.1) (Eq. 5.9.1), and (2) a two-electron oxidase in the oxidation of *o*-diphenols to *o*-quinones (1,2-benzenediol:oxygen oxidoreductase, EC 1.10.3.1) (Eq. 5.9.2). The former reaction is sometimes referred to as cresolase activity (based on the common substrate *p*-cresol) and the latter catecholase activity (based on the common substrate catechol). The recommended and more appropriate names reflecting the two enzyme activities are monophenol oxidase and *o*-diphenol oxidase, respectively.

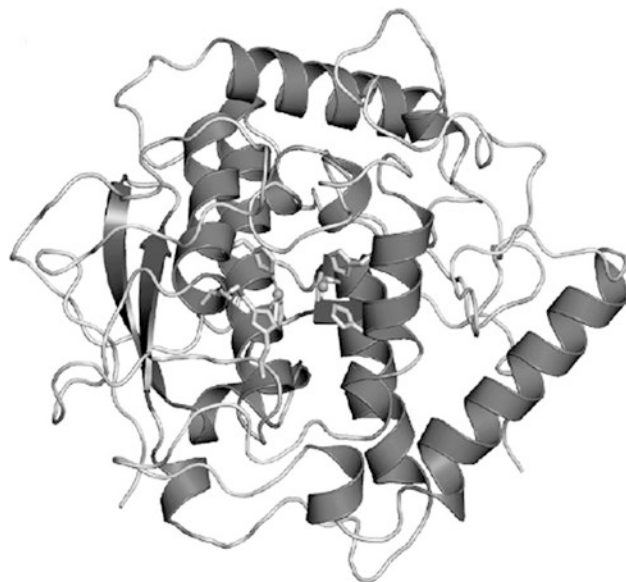


Polyphenol oxidases have broad substrate specificity. However, enzymes from different sources tend to differ from each other in their relative activity toward specific substrates. All polyphenol oxidases oxidize *o*-diphenol, but some may not have monophenol oxidase-type activity. In the literature, the enzyme is named variously as tyrosinase, polyphenolase, catechol oxidase, catecholase, diphenol oxidase, monophenol oxidase, and cresolase, referring to its action on a rather broad range of substrates.

5.3.1 Enzyme Characteristics

Many studies have been conducted on the polyphenol oxidases isolated from *Agaricus bisporus* (common mushroom) and *Neurospora crassa*. Polyphenol oxidase from the common mushroom has a molecular mass of 120 kDa, composed of two H subunits of 392 residues and two L subunits of 150 residues. The enzyme protein has a quaternary structure of L_2H_2 [71]. The H subunit is the enzyme proper, which assumes a globular domain of 13 α helices, 8 short β strands, and many loops. The binuclear copper site is located at the heart of two pairs of antiparallel α helices ($\alpha 3/\alpha 4$ and $\alpha 10/\alpha 11$). Each copper ion (Cu-A and Cu-B) is coordinated to three His residues that are highly conserved in bacterial enzymes as well [30]. The His ligands maintain the copper ions in tetragonal positions to be functionally reactive. The L subunit has a lectin-like fold and does not contribute to the activity of the enzyme. Grape (*Vitis vinifera* L.) and sweet potato (*Ipomoea batatas*)

Fig. 5.7 Ribbon model structure of PPO from grape *Vitis vinifera* showing the overall ellipsoidal shape, and the binuclear copper site within a four-helix bundle (From Virador et al. [81] with permission. Copyright 2010 American Chemical Society. PDB 2P3X)



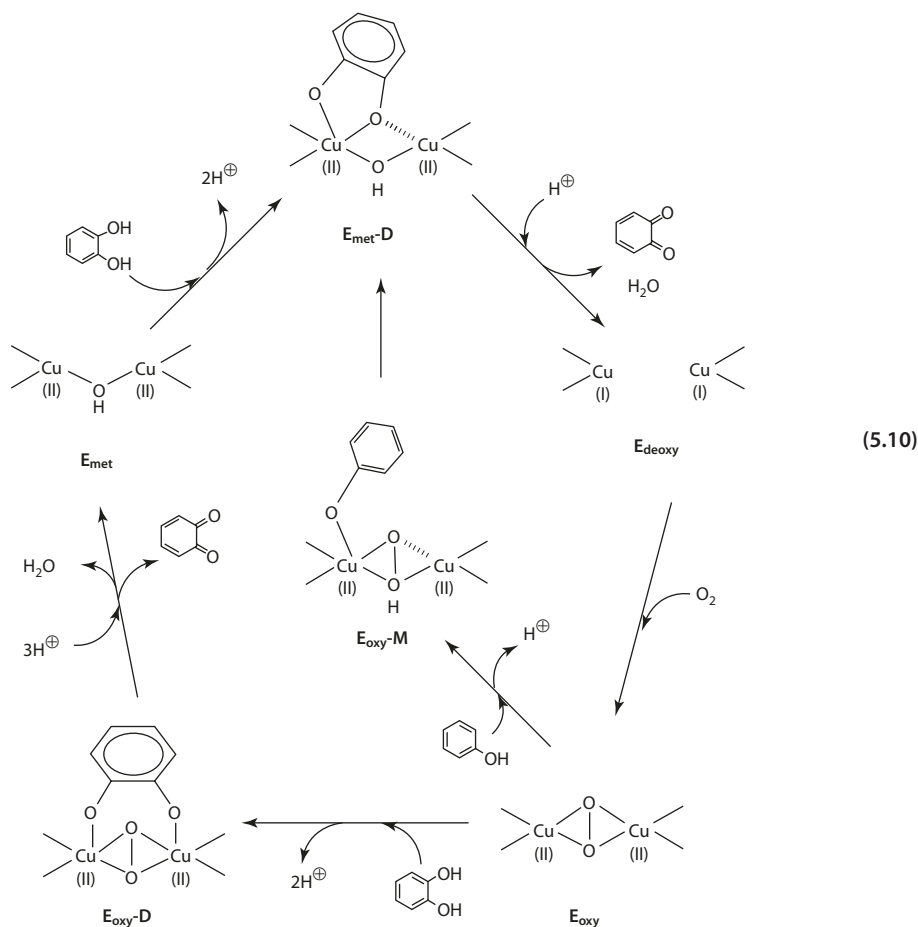
enzymes are monomeric proteins, but have architectural structures very similar to that of the mushroom enzyme H subunit [37, 81]. The structure of the grape enzyme protein is shown in **Fig. 5.7**.

5.3.2 Reaction Mechanism

The binuclear copper active site exists in three forms: met, oxy, and deoxy forms.

1. The met form: $E_{\text{met}}:[\text{Cu(II)-Cu(II)}]$ is the resting enzyme (native state), where the Cu(II) ions are bridged by solvent-derived ligand such as water molecule or hydroxide ion (instead of peroxide in the oxy form). The met form is converted to the deoxy form by a $2e^-$ reduction of Cu(II) to Cu(I).
2. The deoxy form: $E_{\text{deoxy}}:[\text{Cu(I)-Cu(I)}]$ is a reduced species containing a bicuprous structure without exo- or endogenous bridging. The deoxy form binds oxygen to give the oxy form.
3. In the oxygenated form: $E_{\text{oxy}}:[\text{Cu(II)-O}_2\text{-Cu(II)}]$, the molecular oxygen is bound to the two Cu(II) ions as peroxide in a side-on bridging mode. The oxy form and the met form are the oxidized species of the enzyme.

The mechanism of PPO consists of two catalytic cycles. The monophenol oxidase cycle requires one phenol substrate and one dioxygen for each turnover. The *o*-diphenol oxidase cycle consists of two phases (reductive and oxidative), each turnover requiring two substrates and one dioxygen (Eq. 5.10) [29, 41, 69].



■ Hydroxylation and Oxidation of Monophenol

The cycle begins with the addition of dioxygen as side-on peroxide bridge to the deoxy form (E_{deoxy}) generating the oxy enzyme (E_{oxy}). In the next step, a monophenol substrate is coordinated to the axial position of one of the coppers, followed by a distortion of the tetragonal site to a trigonal bipyramidal intermediate, oxy enzyme-monophenol complex ($E_{\text{oxy}}\text{-M}$) (Eq. 5.10, the inner cycle). This rearrangement of the copper coordination geometry labilizes the peroxide, introducing polarization into the O–O bond to yield an activated peroxide for the hydroxylation of the phenol substrate (Eq. 5.10) [69, 86]. Electrophilic attack of the peroxide oxygen at the ortho position of the substrate produces the met enzyme-diphenol complex ($E_{\text{met}}\text{-D}$) with a diphenol as the exogenic ligand. Finally, oxidation of the diphenol occurs with the product *o*-quinone dissociated from the enzyme, while Cu(II) is reduced to Cu(I). The deoxy form (E_{deoxy}) then binds O_2 to yield the oxy enzyme (E_{oxy}), allowing another turnover.

■ Oxidation of Diphenol

In the oxidation of *o*-diphenol, the tetragonal site has the correct geometry for both phenolic oxygens to coordinate in the deoxy (E_{deoxy}), oxy (E_{oxy}), or the met (E_{met}) forms [85]. Rearrangement of the coordination geometry of the copper site is not required for the

5.4 Glucose Oxidase

Glucose oxidase (β -D-glucose:oxygen 1-oxidoreductase, EC 1.1.3.4) has been highly purified from *Penicillium notatum*, *Penicillium amagasakiense*, and *Aspergillus niger*, with the latter being the major commercial source.

5.4.1 Enzyme Characteristics

The enzyme is a homodimer of 140–160 kDa, containing 10–18% (w/w) carbohydrates and two moles of firmly bound FAD per protein molecule. The coenzyme FAD acts as a redox carrier in catalysis. The enzyme contains no sulfhydryl or disulfide groups [31]. Removal of 95% of the carbohydrate moiety does not significantly affect the catalytic activity or the stability. The monomeric unit of the *Aspergillus niger* enzyme consists of a polypeptide chain of 583 amino acid residues.

The monomeric molecule is a compact spheroid of $60 \times 52 \times 27 \text{ \AA}$, with two separate domains, between which the flavin site is located inside a deep pocket (■ Fig. 5.8). The domain that binds FAD consists of a $\beta\alpha\beta$ motif. The second domain contains a large 6-stranded antiparallel β sheet with helices on both sides. This domain provides most of the contacts of the dimer interface, where the active site is located [26].

Glucose oxidase catalyzes the irreversible oxidation of a number of aldoses to the corresponding lactones (Eq. 5.13). Glucose, deoxyglucose, mannose, and galactose are some of substrates studied (■ Table 5.5). It is evident that glucose is a far better substrate than the other sugars [25]. The enzyme also shows high anomeric specificity with activity 160 times greater for the β -D-glucose than the α -anomer.

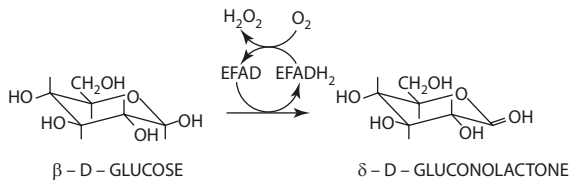


■ Fig. 5.8 A stereo drawing of the *Aspergillus niger* glucose oxidase monomer (From Hecht et al. [26] with permission. Copyright 1993 Elsevier. PDB 1GAL)

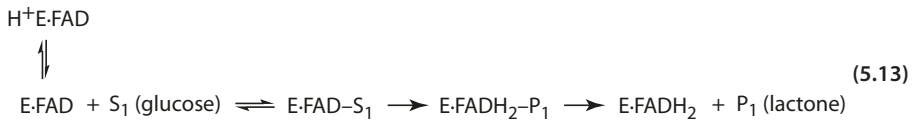
■ **Table 5.5** Relative activity of glucose oxidase on various substrates

Substrate	Source of enzyme		
	<i>A. niger</i>	<i>P. notatum</i>	<i>P. amagasakiense</i>
Glucose	100	100	100
2-Deoxy-D-glucose	3.3	—	—
Mannose	0.9	1.0	0
Galactose	0.55	0.14	0

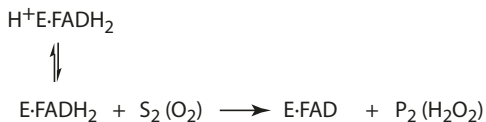
From Gibson et al. [25]



REDUCTIVE HALF-REACTION



OXIDATIVE HALF-REACTION



5.4.2 Reaction Mechanism

The reaction described in Eq. 5.13 refers to glucose as the substrate. The product in this case is δ -D-gluconolactone. The mechanism is composed of two redox half reactions [7, 87].

1. Reductive half-reaction: Reduction of E-FAD (oxidized form of the enzyme) to E-FADH (reduced form), with the substrate β -D-glucopyranose oxidized to δ -D-gluconolactone
2. Oxidative half-reaction: Oxidation of E-FADH to E-FAD with the electron acceptor (O_2) reduced to H_2O_2

Both the reductive and oxidative steps are pH dependent, involving a prototropic group in the enzyme. In the reductive reaction, the substrate (glucose) can only bind with the unprotonated enzyme (E-FAD) and the pK_a of the prototropic group is 3.4. This ionization group has been attributed to the Glu412 carboxylate (pK_1) which is hydrogen bonded to His559 (numbering based on the *Aspergillus niger* mature protein). Protonation of the glutamyl carboxylate group would disrupt the bonding and partially block the active site and binding of the flavin. The dissociation in the Glu412/His559 system therefore modulates the activity of the enzyme [42, 87].

In the oxidative reaction, the binding of O_2 to the reduced enzyme is an acid-catalyzed process, requiring the protonation of a group with pK_a of 6.9. This ionization group is attributed to the His516 imidazole, which is the catalytic base involved in the oxidative and the reductive reactions of the catalytic cycle.

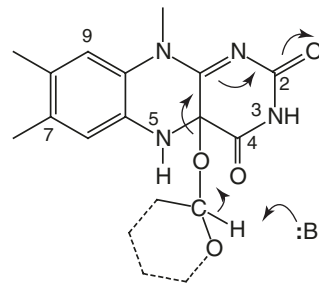
■ ■ The Two-Electron Transfer Process

The reduction of flavin by the substrate (β -D-glucose) and the oxidation of glucose to δ -lactone involve a hydride transfer (a $2e^-$ reduction) from the substrate to the flavin. The hydride is generated from C1–H bond breaking in the substrate (β -D-glucose). The process is promoted by a general base catalysis, involving His516 (as the catalytic base) in accepting a proton from the C1 hydroxyl group of glucose. A concerted hydride transfer occurs from the C1 position of the glucose to the flavin N5F, with the glucose oxidized to lactone (■ Fig. 5.9) [42, 82].

5.4.3 Industrial Uses

Applications of the enzyme glucose oxidase in food, usually with catalase to decompose the H_2O_2 , are summarized in two categories according to its function (■ Table 5.6).

■ Fig. 5.9 Proposed mechanism for the reductive half-reaction (Leskovac et al. [42])



■ Table 5.6 Applications of glucose oxidase

Function	Specific application
1. Removal of glucose	To prevent Maillard reaction in egg solids, dried meats, potatoes
2. Removal of oxygen	To prevent oxidation in beer
	To prevent browning in white wine
	To stabilize oil in water emulsion against rancidity

5.5 Amylases

The amylases are glycosidases that catalyze the hydrolysis of α -1,4-glucose polymers by the transfer of a glucosyl residue (donor) to H_2O (acceptor). α -Amylase (1,4- α -D-glucan glucohydrolase, EC 3.2.1.1) occurs widely in all living organisms. The commercially used α -amylase is mostly obtained from *Bacillus licheniformis* or *Aspergillus oryzae* var. [15]. β -Amylase (1,4- α -D-glucan maltohydrolase, EC 3.2.1.2) is widely distributed in seeds of higher plants. β -Amylase is found in cereal crops, such as barley, wheat, and leguminous crops. The barley-derived enzyme has been the primary source of industrial production. Glucoamylase (1,4- α -D-glucan glucohydrolase, EC 3.2.1.3) (also known as amyloglucosidase in the literature) is commercially produced from *Aspergillus awamori* and *A. niger*.

5

5.5.1 Enzyme Characteristics

α -Amylase cleaves α -1,4-glucose polymers at internal positions (endo-attack) to yield oligosaccharide fragments with the C1 hydroxyl group in the α -configuration. The enzyme has a molecular mass in the range of 50 kDa. It contains one Ca^{2+} per mole of protein, which is essential for the stabilization of the enzyme. The optimum pH of α -amylase varies depending on the source (6.0–7.0 for mammalian, 5.5–7.0 for *Bacillus licheniformis*, 4.8–5.8 for *Aspergillus oryzae*).

β -Amylase is an exoglycosidase that successively cleaves maltosyl units from the non-reducing end of the polymer to yield maltose in the β configuration (■ Table 5.6) [73]. Inherent in its sequential attack, the action of β -amylase stops at the α -1,6 branch point in the starch molecule. α -Amylase, with its random attack, can bypass the branch points in the polymer. However, the presence of an α -1,6 branching point is known to cause the neighboring α -1,4 linkage resistant to attack by β -amylases [72]. β -Amylases have a molecular mass in the range of 50 kDa, except sweet potato β -amylase, which is a tetramer of 197 kDa. The pH optimum for activity ranges from 5.0 for wheat, malt, and sweet potato to 6.0 for soybean. In contrast to α -amylase, β -amylase requires no metal ions.

Glucoamylase is an exoglycosidase that removes glucose units successively from the non-reducing end of the polymeric substrate. The end product is exclusively glucose in the β configuration. The enzyme hydrolyzes both α -D-1,4- and α -D-1,6-glucosidic bonds at the branch point, however, with the latter reaction occurring at a slower rate. Glucoamylase is a glycoprotein containing 5–20% carbohydrate, and mostly exists in isoforms. Fungal glucoamylases have a molecular mass in the range of 70 kDa, and an optimum pH 4.0–4.4 (■ Table 5.7).

The three-dimensional structures of several α -amylases have been solved. The central core of α -amylase is an $(\alpha/\beta)_8$ barrel (domain A), consisting of eight parallel β strands alternating with eight helices joined by loops (■ Fig. 5.10). The molecule also contains domain B, which occurs as insertion between β strand 3 and helix 3. Domain C forms an extension from the $(\alpha/\beta)_8$ barrel. The active site is located in a deep cleft formed on the C-terminus side of the parallel β strands of the central core. Domain B contains a calcium-binding site conferring structural stability to the enzyme. Pancreatic and cereal α -amylases contain a surface-located starch granule-binding site, which facilitates protein-carbohydrate interaction and the digestion of starch (insoluble) granules [13, 55].

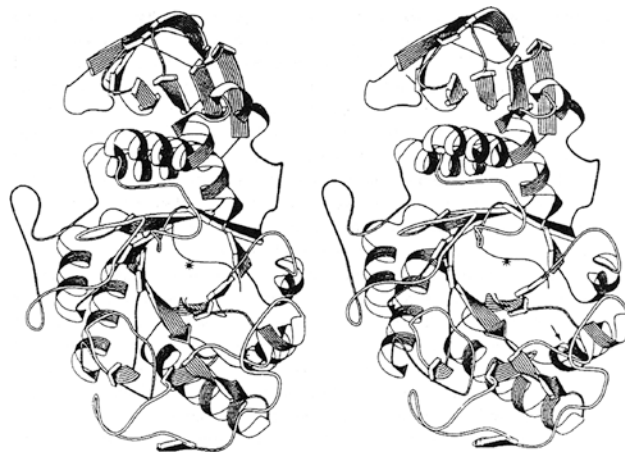
The core structure of β -Amylase consists of a large $(\alpha/\beta)_8$ barrel, similar to that of the α -amylase. However, the enzyme active site is a cleft that opens into a pocket that contains the catalytic Glu/Glu residues, instead of a long open cleft typically found in endo-acting

■ **Table 5.7** Similarities and differences between α and β -Amylases

Characteristics	α -Amylase	β -Amylase
Source	Widespread in nature	Plant seeds
Molecular weight	~50,000	~50,000
Cleavage point	α -1,4 glucosidic bond	α -1,4 glucosidic bond
Configuration of new unit	α	β
Mechanism	Endo	Exo
Product	Oligosaccharides	Maltose
Action at branch point	Bypass	Cannot bypass
Decrease in viscosity	Rapid	Slow

From Thomas et al. [73]

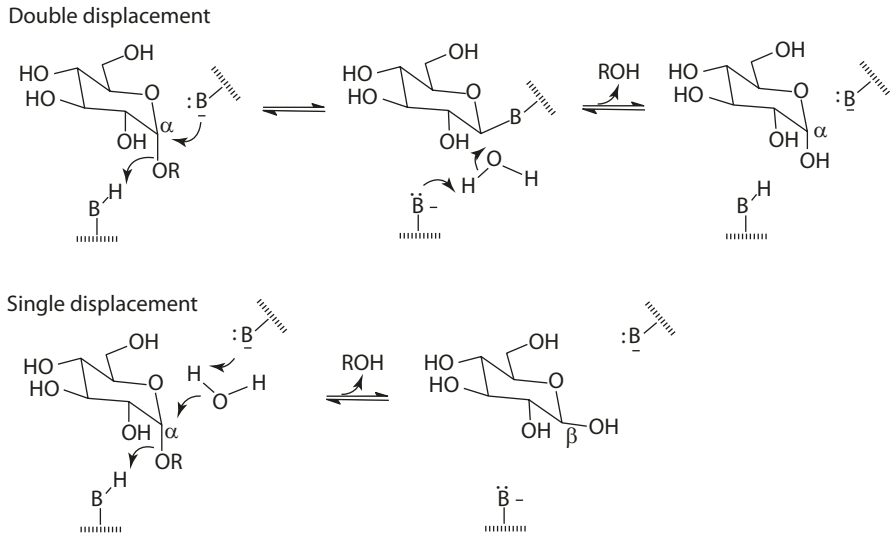
■ **Fig. 5.10** A stereo view of the structure of porcine pancreatic α -amylase. The chloride ion is shown as an asterisk near the axis of the β barrel. The arrow points to the calcium-binding site (From Qian et al. [60] with permission. Copyright 1993 Elsevier)



enzymes. The catalytic domain of glucoamylase is an $(\alpha/\alpha)_6$ barrel with six interior α helices surrounded by six exterior α helices. The active site is located in a deep well with Glu/Glu residues as the general acid and base. Most fungal enzymes contain a starch-binding domain connected to the catalytic domain by an extended, rigid, highly glycosylated linker. In catalysis, the starch-binding domain is tethered onto the surface of a starch granule, and the long linker allows the catalytic domain to attack a large area of the starch substrate.

5.5.2 Reaction Mechanism

Amylolytic hydrolysis proceeds by nucleophilic displacement involving two catalytic residues: Asp/Asp, Glu/Glu, and Glu/Glu for α -amylase, β -amylase, and glucoamylase, respectively. One residue acts as a proton donor to protonate the glycosidic oxygen, and the other serves as a nucleophile to activate the hydrolytic water molecule.



■ Fig. 5.11 Nucleophilic displacement mechanism (From McCarter and Withers [48])

■ ■ Double Displacement Mechanism

The retention of configuration in α -amylase-catalyzed hydrolysis suggests a double displacement mechanism. The concerted protonation of the glycosidic oxygen and the nucleophilic attack of the carboxylate anion at C1 cleaves the glycosidic bond, resulting in the formation of a covalent glycosyl-enzyme intermediate with an inverted configuration [38, 48]. A second displacement by a general base catalysis dissociates the glycosyl-enzyme covalent bonding to yield a product with the anomeric sugar in the α configuration (■ Fig. 5.11).

■ ■ Single Displacement Mechanism

Inversion of configuration by β -amylase- and glucoamylase-catalyzed hydrolysis can be explained by a single displacement mechanism. In this case, the protonated glycosidic oxygen is attacked by a H_2O molecule directed towards the carboxyl carbon on the β side of the substrate assisted by a general base (■ Fig. 5.11). In the single displacement, there is no formation of a covalent glycosyl-enzyme intermediate.

5.5.3 Action Pattern

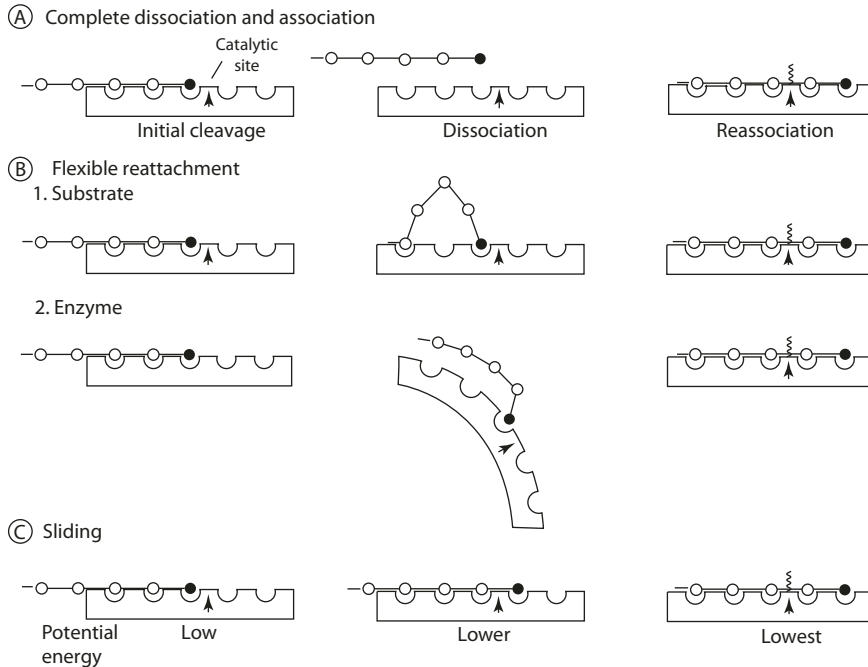
The action pattern of amylase-catalyzed reactions describes the relative susceptibility to cleavage of a given substrate molecule in a population.

In a single-chain action pattern, the amylase once complexed with a substrate molecule continuously acts on it to complete degradation. Another possibility is a multichain action pattern, in which the amylase, having cleaved once a given substrate molecule, dissociates and attacks another substrate molecule. This type of action pattern leads to the simultaneous shortening of all substrate molecules. It is also conceivable that the enzyme, in a multiple attack pattern, cleaves a given substrate more than once before it dissociates and acts on another substrate molecule. Note that the dissociated products in all these cases can in themselves serve as a substrate for the enzyme [73].

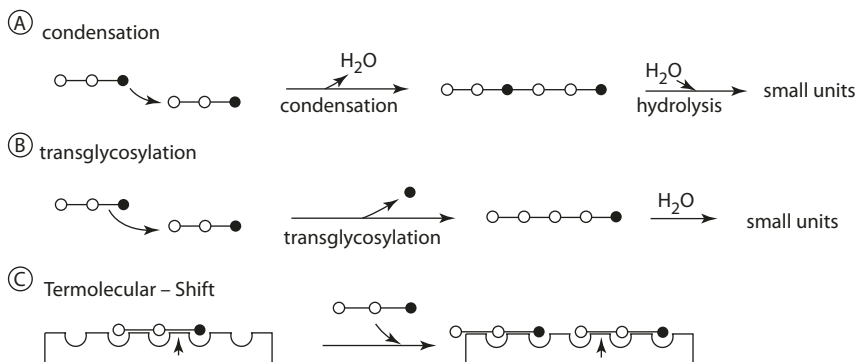
Both β - and α -amylases have been shown to have a multiple attack pattern. The direction of multiple-attack is towards the nonreducing end of the substrate [64]. The mechanism of multiple attack can be visualized in the following schemes (■ Fig. 5.12) to consist of three routes [64]:

1. The substrate, after initial cleavage, dissociates completely and reassociates to a new position (■ Fig. 5.12a).

a Multi-attack mechanism



b Multimolecular process



■ Fig. 5.12 a Mechanism of multiple attack (Robyt and French [65]). b Hydrolysis via multimolecular processes (Allen and Thoma [2])

2. A segment of the product substrate remains attached to the enzyme, while the rest dissociates and realigns to a new position. Such mechanism requires a certain degree of flexibility either in the substrate or the enzyme or both.
3. Another possibility is for the product substrate to slide on the enzyme surface to a position of minimum potential energy having all the subsites completely filled.

5.5.4 The Multimolecular Process

5

Amylases do not exclusively catalyze simple unimolecular hydrolysis. Very often the degradation of oligosaccharide substrates proceeds via multimolecular process in which more than one substrate molecule is involved [2]. Realignment of substrate molecules, such as condensation, transglycosylation, and shifting among substrates, occurs at increasing concentration of substrates.

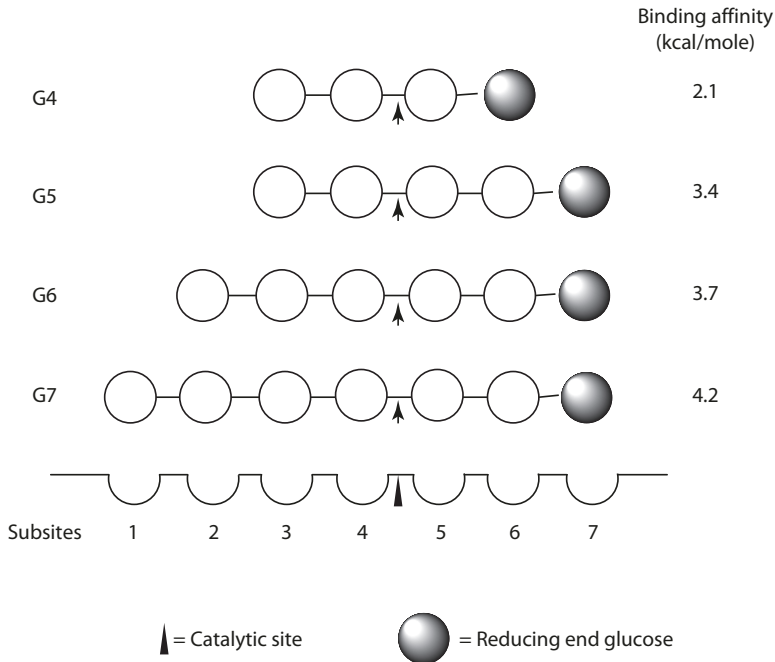
1. Condensation. Two molecules of substrate polymerize to form a new glycosidic bond. The product then undergoes rapid hydrolysis to smaller units (■ Fig. 5.12b).
2. Transglycosylation. A glycosyl group of a substrate donor is transferred to another substrate acceptor, similar to hydrolysis, except that water is not the cosubstrate.
3. Termolecular-shift binding: A second substrate molecule binds to the enzyme in a way that pushes the first bound substrate molecule into a new position, promoting the hydrolysis at a different bond.

5.5.5 Subsites of Amylases

As implicated by the processes described above, the binding site of the enzyme consists of subsites geometrically complementary to the monomer units in the substrate. Pancreatic α -amylase has been shown to contain five subsites, with the catalytic site located asymmetrically [64]. α -Amylase from *Bacillus amyloliquefaciens* has ten subsites [1]. The binding of substrate which covers the catalytic site yields a "productive complex", whereas the binding not conducive to hydrolysis yields a "nonproductive complex". Both types can occur in a number of ways. The interaction between the substrate molecule and the covered subsites results in the increase in the affinity (decrease in the free energy) of the binding. The most probably binding mode for a substrate should retain the highest molecular binding affinity. For example, the *Aspergillus oryzae* α -amylase consists of seven subsites, with the catalytic site between subsites 4 and 5 [52]. The predominant mode of productive binding for various maltooligosaccharides is illustrated in ■ Fig. 5.13. Subsite structure and arrangement has been described for β -amylases and glucoamylases as well.

5.5.6 Industrial Uses

Amylases are used in the baking industry. Yeast fermentation ceases when the sugar in the dough is depleted. There are three sources of sugar: the sugar originally present in the flour, added sugar, and breakdown from starch by amylases. Flour from grains



■ **Fig. 5.13** Schematic illustration of the predominant productive binding mode of *A. oryzae* α -amylase with various maltooligosaccharides (Nita et al. [52])

grown in certain geographic regions may contain a low content of α -amylase. Addition of amylases provides a gradual and constant supply of sugar for continuous fermentation.

In combination with glycoamylase and isomerase, α -amylase is essential in the production of certain types of corn syrup (► Chap. 7). α -Amylase is also used in the clarification of starch haze in beer and wine processing.

β -Amylase is used in the production of maltose syrup, which is used as sweetener in confectionery, ice cream, and other foods, because maltose is less prone to the Maillard browning reaction and resistant to crystallization. The addition of β -amylase is known to inhibit starch retrogradation, and useful in maintaining the softness of starch foods.

5.6 Pectic Enzymes

Pectic enzymes constitute a unique group of enzymes that catalyze the breakdown of pectic substances in plant cell walls. Pectic enzymes are classified according to the type of cleavage [63].

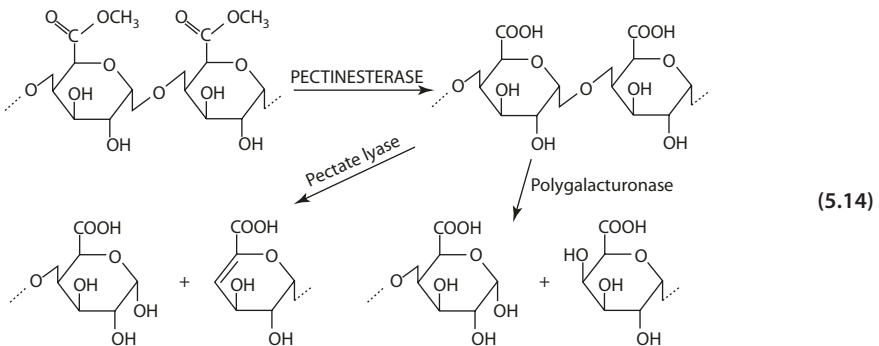
1. Pectinesterase (PE) or pectin methylesterase (PME) (pectic pectylhydrolase, EC 3.1.1.11) catalyzes the deesterification of pectin.
2. Polygalacturonases (PG) catalyze the hydrolytic cleavage of the α -1,4-glycosidic linkage next to a free carboxyl group. The exo-PG, poly(1,4- α -D-galacturonide)

galacturonohydrolase (EC 3.2.1.67), cleaves from the nonreducing end, whereas the endo-PG, poly(1,4- α -D-galacturonide)glycanohydrolase (EC 3.2.1.15), cleaves the pectic chain randomly.

- Pectate lyases catalyze the cleavage of the glycosidic linkage next to a free carboxyl group via β -elimination. Both the exoenzyme, poly(1,4- α -D-galacturonide)exo-lyase (EC 4.2.2.9) and the endoenzyme, poly(1,4- α -D-galacturonide)lyase (EC 4.2.2.2) exist, and pectate is the preferred substrate. Pectate lyases require Ca^{2+} for catalysis.

5.6.1 Pectinesterases

Pectinesterases are highly specific for methyl esters of polygalacturonate (Eq. 5.20). Methyl esters of other uronides or polymers of less than 10 galacturonic acids are not deesterified. Deesterification starts (1) from the reducing end or (2) at some secondary locus, next to free carboxyl groups, and proceeds along the chain, creating blocks free of carboxyl groups [49].



Pectinesterases is ubiquitous in plants, with the primary function in cell wall metabolism during fruit ripening. Most plant pectinesterases have optimum pH between 7 and 9. It is not unusual to find two or more PE isoforms. Pectinesterases of common vegetable origin are small glycoproteins ranging from 10 kDa found in banana, 25 kDa in carrot, to 57 kDa in kiwi. Divalent cations increase the activity of PE in higher plants several times, and the product, polygalacturonic acid, has been shown to act as a competitive inhibitor in tomato PE and orange PE. Pectinesterases are also found in bacterial and fungal pathogens. The enzyme is involved in maceration and softening of plant tissues.

■ ■ Molecular Structure

Pectinesterase has a molecular structure typically of that observed for the other pectinolytic enzymes, representing a family of right-handed parallel β -helical proteins (■ Fig. 5.14a) [32]. The β -helical fold is formed by three parallel β sheets (named PB1, PB2a, PB2b, PB3) [35]. The loops connecting the β helical strands are named T1-, T2-, and T3-turns. The β strands forming each of the β sheets is referred to as β A1, β B2, etc. where the number refers to the β sheets (PB1, PB2, PB3), and the letters refer to the layer of the β strand in the helical coil structure (counting up from the N terminus). Some segments of the loops/turns form bulky extensions on the exterior of the β -helical structure, result-

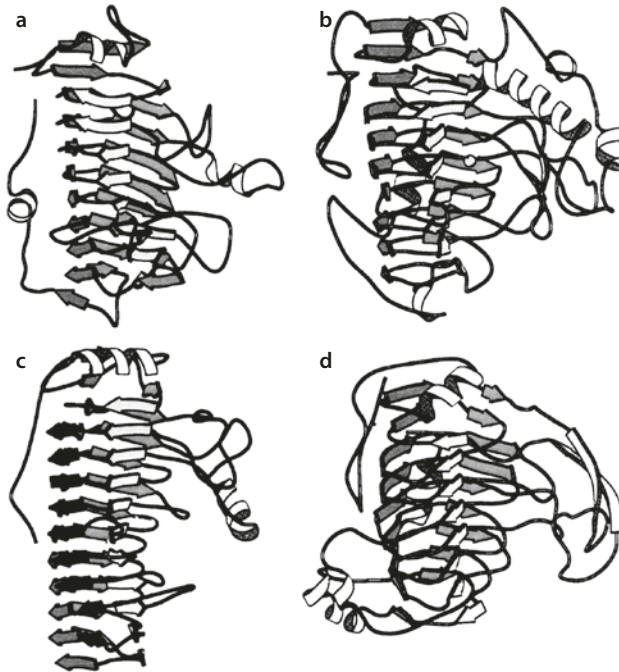


Fig. 5.14 The overall architectures of **a** pectin methylesterase from *Erwinia chrysanthemi* (PDB 1QJV), **b** pectate lyase from *Bacillus subtilis* (1BN8), **c** polygalacturonase from *Erwinia carotovora* (1BHE), and **d** pectin lyase A from *Aspergillus niger* (1IDK). Arrows represent β sheets. Coils represent α helices. The parallel β sheets (PB1, PB2, PB3) are represented by different shades: light gray, gray, dark gray, and so on (From Jenkins et al. [32] with permission. Copyright 1999 American Society of Biochemistry and Molecular Biology)

ing in a long shallow cleft lined with aromatic residues characteristic for carbohydrate binding. The active site contains two Asp residues at the center, a distinguishing feature of aspartyl esterases. The reaction mechanism involves Asp-activated water molecule in the nucleophilic attack on the ester bond of the carboxymethyl group of the polygalacturonan substrate. The second Asp residue acts as a proton donor. *N*-protonation facilitates cleavage of the tetrahedral intermediate to release methanol. (Refer to sections on “Papain” and “Lipase”.)

5.6.2 Polygalacturonases

Polygalacturonases catalyze the hydrolysis of α -D-1,4-glycosidic bonds of nonesterified residues (Eq. 5.14). Deesterified pectin or low methoxy pectins are the preferred substrates.

Both exo- and endo-PGs have weakly acidic pH optima: pH 4.6 for both papaya exo- and endo-PGs; pH 5.5 and 4.0 for peach exo- and endo-PGs, respectively; pH 5.0 for the endo-enzyme from *Rhizopus arrhizus*; and pH 5.5 for *Aspergillus niger* endo-PG [10, 45, 58, 62].

■ ■ Endopolygalacturonases

Endo-PGs usually exist in multiple forms, and the molecular weight varies widely depending on the source. For example, papaya PG has a molecular mass of 164 kDa, *Rhizopus arrhizus* PG 30 kDa, and *Aspergillus niger* 35 kDa. All endo-PGs depolymerize pectic randomly, accompanied by a rapid decrease in viscosity of the substrate solution.

■ ■ Three-Dimensional Structure

Endopolygalacturonase II from *Aspergillus niger* assumes a right-handed parallel β helical fold, comprising 10 complete turns (■ Fig. 5.14c). The β -helical structure is formed by four parallel β sheets (named PB1, PB2a, PB2b, PB3) [78]. The loops connecting the β helical strands are named T1-, T2-, and T3-turns. Some segments of T1- and T2-turns form bulky extensions on the exterior of the β -helical structure, resulting in a large cleft where substrate binding occurs. The catalytic mechanism involves a single displacement reaction. In this case, an Asp residue acts as the acid (proton donor) to protonate the glycosidic oxygen of the scissile bond. A second Asp residue acts as a general base, which activates a water molecule for nucleophilic attack at the anomeric carbon. (This is similar to the single displacement reaction with the products in a retaining configuration described in the Section “Amylases”.)

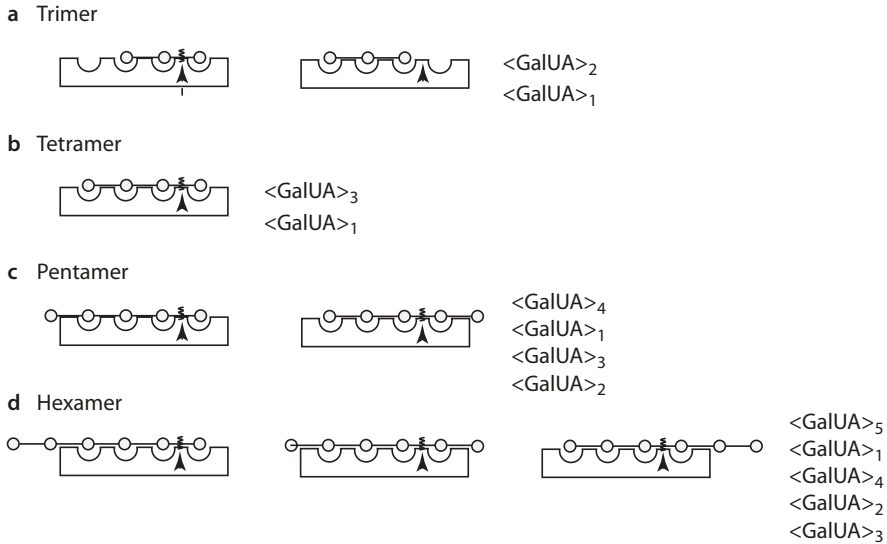
■ ■ Action Pattern

The action pattern of the *Aspergillus niger* endo-PG has been studied using oligogalacturonic acids as the substrate (■ Fig. 5.15). The binding site of the enzyme is composed of four subsites, with the catalytic site situated between subsites 1 and 2 [62].

Trimer substrates do not occupy the complete set of subsites. In the case where the trimer complexes with the subsites without the catalytic groups, the resulting complex is inactive (i.e., a nonproductive complex is formed.) For tetramers, the most probable complex is to have all the subsites occupied, and the product of hydrolysis consists of a trimer and a monomer. Pentamers can complex with the active site in two ways, both satisfying the complete occupancy of all four subsites. With hexamers, three productive complexes can be formed. With high-molecular-weight substrates, the number of productive binding modes in which all the subsites (m) are occupied by the substrate with the degree of polymerization (n), equals $(n - m + 1)$ [62], the mode of hydrolysis becomes random.

■ ■ Exopolygalacturonases

Exo-PGs hydrolyze the substrate starting from the nonreducing end to yield galacturonic acid. However, the degradation of pectate is usually not complete, because the hydrolysis is restricted only to the α -D-1,4-linkage and interrupted by branching. The rate of hydrolysis increases with substrate size and reaches a maximum for polygalacturonate with a degree of polymerization of 20 for carrot and peach ex-PGs [59]. The terminal action pattern is shown by a large increase in reducing groups formation and a slow increase in viscosity.



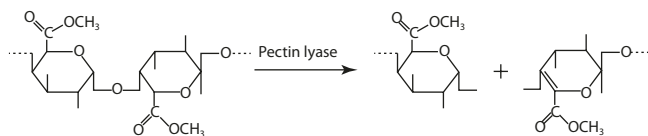
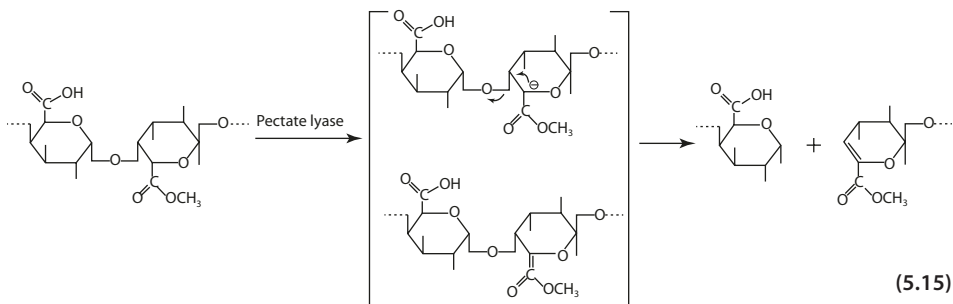
■ **Fig. 5.15** Action pattern of endo-polygalacturonase on **a** trimer, **b** tetramer, **c** pentamer, and **d** hexamer substrates (Rexova-Benkova [62])

5.6.3 Pectate Lyases

Pectate lyases catalyze the degradation of glycosidic bonds next to a free carboxyl group by the mechanism of β -elimination [57]. Deesterified or low-methoxy pectins are the preferred substrates for the enzyme.

The core structure of pectate lyase consists of three parallel β sheets wound into a right-handed parallel β helical fold of seven complete turns [88]. The three parallel β sheets are named PB1, PB2, PB3 (■ Fig. 5.14b). The β helical strands in PB1, PB2, and PB3 are connected by short loops consisting of 3–5 residues. The substrate-binding groove is rich in charged residues, providing an electrostatic environment suitable for the pectate molecule.

In the β -elimination mechanism, the calcium ion at the active site neutralizes the charge on the carboxylate anion at the C6 position of the galacturonic acids in the pectate substrate. This metal interaction results in increasing the electron withdrawing effect of the C5 carbon and lowering the $\text{p}K_a$ of the C5 α proton. Abstraction of the α proton from C5 is achieved by a general base catalysis, involving an Arg residue adjacent to the scissile bond acting as a nucleophile. The resulting carbanion intermediate is stabilized by the C6 carboxyl group. Transfer of the proton to the glycosidic bond with simultaneous bond cleavage (at the β position to the carboxyl group) leads to the formation of a double bond between C4 and C5 (Eq. 5.15). The reaction therefore generates oligosaccharides with unsaturated galacturonosyl residues at their nonreducing ends.



5

Both the exo- and the endoenzymes have an alkaline pH optimum ranging from 8.0 to 9.5 and a requirement for Ca^{2+} for activity. The exoenzyme starts the cleavage from the reducing end of the substrate. In contrast to the endoenzyme, the rate of cleavage does not depend on the size of the substrate. Pectate lyases are mostly reported in bacteria and molds, some of which are involved in the softening of fruits and vegetables.

Another similar enzyme, pectin lyase (EC 4.2.2.10), catalyzes similar reactions, except the preferred substrate is methyl esterified (Eq. 5.15). The substrate-binding groove is rich in aromatic side chains, which favor the binding of noncharged (highly esterified) substrates. The presence of methyl ester substitution plays a crucial role in the substrate recognition in pectin lyase. Removal of the methyl ester groups results in a loss of activity. The rate of reaction decreases as the degree of esterification decreases. The reaction product has 4-deoxy-6-*O*-methyl- α -D-galacturonosyl residues at the nonreducing end.

5.6.4 Industrial Importance

The study of pectic enzymes is important to food science in three aspects. Pectic enzymes are known to play an important role in textural changes during the ripening of fruits. The softening of fruits is correlated to increasing enzyme activity on the degradation of pectic substances.

Post-harvest loss due to rotting of fruits and vegetables has been attributed in part to the action of microbial pectic enzymes. Examples include the softening of cucumber and olives in brine due to the actions of yeast polygalacturonase and bacterial pectate lyase, and the softening of apricots caused by *Rhizopus arrhizus* PGs [45].

Pectic enzymes are studied also for reasons of technological applications, the largest use being in the wine and fruit industry. During the production of apple juice, for example, the enzyme mix is added to increase the yield of extraction and also for juice clarification. In the manufacture of red wine, enzyme treatment of grape pulp results in better color extraction and higher juice yield.

■ **Table 5.8** Lipolytic enzymes, substrates, and products

Enzyme	Systematic name ^a	Substrate	Products
Triacylglycerol lipase (3.1.1.3)	Triacylglycerol hydrolase	Triacylglycerols	Diacylglycerol, fatty acid anion
Phospholipase A ₂ (3.1.1.4)	Phosphatide 2-acylhydrolase	Lecithin	1-Acylglycerol-phosphocholine, fatty acid anion
Phospholipase A ₁ (3.1.1.32)	Phosphatidate 1-acylhydrolase	Lecithin	2-Acylglycerol-phosphocholine, fatty acid anion
Lysophospholipase (3.1.1.5)	Lysolecithin acylhydrolase	Lysolecithin	Glycerophosphocholine, fatty acid anion
Phospholipase C (3.1.4.3)	Phosphatidylcholine cholinephosphohydrolase	Phosphatidylcholine	1,2-diacylglycerol, choline phosphate
Phospholipase D (3.1.4.4)	Phosphatidylcholine phosphatidohydrolase	Phosphatidylcholine	Choline, phosphatidate
Sphingomyelin phosphodiesterase (3.1.4.12)	Sphingomyelin cholinephosphohydrolase	Sphingomyelin	<i>N</i> -acylsphingosine, choline phosphate

^aIUBMB enzyme nomenclature [51]

5.7 Lipolytic Enzymes

Lipolytic enzymes consist of two major groups, the lipases which are triacylglycerol acyl hydrolases, and the phospholipases A₁ and A₂ which are phosphoglyceride acyl hydrolases [34]. Although phospholipases C and D are not acyl hydrolases, they are nonetheless commonly included as lipolytic enzymes (■ Table 5.8).

Lipases constitute a class of esterases that exhibits interfacial activation. These enzymes act specifically on water-insoluble esters (lipid substrates) at the oil-water interfaces. The following discussion will mostly focus on the extensively studied porcine pancreatic lipase.

5.7.1 Pancreatic Lipases

Porcine pancreatic lipase is a single polypeptide containing 449 amino acids with a molecular mass of 50 kDa. A single carbohydrate chain of fucose, galactose, mannose, and *N*-acetylglucosamine is linked to Asn66 [83]. The porcine lipase comprises two domains: (1) The N-terminal domain has an α/β structure containing the catalytic Ser-His-Asp triad. (2) The C domain assumes a β -sandwich structure containing the binding site for colipase to facilitate catalysis at the oil-water interface (■ Fig. 5.16). Unique to pancreatic lipases is the existence of a surface loop forming a "lid" that covers the active site. The lid



Fig. 5.16 A stereo representation of the overall fold of horse pancreatic lipase. The catalytic triad and the disulfide bridges are represented in ball-and-stick. The eight β strands are represented in dark shading (From Bourne et al. [6] with permission. Copyright 1994 Elsevier. PDB 1HPL)

is repositioned by a conformational change during interfacial activation to catalyze the hydrolysis of triacylglycerols. Similar architectural structures are observed in human and horse pancreatic lipases.

Pancreatic lipase requires a protein cofactor, colipase, to facilitate its catalytic function. Colipase in its native form (procolipase) contains 101 amino acid residues. It is activated by low concentrations of trypsin, which hydrolyzes the N-terminal pentapeptide to form colipase₉₀. Higher concentrations of trypsin result in the formation of colipase₈₅, with the loss of 11 amino acid residues at the C terminus. The specific activities of both are about five times higher than that of the procolipase [39].

5.7.2 The Role of Colipase

Contrary to conventional enzyme reactions that normally occur in aqueous solution, lipolytic enzymes catalyze the hydrolysis reaction by heterogeneous catalysis at the interface between two immiscible phases, the aqueous phase and the apolar phase containing the lipid substrate.

Lipolytic enzymes are irreversibly denatured at the interfaces. In the physiological environment, the absorption and denaturation of pancreatic lipase is prevented by the presence of bile salt at the interface. The bile salt inhibits the adsorption by physically excluding the enzyme from the interface or by a general detergent effect. Inhibition may also result from the increasing surface pressure due to the bile salt. Lipase has been shown to be unable to penetrate the lipid film above a critical surface pressure.

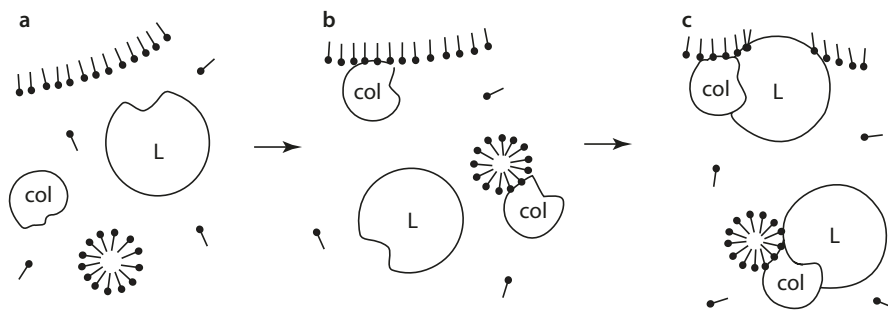


Fig. 5.17 The role of colipase for the functioning of lipase in the presence of bile salts. **a** When alone, lipase recognizes neither the micelles nor the interface. **b** Colipase recognizes both, creating a binding site for lipase. **c** Binding of lipase mediated by colipase (From Chapus et al. [11] with permission. Copyright 1975 Elsevier)

For the lipase to act on the triacylglycerol substrate at the interface in the presence of bile salts, colipase is required. Colipase and lipase bind in a 1:1 complex with a dissociation constant of 10^{-6} M. Both hydrophobic and ionic interactions are involved. The presence of colipase increases the critical surface pressure to allow lipase penetration. It has also been shown that colipase has a high affinity for bile salt micelles and monolayers. The binding of colipase to the interface leads to a conformational change, unmasking a specific binding site for lipase to complex [11], and adsorb to the bile salt-covered interface. The formation of the bile salt-colipase-lipase ternary complex stabilizes the lipase against surface denaturation and thus anchors the lipase to the interface where hydrolysis can occur (Fig. 5.17). It is also conceivable that the colipase and lipase complex before anchoring to the interface.

5.7.3 Mechanism of Catalysis

The hydrolysis reaction catalyzed by pancreatic lipase consists of a mechanism resembling that of the serine proteases such as chymotrypsin, in which the hydroxyl group of Ser is activated by a His-carboxylate anion in a charge-relay system (Fig. 5.18). The Ser-OH reacts with the substrate to form an acylenzyme, which is then deacylated to give the product [8].

The reaction mechanism proposed for lipoprotein lipase catalysis is also similar to that of serine proteases. The one shown in Eq. 5.16 is for the action on a *p*-nitrophenyl ester substrate [61, 67]. The acylenzyme is formed via the formation of a tetrahedral intermediate. (Refer to the section on "Papain".) The transition state is stabilized by a general base proton bridge between the Ser and the His. Expulsion of the *p*-nitrophenoxide breaks down the tetrahedral intermediate to form the acylenzyme. Hydrolysis of the acylenzyme occurs by general base catalysis.

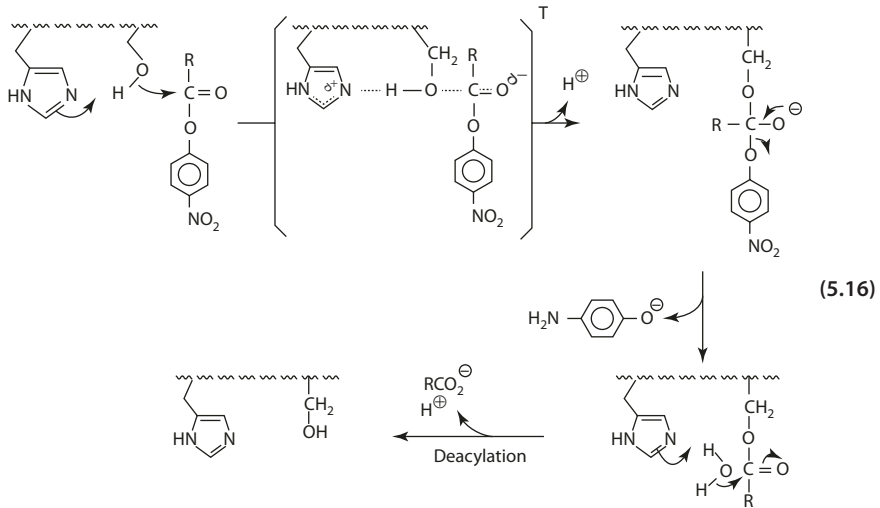
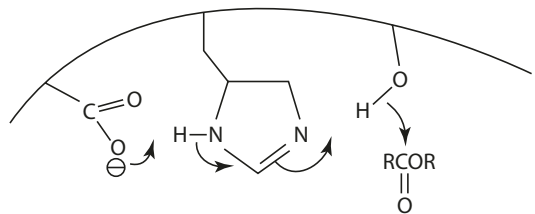


Fig. 5.18 Mechanism of lipase catalysis (Brockenhoff [8])



5.7.4 Specificity

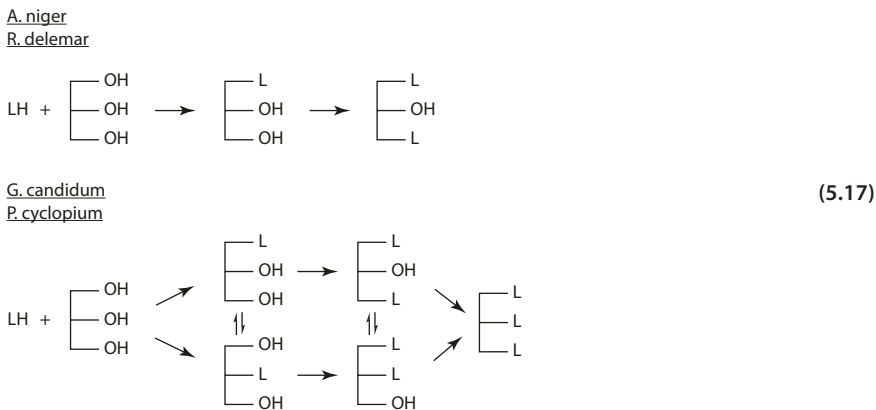
Lipases exhibit three types of specificity [33]:

1. **Substrate specificity:** The enzyme hydrolyzes acylglycerols (TG, DG, MG) or types of fatty acids at different rates. For example, *Geotrichum candidum* lipase hydrolyzes oleic acid and palmitic acid in preference to stearic acid.
2. **Positional specificity:** The enzyme catalyzes the release of fatty acids at preferential positions on the acylglycerol molecule. Pancreatic lipase is specific for the primary esters of acylglycerols, and the sequence of hydrolysis follows TG > 1,2(2,3)-DG > 2-MG. Lipases from *G. candidum* and *Penicillium cyclopium* show no specificity with regard to the position, whereas lipases from *Aspergillus niger* and *Rhizopus delemar* do not hydrolyze the ester bond in position 2. In general, 1,3-specificity is common among microbial lipases.
3. **Stereospecificity:** Pancreatic lipase and most microbial lipases show no distinction in catalytic activity at position 1 and 3. However, lipoprotein lipase and heparin-releasable lipase preferentially attack the *sn*-1 position, and lingual lipase prefers the *sn*-3 position of the acylglycerol molecule. (Refer to ► Chap. 1 for the stereochemistry and nomenclature.)

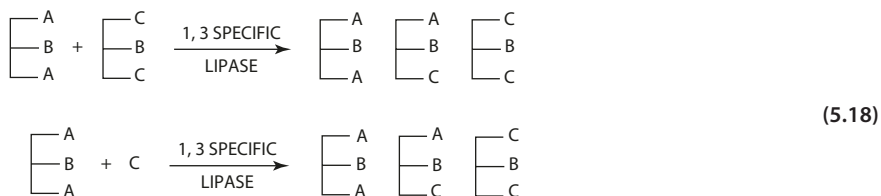
5.7.5 The Acyl Transfer Reaction

Under specific and controlled conditions, lipase catalyzes acyl transfer between acylglycerols and fatty acids. In these types of reactions, the acyl group is transferred to the glycerol instead of water. Obviously, the presence of water in the reaction system favors the hydrolysis pathway. Increasing the proportion of organic solvent facilitates the acyl transfer reaction.

The acyl transfer reaction offers a novel method of synthesizing acylglycerols starting with glycerol and fatty acids [74]. Using lipase with the desirable specificity, it is possible to manipulate the synthesis to obtain a particular esterification product. Lipases from *A. niger* and *R. delemar* synthesize only 1(3)-MG and 1,3-DG (Eq. 5.17) whereas lipases from *G. candidum* and *P. cyclopium* make ester bonds at all three positions. Esterification of glycerol with oleic acid using *Candida rugosa* lipase gives 2-MG, 1-MG, 1,2-DG, 1,3-DG, and TG [44].

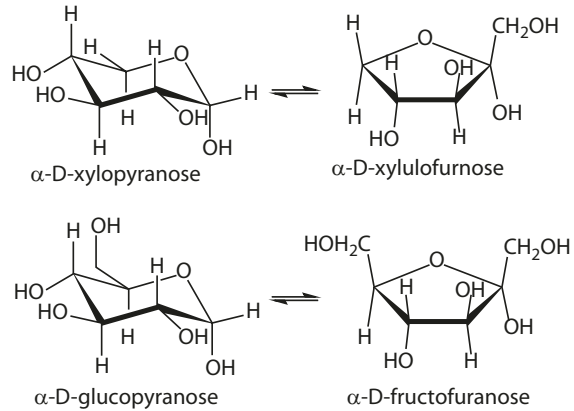


The acyl transfer reaction, however, is most useful for the food industry in its application in the interesterification process [46, 47]. Hydrolysis and resynthesis cause acyl exchange (1) between acylglycerol molecules to form interesterified products (Eq. 5.18), or (2) between acylglycerol and free fatty acids to produce new acylglycerols enriched with the added fatty acid.



Using lipases with appropriate specificity, it becomes possible to direct the process of interesterification to produce the desired product. While chemical interesterification gives products in which the fatty acyl residues are randomly distributed, the enzymatic process provides interesterification at specific positions with specific acyl groups. Considering that the physical characteristics of fats and oils depend on the position of a particular fatty acid in the glycoside, the advantage of enzymatic interesterification and its practical usage are significant.

Fig. 5.19 Reversible isomerization of D-xylose and D-glucose to respective ketoses



5.8 Xylose Isomerase

Xylose (glucose) isomerase (EC 5.3.1.5) is well known for its large-scale application in the starch processing industry for the production of high-fructose corn syrup. The enzyme catalyzes the reversible isomerization of D-xylose and D-glucose to their respective ketoses, D-xylulose and D-fructose, respectively, in the presence of divalent metal ions (Mg^{++} , Mn^{++} , or Co^{++}) (Fig. 5.19). The enzyme is essentially a xylose isomerase. Glucose isomerization is not the primary physiological function. Although xylose isomerase acts on D-glucose, and also L-arabinose, L-rhamnose, D-ribose, and other sugar substrates, xylose is clearly the preferred substrate. The K_m for D-xylose is 2 orders of magnitude smaller and the k_{cat} is two to tenfold higher than for D-glucose or D-fructose.

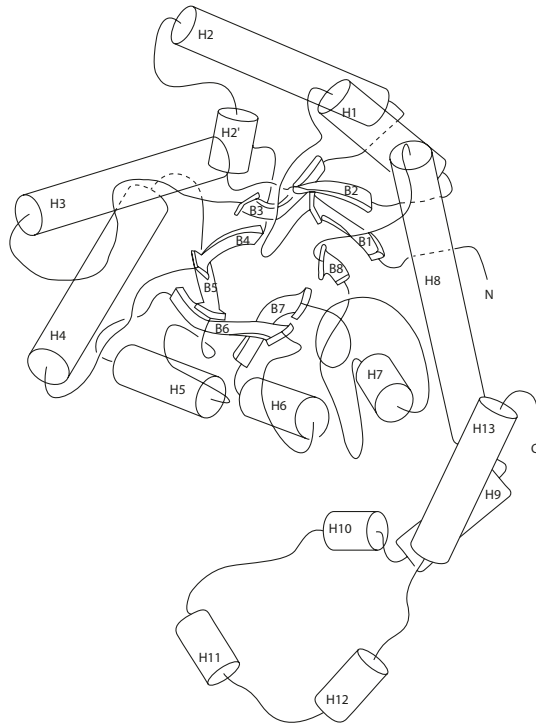
Xylose isomerases are microbial enzymes widely present in prokaryotic organisms. The enzymes used in the industry are mostly derived from selected bacterial species (e.g., *Streptomyces*), developed by protein engineering, and usually immobilized for high performance[50].

5.8.1 Protein Structure

With few exceptions, xylose isomerases are tetramers of identical subunits. Depending on the microbial source, the molecular mass varies in the range of 170–200 kDa. Xylose isomerases are encoded by a single gene, and therefore do not exist in isoforms.

The crystal structures of xylose isomerase from *Streptomyces* as well as other bacterial sources have been investigated [9, 40]. The subunit consists of two domains: (1) Domain I (320 residues) is composed of eight strands of parallel β sheet connected by helices anti-parallel to the strands forming an $(\alpha/\beta)_8$ barrel. (2) Domain II (65 residues) contains five helices connected by random coils forming a large loop away from Domain I (Fig. 5.20). Interactions between Domain I of one subunit with Domain II of another subunit result in a dimer, with the interface mostly hydrophobic. Two dimers then align in a twofold symmetry to form a tetramer. The dimer structures are active, whereas the monomers are

Fig. 5.20 The subunit structure of xylose isomerase from *Arthrobacter*, viewed down the barrel axis from the carboxyl end of the sheet (From Henrick et al. [28] with permission. Copyright 1989 Elsevier)

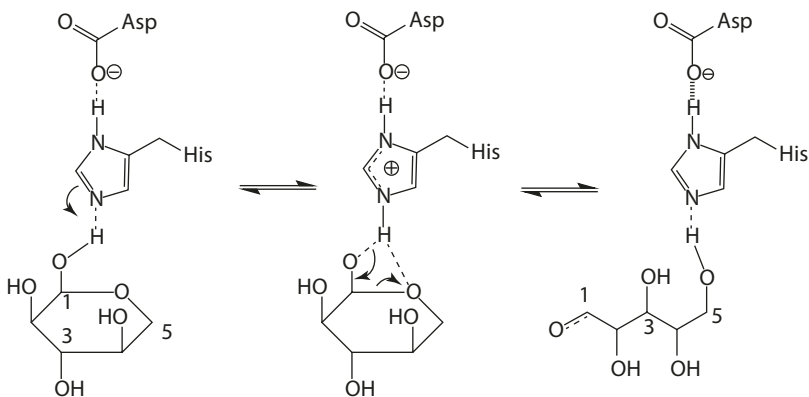


inactive. The active site is located in a deep pocket (amphipathic in nature) close to the twofold axis of the tetramer molecule. It is lined with a cluster of aromatic side chains for interaction with the sugar substrate, and several acidic and polar residues forming ligands to the metal cation.

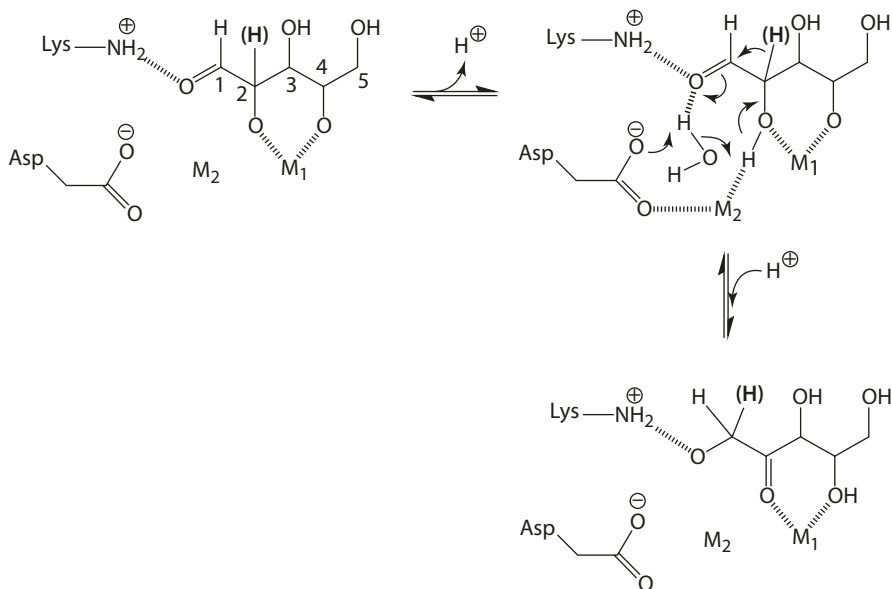
Inactivation of xylose isomerase occurs at high glucose concentration and high heat as observed in industrial application. Glucose reacts with the Lys residues exposed on the subunit interfaces, forming Schiff base followed by Amadori rearrangement as known in the Maillard reaction.

5.8.2 Metal Cations

All xylose isomerases contain two metal ion binding sites per subunit, one of high affinity and one of weak binding. The enzymes are active only when the two sites have bound metal cations. Studies of dissociation constants suggest that the binding affinity is in the order of $Mn^{++} > Co^{++} > Mg^{++}$. The two metal binding sites also vary in their affinity for different metal cations [76]. A particular metal ion may have the same K_d for both sites, or exhibit big difference for the two sites, depending on the bacterial source. In most literature, site 1 is designated to the site responsible for stabilizing effect of the structure. Site 2 is the one closer to the C1 and C2 of the substrate, involving mainly in the catalytic process.



■ Fig. 5.21 The hydride shift mechanism of xylose isomerase, illustrating His-catalyzed opening of the aldose (Collyer et al. [14])



■ Fig. 5.22 The metal-catalyzed stereospecific hydride transfer indicating the role of the Asp side chain (Collyer et al. [14]; Whitlow et al. [84])

5.8.3 Reaction Mechanism

The mechanism for aldose-ketose isomerization by xylose isomerase involves ring opening of the substrate, followed by 1,2-hydride shift mediated by the metal ion [14, 19, 84]. Xylose isomerase reacts specifically with the sugar substrate in its α -anomeric form, and the product maintains the α configuration. The 1,2-hydride shift isomerization is the rate limiting step.

1. The enzyme binds the closed ring substrate, which positions to undergo ring opening to form an open extended form. (Glucose is represented in  Fig. 5.21.) Ring opening of the substrate is catalyzed by the His54–Asp57 charge relay system, in which the His acts as a base catalyst in transferring the C1–OH proton to the ring oxygen. (The numbering of amino acid residues is based on the *Streptomyces rubiginosus* enzyme.) The open form of the substrate is now bound to the enzyme in an extended configuration.
2. The isomerization reaction involves the transfer of two hydrogen atoms: from C2–OH to C1–O and C2–H to C1, resulting in a 1,2-hydride shift of the sugar substrate ( Fig. 5.22). The initial step is proton abstraction of the C2 hydroxyl (C2–OH), in which the site 2 metal ion-bound hydroxide ion (solvent water molecule) acts as the proton acceptor. The anion intermediate (the negative charge at C2–O) is then stabilized by coordination with the metal ions.
3. Polarization of the C–O bonds at C1 and C2 facilitates 1,2-hydride shift (transfer of the hydrogen as hydride ion H[−]) from C2 to C1. Disengagement of metal coordination converts the intermediate to a stable ketose, followed by ring closure yielding the ketose product.

References

1. Allen JD, Thoma JA (1976) Subsite mapping of enzymes. *Biochem J* 159:121–132
2. Allen JD, Thoma JA (1979) Multimolecular substrate reaction catalyzed by carbohydrates. *Aspergillus oryzae* α -amylase degradation by maltooligosaccharides. *Biochemistry* 17:2338–2344
3. Baker EN, Drenth J (1987) The thiol proteases: structure and mechanism. In: *Jurnak FA, McPherson A (eds) Biological macromolecules and assemblies, vol 3*. Wiley, New York
4. Boyington JC, Gaffney BJ, Amzel LM (1993) Structure of soybean lipoxygenase-1. *Biochem Soc Trans* 21:744–748
5. Boyington JC, Gaffney BJ, Amzel LM (1993) The three-dimensional structure of an arachidonic acid 15-lipoxygenase. *Science* 260:1482–1486
6. Bourne Y, Martinez C, Kerfelec B, Lombardo D, Chapus C, Cambillau C (1994) Horse pancreatic lipase: the crystal structure refined at 2.3 Å resolution. *J Mol Biol* 238:709–732
7. Bright HJ, Appleby M (1969) The pH dependence of the individual steps in the glucose oxidase reaction. *J Biol Chem* 244:3625–3634
8. Brockerhoff H (1973) A model of pancreatic lipase and the orientation of enzymes at interfaces. *Chem Phys Lipids* 10:215–222
9. Carrell HL, Glusker JP, Burger V, Manfre F, Tritsch D, Biellmann J-F (1989) X-ray analysis of D-xylose isomerase at 11.9 Å: native enzyme in complex with substrate and with a mechanism-designed in activator. *Proc Natl Acad USA* 86:4440–4444
10. Chan HT, Tam SNY (1982) Partial separation and characterization of papaya endo- and exo-polygalacturonase. *J Food Sci* 47:1478–1483
11. Chapus C, Sari H, Semeriva M, Desnuelle P (1975) Role of colipase in the interfacial adsorption of pancreatic lipase at hydrophilic interfaces. *FEBS Lett* 58:155–158
12. Cheesbrough TM, Axelrod B (1983) Determination of the spin state of iron in native and activated soybean lipoxygenase 1 by paramagnetic susceptibility. *Biochemistry* 22:3837–3840
13. Chung H, Friedberg F (1980) Sequence of the N-terminal half of *Bacillus amyloliquifaciens* α -amylase. *Biochem J* 185:387–395
14. Collyer CA, Henrick K, Blow DM (1990) Mechanism for aldose-ketose interconversion by D-xylose isomerase involving ring opening followed by a 1,2-hydride shift. *J Mol Biol* 212:211–235
15. Dawson HG, Allen WG (1984) *The use of enzymes in food technology*. Miles Laboratories, Inc., Biotech Products Division, Elkhart
16. deGroot JJM, Veldink GA, Vliegthart JFG, Boldingh J, Wever R, van Gelder BF (1975) Demonstration by EPR spectroscopy of the functional role of iron in soybean lipoxygenase-1. *Biochim Biophys Acta* 377:71–79

17. Drenth J, Jansonius JN, Kockock R, Wolthers BG (1971) Papain, X-ray structure. In: Boyer PD (ed) The enzymes, vol III. Academic, New York
18. Egmond MR, Vliegthart JFG, Boldingh J (1972) Stereospecificity of the hydrogen abstraction at carbon atom n-8 in the oxygenation of linoleic acid by lipoxygenases from corn germs and soya beans. *Biochem Biophys Res Commun* 48:1055–1060
19. Farber GK, Glasfeld A, Tiraby G, Ringe D, Petsko GA (1989) Crystallographic studies of the mechanism of xylose isomerase. *Biochemistry* 28:7289–7297
20. Galliard T, Chan HWS (1980) Lipoxygenase. In: Stumpf PK, Conn EE (eds) The biochemistry of plants, a comprehensive treatise, vol 4. Academic, New York
21. Galliard T, Phillips DR, Reynolds J (1976) The formation of *cis*-3-nonenal, *trans*-2-nonenal and hexanal from linoleic acid hydroperoxide isomers by a hydroperoxide cleavage enzyme system in cucumber (*Cucumis sativus*) fruits. *Biochim Biophys Acta* 441:181–192
22. Gardner HW (1979) Stereospecificity of linoleic acid hydroperoxide isomerase from corn germ. *Lipids* 14:208–211
23. Garssen GJ, Vliegthart JFG, Boldingh J (1971) An anaerobic reaction between lipoxygenase, linoleic acid and its hydroperoxide. *Biochem J* 22:327–332
24. Garssen GJ, Vliegthart JFG, Boldingh J (1972) The origin and structures of dimeric fatty acids from the anaerobic reaction between soya-bean lipoxygenase, linoleic acid and its hydroperoxide. *Biochem J* 130:435–442
25. Gilson QH, Swoboda BEP, Massey V (1964) Kinetics and mechanism of action of glucose oxidase. *J Biol Chem* 239:3927–3934
26. Hecht HJ, Kalisz HM, Hendle J, Schmid RD, Schomburg D (1993) Crystal structure of glucose oxidase from *Aspergillus niger* refined at 2.3 Å resolution. *J Mol Biol* 229:153–172
27. Heller MJ, Walder JA, Klotz IM (1977) Intramolecular catalysis of acylation and deacylation in peptides containing cysteine and histidine. *J Am Chem Soc* 99:2780–2785
28. Henrick CA, Collyer A, Blow DM (1989) Structures of D-xylose isomerase from *Arthrobacter* strain B3728 containing the inhibitors xylitol and D-sorbitol at 2.5 Å and 2.3 Å resolution, respectively. *J Mol Biol* 208:129–157
29. Himmelwright RS, Eickman NC, Lubien CD, Lerch K, Solomon EI (1980) Chemical and spectroscopic studies of the binuclear copper active site of *Neurospora* tyrosinase: comparison to hemocyanins. *J Am Chem Soc* 102:7339–7344
30. Ismaya W, Rozeboom HJ, Weijn A, Mes JJ, Fusetti F, Wichers HJ, Dijkstra BW (2011) Crystal structure of *Agaricus bisporus* mushroom tyrosinase: identity of the tetramer subunits and interaction with tropolone. *Biochemistry* 50:5477–5486
31. James TL, Edmondson DE, Husain M (1981) Glucose oxidase contains a disubstituted phosphorus residue. Phosphorus-31 nuclear magnetic resonance studies of the flavin and nonflavin phosphate residues. *Biochemistry* 20:617–621
32. Jenkins J, Mayans O, Smith D, Worboys K, Pickersgill RW (2001) Three-dimensional structure of *Erwinia Chrysanthemi* pectin methylesterase reveals a novel esterase active site. *J Mol Biol* 305:951–960
33. Jensen RG, Dejong FA, Clark RM (1983) Determination of lipase specificity. *Lipids* 18:239–253
34. Jensen RG, Gerrior SA, Hagerty MM, McMahon KE (1978) Preparation of acylglycerols and phospholipids with the aid of lipolytic enzymes. *JAOCS* 55:422–427
35. Johansson K, El-Ahmad M, Fridmann R, Jornvall H, Markovic O, Eldund H (2002) Crystal structure of plant pectin methylesterase. *FEBS Lett* 514:243–249
36. Kang CK, Rice EE (1970) Degradation of various meat fractions by tenderizing enzymes. *J Food Sci* 35:563–565
37. Klabunde T, Eicken C, Sacchettini JC, Krebs B (1998) Crystal structure of a plant catechol oxidase containing a dicopper center. *Nat Struct Biol* 5:1084–1090
38. Lai H-L, Butler LG, Axelrod B (1974) Evidence for a covalent intermediate between α -glucosidase and glucose. *Biochem Biophys Res Commun* 60:635–640
39. Larsson A, Erianson-Albertsson C (1981) The identity and properties of two forms of activated colipase from porcine pancreas. *Biochim Biophys Acta* 664:538–548
40. Lavie A, Allen KN, Petsko GA, Ringe D (1994) X-ray crystallographic structures of D-xylose isomerase-substrate complexes position the substrate and provide evidence for metal movement during catalysis. *Biochemistry* 33:5469–5480
41. Lerch K (1982) Primary structure of tyrosinase from *Neurospora crassa*. *J Biol Chem* 257:6414–6419

References

42. Leskovac V, Trivic S, Wohlfahrt G, Kandrac J, Pericin D (2005) Glucose oxidase from *Aspergillus niger*: the mechanism of action with molecular oxygen, quinones, and one-electron acceptors. *Int J Biochem Cell Biol* 37:731–750
43. Lewis SD, Johnson FA, Shafer JA (1981) Effect of cysteine-25 on the ionization of histidine-159 in papain as determined by proton nuclear magnetic resonance spectroscopy. Evidence for a His-159-Cys-25 ion pair and its possible role in catalysis. *Biochemistry* 20:48–51
44. Linfield WM, Barauskas RA, Sivieri L, Serota S, Stevenson RW Jr (1984) Enzymatic fat hydrolysis and synthesis. *JAOCS* 61:191–195
45. Liu YK, Luh BS (1978) Purification and characterization of endopolygalacturonase from *Rhizopus arrhizus*. *J Food Sci* 43:721–726
46. Macrae AR (1983) Lipase-catalyzed interesterification of oils and fats. *JAOCS* 60:291–294
47. Macrae AR (1989) Tailored triacylglycerols and esters. *Biochem Soc Trans* 17:1146–1989
48. McCarter JD, Withers SG (1994) Mechanisms of enzymatic glycoside hydrolysis. *Curr Opin Struct Biol* 4:885–892
49. Miller L, McMillan J (1971) Purification and pattern of action of pectinesterase from *Fusarium oxysporum* sp. vasinfectum. *Biochemistry* 10:570–576
50. Misset O (2003) Xylose (Glucose) isomerase. In: Whitaker JR, Voragen AGJ, Wong DWS (eds) *Handbook of food enzymology*. Marcel Dekker, New York
51. NC-IUBMB (2015) Enzyme nomenclature, recommendations of the nomenclature committee of the international union biochemistry and molecular biology on the nomenclature and classification of enzymes by the reactions they catalyze. www.chem.qmul.ac.uk/ubmb/enzymes
52. Nita Y, Mizushima M, Hiromi K, Ono S (1971) Influence of molecular structures of substrates and analogues on Taka-amylase A catalyzed hydrolyses. *J Biochem* 69:567–576
53. Palmer JK (1963) Banana polyphenoloxidase. Preparation and properties. *Plant Physiol* 38:508–513
54. Pariza MW, Johnson EA (2001) Evaluating the safety of enzyme preparations used in food processing: update for a new century. *Regul Toxicol Pharmacol* 33:173–186
55. Payan F, Haser R, Pierrot M, Frey M, Astler JP (1980) The three-dimensional structure of α -amylase from porcine pancreas at 5 Å resolution – the active site location. *Acta Cryst B* 36:416–421
56. Polgar L (1973) On the mode of activation of the catalytically essential sulfhydryl group of papain. *Eur J Biochem* 33:104–109
57. Press J, Ashwell G (1963) Polygalacturonic acid metabolism in bacteria. *J Biol Chem* 238:1571–1576
58. Pressey R, Avants JK (1975) Separation and characterization of endo-polygalacturonase and exopolygalacturonase from peaches. *Plant Physiol* 52:252–256
59. Pressey R, Avants JK (1975) Modes of action of carrot and peach exopolygalacturonases. *Phytochemistry* 14:957–961
60. Qian M, Haser R, Fayon F (1993) Structure and molecular model refinement of pig pancreatic α -amylase at 2.1 Å resolution. *J Mol Biol* 231:785–799
61. Quinn DM (1985) Solvent isotope effects for lipoprotein lipase catalyzed hydrolysis of water-soluble *p*-nitrophenyl esters. *Biochemistry* 24:3144–3149
62. Rexova-Benkova L (1973) The size of the substrate-binding site of an *Aspergillus niger* extracellular endopolygalacturonase. *Eur J Biochem* 39:109–115
63. Rexova-Benkova L, Markovic O (1976) Pectic enzymes. *Adv Carbohydr Chem Biochem* 33:323–385
64. Robyt JF, French D (1970) The action pattern of porcine pancreatic α -amylase in relationship to the substrate binding site of the enzyme. *J Biol Chem* 10:3917–3927
65. Robyt JF, French D (1970) Multiple attack and polarity of action of porcine pancreatic α -amylase. *Arch Biochem Biophys* 138:662–670
66. Schieberle P, Grosch W, Kexel H, Schmidt H-L (1981) A study of oxygen isotope scrambling in the enzyme and non-enzymic oxidation of linoleic acid. *Biochim Biophys Acta* 666:322–326
67. Semeriva M, Desnuelle P (1979) Pancreatic lipase and colipase. An example of heterogeneous biocatalysis. *Adv Enzymol* 48:320–371
68. Slappendel S, Veldink GA, Vliegthart JFG, Aasa R, Malmström BG (1981) EPR spectroscopy of soybean lipoxygenase-1. Description and quantification of the high-spin Fe(III) signals. *Biochim Biophys Acta* 667:77–86
69. Solomon EI, Heppner DE, Johnston EM, Ginsbach JW, Cirera J, Qayyum M, Kieber-Emmons MT, Kjaergaard CH, Hadt RG, Li T (2014) Copper active sites in biology. *Chem Rev* 114:2659–3853
70. Storer AC, Carey PR (1985) Comparison of the kinetics and mechanism of the papain-catalyzed hydrolysis of esters and thiono esters. *Biochemistry* 24:6808–6818

71. Strothkamp KG, Jolley RL, Mason HS (1976) Quaternary structure of mushroom tyrosine. *Biochem Biophys Res Commun* 70:519–524
72. Takeda Y, Hizukuri S (1981) Re-examination of the action of sweet-potato beta-amylase on phosphorylated(1->4)- α -D-glucan. *Carbohydr Res* 89:174–178
73. Thoma JA, Spradin JE, Dygert S (1971) Plant and animal amylases. In: Boyer PO (ed) *The enzymes*, vol V, 3rd edn. Academic, New York
74. Tsujisaka Y, Okumura S, Iwai M (1977) Glyceride synthesis by four kinds of microbial lipase. *Biochim Biophys Acta* 489:415–422
75. Uhlig H (1998) *Industrial enzymes and their applications*. Wiley, New York
76. van Bastelaere PBM, Callens M, Vangrysperre WAE, Kersters-Hilderson HLM (1992) Binding characteristics of Mn^{2+} , Co^{2+} , and Mg^{2+} ions with several D-xylose isomerases. *Biochem J* 286:729–735
77. van Os CPA, Rike-Schider GPM, van Halbeek H, Verhagen J, Vliegthart JFG (1981) Double dioxygenation of arachidonic acid by soybean lipoxygenase-I. *Biochim Biophys Acta* 663:177–193
78. van Santen Y, Benen JAE, Schroter K-H, Kalk KH, Armand S, Visser J, Dijkstra BW (1999) 1.68-Å Crystal structure of endopolygalacturonase II from *Aspergillus niger* and identification of active site residues by site-directed mutagenesis. *J Biol Chem* 274:30474–30480
79. Verhagen J, Veldink GA, Egmond MR, Vliegthart FG, Boldingh J, van der Star J (1978) Steady-state kinetics of the anaerobic reaction of soybean lipoxygenase-1 with linoleic acid and 13-L-hydroperoxylinoleic acid. *Biochim Biophys Acta* 529:369–379
80. Vick BA, Zimmerman DC (1981) Lipoxygenase, hydroperoxide isomerase, and hydroperoxide cyclase in young cotton seedlings. *Plant Physiol* 67:92–97
81. Virador VM, Grajeda JPR, Blanco-Labra A, Mendiola-Olaya E, Smith GM, Moreno A, Whitaker JR (2010) Cloning, sequencing, purification, and crystal structure of Grenache (*Vitis vinifera*) polyphenol oxidase. *J Agric Food Chem* 58:1189–1201
82. Weibe MK, Bright HJ (1971) The glucose oxidase mechanism. *J Biol Chem* 246:2734–2744
83. Wells MA, DiRenzo NA (1983) Glyceride digestion. In: Boyer PD (ed) *The enzymes*, vol XVI, 3rd edn. Academic, New York
84. Whitlow M, Howard AJ, Finzel BC, Poulos TL, Winborne E, Gilliland GL (1991) A metal-mediated hydride shift mechanism for xylose isomerase based on the 1.6 Å *Streptomyces rubiginosus* structures with xylitol and D-xylose. *Proteins Struct Funct Genet* 9:153–173
85. Wilcox DE, Porras AG, Hwang YT, Lerch K, Winkler ME, Solomon EI (1985) Substrate analogue binding to the coupled binuclear copper active site in tyrosinase. *J Am Chem Soc* 107:4015–4027
86. Winkler ME, Lerch K, Solomon EI (1981) Competitive inhibitor binding to the binuclear copper active site in tyrosinase. *J Am Chem Soc* 103:7001–7003
87. Wohlfahrt G, Trivic S, Zeremski J, Pericin D, Leskovic V (2004) The chemical mechanism of action of glucose oxidase from *Aspergillus niger*. *Mol Cell Biochem* 260:69–83
88. Yoder MD, Lietzke SE, Jurnak F (1993) Unusual structural features in the parallel β -helix in pectate lyases. *Structure* 1:241–251
89. Yoon S, Klein BP (1979) Some properties of pea lipoxygenase isoenzymes. *J Agric Food Chem* 27: 955–962

Flavors

- 6.1 The Sensation of Taste – 265
- 6.2 The Mechanism of Taste Sensations – 266
- 6.3 Glutamate and Umami Receptor – 267
- 6.4 Taste Enhancers – 268
- 6.5 Odor: The Stereochemical Theory for Olfaction – 269
- 6.6 Character-Impact Compounds – 271
- 6.7 Odorant Receptors: Molecular Mechanism of Odor Recognition – 271

- 6.8 The Origin of Flavor – 272
 - 6.8.1 Biosynthesis – 272
 - 6.8.2 Chemical Reactions During Processing – 276

- 6.9 Beverage Flavor – 280
 - 6.9.1 Tea – 280
 - 6.9.2 Beer – 283
 - 6.9.3 Coffee – 285

- 6.10 Spice Flavor – 287
 - 6.10.1 Garlic and Onion – 287
 - 6.10.2 Black Pepper – 290
 - 6.10.3 Hot Pepper – 292
 - 6.10.4 Ginger – 293
 - 6.10.5 Peppermint – 293
 - 6.10.6 Cinnamon – 294

6.11 Fruits and Vegetables – 294

6.11.1 Fruit Flavor – 294

6.11.2 Vegetables – 298

6.12 Meat Flavor – 302

6.12.1 Simulated Meat Flavors – 305

6.13 Microencapsulation of Flavors – 305

References – 306

Flavor is the sensation produced by a material perceived principally by the senses of taste and smell. In certain cases, flavor also denotes the sum of the characteristics of the materials which produce the sensation. The primary role of flavor in food processing is to make the food palatable. Many food products may become unattractive for consumption without the supplementation of flavors, either unintentionally or intentionally. The use of flavors also adds variety to the diet and the functional and economic values of food products. The application of flavor technology depends often on the identification of the sensory active compounds. Most synthetic flavor compounds are imitates of the key flavor constituents of natural origin.

The biochemical and chemical reactions that generate the many characteristic flavors in food are extremely complex. There are about 4000 flavor compounds identified in approximately 200 types of fruits, spices, and other foods. Few detailed pathways are known, and many of these mechanisms are postulated from model studies. The structure-activity relationship of flavor compounds is an area of great interest for food applications.

6.1 The Sensation of Taste

Taste is a combination of chemical sensations perceived by the papillae of the tongue. There are five basic taste sensations: sourness, saltiness, sweetness, bitterness, and umami. Many substances do not have a single taste, but a complex sensation comprising more than one of the five basic components.

Sour taste is caused by hydrogen ions: acids, acid salts, and other substances that generate hydrogen ions in contact with water to give the sour taste. The threshold is about 0.002 *N* acid. Sour taste can also be induced by passing electric current through the tongue, presumably due to the hydrolysis of acid or water with the generation of hydrogen ions. Strong currents, however, induce a bitter taste. Some acid substances, for example, potassium acid oxalate and protocatechuic acid, stimulate both sour and bitter tastes.

Saltiness is stimulated by soluble salts. Most salts of high molecular weight are bitter rather than salty. Low-molecular-weight salts, notably chlorides of sodium, potassium, and calcium, are salty. The threshold level is 0.007–0.016% salt solution.

Sweetness of a substance is related to the functional groups that make up the glyco-phore units in a tripartite model. The molecular theory of sweet taste is well developed and will be discussed in ► Chap. 7.

Bitter compounds require a polar (electrophilic or nucleophilic) group and a hydrophobic group. The structure-activity relationship of bitter-tasting compounds has not been firmly established [4]. There are large numbers of bitter substances in plants, which are classified into alkaloids and glycosides.

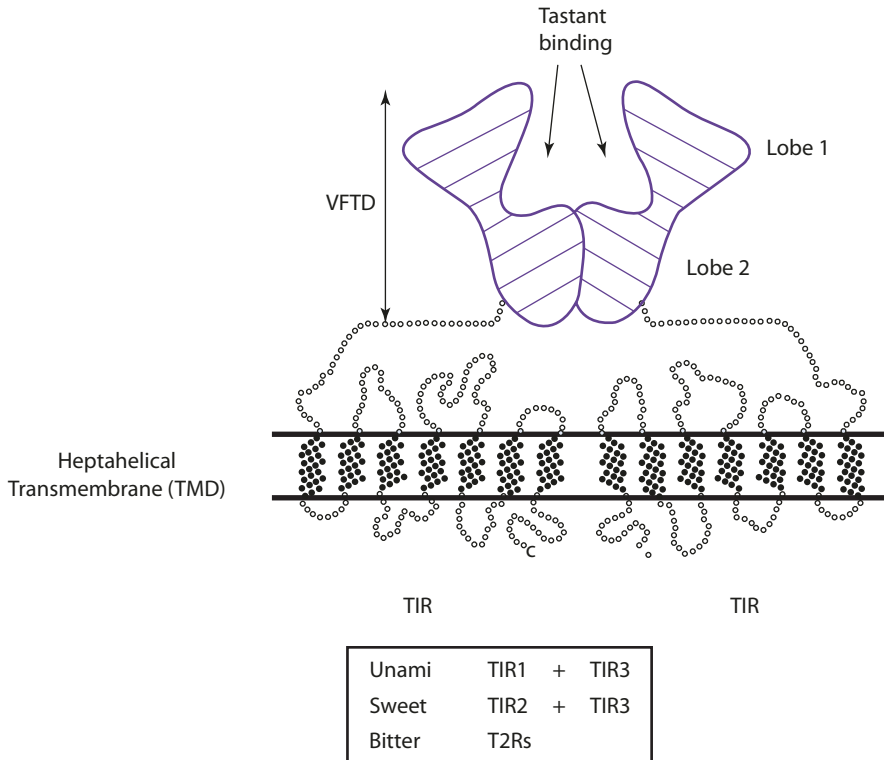
The fifth basic taste, umami, is a delicious savory taste sensation, relating to L-amino acids. The first umami amino acid, monosodium glutamate (MSG), was isolated from dashi (a fish) and seaweed in 1908. Several umami enhancers (potentiators) have been since discovered, including: IMP (inosine 5'-monophosphate) isolated from dried bonito tuna in 1914; and GMP (guanosine 5'-monophosphate) from shitake broth in 1960. A synergistic effect often occurs between glutamate and inosinate or guanylate. (Refer to section "Taste Enhancers".)

6.2 The Mechanism of Taste Sensations

During ingestion and chewing of foods, chemicals from the food enter the taste pores of taste buds on the tongue, where they interact with specialized epithelial cells, known as taste receptor cells (TRC). Each taste bud has 50–150 taste receptor cells, each of which consists of chemoreceptors that detect one of the five taste sensations. Binding of a food chemical (tastant) to a specific receptor triggers a reaction sending signals to the medulla in the brain. Two types of mechanisms are utilized in generating the basic sensations [11, 26].

1. Salty and sour sensations rely on the control of ion channels. Sodium chloride triggers taste cells when Na^+ ions enter through the ion channel. Accumulation of sodium ions causes depolarization allowing calcium ions (Ca^{2+}) entering the cell. The calcium ions in turn trigger the cell to release neurotransmitters. Repolarization occurs with potassium ions exiting the cell. For sour taste, the acid generates hydrogen ions (H^+) entering into the cell, blocking potassium ions (K^+) channels, or facilitating other positive ions entering the cell. The accumulation of positive ions/charges inside the cell (intracellular acidification) causes depolarization and release of neurotransmitters.
2. Bitter, sweet, and umami rely on a G protein-coupled receptor (GPCR) cascade systems (involving regulation by GTP, guanosine triphosphate) [2, 11]. Sequence comparison of all known GPCRs defines three families: (1) Family A GPCR is composed of rhodopsin and related receptors, including odorant receptors; (2) Family B is composed of receptors activated by large peptides, such as secretin and glucagon; and (3) Family C includes metabotropic glutamate receptors, some hormone receptors, as well as taste receptors. Relating to sweet and umami tastes, the GPCRs are membrane proteins of about 850 amino acids, carrying (1) a large N-terminal extracellular domain that resembles a venus flytrap (VFTD), which is the ligand (tastant) binding region, and (2) a transmembrane segment consisting of hydrophobic stretches, linked by (3) a cysteine-rich domain (■ Fig. 6.1). Two distinct families of taste receptors are known to exist. The taste receptor type 1 family comprises 3 members (T1R1, T1R2, and T1R3). These T1Rs assemble in combination to form heterodimers: (1) the T1R1 plus T1R3 heterodimer functions as the umami receptor; (2) the T1R2 plus T1R3 heteromer forms a sweet taste receptor (See ► Chap. 7). In contrast, the taste receptor type 2 family, which functions to recognize bitter substances, comprises about 35 highly divergent T2R members. These proteins contain 300–330 amino acids with a short N-terminal extracellular domain (without a Venus flytrap structure). Most T2Rs are expressed in the same TRCs, functioning as broadly tuned sensors for bitter chemicals.

Gustducin, the G-protein for the mechanism has been identified. The binding interaction between ligands (tastants, taste compounds) and receptors causes the dissociation of the subunits of gustducin and initiates a cascade of reactions in the release of neurotransmitters. Two hypotheses have been put forward to explain how taste information is processed. (1) The "labeled-line model" refers to a coding model in which the peripheral or central neurons that respond to a given taste stimulus carry the information to the brain in an individual pattern. Receptor cells are tuned to respond to single taste modalities, and are innervated by individually tuned nerve fibers. (2) The "across fiber pattern" refers to



■ **Fig. 6.1** Schematic representation of human taste receptors (From Assadi-Porter et al. [2] with permission. Copyright 2010 Elsevier)

ensemble coding in which the information about a taste stimulus is extracted by comparative activities across a neuron population or ensemble that responds with different intensity levels to multiple stimuli. Neurons activated in response to TRC activation are often broadly tuned. Each neuron cell type responds typically to more than one tastant with dissimilar taste qualities, but responds more strongly (higher intensity or activity) to one type of the basic taste stimuli. Taste discrimination will depend on the relative activity of different neuron types to multiple taste stimuli.

6.3 Glutamate and Umami Receptor

Only the L-form glutamate possesses umami activity, and dicarboxylates with four to seven carbons have been shown to have similar property. The pK_a of α -COOH, γ -COOH, and α -NH₂ in glutamic acid are 2.19, 4.25, and 9.67, respectively. At low pH, the free acid form is predominant and MSG becomes less soluble. MSG is prepared in monosodium form, and is most effective in food systems in the pH range of 5.5–8.0.

In the umami receptor, L-glutamate binds close to the hinge region formed by the two lobes in the VFTD of T1R1. In the active form, T1R1 is in the "closed" conformation and T1R3

is in the “open” conformation. In the T1R1 binding site, the glutamate α -carboxylate group maintains favorable interactions with the backbone NH group of Thr149 and Ser172, and the side chain OH of Ser148 and Thr149. The glutamate amino nitrogen maintains favorable interactions with the backbone oxygen of Ala170, the side chain oxygen of Ser172, and side chain carboxylate of Glu301. The γ -carboxylate of the glutamate molecule interacts with the backbone NH group of Arg277 and the side chain guanidium group of Arg151 and Arg277 [10].

6.4 Taste Enhancers

Purine ribonucleotides, such as inosine 5′ monophosphate (IMP) and guanosine 5′ monophosphate (GMP), are naturally occurring enhancers known to strongly potentiate the umami intensity by allosteric modulation.

Structurally, the binding site for the 5′-ribonucleotides (such as IMP, GMP) lies adjacent to the glutamate binding site close to the hinge opening of the VFTD of T1R1. The binding provides synergistic effect in activating the umami taste receptor via allosteric modulation [53]. It further stabilizes the closed conformation by coordinating the positively charged residues via their phosphate groups.

The enhancers MSG, IMP, and GMP are disodium salts at neutrality (■ Fig. 6.2). Only the 5′-nucleotides are active, although three possible isomers (2′, 3′, and 5′) can exist. GMP and IMP are produced by enzymatic degradation of yeast RNA, using 5′-phosphodiesterases. The products are usually an equal mixture of IMP and GMP. The threshold levels for the nucleotides are in the range of 0.01–0.03%. The threshold levels are greatly reduced when the nucleotides are combined synergistically with MSG (■ Table 6.1). Maximum flavor-enhancing activity is obtained when the nucleotide and MSG are in a 1:1 mix. Lower or higher ratio of mixing tends to reduce the effectiveness. GMP shows about four times the effectiveness in the synergistic action compared to IMP (■ Table 6.2) [24].

It has been postulated that the nucleotide interacts with its receptor at three sites. Sites A and B are electrophilic and interact with the two phosphoryl oxygens and the C6 oxygen, respectively. Site X interacts with the substituent at C2 [25]. The distance between sites A and B is about 8 Å. The flavor-enhancing activity depends on the electron density of the C6 oxygen. The site X interaction depends largely on the ability of delocalization of

■ Fig. 6.2 Nucleotide flavor potentiators

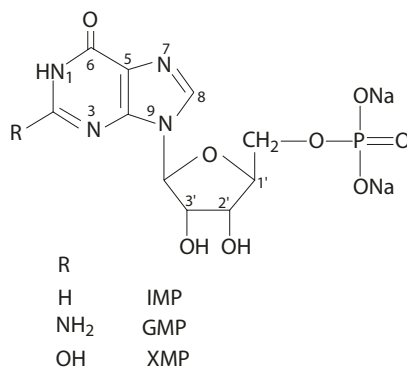


Table 6.1 Synergistic interaction between MSG and 5'-nucleotide in the reduction of individual threshold levels

	Threshold level (%)		
	IMP	GMP	MSG
Water	0.012	0.0035	0.03
0.1% MSG	0.0001	0.00003	—
0.01% IMP	—	—	0.002

From Kuninaka [24, 25]

Table 6.2 Flavor activity of mixtures of MSG and 5'-nucleotide

Mixture		Relative flavor activity per unit weight	
MSG	IMP OR GMP	IMP	GMP
1	0	1.0	1.0
1	1	7.5	30.0
10	1	5.0	19.0
20	1	3.4	12.4
50	1	2.5	6.4
100	1	2.0	5.5

From Kuninaka [24, 25]

the substituent at C2. Thus GMP, with the C2 substituent being NH_2 , has a comparatively higher activity than IMP. Association of the molecule with a receptor initiates an umami sensation, and simultaneously activates other receptors whose sensitivity for their respective flavor compounds are enhanced.

6.5 Odor: The Stereochemical Theory for Olfaction

In order to be odorous, a compound must be sufficiently volatile, and there has to be physical interactions between the odorous compound and the receptor site. Based on the relationship between odor and chemical structure of the odor compound [1], there are seven primary odors: camphoraceous, ethereal, musky, floral, minty, pungent, and putrid. For each class of these odorous compounds, there are receptor sites that are complementary to the size, shape, and electronic status of the molecule. The ethereal, camphoraceous, and musky odors depend primarily on the size of the molecule, and the floral and the minty depend on the shape, whereas pungent and putrid are caused by electrophilic and nucleophilic molecules, respectively. The minty structure also has an additional requirement of possessing, near the point of the wedge-shaped molecules, a group capable of

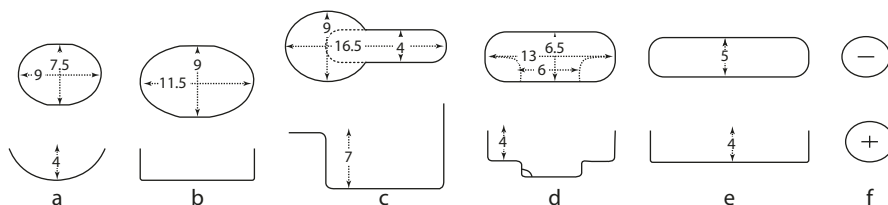


Fig. 6.3 Olfactory receptor sites: **a** Camphoraceous (δ -camphor, 2,3-dinitropentane, acetylenetetrabromide); **b** musky (androstan-3 α -ol, 3-methylcyclopentadecanone, undecyl- γ -butyrolactone); **c** floral (diphenylamine, geraniol, anisole); **d** minty (1-menthone, methyl 2,4-dimethylphenyl ketone, cyclopentanone); **e** ethereal (diethyl ether, ethylene, acetylenetetrabromide); and **f** pungent (electrophilic compounds, such as isocyanate, isothiocyanate, and chloraminel), and putrid (nucleophilic compounds such as mercaptan and amines) (From Amoore [1] with permission. Copyright 1964 John Wiley & Sons)

forming a hydrogen bond with the receptor site. The primary odors are perceived when there is a fit between a molecule and the corresponding receptor site, in a way similar to the lock-and-key mechanism (■ Fig. 6.3).

A compound can develop more than one primary odor if the molecule can fit more than one type of receptor site. For example, acetylene tetrabromide fits both sites for camphoraceous and ethereal. It is also possible for molecules to come together to fill a common site, giving complex odors. In short, a given complex odor is a mixture of the appropriate primary odors. The following are some examples of complex odors and their primary odor compounds.

Odor	Components (primary odor)
Almond	Camphoraceous, floral, minty
Lemon	Camphoraceous, floral, minty, pungent
Garlic	Ethereal, pungent, putrid
Rancid	Ethereal, minty, pungent

The molecular shape requirements are inadequate to explain the distinct odors exhibited by many small molecules. The use of electrophilic and nucleophilic properties to relate pungent and putrid recognizes, to a certain degree, the importance of a particular functional group in the molecule. The profile-functional group theory [3] postulates that while the shape and size of an odorous molecule is responsible for the quality of the odor, the functional group determines the orientation of the molecule at the receptor site. It has an important influence on the homogeneity of the orientation pattern and on the affinity of the interaction complex. Removal of the functional group changes the orientation pattern, resulting in randomness and decreased affinity in absorption to the receptor site. For example, the isochromene in ■ Fig. 6.3 has a musk odor, but substitution with a methyl group at positions causing steric hindrance of the functional ether oxygen results in the loss of odor. Replacing the oxygen with nitrogen decreases the intensity.

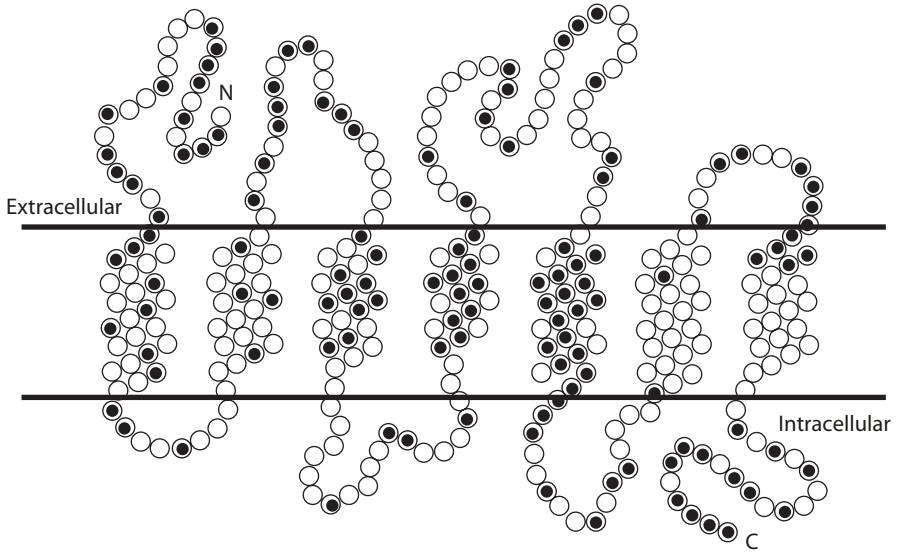
6.6 Character-Impact Compounds

A characteristic taste of a food can usually be related to a particular compound or a class of compounds. However, an odor is usually attributed to a combination of numerous volatile compounds, each of which individually smells very differently. The difference in the characteristics of certain odors is partially due to varying proportions of many widely distributed volatiles, such as esters, acids, alcohols, aldehydes, and ketones that occur in the food. These volatiles are called "contributing flavor compounds." However, some substances contain trace amounts of a few unique volatile compounds which possess the characteristic essence of the odor. These are called "character-impact compounds." Unfortunately, there are not very many character-impact compounds that have been identified. Nonetheless, the focus in this chapter will focus on unique compounds which contribute the most significant characteristic flavor to a particular food.

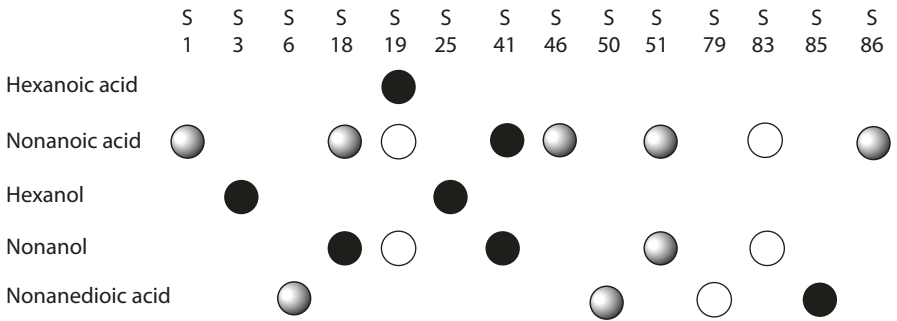
6.7 Odorant Receptors: Molecular Mechanism of Odor Recognition

With the advent of molecular biology techniques, it is now known that humans have about 500 (G-protein coupled) odorant receptors. The olfactory epithelium in the nasal cavity contains millions of olfactory sensory neurons, and each olfactory neuron expresses one odorant receptor (OR) gene. The number of OR genes amounts to roughly 1–5% of the total genes in the genome devoted to the detection of odorants. OR proteins belong to the superfamily of seven transmembrane domain proteins that interact with G proteins to generate intracellular signal transduction (GPCR) Family A. (Refer to section on "Chapter 7: Sweet Taste Receptors"). The primary structure of OR proteins contains 300–330 amino acids, with seven hydrophobic stretches of 19–26 amino acids that transverse the cell plasma membrane, linked by six loops (four extra- and three intracellular), which serve as binding sites of odorous chemicals (▶ Fig. 6.4) [8].

It has been estimated that humans can smell 10,000 and more chemicals as distinct odors. How can the binding interactions between ORs and odorous chemicals be transmitted and organized into a signal input? First, each OR can recognize multiple odorants. Second, each odorant is detected by multiple different ORs. Third, different odorants are recognized by different combinations of ORs. In summary, different odorants are encoded by different combinations of ORs, known as "receptor codes." Given the number of possible combinations of 500 different ORs in humans, this coding scheme would allow the detection and discrimination of an astronomical number of odorants [29]. ▶ Figure 6.5 illustrates the combination codes for a number of volatile compounds, clearly showing different odorants encoded by different combinations of receptors. The binding interactions of odors with OR proteins initiate a cascade of G-protein coupled signaling events propagated by olfactory neuron to the olfactory bulb of the brain. From there, the signals are relayed to the primary olfactory cortex, thereby allowing both perception of and physiological response to the odors.



■ Fig. 6.4 Schematic illustration of an odorant receptor protein showing it traversing the plasma membrane seven times with loops extending intra- and extracellularly. More variable amino acid residues are drawn in dotted circles (From Buck and Axel [8] with permission. Copyright 1991 Elsevier)



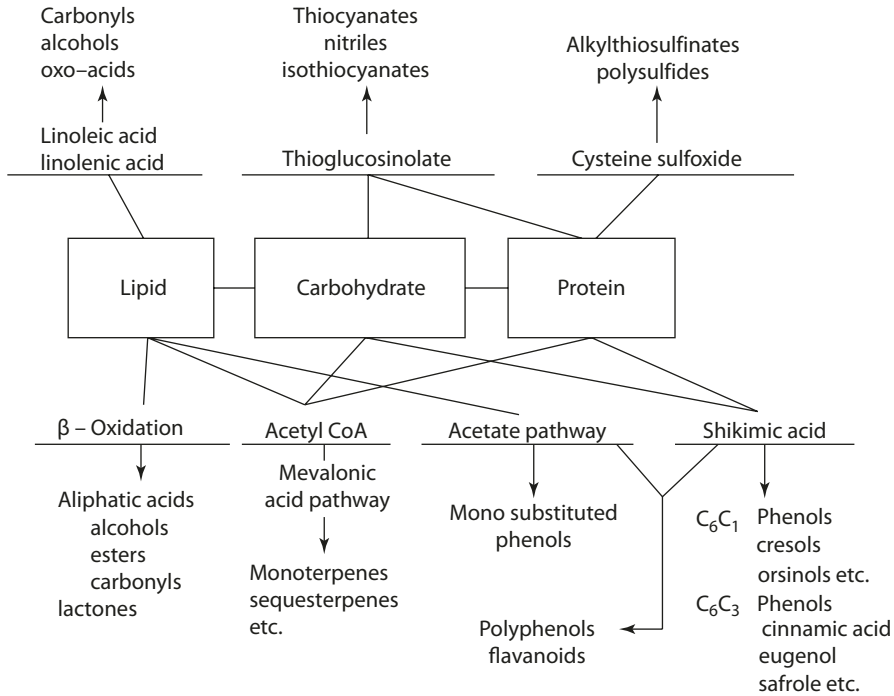
■ Fig. 6.5 The combinatorial profiles of individual odorant receptors in the recognition of odorants. Shade intensity reflect the level of response (Malnic et al. [29])

6.8 The Origin of Flavor

6.8.1 Biosynthesis

Many flavors, especially those in fruits and vegetables, are the products or byproducts of metabolic pathways. Schematically, the biosynthesis of these flavors is represented by

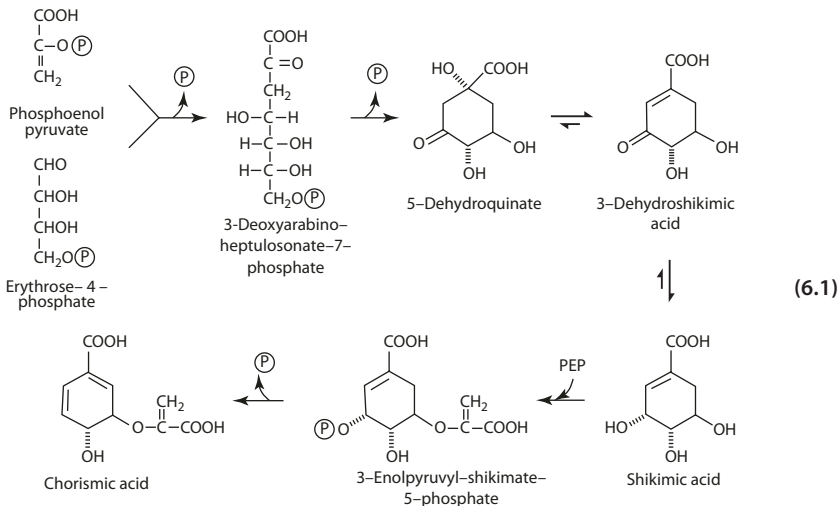
■ Fig. 6.6.



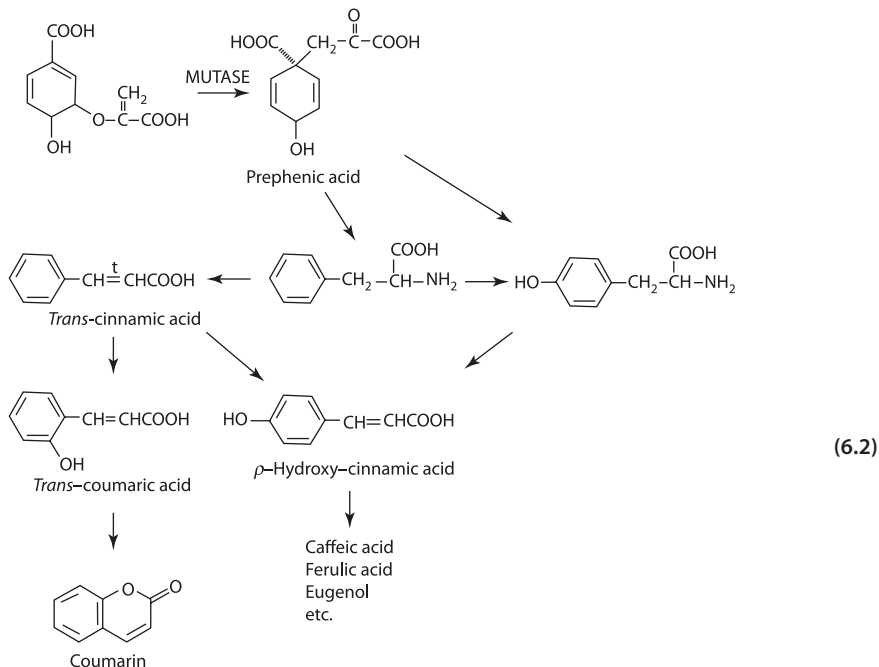
■ Fig. 6.6 Biosynthesis of flavor compounds

■ ■ The Shikimic Pathway

The initial step is the condensation of phosphoenolpyruvate, an intermediate from glycolysis, and erythrose-4-phosphate (from the pentose phosphate pathway). The C7 product cyclizes and undergoes further dehydration and reduction to yield shikimic acid. Condensation with a second molecule of phosphoenolpyruvate yields chorismic acid (Eq. 6.1).

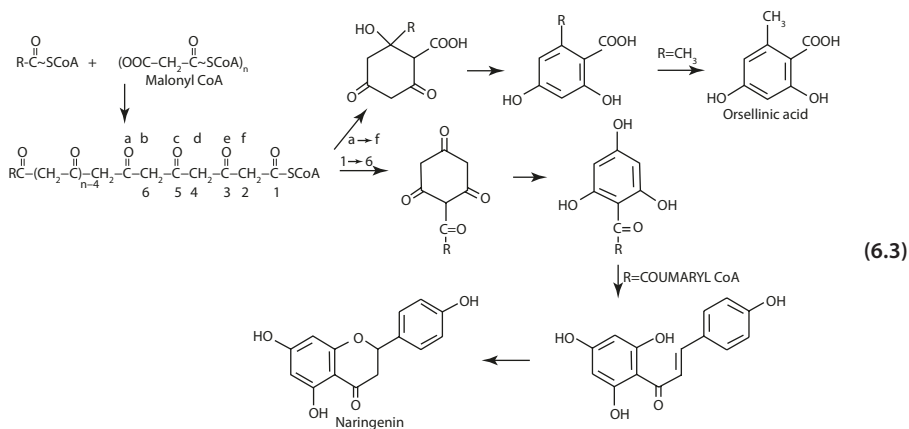


Chorismic acid is the precursor of the aromatic amino acids phenylalanine and tyrosine, which undergoes deamination to yield *trans*-cinnamic acid, the parent compound of many C6C3 phenolic compounds (Eq. 6.2)



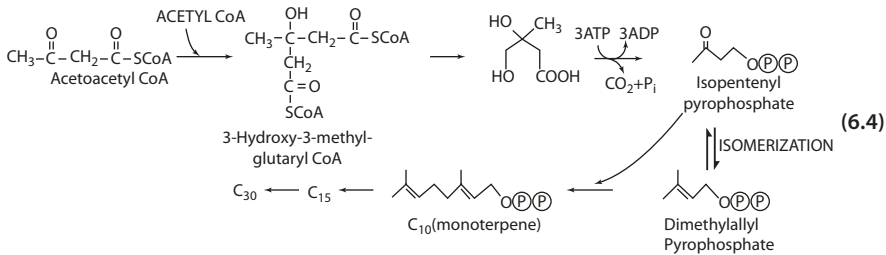
■ The Polyketide Pathway

The main reaction involves the addition of malonyl CoA to acyl CoA. Successive additions of malonyl CoA extend the chain to give a ketide unit, which then cyclizes to form various phenolic compounds (Eq. 6.3). All phenols synthesized via the polyketide pathway are meta-substituted.



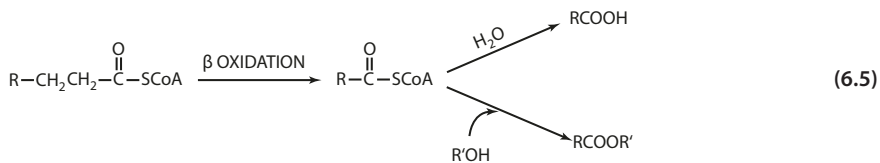
■ ■ The Isoprene Pathway

The isoprene pathway involves the condensation between acetyl CoA with the formation of mevalonic acid. Decarboxylation and phosphorylation of mevalonic acid gives isopentenyl pyrophosphate, which through self-condensation yields the terpenes (Eq. 6.4). Monoterpenes are usually volatile and odorous. Mevalonate is also the key intermediate in the synthesis of cholesterol.



■ ■ β -Oxidation

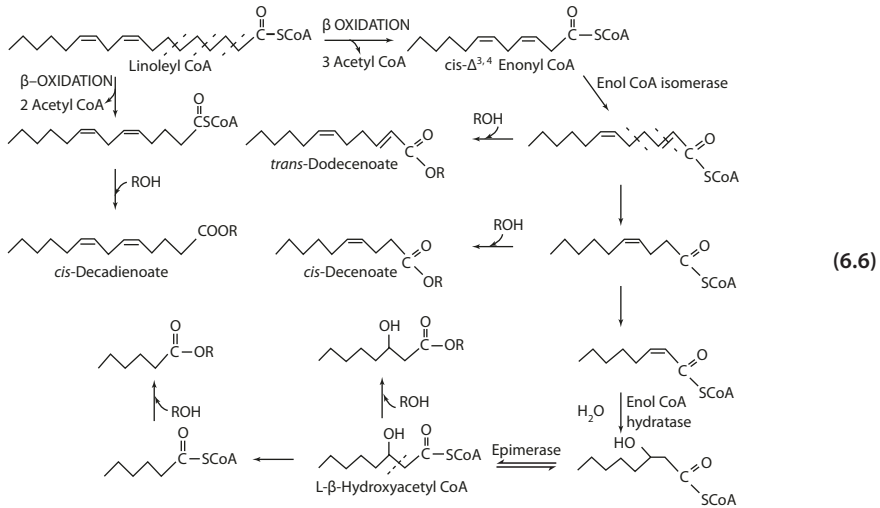
Saturated fatty acids are degraded to short acyl chains by the β -oxidation pathway, which involves the reaction sequence of oxidation, hydration, oxidation, and hydrolysis (Eq. 6.5). This pathway gives rise to many of the naturally occurring acids, esters, and lactones.



The oxidation of unsaturated fatty acids undergoes many reactions similar to those of saturated fatty acids. However, as is now well known, *cis*- Δ 3,4 enonyl CoA is not a substrate for acyl CoA dehydrogenase. The position and configuration of the *cis*- Δ 1,4 double bond must be isomerized in position and configuration. A similar rearrangement also occurs with the *cis*- Δ 2,3 double bond (Eq. 6.6). Unsaturated fatty acids are the precursors of numerous unsaturated esters, which characterize various flavors in many food systems.

■ ■ Lipoygenase and Lipase

In plant tissues, lipid hydroperoxides are both enzymatically formed and decomposed (refer to ► Chap. 5), yielding specific aldehydes and corresponding alcohols. For example, the characteristic flavor of cucumber is due to 2-nonenal and 2,6-nonadienal and their alcohols. In tomatoes, *cis*-2-hexenal and *cis*-3-hexenal contribute to the fresh flavor. The flavor of green beans is partly due to 2-hexenal and 1-octen-3-ol. Hydrolysis of milk fat in milk by lipase is responsible for the development of rancid flavor.

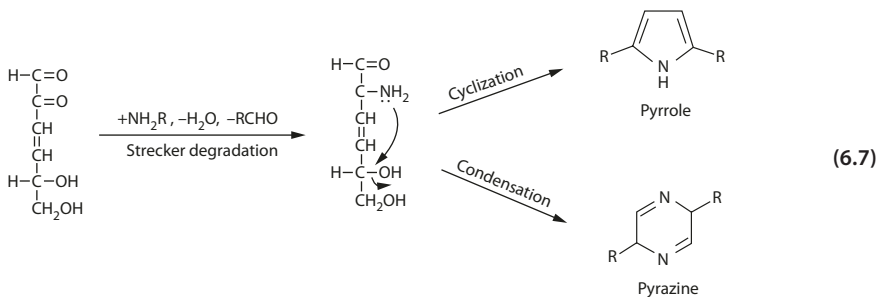


6.8.2 Chemical Reactions During Processing

The Maillard reaction occupies a unique position in the generation of flavor compounds in processed food products. The primary reactions have been described in ► Chap. 3 in connection with the chemistry of monosaccharides. Only the secondary reactions that are best understood and are significant in their contribution to flavors are presented here. Flavor products of the Maillard reaction include furans, pyrones, carbonyls, and acids from dehydration and/or fragmentation; and pyrroles, pyrazines, oxazoles, thiazoles, and sulfur compounds formed via the Strecker degradation, condensation, and further reactions. The reaction intermediates in the Maillard reaction that are responsible for generating flavor products are the dicarbonyl compounds. For simplicity, glucose is the aldohexose used in the following reaction schemes.

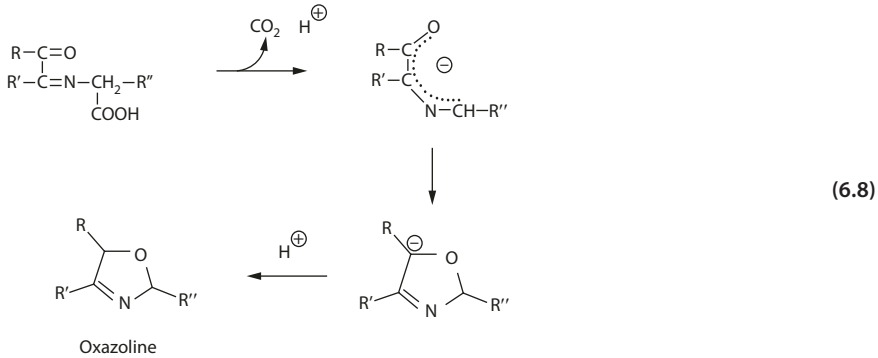
■ ■ Formation of Pyrrole and Pyrazine

The 3-deoxyglycosulose and the unsaturated glycosulos-3-ene formed by 1,2-enolization of the amadori compound produce furfurals, pyrroles, and pyrazine derivatives. Formation of the latter two types of compounds is due to the Strecker degradation, where the heterocyclic nitrogen is derived from the α -amino acid. Pyrroles are formed by cyclization of the aminocarbonyl product of Strecker degradation. Condensation of the aminocarbonyl compound followed by oxidation yields pyrazines (Eq. 6.7) [37].



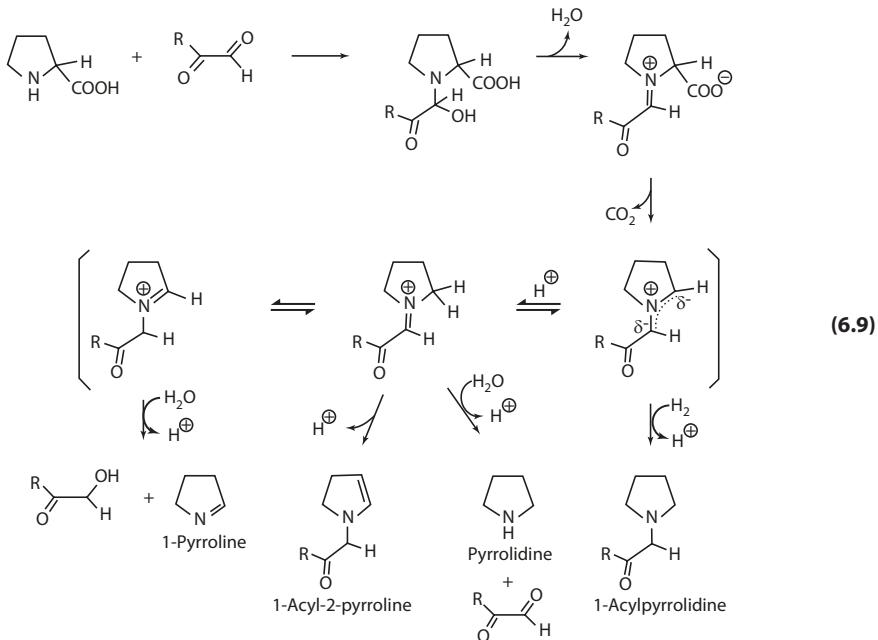
■ Oxazoles and Derivatives

Oxazoline formation is favored when, in the reaction in Eq. 6.8, cyclization occurs before hydrolysis of the Schiff base, followed by protonation of the resulting oxazolidine ion (Eq. 6.8) [36].

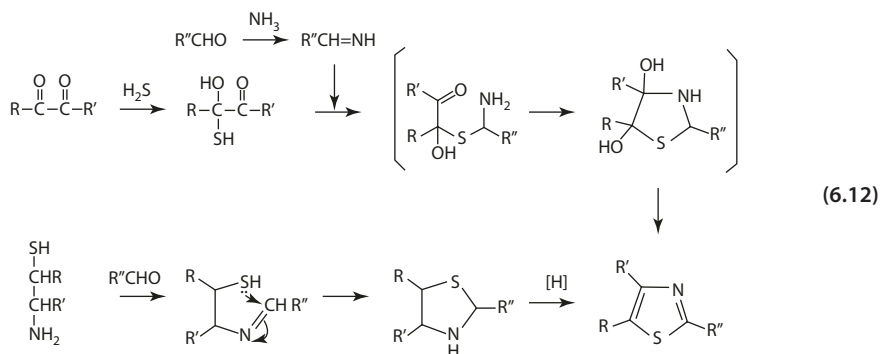


■ Pyrrolines and Pyrrolidines

Both pyrrolines and pyrrolidines form via the Strecker degradation of proline with a dicarbonyl compound. Condensation of the aldehyde and the secondary amine forms an iminium carboxylate intermediate that is transformed by decarboxylation into a reactive ylide or iminium ion [48]. Further hydrolysis yields pyrroline and pyrrolidine, while reduction yields *N*-acylpyrrolidine (Eq. 6.9).

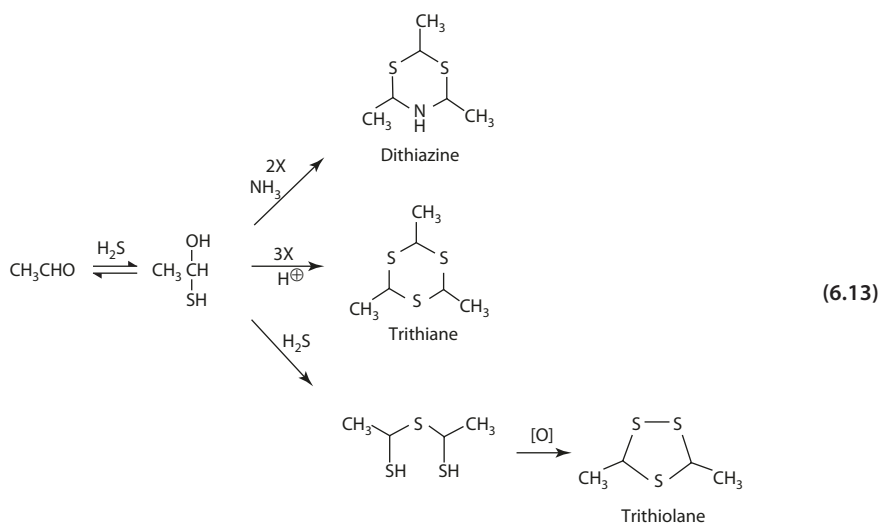


6.8 • The Origin of Flavor



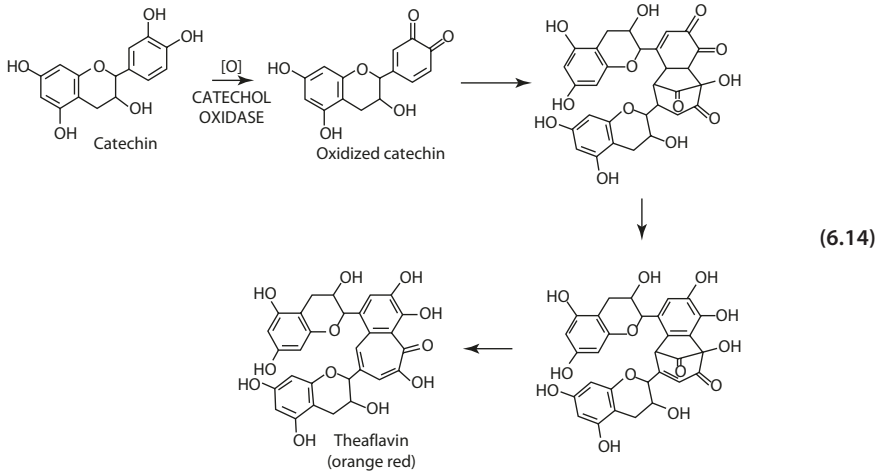
Polysulfide Heterocyclic Compounds

Cyclic polysulfide compounds are found in cooked meat products. The formation of these products may result from the reaction of H_2S with aldehyde and ammonia via condensation reactions (Eq. 6.13).



Lipid Degradation

Lipid degradation during food processing contributes a significant part in flavor formation, both desirable and undesirable. Numerous saturated and unsaturated acids, aldehydes, alcohols, ketones, esters, hydrocarbons, lactones, and aromatic compounds originate from the lipid constituents in food. These may be due to autoxidation, photosensitized oxidation, irradiation, thermal degradation, or enzymatic breakdown. All these processes have been covered ▶ Chaps. 2 and 5.

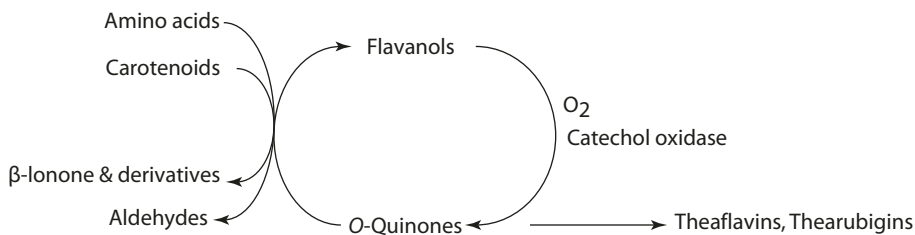


the relationship between various oxidative changes of carotenoids, lipids, amino acids, and glycoside precursor induced by the oxidation of tea flavanols [38].

The major volatile aroma compounds in tea are β -damascenone (fruity) and ionones (woody) and their epoxy derivatives (■ Fig. 6.9a). β -Damascenone is an essential odor in black tea infusion, derived from the enzymatic oxidation of neoxanthin. β -Ionone derived from the oxidation of β -carotene contributes significantly to green and black tea.

Fatty acid-derived volatiles include saturated and unsaturated C6 aldehydes and alcohols, such as *cis*-3-hexenol and *trans*-2-hexenal from α -linolenic acid, and *n*-hexanol from linoleic acid, which are known to contribute to the fresh green odor. Methyl jasmonate and its derivatives derived from α -linolenic impart the jasmine-like (floral, sweet) aroma in green and oolong tea (■ Fig. 6.9b).

During processing, the oxidized flavanols (the catechin quinones) react with amino acids to yield various aldehydes via the Strecker degradation. Isobutanal, 2-methylbutanal, isovaleraldehyde, and phenylacetaldehyde found to be present in fermented tea aroma are produced from the amino acids valine, isoleucine, leucine, and phenylalanine, respectively (Eq. 6.15).



■ Fig. 6.8 Oxidative changes induced by the oxidation of tea flavanols

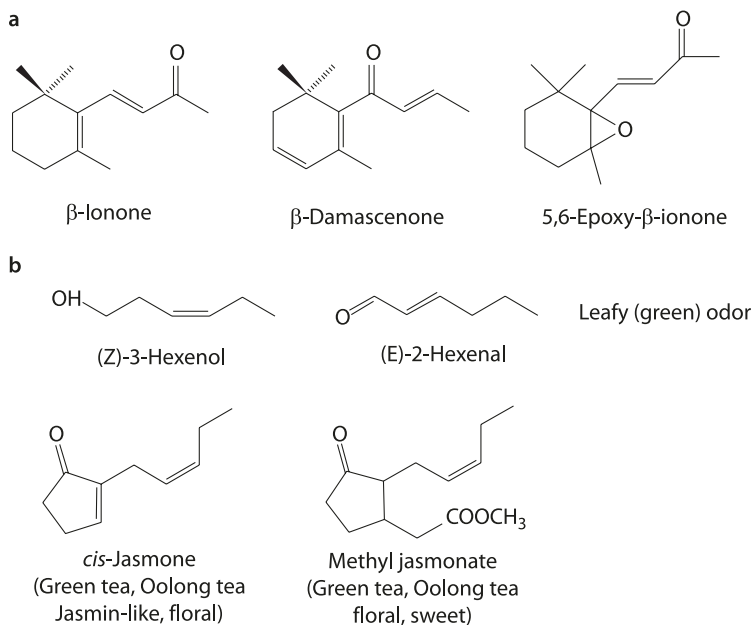
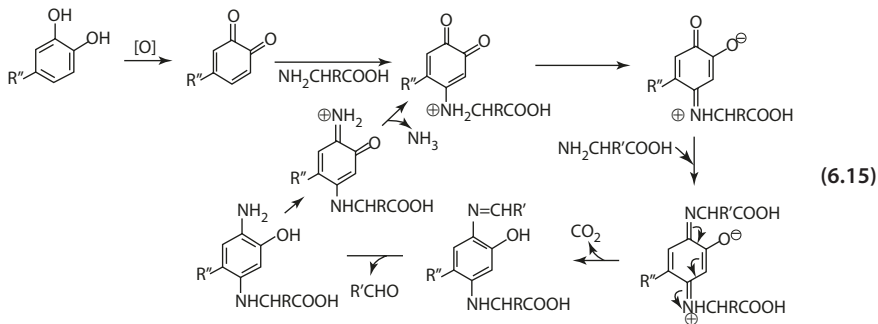
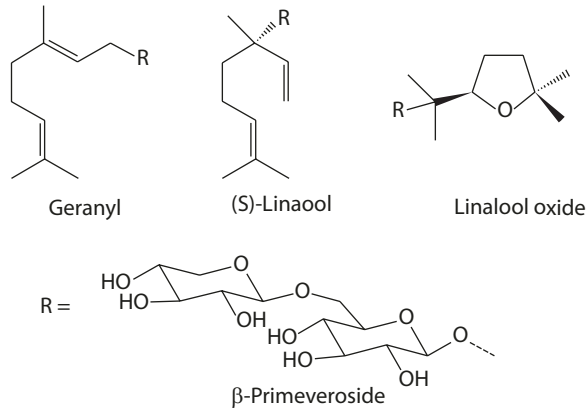


Fig. 6.9 Aroma compounds of tea derived from **a** carotenoids, and **b** lipids (Ho et al. [19])



Volatile compounds in tea occur not only in free forms, but some are derived from glycosidic precursors. The release of the free volatile compound from its glycosidic precursor requires the enzymatic action of glycosidases. The characteristic floral aroma of oolong and particularly black tea are due to the enzymatic release of geraniol (sweety green), linalool (floral, citrus like), and linalool oxides (sweet floral, fruity) from their glycoside precursors (Fig. 6.10).

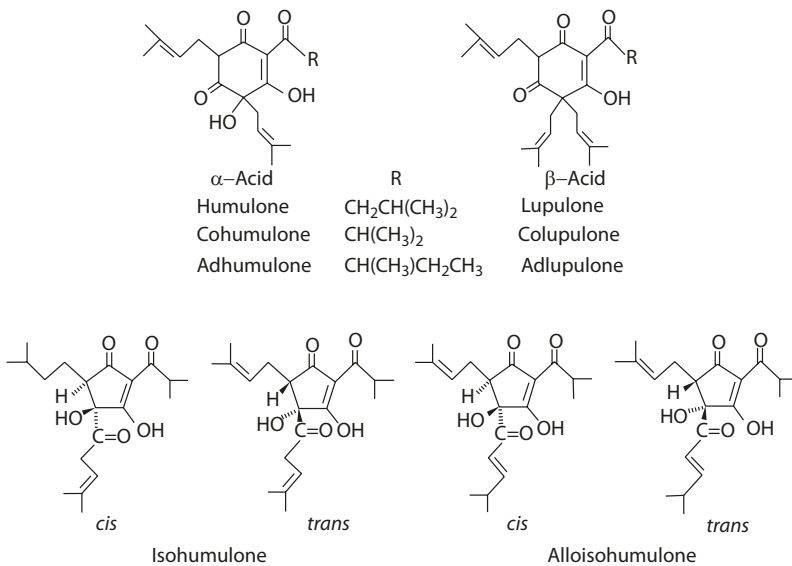
■ Fig. 6.10 Tea aroma compounds released from glycoside precursors



6.9.2 Beer

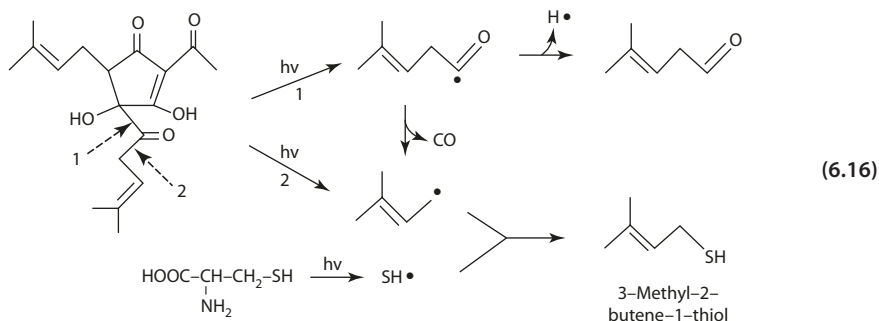
The characteristic bitter note in beer is ascribed to hop "resins." Hop resins are classified into soft (soluble in water) and hard (insoluble in hexane). Soft resins include α -acids (humulone, cohumulone, adhumulone) and β -acids (lupulone, colupulone, adlupulone) (■ Fig. 6.11).

In the brewing process, the α -acids isomerize into iso- α -acids, which possess a bitter taste. Isomerization of an α -acid produces two pairs of stereoisomers as indicated for humulone in ■ Fig. 6.11.



■ Fig. 6.11 α -Acids and β -acids in hop resins

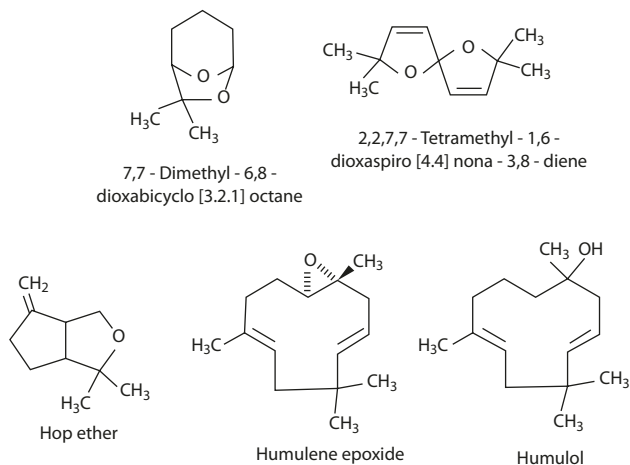
Beer, when exposed to sunlight, develops an unpleasant sulfur odor, termed "sun-struck" flavor. Its formation has been attributed to 2-methyl-2-butene-1-thiol, which is derived from the photolysis of hop-derived bitter iso- α -acids in the presence of sulfur-containing amino acids [17] (Eq. 6.16).



The characteristic hop flavor in beer is due to the transfer of some essential oil-derived compounds to beer. More than 100 aroma constituents have been identified, including esters, ketones, alcohols, ethers, terpenoids, and sesquiterpenoids. The cyclic esters and the oxygenated sesquiterpenoids are constituents with a strong hop aroma. The esters have predominantly bicyclic structures, and the sesquiterpenoids have either an epoxide or a hydroxyl constituent [47]. A few examples are given in

Fig. 6.12.

Fig. 6.12 Cyclic esters present in hop flavor

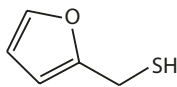


6.9.3 Coffee

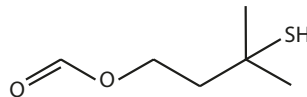
More than 1000 compounds have been identified in roasted coffee. The aroma in roasted ground coffee is derived from a complex collection of many volatile compounds. The potent ones include: (1) sulfur-containing compounds, (2) alkyl pyrazines, (3) furanones, (4) aldehydes and dicarbonyls, and (5) phenolics. The chemical structures of some examples are presented in [Fig. 6.13](#). In coffee brews, the aroma change (from that of the roasted ground coffee) is caused by a shift in the concentrations of the odorants due to hot water extraction and not by the appearance of new potent odorants.

The significant contributions of sulfur-substituted furans have been characterized in green and roasted coffee. The compound 2-furylmethanethiol (2-furfurylthiol) has long been considered a character-impact compound of roasted coffee [45]. The threshold is 0.01 ppb in water, and at concentrations of 0.1–5 ppb, the compound has the aroma of roasted coffee. At increasing concentrations (as occurred during storage of roasted coffee beans), it develops a strong sulfur odor.

Sulfur-containing

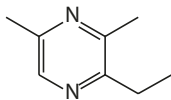


2-furfurylthiol
(roasted coffee)



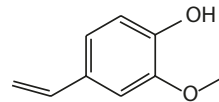
3-mercapto-3-methylbutylformate
(catty, roasted)

Pyrazines



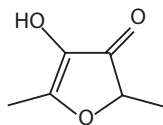
3-ethyl-3,5-dimethylpyrazine
(earthy, roasted)

Phenolics



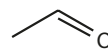
4-vinylguaiacol
(spicy, smoky)

Furans



4-hydroxy-2,5-dimethyl-3(2H)-
furanone (furanol)
(caramel-like, sweet)

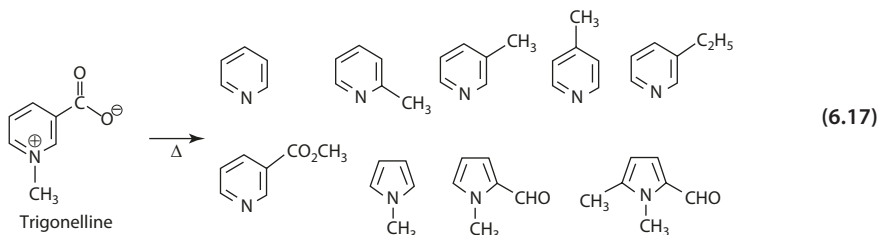
Aldehydes



acetaldehyde
(fruity, pungent)

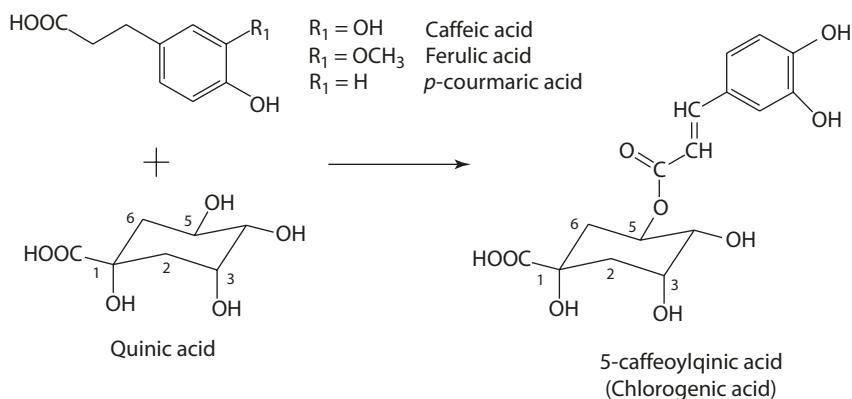
Fig. 6.13 Some volatile compounds in roasted coffee

Nonvolatiles may also be important contributors to the flavor of coffee beverages after roasting. The compound worth mentioning is trigonelline, which is present at a 1% level in coffee beans. Unlike caffeine, which is thermally stable, trigonelline decomposes readily at roasting temperatures to give a series of aroma compounds, pyridines and pyrroles [5] (Eq. 6.17).



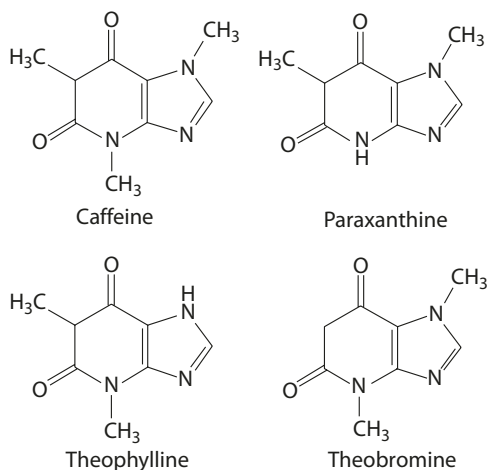
The "acid" flavor in coffee is caused by the presence of organic acids. Phenolic acids, in particular, average about 7.5% total dry weight in coffee beans. The major phenolic acids belong to a family of chlorogenic acids (■ Fig. 6.14), which are esters formed between cinnamic acids (caffeic, ferulic, *p*-coumaric) with quinic acid. Esterification may occur at the hydroxyl groups at C3, C4, and C5. Diesters are also formed. The most abundant chlorogenic acid in coffee beans is 5-caffeoylquinic acid (commonly called chlorogenic acid). Chlorogenic acid confers astringent, bitter, and acid flavors to the coffee brew.

Aside from taste and smell, the most attractive ingredient is caffeine, a methylxanthine with bitter characteristics. Caffeine acts as a stimulant by binding to and blocking the



■ Fig. 6.14 Phenolic compounds contributing to the "acid" flavor of coffee

■ Fig. 6.15 Caffeine and its metabolites



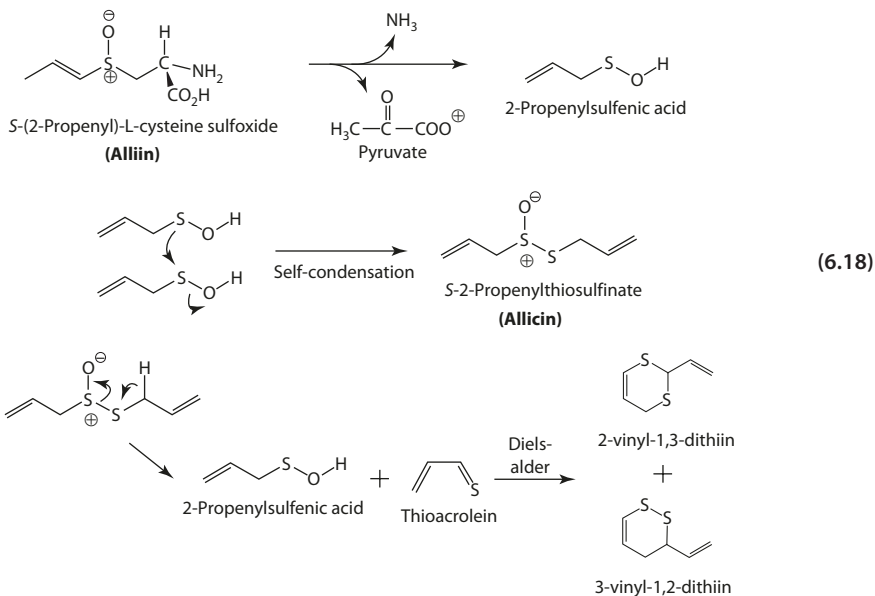
adenosine receptors from interactions involved in nerve cell activities in the brain and the heart. The primary metabolites of caffeine include paraxanthine, theophylline, and theobromine, each of which has its own physiological effects on the body (■ Fig. 6.15).

6.10 Spice Flavor

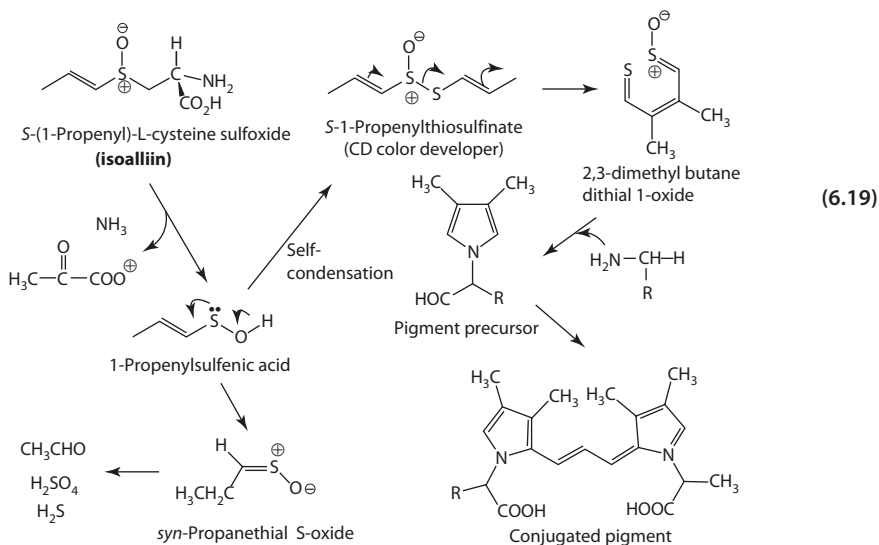
In food processing, spices are often applied in the form of essential oils or oleoresins. Essential oils are prepared by water and steam distillation of the dried ground spices. The oil contains the volatile flavor compounds. Oleoresins are extracts of freshly ground spices. The ground spice is repeatedly extracted with an organic solvent that is eventually removed to give a product that consists of volatile essential oil, nonvolatile resinous materials, and the active principle characteristics of the spice.

6.10.1 Garlic and Onion

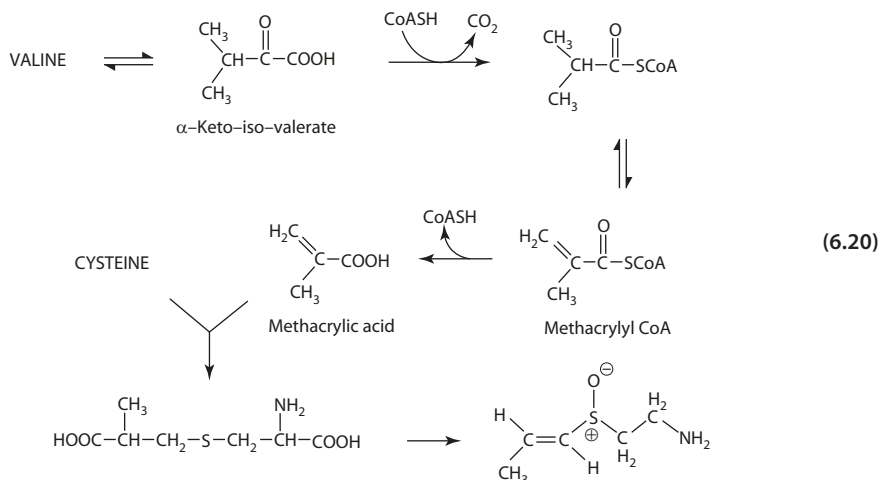
The odor of garlic is derived from *S*-2-propenylthiosulfinate (allicin). The odor develops only when the garlic is cut or crushed. The enzyme alliinase (EC 4.4.1.4, pyridoxal 5'-phosphate dependent α,β -eliminating lyase) present in the cell vacuole comes in contact with the odorless substrate, *S*-(2-propenyl)-*L*-cysteine sulfoxide (alliin) in the cytosol. The resulting product is 2-propenesulfenic acid (Eq. 6.18.1), which then dimerizes (self-condensation) to form allicin (Eq. 6.18.2). Allicin readily decomposes to 2-propenesulfenic acid and thioacrolein. The latter self-condenses via a Diels-Alder reaction to form cyclic sulfur compounds (Eq. 6.18.3) [5, 6].



In onion, the precursor is *S*-(1-propenyl)-L-cysteine sulfoxide (isoalliin), a positional isomer of alliin. Garlic also contains isoalliin as a minor metabolite, but with increased concentration upon storage. The alliinase in onion converts isoalliin into 1-propenylsulfenic acid, which rearranges to form *syn*-propanethial-*S*-oxide, the lacrimatory factor that causes the eye to tear. The oxide readily hydrolyzes to yield propionaldehyde and hydrogen sulfide (Eq. 6.19). The 1-propenylsulfenic acid can also dimerize to form *S*-1-propenylthiosulfinate, a key compound involved in allium discoloration (Eq. 6.19).



The flavor precursor, *S*-(1-propenyl)cysteine sulfoxide, is biosynthetically derived from valine and cysteine (Eq. 6.20). In nature, as much as half of the precursor is bound as a peptide, γ -L-glutamyl-*S*-allylcysteine sulfoxide. The peptide is not susceptible to the action of alliinase. The enzyme γ -glutamyl transpeptidase is required for the formation of the alk(en)yl cysteine sulfoxide.

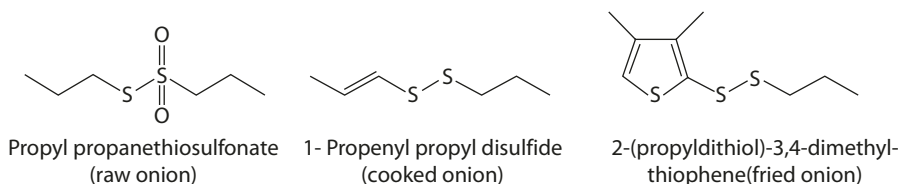


Many other compounds, including sulfides (mono-, di-, tri-, and tetra-), thiophenes, and thiosulfonates, found in the essential oils also contribute to the flavor [7]. Disulfides and thiosulfonates are formed by disproportionation of the unstable thiosulfinate (allicin is an alkenyl thiosulfinate) (Eq. 6.21). Thiosulfonates with four or more carbon atoms possess the distinct odor of freshly cut onions. Propyl and propenyl di- and tri-sulfides possess cooked-onion flavor.

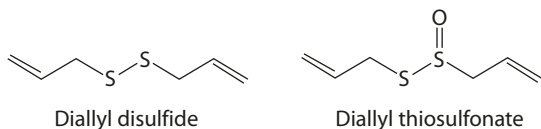


The character-impact compounds of onion and garlic are primarily sulfur-containing molecules (■ Fig. 6.16). In raw, fresh onion, the aroma contributors are propyl propanethiosulfinate, propenyl propanethiosulfinate, thiopropanal *S*-oxide, and propyl methanethiosulfinate. For cooked onion, dipropyl disulfide and 1-propenyl propyl disulfide are the potent aroma compounds. The distinct fried onion aroma is characterized by 2-(propyldithiol)-3,4-dimethylthiophene with a threshold of 10–50 ppm in water. For garlic, di-2-propenyl disulfide and the corresponding diallylthiosulfinate (allicin) are character-impact compounds. Thiophenes are formed, along with mono- and tri-sulfides, from the decomposition of alkyl and alkenyl disulfides (Eq. 6.22).

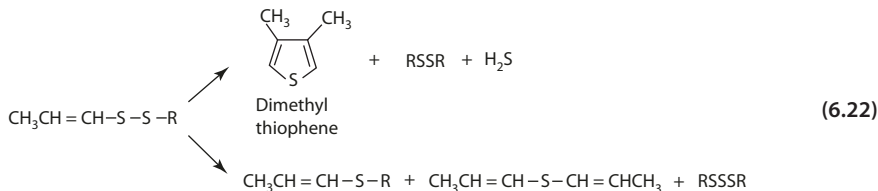
a Character-impact aroma compounds of onion



b Character-impact aroma compounds of garlic



■ Fig. 6.16 Some character-impact compounds of onion and garlic



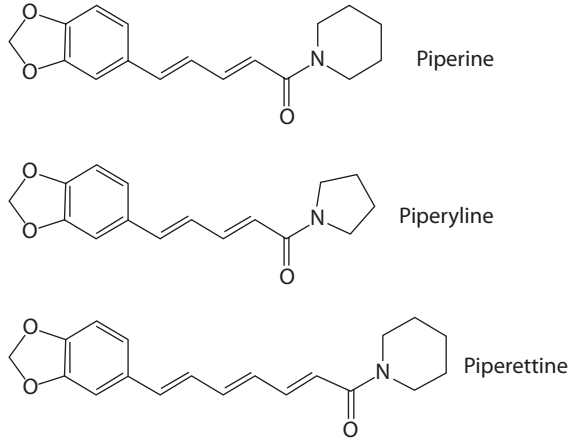
Discoloration in processed garlic and onion, such as maceration in the production of powder, puree, or paste, occurs slowly when in storage, and more quickly at low temperature and acidic pH. The development of pink-red color (pinkening or reddening) in onion and green-blue color (greening) in garlic involves mainly 1-propenyl-containing thiosulfonates (such as S-1-propenylthiosulfonate) (Eq. 6.19). The thiosulfonate reacts with amino acids to form pyrrole compounds, as pigment precursors [21].

The pigment precursor molecules are crosslinked by reacting with carbonyl compounds (such as pyruvate, formaldehyde, acetaldehyde, propionaldehyde, acrolein, allacin, etc.). The colored pigment may be di, tri, tetra, and polypyrrole compounds. The color depends on (1) the structure of the 1-propenyl-containing thiosulfonate, (2) structure of the amino acid side groups, (3) the carbonyl compound, and (3) the degree of oligomeric crosslink.

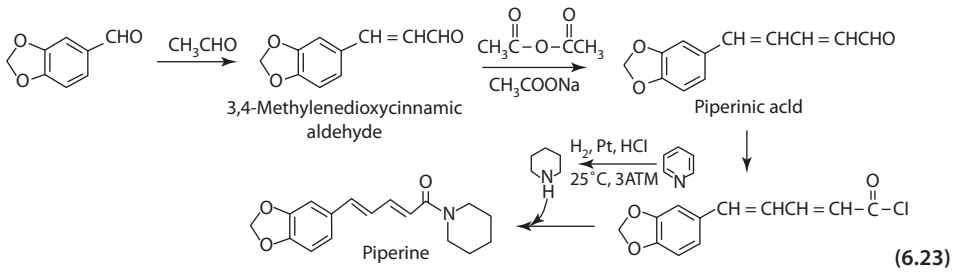
6.10.2 Black Pepper

Pepper (*Piper nigrum* L.) oleoresin contains the pungent alkaloid piperine: 5-(3,4-methylenedioxyphenyl)-2,4-*trans,trans*-pentadienoic acid. Geomeric isomers of piperine are found to be present; however, only the *trans, trans*-piperine has a strong pungent taste. Other piperamides, such as piperlyne and piperettine, with higher threshold concentrations for pungency have also been identified (■ Fig. 6.17). On average, the total piperamide content (40–50 mg/100 g) of peppers consists of 84% piperines and 16% other piperamides [13].

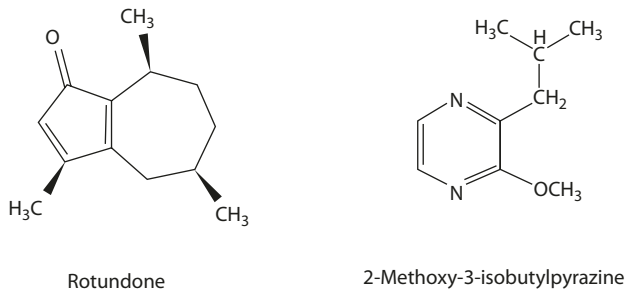
■ Fig. 6.17 Piperines and piperamides



Piperine can be synthesized by the aldol condensation of piperonal with acetaldehyde. Further reaction with acetic anhydride yields piperinic acid, which then reacts with an acid chloride to yield the piperine [16] (Eq. 6.23).



Rotundone, a sesquiterpene, has been identified as a character-impact compound with a strong, spicy peppery aroma (■ Fig. 6.18). Its concentration reaches 1.2 ppm and 2.0 ppm in black and white pepper, respectively [40].



(3S,5R,8S)-3,8-Dimethyl-5-prop-1-en-2-yl-3,4,5,6,7,8-hexahydro-2H-azulen-1-one

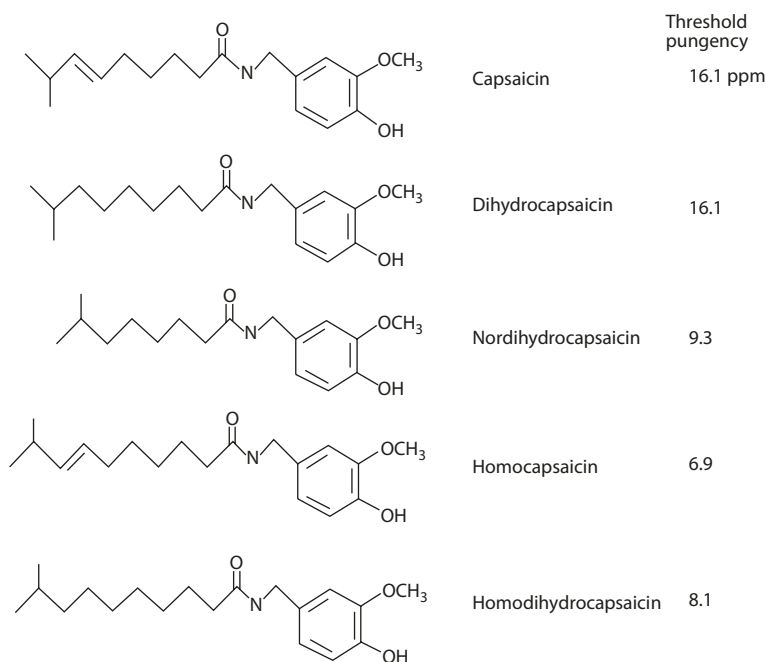
■ Fig. 6.18 Character-impact aroma compounds of pepper

6.10.3 Hot Pepper

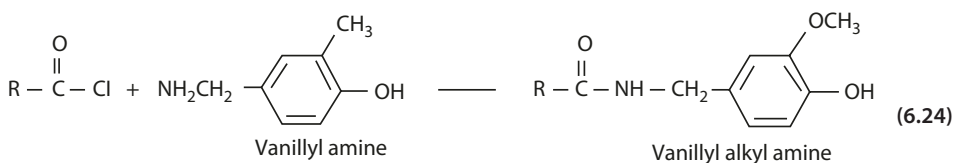
Mild and hot peppers belong to the genus *Capsicum*. The common domesticated species include: *C. annuum* (cayenne or red chili pepper, jalapeno), *C. chinense* (habanero or yellow-lantern chili), and *C. frutescens* (variety tabasco). Bell peppers, also belong to *C. annuum*, but do not have the "hot" taste associated with hot peppers.

The "hot" taste is due to the presence of the nonvolatile compound capsaicin, which is attributed mainly to a class of alkaloid compound collectively known as capsaicinoids [44] (■ Fig. 6.19). Synthetically, capsaicinoids can be made by reacting vanillyl amide with an acid chloride (Eq. 6.24).

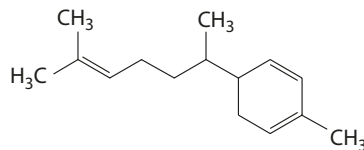
The aroma profiles of both red chili pepper and green bell pepper suggest that 2-isobutyl-3-methoxy-pyrazine process a characteristic pepper-like note, with a very low detection threshold of 2 ppt in water (■ Fig. 6.18) [9]. 2-Heptanethiol has also been identified to produce bell pepper-like smell, with thresholds of 3 ppm [41].



■ Fig. 6.19 Capsaicinoids and their pungency thresholds



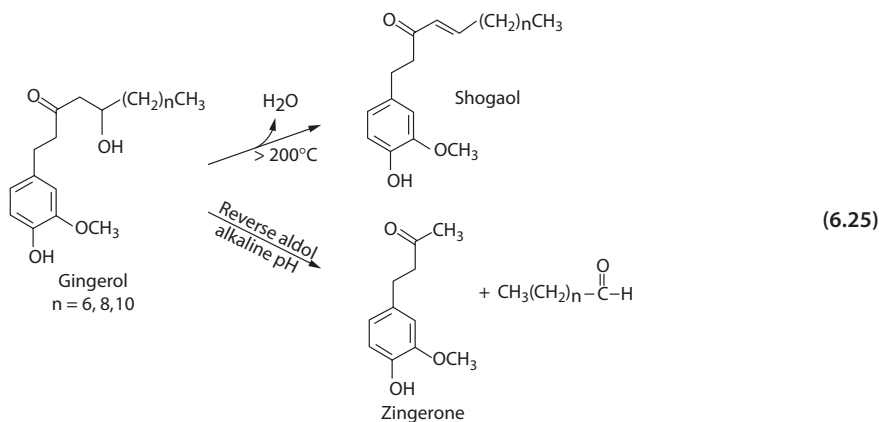
■ Fig. 6.20 Zingiberene



6.10.4 Ginger

Ginger (*Zingiber officinale* Roscoe) is a fibrous-rooted perennial plant. The oil and oleoresin are obtained from the rhizome. The essential oil is made up largely of terpenoids (4% monoterpenes, 63% sesquiterpenes, and 17% of terpene alcohols). Zingiberene is the most abundant sesquiterpene, making up to 30% of the root's essential oil (■ Fig. 6.20).

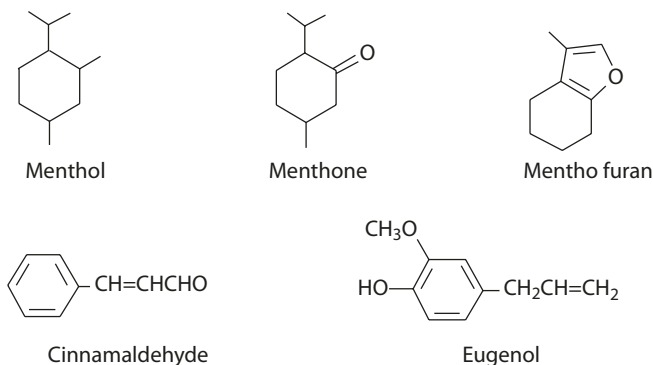
The pungent substance in the ginger oleoresin is gingerol, with the amount present in older ginger twice that in green ginger. The aliphatic chain in the structure may range from 6, 8, 10 carbons, but [6]-gingerol is the major form. Gingerols are thermally labile due to the presence of a β -hydroxy-keto function. Gingerol undergoes dehydration to shogaol or reverse aldol reaction to zingerone and aldehyde (Eq. 6.25). The former reaction is accelerated by alkaline pH, and the latter reaction occurs at a high temperature [12]. Both zingerone and shogaol are less pungent than gingerol. The aliphatic aldehyde causes the formation of off-flavors. These undesirable changes occur rarely in fresh ginger but more often in preparing and storing the oleoresin.



6.10.5 Peppermint

Peppermint oil is obtained from *Mentha piperita* plants. The important aroma constituents are the monocyclic monoterpenoids, menthol (50–60%), and to a lesser extent, menthone and menthofuran (■ Fig. 6.21).

Fig. 6.21 Flavor compounds in peppermint and cinnamon



6

6.10.6 Cinnamon

The spice cinnamon is obtained from commercial species *Cinnamomun cassia* (China) and *C. zeylanicum* Blume (Ceylon). The traditional commercial cinnamon is the “quills” – rolled pieces of peeled bark. Essential oils are produced by distillation of bark oil or leaf oil. Cinnamaldehyde and eugenol are two main flavor compounds in the oil (■ Fig. 6.21).

6.11 Fruits and Vegetables

The most important category of flavor ingredients obtained from fruits, especially citrus, is included in the essential oils. An essential oil is an oil substance obtained from a plant material, and it retains the characteristic flavor of that material.

There are two common processes for the production of essential oils of citrus fruits. Most of the oil is found in the rind of the fruit. Citrus fruits that contain high concentrations of essential oil (>3%) include orange, lemon, lime, tangerine, mandarin, and grapefruit. Commercially, the oil is obtained as a byproduct of fruit juice production. When juice is pressed from the fruit, the oil is also carried through. It is removed by centrifugation and becomes what is known as cold-pressed peel oil. The essential oils used in industry are the distilled oil obtained as a by-product of various types of essence recovery processes.

The natural essence of citrus fruits is obtained when the fruit juice is concentrated in high-temperature evaporators. Approximately 25% of the juice water is removed. The volatile flavors carried in the vapor are recovered and concentrated in the essence units (fractionation stills with condensers). The flavor components collected are separable into an aqueous (aroma) and oil phase (essential oil). Essence is a common name that includes fractions of both aroma and essence oil. Since essence oil is distilled oil, it lacks the non-volatile components and, therefore, many natural antioxidants found in cold-pressed oils. For this reason, essence oil is relatively less stable than cold-pressed oil.

6.11.1 Fruit Flavor

Citrus essential oils consist mainly of aldehydes, ketones, esters, alcohols, and acids (■ Table 6.3). Many of these are isoprenoids, with smaller amount of phenylpropanoids or short-chain aliphatics and their derivatives.

Table 6.3 Components of orange (valencia) oil

Compound	Concentration
Ethanol	0.1%
Ethyl acetate	50 ppm
Acetal	20 ppm
Hexanal	200 ppm
Ethyl butyrate	0.1%
<i>Trans</i> -2-hexenal	50 ppm
α -Pinene	0.4%
Sabinene	0.4%
Myrcene	1.8%
Octanal	0.5%
δ -Limonene	93.6%
Linalool	0.5%
Decanal	0.6%
Neral	0.2%
Geranial	0.1%
Valencene	1.7%

From Johnson and Vora [22]

The cyclic terpene δ -limonene is one of the abundant constituents (~90%) present in oranges and other citrus oils. It possesses the flavor characteristic of lemon, orange, and caraway [22]. Another major sesquiterpene present in orange oil is valencene (1–2%). Nootkatone, the character-impact compound of grapefruit, is chemically synthesized from valencene (Fig. 6.22). Another compound, α -*p*-menthene-8-thiol, has been

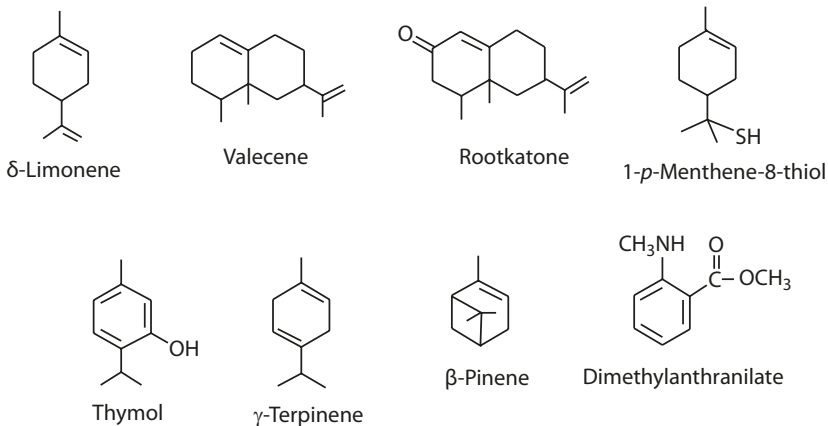


Fig. 6.22 Isoprenoids in fruit flavor

Table 6.4 Major components of tangerine and mandarin oil

Component	Tangerine oil (WT%)	Mandarin oil (WT%)
Thymol	0.022	0.182
Methyl- <i>N</i> -methylanthranilate	0.072	0.652
γ -Terpinene	1.74	14.0
β -Pinene	0.17	1.8

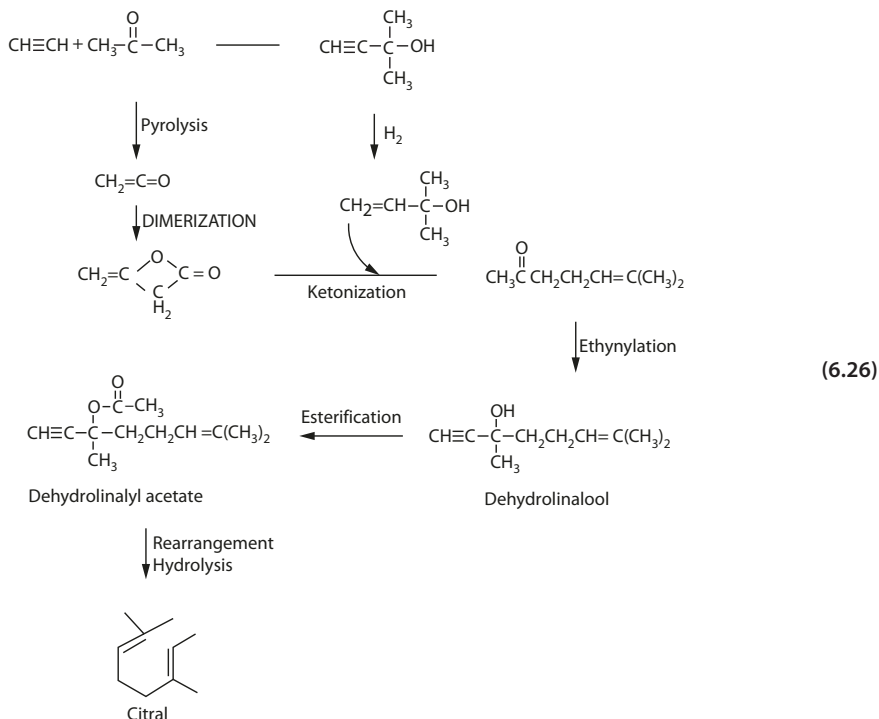
From Wilson and Shaw [51]

6

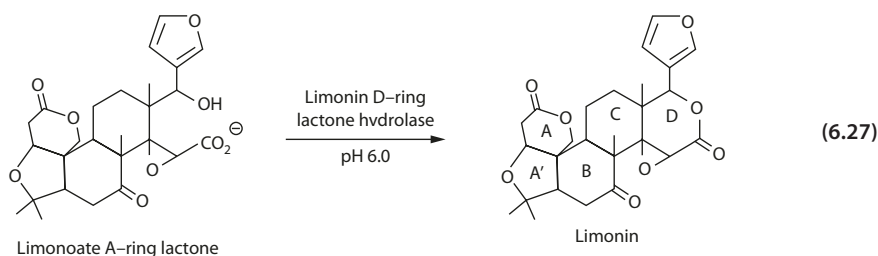
isolated which also displays a character aroma of fresh grapefruit juice. Its flavor threshold is in the range of 1×10^{-4} ppb in water, among the lowest detection thresholds for naturally occurring flavor compounds [14].

Essential oils of tangerine and mandarin contain thymol, dimethylantranilate, γ -terpinene, and β -pinene (Table 6.4). The latter two compounds are shown to contribute to the flavor of mandarin oranges as distinct from other oranges [51].

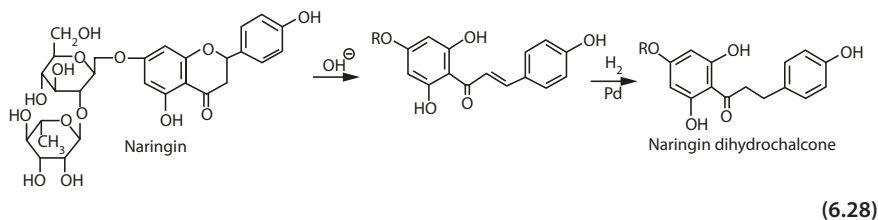
Citral, a terpene aldehyde with a powerful lemon flavor, is present in the essential oils of lemon, lemon grass, and lime. Citral is commercially synthesized from acetylene and acetone (Eq. 6.26).



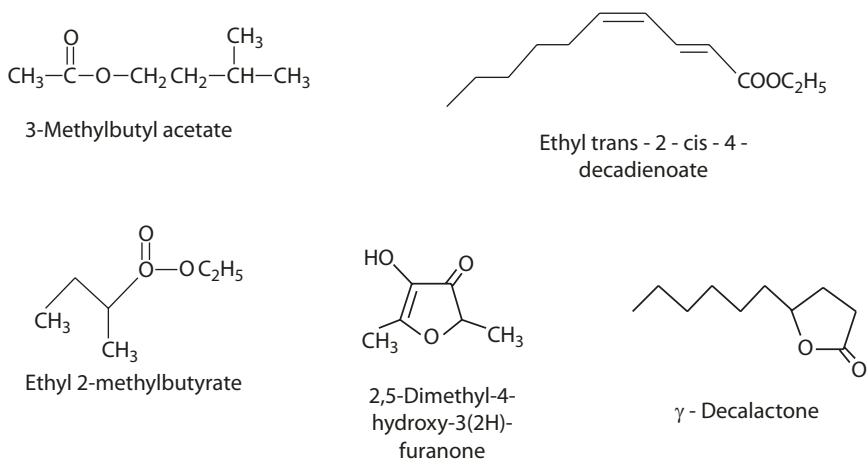
The bitterness of citrus fruits is ascribed to flavonoid compounds, especially naringin and limonin. Limonin belongs to a class of triterpene derivatives known as limonoids. It consists of two lactone rings, one of which has a furan substituent and an epoxide group. Limonin is the cause of the problem known as delayed bitterness, in which citrus fruit juice turns bitter after extraction. This is due to the conversion of the major natural limonoate A-ring lactone to limonin catalyzed by the enzyme limonin D-ring lactone hydrolase [18] (Eq. 6.27).



Another bitter compound is naringin, a flavanone neohesperidoside. The aglycone part is the flavanone naringenin, and the disaccharide part is neohesperidose, which is 2-*O*- α -L-rhamnosyl- β -D-glucose [20]. Alkaline hydrolysis of naringin converts it to the intensely sweet dihydrochalcone (Eq. 6.28). (See ► Chap. 7 for a detailed discussion.)



The typical flavor compounds of noncitrus fruits such as banana, pears, peaches, and apples are produced during the climacteric rise. Many aliphatic acids and amino acids in the unripe fruit are converted to esters, alcohols, and ethers that are mostly responsible for the characteristic fruit odor [33]. Esters, especially acetates and butyrates, are most abundant in bananas, and so are some phenol ethers. The main component that gives a banana aroma is isobutyl acetate (► Fig. 6.23). In Bartlett pears, ethyl *trans*-2-*cis*-4-decadienoate is identified as the important flavor compound. Ethyl 2-methylbutyrate in apple, 2,5-dimethyl-4-hydroxy-3(2*H*)-furanone in pineapple and strawberry, and γ -decalactone in peaches are some more examples of character-impact compounds.

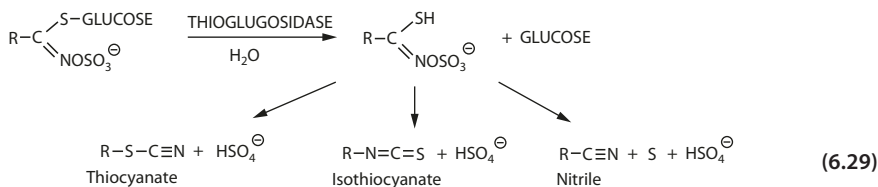


■ Fig. 6.23 Character-impact compounds in some noncitrous fruits

6.11.2 Vegetables

Cruciferous vegetables, such as cabbage, cauliflower, brussels sprouts, turnips, and mustards, contain glucosinolates that can be enzymatically degraded to yield the pungent sulfur compound isothiocyanate.

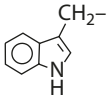
The formation of isothiocyanate involves a process similar to the Lossen rearrangement in which the alkyl group of a hydroxamic acid salt migrates from the carbon to the nitrogen (Eq. 6.29) (See ► Chap. 8).

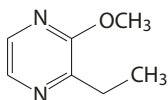


More than 90 glucosinolates have been identified. Some of the more important ones are listed in ■ Table 6.5 (with only the side group R shown).

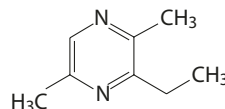
Alkoxyalkylpyrazines are widespread in vegetables, especially in pea, pepper, bean, asparagus, beetroot, carrot, and lettuce. These compounds possess a notably green odor. Bell pepper contains 20,000 ppm of 3-isobutyl-2-methoxy pyrazine and 1400 ppm of 3-isopropyl-2-methoxy pyrazine (■ Fig. 6.18) [42].

■ **Table 6.5** Structures and occurrence of selected glucosinolates

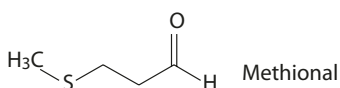
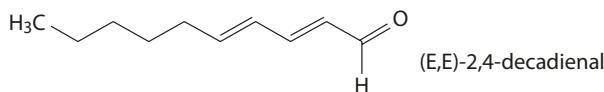
Side chain	Glucosinate (common name)	Occurrence
$\text{CH}_2=\text{CHCH}_2-$	Sinigrin	Brown or black mustard
$\text{HO}-\text{C}_6\text{H}_4-\text{CH}_2-$	Sinalbin	White mustard
$\text{CH}_2=\text{CH}(\text{OH})\text{CH}_2-$	Progoitrin	Turnip
	Glucobrassicin	Cabbage



2-Ethyl-3-methoxypyrazine



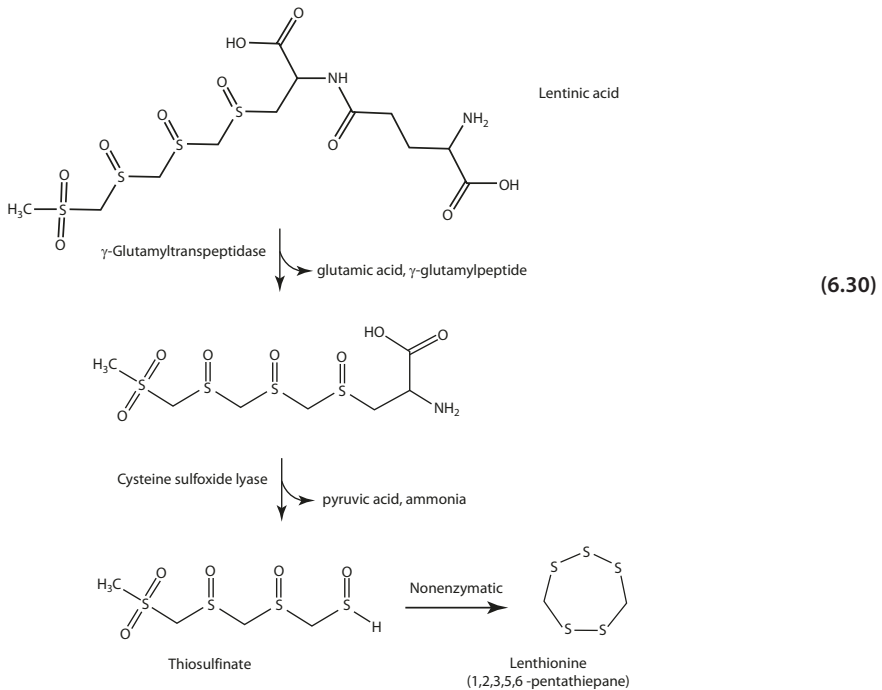
2-Ethyl-3,6-dimethylpyrazine



■ **Fig. 6.24** Aroma compounds in raw and processed potatoes

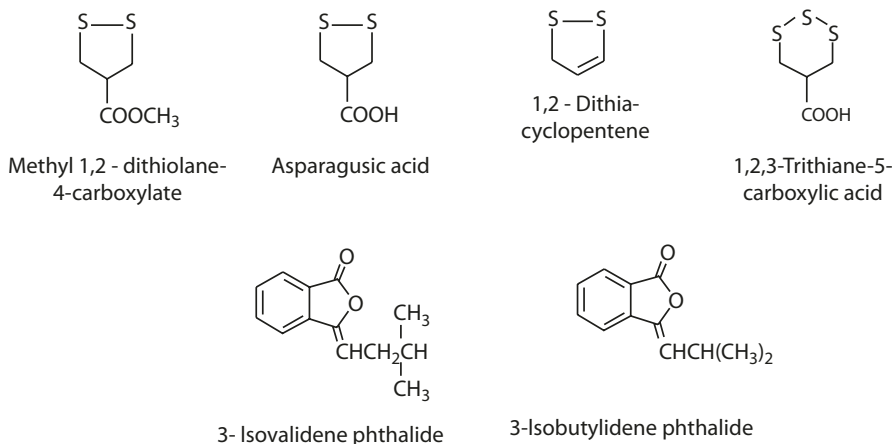
The earthy aroma of raw potato is attributed to 2-ethyl-3-methoxypyrazine. An important aroma in baked potato flavor has been identified to be 2-ethyl-3,6-dimethylpyrazine (Fig. 6.24). The alkylpyrazines, 2-isobutyl-3-methylpyrazine, 2,3-diethyl-5-methylpyrazine, and 3,5-diethyl-2-methylpyrazine, taken as a mixture, have a characteristic baked-potato flavor [34]. In potato chips and fries, the key character-impact compound is (*E,E*)-2,4-decadienal thermally generated from frying oils. Another notable aroma in potato chips is methional, a degradation product of methionine. The compound is also found in both boiled and baked potatoes.

In mushroom, the characteristic volatile flavor is associated with the unsaturated alcohol and ketone, 1-octen-3-ol and 1-octen-3-one. The latter occurs in increasing amounts in cooked mushroom and also has been related to metallic or mushroom off-flavors in dairy products [28]. The predominant sulfur compounds, bis(methylthio)methane and 1,2,4-trithiolane, are responsible for the characteristic aroma of truffles [35]. Lenthionine (1,2,3,5,6-pentathiepane, a cyclic polysulfide is known to possess the characteristic aroma of black mushroom (Shiitake, *Lentinus edodes*). This distinct aroma intensifies upon drying of the mushroom due to enzymatic conversion of lenthinic acid to lenthionine. γ -Glutamyl transpeptidase removes the glutamyl moiety from lenthinic acid, and *S*-alkyl-L-cysteine sulfoxide lyase acts next to produce an unstable intermediate which is spontaneously converted to the polythiepane (Eq. 6.30) [52].



Asparagus consists of sulfur-containing acids and esters as principal flavor compounds. The strong concentrated (~7 ppm) component, methyl 1,2-dithiolane-4-carboxylate, possesses an aroma characteristic of raw asparagus. During cooking of asparagus, the asparagusic acid (1,2-dithiolane-4-carboxylic acid) is decomposed to 1,2-dithiacyclopentene and 1,2,3-trithiane-5-carboxylic acid (Fig. 6.25) [46]. Besides the breakdown products of asparagusic acid, methyl disulfide has also been suggested to be a major aroma constituent (2–10 ppm) in cooked asparagus, formed by thermal fragmentation of *S*-methylmethionine.

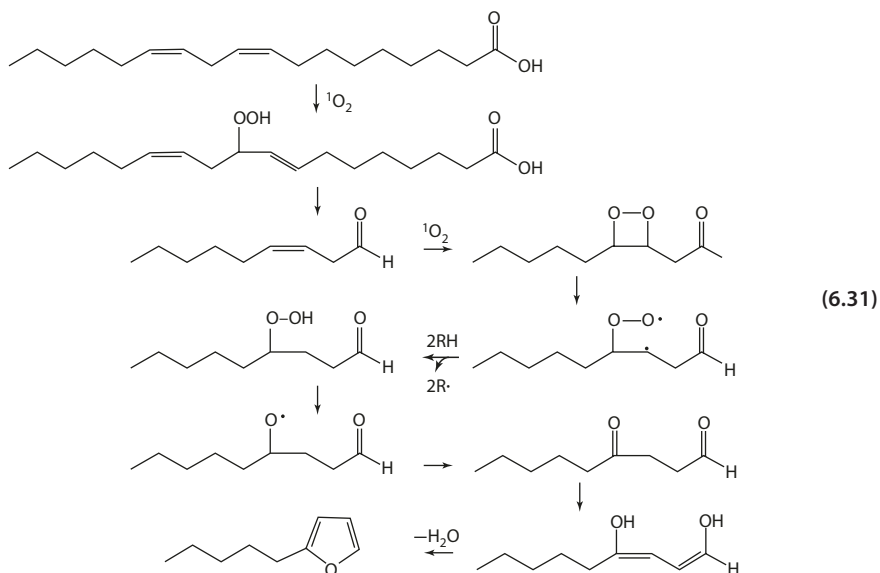
6.11 · Fruits and Vegetables



■ Fig. 6.25 Sulfur-containing compounds and phthalides

Phthalides and their derivatives are implicated in the characteristic odor of celery. These are the 3-isovalidene phthalide, 3-isobutylidene phthalide, and their dihydro-derivatives [15] (■ Fig. 6.25).

The undesirable beany off-flavor in soybean products, especially in soybean oil, has been attributed to 2-pentylfuran and 2-pentenylfuran (Eq. 6.31). These products are formed by oxidation of linoleic and linolenic acids by singlet oxygen. Traces of chlorophyll acting as sensitizer may be involved [31].



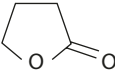
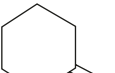
6.12 Meat Flavor

The chemistry of meat flavor represents the utmost complexity in flavor research. Meat must be cooked before it develops flavor, and numerous reactions can occur during the process.

There are well over 200 volatile compounds identified in cooked (boiled, roasted) beef. It is generally believed that the heterocyclic compounds are the important components in meat flavor. Table 6.6 list classes of volatile compounds in beef aroma [27]. The Maillard reaction and the Strecker degradation contribute to several important classes of flavor compounds: furans, pyrazines, pyrroles, oxazoles, thiophenes, thiazoles, and other heterocyclic compounds. Thermal degradation of lipids is another major source contributing to meat flavor, especially alkypridines, alkythiophenes, trithiolanes, and alkyl-substituted heterocyclic compounds.

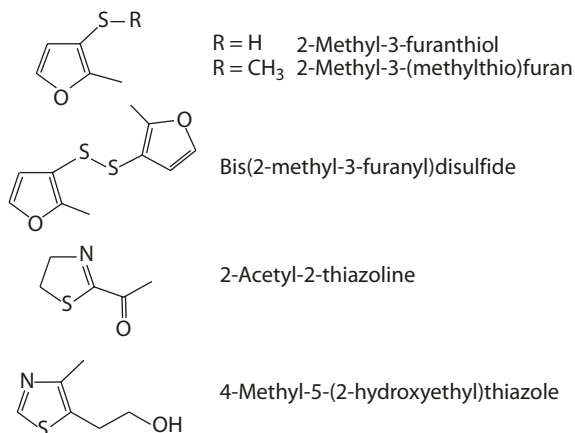
Furans and thiophenes with a thiol group in the 3- and 4-positions, and related disulfides, possess strong meat-like aromas with very low odor threshold values. 2-Methyl-3-furanthiol and its corresponding disulfide, bis-(2-methyl-3-furanyl) disulfide, are major contributors to the meaty aroma of cooked beef (Fig. 6.26). The odor threshold of the

Table 6.6 Classes of volatile heterocyclic compounds of beef aroma

Thiophene		Furan	
Thiazole	 Thiazole	Oxazole	 Oxazole
	 Thiazoline		 Oxazoline
Thiopane		Pyrrole	
Pyrazine		Pyridine	
Benzenoid		Lactone	 γ
			 δ

6.12 · Meat Flavor

Fig. 6.26 Furans and thiophenes contributing to meaty aroma in cooked beef



disulfide has been reported to be 0.02 ppb (ng/kg) [32]. 2-Acetyl-2-thiazoline is a potent aroma of cooked chicken and broth.

The compound 4-hydroxy-5-methyl-3(2*H*)-furanone (DMHF) and its 2,5-dimethyl homologs have been detected in beef broth. These are α -dicarbonyl compounds that can thermally react with H₂S to form a whole array of compounds with meaty flavors in model systems (Table 6.7). Mercapto-substituted furans and thiophenes identified with meaty

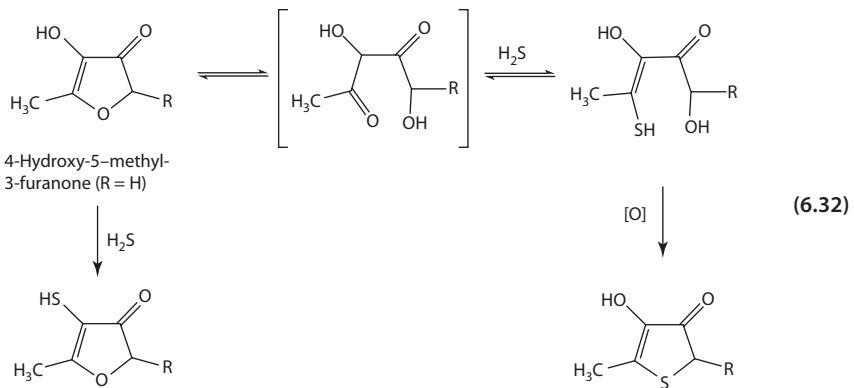
Table 6.7 Meaty flavors formed in the reaction of 4-hydroxy-5-methyl-3(2*H*)-furanone with hydrogen sulfide

4-Mercapto-2-methylfuran		Green, meaty
3-Mercapto-2-methyl-4,5-dihydrofuran		Roasted meat
4-Mercapto-3-oxo-tetrahydrofuran		Green, meaty
3-Mercapto-2-methyl-thiophene		Roasted meat
4-Mercapto-2-methyl-2,3-dihydrothiophene		Rubbery, meaty
3-Mercapto-4-hydroxy-2-methyl-2,3-dihydrothiophene		Meaty, savory

From Mottram [32], Van den Ouwedand and Peer [49]

flavors may derive from this reaction pathway [49]. The reaction between dihydrofuranone and hydrogen sulfide involves substitution of the ring oxygen by sulfur to give thio analogs, via the intermediate, 2,4-diketone (Eq. 6.32). Study of the reaction using cysteine also results in the formation of roasted meat flavor.

The off-flavor, known as warm-over flavor, which develops in reheating cooked and refrigerated meats is formed by the autoxidation of lipids, primarily the phospholipids in the meat. This is the major cause of rancidity during frozen storage of meat and meat products. The autoxidation is catalyzed by heme and nonheme irons, followed by decomposition to secondary products. Of these compounds, hexanal and *trans*-4,5-epoxy-(*E*)-2-decenal contribute most strongly to the warm-over flavor of refrigerated cooked beef [23].



Fish meat has short shelf life due to the development of unpleasant odor from the breakdown of trimethylalkylammonium compounds to trimethylamine (TMA) by bacteria in the fish gut. The TMA is converted to TMAO by a monooxygenase (trimethylamine oxidase) in the digestive gland or liver, to be transported to the tissues, accumulated or excreted (Fig. 6.27). In addition, bacterial actions on amino acids in the tissue also produce biogenic amines, such as histamine, putrescine, and cadaverine. TMAO and biogenic amines are common indicators for freshness of fish meat.

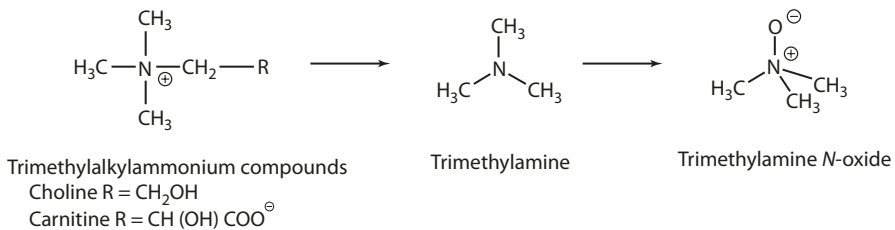
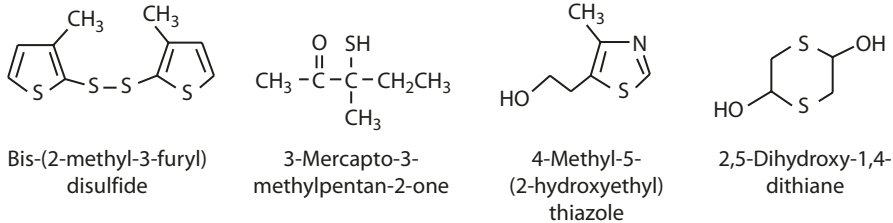


Fig. 6.27 Formation of trimethylamine and trimethylamine N-oxide

6.13 · Microencapsulation of Flavors



■ Fig. 6.28 Synthetic flavoring compounds

6.12.1 Simulated Meat Flavors

Most simulated meat flavorings have been produced by thermal processing a mixture of "precursor" compounds, some of which are listed below.

Amino acids – cysteine, cystine, methionine, glutamic acid, glycine, valine

Proteins – glycoproteins, hydrolyzed vegetable, yeast, animal proteins

Nucleotides – adenosine-5'-monophosphate, guanosine-5'-monophosphate

Carbohydrates (reducing sugars) – ribose, glucose, xylose, ribose-5-phosphate

Acids – α -ketobutyrate, succinate, lactate, aliphatic carboxylic acid

Vitamins – thiamin

Sulfur compounds – thiols, sulfides, furanones, sulfur amino acids

In general, the reaction mixture always contains: (1) an amino-containing compounds (such as amino acid), (2) a sulfur-containing compound (such as cystine, thiamin), and (3) a reducing sugar or carbonyl compound. Other flavor chemicals are sometimes added to the reaction mixture to improve the meaty flavor. These meat flavor chemicals include many of the naturally occurring flavor compounds that are not replaced as naturally occurring meat. Some of these are listed in ■ Fig. 6.28 [50].

6.13 Microencapsulation of Flavors

There are increasing numbers of food products containing microencapsulated flavors and ingredients. The flavor ingredients are coated with edible film matrix. The coated particle has a size of less than 5000 μ . The coating materials include the following:

1. Polysaccharides, such as gum arabic, starch
2. Maltodextrin
3. Protein – gelatin
4. Hydrolyzed gelatin
5. Modified proteins – succinylated gelatin, alkylated starch

Microencapsulation has the advantages of: (1) converting liquid flavor concentrate to solid or powder form, (2) protecting flavor loss during food processing and storage, and (3) controlling the rate of release of volatiles and nonvolatiles into a food system. An example of the last is the use of slow-release capsules of ascorbic acid and calcium peroxide in bread making.

References

1. Amoore JE (1964) Current status of the steric theory of odor. *Ann NY Acad Sci* 116:457–476
2. Assadi-Porter FM, Maillet EC, Radeh JT, Quijada J, Markley JL, Max M (2010) Key amino acid residues involved in multi-point binding interactions between Bazein, a sweet protein and the TIR2-TIR3 human sweet receptor. *J Mol Biol* 398:584–599
3. Beets MGJ (1971) Relationship of chemical structure to odor and taste. In: Proceedings third international congress on food science and technology. Institute of Food Technologists, Chicago
4. Belitz H-D, Chen W, Jugel H, Stempf H, Treleano R, Wieser H (1983) Quantitative structure activity relationships of bitter tasting compounds. *Chem Ind* 3:23
5. Block E (1985) The chemistry of garlic and onions. *Sci Am* 252(3):114–119
6. Block E (1992) The organosulfur chemistry of the genus *Allium* – Implications for the organic chemistry of sulfur. *Angew Chem Int Ed Engl* 31:1135–1178
7. Boelens M, deValois PJ, Wobben HJ, van der Gen A (1971) Volatile flavor compounds from onion. *J Agric Food Chem* 19:984–991
8. Buck L, Axel R (1991) A novel multigene family may encode odorant receptors: a molecular basis for odor recognition. *Cell* 65:175–187
9. Buttery RG, Seifert RM, Guadagni DG, Ling LC (1969) Characterization of some volatile constituents of bell peppers. *J Agric Food Chem* 17:1322–1327
10. Cascales JLL, Costa SDO, de Groot BL, Walters DE (2010) Binding of glutamate to the umami receptor. *Biophys Chem* 152:139–144
11. Chandrashekar J, Hoon MA, Ryba NJ, Zuker CS (2006) The receptors and cells for mammalian taste. *Nature* 444:288–294
12. Connell DW (1970) The chemistry of the essential oil and oleoresin of ginger (*Zingiber officinale* Roscoe). *Flavor Industry* 1(10):677–693
13. David C, Henze A, Frank O, Glabasnia A, Rupp M, Buning K, Orlikowski D, Bader M, Hofmann T (2012) Structural and sensory characterization of key pungent and tingling compounds from black pepper (*Piper nigrum* L.). *J Agric Food Chem* 60:2884–2895
14. Demole E, Enggist P, Ohloff G (1982) 1-*p*-Menthene-8-thiol. A powerful flavor impact constituent of grapefruit juice (*Citrus paradisi* Macfayhden). *Helv Chim Acta* 65:1785–1794
15. Gold HJ, Wilson CW (1963) The volatile flavor substances of celery. *J Food Sci* 28:484–488
16. Govindarajan VS (1977) Pepper-chemistry, technology, and quality evaluation. *CRC Crit Rev Food Sci Nutr* 9:115–225
17. Gunst F, Verzele M (1978) On the sunstruck flavor of beer. *J Inst Brew* 84:291–292
18. Hasegawa S, Maier VP (1983) Solutions to the limonin bitterness problem of citrus juices. *Food Technol* 37(6):73–77
19. Ho C-T, Zheng X, Li S (2015) Tea aroma formation. *Food Sci Hum Wellness* 4:9–27
20. Horowitz RM, Gentili B (1979) Taste and structure relations of flavonoid compounds. In: Chiba H (ed) Proceedings of the fifth international congress of food science and technology. Elsevier Scientific Publishing Co., New York
21. Imai S, Akita K, Tomotake M, Sawada H (2006) Identification of 2 novel pigment precursors and a reddish-purple pigment involved in the blue-green discoloration of onion and garlic. *J Agric Food Chem* 54:843–847
22. Johnson JD, Vora JD (1983) Natural circus essences. *Food Technol* 37(12):92–93. 97
23. Kerler J, Grosch W (1996) Odorants contributing to warmed-over flavor (WOF) of refrigerated cooked beef. *J Food Sci* 61:1271–1275
24. Kuninaka A (1967) Flavor potentiator. In: Schultz HW (ed) The chemistry and physiology of flavors. AVI, Westport
25. Kuninaka A (1981) Taste and flavor enhances. In: Teranish R, Flath RA, Sugisawa H (eds) Flavor research, recent advances. Marcel Dekker, New York
26. Liman ER, Zhang YV, Montell C (2014) Peripheral coding of taste. *Neuron* 81:984–1000
27. MacLeod G, Seyyedain-Ardebili M (1981) Natural and simulated meat flavors (with particular reference to beef). *CRC Crit Food Sci Nutr* 14:308–437
28. Maga JA (1981) Mushroom flavor. *J Agric Food Chem* 29:1–4
29. Malnic B, Hirono J, Sato T, Buck LB (1999) Combinatorial receptor codes for odors. *Cell* 96:713–723
30. Miles FD, Baker BG, Hodge JE (1969) Amadori compounds as nonvolatile flavor precursors in processed foods. *J Agric Food Chem* 17:723–727

References

31. Min DB, Callison AL, Lee HO (2003) Singlet oxygen oxidation of 2-pentylfuran and 2-pentenylfuran in soybean oil. *J Food Sci* 68:1175–1178
32. Mottram DS (1998) Flavour formation in meat and meat products: a review. *Food Chem* 62:415–424
33. Nursten HE (1978) Flavor chemistry of fruits and vegetables. In: Teranishi R (ed) *Agricultural and food chemistry: past present, future*. AVI, Westport
34. Pares SR, Chang SS (1974) Identification of compounds responsible for baked potato flavor. *J Agric Food Chem* 22:339–340
35. Pelusio F, Nilsson T, Montanarella L, Tilio R, Larsen B, Facchetti S, Madsen JO (1995) Headspace solid-phase microextraction analysis of volatile organic sulfur compounds in black and white truffle aroma. *J Agric Food Chem* 43:2138–2143
36. Rizzi GP (1969) The formation of tetramethylpyrazine and 2-isopropyl-4,5-dimethyl-3-oxazoline in the Strecker degradation of DL-valine with 2,3-butanedione. *J Org Chem* 34:2002–2004
37. Rizzi GP (1972) A mechanistic study of alkylpyrazine formation in model systems. *J Agric Food Chem* 20:1081–1085
38. Sanderson GW, Co H, Gonzalez JG (1971) Biochemistry of tea fermentation: the role of carotenes in black tea aroma formation. *J Food Sci* 36:231–236
39. Sanderson GW, Graham HN (1973) On the formation of black tea aroma. *J Agric Food Chem* 21:576–585
40. Siebert TE, Wood C, Eley GM, Pollnitz AP (2008) Determination of rotundone, the pepper aroma impact compound, in grapes and wine. *J Agric Food Chem* 56:3745–3748
41. Simian H, Robert F, Blank I (2004) Identification and synthesis of 2-heptanethiol, a new flavor compound found in bell peppers. *J Agric Food Chem* 52:306–310
42. Takken HJ, van der Linde LM, Boelens M, van Dort JM (1975) Olfactive properties of a number of poly-substituted pyrazines. *J Agric Food Chem* 23:638–642
43. Takken HJ, van der Linde LM, deValois PJ, van Dort HM, Boelens M (1976) Reaction products of α -dicarbonyl compounds, aldehydes, hydrogen sulfide, and ammonia. In: *Phenolic, sulfur, and nitrogen compounds in food flavors*. ACS symposium series, vol 26. American Chemical Society, Washington, D.C.
44. Todd PH Jr, Bensinger MG, Biftu T (1977) Determination of pungency due to capsaicin by gas-liquid chromatography. *J Food Sci* 42:660–680
45. Tressl R, Silwar R (1981) Investigation of sulfur-containing components in roasted coffee. *J Agric Food Chem* 29:1078–1082
46. Tressl R, Bahri D, Holzer M, Kossa T (1977) Formation of flavor components in asparagus. 2. Formation of flavor components in cooked asparagus. *J Agric Food Chem* 25:459–463
47. Tressl R, Friese L, Fendesack F, Koppler H (1978) Gas chromatographic – mass spectrometric investigation of hop aroma constituents in beer. *J Agric Food Chem* 26:1422–1426
48. Tressl R, Rewicki D, Helak B, Kamperschroer H (1985) Formation of pyrrolidines and piperidines on heating L-proline with reducing sugars. *J Agric Food Chem* 33:924–928
49. van den Ouwedand GAM, Peer HG (1975) Components contributing to beef flavor. Volatile components produced by the reactions of 4-hydroxy-5-methyl-3(2H)-furanone and its thio analog with hydrogen sulfide. *J Agric Food Chem* 23:501–505
50. Wilson RA, Katz I (1974) Synthetic meat flavors. *Flavor Industry* 5(30–35):38
51. Wilson CW III, Shaw PE (1981) Importance of thymol, methyl N-methyl-anthranilate, and monoterpene hydrocarbon to the aroma and flavor of mandarin cold-pressed oils. *J Agric Food Chem* 29:494–496
52. Yasumoto K, Iwami K, Mitsuda H (1971) Enzyme-catalyzed evolution of lenthionine from lenthionine. *Agric Biol Chem* 33:2070–2080
53. Zhang F, Klebansky B, Fine RM, Xu H, Pronin A, Liu H, Tachdjian C, Li X (2010) Molecular mechanism for the umami taste synergism. *Proc Natl Acad Sci U S A* 105:20930–20934

Sweeteners

- 7.1 The Tripartite Theory of Sweetness – 310
- 7.2 Sweet Taste Receptors – 312
- 7.3 Amino Acids and Dipeptides – 313
 - 7.3.1 Aspartame – 313
 - 7.3.2 Neotame – 316
- 7.4 The Aminosulfonates – 316
- 7.5 Dihydrochalcone – 317
- 7.6 Glycyrrhizin – 319
- 7.7 Stevioside – 320
- 7.8 Sugar Alcohol – 321
- 7.9 Corn Sweeteners – 322
- 7.10 Sweet Proteins – 323
- References – 325

Sweeteners are classified into two basic categories: nutritive and nonnutritive. Nutritive sweeteners include sugars, sugar alcohols, corn syrups, and high-fructose corn syrups. Nonnutritive sweeteners include acesulfame K, sucralose, and neotame. Most nutritive sweeteners are obtained from plant sources, and nonnutritive sweeteners are synthetic. However, stevioside, a sweet diglycoside extracted from the wild plant *Stevia rebaudiana*, is noncaloric. Aspartame is a synthetic but low-caloric sweetener.

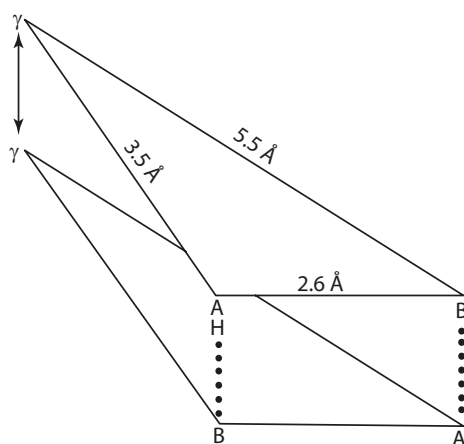
Each individual sweetener has its specific properties and limitations. Development of new and sweet-tasting compounds with desirable properties becomes increasingly attainable due to the numerous investigations in recent years on the chemistry of the nature of sweetness. Theoretically, sweet compounds could be constructed if the basic chemistry of sweetness was understood. In fact, sweet compounds designed for research studies provide much of the present knowledge on the theory of taste perception.

7.1 The Tripartite Theory of Sweetness

The chemical nature of sweetness of a substance can be correlated based on the widely accepted tripartite model. The glycochore (sweet-carry moiety) in a sweet-tasting compound consists of two units, AH and B, together with a third component, γ , arranged in a tripartite structure. The unit AH is a group consisting of oxygen or nitrogen carrying a hydrogen atom such as OH, NH, or NH₂. The unit B is a group consisting of O, N, or any electronegative center that is capable of attracting a hydrogen atom to form hydrogen bonding. The γ unit is a hydrophobic site and needs not be present as a specific functional group. The distance parameters are A–B = 2.6 Å, B– γ = 5.5 Å, and A– γ = 3.5 Å. The orbital distance between the AH proton and B is about 3.0 Å (■ Fig. 7.1) [20].

In a three-dimensional picture, the glycochore binds to the receptor site. The sweet taste is initiated by intermolecular hydrogen bonding between this glycochore (AH, B)

■ Fig. 7.1 The tripartite model

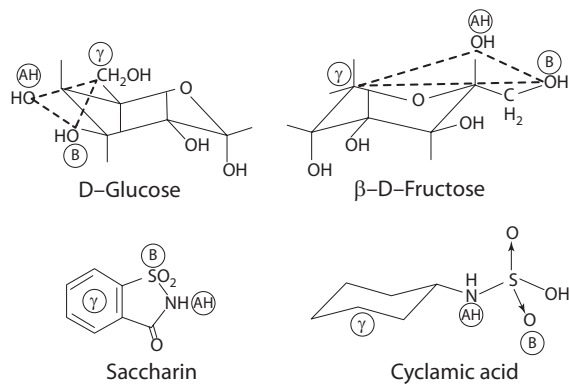


and a similar AH, B units on the receptor. The γ component functions to direct and align the molecule as the AH, B glycochore approaches the receptor site (■ Fig. 7.1)

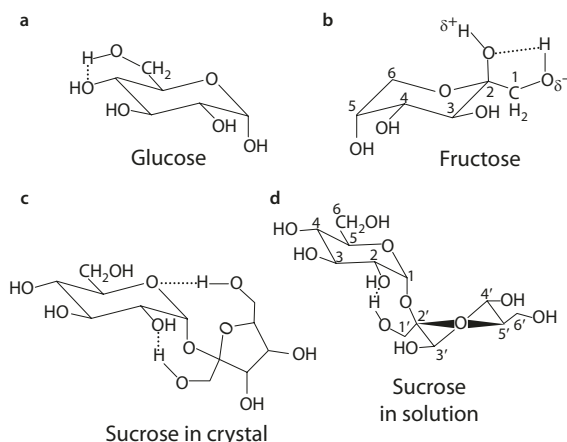
The AH, B glycochore can be found in many carbohydrates with 1,2-glycol structures. In the sugars, the 1,2-glycol has to be in the gauche conformation to satisfy the distance requirement. For a pyranose sugar, both α -D-C1 and α -D-1C acquires a 60° angle. Anticonformation as in β -D-1C elicits no sweet taste. Eclipsed vicinal OH groups as in α -D-B3 conformer tastes less sweet due to strong intramolecular hydrogen bonding.

Experimentally, it is possible to locate the AH, B glycochore in a particular sweet compound. Some representative compounds and their AH, B glycochore assigned to be responsible for the sweet taste are listed in ■ Fig. 7.2. Note that for glucose, the C4–OH has the AH function, and C3–O is the B unit. The reason for this assignment is based on the studies that C6–OH is so positioned to hydrogen bond to C4–O, and consequently the proton of C4–OH becomes more acidic and more capable of intermolecular hydrogen bonding with the receptor site B (■ Fig. 7.3a). This "activation" of the proton of C4–OH by C6–OH and thus the enhancement of the AH, B functions is known as "Lemieux

■ Fig. 7.2 Glycochore structures of some sweet compounds



■ Fig. 7.3 The "Lemieux effect" in a glucose, b fructose, c sucrose crystal, and d sucrose in solution



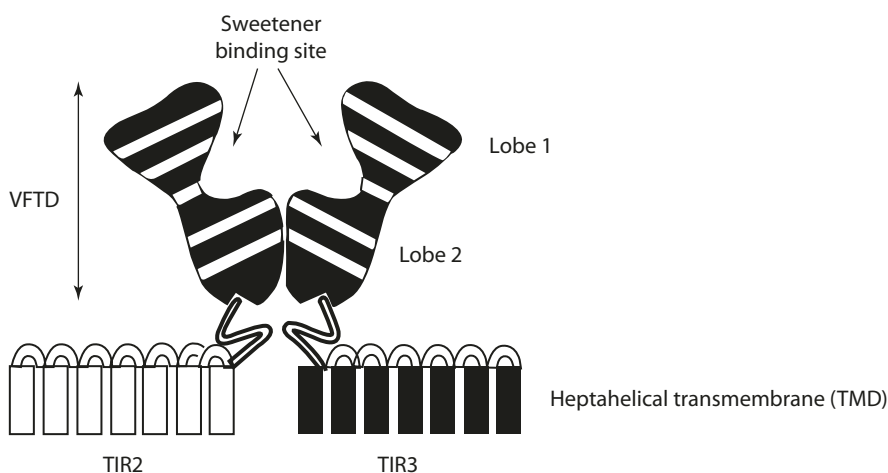
effect.” Analogous bonding in fructose fixes the position of C1–O in space and enhances the proton-donating group C2–OH (■ Fig. 7.3b) [19].

Sucrose contains eight hydroxyl groups arranged in the crystal in which the fructose and glucose units are bridged by two intramolecular hydrogen bonds from C6'–OH to C5–O and from C1'–OH to C2–O (■ Fig. 7.3c). In solution, sucrose exists in a form wherein the C1'–OH to C2–O hydrogen bond is maintained (■ Fig. 7.3d) [3]. In addition to the glycopore in the glucopyranosyl unit, a second glycopore can be established involving C2–OH (AH), C3–O (B), and C1' (γ).

This Shallenberg and Acree model has found widespread acceptance. This model and subsequent extensions of it describe beautifully the structure-activity of many sweet compounds and interpret the various effects of geometric or conformational differences. The biological half of the binding system, that is, the structure and mechanism of the taste receptor, has also recently become the subject of intense study as well.

7.2 Sweet Taste Receptors

Sweet taste perception in human is characterized by its broad tuning to chemically diverse molecules: simple sugars, D-amino acids, peptides, proteins, heterocyclic molecules, such as saccharin and cyclamate, and other classes of compounds. The sweet receptor protein consists of a heterodimer of two sequence-related subunits that belong to the class C G-protein-coupled receptor (GPCR) family: Type 1 Receptor 2 (T1R2) and Type 1 Receptor 3 (T1R3). Each subunit consists of three structural domains: (1) a large extracellular amino-terminal domain (resembling a venus flytrap, VFTD) composed of lobes 1 and 2, (2) a heptahelical transmembrane domain (TMD), and (3) a cysteine-rich domain (CRD) connecting the two domains (■ Fig. 7.4). The two lobes of T1R2 and T1R3 flexibly change in arrangement to form an "open" or "closed" conformation [15]. There are two active closed-open forms: T1R2 open and T1R3 closed or T1R2 closed and



■ Fig. 7.4 Schematic representation of human T1R2-T1R3 sweet receptor (Assadi-Porter et al. [2])

T1R3 open. The open-open form is inactive, whereas the closed-open form is active. Binding of a small molecular sweetener to the receptor activates the receptor by closure of the two lobes, transforming the inactive (free) form to the active form. Aspartame, sodium saccharin, acesulfame K, cyclamate, and sucralose are all recognized in the cleft composed of lobes 1 and 2 of T1R2, involving multipoint binding interactions [14]. Sweet proteins seem to bind to a secondary surface site (without entering the lobe 1-2 cleft) belonging mostly to the T1R3 receptor. The mode of binding between human sweet taste receptor and low-molecular-weight sweet compounds has been studied (14). It is proposed that individual sweetener molecules each has a unique set of specific amino acid residues in the receptor for binding in corresponding to the chemical structure, although some residues are responsible for interacting with multiple sweeteners. The detailed chemistry of the structural binding interaction between a sweetener and its receptor is not yet available.

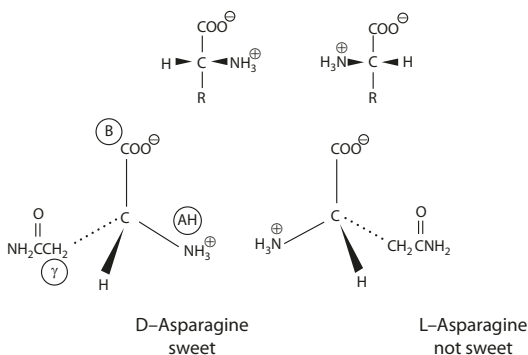
7.3 Amino Acids and Dipeptides

A number of D-amino acids, including Trp, His, Phe, Tyr, Leu, Gly, and Apn, are sweet, but their enantiomers, the L-amino acids, are known to be tasteless or bitter (■ Fig. 7.5). The difference in sweetness in the enantiomeric amino acids can be explained by the fact that the D-amino acids are superimposable upon the receptor sites, while the L-amino acids are not, as shown in ■ Fig. 7.6.

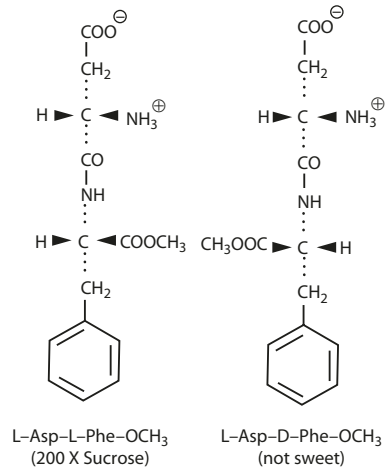
7.3.1 Aspartame

The low-calorie sweetener aspartame is a methyl ester of a dipeptide L-aspartyl-L-phenylalanine (L-Asp-L-Phe-OCH₃). The dipeptide is 180–200 times sweeter than sucrose and exhibits no bitter aftertaste generally associated with some other artificial sweeteners. Furthermore, aspartame acts synergistically with other sweeteners.

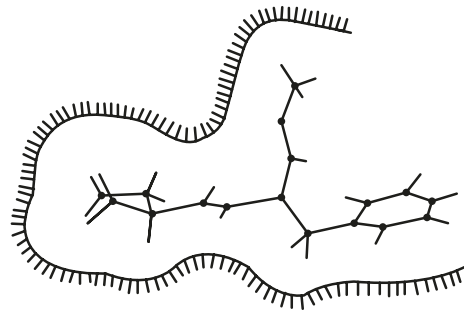
■ Fig. 7.5 Fischer projection formula and the corresponding configurations of D and L-asparagine



■ **Fig. 7.7** L-Asp-L-Phe-OCH₃ and L-Asp-D-Phe-OCH₃ represented by Fischer projection formula



■ **Fig. 7.8** Schematic model of L-Asp-L-Phe-OCH₃ inside the receptor site (From Lej et al. [12] with permission. Copyright 1976 American Chemical Society)

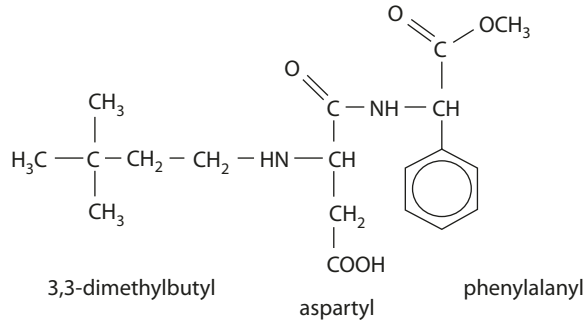


–OCH₃ portion of the molecule could be replaced by various esters of amino acids without losing the sweetness, since the taste receptor site recognizes only the shape and size and the hydrophobic portion of the molecule.

Only the L-L isomer is intensively sweet. L-Asp-D-Phe-OCH₃ is not sweet. This structural-taste relationship can readily be explained by considering the receptor site as a "pocket" with the AH, B, γ system inside a spatial barrier. The L-D isomer has the methyl ester group so positioned that the molecule cannot fit into the pocket for the interaction with the receptor site to occur. In the case of the L-L isomer, the conformation of the molecule allows it to interact with the receptor site within the spatial barrier (■ Fig. 7.8) [12].

Aspartame has a pI of pH 5.2, where minimum solubility occurs. The phenylalanine portion of aspartame is highly hydrophobic, since the carboxyl group is esterified.

Fig. 7.9 Neotame structure



Therefore, aspartame is only fairly soluble in water (about 1% at 24 °C, pH 5.2). In practice, food grade citric or malic acid is used to convert the aspartame into salt which is readily soluble.

7.3.2 Neotame

Neotame, a derivative of aspartame, has a 3,3-dimethylbutyl group attached to the amino group of the aspartyl residue of aspartame [16]. This group provides a second hydrophobic site (γ unit), in addition to the phenyl ring (γ unit) provided by the phenylalanine residue. Neotame has an intensity of sweetness about 8000 times that of sucrose on a 2% solution weight basis and about 40 times that of aspartame (Fig. 7.9).

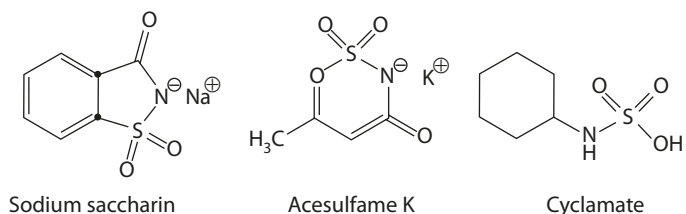
Neotame can be synthesized by reductive alkylation of aspartame with 3,3-dimethylbutyraldehyde. The presence of the 3,3-dimethylbutyl group renders the structure unsusceptible to peptidase-catalyzed hydrolysis, as aspartame would be. Neotame is therefore non-caloric. In contrast to the primary amino group in aspartame, the secondary amino group in neotame is unreactive with reducing sugars and aldehyde derivatives to form Maillard products, resulting in broader applications in food formulations.

7.4 The Aminosulfonates

Another group of high-intensity sweeteners is the aminosulfonates, which include cyclamate, saccharin, and acesulfame K (Fig. 7.10).

Cyclamate is a cyclohexane sulfonic acid, which is a white crystalline powder 30–60 times the sweetness of sucrose. Its unpleasant aftertaste can usually be minimized by blending with saccharin.

Fig. 7.10 Structure of some synthetic sweeteners



Saccharin is supplied in the sodium or calcium form, with a solubility of 6.5% in water at 25 °C and a sweetness intensity 450 times that of sucrose.

Acesulfame K differs from saccharin by having an oxygen atom in between the SO₂ group and the π ring. In both compounds, altering the imide function destroys the sweet taste. Acesulfame K is 200 times sweeter than sucrose, and more stable. It shows no loss of stability at pH values of 3 and higher and only decomposes at a temperature higher than 225 °C. Its solubility at 20 °C in water is about 27%.

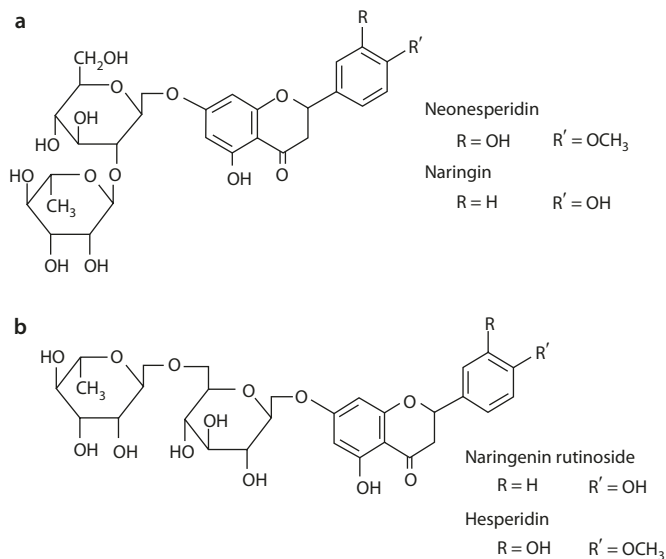
These aminosulfonate sweet compounds have the AH group (NH) and B group (oxygen of the SO₃) in the gauche conformation. The great sweetness found in these compounds is due to the large hydrophobic surface contact provided by the ring structure. Ring substituents with various lengths indicate a loss of sweetness when the length of the hydrophobic group on the nitrogen exceeds 0.7 Å. This relationship may be explained by the presence of a spatial barrier in the receptor site, located at 0.7 Å from the NH interaction point [18]. A bulky substituent would displace the molecule that interaction with the receptor AH, B units becomes impossible.

7.5 Dihydrochalcone

The bitter flavanone glycosides in citrus fruits include the neohesperidin in oranges and lemons and the naringin in grapefruits.

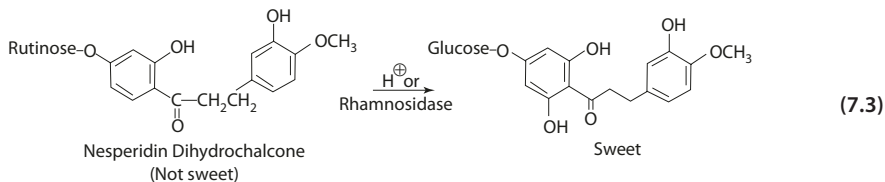
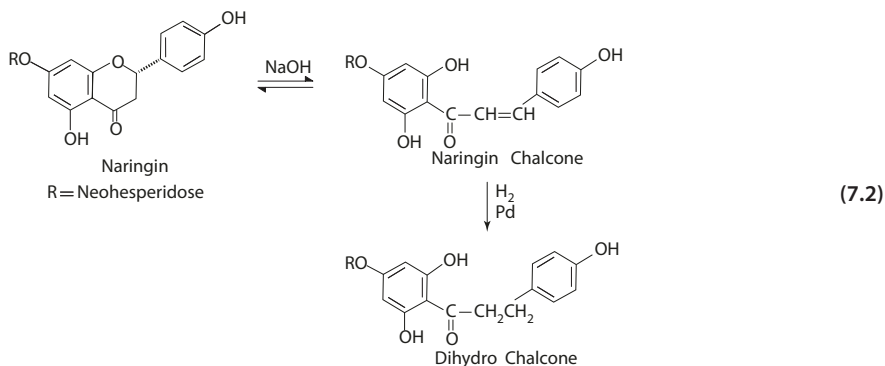
In neohesperidin, the disaccharide component linked to the 7-hydroxyl group of the aglycone is neohesperidose (2'-O-α-L-rhamnopyranosyl-D-glucose) (■ Fig. 7.11a). The aglycone in these structures has a 2(S) configuration. When the rhamnose is linked to the

■ Fig. 7.11 Structure of a neohesperidin and naringin, and b hesperidin and naringenin rutinoside



6-position of the glucose instead, the product exhibits a loss of sweetness. The disaccharide now becomes 6-*O*- α -L-rhamnosyl- β -D-glucose with the trivial name rutinose (■ Fig. 7.11b)

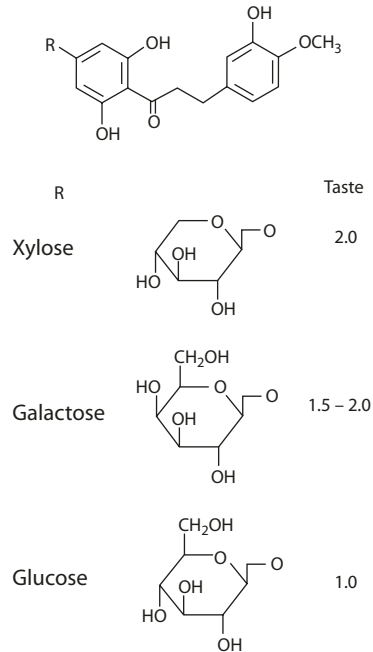
The compounds naringin, neohesperidin, and other neohesperidose-containing flavanones can be hydrolyzed to the chalcones and dihydrochalcones (Eq. 7.2). Both the chalcones and dihydrochalcones are sweet [8]. The rutinose-containing flavanones such as hesperidin and naringenin rutinoside yield tasteless dihydrochalcones which become sweet when the rhamnose is removed enzymatically or by acid hydrolysis (Eq. 7.3).



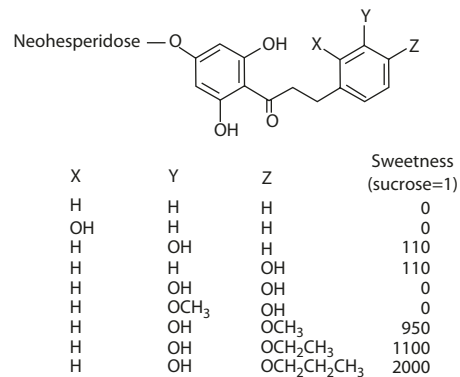
In the chalcone and dihydrochalcone, the rhamnose linking to the C2 hydroxyl of glucose enhances sweetness but causes a complete loss of sweetness when it is linked to the C6 hydroxyl group. The C6 substituent is not necessary for sweet taste. Hesperetin dihydrochalcones with the disaccharide replaced by xylose or galactose are twice as sweet as a glucose substituent (■ Fig. 7.12) [9].

The C3 and C4 hydroxyl groups are the AH, B glycoflavone unit. Aside from the glucoside position, there is a very specific requirement of the substituents in ring B of the flavanone of the dihydrochalcone, as indicated in ■ Fig. 7.13 [9]. A hydroxyl substitution at the B ring and its position are important for the intensity of sweetness.

■ **Fig. 7.12** Sweetness of hesperetin dihydrochalcone modified with various monosaccharide substituents



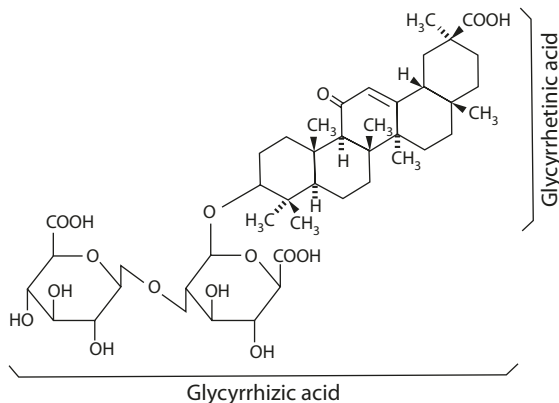
■ **Fig. 7.13** Sweetness of hesperetin dihydrochalcone modified with various substituents in ring B (Inglett [9])



7.6 Glycyrrhizin

The sweetener glycyrrhizin occurs naturally as mixed calcium and potassium salts of glycyrrhizic acid, which is mainly found 6–10% in the licorice root (*Glycyrrhiza glabra L.*). Glycyrrhizin is a triterpenoid glycoside, having two glucuronic acid units. The aglycone is the glycyrrhetic acid (■ Fig. 7.14). Licorice extracts are used in the flavoring of cigarettes

■ Fig. 7.14 Structure of glycyrrhizic acid



and tobaccos, confectionary, beverages such as root beer, and pharmaceutical products. Glycyrrhizin is isolated from the extract as the fully ammoniated salt (ammonium glycyrrhizinate, AG) available in spray-dried brown powder form. Mono-ammonium glycyrrhizinate (MAG), which is a white crystalline powder, is also available [1].

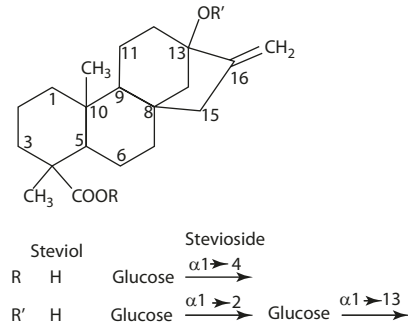
Ammonium glycyrrhizinate has an effective use level of 20–1000 ppm. It is soluble in water, alcohol, and propylene glycol. At pH below 4.5, AG tends to precipitate. Heating above 105 °C causes deterioration of the flavor. AG is about 50 times sweeter than sucrose. The sweetener is potentiated to 100 times in the presence of sucrose. MAG has poor solubility in water and alcohol, but it is stable over a wide pH range.

7.7 Stevioside

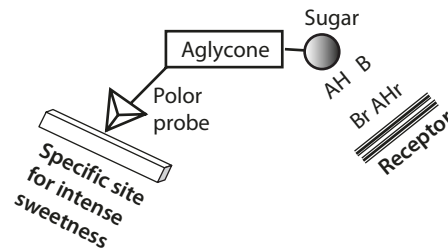
Stevioside is the sweet diterpenoid glycoside found in the leaves of *Stevia rebaudiana* (Bert.). It is a white crystalline, hygroscopic powder 250–300 times sweeter than sucrose, but has a bitter and unpleasant aftertaste. The aglycone is a diterpenoid called steviol (■ Fig. 7.15a). The α -hydroxyl group at C13 is linked to the disaccharide sophorose (2-*O*- β -D-glucopyranosyl- β -D-glucopyranose), and the α -carboxyl at C4 is condensed with β -D-glucopyranose (■ Fig. 7.15b). The aglycone steviol has been shown to be weakly antiandrogenic.

All the aglycoside sweeteners mentioned above contain the hydrophilic disaccharide and the hydrophobic aglycone. To explain the intense sweetness of these large molecules, the tripartite theory is extended to include another hydrophilic function, designated as the polar "probe." The probe may be the β -D-glucose in stevioside, the C20 carboxylate anion of ammonium glycyrrhizinate, and the phenolate ion of naringin dihydrochalcone and neohesperidin dihydrochalcone. It is postulated that the probe binds to a more specific type of receptor site, which by electron transfer or charge displacement elicits a strong response to the taste of sweetness. Schematically, the mode of interaction is presented in ■ Fig. 7.16 [10]. The entire molecule positions so that the hydrophobic and hydrophilic units are attracted to the corresponding sites of the receptor, placing the probe to a specific receptor for inducing the intensity sweet taste.

■ Fig. 7.15 Structure of a steviol and b stevioside



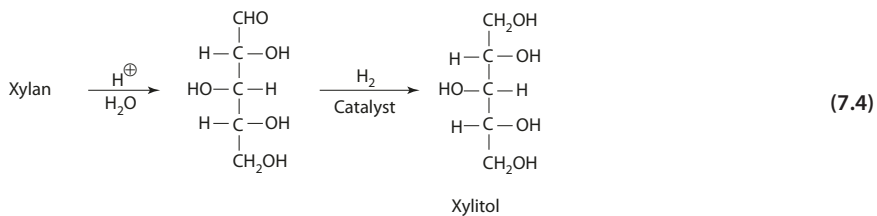
■ Fig. 7.16 Schematic representation of interaction between glycoside and receptor (Inglett [10])



7.8 Sugar Alcohol

Sugar-derived polyhydric alcohols are less sweet when compared with sucrose as shown in Table 7.1. The last two listed are polyhydric glycosides, although they are usually regarded as alcohols.

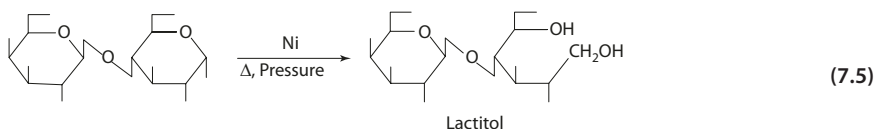
Xylitol is produced by the hydrogenation of xylose obtained from the hydrolysis of xylan. Raw materials such as corn cob, hardwood chips, and sugar cane bagasse typically contain 20–35% xylan (Eq. 7.4) [13].



Lactitol can be synthesized by the catalytic hydrogenation of lactose under high pressure and temperature (Eq. 7.5).

■ **Table 7.1** Sweetness of polyhydric alcohols

Alcohol	Sweetness
Sucrose	100
Xylitol	95
Sorbitol	54
Galactitol	46
Mannitol	62
Maltitol	63
Lactitol	34



7.9 Corn Sweeteners

Sweeteners prepared by the hydrolysis of cornstarch have found large-scale applications in the food industry. Corn sweeteners can be classified into three basic categories: (1) conventional corn syrups, (2) dextrose solids, and (3) high-fructose corn syrups.

The key step in the manufacture of the above sweeteners is hydrolysis, using a combination of a starch-liquefying enzyme (α -amylase) and a starch-saccharifying enzyme (glucoamylase) (Eq. 7.6). The former enzyme hydrolyzes the α -1,4 bonds randomly along the chain, while the latter is exo-acting, hydrolyzing glucose units successively from the non-reducing end and also the α -1,6 linkages at the branching points. The process results in a mixture of dextrose, maltose, and whole range of higher saccharides depending on the degree of hydrolysis. The total reducing sugar in the product is compared to the reducing power of pure dextrose to yield a number known as the dextrose equivalent (D.E.). Thus, the higher the D.E. of the product, the more low-molecular-weight saccharides it contains. The product is sweeter and more fermentable, has a greater freezing point depression and lower viscosity, and is more susceptible to nonenzymatic browning reaction. Commercially, the hydrolysate is refined (removal of impurities) and concentrated to yield the conventional corn syrups. There are four types of corn syrups for various applications [7].

Type	D. E	Applications
I	20–38	Relatively nonsweet, used as bulking agents, provide body and mouth feel
II	38–58	Commonly used as sweeteners in combination with sucrose or HFCS
III	58–73	Used mainly as sweeteners
IV	>73	Used for further processing into HFCS



Alternatively, the dextrose in the refined hydrolysate can be crystallized out to give a product of alpha dextrose monohydrate or alpha dextrose anhydrate. Dextrose is three-fourths as sweet as sucrose.

High-fructose corn syrup is derived from the high-D.E. (92-96 D.E.) corn syrup. The corn syrup is treated with glucose isomerase which catalyzes the isomerization of glucose and fructose. The product contains a liquid mixture of glucose and fructose that is similar to sucrose in sweetness and chemical composition. Since the fructose comprises 42% of the total solids, these syrups are known as 42% HFCS. The 42% HFCS is pumped past a calcium or other cation affinity carrier, where it is further concentrated to yield the 90% HFCS. Blending the 90 and 42% HFCS gives the 55% HFCS. The high-fructose corn syrups have replaced sucrose in many food applications.

7.10 Sweet Proteins

Sweet proteins include monellin found in red berries (serendipity berries) of the tropical plant *Dioscoreophyllum cumminsii*, thaumatin isolated from the fruit of *Thaumatococcus danielli* in western Africa, and miraculin from miracle fruit, *Synsepalum dulcificum*. These proteins are about 100,000 times sweeter than sucrose on a molar basis and several thousand times on a weight basis.

Thaumatococcus I is a basic protein (pI = 12) of 22 kDa, consisting of a single polypeptide chain of 207 amino acids, with eight disulfide bonds and no histidine. The complete amino acid sequence of the protein and its tertiary structure are known. The protein consists of a very low α helix or random coil. The main domain (I) is a long β sheet folded into a flattened β barrel (■ Fig. 7.17). The β strands are arranged antiparallely except the N- and C-terminal strands, which are parallel to each other. The two other domains, II and III, are loops linked and stabilized by disulfide bonds [4, 17].

Monellin is composed of two polypeptide chains held by noncovalent bonds. Subunits I and II contain 50 and 44 amino acid residues, respectively. Monellin contains a single sulfhydryl group (in subunit II), and contrary to thaumatococcus I, no disulfide bond. The protein structure consists of a single antiparallel β sheet of five strands and a 17-residue α helix on the concave side of the β sheet. Only the undissociated protein is found to be sweet; subunits are not sweet. Chemically blocking the SH group results in the loss of sweetness.

Five homologous tripeptide sequences are found in monellin and thaumatococcus I. Four of these are located in domain I of thaumatococcus I, and one is in between domain I and II (■ Fig. 7.18). In monellin, three homologous sequences are in subunits I and two in subunit II [11]. The significance of this homology in sequences is not clear. There is no similarity of apparent importance in the backbone structure of the two proteins. It has been suggested that sweet proteins can bind to a secondary surface site in the T1R1-T1R3 receptor without entering the lobe 1-2 cleft. The absence of sequence or structural motifs common to sweet proteins has led to various proposals, including large hydrophobic surface that forms chemically and sterically complementary contact with the receptor. (Refer to the section on "Sweet Taste Receptors".)

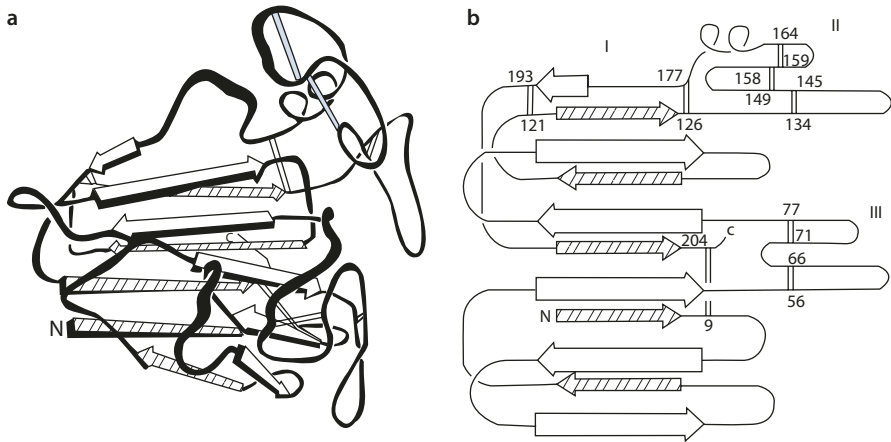


Fig. 7.17 a Backbone structure of thaumatin I. The main structure consists of two β sheets forming a flattened β barrel. Beta strands in the top sheet are clear, and those in the bottom sheet are shaded. Open bars represent disulfide bonds. b Topological structure of thaumatin I. There are two β sheets in the structure. The β strands of the top sheet are indicated by wide arrows. There are three domains of the protein and a crystallographic assignment of disulfide bonds shown in open bars (From de Vos et al. [4] with permission. Copyright 1985 National Academy of Science, courtesy of Prof. Sung-Hou Kim)

Thaumat	116	- Pro - Thr -	Thr - Arg - Gly	- Cys - Arg -
Monellin A	27	- Tyr - Lys -	Thr - Arg - Gly	- Arg - Lys -
Thaumat	126	- Cys - Ala -	Ala - Asp - Ile	- Val - Gly -
Monellin A	19	- Phe - Arg -	Ala - Asp - Ile	- Ser - Glu -
Thaumat	98	- Asp - Tyr -	Ile - Asp - Ile	- Ser - Asn -
Monellin B	4	- Glu - Ile -	Ile - Asp - Ile	- Gly - Pro -
Thaumat	99	- Tyr - Ile -	Asp - Ile - Ser	- Asn - Ile -
Monellin A	20	- Arg - Ala -	Asp - Ile - Ser	- Glu - Asp -
Thaumat	92	- Leu - Asn -	Gln - Tyr - Gly	- Lys - Asp -
Monellin B	26	- Ile - Gly -	Gln - Tyr - Gly	- Arg - Leu -

Fig. 7.18 Sequence similarities between thaumatin and monellin (Iyengar et al. [11])

References

1. Anonymous (1984) Magnasweet. Macandrews & Forbes Co., Camden
2. Assadi-Porter FM, Mailliet EC, Radeh JT, Quijada J, Markley JL, Max M (2010) Key amino acid residues involved in multi-point binding interactions between Bazein, a sweet protein and the T1R2-T1R3 human sweet receptor. *J Mol Biol* 398:584–599
3. Boch K, Lemieux RU (1982) The conformational properties of sucrose in aqueous solution: intramolecular hydrogen-bonding. *Carbohydr Res* 100:63–74
4. deVos AM, Hatada M, van der Wei H, Krabbendam H, Peerdeman AF, Kim S-H (1985) Three dimensional structure of thaumatin I, an intensely sweet protein. *Proc Natl Acad Sci U S A* 82:1406–1409
5. Hatada M, Jancarik J, Graves B, Kim SH (1985) Crystal structure of aspartame, a peptide sweetener. *J Am Chem Soc* 107:4279–4282
6. Homler BE (1984) Properties and stability of aspartame. *Food Technol* 38(7):50–55
7. Horn HE (1981) Corn sweeteners: functional properties. *Cereal Foods World* 26(5):219–223
8. Horowitz RM, Gentili B (1974) Dihydrochalcone sweeteners. In: Englert GE (ed) *Sweeteners*. AVI, Westport
9. Inglett GE (1969) Dihydrochalcone sweeteners – sensory and stability evaluation. *J Food Sci* 34:101–103
10. Inglett GE (1974) Sweeteners in perspective. *Cereal Sci Today* 19(7):259–261, 292–295
11. Iyengar RB, Smits P, van der Ouderaa F, van der Wei H, van Brouwershaven J, Ravesteyn P, Richters G, van Wassenaar PD (1979) The complete amino-acid sequence of the sweet protein Thaumatin I. *Eur J Biochem* 96:193–194
12. Leij F, Taneredit T, Temussi PA, Tonioto C (1976) Interaction of α -L-aspartyl-1-phenylalanine methyl ester with the receptor site of the sweet taste bud. *J Am Chem Soc* 98:6669–6675
13. Linko P, Saijonmaa T, Heikonen M, Kreula M (1980) Lactitol. In: Koivistonen P, Hyvonen L (eds) *Carbohydrate sweeteners in foods and nutrition*. Academic, New York
14. Masuda K, Koizumi A, K-i N, Tanaka T, Abe K, Misaka T, Ishiguro M (2012) Characterization of the modes of binding between human sweet taste receptor and low-molecular weight sweet compounds. *PLoS One* 7(4):e35380
15. Morini G, Bassoli A, Temussi PA (2005) From small sweeteners to sweet proteins: anatomy of the binding sites of the human T1R2-T1R3 receptor. *J Med Chem* 48:5520–5529
16. Nofre C, Tinti J-M (2000) Neotame: discovery, properties, utility. *Food Chem* 69:245–257
17. Ogata CM, Gordon PL, de Vos AM, Kim S-H (1992) Crystal structure of a sweet tasting protein thaumatin I at 1.65 Å resolution. *J Mol Biol* 228:893–908
18. Pautel F, Nofre C (1978) Correlation of chemical structure and taste in the cyclamate series and the steric nature of the chemoreceptor site. *Z Lebensm Unters-Forsch* 166:167–170
19. Shallenberger RS (1979) Taste and chemical structure. In: Chiba H (ed) *Proceedings of the fifth international congress of food science and technology*. Kodansha Ltd./Elsevier Scientific Publishing Co., Tokyo/New York
20. Shallenberger RS (1983) The chiral principles contained in structure-sweetness relations. *Food Chem* 12:89–107

Natural Toxicants

- 8.1 Cyanogenic Glycosides – 329**
 - 8.1.1 Chemical Structure – 329
 - 8.1.2 Mechanism of Toxicity – 330
- 8.2 Glycoalkaloids – 330**
 - 8.2.1 Chemical Structure – 330
 - 8.2.2 Mechanism of Toxicity – 331
- 8.3 Glucosinolates – 332**
 - 8.3.1 Chemical Structure – 332
 - 8.3.2 Mechanism of Toxicity – 333
- 8.4 Methylxanthines – 335**
 - 8.4.1 Metabolic Pathway – 335
 - 8.4.2 Mechanism of Toxicity – 337
- 8.5 Amino Acids, Peptides, and Proteins – 338**
 - 8.5.1 Nonprotein Amino Acids – 338
 - 8.5.2 Mechanism of Toxicity – 338
 - 8.5.3 Toxic Peptides – 340
 - 8.5.4 Proteins: Botulinum Neurotoxins – 341
- 8.6 Amines – 343**
 - 8.6.1 Metabolism – 345
- 8.7 Mycotoxins – 345**
 - 8.7.1 Chemical Structure – 345
 - 8.7.2 Mechanism of Toxicity – 346
- 8.8 Polycyclic Aromatic Hydrocarbons – 348**
 - 8.8.1 Chemical Structures – 348
 - 8.8.2 Mechanism of Toxicity – 349

8.9 Heterocyclic Amines – 349

- 8.9.1 Mutagenicity – 351
- 8.9.2 Mechanism of Toxicity – 351

8.10 Nitrosamines – 352

- 8.10.1 The General Chemistry of *N*-Nitrosation – 352
- 8.10.2 Inhibition of Nitrosation – 353
- 8.10.3 Nitrosamines in Cured Meat – 354
- 8.10.4 In Vivo Nitrosation – 355
- 8.10.5 Chemical Reactions of Nitrosamine – 356
- 8.10.6 Metabolic Mechanism – 357

References – 358

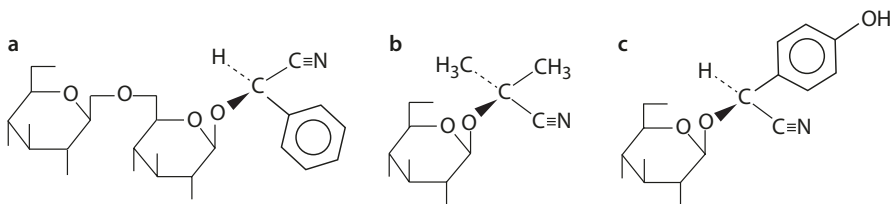
We consume a large number of toxic chemicals daily in our perfectly natural diet. The toxicants may be chemical constituents of the food itself, contaminants from microbial infestation, or degradation products from chemical changes during food processing (including cooking). Toxicants vary in chemical structures ranging from amino acids to proteins, from simple amines to alkaloids, and from phenolic compounds to their glycosides and derivatives. The biological effects of these chemicals are diverse and complex, and only a small percentage of these studies have been directed to the mechanism of action at the molecular level. A thorough understanding of the structural activity and biochemical mechanism of these naturally occurring toxicants is essential to ensure proper preparation and processing of foods. Caution must be taken to the fact that toxicity is determined not only by the chemical and biological properties of the compound but also the level and duration of exposure an individual is subjected to. While it is true that many food plants contain toxicants, the generally low level of these compounds combined with the variety of choices in human diet usually precludes the risk of intoxicification.

8.1 Cyanogenic Glycosides

Cyanogenic glycosides are known to be present in several plant species used for food. They are found in (1) seeds of bitter almond, apricot, and peach, (2) green leaves of sorghum, and (3) cassava and lima bean. Poisoning due to consumption of a large amount of cyanogenic glycosides is rare, since the edible portion of the plants mentioned above, in general, contains no glycosides. In the case of cassava, the edible tuber contains far less cyanogenic glycosides than the leaves. Proper processing, such as boiling, roasting, sundrying, soaking in water, or fermentation, eliminates most of the toxicity.

8.1.1 Chemical Structure

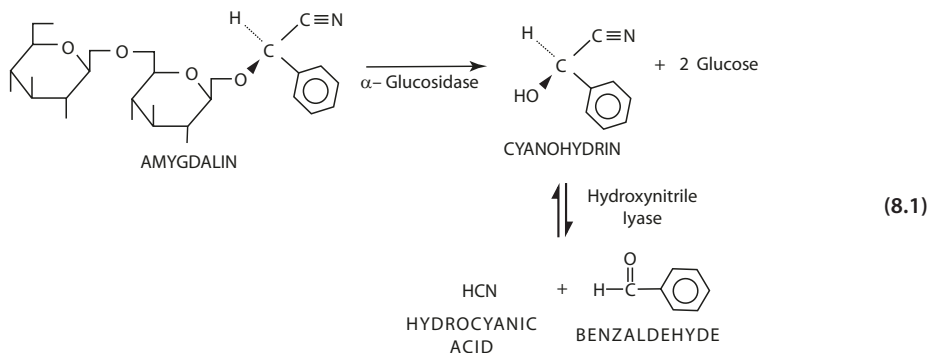
Cyanogenic glycosides consist of a sugar moiety (usually D-glucose or disaccharides such as gentiobiose) linked to a cyanohydrin. ■ Figure 8.1 shows the structure of some of the better known cyanogenic glycosides [9].



■ Fig. 8.1 Cyanogenic glycosides. a Amygdalin. b Linamarin. c Dhurrin

8.1.2 Mechanism of Toxicity

The toxicity of these glycosides is due to the release of hydrocyanic acid (HCN) caused by enzymatic actions. Two enzymes are involved: (1) the β -glucosidase, which hydrolyzes the glycoside into the corresponding cyanohydrin and sugar, and (2) the hydroxynitrile lyase, which dissociates the cyanohydrin to yield the corresponding aldehyde or ketone and HCN (Eq. 8.1) [10]. Both enzymes are found in plants containing cyanogenic glycosides. Reactions occur when the plant tissue is crushed, as in processing or injection, to allow the enzyme and substrate to come in contact.



The lethal level of HCN taken orally in a single dose in human is 0.5–3.5 mg/kg body weight. The primary action of HCN is the inhibition of cytochrome oxidase, resulting in the interruption of cellular respiration. Small amounts of HCN can be detoxified by the enzyme rhodanese in the liver (Eq. 8.2) [10]. The reaction requires a supply of thiosulfate and the product is thiocyanate, which is goitrogenic.

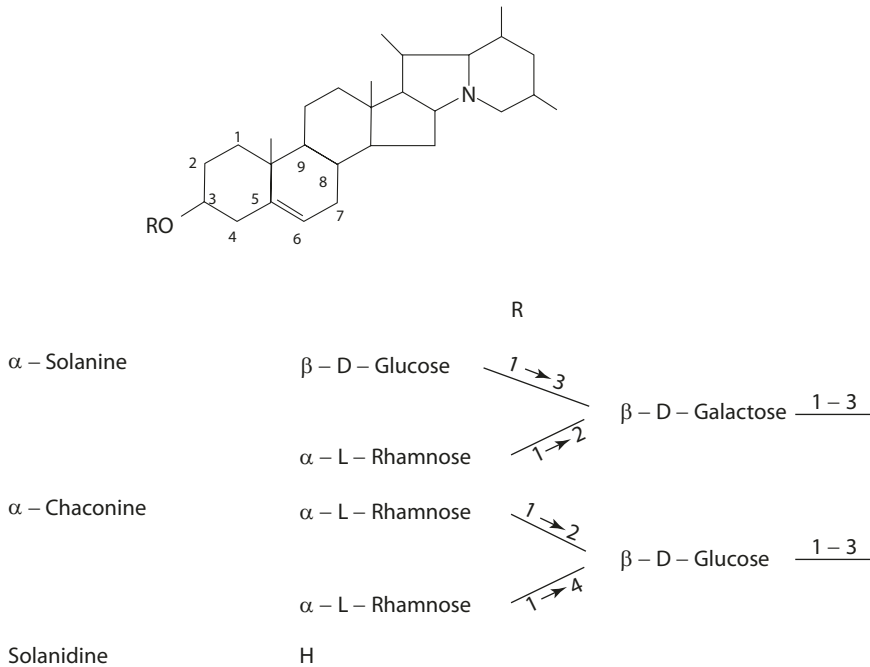


8.2 Glycoalkaloids

Glycoalkaloids are toxic compounds found in Solanaceae plants, notably the cultivated potato (*Solanum tuberosum* L.). There have been recorded cases of poisoning in humans involving the consumption of potato glycoalkaloids. Other Solanaceae plants also contain alkaloids, for example, tomatine and dehydrotomatine in tomatoes, and solasonine and solarmargine in eggplants.

8.2.1 Chemical Structure

Glycoalkaloids are alkaloids (the aglycone portion) glycosylated with a carbohydrate moiety. The two major glycoalkaloids found in potatoes are α -solanine (~40%) and α -chaconine (~60%). Both have the same alkaloidal aglycone, solanidine, but contain β -solutriose and β -chacotriose, respectively, as the carbohydrate moiety (■ Fig. 8.2).



■ Fig. 8.2 α -Solanine and α -chaconine

8.2.2 Mechanism of Toxicity

Potatoes usually contain glycoalkaloids at the level of approximately 10 mg total per 100 g fresh weight. The highest concentration is found in the peel and sprouts. Differences also exist among different cultivars with as high as 30 mg/100 g [37]. The synthesis of glycoalkaloids can be induced by light or mechanical damage. Injury such as cutting and slicing results in increasing synthesis of glycoalkaloids by the plant. "Greening" occurs when potato is exposed to light. Associated with the increasing accumulation of chlorophyll is an increase in glycoalkaloids. To safeguard against poisoning, potato cultivars with total glycoalkaloid levels over 20 mg/100 g are not commercially acceptable [29]. Since potato is a major staple food, greening can cause considerable loss to the potato industry.

Glycoalkaloids are strong inhibitors of cholinesterase and the cause of neurological disorder symptoms. Other toxic action includes disruption of the cell membranes in the gastrointestinal tract. Absorption of glycoalkaloids is usually enhanced by alkaline pH conditions where binding with sterols in cell membranes causes extra disruption [32]. Lethal doses for humans range from 3 to 6 mg/kg body weight, although susceptibility varies considerably among individuals. Doses of greater than 2 mg/kg are normally considered toxic. Symptoms of poisoning include vomiting, diarrhea, abdominal pain, apathy,

weakness, and unconsciousness. Birth abnormalities including cranial defects, neural defects, high fetal mortality rate, and resorption of fetus have been implicated in the consumption of high dose of glycoalkaloids in animal studies.

8.3 Glucosinolates

Glucosinolates occur predominantly in cruciferous plants (order Brassicales, genus *Brassica*). The concentrations of glucosinolate found in some common vegetables are presented in [Table 8.1](#) [15].

8.3.1 Chemical Structure

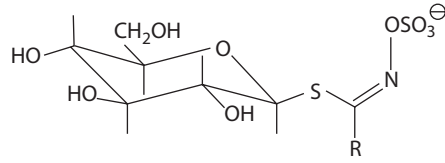
Glucosinolates consist of a β -thioglucose, a sulfonate oxime, and a side chain R ([Fig. 8.3](#)). The side chain R and the *O*-sulfonate group have a *trans*-configuration. Numerous glucosinolates have been identified in plants. Glucosinolates are classified into (1) aliphatic, (2) aromatic, and (3) indole glucosinolates, based on the variable side chain of the basic chemical structure that results from the amino acid precursor. More than half of the

Table 8.1 Glucosinolate content in edible parts of plants

Plants	Glucosinolate ($\mu\text{g/g}$ vegetable)	
	Range	Mean
Cabbage		
Red	410–1090	760
White	260–1060	530
Chinese	170–1360	540
Cauliflower	270–830	480
Turnip	210–600	420
Radish		
Red	90–130	110
White	70–210	140
Mustard		
White	45,100–82,300	64,100
Black	32,800–59,800	46,300

From Fenwick et al. [15]

■ **Fig. 8.3** General structure of glucosinolate



■ **Table 8.2** Various glucosinolates in vegetables

Common name	R group	Occurrence
Sinigrin	Allyl-	Cabbage, brussels sprouts, cauliflower, mustard greens
Glucobrassicin	3-Indoymethyl-	Cabbage, brussels sprouts, cauliflower, broccoli
Progoitrin	(R)-2-Hydroxy-3-butenyl	Cabbage, Chinese cabbage, turnips, rutabaga
Gluconapin	3-Butenyl-	Cabbage, Chinese cabbage, brussels sprouts, cauliflower, mustard spinach
Neoglucobrassicin	N-Methoxy-3-inodylmethyl	Brussels sprouts, cauliflower, broccoli, rutabagas, radishes
Gluconasturtiin	2-Phenylethyl-	Cabbage, Chinese cabbage, brussels sprouts, cauliflower, broccoli, mustard greens, mustard spinach, turnips
Glucotropaeolin	Benzyl-	Mustard greens, cabbage, mustard spinach
Glucobrassicinapin	4-Pentenyl-	Chinese cabbage, mustard spinach, mustard greens
Glucoalyssin	4-Methylsulfinylbutyl-	Cabbage, brussels sprouts, broccoli
Glucoiberin	3-Methylsulfinylpropyl-	Cabbage, brussels sprouts, cauliflower

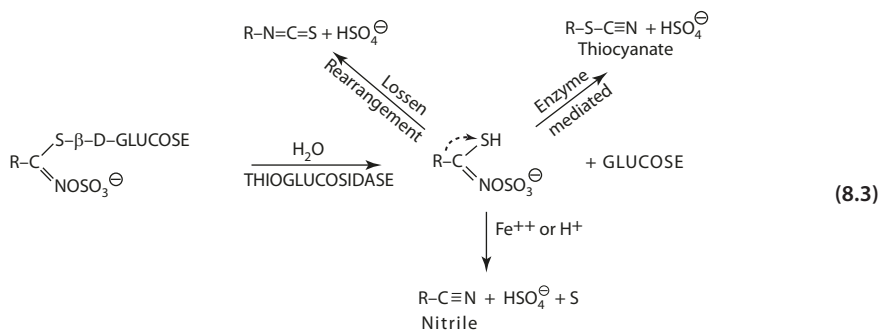
From van Etten et al. [45]

glucosinolates identified are aliphatic. Some common glucosinolates found in vegetables are listed in ■ Table 8.2 [45].

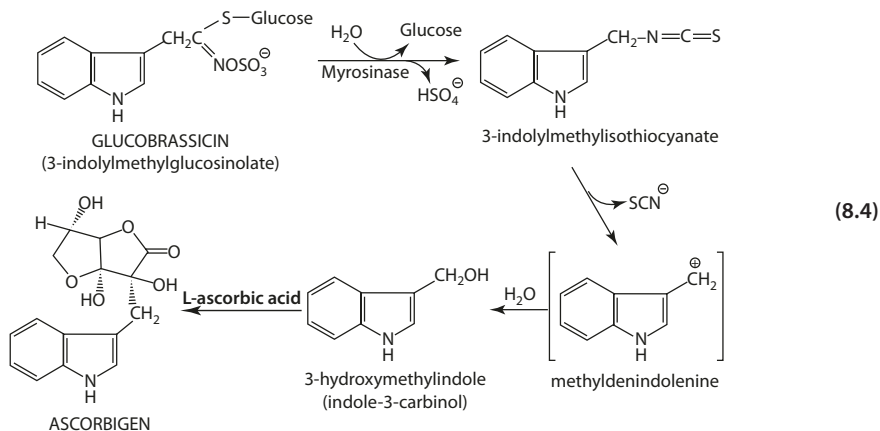
8.3.2 Mechanism of Toxicity

Hydrolysis of glucosinolates is catalyzed by thioglucoside glucohydrolase (EC 3:2:3:1, also commonly known as myrosinase) located separately from the substrate in intact tissues. The reaction occurs only when the plant tissue is crushed. The enzyme exhibits optimum activity near neutral pH and is activated markedly by the addition of ascorbic acid.

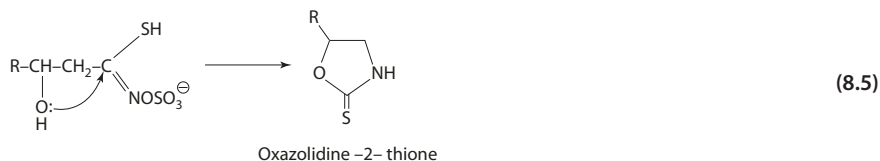
The unstable aglycone produced from enzymatic hydrolysis forms predominantly isothiocyanates in a process similar to the Lossen rearrangement [4]. Thiocyanates and nitrile may also form to a limited extent (Eq. 8.3). Thiocyanate lacks the pungent flavor of isothiocyanate and has also been implicated in the off-flavors in milk. The formation of nitrile is enhanced by acidic pH and metal ion.



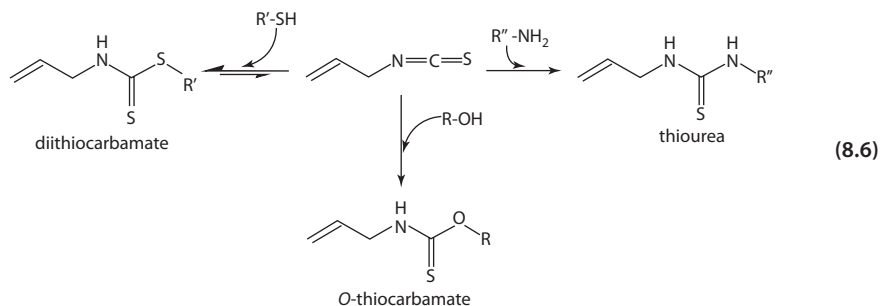
Indole glucosinolates (e.g., glucobrassicin) form isothiocyanates that degrade to 3-hydroxymethylindole. The product condenses or, in the presence of ascorbic acid, forms a complex compound, ascorbigen (Eq. 8.4). The aglycone from glucosinolates containing a β -hydroxyl group (e.g., 2-hydroxy-3-butenyl glucosinolate) can cyclize to the corresponding oxazolidine-2-thione (Eq. 8.5) [15].



Isothiocyanate is metabolized *in vivo* to thiocyanate, which is a goitrogen. The goitrogenic effect of thiocyanate, resulting from its competition with iodine, is shown only under iodine-deficient diets. Oxazolidine-2-thione, however, acts by interfering with the synthesis of thyroxine. The antithyroid effect is not alleviated by supplementing with iodide. The compound 5-vinylloxazolidine-2-thione present in rape, rutabaga, and cabbage seeds is one of the potent goitrogens reported.



Isothiocyanates contain a highly electrophilic carbon center and readily react with nucleophiles that are present in most foods in the form of amino acids, peptides, and proteins [19]. Functional substituents such as hydroxyl, amino, and thiol groups, which in their base forms (i.e., at high pH values), react with isothiocyanates via nucleophilic addition reactions, forming *O*-thiocarbamates, thiourea derivatives, and dithiocarbamates, respectively (Eq. 8.6). These products may further undergo cyclization and cleavage to smaller molecules. The reactivity of the nucleophilic addition reaction increases with increasing basicity of the nucleophiles, side chain structure (e.g., electron-withdrawing substituents), and concentration of the isothiocyanate.



8.4 Methylxanthines

The best known methylxanthine is caffeine, with the chemical structure 1,3,7-trimethylxanthine. The familiar sources of caffeine are coffee, cocoa beans, cola nuts, and tea. The amounts of caffeine present in various beverages, including soft drinks, are shown in Table 8.3. Although coffee contains only caffeine, tea and cocoa contain other methylxanthines besides caffeine, notably theophylline and theobromine (Fig. 8.4).

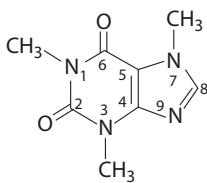
8.4.1 Metabolic Pathway

More than 90% of the caffeine ingested is absorbed rapidly from the gastrointestinal tract, and its concentration in the blood plasma rises to a peak level within 30 min. Once in the blood stream, caffeine effectively penetrates through all body tissues. Because of the high permeation of caffeine through biological membranes, caffeine must be transformed into metabolites for effective excretion and elimination from the body.

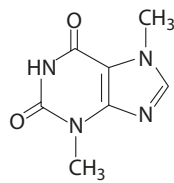
■ **Table 8.3** Caffeine contents in various beverages

Type of drink	Caffeine (mg)
Coffee (5-oz cup)	
Drip method	110–150
Precoated	64–124
Instant	40–108
Decaffeinated	2–5
Tea (5-oz cup)	
1 min brew	9–33
3	20–46
5	20–50
Instant	12–28
Iced tea	22–36
Cocoa	
Mix	6
Milk chocolate (1 oz)	6
Baking chocolate (1 oz)	35
Soft drink (12 oz)	
Colas and pepper type	30–60

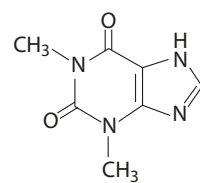
From Roberts and Barone [31]



Caffeine



Theobromine

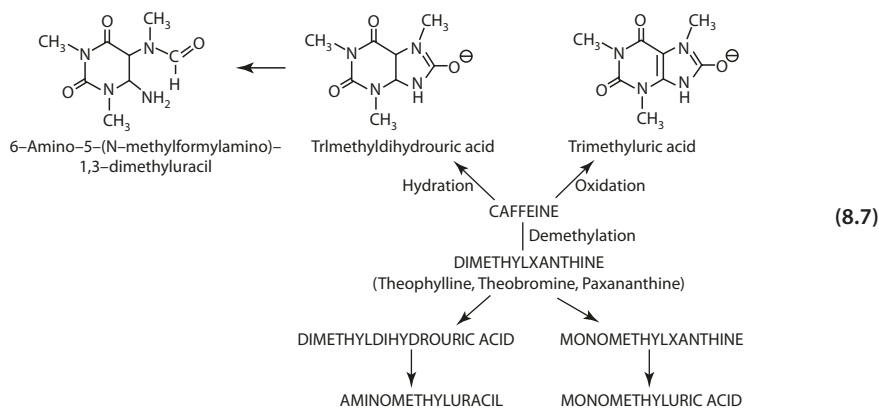


Theophylline

■ **Fig. 8.4** Some common methylxanthines

The half-life of caffeine (time required for the body to eliminate one-half of the plasma caffeine) varies from hours to days, depending on age, sex, medication, and health conditions. Newborns lack the many enzymes required to metabolize caffeine, and the half-life is 3–4 days. Smokers have a shorter half-life (3 h) than nonsmokers (3–7 h). Pregnant women require 18 or more hours, and patients with liver problem also have a long half-life [44].

Metabolically, caffeine undergoes (1) initial demethylation to the dimethylxanthines—theophylline, theobromine, and paraxanthine (1,7-dimethylxanthine); (2) oxidation at C8 to form 1,3,7-trimethyluric acid; and (3) hydration and ring cleavage at the C8–N9 bond to form dimethyluracil (Eq. 8.7). The dimethylxanthines are further demethylated and metabolized via reactions similar to (2) and (3) [42].

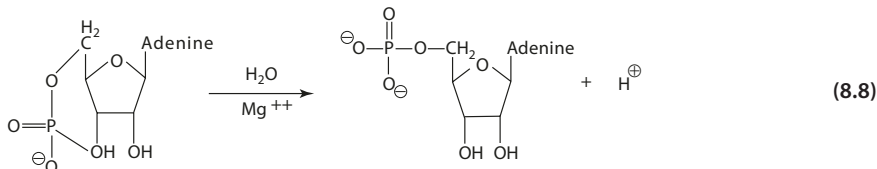


8.4.2 Mechanism of Toxicity

Caffeine is listed in the GRAS list and widely used in soft drinks and medicine, although it is generally considered to be a stimulant at low doses. One cup of coffee, amounting to the consumption of 1–2 mg/kg body weight, gives a peak plasma level of 1–10 μM . Excessive consumption ($>50 \mu\text{M}$) leads to symptoms of "caffeinism"—anxiety, restlessness, sleep latency, diarrhea, muscular tension, and heart palpitation. The oral LD_{50} for humans is 150–200 mg/kg (0.75–1 mM plasma concentration), which amounts to a single consumption of over 75 cups of strong coffee [1].

At the molecular level, methylxanthines are known to inhibit the enzyme cyclic adenosine 3,5-monophosphate (cAMP) phosphodiesterase, which catalyzes the hydrolysis of cAMP (Eq. 8.8). Cyclic AMP mediates the action of many hormones, for example, calcitonin, epinephrine, glucagon, norepinephrine, vasopressin, thyroid-stimulating hormone, lipoprotein, parathyroid hormone, and corticotropin. However, the concentrations required to inhibit phosphodiesterases are substantially higher than the dose levels for neurophysiological responses.

The effect of methylxanthines may also be attributed to their involvement in blocking certain receptor sites on cell membranes for adenosine [39]. Since endogenous adenosine is generally inhibitory on neurophysiological reactions, it is postulated that methylxanthines exert a stimulatory action by blocking the receptor sites.



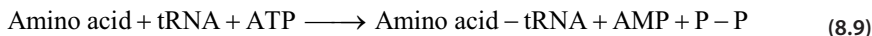
8.5 Amino Acids, Peptides, and Proteins

8.5.1 Nonprotein Amino Acids

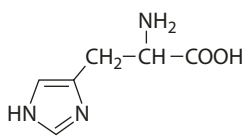
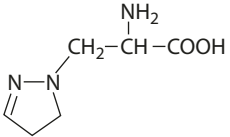
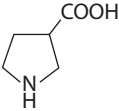
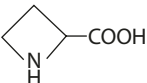
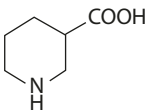
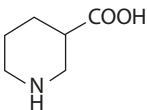
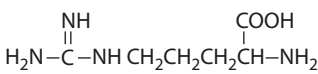
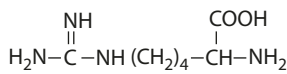
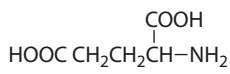
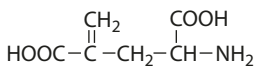
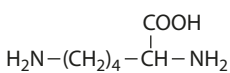
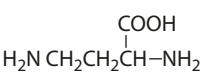
There are more than 250 nonprotein amino acids found in plants and microorganisms. Many of these nonprotein amino acids are structurally related to the protein amino acids. They are usually homologs, isomers, or products of substitution of protein amino acids. The structural relationships between a few protein and nonprotein amino acids are illustrated in [Fig. 8.5](#).

8.5.2 Mechanism of Toxicity

Not all nonprotein amino acids are toxic. For example, homoarginine is enzymatically converted to lysine and urea in rat liver. The mechanism of toxicity of nonprotein amino acids [3] is usually due to (1) competition with structurally similar protein amino acids or enzymes, forming inactivated complexes; (2) incorporation into proteins, resulting in functionally defective proteins; and (3) interference with protein synthesis in the transfer of protein amino acids to transfer RNA (Eq. 8.9).

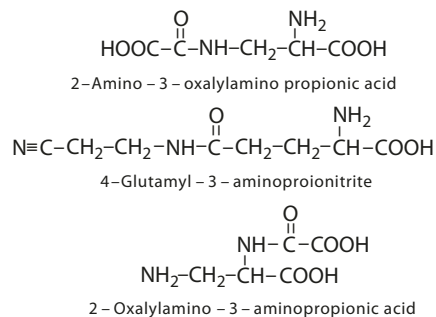


Seeds of the legume *Lathyrus sativus* (grass pea) are included in diets in certain areas, especially during drought famine. *Lathyrus* species include toxic symptoms known as lathyrism, characterized by skeletal defects (osteolathyrism) and damage in the nervous system (neurolathyrism). The neurological effect is attributed to the oxalyldiaminopropionic acids ([Fig. 8.6](#)) present in the legume. One of the ODAPs, γ -glutamylaminopropionitrile, has been shown to inhibit the enzymes for the crosslinkages in collagen synthesis. Another compound, 2,4-diaminobutyric acid, has been found to be toxic by inhibiting the enzyme ornithine transcarbamylase. Disruption of the urea cycle induces ammonia toxicity.

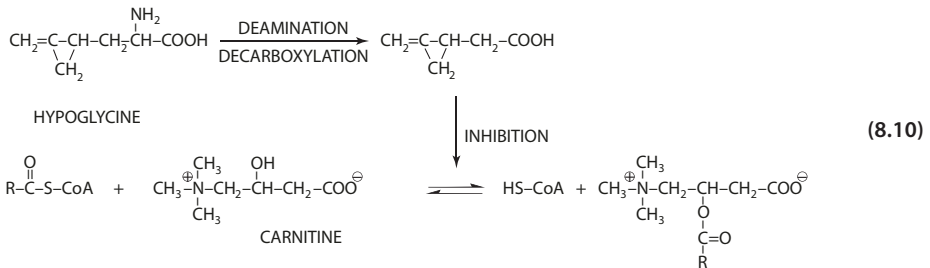
		Occurrence
		Cucurbitaceae (Seed)
β-Pyrazol-1-ylalane		
		Liliaceae
Azetidine - 2 - carboxylic acid		
		Legumes
Pipecolic acid		
		Lathyrus sp.
Homoarginine		
		Peanut, Turnip
γ-Methyleneglutamic acid		
		
α,γ-Diaminobutyric acid		

■ Fig. 8.5 Structural relationships between protein and nonprotein amino acids

■ Fig. 8.6 Oxalyldiamino-propionic acids



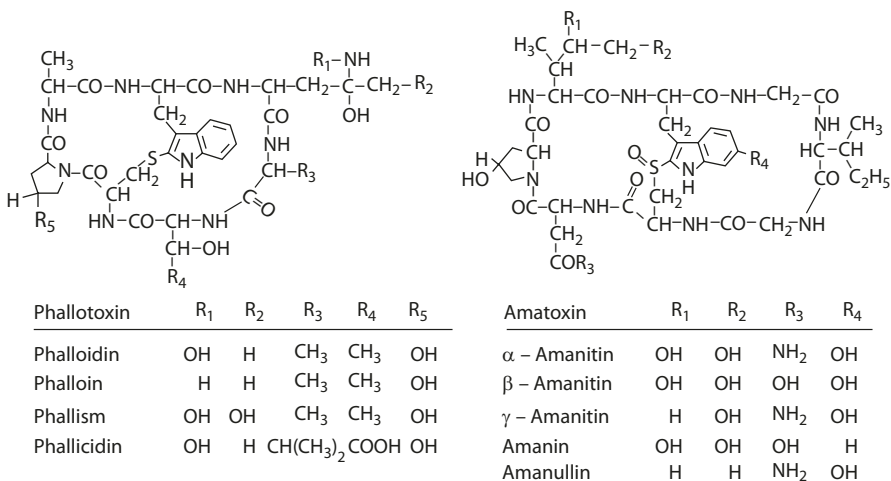
Unripe fruit of tropical tree ackee (*Blighia sapida*) contains hypoglycine A (β -methylene cyclopropylalanine), which causes severe vomiting and hypoglycemia. In the body, hypoglycine A is metabolized to α -(methylene cyclopropyl)acetate. The metabolite interferes with the transacylation reaction in which the long-chain fatty acid CoA molecules are transferred to carnitine to form acyl carnitine (Eq. 8.10). The reaction is crucial to the effective oxidation of long-chain fatty acids, since only acyl carnitine can diffuse across the mitochondrial membrane to the matrix where β -oxidation takes place. Hypoglycine A, therefore, interrupts β -oxidation so that glycogen has to be metabolized for energy instead. The resulting depletion of carbohydrate causes hypoglycemia.



8.5.3 Toxic Peptides

The two notable toxic peptides are the phallotoxins and amatoxins of wild mushroom (genus *Amanita*). Both are cyclic peptides; the former contains a thioether bridge and the latter a sulfoxide group (■ Fig. 8.7).

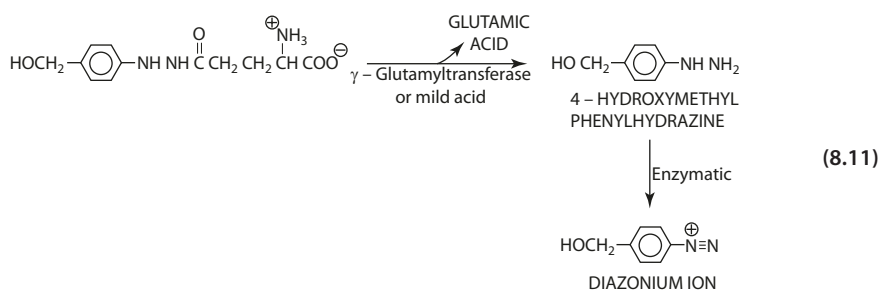
Phallotoxins inhibit the conversion of F-actin to G-actin in liver cells, resulting in irreversible polymerization of actin filaments. Amatoxins cause fragmentation of the



■ Fig. 8.7 Phallotoxins and amatoxins (From Wieland [47])

nucleoli of liver cells. Alpha-amanitin has been shown to inhibit DNA-dependent RNA polymerase II. Fragmentation begins 15 h after administration of α -amanitin to rats, while the cytological effects of phallotoxin occurs in 1–2 h [47]. Symptoms of toxicity include fatty generation, acute liver dystrophy, and centrilobular necroses.

The commercial cultivated mushrooms, although they contain no phallotoxins or amatoxins, are found to contain up to 0.04% fresh weight of agaritine (β -N[γ -L(+)-glutamyl]-4-hydroxymethyl-phenylhydrazine). The enzyme γ -glutamyltransferase, found in mushroom sporophores, hydrolyzes agaritine to L-glutamate and 4-hydroxymethyl-phenylhydrazine (Eq. 8.11), which is further converted to the 4-hydroxymethyl-benzene-diazonium ion. Hydrolysis of agaritine with hot, dilute acid also results in the liberation of L-glutamate and the hydrazine [18, 33]. The diazonium ion is chemically reactive that can couple with aromatic compounds to form azo derivatives.

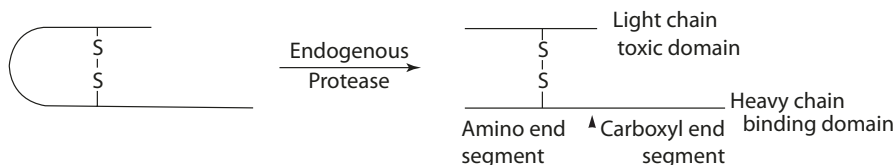


8.5.4 Proteins: Botulinum Neurotoxins

The neurotoxins found in *Clostridium botulinum* are proteins. There are seven distinct toxins, types A, B, C, D, E, F, and G, produced by various strains of *C. botulinum*. Serotypes A, B, and E are known common causes of human botulinum. Most strains produce one toxin serotype, but a single bacterium may also be capable of producing multiple neurotoxin types. Botulinum toxins cause neuromuscular paralysis by blocking neurotransmitter release at the neuromuscular junction.

■ Structure of the Protein Molecule

Botulinum neurotoxins are synthesized intracellularly as an inactive precursor, a single polypeptide of 150 kDa. The molecule is "nicked" by an endogenous protease to yield an active double-chain molecule composed of a heavy chain (100 kDa) and a light chain (50 kDa) linked by an intrachain disulfide bond. (■ Fig. 8.8) [35]. The light chain (Lc) is



■ Fig. 8.8 Activation of *C. botulinum* neurotoxin

the catalytic domain, containing the catalytic zinc atom in a conserved zinc-binding motif characteristic of zinc-dependent proteases. The heavy chain (Hc) contains two domains of roughly equal size: The C domain (receptor-binding domain) binds to the target cell membrane as the initial step for internalization. The N-terminal (translocation) domain forms ion channels (pores) in the lipid bilayer to facilitate translocation of the catalytic domain into the neuron cytosol.

■ ■ Mechanism of Toxicity

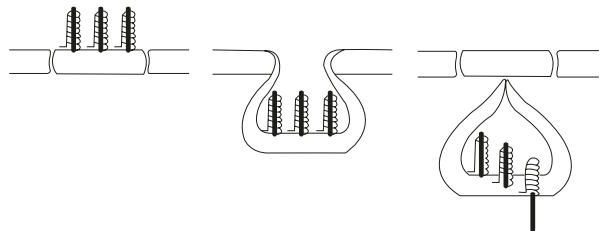
The botulinum toxin must penetrate into the cholinergic nerve cell before it can exert its blocking effect on the release of acetylcholine. The initial step of binding of the toxin molecule (directed by the Hc C domain) in a dual receptor model involves (1) a polysialoganglioside receptor site and (2) a protein receptor site, located closely on the plasma membrane of the cholinergic nerve [25].

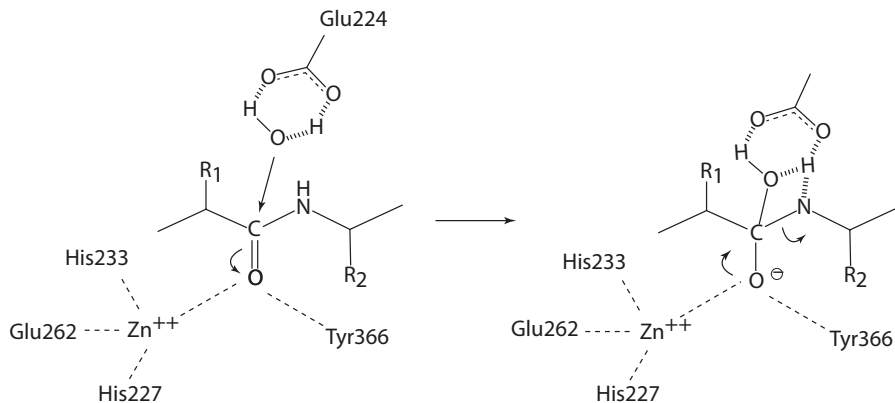
A membrane translocation occurs by receptor-mediated endocytosis. The endocytic vesicle (for receptosome) migrates toward the lysosome, with a gradual buildup of pH gradient across the membrane. The fall in pH causes a conformational change in the toxin molecule, allowing the amino-terminal segment of the heavy chain to penetrate across the membrane, creating a channel for the light chain to enter into the cytoplasm (■ Fig. 8.9) [36].

Activation of the toxin occurs with the reduction of the intrachain disulfide bond (Cys430-Cys454 in botulinum A) rendering the light chain (Lc) free to enter the neuron cytosol. The Lc disrupts neurotransmission by cleaving one or more components of the synaptic vesicle docking-fusion complex known as soluble *N*-ethylmaleimide-sensitive factor attachment protein receptor (SNARE) complex. Synaptic SNARE proteins play a critical role in forming a protein bridge to promote membrane fusion and subsequently vesicle exocytosis of neurotransmitters into the synapse junction. Cleavage of SNARE proteins, therefore, causes a sustained inhibition of the exocytosis synaptic activity (blockade of neurotransmitter release). The cleavage occurs in a highly specific manner, with different botulinum types acting on different types of SNARE proteins.

The catalytic mechanism is similar to that of thermolysin [16, 34]. In the botulinum neurotoxin (serotype A as the example), the active site zinc ion assumes tetrahedral coordination, with two His residues (in the Zn²⁺ binding motif HisGluXXHis), a water

■ Fig. 8.9 Schematic representation of *C. botulinum* toxin entry into cell by receptor-mediated endocytosis (From Simpson [36] with permission. Copyright 1986 Annual Reviews Inc.)





■ Fig. 8.10 Proposed catalytic mechanism of botulinum neurotoxin (From Silvaggi et al. [34])

molecule hydrogen-bonded to the Glu residue of the motif, and a fourth ligand provided by another Glu residue (■ Fig. 8.10)

1. In the enzyme-substrate complex, the zinc ion interacts with the carbonyl oxygen in the P1 position of the scissile peptide bond, causing polarization of the C–O bond. Hydrogen bonding provided by the active site Tyr366 further assists the polarization.
2. The carbonyl carbon becomes susceptible to nucleophilic attack by the water molecule, which is activated by hydrogen bonding to the Glu224 residues of the HisGluXXHis motif.
3. The resulting tetrahedral intermediate involves residues Glu350 and Arg362 in stabilization of the negative charged oxyanion. Peptide (C–N) bond cleavage occurs by a proton transfer from the same nucleophilic water to the scissile peptide bond nitrogen. The protonated amine serves as the leaving group in the breakdown of the peptide bond.

Botulinum toxins are protected against denaturation and proteolysis in the gastrointestinal environment upon ingestion. The toxins are synthesized as large high-molecular-weight progenitor-toxin complexes (PTCs), in which the toxin is noncovalently associated with nontoxic neurotoxin-associated proteins (nontoxic non-hemagglutinins and hemagglutinins) [24]. The formation of PTCs provides the protection for the botulinum protein. Also, the association of these proteins is pH dependent, allowing the release of the toxin upon entry into the bloodstream.

8.6 Amines

Amine compounds are naturally occurring in food plants at relatively high levels. Foods subjected to bacterial contamination or fermentation processes may also have certain amino acids converted to amines that are vasoactive. Most amines found in animal products are the result of bacterial action, since natural amines are rarely found in significant concentrations in animal tissues.

■ **Table 8.4** Content of some common amines found in fruits ($\mu\text{g/g}$)

Fruit	Serotonin	Tyramine	Dopamine
Banana	28	7	8
Tomato	12	4	0
Plum (red)	10	6	0
Avocado	10	23	4–5
Pineapple	20	–	–
Orange	0	10	0

From Lovenberg [26]

■ **Table 8.5** Amines from bacterial action

Product	Tyramine ($\mu\text{g/g}$)	Histidine ($\mu\text{g/g}$)
Cheese (fermented aged)	0–2200	0–2500
Beer and ale	1.8–11.2	–
Wine	0–25	0.3–30
Yeast extract	0–2250	250–2830
Fish	0–470	10–300
Meat extract	95–304	–
Beef liver (stored)	274	65

From Smith [38]

The commonly known amines found in food plants include tyramine, dopamine, and serotonin (5-hydroxytryptamine) (■ Table 8.4) [26]. All the amines are biosynthesized by the decarboxylation and, in some, hydroxylation of the corresponding amino acid precursors.

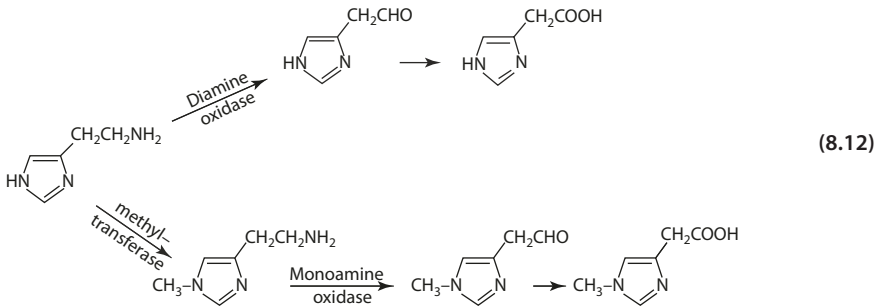
The amines tyramine and histamine found in cheese, dairy products, alcoholic beverages, and putrefying meat products (■ Table 8.5) result from the actions of bacteria containing amino acid decarboxylases that can convert amino acids to amines. Histamine, formed from bacterial decarboxylation of histidine, has caused food poisoning in fish consumption. *Enterobacteria*, especially *Proteus* species, are histamine-producing bacteria found in fish. *Proteus morgani* and *Enterobacter aerogenes* are among the known examples.

Histamine is a vasodilator that causes characteristic skin flushing. Less common symptoms include vomiting, nausea, diarrhea, and hypertension. Fish also contains trimethylamine, formed from the breakdown of choline and carnitine (trimethylalkyammonium salts) by bacteria in the fish gut. (Refer to ► Chap. 6, section on "Meat Flavor".)

8.6.1 Metabolism

Under normal conditions, amines are rapidly detoxified once absorbed into the body. The mitochondrial amine oxidase catalyzes the oxidative deamination of amines to the corresponding aldehyde, which is relatively inactive.

For example, histamine is metabolized by diamine oxidase to imidazole acetaldehyde and the acid. Alternatively, the histamine may be *N*-methylated by the enzyme histamine-*N*-transferase before conversion to *N*-methylimidazole acetic acid by monoamine oxidase (Eq. 8.12) [43].



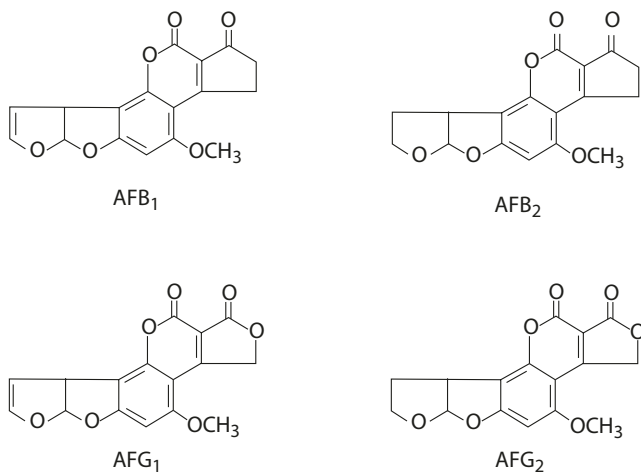
8.7 Mycotoxins

Mycotoxins are toxic fungal metabolites that may contaminate peanuts, rice, soybean, wheat, barley, corn, sorghum, cottonseed meal, and dairy products. Many known mycotoxins are attributed to *Aspergillus* and *Penicillium* species.

8.7.1 Chemical Structure

The most extensively studied aflatoxins are a group of toxic metabolites of *Aspergillus flavus* and *parasiticus*. These are furanocoumarin compounds, consisting of a coumarin nucleus fused to a furan and lactone. The two major types are aflatoxins B and G (► Fig. 8.11).

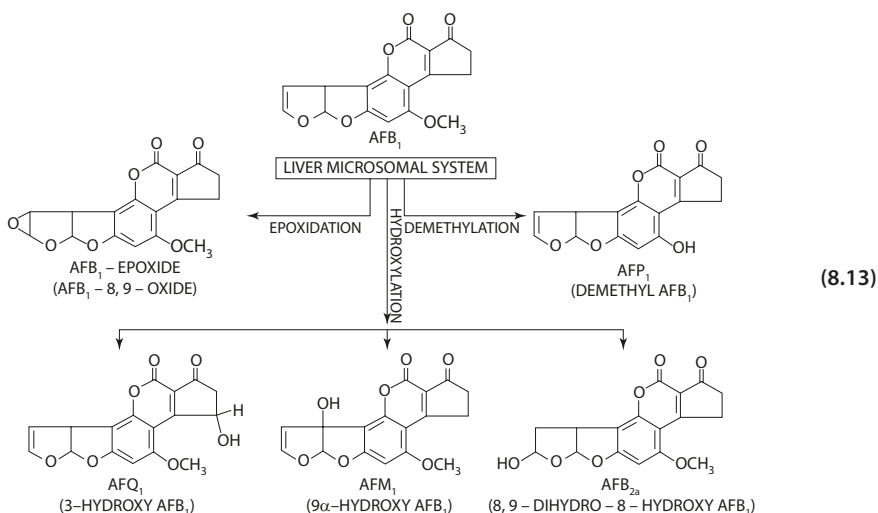
■ Fig. 8.11 Chemical structures of aflatoxins

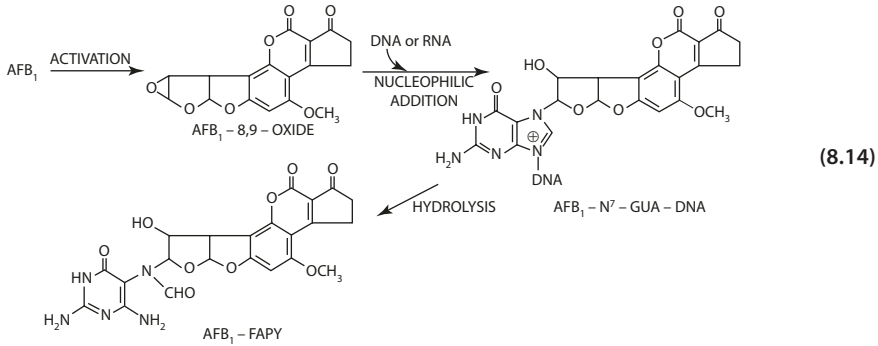


8.7.2 Mechanism of Toxicity

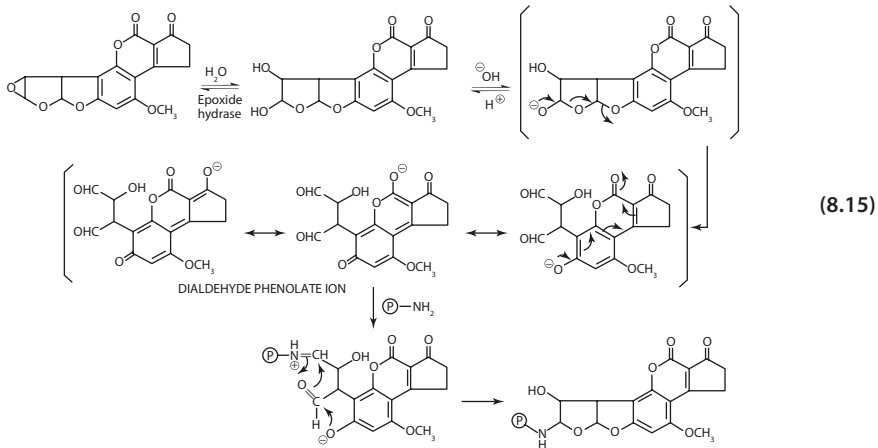
Aflatoxin contamination is widespread in many foods and has prompted numerous investigations into every aspect of aflatoxin B₁, the most notorious mycotoxin in the group, which is known to cause liver cancer (oral LD₅₀ for rat = 5.5–7.5 mg/kg).

Aflatoxin B₁ is biologically metabolized to form various products [41]. Microsomal detoxification occurs when aflatoxin B₁ undergoes hydroxylation or demethylation resulting in aflatoxin M₁, Q₁, B_{2a}, and P₁ (Eq. 8.13). Aflatoxin B₁ also undergoes epoxidation to the reactive aflatoxin B₁-8,9-oxide, which forms covalent conjugates with DNA and proteins (Eq. 8.14). The major aflatoxin-DNA conjugate has been identified to be 8,9-dihydro-8-(*N*⁷-guanyl)-9-hydroxy-aflaxin B₁ (AFB₁-*N*⁷-GUA). In vivo kinetic studies show that AFB₁-*N*⁷-GUA undergoes a rapid decrease in the liver due to the spontaneous hydrolysis of the imidazole ring. One of the identified products, 8,9-dihydro-8-(*N*⁵-formyl-2',5',6'-triamino-4'-oxo-*N*⁵-pyrimidyl)-9-hydroxy-aflatoxin B₁ (AFB₁-FAPY), has been shown to be the persistent DNA conjugate that accumulates in the liver [12].

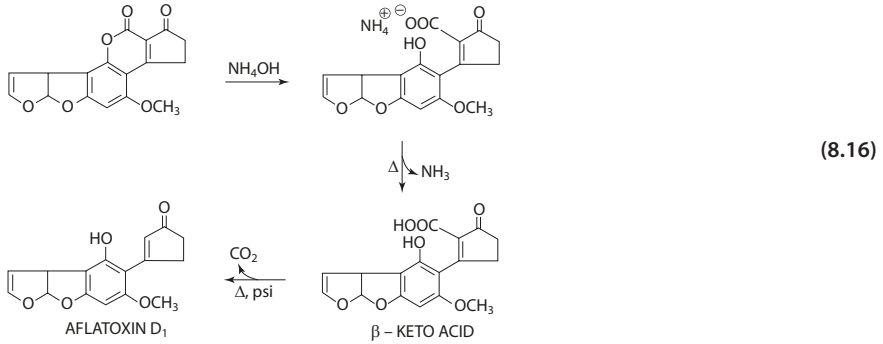




The aflatoxin B_1 -epoxide may also undergo hydrolysis to AFB_1 -8,9-dihydrodiol. The product is a dialdehyde phenolate ion, which is stabilized by resonance (Eq. 8.15). The 8-hydroxy aflatoxins (AFB_{2a} , AFG_{2a}) also can rearrange to yield dialdehyde phenolate ions [30]. The aldehyde groups in the dialdehyde phenolate ion can form Schiff base with protein amino groups.



Cows fed with aflatoxin B_1 -contaminated feeds produce milk containing aflatoxin M_1 . Although less toxic, aflatoxin M_1 is still considered undesirable. Various treatments have been studied to remove aflatoxin. Roasting removes 60–70% of aflatoxin in peanuts, although heat treatment of milk does not cause a decrease in aflatoxin M_1 . Chemicals such as hydrogen peroxide, sodium hypochlorite, calcium hydroxide, formaldehyde, and lime can destroy aflatoxin. The detoxification process for cattle and chicken feeds in practice is by ammonium treatment under high temperature and pressure (Eq. 8.16). Treatment with ammonia rapidly opens the lactone ring to yield the open-ring salt. Loss of ammonium results in the formation of the α -keto acid, which undergoes decarboxylation to aflatoxin D_1 or decomposition to a benzofuran [28].



8.8 Polycyclic Aromatic Hydrocarbons

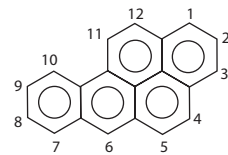
Carcinogenic polycyclic aromatic hydrocarbons (PAHs) are known to form in grilled meat products. These PAH compounds are formed in the smoke and adsorbed on the meat when fats are pyrolyzed by high temperature of hot coals.

The concentration of PAH depends on the fat content in the meat, the grilling process (contact of melted fat drips with the heat source), and the heat source (amount of smoke formed) and may vary from undetectable amounts to as high as 50 ppm benzo[*a*]pyrene in some cases. PAHs have been reported in sausages, beef, pork, lamb, turkey, chicken, hamburgers, and bacon [17].

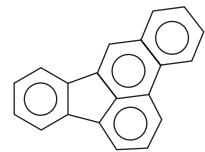
8.8.1 Chemical Structures

The four PAHs commonly detected in grilled meat products are benzo[*a*]pyrene, benzo[*b*]fluoranthene, benzo[*a*]anthracene, and chrysene (■ Fig. 8.12).

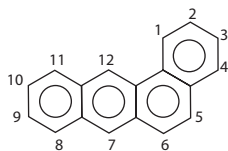
■ Fig. 8.12 Polycyclic aromatic hydrocarbons



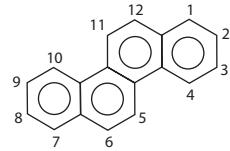
Benzo [*a*] pyrene



Benzo [*b*] fluoranthene



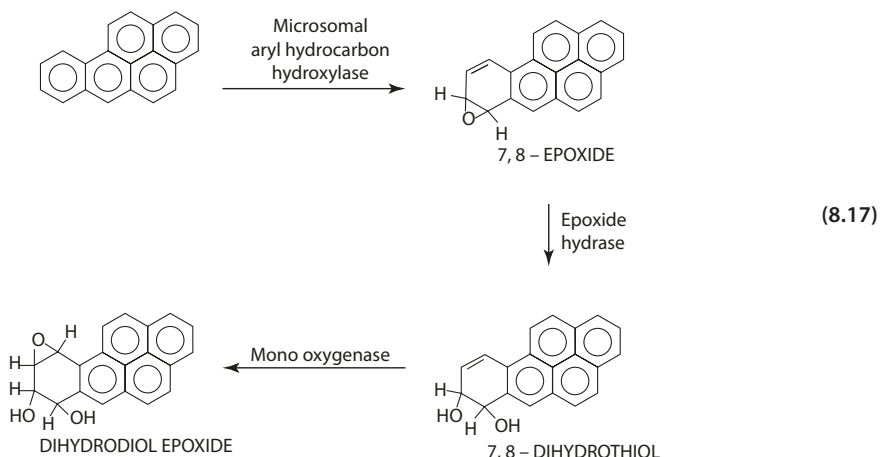
Benzo [*a*] anthracene



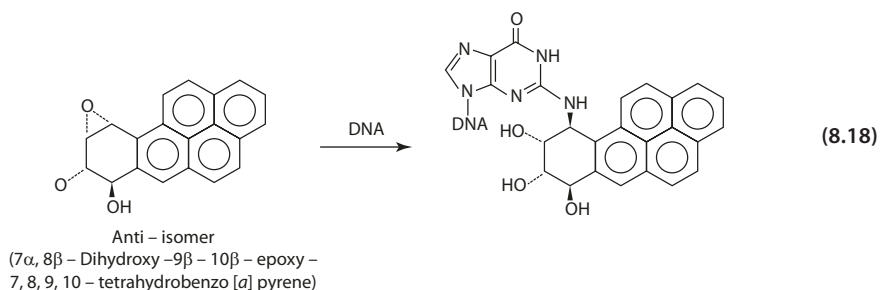
Chrysene

8.8.2 Mechanism of Toxicity

Polycyclic aromatic hydrocarbons undergo metabolic activation to reactive intermediates that are responsible for their carcinogenic effects [22]. Benzo[*a*]pyrene is converted to the 7,8-epoxide (7,8-dihydro-7,8-epoxybenzo[*a*]pyrene). The enzyme aryl hydrocarbon hydroxylase catalyzing the conversion is located in the microsomal fraction and requires NADPH. The epoxide product is further converted to the dihydrodiol (8-dihydro-7,8-dihydroxybenzo[*a*]pyrene) by the enzyme epoxide hydrase. A second epoxidation by the microsomal monooxygenase yields the dihydrodiol epoxide (7,8-dihydroxy-9,10-epoxy-7,8,9,10-tetrahydrobenzo[*a*]pyrene) (Eq. 8.17).



The diol epoxide of PAH exists in isomers (i.e., the 7-OH is either *cis* or *trans* to the epoxy group), and it is the *trans*-isomer that is exclusively involved in the binding of DNA (Eq. 8.18) [23].

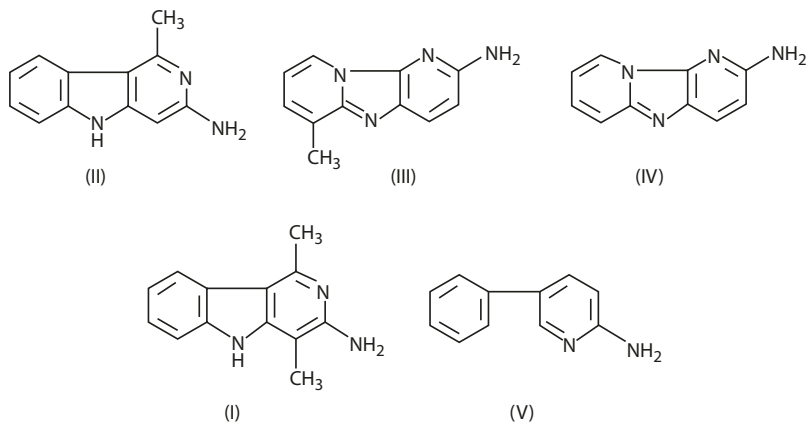


8.9 Heterocyclic Amines

A number of mutagenic heterocyclic amines are known to form by the pyrolysis of amino acids. The structures and sources of these compounds are listed in [Table 8.6](#) [20].

■ **Table 8.6** Heterocyclic amines and their sources

Source	Mutagen
Tryptophan	I. Trp-P-1 3-Amino-1,4-dimethyl-5 <i>H</i> -pyrido[4,3- <i>b</i>]indole
	II. Trp-P-2 3-Amino-1-methyl-5 <i>H</i> -pyrido[4,3- <i>b</i>]indole
Glutamic acid	III. Glu-P-1 2-Amino-6-methyldipyrido[1,2- <i>a</i> :3',2'- <i>d</i>]imidazole
	IV. Glu-P-2 2-Aminodipyrido[1,2- <i>a</i> :3',2'- <i>d</i>]imidazole
Phenylalanine	V. Phe-P-1 2-Amino-5-phenylpyridine



From Hashimoto et al. [20]

As in the case of PAH, the formation of these amine mutagens in food requires high temperatures in excess of 300 °C. However, some mutagenic amines are also found in moderate-temperature cooking (< 200 °C), such as frying and boiling. Most studies have been on commercial beef extracts, broiled and fried beef, and broiled and roasted fish. These mutagens have been isolated and characterized as 2-amino-3-methylimidazo[4,5-*f*]quinoline (IQ), 2-amino-3,4-dimethylimidazo[4,5-*f*]quinoline (MeIQ), and 2-amino-3,8-dimethylimidazo[4,5-*f*]quinoxaline (MeIQ_x). Their chemical structures are presented in

■ Fig. 8.13.

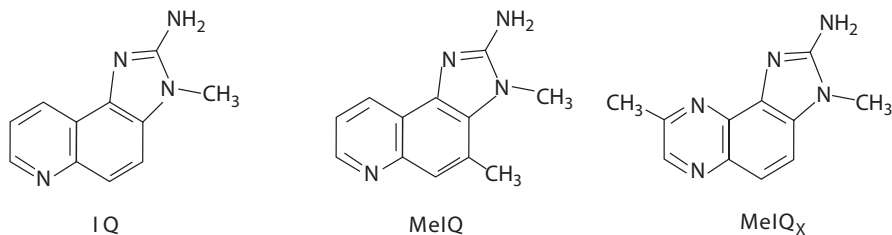


Fig. 8.13 Chemical structures of IQ (2-amino-3-methylimidazo[4,5-*f*]quinoline), MeIQ (2-amino-3,4-dimethylimidazo[4,5-*f*]quinoline), and MeIQ_x (2-amino-3,8-dimethylimidazo[4,5-*f*]quinoxaline)

Table 8.7 Mutagenic activity of heterocyclic amines

Common abbreviation	Full name	Revertants of TA98 per mg
MeIQ	2-Amino-3,4-dimethylimidazo[4,5- <i>f</i>]quinoline	661,000
IQ	2-Amino-3-methylimidazo[4,5- <i>f</i>]quinoline	433,000
MeIQ _x	2-Amino-3,8-dimethylimidazo[4,5- <i>f</i>]quinoxaline	145,000
Trp-P-2	3-Amino-1-methyl-5 <i>H</i> -pyrido[4,3- <i>b</i>]indole	104,000
Glu-P-1	2-Amino-6-methyldipyrdo[1,2- <i>a</i> :3',2'- <i>d</i>]imidazole	49,000
Trp-P-1	3-Amino-1,4-dimethyl-5 <i>H</i> -pyrido[4,3- <i>b</i>]indole	39,000
AFB ₁	Aflatoxin B ₁	6000
Glu-P-2	2-Aminodipyrdo[1,2- <i>a</i> :3',2'- <i>d</i>]imidazole	1900
Phe-P-1	2-Amino-5-phenylpyridine	41

From Miller [27]

8.9.1 Mutagenicity

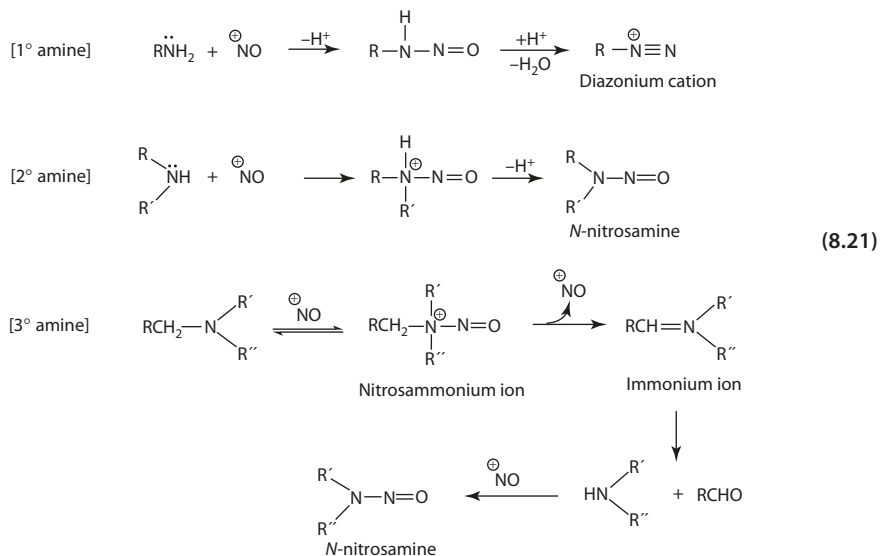
The mutagenicity of the abovementioned heterocyclic amines to *Salmonella typhimurium* TA98 is compared with other mutagens such as aflatoxin B₁ and benzo[*a*]pyrene in Table 8.7 [20, 27, 40].

8.9.2 Mechanism of Toxicity

Metabolically, heterocyclic amine is enzymatically modified by liver microsomal cytochrome P-450 to the active mutagen, *N*-hydroxyamine, which is further converted to the corresponding *O*-acyl derivative. Possible acylation catalyzed by enzymes in the

8.10 · Nitrosamines

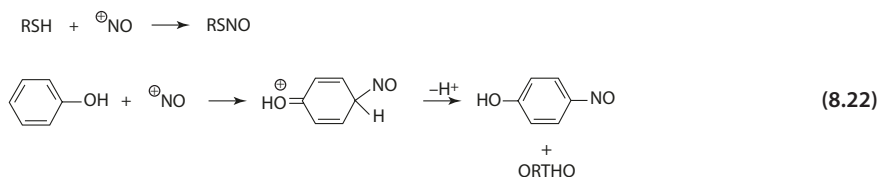
ion formed in this case undergoes *cis*-elimination of the nitrosyl to form an immonium ion, which then hydrolyzes to a secondary amine. A second nitrosation of the product then yields the corresponding stable nitrosamine (Eq. 8.21). Primary amines do not yield nitrosamine. Instead, the product is an unstable diazonium ion, which decomposes to carbocation and nitrogen.

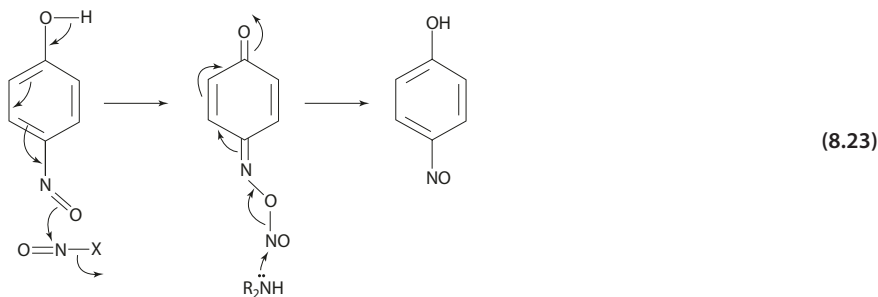


The rate of *N*-nitrosation depends on the pH of the reaction medium and basicity of the amine. The higher the pK_a (i.e., stronger base) of the amine, the lower is the nitrosation rate, since protonated amine is not reactive. The effect of pH is twofold. Low pH favors the formation of the unreactive protonated amine but shifts the equilibrium of nitrite ion \rightleftharpoons nitrous acid to the right. The nitrosation reaction is, therefore, best carried out with highly basic amines in weakly acidic media (pH 3 to 3.4).

8.10.2 Inhibition of Nitrosation

Nitrosation is known to be inhibited by ascorbate. Most curing systems contain 550 ppm sodium ascorbate. Phenolics, thiols, and other aromatic compounds compete with amines for nitrite, forming *C*- and *S*-nitroso compounds, respectively (Eq. 8.22) [14]. Both *p*-nitrophenols and *S*-nitrosocysteine have been shown to catalyze nitrosamine formation via transnitrosation. A nitrosating intermediate is involved in the nitrosophenol reacting with nitroso compounds [13]. Nucleophilic attack on the intermediate by an amine produces the corresponding nitrosamine and regenerates the nitrosophenol (Eq. 8.23).





8.10.3 Nitrosamines in Cured Meat

A number of nitrosamines have been identified in cured meat and fish products. These include *N*-nitrosodimethylamine (NDMA), *N*-nitrosodiethylamine, *N*-nitrosopyrrolidine (NPYR), and *N*-nitrosopiperidine (Fig. 8.14). Of these, NDMA and NPYR are found consistently in cooked bacon, and their concentrations are two times higher in the cook-out fat than the rasher (Table 8.8) [8]. The nitrosamine NPYR is formed during frying of bacon, largely in the fat phase. During frying, up to 70% of the total NDMA and 50% of the total NPYR appear in the vapor. Since pyrrolidine is not found in raw bacon, free proline is the most likely precursor of NPYR in bacon [5]. At high temperature (> 100 °C) as in frying, nitrous anhydride (N₂O₃) dissociates to form NO₂· and NO· radicals. The nitrous oxide radical abstracts the amino proton from proline to yield a radical that combines with NO· to yield nitrosoproline. Further decarboxylation converts the nitrosoproline to NPYR (Eq. 8.24).

Fig. 8.14 Nitrosamines found in cured meat

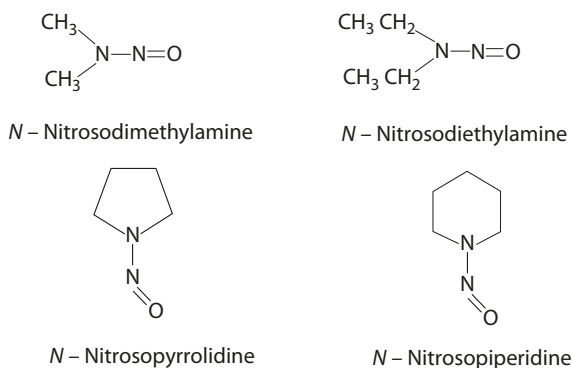
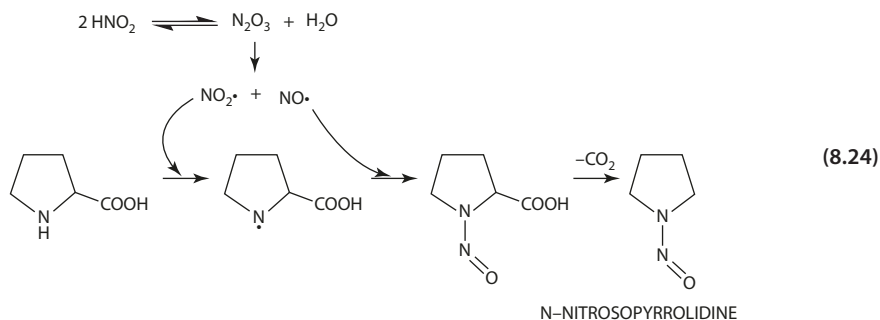


Table 8.8 Distribution of nitrosamine in cooked bacon

Bacon	NDMA (PPB)	NPYR (PPB)
Rasher	3.8	10.4
Cook-out fat	9.9	21.6

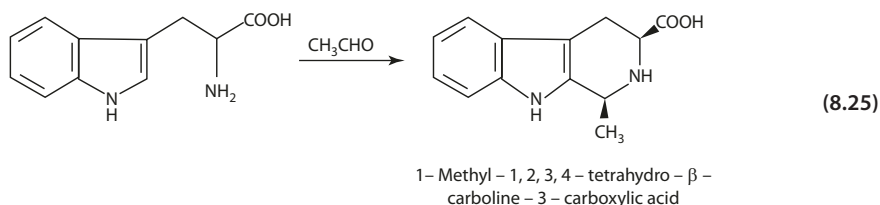
From Coleman [8]



8.10.4 In Vivo Nitrosation

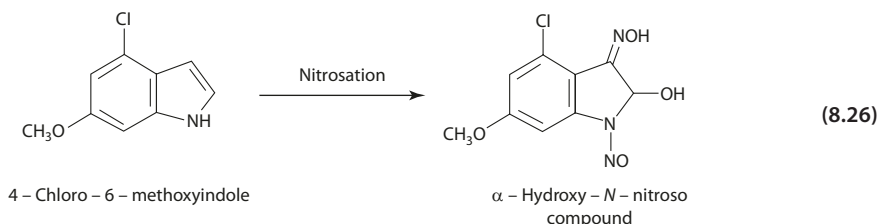
It has been shown that nitrate and nitrite are formed endogenously, and the conversion of nitrate to nitrite occurs in the oral cavity and intestine via microbial nitrification. Therefore, *N*-nitroso compounds are likely to form when suitable precursor compounds are present to react with nitrite.

The precursor for nitrosation found in certain brands of soy sauce and fish sauce has been identified to be 1-methyl-1,2,3,4-tetrahydro- β -carboline-3-carboxylic acid (Eq. 8.25) [38]. The nitroso compound, after reacting with nitrite, is a mutagen (17.4 resertants of TA100 without S9 per μg).

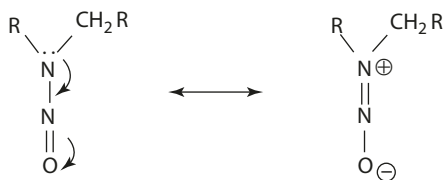


The same compound, along with tetrahydro- β -carboline-3-carboxylic acid, is found in alcoholic beverages. The concentrations range between 300–400 and 1000–10,000 ppm in beer and wine, respectively [6]. Other tetrahydro- β -carbolines have also been found in alcoholic beverages and other foods, including 6-hydroxy-1-methyl-1,2,3,4-tetrahydro- β -carboline (in beer, certain fruits such as banana and plum, and cheese), 6-hydroxy-1,2,3,4-tetrahydro- β -carboline, and 1-methyl-1,2,3,4-tetrahydro- β -carboline (in alcoholic beverages prepared by fermentation processes). However, these compounds are present at much lower concentrations.

Fava beans treated with nitrite under gastric conditions form a mutagenic α -hydroxy-*N*-nitroso compounds (4-chloro-6-methoxyindole-2-hydroxy-1-nitrosoindoline-3-one oxime) that is 2,000 times more potent than the mutagen in soy sauce. The precursor in this case is 4-chloro-6-methoxyindole (Eq. 8.26) [48].



■ Fig. 8.15 Resonance structure of nitrosamine



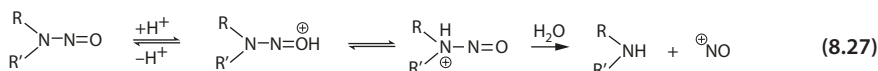
8

8.10.5 Chemical Reactions of Nitrosamine

The chemistry of *N*-nitrosamine is based on the polar resonance structure due to the partial N–N bond character and the negative charge on the oxygen atom (■ Fig. 8.15) [7, 11].

■ Denitrosation

Nitrosamines undergo denitrosation on heating with mineral acids. While initial protonation occurs at the oxygen atom, it is the *N*-protonated form that undergoes hydrolysis to the amine and nitrosonium ion (Eq. 8.27).



■ Oxidation and Reduction

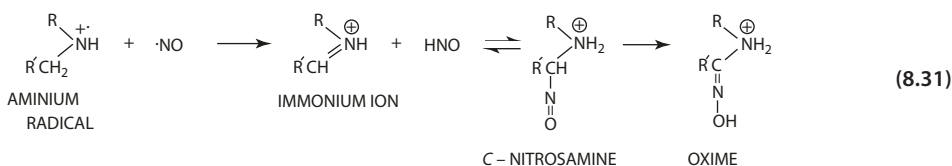
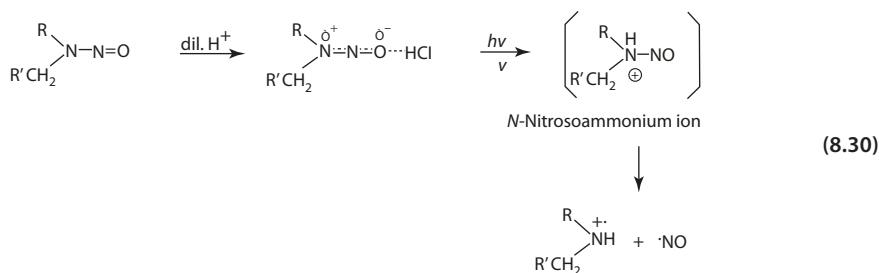
Nitrosamines are oxidized to the corresponding *N*-nitramines. Oxidizing agents include hydrogen peroxide/nitro acid and nitric acid/ammonium persulfate (Eq. 8.28). The nitroso group can also undergo reduction to *N,N*-disubstituted hydrazines and secondary amines (Eq. 8.29).



■ Photoreaction

In dilute acid (0.001–0.1 N), *N*-nitrosamines undergo photoreaction, rapidly generating NO· and aminium radical (R₂NH^{·+}). Excitation causes proton migration to the electron-rich amine nitrogen in the nitrosamine-acid complex, forming an *N*-nitrosoammonium

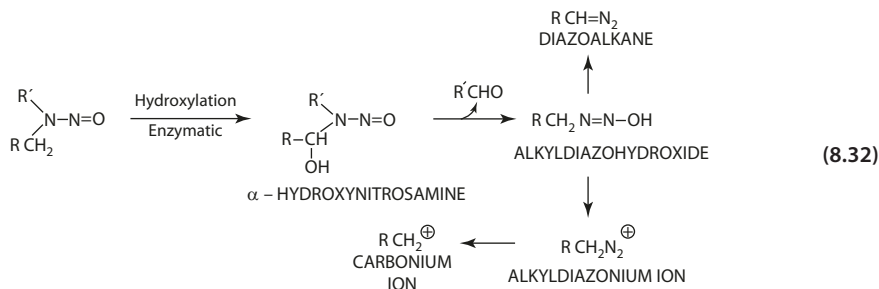
ion, which decomposes to aminium and nitrous oxide radical (Eq. 8.30). In aqueous solution, the radical disproportionates to form HNO and the immonium ion. Nucleophilic attack of HNO on the immonium ion yields the C-nitroso product, which tautomerizes to the stable oxime (Eq. 8.31). In the absence of an α -hydrogen, tautomerization cannot occur, and reverse elimination of the C-nitrosamine regenerates the more stable immonium ion.



8.10.6 Metabolic Mechanism

Metabolically, nitrosamines undergo enzymatic α -hydroxylation to the α -hydroxynitrosamine. Cleavage of the C–N bond yields the aldehyde and the alkyldiazoaldehyde. The latter then breaks down to diazoalkane or cationic species (Eq. 8.32). It is believed that the electrophilic intermediate, alkyldiazonium ion, and alkyldiazoaldehyde react with DNA to form covalent conjugates [2].

Numerous nitroso compounds have been tested on animals and are known to be carcinogenic. Nitrosamines are widely distributed in body tissues following oral administration, often producing tumors at various sites, including the liver, nasal cavities, kidney, and stomach. However, all these animal tests have been conducted using dosage levels in the range of mg/kg well above the ppb range found in any food products.



References

1. Anonymous (1983) Caffeine. *Food Technol* 37(4):87–91
2. Archer MC (1982) Reactive intermediates from nitrosamines. In: Snyder R (ed) *Biological reactive intermediates – II. Advances in experimental medicine and biology*, vol 136B. Plenum Press, New York
3. Bell EA (1980-1981) The structure and biosynthesis of lathrogens and related compounds. *Food Chem* 6:213–222
4. Benn M (1977) Glucosinolates. *Pure Appl Chem* 49:197–210
5. Bharucha KR, Cross CK, Rubin LJ (1979) Mechanism of *N*-nitrosopyrrolidine formation in bacon. *J Agric Food Chem* 27:63–69
6. Bosin TR, Krogh S, Mais D (1986) Identification and quantitation of 1,2,3,4-tetrahydro- β -carboline-3-carboxylic acid and 1-methyl-1,2,3,4-tetrahydro- β -carboline-3-carboxylic acid in beer and wine. *J Agric Food Chem* 34:843–847
7. Chow YL (1973) Nitrosamine photochemistry: reactions of aminium radicals. *Acc Chem Res* 6:354–360
8. Coleman MH (1978) A model system for the formation of *N*-nitrosopyrrolidine in grilled or fried bacon. *J Food Technol* 13:55–69
9. Conn EE (1969) Cyanogenic glycosides. *J Agric Food Chem* 17:519–526
10. Conn EE (1981) Unwanted biological substances in foods: cyanogenic glycosides. In: Ayres JC, Kirschman JC (eds) *Impact of toxicology on food processing*. AVI, Westport
11. Crosby NT, Sawyer R (1976) *N*-nitrosamines: a review of chemical and biological properties and their estimation in foodstuffs. *Adv Food Res* 22:1–56
12. Croy RG, Wogan GN (1981) Temporal patterns of covalent DNA adducts in rat liver after single and multiple doses of aflatoxin B1. *Cancer Res* 41:197–203
13. Davies R, Massey RC, McWeeny DJ (1980-1981) The catalysis of the *N*-nitrosation of secondary amines by nitrophenols. *Food Chem* 6:115–122
14. Fan T-Y, Tannenbaum SR (1973) Factors influencing the rate of formation of nitrosamorpholine from morpholine and nitrite: acceleration by thiocyanate and other anions. *J Agric Food Chem* 21:237–240
15. Fenwick GR, Heaney RK, Mullin WJ (1983) Glucosinolates and their breakdown products in food and food plants. *CRC Crit Rev Food Technol* 18:123–200
16. Fernandez M, Liu X, Wouters MA, Heyberger S, Husain A (2001) Antiotensin I-converting enzyme transition state stabilization by His¹⁰⁸⁹. *J Biol Chem* 276:4998–5004
17. Fretheim K (1983) Polycyclic aromatic hydrocarbons in grilled meat products – a review. *Food Chem* 10:129–139
18. Gigliotti HJ, Levenberg B (1964) Studies in the γ -glutamyltransferase of *Agaricus bisporus*. *J Biol Chem* 239:2274–2284
19. Hanschen FS, Lamy E, Schreiner M, Rohn S (2014) Reactivity and stability of glucosinolates and their breakdown products in foods. *Angew Chem Int Ed* 53:11430–11450
20. Hashimoto Y, Shudo K, Okamoto T (1984) Mutagenic chemistry of heteroaromatic amines and mitomycin C. *Acc Chem Res* 17:403–408
21. Hashimoto Y, Shudo K, Okamoto T (1980) Activation of a mutagen, 3-amino-methyl-5H-pyrido[4,3-*b*]indole. Identification of 3-hydroxyamino-1-methyl-5H-pyrido[4,3-*b*]indole and its reaction with DNA. *Biochem Biophys Res Commun* 96:355–362
22. Huberman E, Sachs L, Yang SK, Gelboin HV (1976) Identification of mutagenic metabolites of benzo[*a*]pyrene in mammalian cells. *Proc Natl Acad Sci U S A* 73:607–611
23. King HW, Osborne MR, Beland FA, Harvey RG, Brookes P (1976) (\pm)-7 α ,8 β -dihydroxy-9 β ,10 β -epoxy-7,8,9,10-tetrahydrobenzo[*a*]pyrene in an intermediate in the metabolism and binding to DNA of benzo[*a*]pyrene. *Proc Natl Acad Sci USA* 73:2679–2661
24. Lam K-H, Jin R (2015) Architecture of the botulinum neurotoxin complex: a molecular machine for protection and delivery. *Curr Opin Struct Biol* 31:89–95
25. Lam K-H, Yao G, Jin R (2015) Diverse binding modes, same goal: the receptor recognition mechanism of botulinum neurotoxin. *Prog Biophys Mol Biol* 117:225–231
26. Lovenberg W (1974) Psycho- and vasoactive compounds in food substances. *J Agric Food Chem* 22:23–26
27. Miller AJ (1985) Processing-induced mutagens in muscle foods. *Food Technol* 39(2):75–79. 109-113
28. Norred WP (1982) Ammonia treatment to destroy aflatoxins in corn. *J Food Protection* 45:972–976

References

29. Osman SF (1983) Glycoalkaloids in potatoes. *Food Chem* 11:235–247
30. Patterson DSP, Roberts BA (1970) The formation of alatoxins B_{2a} and G_{2a} and their degradation products during the in vitro detoxification of aflatoxin by livers of certain avian and mammalian species. *Food Cosmet Toxicol* 8:527–538
31. Roberts HR, Barone JT (1983) Biological effects of caffeine, history and use. *Food Technol* 37(9):32–39
32. Roddick JG (1979) Complex formation between solanaceous steroidal glycoalkaloids and free sterols in vitro. *Phytochemistry* 18:1467–1470
33. Ross AE, Nagel DL, Toth B (1982) Evidence for the occurrence and formation of diazonium ions in the *Agaricus bisporus* mushroom and its extracts. *J Agric Food Chem* 30:521–525
34. Silvaggi NR, Wilson D, Tzipori S, Allen KN (2008) Catalytic features of the botulinum neurotoxin A light chain revealed by high resolution structure of an inhibitory peptide complex. *Biochemistry* 47:5736–5745
35. Simpson LL (1981) The origin, structure, and pharmacological activity of botulinum toxin. *Pharmacol Rev* 33:155–188
36. Simpson LL (1986) Molecular pharmacology of botulinum toxin and tetanus toxin. *Pharmacol Rev Pharmacol Toxicol* 26:427–453
37. Sinden SL, Webb RE (1972) Effect of variety and location on the glycoalkaloid content of potatoes. *Am Potato J* 49:334–338
38. Smith TA (1980–1981) Amines in food. *Food Chem* 6:169–200
39. Snyder SH, Katims JJ, Annau Z, Bruns RF, Daly JW (1981) Adenosine receptors and behavioral action of methylxanthines. *Proc Natl Acad Sci U S A* 78:3260–3264
40. Sugimura T, Wakabayashi K, Nakagama H, Hagao M (2004) Heterocyclic amines: mutagens/carcinogens produced during cooking of meat and fish. *Cancer Sci* 95:290–299
41. Swenson DH, Miller JA, Miller EC (1975) The reactivity and carcinogenicity of aflatoxin B₁. *Cancer Res* 35:3811–3823
42. Tarka SM Jr (1982) The toxicology of cocoa and methylxanthines: a review of the literature. *CRC Crit Rev Toxicol* 9:275–310
43. Taylor SL (1986) Histamine food poisoner: toxicology and clinical aspects. *CRC Crit Rev Toxicol* 17:91–128
44. van Borstel RW (1983) Biological effects of caffeine. *Food Technol* 37(9):40–43, 46
45. van Etten CH, Daxenbichler ME, Wolff IA (1969) Natural glucosinolates (thioglucosides) in foods and feeds. *J Agric Food Chem* 17:483–491
46. Wakabayashi K, Ochiai M, Saito H, Tsuda M, Suwa Y, Nagao M, Sugimura T (1983) Presence of 1-methyl-1,2,3,4-tetrahydro- β -carboline-3-carboxylic acid, a precursor of a mutagenic nitroso compounds, in soy sauce. *Proc Natl Acad Sci U S A* 80:2912–2916
47. Wieland T (1968) Poisonous principles of mushrooms of the genus *Amanita*. *Science* 159:946–952
48. Yang D, Tannenbaum SR, Buchi G, Lee GCM (1984) 4-Chloro-6-methoxyindol is the precursor of a potent mutagen (4-chloro-6-methoxy-2-hydroxy-1-nitroso-indolin-3-one oxime) that forms during nitrosation of the fava bean (*Vicia faba*). *Carcinogenesis* 5:1219–1224

Additives

9.1 Phosphates – 362

- 9.1.1 Chemical Structure – 362
- 9.1.2 Sequestering – 365
- 9.1.3 Water Holding Capacity – 366
- 9.1.4 Stabilizing Emulsion – 367
- 9.1.5 Leavening – 367

9.2 Citric Acid – 368

- 9.2.1 Acidification – 368
- 9.2.2 Buffering – 368
- 9.2.3 Flavor Enhancing – 369
- 9.2.4 Sequestering – 369
- 9.2.5 Phosphoric Acid and Others – 371

9.3 Antimicrobial Short-Chain Acid Derivatives – 371

- 9.3.1 Mechanism of Inhibition – 372

9.4 Sulfite – 372

- 9.4.1 Chemical Equilibrium of the Oxospecies – 373
- 9.4.2 Inhibition of Nonenzymatic Browning – 373
- 9.4.3 Inhibition of Enzymatic Browning – 374
- 9.4.4 Antimicrobial Action – 374
- 9.4.5 Reaction with Pyrimidines – 374
- 9.4.6 Transamination – 375
- 9.4.7 Free-Radical Reactions – 376
- 9.4.8 Mutagenicity – 378
- 9.4.9 Metabolic Pathway – 379

References – 379

The use of food additives is essential for an industry that has to meet the demand of a continuous, adequate supply of a substantial variety of food items to a large and diverse population of consumers. Chemicals, natural or synthetic, are deliberately added to various foods for the purpose of changing the chemical and physical properties of a food. A number of additives have been discussed in various chapters. These include antioxidants, emulsifiers, colors, flavoring ingredients, preservatives, textural modifiers, and enzymes. In this chapter, only those additives that are of importance, but have not been covered elsewhere in this book, are presented. The chemistry of their functional properties, their fate in the food system, and their metabolic pathway after consumption will help our understanding of why additives are used, how to assure their safe use, and how to establish the conditions for effective utilization.

9.1 Phosphates

There are more than 20 available phosphates with wide applications in processed food products. Much of the confusion comes from naming the phosphates, especially when trade names are used.

9.1.1 Chemical Structure

Food phosphates can be conveniently classified into (1) orthophosphates and (2) condensed phosphates. The latter is composed of polyphosphates and metaphosphates. Their general structures are shown in [Fig. 9.1](#). Cyclic phosphates of three and larger rings also exist. Long-chain polyphosphates commonly exist in glasslike crystals. [Table 9.1](#) lists some common food phosphates with chemical formula under each of the three groups [[1](#), [6](#)].

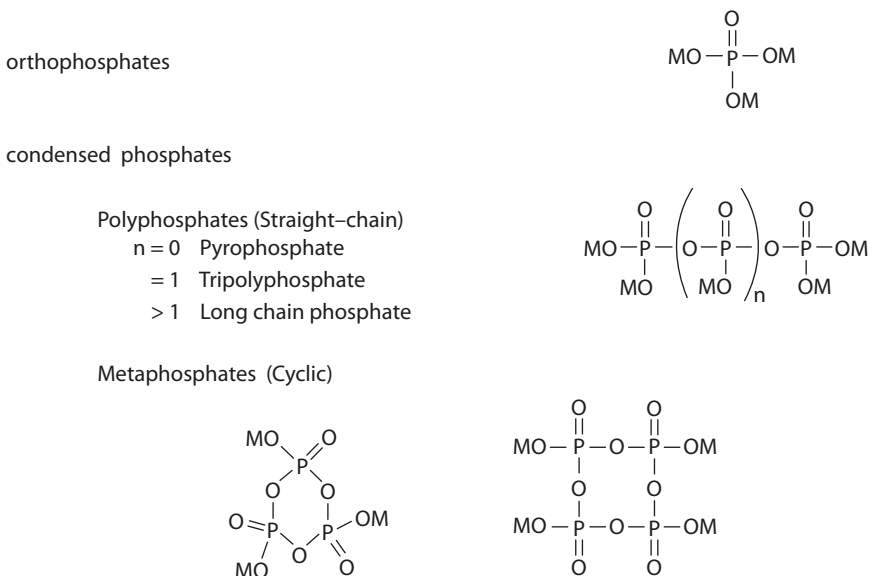


Fig. 9.1 Food phosphates

■ **Table 9.1** Commonly used food phosphates

Chemical names and synonyms	Formula	pH (1% solution)	Neutralizing value
The orthophosphates			
1. Phosphoric acid ^a	H ₃ PO ₄	1.6	–
Orthophosphoric acid			
Monophosphoric acid			
2. Monosodium dihydrogen monophosphate	NaH ₂ PO ₄ (anhydrous)	4.6	70
Monosodium Phosphate ^a	NaH ₂ PO ₄ ·H ₂ O (monohydrate)		
Monosodium monophosphate	NaH ₂ PO ₄ ·2H ₂ O (dihydrate)		
Sodium dihydrogen phosphate			
Sodium phosphate, monobasic			
Sodium biphosphate			
Primary sodium phosphate			
3. Disodium monohydrogen monophosphate	Na ₂ HPO ₄ (anhydrous)	9.0	–
Disodium phosphate ^a	Na ₂ HPO ₄ ·2H ₂ O (dihydrate)		
Disodium monohydrogen phosphate	Na ₂ HPO ₄ ·7H ₂ O (heptahydrate)		
Sodium phosphate, dibasic	Na ₂ HPO ₄ ·12H ₂ O (dodecahydrate)		
Neutral sodium phosphate			
Disodium monophosphate			
Disodium phosphate			
Secondary sodium phosphate			
4. Monocalcium phosphate ^a	Ca(H ₂ PO ₄) ₂ (anhydrous)	4.6	8
Calcium phosphate, monobasic	Ca(H ₂ PO ₄) ₂ ·H ₂ O (monohydrate)		
Calcium acid phosphate			
Calcium biphosphate			
Primary calcium phosphate			

(continued)

■ **Table 9.1** (continued)

Chemical names and synonyms	Formula	pH (1% solution)	Neutralizing value
5. Dicalcium phosphate ^a	CaHPO ₄ ·H ₂ O (dihydrate)	7.5	33
Calcium phosphate, dibasic			
Calcium phosphate, secondary			
6. Tricalcium phosphate ^a	Ca ₁₀ (OH) ₂ (PO ₄) ₆	7.3	–
Calcium phosphate, tribasic			
Tertiary Calcium phosphate			
7. Monoammonium phosphate ^a	NH ₄ H ₂ PO ₄	4.6	62
Ammonium biphosphate			
Ammonium phosphate, monobasic			
8. Diammonium phosphate ^a	(NH ₄) ₂ HPO ₄	8.0	–
Ammonium phosphate, dibasic			
9. Monopotassium phosphate ^a	KH ₂ PO ₄	4.6	–
Acid potassium phosphate			
Potassium phosphate, monobasic			
10. Tripotassium phosphate ^a	K ₃ PO ₄	11.5	–
Basic potassium phosphate			
Potassium phosphate, tribasic			
11. Sodium aluminum phosphate	Na ₃ Al ₂ H ₁₅ (PO ₄) ₈ NaH ₁₄ Al ₃ (PO ₄) ₈ ·4H ₂ O	3.4	100
The polyphosphates			
1. Sodium pyrophosphate	Na ₂ H ₂ P ₂ O ₇	4.2–4.8	74
Sodium acid pyrophosphate ^a			
Disodium dihydrogen diphosphate			
Dibasic sodium pyrophosphate			
Disodium pyrophosphate			
2. Sodium tripolyphosphate ^a	Na ₅ P ₃ O ₁₀	9.8	—
Pentasodium triphosphate			
Sodium triphosphate			

■ **Table 9.1** (continued)

Chemical names and synonyms		Formula	pH (1% solution)	Neutralizing value
3.	Sodium hexametaphosphate ^a	mixture of various chain lengths $\text{Na}_{n+2}\text{P}_n\text{O}_{3n+1}$	6.9	
	Sodium phosphate glass			
	Graham's salt			
	Sodium polyphosphate			
The metaphosphates				
1.	Sodium trimetaphosphate	$\text{Na}_3\text{P}_3\text{O}_9$		

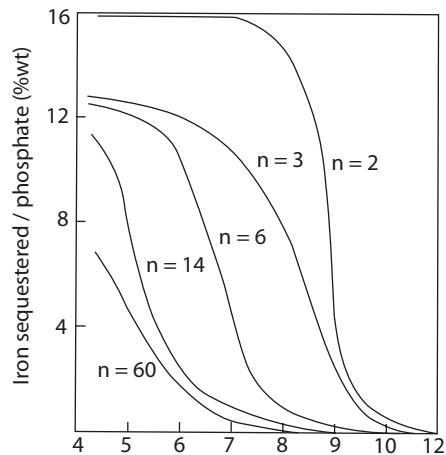
From Anon [1]

^aCommon names for commercial products

9.1.2 Sequestering

One important function of phosphates is their effectiveness in sequestering metals. A sequestrant is an anion that forms a soluble complex with metal ions in the presence of other complexing or precipitating anions. Based on the amount of the free metal ion in equilibrium with solutions of sequestrants and of precipitating anions, the complexing ability of the sequestrants for the metal ion can be compared [17]. Hence, as suggested in ■ Fig. 9.2, the long-chain phosphates are stronger anions than the orthophosphates, and sequestration of iron decreases with increasing pH.

■ **Fig. 9.2** Sequestration of iron (III) (Irani and Morgenthaler [17])



9.1.3 Water Holding Capacity

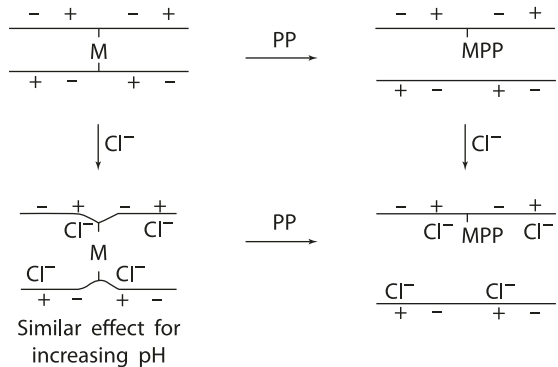
Polyphosphates are used in processed meat, poultry, and seafood largely for controlling fluid loss to give a more tender and juicy product. The polyphosphates used in this regard include sodium tripolyphosphate, often blended with sodium hexametaphosphate for better effect. The phosphates added are usually hydrolyzed to pyrophosphate which is believed to be the active agent. In meat processing, a combination of 2% salt and 0.3% phosphate is commonly used to increase water uptake. Approximately 0.8–1.0 M (4.6–5.9%) sodium chloride is required for maximum swelling, but the addition of phosphate reduces the concentration of chloride needed.

The effect of polyphosphate on meat hydration is related to three factors: (1) increase in pH, (2) increase in ionic strength, and (3) sequestration of metal ions. The greater the increase of pH from the isoelectric point of meat (pH ~ 5.4), the stronger is the electrostatic repulsion due to increasing negative net charge of the protein. Screening of the positive charges by phosphate anions causes further weakening of electrostatic attractions. The increase in the water-holding capacity is also related to the sequestering property of the phosphate anions. Polyphosphates form complexes with protein-bound muscle calcium and magnesium, freeing the protein molecules from crosslinking by these cations. The polypeptide chain, once separated, gives way to electrostatic repulsion. More water molecules are immobilized in the loosened protein network. The effect is greatly enhanced in the basic pH range (>pI) or by the addition of salt, which causes increasing electrostatic repulsion and further loosening of the protein molecule (■ Fig. 9.3) [11].

It has been observed by phase-contrast microscopy that the increase in water-holding capacity is reflected in the expansion of the volume of the myofibrils. Based on the structural organization of muscle myofibrils, the swelling by water hydration is constrained at the Z- and M-lines, as well as the cross-bridges that tie together the thick and thin filaments. Both chloride and pyrophosphate have the effect of causing: (1) depolymerization of the myosin filament and (2) dissociation of the actomyosin complex [20]. Such action releases the structural constraint in the myofibril allowing the volume to expand. Similar process also occurs with the cytoskeletal proteins, titin and nebulin.

The use of alkaline salts, such as bicarbonates, shows similar effects resulting in the improvement of water-holding capacity, drip loss, product yield, and tenderness. The effect of bicarbonate is due to the elevated pH, increased net negative charge of the muscle

■ Fig. 9.3 Effect of phosphate ions on meat hydration (Hamm [11])



proteins, and depolymerization/dissociation of myosin and actomyosin, similar to that described for the phosphates. In addition, it has been suggested that bicarbonate generates carbon dioxide during cooking, creating porous structures in the meat, which may also contribute to the reduced toughness. Postmortem injection of sodium bicarbonate or phosphate has been shown to inhibit the development of pale, soft, exudative conditions in pork [26, 35].

9.1.4 Stabilizing Emulsion

Phosphates are employed in the manufacture of processed cheese. They help stabilizing the emulsion of butterfat in the protein-water matrix. It is suggested that phosphates, by sequestering the calcium ions from the para- κ -casein, expose the solubilizing groups in the milk protein. The resulting cheese has smooth texture and melts down with no fat separation. The phosphates used for this purpose are the sodium salts of orthophosphates. Polyphosphates such as sodium acid pyrophosphate and sodium hexametaphosphates are also used [1]. Alkaline orthophosphates tend to give the cheese product a soft texture with lower melting temperature. Acidic phosphates and polyphosphates increase the melting temperature and hardness of the product. Up to 3% by weight of the finished product of these emulsifying salts can be used.

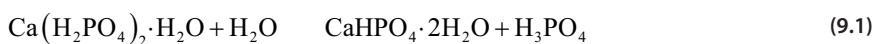
9.1.5 Leavening

The most unique application of phosphates is their functioning as leavening acids that react with sodium bicarbonate to release carbon dioxide. The commonly used phosphates are anhydrous monocalcium phosphate, monocalcium phosphate monohydrate, dicalcium phosphate dihydrate, sodium aluminum phosphate, and sodium acid pyrophosphate. The amount and the types of leavening acids used for a particular product depend largely on the available acidity and the rate of reaction of the leavener. The terms «neutralizing value» (NV) (■ Table 9.1) and «dough reaction rate» (DRR) are used to define the properties of leavening acids [4].

The neutralizing value is defined as the parts by weight of sodium bicarbonate that will be neutralized by 100 parts of leavening acid. Thus, $NV = (\text{wt. sodium bicarbonate}/\text{wt. leavening acid}) \times 100$. In practical terms, NV corresponds to the weight amount of sodium bicarbonate that will completely react with 100 parts of leavening acid to release all the carbon dioxide, with little of the soda or acid phosphate salt remaining after baking.

The dough reaction rate measures the rate of carbon dioxide release during mixing and in the bench stage (holding period) in a dough under standardized conditions. The DRR allows comparing the reactivity of differing leavening acids in a chemical leavening system.

Monocalcium phosphate monohydrate, one of the first acidic phosphates used, reacts rapidly with soda, with much carbon dioxide released during the mixing stage of dough preparation. Further, it disproportionates in water to form dicalcium phosphate and phosphoric acid (Eq. 9.1).



Dicalcium phosphate dihydrate is slow acting and only reacts with soda above 60°C, at which temperature the dicalcium phosphate starts to disproportionate to $\text{Ca}(\text{H}_2\text{PO}_4)_2$ and $\text{Ca}(\text{PO}_4)_3\text{OH}$. Anhydrous monocalcium phosphate is hygroscopic and is used in a form stabilized by a coating of mixed potassium, aluminum, calcium, and magnesium metaphosphate to slow down dissociation and reaction with soda. Sodium aluminum phosphate exhibits slow reaction during holding, and the leavening action starts largely when the product is heated. Sodium acid pyrophosphate comes in several grades, each with a different rate of reaction, ranging from DRR of 20–45 [1]. Many household baking powders are "double acting" – containing monocalcium phosphate monohydrate, to provide rapid reaction during mixing, and sodium aluminum sulfate, which gives little reaction until the dough or batter is heated in the oven. Cake mix, frozen dough, and batter require slow-acting leavening acid. Orthophosphates such as phosphoric acid, monosodium phosphate, disodium phosphate, and sodium acid pyrophosphate are used as buffering and acidifying agents. Long-chain polyphosphates generally have poor buffering capacity.

9.2 Citric Acid

Citric acid is a multifunctional additive suitable for a wide range of applications. It is one of the common acidulants used to control acidity level, enhance flavor, and act as preservatives (to suppress microbial growth).

Citric acid is a tribasic acid with four ionizable groups [2], with $\text{p}K_1 = 3.13$, $\text{p}K_2 = 4.76$, $\text{p}K_3 = 6.40$ for the three carboxyl groups, and a $\text{p}K_4$ of 11 or greater for the hydroxyl group. The carboxyl group α to the hydroxyl group is ionized first, followed by the two terminal carboxyl groups, then finally the hydroxyl group.

9.2.1 Acidification

Citric acid is used for acidifying low-acid foods to a final equilibrium pH of the food of 4.6 or below in the canning process. Foods such as bean, carrot, cucumber, cabbage, cauliflower, spinach, pepper, corn, pea, asparagus, tropical fruit, and fish have a finished equilibrium pH higher than 4.6 (■ Fig. 9.4) and a water activity (a_w) greater than 0.85 [22]. If the pH is lowered, the processing time and temperature in canning these foods can be reduced, since a pH of 4.6 or lower inhibits sporulation of the spoilage organism of the greatest concern, *Clostridium botulinum*. The fermentation of grapes that is low in total acidity results in poor wine quality. Citric acid is often used to make up for the acidity deficiency before fermentation.

9.2.2 Buffering

Citric acid, used in combination with its salts, provides a good buffer that serves to stabilize the pH during various stages of food processing, as well as in the formulation of the finished product.

■ **Fig. 9.4** pH values of canned foods (Schmidt [22])

2.5	Plums Gooseberries
3.0	Prunes Apricots Apples, Blackberries, Strawberries Peaches
3.5	Kraut, Raspberries Sweet cherries Pears
4.0	Tomatoes
4.5	Pimentos Okra Pumpkins, Carrots
5.0	Cabbage, Turnips Beets, Green beans Spinach
5.5	Asparagus, Califlower Lima beans
6.0	Peas Corns
6.5	
7.0	Ripe canned olives

9.2.3 Flavor Enhancing

Due to its high solubility (~160 g per 100 g H₂O at 25°C) and good flavor-blending characteristic, citric acid has long been used by the beverage industry to impart a pleasant sour taste of fruit flavor and also to enhance the natural and artificial flavorings used in various beverages (■ Table 9.2) [18]. Instant tea also utilizes citric acid to enhance the lemon flavor.

9.2.4 Sequestering

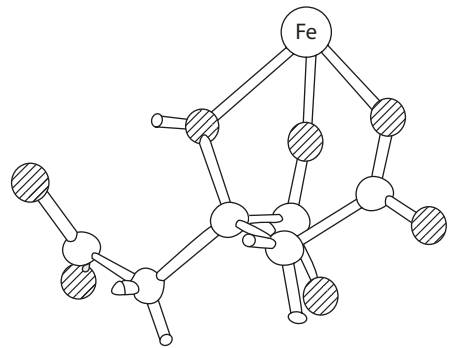
Another important function of citric acid is to sequester metal ions that would otherwise accelerate oxidation (rancidity in fats and oil), browning (color deterioration in beverages), and complex formation (turbidity in wine and ice tea). Citric acid has seven ligating groups (seven oxygen atoms), which can coordinate with metal ions [7]. The citric ion forms a tridentate chelate with ferrous ion in which one terminal carboxyl, the central carboxyl, and the hydroxyl group are coordinated to a single

■ **Table 9.2** Citric acid usage in beverages

Beverage	% citric acid (w/v)
Carbonated beverage	
Orange	0.133
Diet orange	0.173
Lemon lime	0.144
Creme soda	0.046
Ginger ale	0.099
Tonic	0.363
Still beverage	
Citrus drink	0.14
Cherry	0.14
Peach	0.14
Orange	0.19

From Irwin [18]

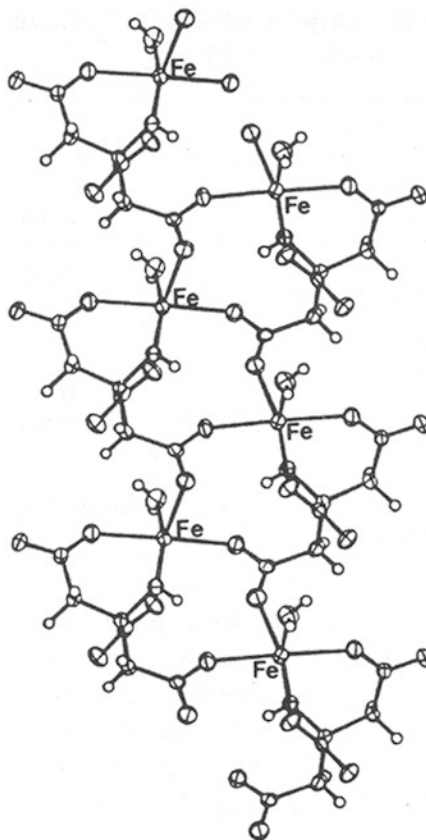
■ **Fig. 9.5** Molecular structure of citric acid-iron complex (From Clusker [2] with permission. Copyright 1980 American Chemical Society)



ferrous ion (■ Fig. 9.5). The remaining terminal carboxyl group is coordinated to two other ferrous ions. The metal ions are each, in turn, coordinated with other citrate ions, thus forming a chain structure. Adjacent chains of ferrous citrate are linked by extensive hydrogen bonding through water molecules and hexaquoiron counter ions $[\text{Fe}(\text{II})(\text{H}_2\text{O})_6]$ (■ Fig. 9.6). Magnesium and manganese form similar structures in solution [28].

Citric acid is used in fats and oils to increase the effectiveness of the antioxidants and in wines for protection against haze formation in the finishing process. Trace metals present in fruits and vegetables often cause discoloration in processing. Some known examples are surface darkening of cauliflower, kidney beans, potatoes, and mushrooms and the formation of pink color in canned pears. Citric acid can help control discoloration during fruit and vegetable processing by removing the trace metals.

■ **Fig. 9.6** Infinite chain of $\text{Fe(II)C}_6\text{H}_5\text{O}_7(\text{H}_2\text{O})$ along a 2_1 axis of the unit cell (From Strouse et al. [28] with permission. Copyright 1977 American Chemical Society)



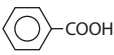
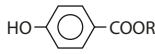
9.2.5 Phosphoric Acid and Others

Phosphoric acid is the acid of choice particularly for nonfruit drinks. Its flat and dry flavor is well suited for the application. Other commonly used acids, such as carbonic acid, give a «sparkling» mouthfeel and bite. Tartaric acid gives a sharper flavor spike than citric acid and may be used at lower concentrations. Ascorbic acid is used for its antioxidant properties.

9.3 Antimicrobial Short-Chain Acid Derivatives

Included in the category of antimicrobial short-chain acid derivatives are the sodium benzoate, alkyl esters of *p*-hydroxybenzoate (parabens), sorbate and its salts (commonly sodium or potassium), propionate, and sulfite. Sulfite, due to its unique chemistry and functions, is to be discussed in a separate section.

■ **Table 9.3** The pK_a and undissociated forms of selected acids

Name	pK_a	Undissociated acid form
Benzoate	4.2	
Paraben	8.47	
Propionate	4.87	$\text{CH}_3\text{CH}_2\text{CH}_2\text{COOH}$
Sorbate	4.8	$\text{CH}_3\text{CH}=\text{CHCH}=\text{CHCOOH}$

From Freese et al. [7]

9.3.1 Mechanism of Inhibition

The antimicrobial effect of these short-chain acids comes from the undissociated form [7], the concentration of which is determined by the pK_a of the acid and the pH of the medium (■ Table 9.3). Ionized species fail to penetrate the cell membrane to any great extent. Maximum usage levels are in the range of 0.1%.

Inhibition of microbial growth is slowly reversible and concentration dependent. The amount needed for inhibition decreases with increasing chain length of the acid. It is generally believed that inhibition of microbial growth by these acid preservatives involves disruption of the cellular membrane transport system, although the exact mechanism is not entirely clear.

It has been shown in *Bacillus subtilis* and *Escherichia coli* that cellular uptake of amino acids, organic acids, phosphates, and other compounds is inhibited by added preservatives [27]. Similar inhibition of transport activity is also observed in the fungus *Penicillium chrysogenum* [15]. The undissociated acids penetrate through the lipophilic cell membrane and then become ionized after reaching the interior cell compartments of low protein concentration. The intracellular concentration of the organic acids upsets the proton or charge gradient involved in energizing membrane transport.

Intracellular accumulation of high concentration of preservatives has also been shown to occur in yeast. But one particular species, *Saccharomyces bailli*, grows in the presence of 600 mg/L benzoic acid or sorbic acid and at a pH less than the pK_a of the acids [31].

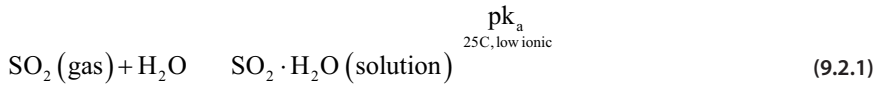
9.4 Sulfite

Sulfur (IV) oxospecies are used as food preservatives, which include sulfur dioxide (SO_2) and salts of sulfite (SO_3^{2-}) and bisulfite (HSO_3^-). Gaseous sulfur dioxide generated from burning sulfur solution is applied to preserve dried fruits and vegetables, while solutions of sodium or potassium sulfite are used for liquid foods.

Regardless of the form, the equilibrium between the various sulfur oxospecies always exists. For food applications, sulfur dioxide, sulfite, and bisulfite are used indiscriminately. For convenience, «sulfite» will be used as a general term for any or all of these species.

9.4.1 Chemical Equilibrium of the Oxospecies

The oxospecies exist in an aqueous solution of SO_2 described by the following equations (Eq. 9.2.1) [10, 32]. Dissolved sulfur dioxide exists as SO_2 , denoted as $\text{SO}_2 \cdot \text{H}_2\text{O}$, and not the commonly expected sulfurous acid, H_2SO_3 .



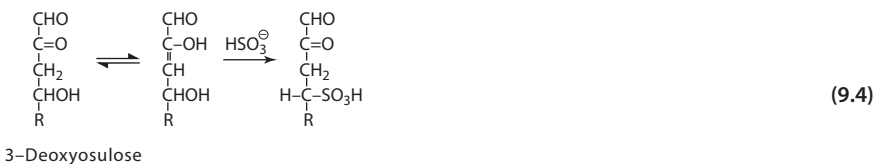
In the normal pH range of food, the predominant species is HSO_3^- as indicated in Eq. 9.2.2 [32]. Increasing ionic strength reduces the $\text{p}K_a$ for Eq. 9.2.3, and SO_3^- is therefore expected to be present in greater proportion.

Also, as the total concentration is increased, the bisulfite ions dimerize to form the disulfite (metabisulfite, pyrosulfite), as in Eq. 9.3. Dimerization is unimportant at concentrations lower than 0.01 M.



9.4.2 Inhibition of Nonenzymatic Browning

Nonenzymatic browning consists of the following reactions: (1) Maillard reaction, (2) ascorbic acid browning, and (3) caramelization, as discussed in ► Chap. 4. One major action of sulfite on the browning reaction is to interrupt the steps leading to the formation of colored products, by forming sulfonates with the carbonyl intermediates such as 3-deoxyosulose and 3,4-dideoxyosulo-3-ene [16, 33]. In the case of 3-deoxyosulose, the hydroxyl group β to the enediol grouping is very labile. Replacement of the 4-hydroxyl group by sulfur oxoanions yields the sulfonate product, 3-deoxy-4-sulfo-osulose, with inversion at C4 (Eq. 9.4). The 3-deoxyosulose can also undergo dehydration to 3,4-dideoxyosulo-3-ene, which is an α,β -unsaturated carbonyl. Nucleophilic 1,4-addition of sulfur oxoanions to the double bond also leads to the formation of the same product (Eq. 9.5).



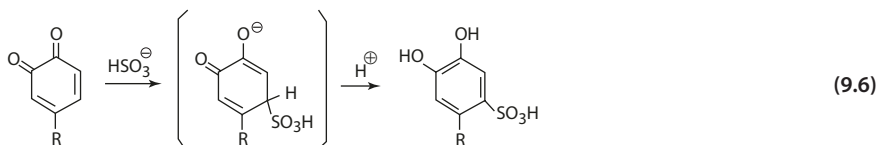
The mechanism involving the addition of sulfur oxoanions to the α,β -unsaturated intermediate constitutes the major route of inhibition of nonenzymatic browning (► Chap. 5).

The irreversible formation of the sulfonate product effectively removes the reaction intermediates from the later stages of browning reactions.



9.4.3 Inhibition of Enzymatic Browning

Inhibition of enzymatic browning by sulfur oxoanions is mainly accomplished by removing the *o*-quinones produced from *o*-diphenols by the action of polyphenol oxidase from further oxidation and polymerization. Nucleophilic addition of sulfite to the *o*-quinone leads to the formation of a sulfonate (Eq. 9.6). There may also be a direct effect of sulfite on the enzyme protein.



9.4.4 Antimicrobial Action

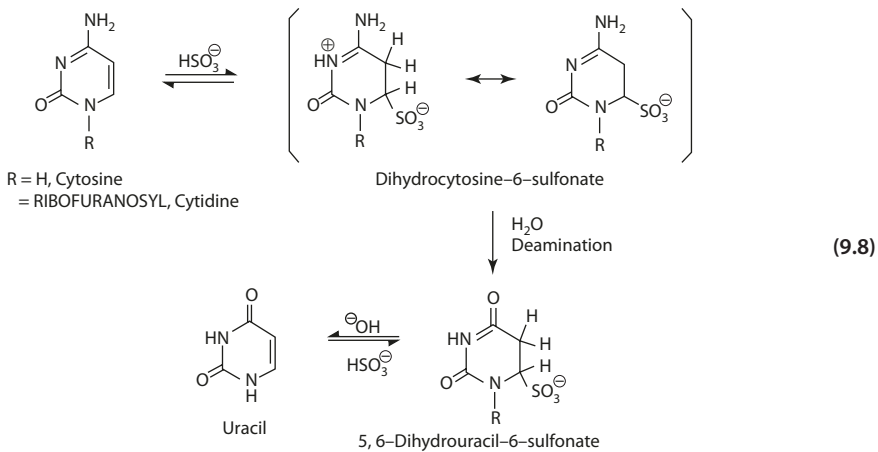
The antimicrobial activity of sulfite depends on the penetration of molecular SO_2 across the cell membrane. It is suggested that sulfur dioxide activates an ATPase system located in the cell membrane. Sulfite concentration as low as 1 mM, at pH 5.0 or below, has been shown to cause rapid depletion of ATP prior to cellular death in yeast [21]. The SO_2 , once inside the cell, may also react with cell components. Sulfite has been shown to react with cofactors and coenzymes, amino acids, pyrimidines, and nucleosides.

9.4.5 Reaction with Pyrimidines

The pyrimidine uracil reacts with NaHSO_3 at pH 6–7 to yield an addition product, 5,6-dihydrouracil-6-sulfonate (Eq. 9.7). The sulfonate is stable at neutral and acidic pH, but hydrolyzed by alkali (pH > 9) to uracil [13]. The rate of addition for uracil is proportional to the concentration of sulfite ion and unionized uracil. Uracil has been shown to be converted to the addition product at bisulfite concentration as low as 0.1 M [23].

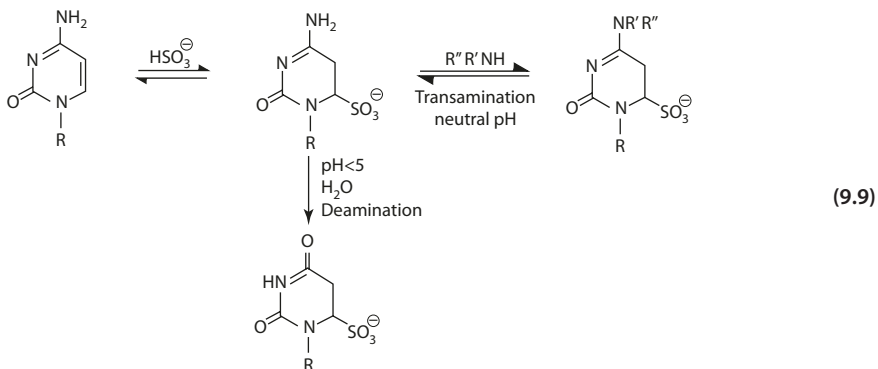


Under similar conditions, cytosine forms an addition product with bisulfite, dihydrocytosine-6-sulfonate, which undergoes deamination to yield the 5,6-dihydrouracil-6-sulfonate (Eq. 9.8). The optimum rate of deamination occurs at acidic pH <5 and in a high sodium bisulfite concentration (>0.5 M). At physiological pH, the rate of deamination declines to only about 1% of that observed at the optimum pH. Furthermore, at low sulfite concentrations compatible with in vivo conditions, the rate can be expected to be extremely low, estimated to be 4.0×10^{-4} /sec for a sulfite concentration of 10^{-1} M [24].



9.4.6 Transamination

At neutral pH, in the presence of sufficient concentration of amines, bisulfite catalyzes transamination reactions of cytosine and derivatives with the formation of *N*-substituted cytosines (Eq. 9.9) [25]. The amines compete with water as nucleophiles for formation of the intermediate, dihydrocytosine-6-sulfonate, at neutral pH, where the deamination reaction is minimal. Crosslinkage of proteins and nucleic acids by bisulfite has been demonstrated in RNA bacteriophage MS2. Therefore, the transamination reaction that occurs optimally at neutral pH raises the possibility of adverse effects at the cellular level.



■ **Table 9.4** Destruction of β -carotene by sulfite at pH 5.7 and 9.2

Time	Relative β -carotene concentration ^a	
	pH 5.7	pH 9.2
0	1.00	1.00
10	0.76	0.15
20	0.51	0.10
30	0.26	0.07
40	0.12	0.05
50	0.09	0.05

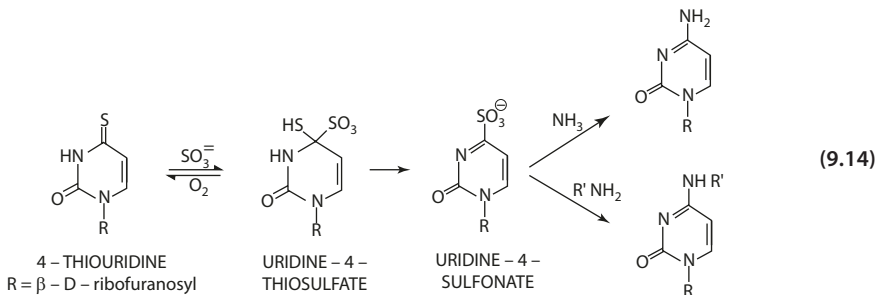
Wedzicha and Lamikanra [34]

^aInitial concentration: β -carotene = 80 μ M, sulfite = 100 μ M, $MnCl_2$ = 52 μ M, glycine = 21 mM, in 0.025 M buffer

Sulfite has also been shown to induce lipid oxidation in emulsified linoleic acid [19]. The formation of hydroperoxide correlates with the loss of sulfite (Eq. 9.13).



The sulfite free radicals also react with nucleic acids. Sulfite at concentrations of 10 mM catalyzes the transformation of 4-thiouridine, a nucleoside in bacterial transfer RNA, to uridine-4-thiosulfate in the presence of oxygen at neutral pH (Eq. 9.14) [12]. The thiosulfate is unstable toward light or acid and decomposes to uridine-4-sulfonate. A high concentration of sulfite inhibits the overall reaction due to the competition between the substrate (4-thiouridine) and sodium bisulfite for the sulfite radical.



The 4-sulfonate group of the product is susceptible to attack by various nucleophiles. Reactions with ammonia or alkyl amines results in the substitution of amino and alkyl amino groups, forming cytidine and its derivatives. Sulfite at 10 mM concentration also reacts with DNA, leading to the cleavage of the nucleotides. The reaction is oxygen dependent and occurs rapidly at pH 7 in the presence of Mn^{2+} ions.

9.4.8 Mutagenicity

Mutagenicity of sulfite is anticipated from the chemistry of all the possible reactions with biological molecules. Although most studies done on viruses, bacteria, and yeast employ 1 M or high concentrations of bisulfite, in a few cases, relatively low concentration of bisulfite (0.01 M) at neutral pH has been shown to promote mutations in *Micrococcus aureus* and *Saccharomyces cerevisiae*. In mammalian cell cultures, low concentrations of sulfite (less than 0.01 M) inhibit DNA, RNA, and protein synthesis, prevent mitosis, reduce cell growth, and cause chromosomal abnormalities [8].

In spite of sulfite-induced chromosomal aberrations in in vitro experiments, no adverse effects have been observed in chronic sulfite feeding studies, unless sulfite is administered at significantly high doses. The effect of high doses can be attributed to the indirect toxicity due to the destruction of thiamine and other vitamins in the feeding diet [9]. Studies on the effect of sulfite on three generations of rats for a 2-year period suggest a noneffect level equivalent to an intake dose of 72 mg SO_2 equivalent/kg/day [30]. Applying a 100-fold safety factor, the estimated maximum acceptable daily intake becomes 0.7 mg/kg, which amounts to a safety level of 42 mg per average adult (60 kg body weight). The estimated total sulfite as SO_2 in some sulfited foods is listed in Table 9.5 [5, 29].

Table 9.5 Sulfite levels (ppm) found in food analyzed by the optimized Monier-Williams method

Food	Mean	Range	
Dried apricots	2791	2259–3722	
Dried peaches	1391	104–2633	
Mashed potatoes	347	91–440	
Fresh shrimp	(unshelled)	175	0.8–569
	(shelled)	52	29–80
Peppers	228	72–411	
White grape juice	43	3.9–83	
Hash browns	41	0–121	
Molasses	4.6	3.0–6.9	
French fries	0.6	0–1.3	
Corn	0.3	0–0.4	
Fresh potato	0.3	0–0.5	

Daniels et al. [5]

9.4.9 Metabolic Pathway

The principal defense against toxicity of sulfite in mammalian systems is the reduction to sulfate by sulfite oxidase (Eq. 9.15), a hemeprotein containing molybdenum located in the intermembrane spaces of mitochondria. Electrons in the oxidation can be transferred to the oxidative phosphorylation system.



The natural function of the enzyme is to participate in the degradation of endogenous sulfur-containing amino acids. Endogenous sulfite produced in the metabolism of sulfur-containing compounds is considerably higher than the estimated daily intake of exogenous sulfite from the diet. Animals deficient in sulfite oxidase are found to be more susceptible to a lower dose of sulfite [3].

References

1. Anonymous (1984) Food phosphates. Monsanto Nutritional Chemicals Division, St. Louis
2. Clusker JP (1980) Citrate conformation and chelations: enzymatic implications. *Acc Chem Res* 13:345–352
3. Cohen HJ, Drew RT, Johnson JL, Rajgopalan KV (1973) Molecular basis of the biological function of molybdenum. The relationship between sulfite oxidase and the acute toxicity of bisulfite and SO_2 . *Proc Natl Acad Sci USA* 70:3655–3659
4. Conn JF (1981) Chemical leavening systems in flour products. *Cereal Foods World* 26(3):119–123
5. Daniels DH, Joe FL, Warner CR, Longfellow SD, Fazio T, Diachenko GW (1992) Survey of sulphites determined in a variety of foods by the optimized Monier-Williams methods. *Food Addit Contam* 9(4):283–289
6. Ellinger RH (1972) Phosphates in food ingredients. CRC Press, Cleveland
7. Freese E, Sheu CW, Galliers E (1973) Function of lipophilic acids as antimicrobial food additives. *Nature* 341:321–325
8. Gunnison AF (1981) Sulphite toxicity: a critical review of *in vitro* and *in vivo* data. *Food Cosmet Toxicol* 19:667–682
9. Gunnison AF, Dulak L, Chiang G, Zaccardi J, Farruggella TJ (1981) A sulphite oxidase-deficient rat model: subchronic toxicology. *Food Cosmet Toxicol* 19:221–232
10. Guthrie JP (1979) Tautomeric equilibria and pK_a values for “sulfurous acid” in aqueous solution: a thermodynamic analysis. *Can J Chem* 57:454–457
11. Hamm R (1971) Interaction between phosphates and meat proteins. In: Deman JM, Melnychyn P (eds) *Phosphates in food processing*. AVI, Westport
12. Hayatsu H (1969) The oxygen-catalyzed reaction between 4-thiouridine and sodium sulfite. *J Am Chem Soc* 91:5693–5694
13. Hayatsu H, Wataya Y, Kal K (1970) The addition of sodium bisulfite and uracil and to cytosine. *J Am Chem Soc* 92:724–726
14. Hayon E, Treinin A, Wilf J (1972) Electronic spectra, photochemistry, and autoxidation mechanism of the sulfite-bisulfite-pyrosulfite system. The SO_2^- , SO_3^- , SO_4^- and SO_5^- radicals. *J Am Chem Soc* 94:47–57
15. Hunter DR, Segel IH (1973) Effect of weak acids on amino acid and transport of *Penicillium chrysogenum*: evidence for a proton or charge gradients as the driving force. *J Bacteriol* 113:1184–1192
16. Ingles DL (1962) The formation of sulphonic acids from the reaction of reducing sugars with sulphite. *Aust J Chem* 15:342–349

17. Irani RR, Morgenthaler WW (1963) Iron sequestration by phosphates. *JAOCS* 40:283–285
18. Irwin WE (1983) The use of citric acid in the beverage industry. Miles Laboratories, Inc., Biotech Products Division, Elkhart
19. Lizada MCC, Yang SF (1981) Sulfite-induced lipid peroxidation. *Lipids* 16:189–194
20. Offer G, Trinick J (1983) On the mechanism of water holding in meat: the swelling and shrinking of myofibrils. *Meat Sci* 8:245–281
21. Schimz K-L (1980) The effect of sulfite on the yeast *Saccharomyces cerevisiae*. *Arch Microbiol* 125:89–95
22. Schmidt TR (1983) The use of citric acid in the canned fruit and vegetable industry. Miles Laboratories Inc., Biotech Products Division, Elkhart
23. Shapiro R, Gazit A (1976) Crosslinking of nucleic acids and proteins by bisulfite. In: Friedman M (ed) Protein crosslinking, biochemical and molecular aspects. Plenum Press, New York
24. Shapiro R, DiFate V, Welcher M (1974) Deamination of cytosine derivatives by bisulfite. Mechanism of the reaction. *J Am Chem Soc* 96:906–912
25. Shapiro R, Welcher M, Nelson V, DiFate V (1976) Reaction of uracil and thymine derivatives with sodium bisulfite. Studies on the mechanism and reduction of the adduct. *Biochim Biophys Acta* 425:115–124
26. Sheard PR, Tali A (2004) Injection of salt, tripolyphosphate and bicarbonate marinade solutions to improve the yield and tenderness of cooked pork loin. *Meat Sci* 68:305–311
27. Shen CW, Konings WN, Freese E (1972) Effects of acetate and other short-chain fatty acids on sugar and amino acid uptake of *Bacillus subtilis*. *J Bacteriol* 111:525–530
28. Strouse J, Layten SW, Strouse CE (1977) Structural studies of transition metal complexes of triionized and tetraionized citrate. Models for the coordination of the citrate ion to transition metal ions in solution and at the active site of aconitase. *J Am Chem Soc* 99:562–572
29. Taylor SL, Bush RK (1986) Sulfites as food ingredients. *Food Technol* 40(6):47–52
30. Til HP, Feron VJ, deGroot AP (1972) The toxicity of sulphite. Long term feeding and multigeneration studies in rats. *Food Cosmet Toxicol* 10:291–310
31. Warth AD (1977) Mechanism of resistance of *Saccharomyces bacilli* to benzoic, sorbic and other weak acids used as food preservatives. *J Appl Bacteriol* 43:215–230
32. Wedzicha BL (1985) Chemistry of sulfur dioxide in foods. Elsevier Applied Science Publ, London/New York
33. Wedzicha BL, McWeeney DJ (1974) Non-enzymatic browning reactions of ascorbic acid and their inhibition. The production of 3-deoxy-4-sulphopentosulose in mixtures of ascorbic acid, glycine and bisulphite ion. *J Sci Food Agric* 25:577–587
34. Wedzicha BL, Lamikanra L (1983) Sulfite mediated destruction of β -carotene. The partial characterization of reaction products. *Food Chem* 10:275–283
35. Wynveen EJ, Bowker BC, Grant AL, Lamkey JW, Fennewald KJ, Henson L, Gerrand DE (2001) Pork quality is affected by early postmortem phosphate and bicarbonate injection. *J Food Sci* 66:886–891
36. Yang SF (1970) Sulfoxide formation from methionine or its sulfide analogs during aerobic oxidation of sulfite. *Biochemistry* 9:5008–5014

Vitamins

10.1 Vitamin A – 383

- 10.1.1 Biological Function – 384
- 10.1.2 Action of Dilute Acid – 385
- 10.1.3 Photochemical Reactions – 386

10.2 Thiamin (Vitamin B₁) – 387

- 10.2.1 Biochemical Mechanism – 387
- 10.2.2 Action of Alkali and Acid – 388
- 10.2.3 Oxidation and Reduction – 389
- 10.2.4 Reaction with Bisulfite – 390
- 10.2.5 Photolysis – 391

10.3 Riboflavin (Vitamin B₂) – 391

- 10.3.1 Biochemical Mechanism – 393
- 10.3.2 Alkaline Degradation – 394
- 10.3.3 Reaction with Sulfite – 394
- 10.3.4 Photochemical Reaction – 395
- 10.3.5 Flavin-Sensitized Reactions – 396

10.4 Pyridoxol, Pyridoxal, and Pyridoxamine (Vitamin B₆) – 397

- 10.4.1 Biochemical Mechanism – 397

10.5 Folic Acid (Vitamin B₉) – 399

- 10.5.1 Biological Functions – 401
- 10.5.2 Degradation of Folates – 401

10.6 Vitamin B₁₂ – 404

- 10.6.1 Biochemical Mechanism – 405
- 10.6.2 Photolytic Degradation – 405
- 10.6.3 Oxidation – 406

10.7 Biotin (Vitamin B₇) – 406

10.7.1 Biochemical Mechanism – 407

10.8 Niacin (Vitamin B₃) – 408

10.8.1 Biochemical Mechanism – 408

10.9 Vitamin C – 409

10.9.1 Biochemical Mechanism – 409

10.9.2 Biological Functions – 410

10.9.3 Loss of Vitamin C – 412

10.9.4 Uses of Vitamin C – 414

10.10 Vitamin D – 415

10.10.1 The Chemical Structures – 415

10.10.2 Biological Functions – 416

10.10.3 Side Reactions of Irradiation – 417

10.10.4 Thermal Reaction – 418

10.11 Vitamin E – 419

10.11.1 Thermal Decomposition – 420

10.11.2 Chemical Oxidation – 420

10.11.3 Free Radical Reactions – 421

10.11.4 Quenching of Singlet Oxygen – 423

References – 424

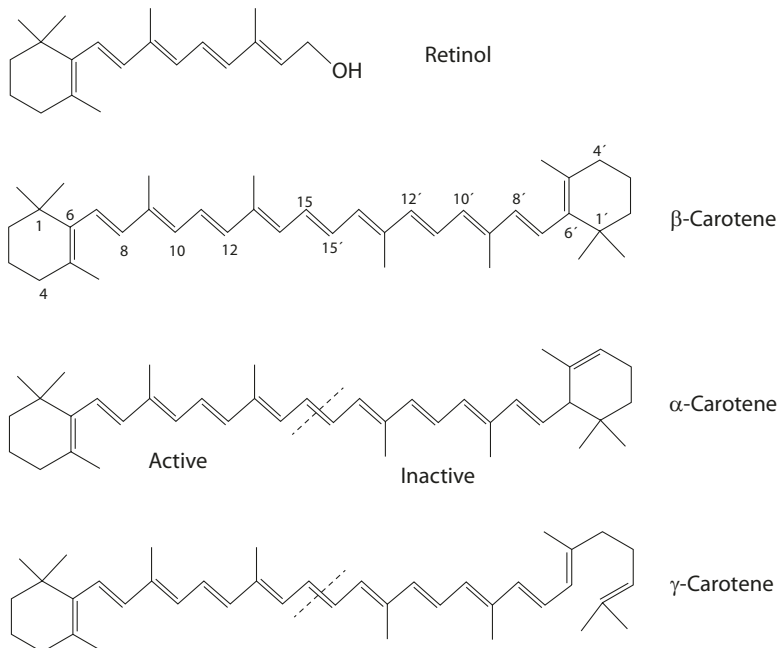
The degradation of vitamins during food processing has always been of great concern and the subject of particular interest to food scientists. The chemical changes of a vitamin in a food system are extremely complex. The assessment of losses in vitamins in a food system is hampered by the lack of systematic studies and by the many variables used in treatment conditions. Most of our present knowledge in this respect results from extrapolating experiments conducted in model systems. While the chemical degradation of vitamins can be used as an index for nutritional loss for a particular food, the fate of the degradation products and their reaction pathways remain largely unknown.

Another area of interest that deserves greater attention concerns the biochemical mechanisms of the vitamins, particularly how the reactions can be understood in terms of known mechanisms of organic reactions. This understanding is particularly important in view of the general misconception regarding vitamins as "natural" miracle treats. An appreciation of the chemical nature of vitamins can help to remove some of the myths and to understand their functional and physiological properties on the basis of good sense and science.

Vitamins are commonly classified into two groups, the fat-soluble vitamins A, D, E, and K and the water-soluble vitamin C and vitamins of the B complex.

10.1 Vitamin A

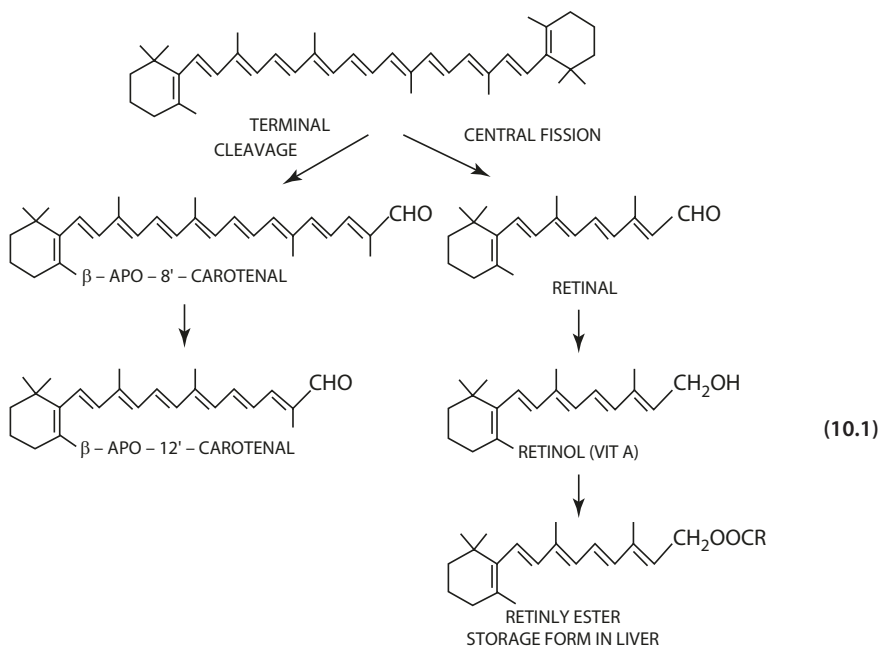
Vitamin A (retinol) is a diterpene alcohol consisting of a trimethylcyclohexenyl ring with a side chain of isoprene units. The main source of vitamin A is β -carotene (■ Fig. 10.1), which is one of the vitamin A precursors found in the carotenoid group. In general, a carotenoid provitamin A compound requires an unsubstituted β -carotene to possess 100% vitamin A activity. While β -carotene has 100% activity, α - and γ -carotenes possess approximately 50% vitamin A activity (■ Fig. 10.1).



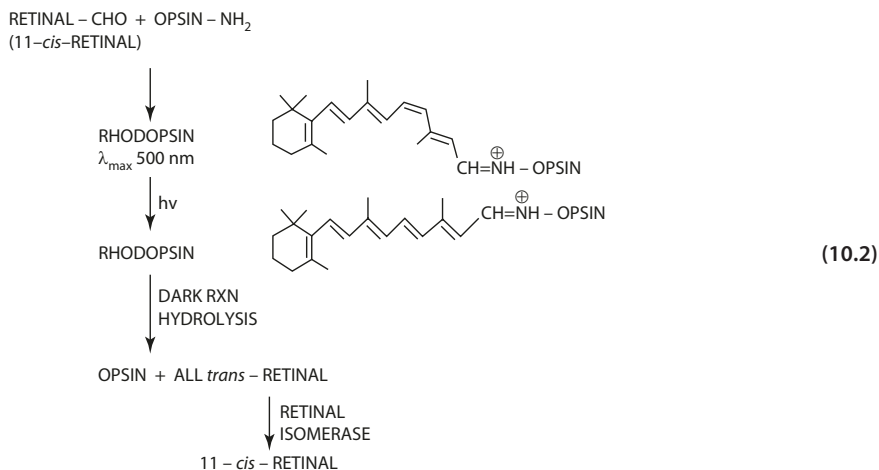
■ Fig. 10.1 Activity of carotenes

10.1.1 Biological Function

Biosynthesis of vitamin A from precursor compounds occurs in the intestinal mucosa. The molecule is cleaved either by (1) symmetric or asymmetric fission or (2) terminal cleavage to yield vitamin A aldehyde (retinal), which is then reduced to the alcohol (retinol) (Eq. 10.1). The enzyme 15,15'-dioxygenase has been demonstrated to cleave precursor compounds in the presence of oxygen to yield retinal.



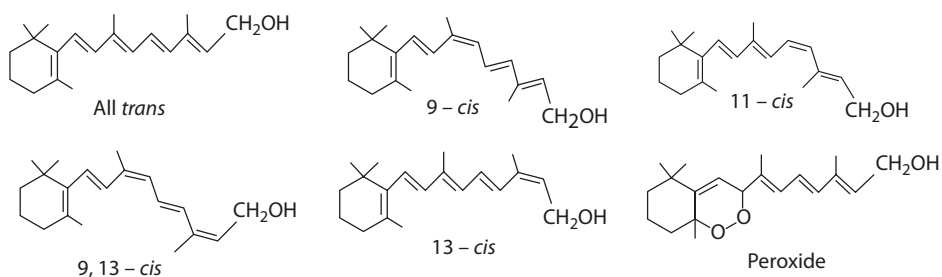
Vitamin A plays a role in development and growth, regulation of stability of biological membranes, maintenance of mucus-secreting cells of epithelia, biosynthesis of glycoprotein, and prevention of keratinization. Vitamin A is known to function in the maintenance of normal vision. The retina consists of photoreceptor cells known as rods and cones. In the rod cells are photosensitive pigments called rhodopsin. Rhodopsin is opsin (a protein) with 11-*cis*-retinal attached to the ϵ -amino group of one of the lysine residues via a Schiff-base linkage [2]. One result of the Schiff-base formation is a marked shift of λ_{\max} to a longer wavelength. Absorption of light by rhodopsin causes isomerization of 11-*cis*-retinal to the all-*trans* configuration. This photochemical event is followed by a series of dark reactions that leads to hydrolysis. The all-*trans* retinal is reconstituted to the *cis*-configuration catalyzed by the enzyme retinal isomerase (Eq. 10.2).



10.1.2 Action of Dilute Acid

The carotenes found in natural sources are in the all-*trans* form. In the presence of dilute HCl, the all-*trans* form isomerizes, yielding a mixture of *trans* and *cis* isomers. Isomerization may also be initiated by light or heat (refer to the next section and ► Chap. 4).

In an isomeric equilibrium mixture of vitamin A, only a few sterically favored isomers exist (► Fig. 10.2), although vitamin A with 5 carbon-carbon double bonds can theoretically comprise 32 stereoisomeric forms. Among the isomers found to exist include the 9-*cis* and 9,13-*cis*.

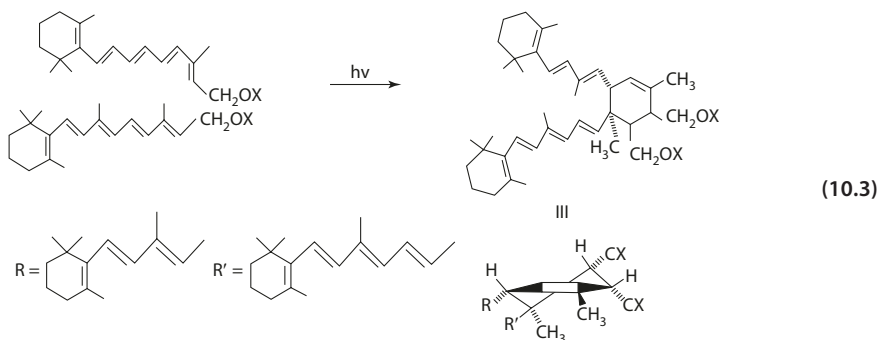


► Fig. 10.2 Isomeric mixture of vitamin A in the presence of dilute acid

10.1.3 Photochemical Reactions

■ ■ Photodimerization

The formation of dimers is expected from a Diels-Alder reaction between two vitamin A molecules. The unsaturated side chains of vitamin A are *trans* to each other and diequatorial. The two CH₂OX groups attached to C14 and C14' are *cis* to each other (Eq. 10.3) [10].

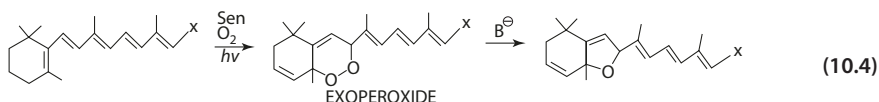


■ ■ Photoisomerization

Irradiation of vitamin A in hexane yields a mixture of *all-trans* (50%), *13-cis* (45%), *9-cis* (8%), and peroxide (5%). Depending on the solvent used, *11-cis* is also formed.

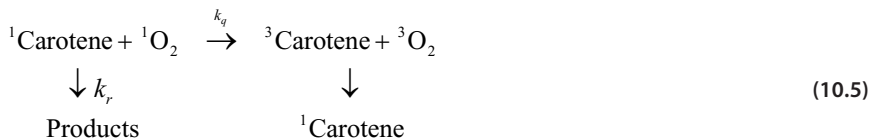
■ ■ Photosensitized Oxidation

When vitamin A is irradiated with ultraviolet light in the presence of a sensitizer, peroxide is formed, analogous to the adducts formed with dienophiles in the Diels-Alder reaction (Eq. 10.4).



■ ■ Quenching

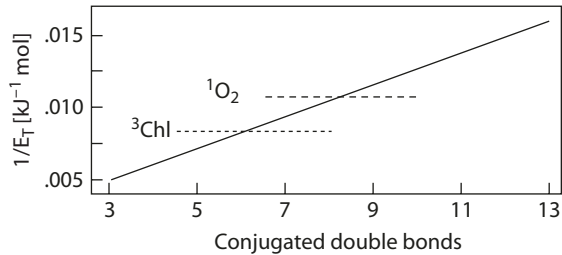
β -Carotene is very efficient in physical quenching of ¹O₂, with a quenching rate constant (k_q) of $1.3 \times 10^{10} \text{ M}^{-1} \text{ s}^{-1}$ (in benzene), close to that expected for diffusion-controlled reactions, and 10^4 times the rate constant (k_r) of the irreversible reaction with ¹O₂ (Eq. 10.5).



The energy difference between ¹O₂ and ³O₂ is estimated to be 95 kJ mol⁻¹. A linear plot of the inverse triplet energy ($1/E_T$) against the number of conjugated double bonds in the carotenoid indicates that only carotenoids with more than nine conjugated double bonds can quench the energy of ¹O₂ (■ Fig. 10.3) [25].

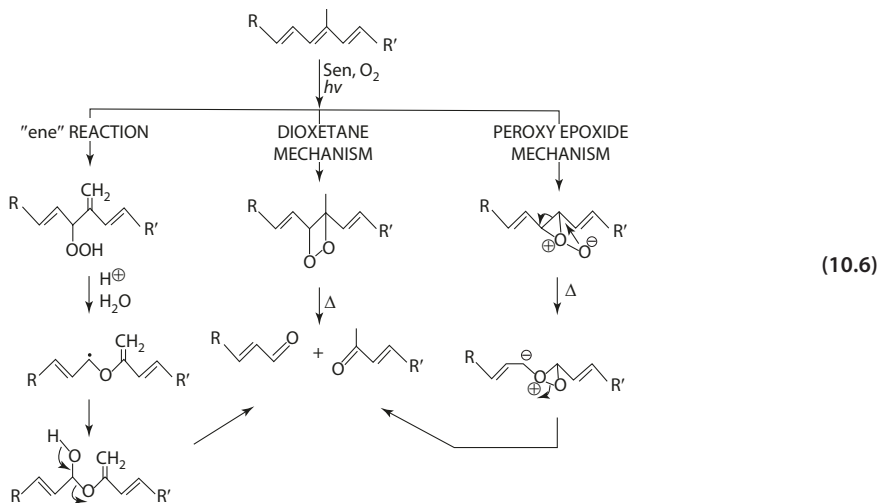
10.2 · Thiamin (Vitamin B₁)

■ **Fig. 10.3** The relationship between the reciprocal of carotenoid triplet energy levels and the number of conjugated double bonds in the pigment (From Krinsky [25] with permission. Copyright 1979 IUPAC)



■ ■ Fragmentation

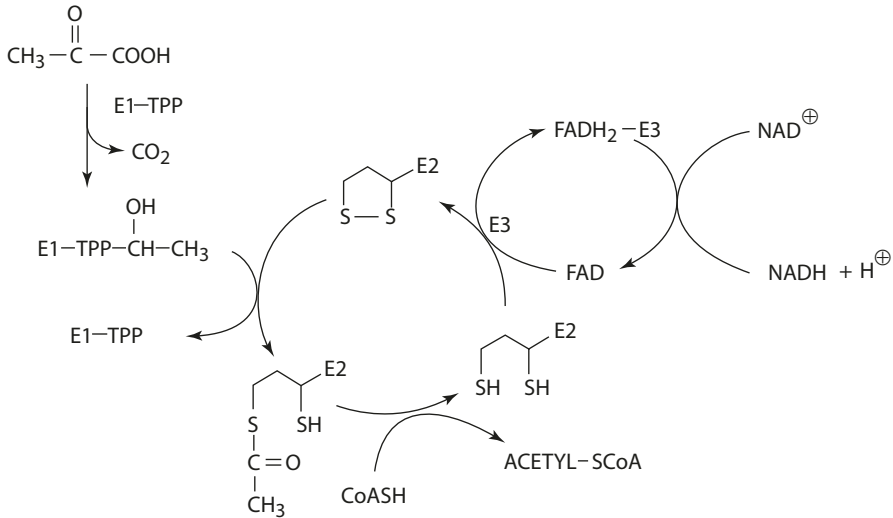
Singlet oxygen reacts with carotene and other carotenoids via (1) the ene-reaction, (2) the dioxane mechanism, and (3) the peroxy epoxide mechanism (Eq. 10.6). Various aliphatic and monocyclic isoprenoids are formed by fragmentation of the oxidation products, including β -13-, β -14-, and β -15-apo-carotenone.

10.2 Thiamin (Vitamin B₁)

Thiamin is present in small quantities in numerous foods; whole cereal grains and organ meat such as liver, heart, and kidney are a good source.

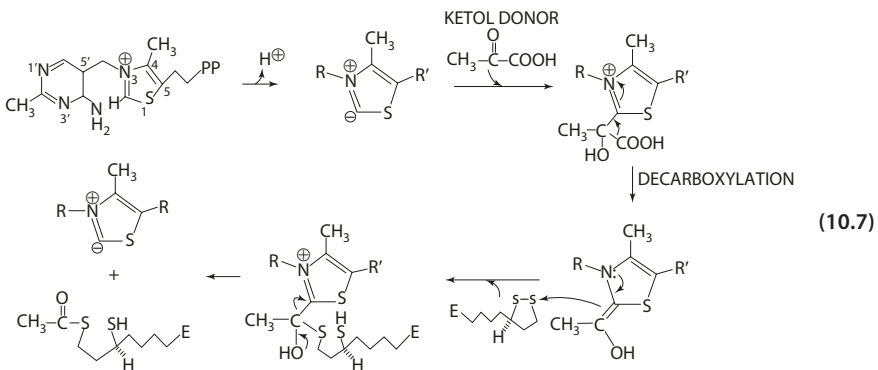
10.2.1 Biochemical Mechanism

Thiamin (as pyrophosphate) participates as a coenzyme in the reactions involving (1) α -keto acid decarboxylase, (2) α -keto acid oxidase, (3) transketolase, and (4) phosphoketolase. The conversion of pyruvate to acetyl CoA serves as an example in ■ Fig. 10.4. Here, thiamin is the cofactor of the pyruvate dehydrogenase complex, which comprises pyruvate decarboxylase (E1), dihydrolipoyl transacetylase (E2), and dihydrolipoyl dehydrogenase (E3).



■ Fig. 10.4 Scheme of reactions catalyzed by the pyruvate dehydrogenase complex

The basic chemistry of the reaction is a benzoin-type condensation. The thiamin molecule consists of a pyrimidine and a thiazolium ring. The C4' amino group acts as a weak base to abstract the proton at C2 in the thiazolium, resulting in the formation of an ylide. The process is enzyme oriented. The ylide carbanion condenses with a ketal donor, such as pyruvate in this case. The thiazolium ion acts as an "electron sink" to accept electrons from the C–C bond cleaved in decarboxylation. The enolic intermediate acts as a nucleophile and acrylates lipoic acid (linked to the lysyl ϵ -amino group of the enzyme lipoyl transacetylase) before being transferred to CoA (Eq. 10.7).

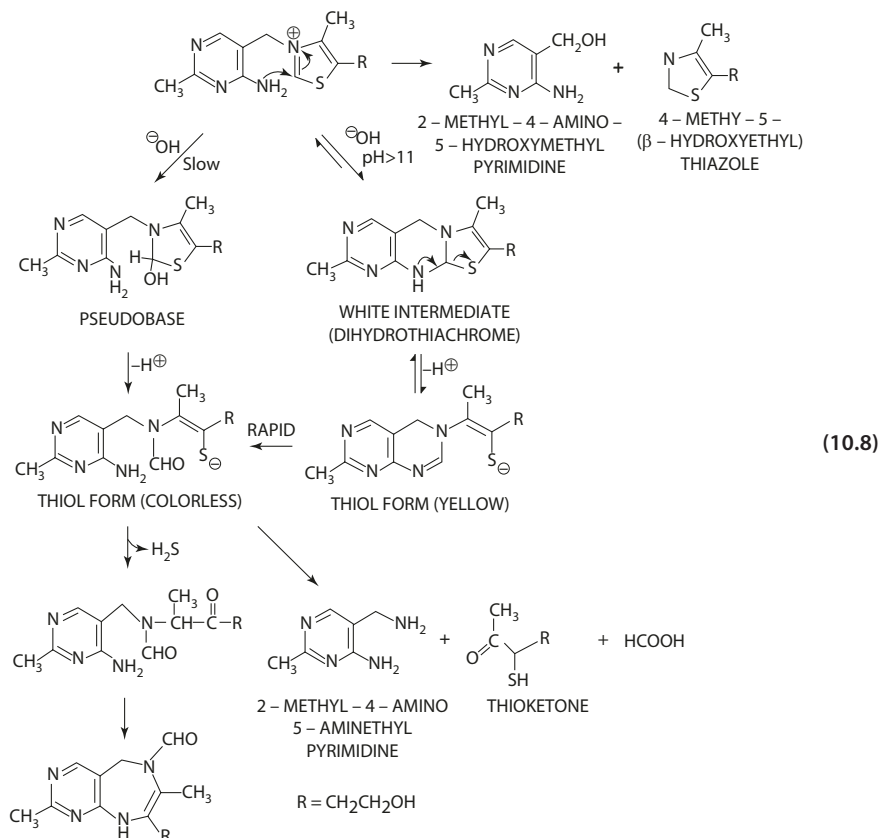


10.2.2 Action of Alkali and Acid

In alkaline solution, the hydroxide ion is added to the C2 of the thiazolium ring, forming an unstable pseudobase. Disruption of the C–S bond yields a colorless thiol form. In a solution of high pH (>11), the amino group of the pyrimidine reacts

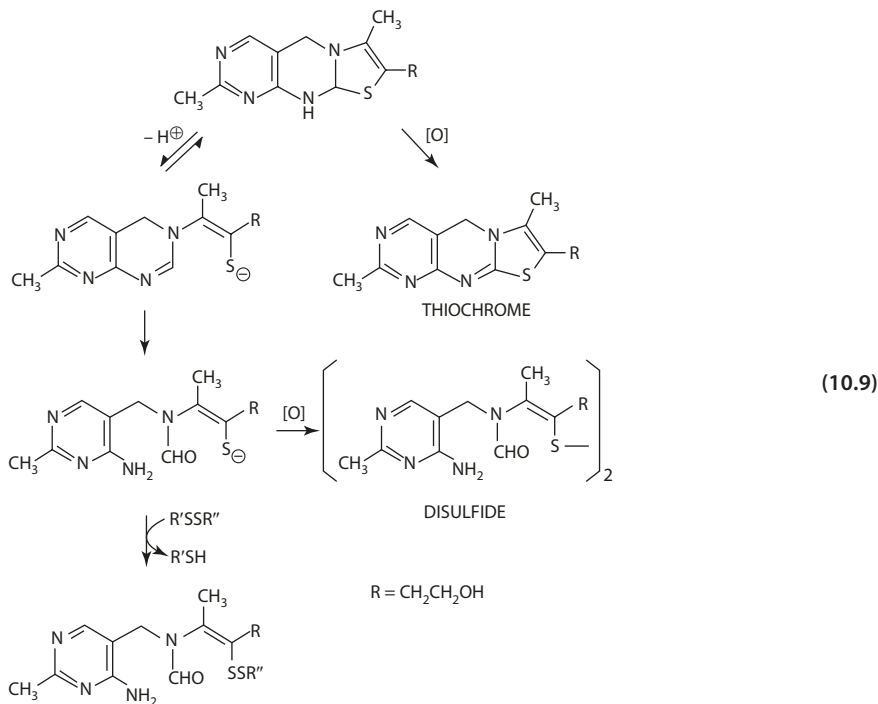
10.2 · Thiamin (Vitamin B₁)

intramolecularly with the C2 in the thiazolium ring to form a tricyclic intermediate, dihydrothiachrome. Ionization of the dihydrothiachrome with opening of the thiazolium ring yields a yellow thiol form, which then converts to the colorless thiol form (Eq. 10.8). Degradation of the thiol form yields hydrogen sulfide and a variety of breakdown products [11]. Heating thiamin solution at pH 6.0 or below results in the cleavage at the methylene bridge to give 2-methyl-4-amino-5-hydroxymethyl pyridine and 4-methyl-5-(β -hydroxyethyl)thiazole.



10.2.3 Oxidation and Reduction

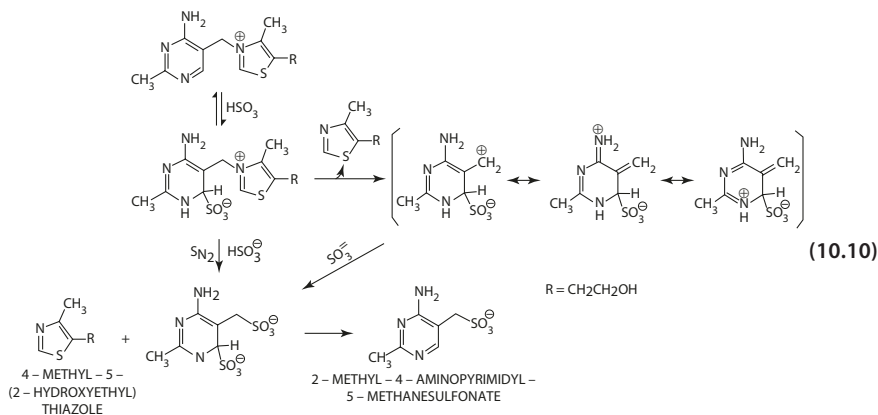
Both the yellow thiol form and the intermediate precursor can be oxidized to the thiochrome with an intense blue fluorescence. The colorless thiol can be oxidized, or undergoes sulfhydryl-disulfide exchange to form dimers (Eq. 10.9). Oxidizing agents such as H₂O₂ and I₂ accelerate the reactions in neutral or alkaline solutions. The thiochrome is not found if the thiamin stays in alkaline solution long enough for the yellow thiol form to disappear before the oxidizing agent is introduced.



10

10.2.4 Reaction with Bisulfite

Thiamin is unstable and undergoes cleavage in bisulfite solution. (Refer also to ► Chap. 9, section on "Reaction with Pyrimidines.") The first step is a bisulfite addition to the 6-position in the pyrimidine ring, followed by nucleophilic substitution at the methylene carbon by a second bisulfite ion via a S_N2 mechanism [9]. It is also suggested that the addition of the first bisulfite ion is followed by the elimination of the leaving group (thiazole) to yield a stabilized carbocation intermediate. Addition of a second bisulfite ion with the loss of the first sulfite ion yields the final sulfonate product (Eq. 10.10) [44].



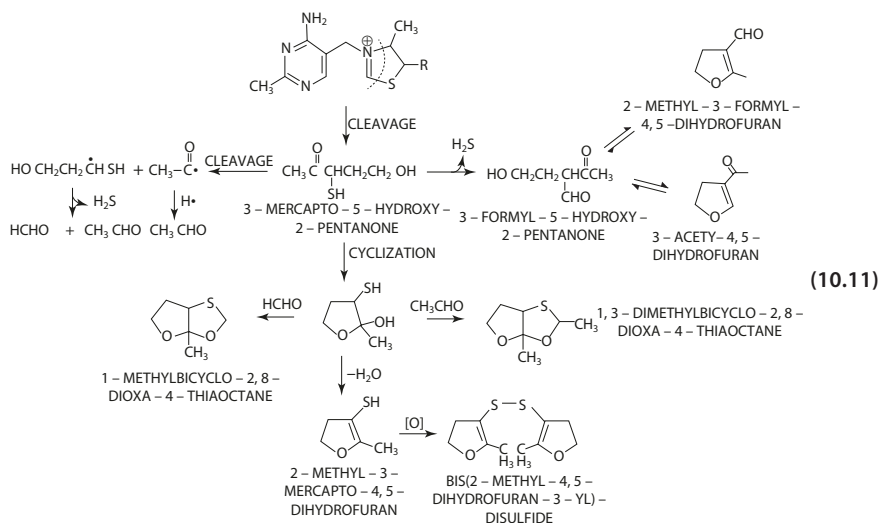
4-METHYL-5-(2-HYDROXYETHYL)THIAZOLE

2-METHYL-4-AMINOPYRIMIDYL-5-METHANESULFONATE

10.2.5 Photolysis

Light irradiation of thiamin causes cleavage at the C–N and C–S bonds, forming 3-mercapto-5-hydroxy-2-pentanone, which is the key intermediate in the formation of various degradation products. Cleavage at the α - and β -position of the intermediate yields hydrogen sulfide, formaldehyde, and acetaldehyde. Elimination of sulfur from the intermediate followed by formylation results in the formation of 3-formyl-5-hydroxy-2-pentanone, which cyclizes readily to an equilibrium mixture of 2-methyl-3-formyl-4,5-dihydrofuran and 3-acetyl-4,5-dihydrofuran.

The intermediate compound may cyclize to form 2-hydroxy-2-methyl-3-mercaptofuran. Dehydration and oxidation of the latter yield a disulfide, bis(2-methyl-4,5-dihydrofuran-3-yl)disulfide. It may also react with formaldehyde or acetaldehyde to form the characteristic thiamin odor, 1-methylbicyclo[3.3.0]-4-thia-2,8-dioxaoctane or 1,3-dimethylbicyclo[3.3.0]-4-thia-2,8-dioxaoctane, respectively. The thresholds of these two thiamin odor compounds are 0.1 ppm and 1 ppm (in water), respectively [38] (Eq. 10.11).



10.3 Riboflavin (Vitamin B₂)

Riboflavin is 7,8-dimethyl-10-(1'-D-ribyl)isalloxazine. The biochemically functional coenzyme is flavin adenine dinucleotide (FAD) (■ Fig. 10.5).

Flavoenzymes catalyze a diverse range of reactions: some typical examples are given in ■ Fig. 10.6. The reaction substrates include amines, amino acids, alcohols, hydroxy acids, dithiols, aldehydes, ketones, and acids.

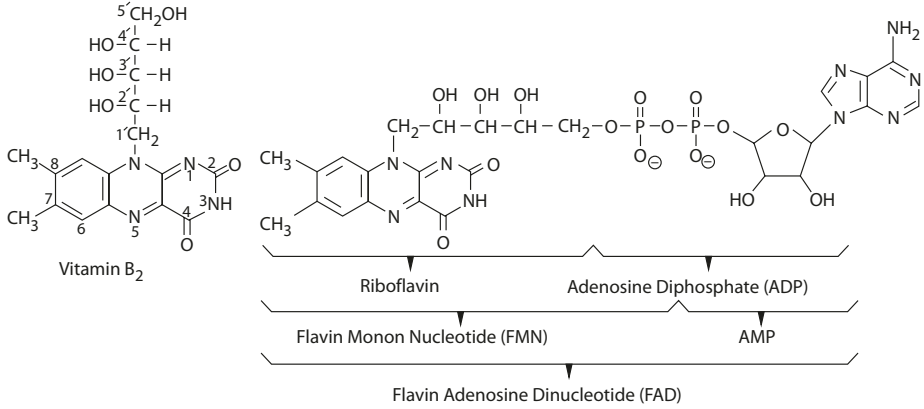


Fig. 10.5 Riboflavin and flavin adenine dinucleotide

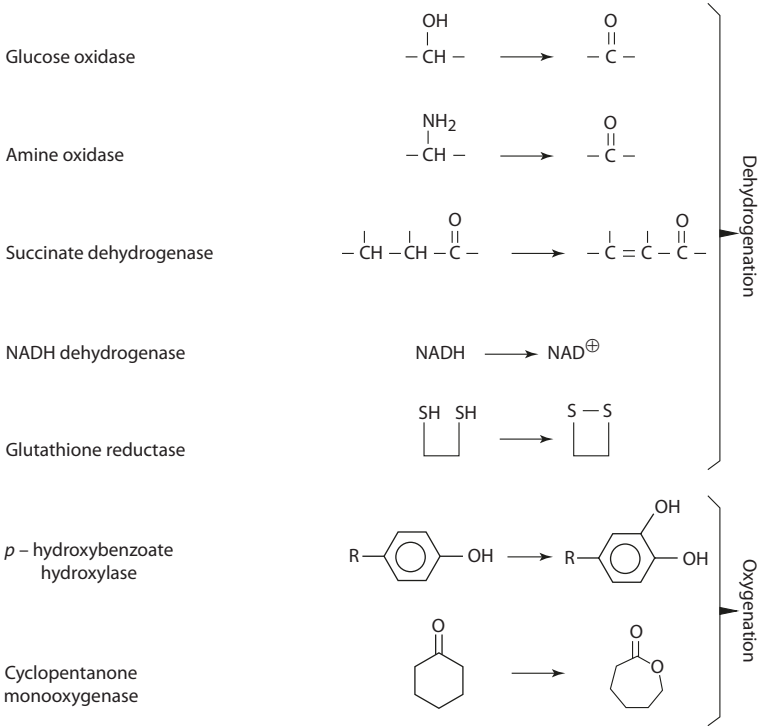
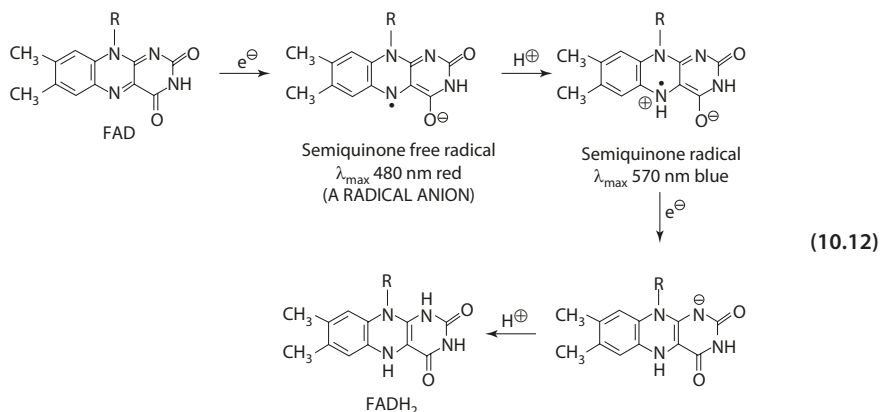


Fig. 10.6 Reactions catalyzed by flavoenzyme

10.3.1 Biochemical Mechanism

Flavin has a unique property of undergoing both $1e^-$ and $2e^-$ reactions. The semiquinone intermediate is a stable radical, with the unpaired electrons delocalized through the conjugated isoalloxazine ring (Eq. 10.12).



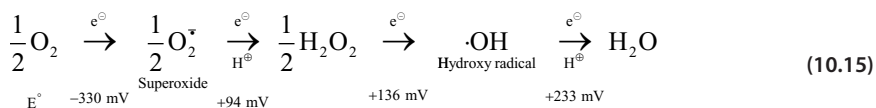
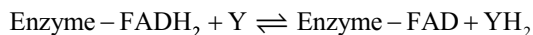
Most flavins bind strongly but noncovalently with the enzyme. The equilibrium constant K is in the order of 10^{-8} M, indicating a strong binding (Eq. 10.13). The flavin coenzyme must complete the redox cycle (two half-reactions) before the enzyme can carry out the next cycle of catalysis (Eq. 10.14). The electron acceptor Y in the oxidation half-reaction is commonly molecular oxygen, which undergoes a $2e^-$ reduction to H_2O_2 or a $4e^-$ reduction to H_2O by successive $1e^-$ reductions (Eq. 10.15).



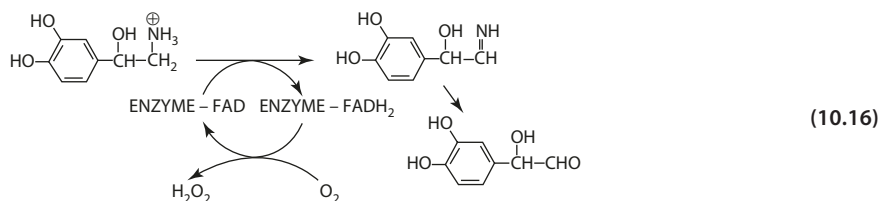
Reduction



Oxidation

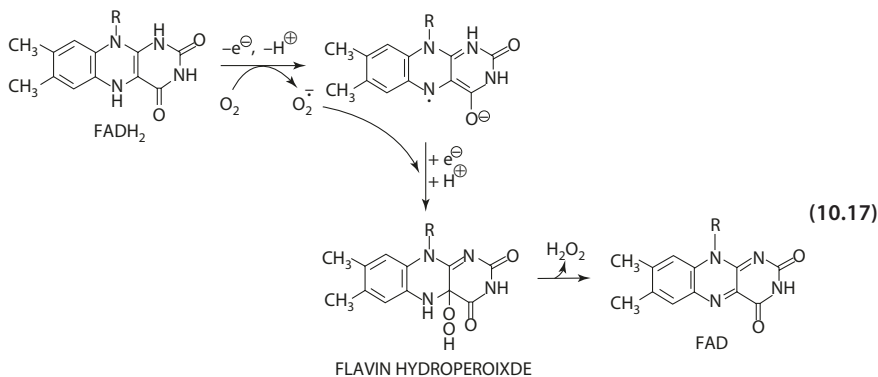


Monoamine oxidase is the flavoenzyme that is involved in the inactivation of catecholamine neurotransmitters by converting the amines to aldehydes. The overall reaction is represented in Eq. 10.16.



The reoxidation of flavin is mediated by a radical mechanism with the oxygen molecule to produce the superoxide anion ($O_2^{\cdot-}$) and the semiquinone radical (flavin-H \cdot). The superoxide anion and flavin-H \cdot recombine to form flavin hydroperoxide, which decomposes to H_2O_2 and oxidized flavin (Eq. 10.17).

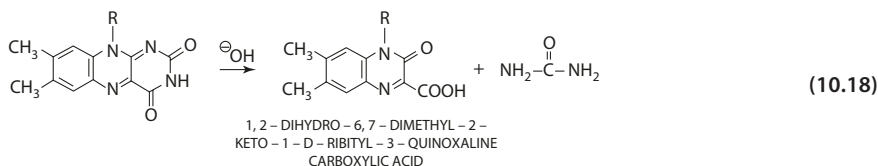
In the reoxidation of enzyme-FADH $_2$, the oxygen undergoes a $2e^-$ reduction to H_2O_2 . Most flavoenzymes involved in the $4e^-$ reduction of oxygen to H_2O are of bacterial origin and therefore will not be discussed.



10

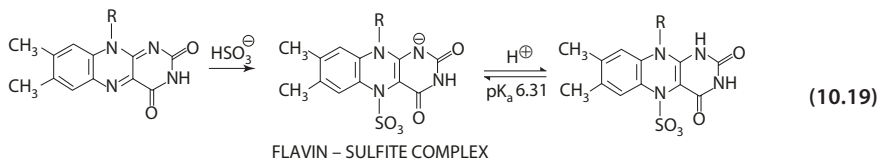
10.3.2 Alkaline Degradation

In alkaline solution, riboflavin is hydrolyzed to urea and oxocarboxylic acid (Eq. 10.18). The hydrolysis occurs even at room temperature.



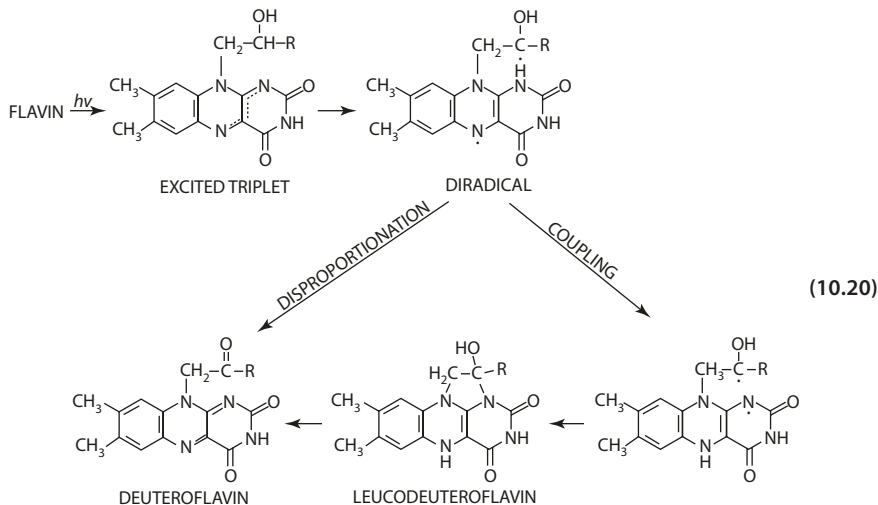
10.3.3 Reaction with Sulfite

Flavoenzymes (particularly the oxidases) and, to a much less extent, the flavins react with sulfite at the N5 position to form an addition complex [18]. Acid hydrolysis under anaerobic conditions yields the reduced flavin and sulfite (Eq. 10.19).



10.3.4 Photochemical Reaction

The photochemistry of flavin can be divided into four categories: photoreduction, photodealkylation, photoaddition, and photosensitized reactions [17].



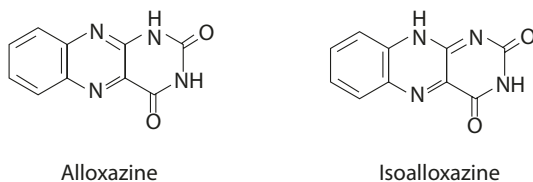
■ Photoreduction

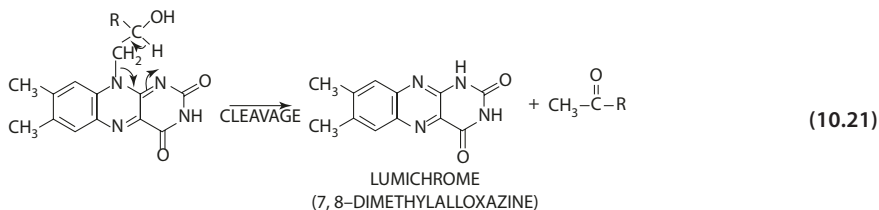
Under anaerobic conditions, flavin undergoes a singlet to triplet excitation, followed by hydrogen abstraction from the ribityl C2'. The diradical intermediate undergoes disproportionation to form deuteroflavin. Alternatively, the diradical undergoes proton exchange to form a N1–N10 bridged leucodeuteroflavin, followed by oxidation to yield the deuteroflavin (Eq. 10.20). (Lumichrome is an alloxazine, and riboflavin and deuteroflavin are isoalloxazines, as indicated in ■ Fig. 10.7).

■ Photodealkylation

Two mechanisms have been proposed for the intramolecular reaction yielding the lumichrome and the ketone. The first involves homolytic cleavage of the N10–C1 bond in the biradical intermediate in Eq. 10.20. The second involves a synchronous fragmentation of a N10–C1' and a C2'–H bond in *cis*-periplanar conformation with direct proton transfer. The second mechanism proceeds without a biradical intermediate (Eq. 10.21).

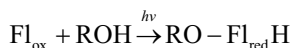
■ Fig. 10.7 Structure of alloxazine and isoalloxazine



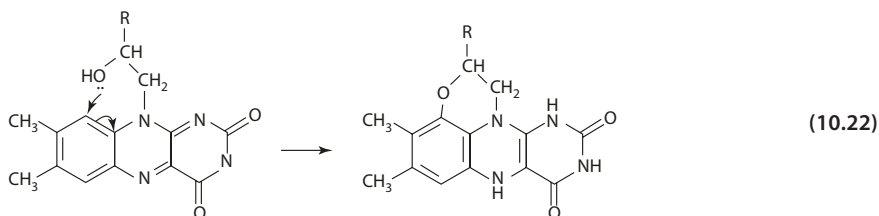


■ ■ Photoaddition

Photoaddition follows the general reaction:



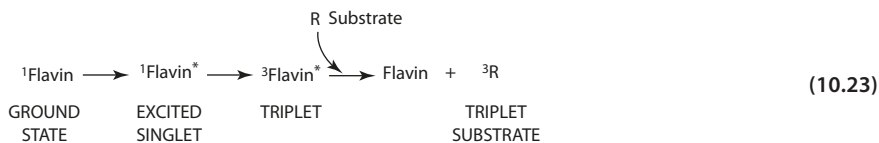
The addition product is hydroxy- or alkoxy-dihydroflavin. While photoreduction and dealkylation occur predominantly through the triplet state $^3\text{Fl}_{\text{ox}}^*$, photoaddition proceeds via the excited singlet $^1\text{Fl}_{\text{ox}}^*$. Intramolecular addition involves a nucleophilic attack of the C2' hydroxyl group at C9. A 9 α ,5-proton shift leads to the formation of 9-alkoxy-flavin (Eq. 10.22).



10.3.5 Flavin-Sensitized Reactions

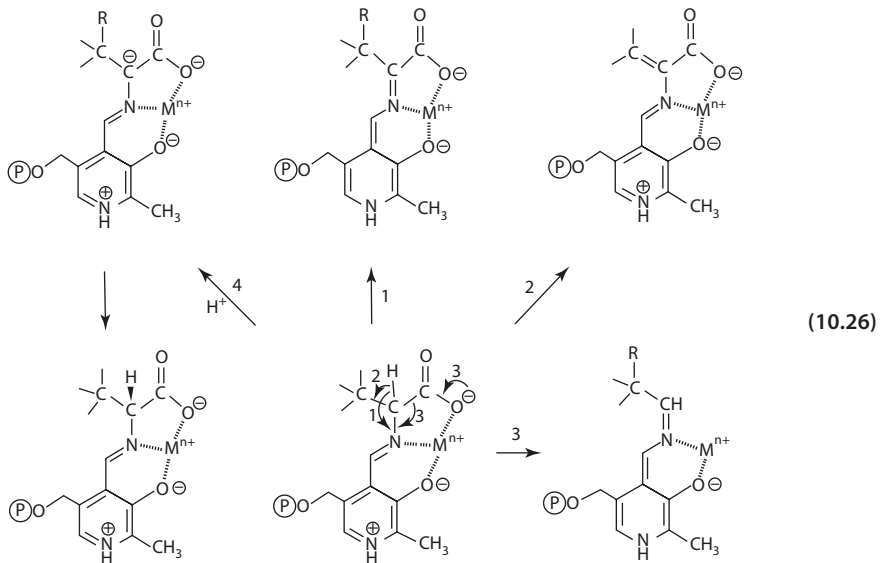
■ ■ Photosensitized Isomerization

Photochemical reactions sensitized by flavins generally proceed via a triplet-triplet energy transfer (Eq. 10.23). Flavins can photosensitize *cis-trans* isomerization of olefinic compounds. Retinol, cinnamic acid, and stilbene-4-carboxylic acid are specific examples.



■ ■ Photosensitized Oxidation

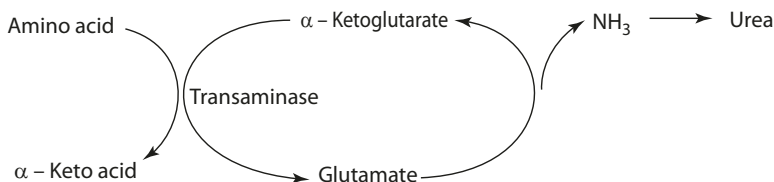
Flavin-sensitized oxidation usually yields complex products. In the case of aliphatic amino compounds, the products are carbon dioxide and an aldehyde (Eq. 10.24).



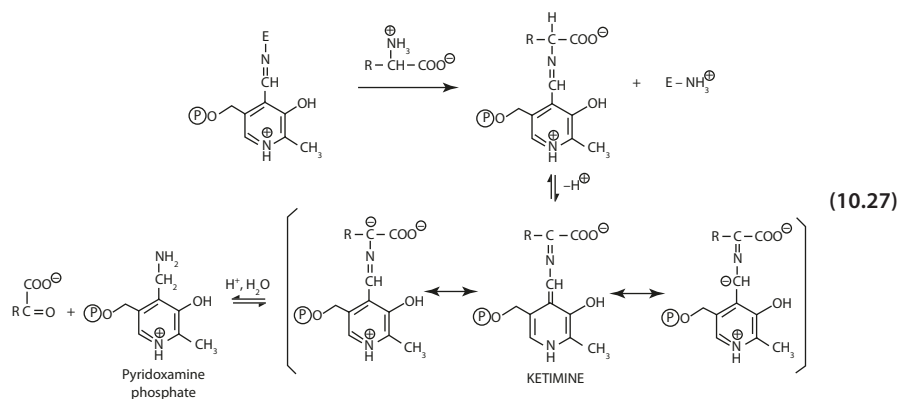
In all cases, hydrolysis of the aldimine yields an amine and pyridoxal, while hydrolysis of the ketimine yields keto acid and pyridoxamine. The metal ion helps stabilize the conjugation system between the Schiff base and the pyridine ring and accelerates the rate of reaction by acting as a general acid catalyst.

To illustrate the biochemical mechanism of pyridoxal phosphate, the reaction of transamination serves as a typical example. In the degradation of amino acids, the α -amino group of the amino acid is transferred to the α -ketoglutarate to form glutamate, which is oxidatively deaminated to yield ammonia (■ Fig. 10.9).

As the initial step, pyridoxal phosphate is linked via the formation of a Schiff base with the ϵ -amino lysine of the transaminase. In transamination, the enzyme-imine is converted to the substrate-imine. The next step involves an abstraction of the α -H from the substrate, followed by aldimine-ketimine conversion. The product is stabilized by resonance. Hydrolysis of the ketimine yields the α -keto acid and the pyridoxamine phosphate. The pyridoxamine phosphate then reacts with α -ketoglutarate (an α -keto acid) to yield glutamate (an α -amino acid) in a reverse mechanism to complete the reaction cycle (Eq. 10.27).

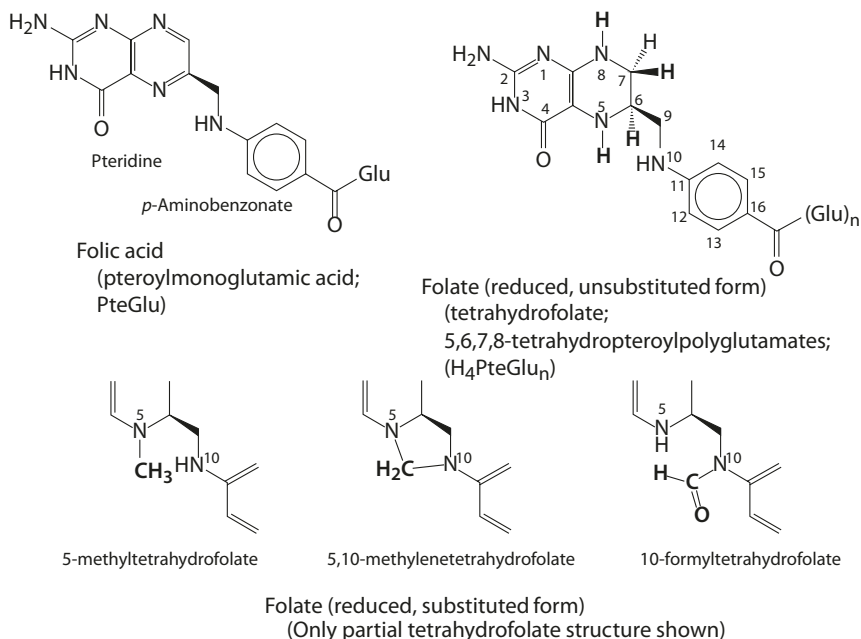


■ Fig. 10.9 The oxidative deamination cycle



10.5 Folic Acid (Vitamin B₉)

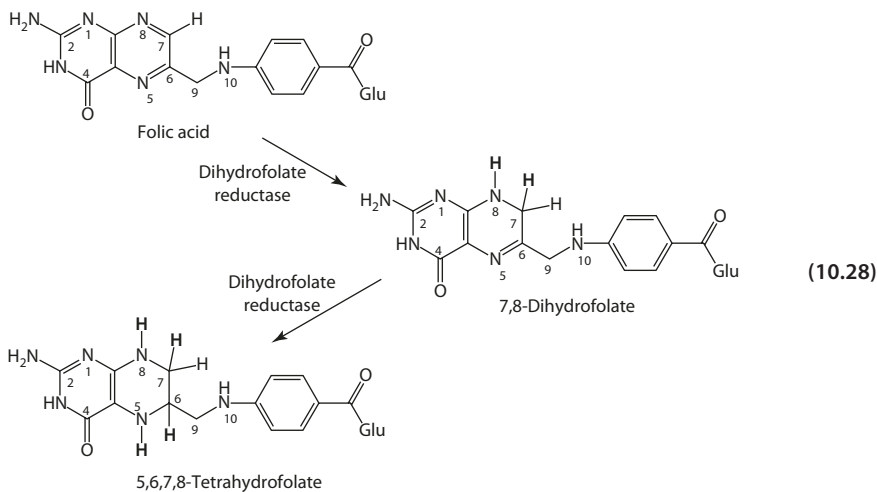
Folates (vitamin B₉) are a group of heterocyclic chemicals based on the 4-[(pteridin-6-ylmethyl)amino]benzoic acid skeleton (called pterotic acid) conjugated with one or more L-glutamate units. The common name is pteroylglutamate. The basic structure consists of three parts: the pteridine bicyclic ring, aminobenzoic acid, and glutamic acid group. The pteridine moiety is in most cases substituted at the N5 and N10 positions with methyl (CH₃), formyl (HCO), methylene (CH₂), methenyl (CH⁺), or formimino (CH=NH) groups. The glutamate part is a polyglutamyl chain of several residues, with the second and subsequent glutamate linked through the γ -carboxyl of the latter (■ Fig. 10.10).



■ Fig. 10.10 Structures of folates

Most naturally occurring folates are in the reduced form, which is indicated by the prefixes "dihydro-", "tetrahydro-", etc. Hence, the name tetrahydropteroylpolyglutamate (or $H_4PteGlu_n$), for example, indicates a reduced folate with " H_4 " indicating reduction at 5,6,7,8 positions of the pteridine ring and " n " equals to the number of glutamic acid units. Folates are found in a wide variety of foods, particularly dark green leafy vegetables, liver, egg yolk, beans and legumes, wheat germ, and yeast. The most common folate found in foods is 5-methyltetrahydrofolate ($5-CH_3-H_4$ folate). In the intestinal mucosal cell, the polyglutamyl chain is removed by the enzyme folate conjugase, and the resulting 5-methyltetrahydrofolate monoglutamate is subsequently absorbed.

Humans do not synthesize folates. Many countries require mandatory fortification of at least one major cereal grains, frequently wheat flour. The vitamin supplement (commonly known as folic acid) is a synthetic unreduced monoglutamic form (pteroylmonoglutamic acid, PteGlu). Since the pteridine ring is not reduced, the supplement is stable under most food processing conditions, but is biologically inactive. In the intestine, folic acid is reduced by the enzyme dihydrofolate reductase to the active fully reduced tetrahydro form (Eq. 10.28). The enzymatic conversion is important, because accumulation of unmetabolized folic acid in plasma or tissues may be harmful. In contrast to the vitamin supplement, folates in the natural reduced form are unstable and subject to degradation. Substantial loss of the vitamin occurs during harvesting, storage, processing, and preparation of foods.



A note on the nomenclature of folates [5]:

Pterotic acid = the 4-[(pteridin-6-ylmethyl)amino]benzoic acid skeleton of folates.

Pteroates = the salts derived from pterotic acid.

Pteroyl = the acyl group derived from pterotic acid.

Pteroylglutamate = compounds in which pterotic acid is conjugated with one or more L glutamate residues (pteroyldiglutamate for 2 glutamate residues, pteroylhexaglutamate for 6 glutamate residues, etc.) (Fig. 10.11). The term is used regardless of the state of reduction of the pteridine ring or one-carbon substitutions.

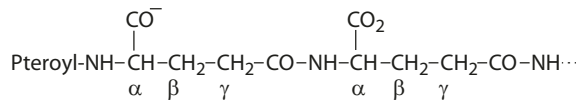
Pteroylglutamic acid = acid form of pteroylglutamate.

Pteroylpolyglutamate = apply to all with more than one glutamate residues.

Folate = the preferred synonym for pteroylglutamate.

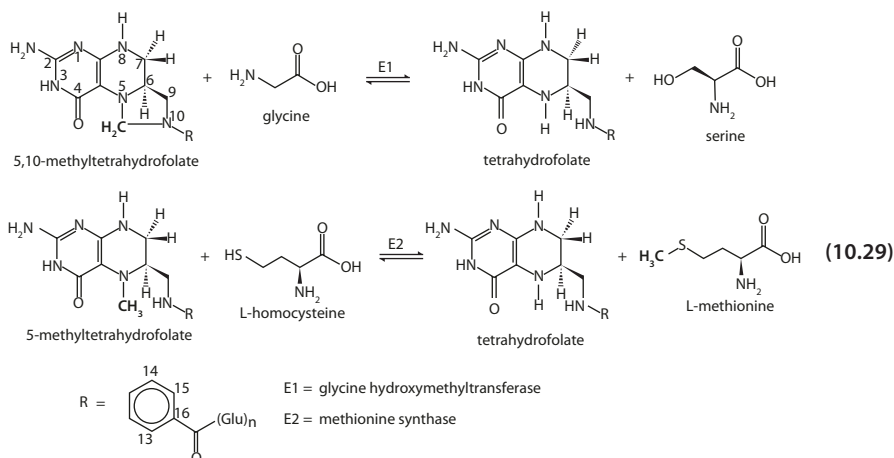
Folic acid = the preferred synonym for pteroylglutamic acid.

■ Fig. 10.11 Pteroyldiglutamate



10.5.1 Biological Functions

In the biological system, folates function to accept, transport, and donate C1 groups, with participation in five major one-carbon transfer reactions within the cell [19, 30]. In accepting the C1 group (originated from the catabolism of serine, histidine, and purines), the H₄PteGlu is transported and enzymatically interconverted into different C1 species. The species 10-HCO-H₄folate donates carbon atoms to the skeleton of each purine molecule in DNA and RNA biosynthesis. The 5,10-CH₂-H₄folate donates its methylene group to dUMP (deoxyuridylate) to form thymidylate (dTMP) in the biosynthesis of one of the pyrimidines. The same folate also involves in the biosynthesis of methionine from remethylation of homocysteine. In the process, the 5,10-CH₂-H₄folate is converted back to the tetrahydrofolate (H₄folate) form (Eq. 10.29).



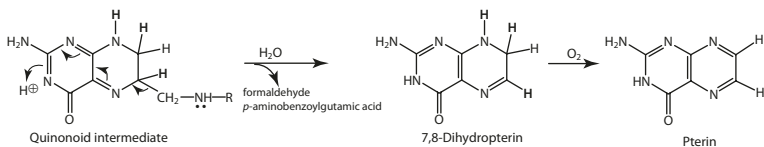
10.5.2 Degradation of Folates

Folate from natural sources (i.e., the reduced form) is sensitive to a wide range of processes, influenced by heat, pressure, pH, radiation, oxygen, light, metal ions, and antioxidants. Degradation follows first-order kinetics, and in all cases, the initial reaction involves cleavage of the C9–N10 bond resulting in irreversible loss of vitamin activity.

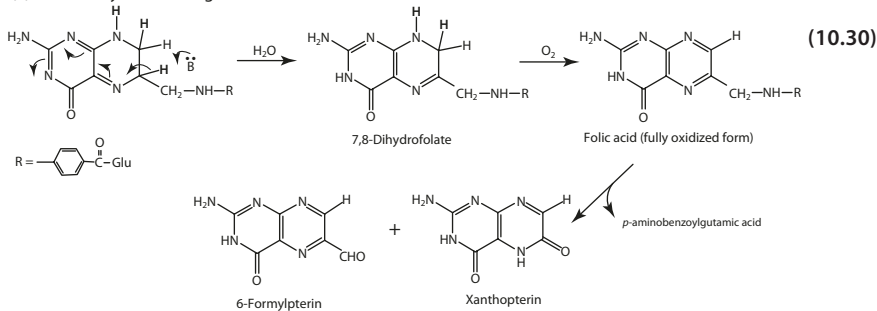
■ Acid- or Base-Catalyzed Rearrangement of the Quinonoid Intermediate

At low pH, the products are 7,8-dihydropterin and *p*-aminobenzoylglutamic acid (Eq. 10.30). At high pH, the product is 7,8-dihydrofolic acid which is further oxidized to the fully oxidized form. Breakdown of the latter yields xanthopterin, 6-formylpterin, and *p*-aminobenzoylglutamic acid.

(1) Acid-catalyzed rearrangement



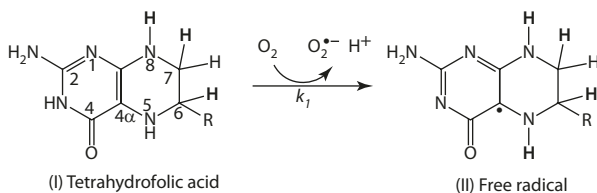
(2) Base-catalyzed rearrangement



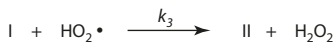
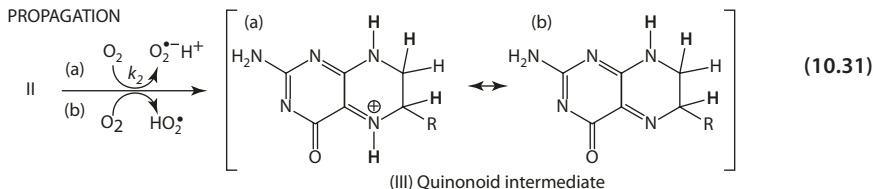
■ Autoxidation of Folates

Folates in the reduced form are highly susceptible to autoxidation. The reaction is first order (on folate), with the rate increases in the region of pH 9–13, in which the 3,4-amide group is deprotonated[4]. Decreasing pH from 6 to 3 decreases the rate due to protonation. Folate autoxidation is a free-radical chain process, with the initiation step occurred by electron abstraction from the 4 α position of the 7,8-dihydro or 5,6,7,8-tetrahydropteridine ring followed by proton loss (Eq. 10.31). The 4 α position is electron dense due to the extensive resonance delocalization caused by the three non-bonded electron pairs on the N2, N4, and N8 of the pteridine ring [13, 14]. Triplet oxygen has two unpaired bonding electrons (see Appendix 1), readily accepting electrons. The resulting folate free radical undergoes further electron abstraction and proton loss to give the quinonoid intermediate. The folate free radical acts as the chain carrier in the autoxidation scheme [36].

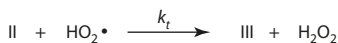
INITIATION STEP



PROPAGATION



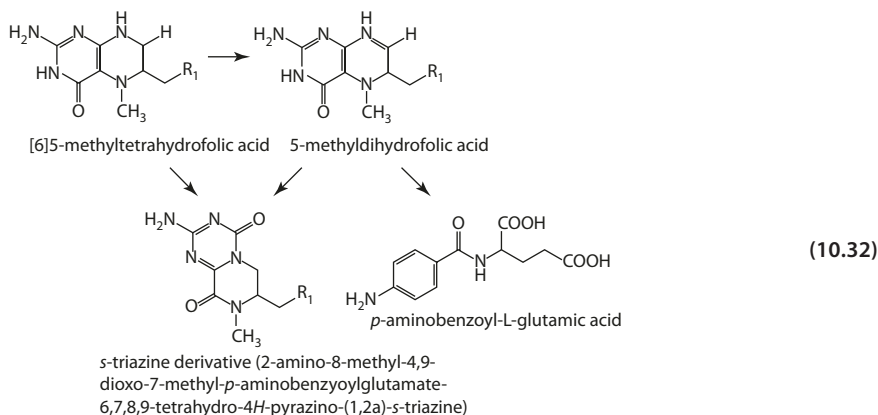
TERMINATION



10.5 · Folic Acid (Vitamin B₉)

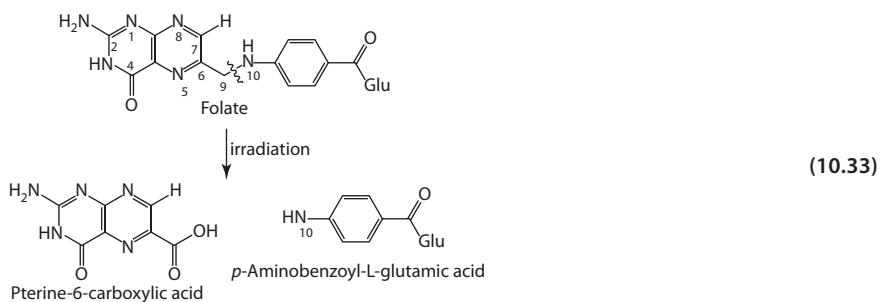
Thermal Oxidation

The most common food folate, 5-methyltetrahydrofolate with optimal stability at neutral pH, undergoes thermal oxidation, following first-order kinetics. Addition of ascorbic acid and other food antioxidants enhances the stability of the folate to temperature and pressure. The predominant degradation products are 5-methyldihydrofolate, *p*-aminobenzoyl-L-glutamate, and a *s*-triazine derivative (2-amino-8-methyl-4,9-dioxo-7-methyl-*p*-aminobenzoylglutamate-6,7,8,9-tetrahydro-4*H*-pyrazino-(1,2*a*)-*s*-triazine) (Eq. 10.32) [39].



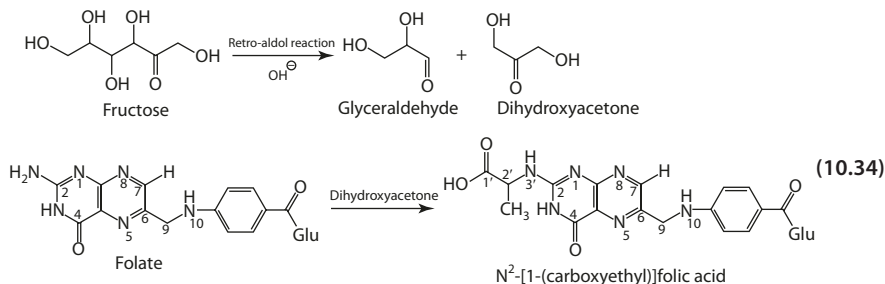
Photodegradation and Radiolysis

Both ultraviolet light and ionizing irradiation cause degradation of folate to produce inactive substituted *p*-aminobenzoylglutamate and 6-formylpterin [3]. The latter is further degraded to pterine-6-carboxylic acid (Eq. 10.33). Both 6-formylpterin and pterine-6-carboxylic acid can act as sensitizers to initiate further chemical reactions. In all cases, the C9–N10 bond is the most susceptible point of attack for bond cleavage.



Nonenzymatic Glycation

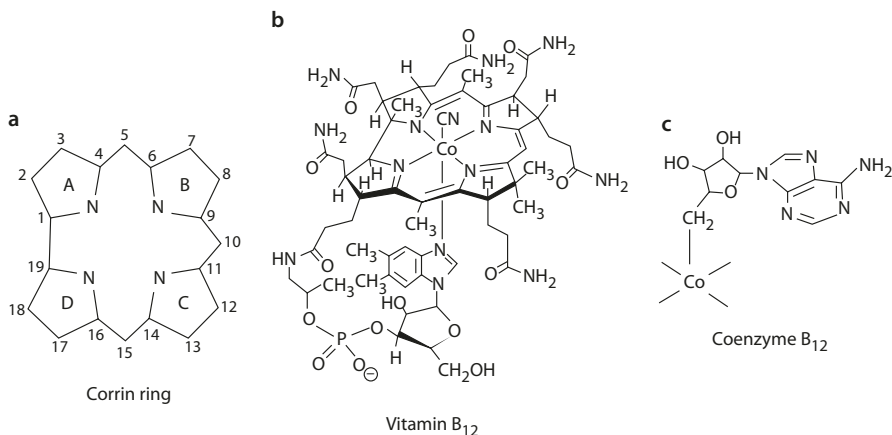
The pteridine ring of folate contains an exocyclic amino group that may react with sugars and sugar degradation products in a mechanism similar to the Maillard reaction. Reducing sugars, such as glucose, fructose, ribose, maltose, and lactose, have been shown to react with folate to form a nonenzymatic glycation product, *N*²-[1-(carboxyethyl)]folic acid during heat treatment (Eq. 10.34) [37, 40]. Fructose as a 2-ketose containing a 1,3-dihydroxy-2-oxo moiety is most effective in generating the glycation product.



10.6 Vitamin B₁₂

The core structure of the vitamin B₁₂ molecule resembles an iron-porphyrin system, but with two of the four pyrrole rings linked directly without a methylene bridge. This corrin system binds Co(III). All side chains consist of acetamide and/or propionamide groups. One side chain consists of an amide-phosphate-ribose bonded to a dimethylbenzimidazole group which coordinates with Co(III). The corrin ring is numbered clockwise, starting from ring A that is involved in the direct linking of the pyrrole ring (■ Fig. 10.12a).

The top axial ligand in the vitamin B₁₂ isolated initially from natural sources is cyanide ion. However, the cyanide was only picked up during isolation and purification steps in the early investigations. The compound has since then also been known as cyanocobalamin (■ Fig. 10.12b). Cyanocobalamin is the form used in dietary supplements. Cyanocobalamin is not biochemically active, and the ingested vitamin must be enzymatically modified to coenzyme B₁₂ by replacing the cyano with a 5'-deoxyadenosyl group (hence known as 5'-deoxyadenosylcobalamin) (■ Fig. 10.12c).

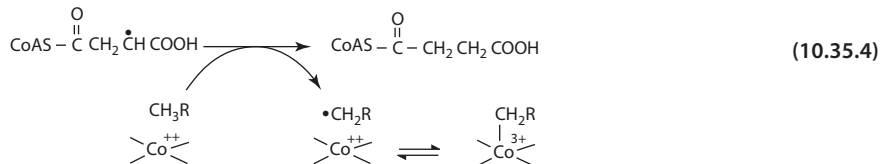
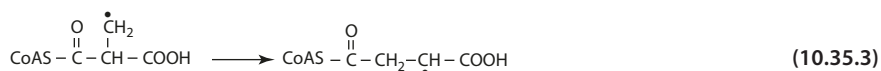
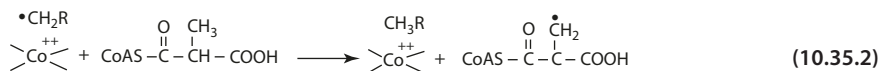
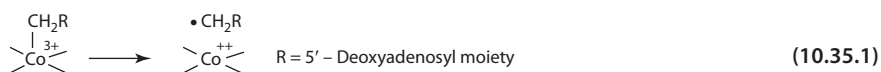


■ Fig. 10.12 a Corrin ring, b vitamin B₁₂, and c coenzyme B₁₂ (From Abels [20])

10.6.1 Biochemical Mechanism

Coenzyme B₁₂ is a cofactor for various enzyme reactions, involving the 1,2-interchange of a hydrogen atom and another substituent. In the case of methylmalonyl-coenzyme A mutase rearrangement, the following steps are depicted [16]:

1. Enzyme-induced homolytic dissociation of the cobalt-carbon bond to generate cobalamin (II) and 5'-deoxyadenosyl radical (Eq. 10.35.1).
2. Abstraction by the 5'-deoxyadenosyl radical of a hydrogen atom from the substrate to yield a substrate radical and 5'-deoxyadenosine (Eq. 10.35.2).
3. Rearrangement of the substrate radical with 1,2-migration of the thioester group (Eq. 10.35.3).
4. Transfer of a hydrogen atom from 5'-deoxyadenosine to the radical (Eq. 10.35.4).

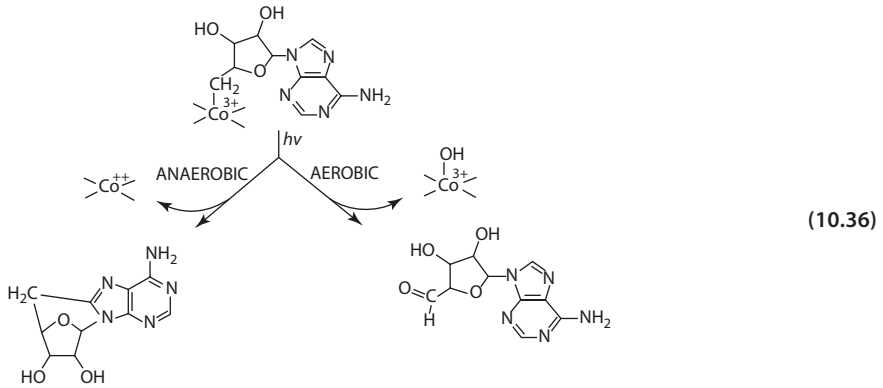


The homolytic fission of the Co–C bond is generally well established. The normal cobalt-alkyl bond is stable with a bond dissociation energy of 18–25 kcal/mol. The binding of substrate to the enzyme induces a conformational change of the apoprotein that, in turn, distorts the cobalt coordination sphere of the coenzyme and labilizes the Co–C bond. The equilibrium in Eq. 10.35 is displaced by a factor of >10⁶ in favor of bond breaking.

Many enzyme systems other than the methylmalonyl CoA mutase are known to require coenzyme B₁₂. These systems include α-methyleneglutarate mutase, glutamate mutase, diol dehydrase, glycerol dehydrase, L-β-lysine mutase, D-α-lysine mutase, and ornithine mutase.

10.6.2 Photolytic Degradation

Light irradiation causes homolytic fission of the cobalt-carbon bond. Under anaerobic conditions, the 5'-deoxyadenosyl radical cyclizes rapidly. Under aerobic conditions, the products are the hydroxocobalamin and 5'-aldehyde of adenosine (Eq. 10.36) [20].



10.6.3 Oxidation

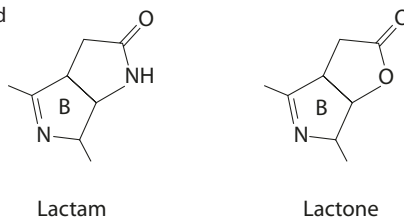
Oxidation of vitamin B₁₂ under mild alkaline conditions yields dehydrovitamin B₁₂. The acetamide side chain at C7 in the corrin B ring cyclizes to form a γ -lactam (cyclic amide). In the presence of an oxidizing agent (e.g., iodine), a γ -lactone (cyclic ester) is formed. Both are biologically inactive (■ Fig. 10.13).

10

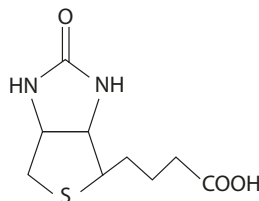
10.7 Biotin (Vitamin B₇)

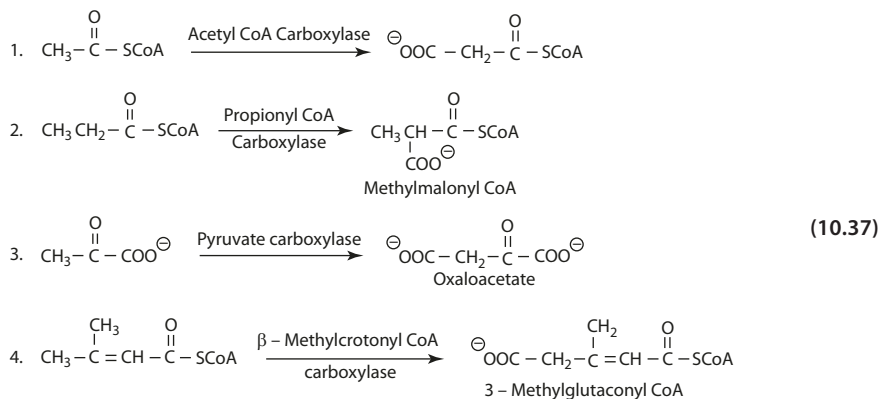
The chemical structure of biotin (vitamin B₇) consists of fused rings of ureido and tetrahydrothiophene, with an aliphatic side chain covalently bound to the ϵ -amino group of a lysine residue of the enzyme (■ Fig. 10.14). Biotin is a cofactor of a number of carboxylases that catalyze the carboxylation of some important metabolic acids (Eq. 10.37).

■ Fig. 10.13 Lactam and lactone



■ Fig. 10.14 Biotin structure

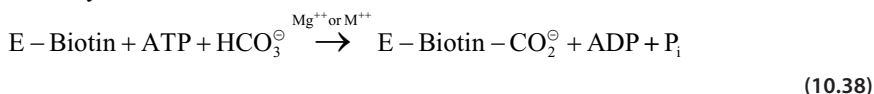


10.7 · Biotin (Vitamin B₇)

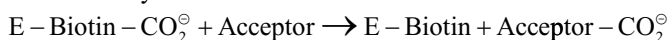
10.7.1 Biochemical Mechanism

The overall reaction is represented by two half-reactions, which occur at different subunits of the enzyme (Eq. 10.38).

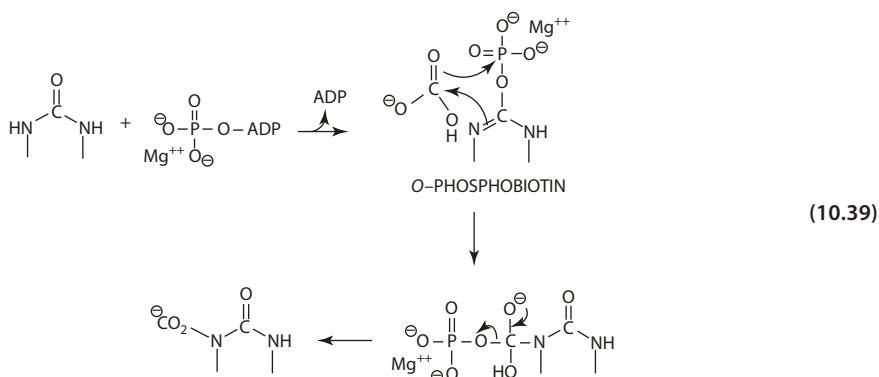
Carboxylation



Transcarboxylation



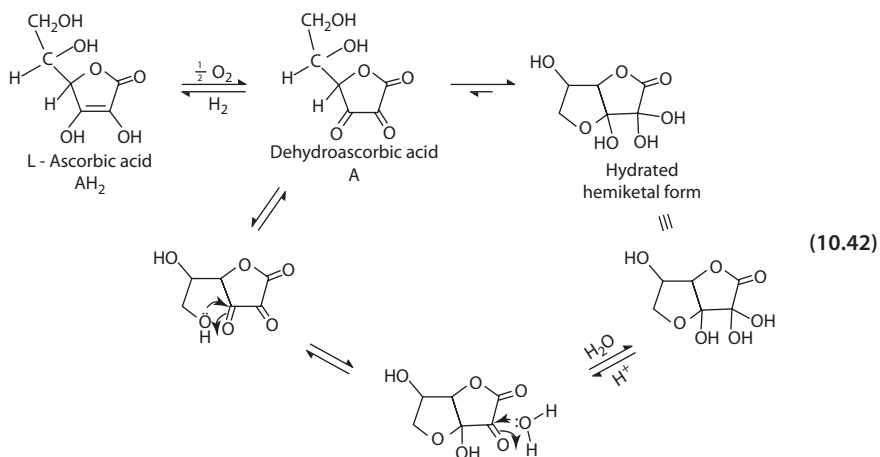
The carboxylation half-reaction involves the formation of *N*-carboxybiotin via *O*-phosphobiotin. The free energy generated by the cleavage of ATP is utilized to form the *O*-phosphobiotin intermediate (Eq. 10.39) [24].



The transcarboxylation reaction proceeds via a stepwise mechanism, in which the proton removal from the acceptor forming the carbanion and the carboxyl addition occurs in separate steps (Eq. 10.40) [34].

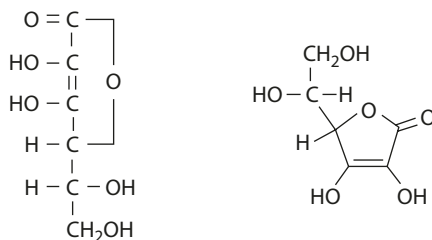
10.9 Vitamin C

Fresh fruits and vegetables have been known for centuries to prevent and cure scurvy. The pure crystalline substance finally isolated is L-ascorbic acid (AH_2). L-Ascorbic acid is a lactone with an enediol group (cyclic ester of a hydroxy carboxylic acid). The oxidized product of ascorbic acid is dehydroascorbic acid (DHA), a 2,3-diketone existing predominantly as a bicyclic hydrated form in solution (Eq. 10.42). Both AH_2 and DHA possess biological activity.



The common substitute for L-ascorbic acid in most food uses is D-isoascorbic acid (■ Fig. 10.16), which possesses essentially no biological activity.

■ Fig. 10.16 Structure of D-isoascorbic acid

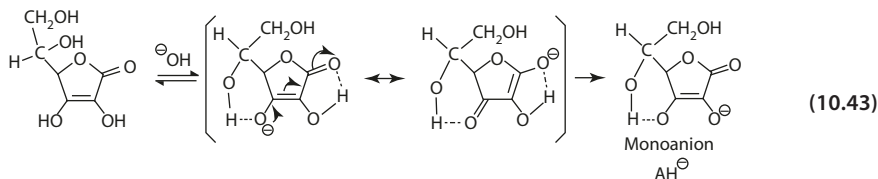


10.9.1 Biochemical Mechanism

■ ■ Acidity

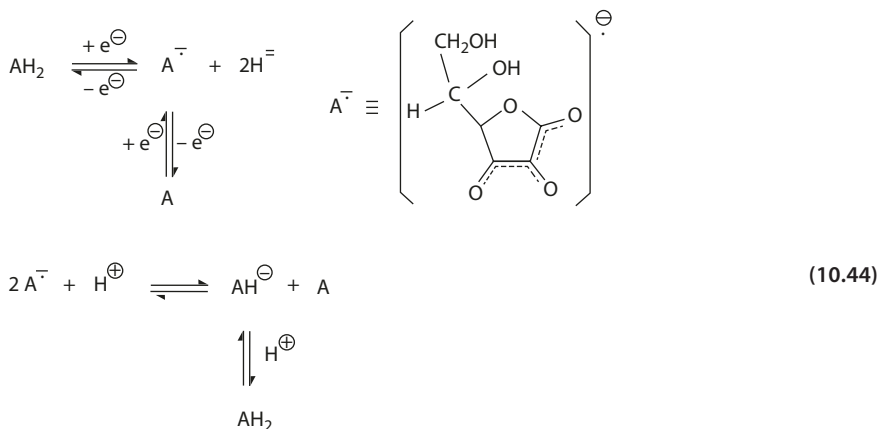
L-Ascorbic acid is dibasic, with the first $pK_a = 4.0$ and the second $pK_a = 11.3$. The acidity of ascorbic acid is mainly due to the monoanion formed by the dissociation of the proton at the 3-hydroxyl group. In contrast, loss of proton from the 2-hydroxyl yields a monovalent anion (L-ascorbate, AH^-) without resonance stabilization (Eq. 10.43). The second dissociation is less favorable, as suggested by the higher pK_a value. Here, a proton is pulled from the 2-hydroxyl that is hydrogen bonded and from a negatively charged molecule to form a

completely dissociated di-anion. At physiological pH, >99% of ascorbic acid is present as the monoanion, which accounts mostly for the antioxidant chemistry of the vitamin.



■ ■ Oxidation of Ascorbic Acid to Dehydroascorbic

The formation of a free-radical intermediate in the oxidation of ascorbic acid to dehydroascorbic acid is probably the most unique characteristic (Eq. 10.44). The oxidation process is reversible and proceeds in a two-step mechanism. The monovalent anion (AH^-) donates a hydrogen atom ($H\cdot$ or $H^+ + e^-$) to an oxidizing radical to form a radical anion ($A^{\cdot-}$) as intermediate [29]. The radical anion ($A^{\cdot-}$) has the unpaired electron spread over the conjugated tricarbonyl system. The resonance-stabilized structure makes it very stable and nonreactive. It decays chiefly by reacting with itself (by dismutation reaction) in terminating the free-chain reaction (Eq. 10.44). In vivo, the radical intermediate is removed by reductase enzymes or cofactors.

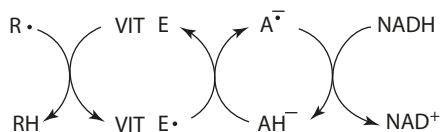


10.9.2 Biological Functions

Vitamin C plays a vital role in the protection against free-radical damage resulting from the metabolic products of oxygen, reactive oxygen species such as hydroxyl radical ($HO\cdot$), perhydroxyl radical ($HO_2\cdot$), superoxide radical ($O_2^{\cdot-}$), and singlet oxygen (1O_2). The protective role of ascorbic acid in biological systems via free-radical reaction has been extensively studied. The general reaction of the oxidation of ascorbate is presented in Eq. 10.45. In terminating free radicals, the AH_2 is oxidized via a radical intermediate, as described in the previous section.

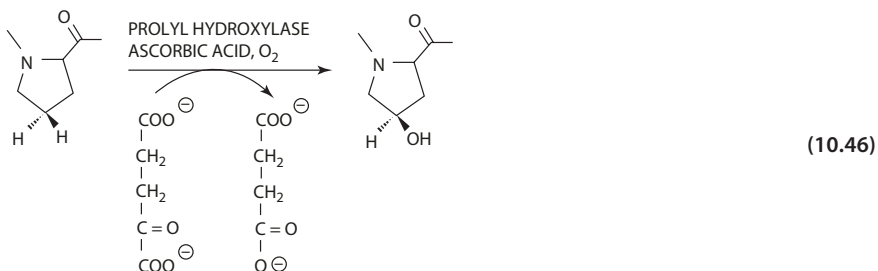


■ **Fig. 10.17** Interaction between vitamin E radical and ascorbate

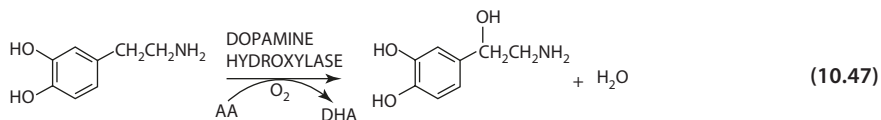


In the biological system, vitamins E and C act synergistically. The reduction potentials for ascorbate ($A^{\cdot-} + H \rightleftharpoons AH^- + DHA$) and tocopherol ($TO\cdot + H^+ \rightleftharpoons TOH$) are +282 mV and +480 mV, respectively. (Refer to Appendix 3.) The common oxidizing radicals in biological systems, such as $HO\cdot$ and $ROO\cdot$, have much higher redox potentials (2310 and 1000 mV, respectively). Vitamin E, also being lipophilic, is generally considered to be the primary antioxidant, especially in lipid peroxidation in cell membranes. α -Tocopherol readily donate an electron (or hydrogen atom) to lipid peroxy radical, eliminating the harmful $ROO\cdot$ and generating the much less reactive tocopherol radical. Ascorbate would then react with the tocopherol radical to regenerate tocopherol, and the resulting ascorbic acid radical can be reduced back to vitamin C by NADH [35] (■ Fig. 10.17). This recycling process of the two vitamins provides major protection to the organism from deleterious free-radical oxidation.

Vitamin C is also involved in collagen synthesis. The enzyme involved in the hydroxylation of proline to hydroxyprolin in collagen synthesis, prolyl collagen proline hydroxylase, requires O_2 , Fe^{3+} , α -ketoglutarate, and ascorbate (Eq. 10.46). An abnormal collagen precursor is formed in the absence of ascorbic acid. Ascorbic acid maintains the activity of the enzyme by stabilizing the iron atom in the reduced ferrous state. Collagen insufficiently hydroxylated has a lower melting point. This abnormal development of the collagen causes skin lesions and fragile vessels evident in scurvy.



In the conversion of 3,4-dihydroxyphenylethylamine to noradrenaline, the enzyme dopamine hydroxylase requires ascorbic acid and oxygen (Eq. 10.47).



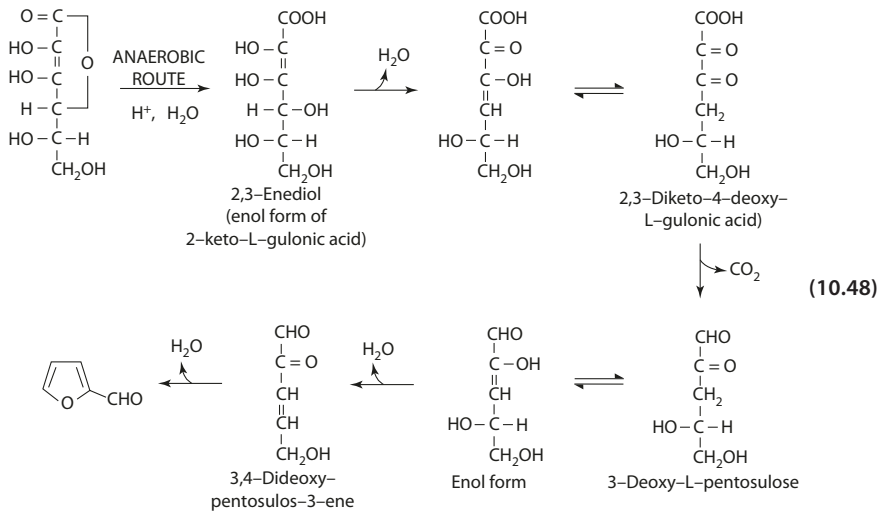
Ascorbic acid is also involved in the metabolism of iron and calcium and the hydroxylation reactions in the metabolism of a number of protein and steroids. All these indicate the importance of the redox balance ($AH_2 \rightleftharpoons A$) of ascorbic acid.

10.9.3 Loss of Vitamin C

Vitamin C is one of the least stable vitamins. Retention of vitamin C is affected by processing, handling, and storage. Enzymes found in fruits and vegetables that oxidize vitamin C are ascorbic acid oxidase, cytochrome oxidase, and peroxidase. However, in food processing, losses of vitamin C due to enzymatic destruction are minimal. Losses are caused by the following reactions.

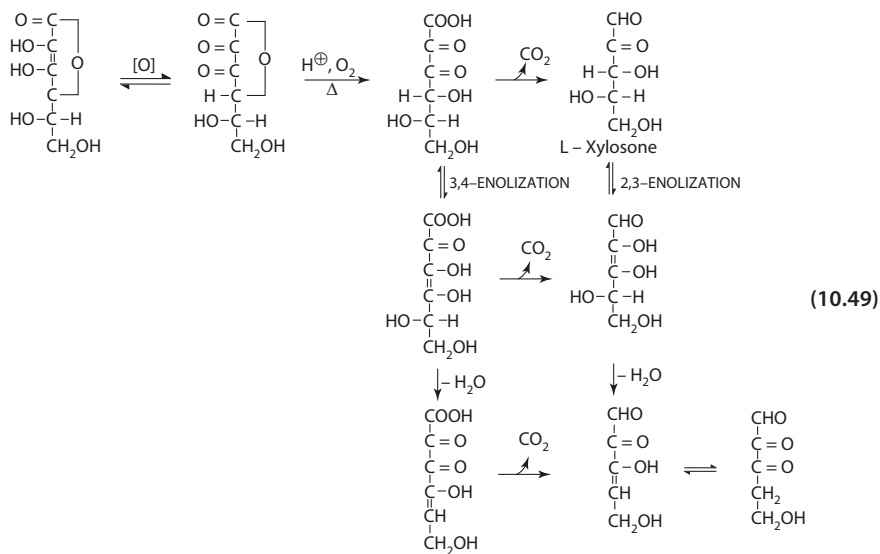
■ ■ Acid-Catalyzed Nonoxidative Degradation

The nonoxidative degradation of ascorbic acid to 2-furaldehyde and carbon dioxide is acid catalyzed under thermal treatment. The initial step involves cleavage of the lactone ring to form 2,3-enediol, which then undergoes dehydration, followed by rearrangement to form the 2,3-diketo acid (Eq. 10.48). Decarboxylation of the diketo acid yields the 3-deoxy-L-pentosulose (corresponding to the 3-deoxyglucosulose in the Maillard reaction) [26]. Nonoxidative reaction is comparatively slow and accelerated by lowering the pH. This type of degradation is responsible for anaerobic loss of vitamin C in canning acid fruits, such as orange and grapefruit juices.



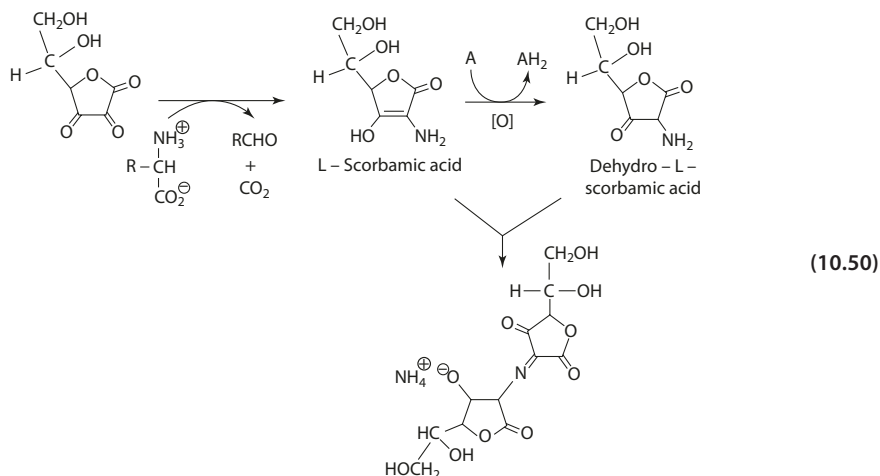
■ ■ Oxidative Degradation

Oxidative browning in an acid medium proceeds by way of dehydroascorbic acid. Cleavage of the lactone ring yields the 2,3-diketogulonic acid, which decarboxylates to pentosulose (L-xylosone) (Eq. 10.49). 2,3-Enolization and dehydration of the xylosone yields a tricarbonyl compound, 3-keto-4-deoxypentosulose. 3,4-Enolization of 2,3-diketogulonic acid, followed by dehydration and decarboxylation, also gives the same product. The route via 2,3-diketogulonic acid may constitute the major pathway [27]. Oxidative browning involving dehydroascorbic acid is found to occur in foods of high ascorbic acid content, such as citrus juices and some dehydrated products.



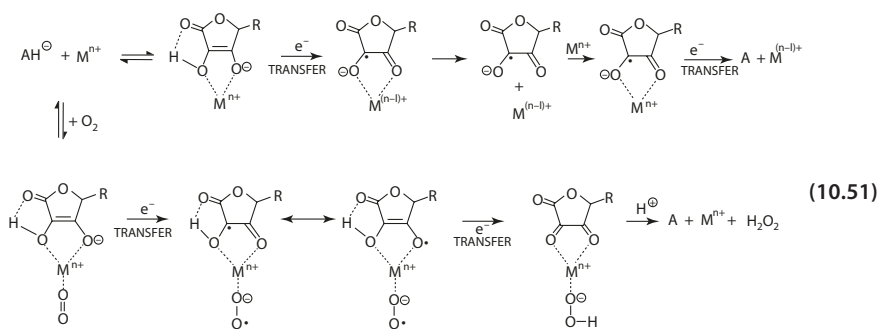
■ The Strecker Degradation

Dehydroascorbic acid may cause the discoloration of foods via the Strecker degradation reaction. The Strecker degradation of an α -amino acid in the presence of dehydroascorbic acid produces the amino-reduction, scorbamic acid, which undergoes oxidation to yield dehydro-L-scorbamic acid. Reaction of the two acids yields the condensation product, 2,2'-nitridodi-2(2')-deoxy-L-ascorbic acid ammonium salt, which has been postulated to be the intermediate compound for further polymerization (Eq. 10.50) [28]. (Refer to ► Chap. 8, section on "Glucosinolates" regarding reaction between glucosinolate breakdown products and ascorbate in the formation of ascorbigen.)



■ Reaction with Metal Ions

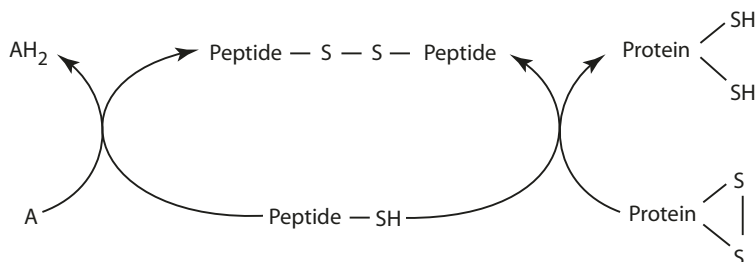
Ascorbic acid is oxidized by metal ions such as Fe^{3+} and Cu^{2+} in a two-sequential one-electron transfer mechanism. The formation of an ascorbate- M^{n+} complex allows a $1e^-$ transfer to yield the ascorbic radical anion- $\text{M}^{(n-1)+}$ complex, which dissociates readily. The resulting radical anion then undergoes a second $1e^-$ transfer by complexing with another metal ion (M^{n+}) to give the final product, dehydroascorbic acid [33] (Eq. 10.51).



Metal ions also catalyze the autoxidation of ascorbic acid. In the reaction, molecular oxygen is reduced by a two-electron transfer to peroxide, but the oxidative state of the metal remains unchanged. The first step involves the formation of an ascorbate-metal-dioxygen complex intermediate, which allows the transfer of one electron to yield the resonance form in which the M^{n+} is coordinated to the ascorbate radical and superoxide anion. A second electron transfer yields a complex of dehydroascorbic acid- M^{n+} -hydroperoxide that rapidly dissociates to dehydroascorbic acid and hydrogen peroxide. It is also possible that a one-step two-electron transfer may occur to give the same products. Autoxidation is the mechanism that accounts for the majority of the loss of ascorbic acid in food.

10.9.4 Uses of Vitamin C

1. Prevention of browning in fruit and vegetables. In the presence of ascorbic acid, the *o*-quinone-type compounds are reduced back to the *o*-phenolic forms. At the exhaustion of the ascorbic acid in the system, the *o*-quinone compounds accumulate and polymerize to browning products (refer to ► Chap. 5, polyphenol oxidase).
2. Inhibition of oxidation in beer, wine, vegetable oil, milk, and dairy products.
3. Stabilization of meat color; color fixing in curing of meat. Ascorbic acid acts as a reductant, similar to sulfhydryl compounds and NADH-flavin found in meat, to generate nitrous oxide and nitrosylmyoglobin (refer to ► Chap. 4, ■ Fig. 4.40).
4. Improvement of dough. During dough mixing, the flour protein gluten undergoes sulfhydryl-disulfide exchange with low-molecular sulfhydryl peptides. The exchange is suggested as one reason for the decrease in dough stability. Dehydroascorbic acid acts as an improver by competing with the gluten in the oxidation of the thiol (■ Figs. 10.16 and 10.18) [31].



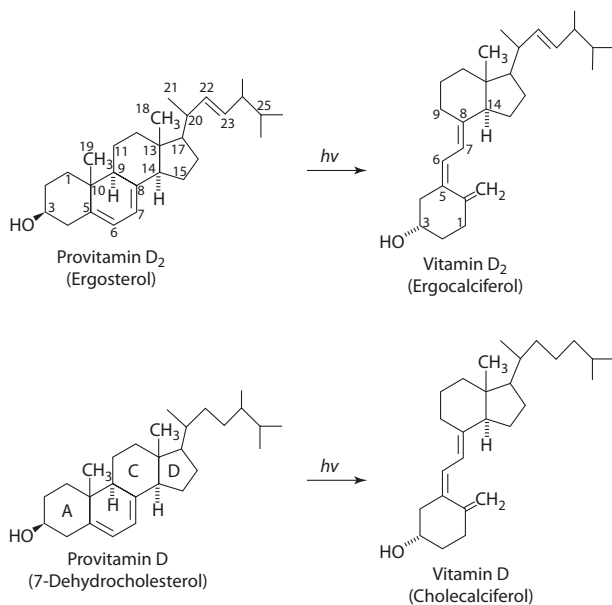
■ Fig. 10.18 Competition for thiol oxidation between vitamin C and flour protein

10.10 Vitamin D

The addition of vitamin D to milk in the United States and the consequent eradication of rickets have been attributed to the antirachitic property of the vitamin. The multiple chemical structures of the D vitamins need clarification. Practically, D vitamins of natural sources are the vitamin D₂ (ergocalciferol) from plants and vitamin D₃ (cholecalciferol) present in animal tissues. Other vitamin D forms with antirachitic activity are also known.

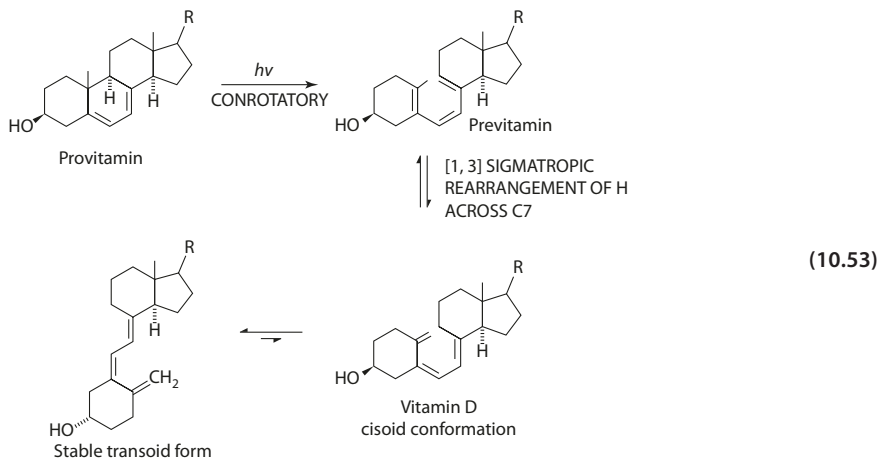
10.10.1 The Chemical Structures

Vitamin D₂ is formed by irradiation of the provitamin D₂ (ergosterol) (Eq. 10.52) and, similarly, D₃ from provitamin D₃ (7-dehydrocholesterol). The only difference between vitamin D₂ and D₃ is exclusively in the side chain attached at C17. Vitamin D₂ has an unsaturated side chain with a double bond between C22 and C23 and with one extra methyl group at C24.

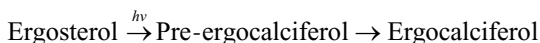


(10.52)

The photochemical reaction involves electrocyclic ring opening of the cyclohexadiene (B ring) of provitamin D. The product (previtamin D) undergoes [1,3] sigmatropic reaction to form vitamin D (Eq. 10.53).



The same reaction is used to convert plant ergosterol into ergocalciferol, the vitamin D₂ that is added to milk:

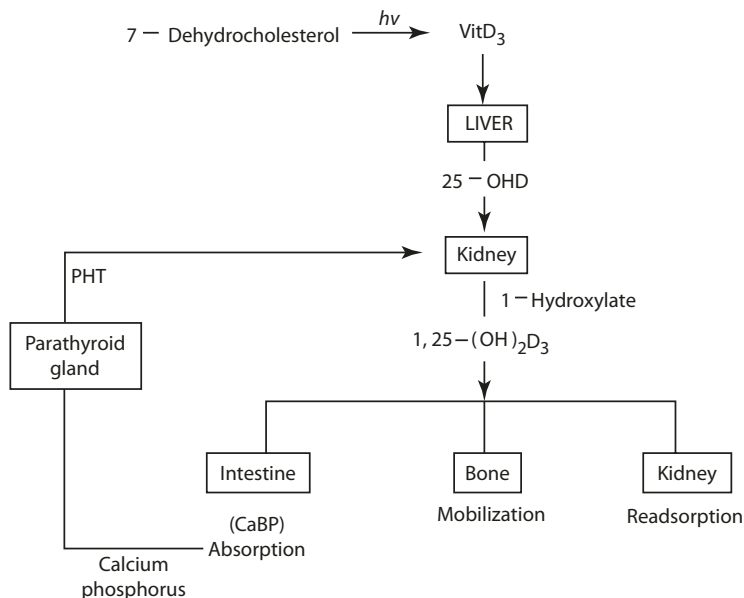


10.10.2 Biological Functions

The biologically active form of vitamin D in the body is the steroid 1,25-dihydroxyvitamin D₃ (1,25(OH)₂D₃). The biosynthesis of 1,25(OH)₂D₃ from vitamin D₃ occurs in the liver, where vitamin D₃ is metabolized to 25-hydroxyvitamin D₃ (25-OHD). Hydroxylation at C1 of 25-OHD occurs only in the kidney and is catalyzed by the enzyme renal 1-hydroxylase. The synthesis of 1,25(OH)₂D₃ is controlled by the calcium demand of the system and the parathyroid hormone PTH (■ Fig. 10.19) [8].

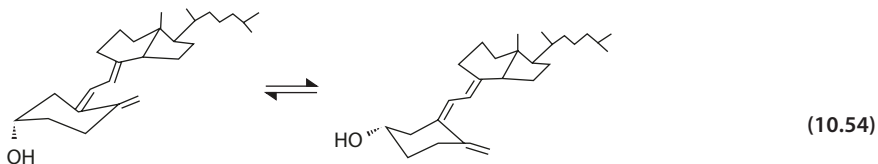
The physiological functions of vitamin D are (1) absorption of calcium and phosphorus in the intestine, possibly involving the vitamin D-dependent calcium-binding protein (CaBP), (2) mobilization of calcium and phosphorus from bone, and (3) renal reabsorption of calcium and phosphorus.

Vitamin D differs from other common steroids in that the B ring is open, resulting in the conformational flexibility of the A-ring. To illustrate this, the structure of 1,25(OH)₂D₃ is presented in the chair form in Eq. 10.54 [41]. Notice the interconversion of the equatorial and axial positions of the two hydroxyl groups in the A-ring. The two chair conformers are in equilibrium, and the interconversion is many thousands of times per second. It is



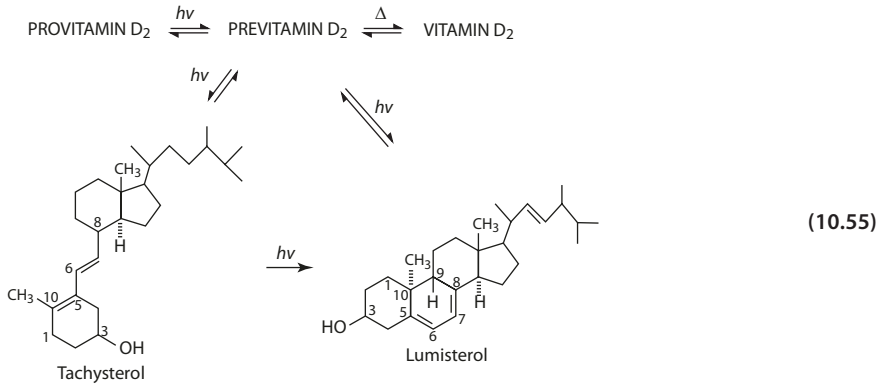
■ Fig. 10.19 Metabolic pathway of vitamin D₃

postulated that the 25-OH group functions to steer the molecule of 1,25(OH)₂D₃ in a position for the receptor protein in the target cell to interact with the A-ring. The resulting 1,25(OH)₂D₃-receptor complex "freezes" the A-ring into a fixed position.

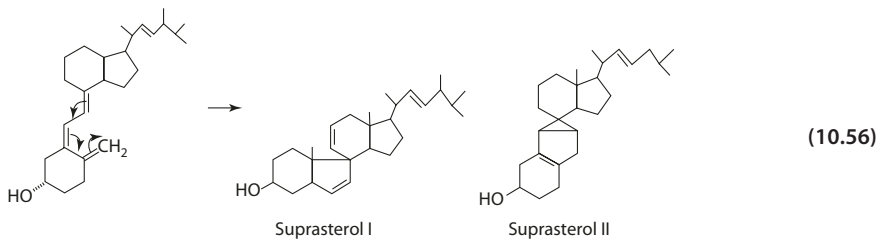


10.10.3 Side Reactions of Irradiation

Irradiation of ergosterol produces tachysterol and lumisterol as side-reaction products. Both reactions proceed from a reversible photochemical side reaction of pre-ergocaliferol. The most effective wavelength for vitamin D production is 280 nm. Irradiation at higher wavelengths favors the formation of lumisterol and at lower wavelengths increases the yield of tachysterol. Lumisterol is also formed irreversibly from tachysterol (Eq. 10.55) [21].

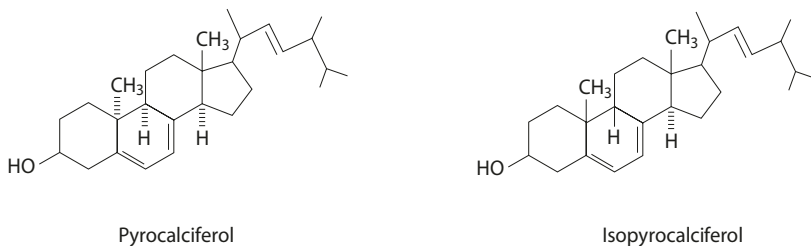


Overexposure to irradiation produces suprasterol (which is biologically inactive) from ring closure of the conjugated triene system (Eq. 10.56). A number of other compounds are also formed by ring closure between other carbons, followed by fragmentation or dimerization.



10.10.4 Thermal Reaction

When vitamin D₂ is heated at 180–190 °C, pyro-ergocalciferols are formed (■ Fig. 10.20). These are isomers (*cis*-9,10) of ergocalciferol, which are biologically inactive.



■ Fig. 10.20 Pyro-ergocalciferols

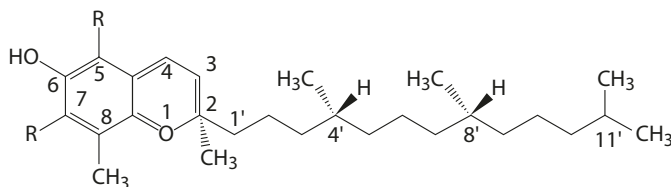
10.11 Vitamin E

Vitamin E (tocopherol) consists of two parts in its molecular structure: (1) a chroman ring (chroman-6-ol) with two rings, one phenolic and one heterocyclic, and (2) a saturated isoprenoid C16 side chain also known as the phytyl tail. Depending on the position of substitution of the methyl groups in the chroman ring, the compounds are referred to α , β , γ , and δ (■ Fig. 10.21).

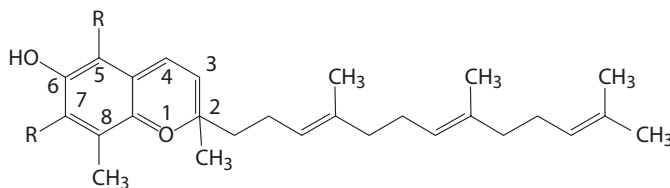
Since the phytyl tail has three chiral centers (2, 4', 8'), there are eight possible stereoisomeric forms. Naturally occurring tocopherols exist only with the configuration of *RRR* (2*D*,4'*D*,8'*D* or simply *d*-), hence the name *d*- (or *RRR*) tocopherol. Tocopherols are exclusively synthesized in higher plants, predominantly in seeds. The natural abundant isomer is *d*- (or *RRR*) α -tocopherol, which is the most biologically active form. Vitamin E activity is conventionally expressed in terms of equivalents of this isomer as mg α -tocopherol (or α -TE) equivalents. Synthetic supplements are a mixture of all eight stereoisomeric forms: 2*D*,4'*D*,8'*D* (*RRR*), 2*L*,4'*D*,8'*D* (*SRR*), 2*D*,4'*D*,8'*L* (*RRS*), 2*L*,4'*D*,8'*L* (*SRS*), 2*D*,4'*L*,8'*D* (*RSR*), 2*L*,4'*L*,8'*D* (*SSR*), 2*D*,4'*L*,8'*L* (*RSS*), and 2*L*,4'*L*,8'*L* (*SSS*) [23].

Besides tocopherols, another group of natural vitamin E analogs consists of the tocotrienols in which the isoprenoid side chain has double bonds at the 3', 7', and 11' positions. The tocotrienols have only one chiral center at position 2 and only 2*R* and 2*S* stereoisomers. However, the double bonds at 3' and 7' positions create *cis/trans* isomers, resulting in a total of eight isomers: 2*D*, 3'*cis*, 7'*cis* (*R*, *cis-cis*); 2*D*, 3'*cis*, 7'*cis* (*R*, *cis-trans*); 2*D*,

a Tocopherol



b Tocotrienol



R5	R7	Homologs
CH ₃	CH ₃	α
CH ₃	H	β
H	CH ₃	γ
H	H	δ

■ Fig. 10.21 Structures of tocopherols and tocotrienols

■ **Table 10.1** Tocopherol and tocotrienol content of selected fats and oils

Fats and oils	Total T+T3 (mg/100 g)	α -TE per 100 g	%T	%T3	Primary homologs
Sunflower	46–67	35–63	100	0	α -T, γ -T
Cottonseed	78	43	100	0	α -T, γ -T
Safflower	49–80	41–46	100	0	α -T, δ -T, γ -T, β -T
Palm	89–117	21–34	17–55	45–80	α -T, α -T3, δ -T3
Canola	65	25	100	0	γ -T, α -T, δ -T, α -T3, β -T
Corn	78–109	20–34	95	5	γ -T, α -T, δ -T, γ -T3, δ -T3
Soybean	96–115	17–20	100	0	γ -T, δ -T, α -T
Peanut	37	16	100	0	γ -T, α -T, δ -T
Olive	5.1	5.1	100	0	α -T
Butter	1.1–2.3	1.1–2.3	100	0	α -T
Lard	0.6	0.6	100	0	α -T

From Ettenmiller [12]

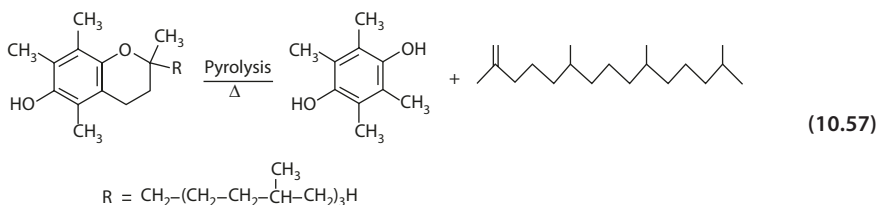
10

3' *trans*, 7' *cis* (*R*, *trans-cis*); 2D, 3' *trans*, 7' *trans* (*R*, *trans-trans*); 2L, 3' *cis*, 7' *cis* (*S*, *trans-cis*); 2L, 3' *cis*, 7' *cis* (*S*, *cis-trans*); 2L, 3' *trans*, 7' *cis* (*S*, *trans-cis*); and 2L, 3' *trans*, 7' *trans* (*S*, *trans-trans*).

Approximately 8% of the vitamin E in the US diet comes from salad and cooking oils. The total vitamin E content (tocopherols plus tocotrienols) of major fats and oils are presented in ■ Table 10.1 [12].

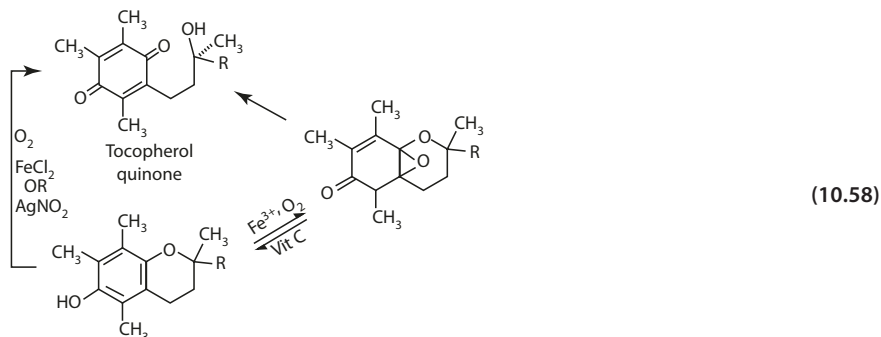
10.11.1 Thermal Decomposition

Pyrolysis of α -tocopherol yields the hydroquinone and unsaturated C19 hydrocarbon (Eq. 10.57).



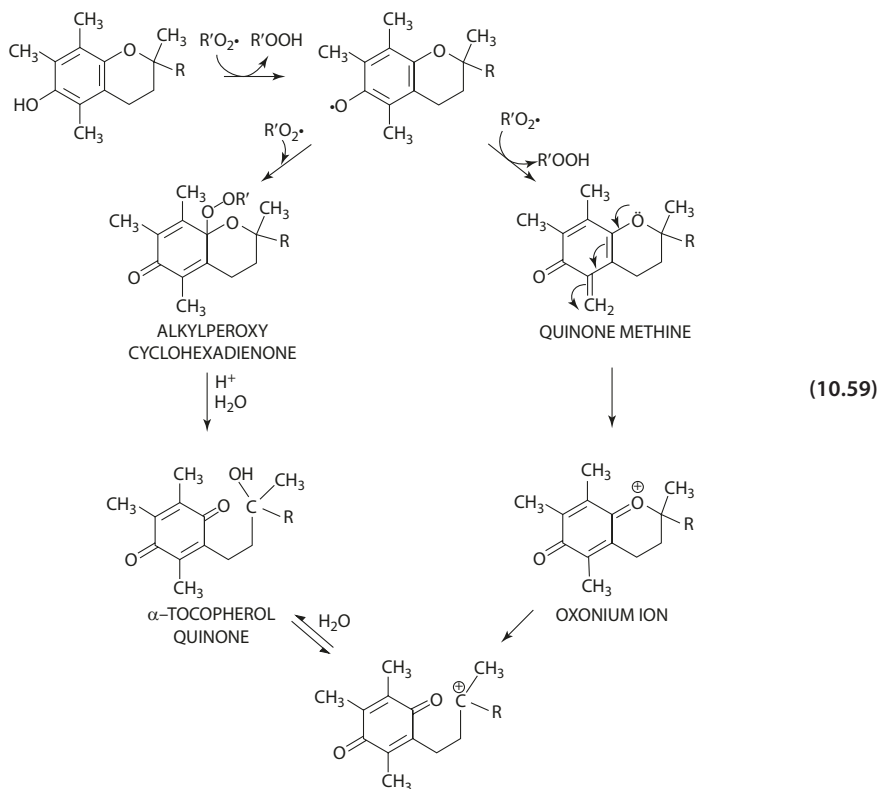
10.11.2 Chemical Oxidation

In many chemical oxidative degradation studies of α -tocopherol, the main product is α -tocopherol quinone (Eq. 10.58).

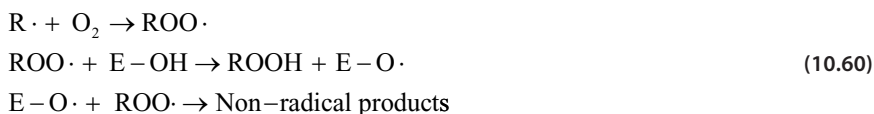


10.11.3 Free Radical Reactions

α -Tocopherol undergoes free-radical oxidation to form α -tocopherol quinone via an intermediate, α -tocopherol quinone methine [15]. The first two steps involve abstraction of two hydrogen atoms, forming an unstable quinone methine, which reacts with a proton to produce an oxonium ion (Eq. 10.59). The oxonium ion rearranges to a carbonium ion, which then adds a water molecule to form the quinone. Alternatively, the tocopherol radical reacts with a second peroxy radical to form 4-(alkylperoxy)cyclohexadienone, which upon acid hydrolysis yields the tocopherol quinone. In both cases, the tocopherol molecule consumes two peroxy radicals to form a nonradical product. Schematically, the reaction sequence is represented by Eq. 10.60.



The high efficiency of tocopherols as a chain-breaking antioxidant is largely attributed to the 6-hydroxychroman system. The alkyl substitution at both ortho- and meta-positions helps to reduce the energy of activation for the transition state and hence increase the formation of the phenoxyl radical. The *p*-alkoxyl group is held in an orientation that the unpaired electron of the phenoxyl radical delocalizes with the oxygen *p* orbital (■ Fig. 10.22) [6]. In contrast, 2,3,5,6-tetramethyl-4-methoxyphenol, although very similar in structure, shows no enhancement in the formation of phenoxyl radical since the methoxyl group is out of the plane of the aromatic ring.

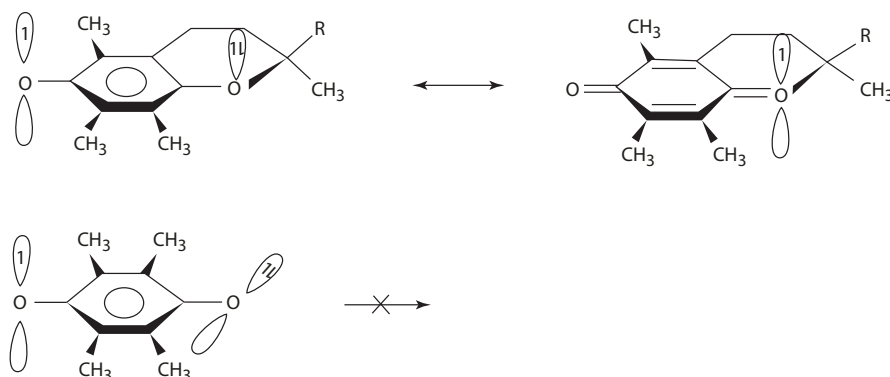


In addition to reacting with peroxy radicals, tocopherols participate in side reactions (i.e., reacting with species other than peroxy radicals) [22]. Tocopherols have been shown to react with lipid hydroperoxides (LOOH) [42], leading to tocopherol radical and alkoxy radical according to the following equation.



10

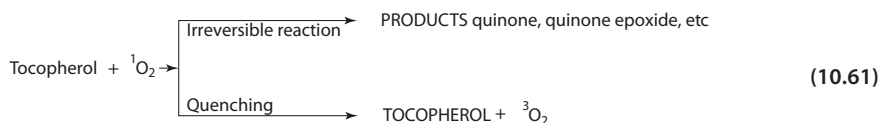
The alkoxy radical initiates new chain reactions resulting in increased lipid oxidation. The consumption of tocopherols in side reactions causes the loss in the antioxidant activity of the vitamin. This reaction (α -tocopherol with LOOH), however, has a very small rate constant of $1.3\text{--}3.6 \times 10^{-1} \text{ M}^{-1} \text{ s}^{-1}$ compared to the almost diffusion rate constant ($1\text{--}8 \times 10^8 \text{ M}^{-1} \text{ s}^{-1}$) of the major reaction involving peroxy radicals. The effect of this and other side reactions is negligible at low concentrations of tocopherol (500–2000 ppm) in vegetable oils. It becomes significant at high concentrations of tocopherol together with high concentrations of unsaturated fatty acids in vegetable oil [43].



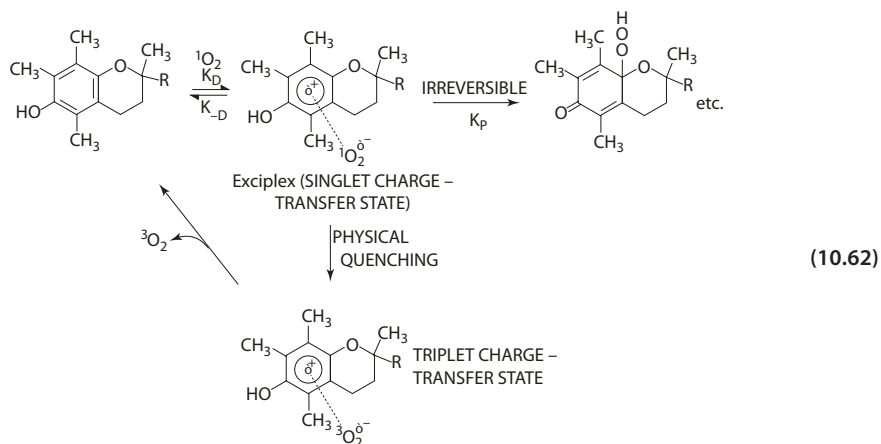
■ Fig. 10.22 Orientation of the *p*-alkoxyl group in α -tocopherol (From Burton and Ingold [533])

10.11.4 Quenching of Singlet Oxygen

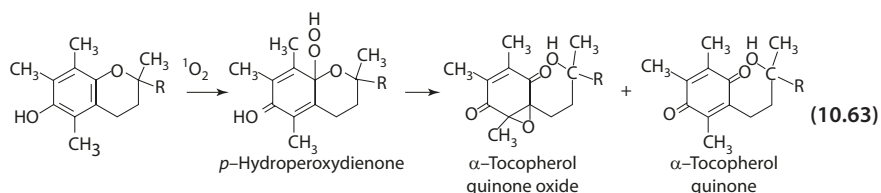
Tocopherols are highly efficient in quenching singlet oxygen by a combination of chemical and physical quenching processes (Eq. 10.61). Between the two processes of scavenging singlet oxygen, the physical quenching process predominates, with the $^1\text{O}_2$ quenching rate 15–100 times the rate of the irreversible reaction. The physical quenching rate constant for α -tocopherol has been determined to be $2.5 \times 10^8 \text{ M}^{-1} \text{ s}^{-1}$ (in benzene). α -Tocopherol is one of the most reactive naturally occurring singlet oxygen acceptors and is the most reactive among the four tocopherols. The singlet oxygen reactivity of α , β , γ , and δ correlates with the vitamin E activity.



Unlike β -carotene, the quenching of singlet oxygen by α -tocopherol does not involve the energy transfer process. Instead, the tocopherol molecule and the singlet oxygen form a charge-transfer exciplex (Eq. 10.62). The contribution of such state perturbs the singlet state of oxygen and causes spin-orbit coupling of the singlet charge-transfer state and the triplet charge-transfer state, allowing a formally forbidden "spin-flip" to occur. Over 95% of the quenching proceeds via this process ($K_D \gg K_p$) [14].



The products of the irreversible process have been studied. α -Tocopherol reacts with singlet oxygen forming tocopherol quinone and quinone epoxide irreversibly with the epoxide as the major product (Eq. 10.63). The intermediate, *p*-hydroperoxydienone, is thermally stable [7].



References

- Abels RH (1976) The vitamin B12 coenzyme. *Acc Chem Res* 9:114–120
- Abrahamson EW (1975) Dynamic processes in vertebrate rod visual pigments and their membranes. *Acc Chem Res* 8:101–106
- Araujo MM, Marchioni E, Villavicencio ALCH, Zhao M, di Pascoli T, Kuntz F, Bergaentzle M (2015) Mechanism of folic acid radiolysis in aqueous solution. *LWT-Food Sci Technol* 63:599–603
- Blair JA, Pearson AJ, Robb AJ (1975) Autoxidation of 5-methyl-5,6,7,8-tetrahydrofolic acid. *J Chem Soc Perkin II* 2(1):18–21
- Blakley RL (1986) Nomenclature and symbols for folic acid and related compounds recommendations 1986. *Eur J Biochem* 168:251–254
- Burton GW, Ingold KU (1981) Autoxidation of biological molecules. 1. The antioxidant activity of vitamin E and related chain-breaking phenolic antioxidants *in vitro*. *J Am Chem Soc* 103:6472–6477
- Clough RI, Yee BC, Foote CS (1979) Chemistry of singlet oxygen. 30. The unstable primary product of tocopherol photooxidation. *J Am Chem Soc* 101:683–686
- DeLuca HF, Schnoes HK (1983) Vitamin D: recent advances. *Annu Rev Biochem* 52:411–439
- Doerge DR, Ingraham LL (1980) Kinetics of thiamine cleavage by bisulfite ion. *J Am Chem Soc* 102:4828–4830
- Drujan BD (1971) Determination of vitamin A. *Meth Enzymol* XVII, Part C
- Dwivedi BK, Arnold RG (1973) Chemistry of thiamine degradation in food products and model systems. A review. *J Agric Food Chem* 21:54–60
- Ettenmiller RR (1997) Vitamin E content of fats and oils – nutritional implications. *Food Technol* 51:78–81
- Fitzhugh AL (1993) Stereoelectronic effects in the O₂-mediated autoxidation of reduced folate derivatives. *Pteridines* 4:187–191
- Gorman AA, Gould IR, Hamblett I, Standen MC (1984) Reversible exciplex formation between singlet oxygen, ¹Δg, and vitamin E. Solvent and temperature effect. *J Am Chem Soc* 106:6956–6959
- Gruger EH Jr, Tappel AL (1970) Reactions of biological antioxidants: 1. Fe(III)-catalyzed reactions of lipid hydroperoxides with α-tocopherol. *Lipids* 5:326–331
- Halpern J (1985) Mechanisms of coenzyme B12-dependent rearrangements. *Science* 227:869–875
- Heelis PF (1982) The photophysical and photochemical properties of flavins (isoalloxazines). *Chem Soc Rev* 11(1):15–39
- Hevesi L, Bruice TC (1973) Reactions of sulfite with isoalloxazines. *Biochemistry* 12:290–297
- Jagerstad M, Jastrebova J (2013) Occurrence, stability, and determination of formyl folates in foods. *J Agric Food Chem* 61:9758–9768
- Johnson AW (1980) Vitamin B₁₂: retrospect and prospects. *Chem Soc Rev* 9(2):125–141
- Jones H, Rasmussen GH (1980) Recent advances in the biology and chemistry of vitamin D. In: Herz W, Grisebach H, Kirby GW (eds) *Progress in the chemistry of organic natural products*. Springer, Wien/New York
- Kamai-Eldin A (2006) Effect of fatty acids and tocopherols on the oxidative stability of vegetable oils. *Eur J Lipid Sci Technol* 58:1051–1061
- Kamal-Eldin A, Appelqvist L-A (1996) The chemistry and antioxidant properties of tocopherols and tocotrienols. *Lipids* 31:671–701
- Kluger R, Adawadkar PD (1976) A reaction proceeding through intramolecular phosphorylation of a urea. A chemical mechanism for enzymic carboxylation of biotin involving cleavage of adenosine 5'-triphosphate. *J Am Chem Soc* 98:3741–3742
- Krinsky NT (1979) Carotenoid protection against oxidation. *Pure Appl Chem* 51:649–660
- Kurata T, Sakurai Y (1967) Degradation of L-ascorbic acid and mechanism of nonenzymatic browning reaction. Part II. Non-oxidative degradation of L-ascorbic acid including the formation of 3-deoxy-L-pentosone. *Agric Biol Chem* 31:170–176
- Kurata T, Fujimaki M (1976) Formation of 3-keto-4-deoxypentosone and 3-hydroxy-2-pyrone by the degradation of dehydro-L-ascorbic acid. *Agric Biol Chem* 40:1287–1291
- Kurata T, Fujimaki M, Sakurai Y (1973) Red pigment produced by the reaction of dehydro-L-ascorbic acid with α-amino acid. *Agric Biol Chem* 37:1471–1477
- Laroff GP, Fessenden RW, Schuler RH (1972) The electron spin resonance spectra of radical intermediates in the oxidation of ascorbic acid and related substances. *J Am Chem Soc* 94:9062–9073

References

30. Lucock M (2000) Folic acid: nutritional biochemistry, molecular biology, and role in disease processes. *Mol Genet Metab* 71:121–138
31. Mair G, Grosch W (1979) Changes in glutathione content (reduced and oxidized form) and the effect of ascorbic acid and potassium bromate on glutathione oxidation during dough mixing. *J Sci Food Agric* 30:914–920
32. Martell AE (1982) Reaction pathways and mechanisms of pyridoxal catalysis. *Adv Enzymol* 53:163–199
33. Martell AE (1982) Chelates of ascorbic acids. Formation and catalytic properties. In: Seib PA, Tolbert BM (eds) *Ascorbic acid: chemistry, metabolism, and uses*. Advances in chemistry series, vol 200. American Chemical Society, Washington, D.C.
34. O'Keefe SJ, Knowles JR (1986) Enzymatic biotin-mediated carboxylation is not a concerted process. *J Am Chem Soc* 108:328–329
35. Packer JE, Slater TF, Wilson RL (1979) Direct observation of a free radical interaction between vitamin E and vitamin C. *Nature* 278:737–738
36. Pearson AJ (1974) Kinetics and mechanism of the autoxidation of tetrahydropterins. *Chem Ind* 6:233–239
37. Schneider M, Klotzsche M, Werzinger C, Hegele J, Waibel R, Pischetsrieder M (2002) Reaction of folic acid with reducing sugars and sugar degradation products. *J Agric Food Chem* 50:1647–1651
38. van Dort HM, van der Linde LM, de Rjke D (1984) Identification and synthesis of new odor compounds from photolysis of thiamin. *J Agric Food Chem* 32:454–457
39. Verlinde PHCJ, Oey I, Deborggraeve WM, Henderickx ME, van Loey AM (2009) Mechanism and related kinetics of 5-methyltetrahydrofolic acid degradation during combined high hydrostatic pressure – thermal treatments. *J Agric Food Chem* 57:6803–6814
40. Verlinde PHCJ, Oey I, Lemmens L, Deborggraeve WM, Hendrickx ME, van Loey AM (2010) Influence of reducing carbohydrates on (6S)-5-methyltetrahydrofolic acid degradation during thermal treatments. *J Agric Food Chem* 58:6190–6199
41. Wing RM, Okamura WH, Rego A, Pirio MR, Norman AW (1975) Studies on vitamin D and its analogs. VII. Solution conformations of vitamin D₃ and 1 α ,25-dihydroxyvitamin D₃ by high-resolution proton magnetic resonance spectroscopy. *J Am Chem Soc* 97:4980–4985
42. Yamauchi R, Goto K, Kato K (1998) Reaction of α -tocopherol in heated bulk phase in the presence of methyl linoleate (13S)-hydroperoxide or methyl linoleate. *Lipids* 33:77–85
43. Yanishlieva NV, Kamai-Eldin A, Marinova EM, Toneva AG (2002) Kinetics of antioxidant action of α - and γ -tocopherols in sunflower and soybean triacylglycerols. *Eur J Lipid Sci Technol* 104:262–270
44. Zoltewicz JA, Uray G, Kauffman GM (1980) Evidence for an intermediate in nucleophilic substitution of a thiamin analogue. Change from first- to second-order kinetics in sulfite ion. *J Am Chem Soc* 102:3653–3654

Supplementary Information

Appendix 1: General Kinetics of Olefin Autoxidation – 428

Appendix 2: Singlet Oxygen – 431

Appendix 3: Where Do the Radicals Come From? – 434

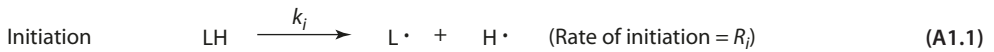
Appendix 4: Flavonoids – 439

Index – 441

Appendix 1: General Kinetics of Olefin Autoxidation

Classical kinetics of lipid autoxidation are formulated based on studies of linoleate (LH) at early stages of oxidation, at low level of substrate-product conversion, and at low temperatures. Under these conditions, the propagation

reactions produce hydroperoxide (LOOH) in high yield, and hydroperoxide decomposition is insignificant. The oxidation proceeds by a free-radical chain mechanism, consisting of initiation, propagation, and termination reactions.



Applying steady state conditions, the rate of change in the concentrations of the alkyl radical (L·) and the peroxy radical (LOO·) is zero.

$$\frac{d[\text{L}\cdot]}{dt} = R_i - k_o[\text{L}\cdot][\text{O}_2] + k_p[\text{LOO}\cdot][\text{LH}] - k_t'[\text{LOO}\cdot][\text{L}\cdot] - k_t''[\text{L}\cdot]^2 = 0 \quad (\text{A1.7})$$

$$\frac{d[\text{LOO}\cdot]}{dt} = k_o[\text{L}\cdot][\text{O}_2] - k_p[\text{LOO}\cdot][\text{LH}] - k_t[\text{LOO}\cdot]^2 - k_t'[\text{LOO}\cdot][\text{L}\cdot] = 0 \quad (\text{A1.8})$$

Addition of (A1.7) and (A1.8),

$$R_i - 2k_t'[\text{LOO}\cdot][\text{L}\cdot] - k_t[\text{LOO}\cdot]^2 - k_t''[\text{L}\cdot]^2 = 0 \quad (\text{A1.9})$$

Assuming $k_t = k_t' = k_t''$,

$$\begin{aligned} \frac{R_i}{k_t} &= [\text{LOO}\cdot]^2 + 2[\text{LOO}\cdot][\text{L}\cdot] + [\text{L}\cdot]^2 \\ &= \{[\text{LOO}\cdot] + [\text{L}\cdot]\}^2 \\ \left(\frac{R_i}{k_t}\right)^{1/2} &= [\text{LOO}\cdot] + [\text{L}\cdot] \end{aligned} \quad (\text{A1.10})$$

$$\begin{aligned} \text{But } k_o [\text{L}\cdot][\text{O}_2] &= k_p [\text{LOO}\cdot][\text{LH}] \\ [\text{L}\cdot] &= \frac{k_p [\text{LOO}\cdot][\text{LH}]}{k_o [\text{O}_2]} \end{aligned} \quad (\text{A1.11})$$

Substituting (A1.11) into (A1.10),

$$\begin{aligned} \left(\frac{R_i}{k_t}\right)^{1/2} &= [\text{LOO}\cdot] + \frac{k_p [\text{LOO}\cdot][\text{LH}]}{k_o [\text{O}_2]} \\ [\text{LOO}\cdot] & \frac{k_o [\text{O}_2] + k_p [\text{LH}]}{k_o [\text{O}_2]} \\ [\text{LOO}\cdot] &= \left(\frac{R_i}{k_t}\right)^{1/2} \frac{k_o [\text{O}_2]}{k_p [\text{LH}] + k_o [\text{O}_2]} \end{aligned} \quad (\text{A1.12})$$

Since $\frac{d[\text{LOOH}]}{dt} = k_p [\text{LOO}\cdot][\text{LH}]$, by substituting (A1.12),

$$\frac{d[\text{O}_2]}{dt} = \frac{d[\text{LOOH}]}{dt} = \left(\frac{R_i}{k_t}\right)^{1/2} \frac{k_p [\text{LH}]k_o [\text{O}_2]}{k_p [\text{LH}] + k_o [\text{O}_2]} \quad (\text{A1.13})$$

The termination reactions (A1.5) and (A1.6) (Alkyl radical L· reacts with oxygen rapidly; become negligible at high pressures of oxygen hence LOO· concentration is much greater than the L· concentration.) Apply steady-state conditions, the peroxy radical (LOO·) is the dominant species.

$$\frac{d[\text{L}\cdot]}{dt} = R_i - k_o [\text{L}\cdot][\text{O}_2] + k_p [\text{LOO}\cdot][\text{LH}] = 0 \quad (\text{A1.14})$$

$$\frac{d[\text{LOO}\cdot]}{dt} = k_o [\text{L}\cdot][\text{O}_2] - k_p [\text{LOO}\cdot][\text{LH}] - k_t [\text{LOO}\cdot]^2 = 0 \quad (\text{A1.15})$$

Addition of (A1.14) and (A1.15),

$$\begin{aligned} R_i - k_t [\text{LOO}\cdot]^2 &= 0 \\ [\text{LOO}\cdot] &= \left(\frac{R_i}{k_t}\right)^{1/2} \end{aligned} \quad (\text{A1.16})$$

Since $\frac{d[\text{LOOH}]}{dt} = k_p [\text{LOO}\cdot][\text{LH}]$, by substituting (A1.16),

$$\underbrace{-\frac{d[\text{O}_2]}{dt}}_{\text{oxygen consumption}} = \underbrace{\frac{d[\text{LOOH}]}{dt}}_{\text{hydroperoxide formation}} = \left(\frac{R_i}{k_t}\right)^{1/2} k_p [\text{LH}] \quad (\text{A1.17})$$

In conditions of elevated temperatures, high conversion, with the presence of metals, antioxidants, or higher degree of unsaturation of the lipid, hydroperoxide decomposition becomes

significant with the formation of a variety of chemical products (refer to ► Chap. 1). The kinetics of such systems are much more complex than those presented above.

Appendix 2: Singlet Oxygen

Oxygen atom has an electronic configuration $1s^2 2s^2 2p_x^2 2p_y^1 2p_z^1$. The diatomic molecule has eight $2p$ electrons. Six of these occupy the σ_{2p} , $\pi_x 2p$, and $\pi_y 2p$ orbitals (two paired electrons each, Pauli exclusion principles). The $\pi_x^* 2p$

and $\pi_y^* 2p$ anti-orbitals are degenerate (with equivalent energy levels), each having one electron with parallel spin (Hund's rule). The molecular orbital scheme for O_2 is shown in **Fig. A2.1**.

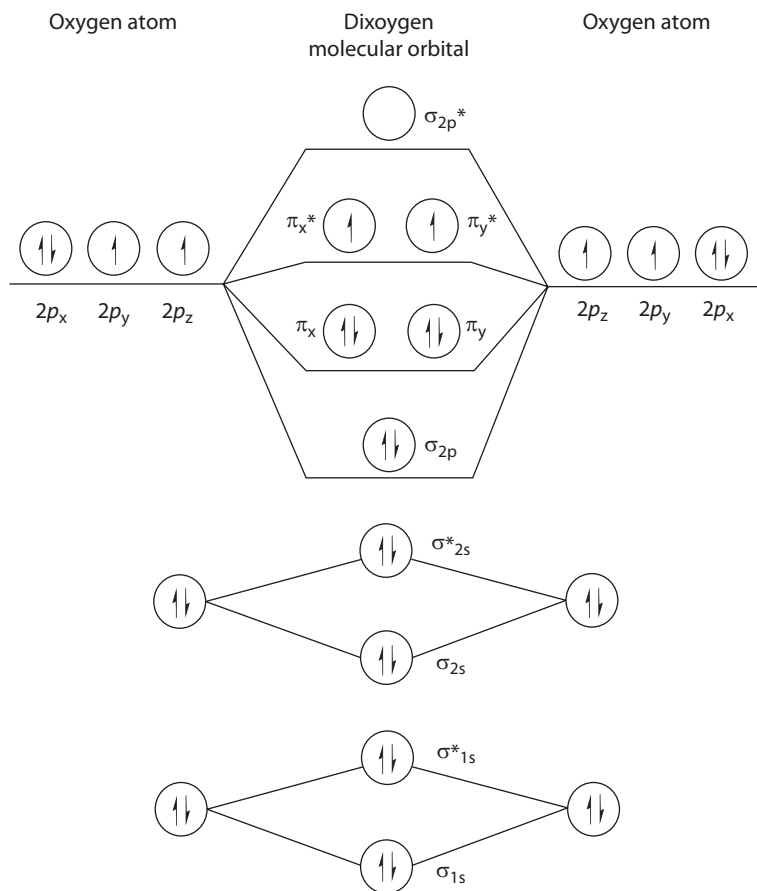


Fig. A2.1 Molecular orbital of oxygen.

The molecule contains two unpaired electrons with parallel spin in the highest molecular orbital (HOMO), each having a magnetic moment. The two magnetic fields interact in three ways:

1. Reinforce each other to augment an extended field.
2. Counteract to decrease an external field.
3. Cancel each other.

The state of possessing two unpaired electrons in the HOMO is called a triplet state, commonly referred to as having a multiplicity of 3. Multiplicity is given by the Eq. A2.1:

$$S = 2s + 1 \quad (\text{A2.1})$$

where S = multiplicity and s = total spin (an electron has spin of $1/2$). For the oxygen molecule,

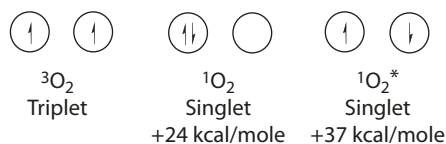
$$S = 2(+1/2 + 1/2) + 1 = 3 \quad (\text{A2.2})$$

The ground state of the oxygen molecule is thus a triplet (represented by $^3\text{O}_2$), which is unusual, since most molecules have singlet ground states. The two excited states of the oxygen molecule are singlets (represented by $^1\text{O}_2$ and $^1\text{O}_2^*$), which are 24 and 37 kcal/mole above the ground state. The electronic configuration of the HOMO of the two singlets is represented in

■ Fig. A2.2.

The $^1\text{O}_2^*$ state is extremely unstable and decays rapidly to the $^1\text{O}_2$ state. The singlet oxygen $^1\text{O}_2$ has one unoccupied π^*2p orbital and therefore is very electrophilic, seeking electrons to fill the empty orbital. The singlet species, therefore, reacts readily with unsaturated fatty acids, for example.

Singlet oxygen can be generated by (1) the chemical reaction between H_2O_2 and strong oxidizing species (e.g., sodium hypochlorite, triphenyl phosphate ozonide) and (2) the action of light in the presence of a sensitizer such as chlorophyll, flavin, heme compounds, porphyrins, and some synthetic colors in food systems. It is the latter reaction that we are most interested.



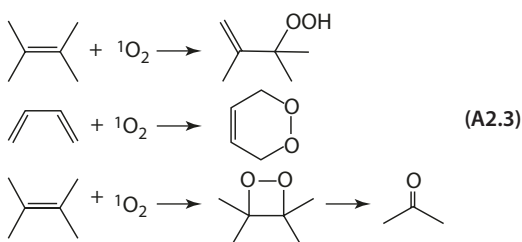
■ Fig. A2.2 Homo of Triplet and Singlet Oxygen

A2.1 Photosensitized Oxygenation

A sensitizer absorbs light and changes from the singlet ground state to the singlet excited state. Intersystem crossing occurs rapidly to yield the triplet state. The energy transfer from the triplet state of the sensitizer is captured by the triplet oxygen to generate the singlet oxygen. (This is type II photosensitized reaction; refer to Appendix 3.)

The singlet oxygen generated can undergo three types of oxygenation reaction, depending on the reactant.

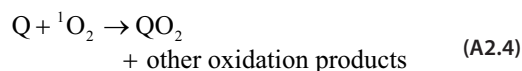
1. The "ene" reaction: Oxygenation of unsaturated olefins to give allylic hydroperoxides, with a shift of the double bond position (Eq. A2.3.1).
2. The 4 + 2 cycloaddition: Oxygenation of cyclic dienes, polycyclic aromatics, and heterocyclic compounds to form cyclic peroxides, analogous to the Diels-Alder reaction (Eq. A2.3.2).
3. The "dioxetane" reaction: Certain olefins react with oxygen by 1,2-cycloaddition to form dioxetane intermediate, which cleaves to carbonyl compounds. This reaction requires the olefins activated by amino or alkoxy groups and the absence of very active allylic hydrogen in the molecule (Eq. A2.3.3).



A2.2 Physical and Chemical Quenching

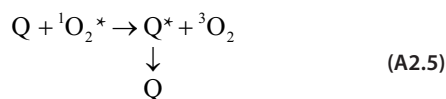
In the above mechanism, the singlet oxygen is converted to its triplet state by transferring the energy to the formation of hydroperoxides and

cycloaddition products. This type of energy quenching, in which the quencher is removed with the formation of new products, is referred to as chemical quenching (or destructive quenching). A general equation for this type of quenching is given in Eq. A2.4.



Another type of quenching process is called physical quenching (or degenerate quenching). The energy is transferred from 1O_2 to the

quencher, resulting in the latter molecule being converted to the excited triplet state, which subsequently decays to the ground state (Eq. A2.5). The structure of the quencher molecule is not chemically changed. Both α -tocopherol and β -carotene are effective physical quenchers of the 1O_2 molecule, although α -tocopherol has been shown to form a charge-transfer exciplex with singlet oxygen. The latter mechanism is discussed in more detail in ► Chap. 10.



Appendix 3: Where Do the Radicals Come From?

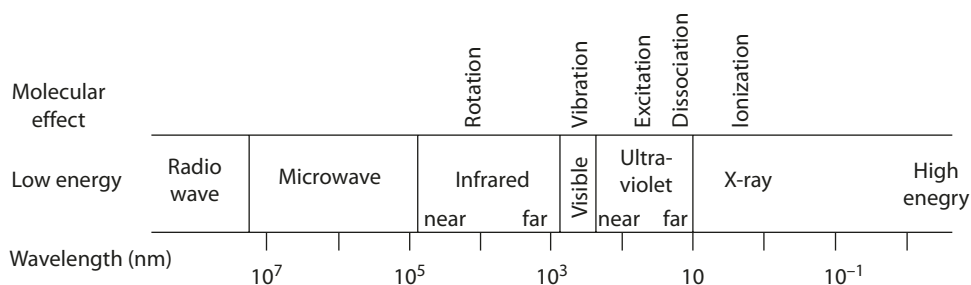
Reaction processes by which free radicals may be produced include (1) photolysis, (2) radiolysis, (3) molecular homolysis, (4) Fenton reaction, and (5) enzyme-catalyzed reactions. Radicals refer to an atom or a group of atoms that have one or more unpaired electrons and can have positive, negative, or neutral charges.

1. Rotation, vibration, and excitation by infrared light
2. Electronic excitation by ultraviolet and visible light

Higher energy radiation may cause ionization of the molecule and will be discussed under radiolysis (■ Fig. A3.1).

A3.1 Photolysis

A molecule can absorb a quantum of energy accompanied by a transition to the higher energy state. Depending on the wavelength, there are different kinds of transitions:

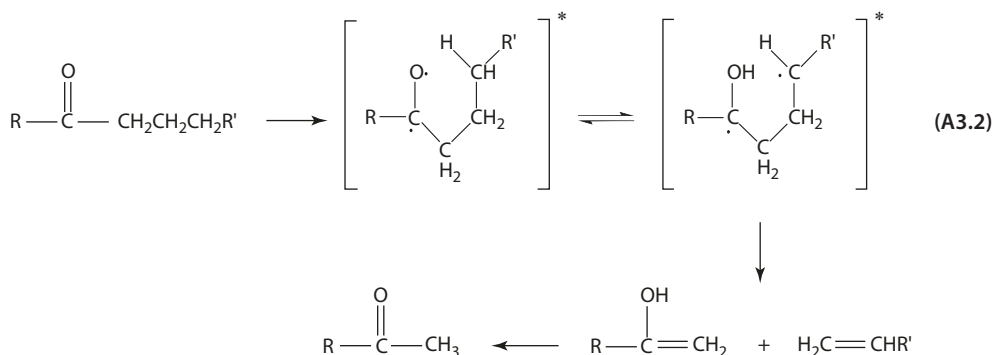
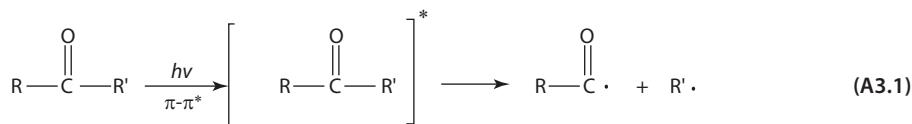


■ Fig. A3.1 Relationship between wavelength and energy.

A3.2 Photodissociation

Most aldehydes and ketones undergo photodissociation reactions (Eq. A3.1). If γ -hydrogen is present, intramolecular hydrogen abstraction

usually occurs, resulting in β -scission (Eq. A3.2).

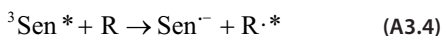
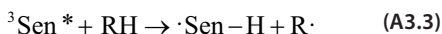


A3.3 Photosensitized Reaction

Light irradiation causes electronic excitation of sensitizers, such as chlorophyll, flavin, heme compounds, and porphyrins, from the ground state to the excited states ($^1\text{Sen}^*$ and $^3\text{Sen}^*$). The excited singlet decays rapidly, while the triplet can initiate two types of reactions.

Type I Reaction

The sensitizer triplet reacts directly with another molecule in the form of hydrogen abstraction (Eq. A3.3), or electron transfer (Eq. A3.4). The radical products can abstract H \cdot from another molecule and initiate other free-radical chain reactions.



Type II Reaction

The $^3\text{Sen}^*$ can transfer the energy to oxygen, resulting in the excitation of the oxygen molecule to the singlet state ($^1\text{O}_2$) (Eq. A3.5). The electrophilic singlet oxygen is reactive to unsaturated systems, for example, and forms oxygenated addition or substitution products with many organic compounds.



A3.4 Radiolysis

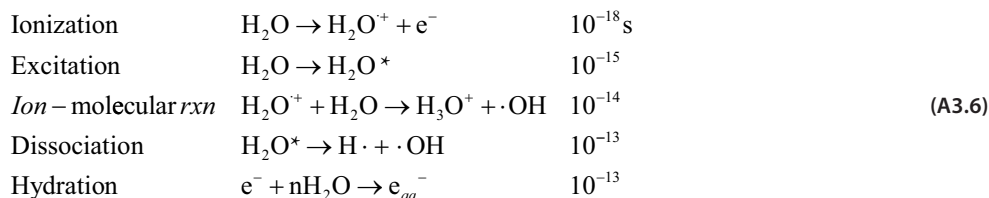
The ionization potentials of most molecules of biological interest are within the range of 10 eV. In practice, radiation chemical studies are carried out with radiation energy in the range of 0.1–20 MeV (■ Fig. A3.2).

	MeV	Charge
Electromagnetic		
x-ray	0.3 - 0.5	0
γ-ray	0.2 - 2.0	0
Particles		
electron	1 - 30	-1
β-particle	0.01 - 2	-1
α-particle	1 - 45	+2
neutron	2 - 30	0
Visible light	0.4 - 3 (eV)	
Ultraviolet	3 - 6 (eV)	

Fig. A3.2 Types of Radiation and Energy.

In biological and food systems, where water is the major constituent, most damage is caused by the indirect effect produced by radiolysis of water. The reactive species produced by the radiolysis of water are (1) hydroxyl radical ($\cdot\text{OH}$), (2) hydrogen atom ($\text{H}\cdot$), and (3) hydrated electron (e_{aq}^-). The G value (number of molecules or radicals formed per 100 eV of energy absorbed) are 2.8, 0.7, and 2.7, respectively. With the typical irradiation energy levels in the MeV range, the energy of radiation is in excess of the bond energies of ionization or excitation potentials of the absorbing molecule.

The chemical changes of water can be expressed by Eq. A3.6.



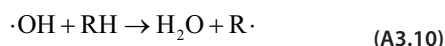
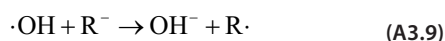
Both $\text{H}\cdot$ and e_{aq}^- are strong reducing agents. The hydrated electron reacts by the following two types of reactions:

1. *Electron capture* (Eq. A3.7)
2. *Dissociation* (Eq. A3.8)



The hydroxyl radical $\cdot\text{OH}$ is a strong oxidizing agent and undergoes the following types of reactions:

1. *Electron transfer* (Eq. A3.9)
2. *Hydrogen abstraction* (Eq. A3.10)
3. *Addition* (Eq. A3.11)



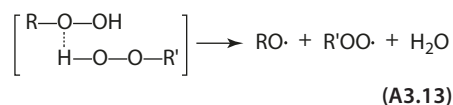
A3.5 Molecular Homolytic Decomposition

The most studied system in this category is the reaction involving decomposition of lipid hydroperoxides. Peroxide bonds $-\text{O}-\text{O}-$ are relatively weak. For example, t-butyl peroxide has a bond energy of 37 kcal/mole compared with the ~ 90 kcal/mole for the normal $\text{C}-\text{C}$ bond. Homolytic scission of the $-\text{O}-\text{O}-$ occurs when sufficient energy is applied.

In the biological and food systems, decomposition is largely induced by other radicals in the system, and the resulting chain reactions are fast even at room temperature (Eq. A3.12):

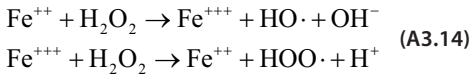


Decomposition is also accelerated by other molecules that can form hydrogen bonding and enhance bond dissociation (Eq. A3.13):

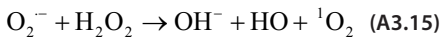


A3.6 The Fenton Reaction

In the Fenton reaction, ferrous iron catalyzes the formation of a hydroxyl radical and a hydroxide ion from hydrogen peroxide. The Fenton reaction is considered a two-step process. The reductive half cycle of Fe^{2+} to Fe^{3+} is a rate-determining step in the reaction (Eq. A3.14):



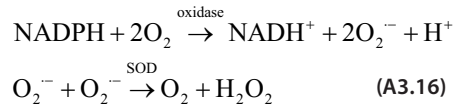
The hydroperoxyl or perhydroxyl radical ($\text{HOO}\cdot$) is the protonated form of superoxide, which exists as superoxide anion ($\text{O}_2^{\cdot-} + \text{H}^+$) at physiological pH environment. In a Fenton-like reaction, the superoxide radical reacts with H_2O_2 to form hydroxyl radical and singlet oxygen (Eq. A3.15).



A3.7 Enzyme-Catalyzed Reactions

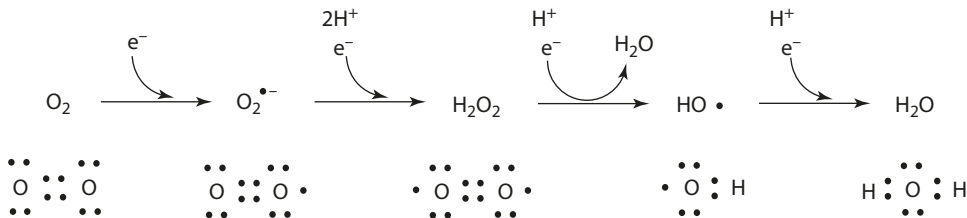
Oxygen-derived radicals are generated at low concentration as metabolites in aerobic cells. Mitochondria, microsomes, peroxisomes, macrophages, and endothelial cells all generate low levels of $\text{O}_2^{\cdot-}$ and H_2O_2 . A number of oxidases, such as NADPH oxidases, xanthine oxidase, and cytochrome P45-dependent oxygenases, are

involved capable of producing superoxide anions by $1e^-$ reduction of oxygen (addition of an electron to the antibonding π^* orbitals of the triplet oxygen). In vivo dismutation of superoxide anion by superoxide dismutase enzymes generates hydrogen peroxide (Eq. A3.16). Catalase and glutathione peroxidase further catalyze the detoxification by breaking down hydrogen peroxide.



Nonenzymatic production of $\text{O}_2^{\cdot-}$ occurs by single e^- transfer mediated by reduced coenzymes or prosthetic groups, such as flavins and iron sulfur clusters. The mitochondrial electron transport chain system consisting of redox centers constitutes a major source of $\text{O}_2^{\cdot-}$ in many cell tissues. Sequential reduction of molecular oxygen (i.e., sequential addition of electrons) produces reactive oxygen species: superoxide anion ($\text{O}_2^{\cdot-}$), peroxide (O_2^{-2}), and hydroxyl radical ($\text{HO}\cdot$) (■ Fig. A3.3).

Reactive oxygen species also include singlet oxygen, which is not a radical (refer to Appendix 1). Radicals such as peroxy radical ($\text{ROO}\cdot$), alkoxyl radical ($\text{RO}\cdot$), and hydroperoxyl radical ($\text{HOO}\cdot$) generated in lipid oxidation also play an important role in food chemistry (refer to ► Chap. 1.)



■ Fig. A3.3 Sequential Reduction of Molecular Oxygen

A3.8 Reduction Potentials

Reduction potential (E_o , measured in V or mV) is a measure of the tendency of a chemical species to acquire electrons and thereby the tendency to be reduced. The larger (more positive) the E_o is, the greater is the tendency for the chemical to gain electrons (be reduced), corresponding to more potent oxidants. This is often reflected in the reaction rate. Below is a list of the E_o values for the major species discussed here. Others that are relevant to foods are also included in the table.

Half cell (Ox/Re forms)	E_o , mV
$O_2/O_2^{\cdot-}$	-330
$^1O_2/O_2^{\cdot-}$	650
$O_2^{\cdot-}, H^+/H_2O_2$	940
$H_2O_2, H^+/H_2O, HO\cdot$	320
$O_2, H^+/HOO\cdot$	-460
$HOO\cdot, H^+/H_2O_2$	1060
$ROO\cdot, H^+/ROOH$	1000
$RO\cdot, H^+/ROH$	1600
PUFA \cdot , $H^+/PUFA-H$ (bisallylic H, polyunsaturated fatty acids)	600
RS \cdot /RS (cysteine)	920
RSSR/RSSR \cdot (cystine)	-1500
Catechol-O \cdot , H^+ /catechol-OH	530
TO \cdot , H^+ /TOH (vitamin E)	500
Ascorbate \cdot , H^+ /ascorbate monoanion	282
Fe(III)/Fe(II) (aqueous)	110

From Buettner, G. R. 1993. *Arch Biochem Biophys* 300, 535-543.

Appendix 4: Flavonoids

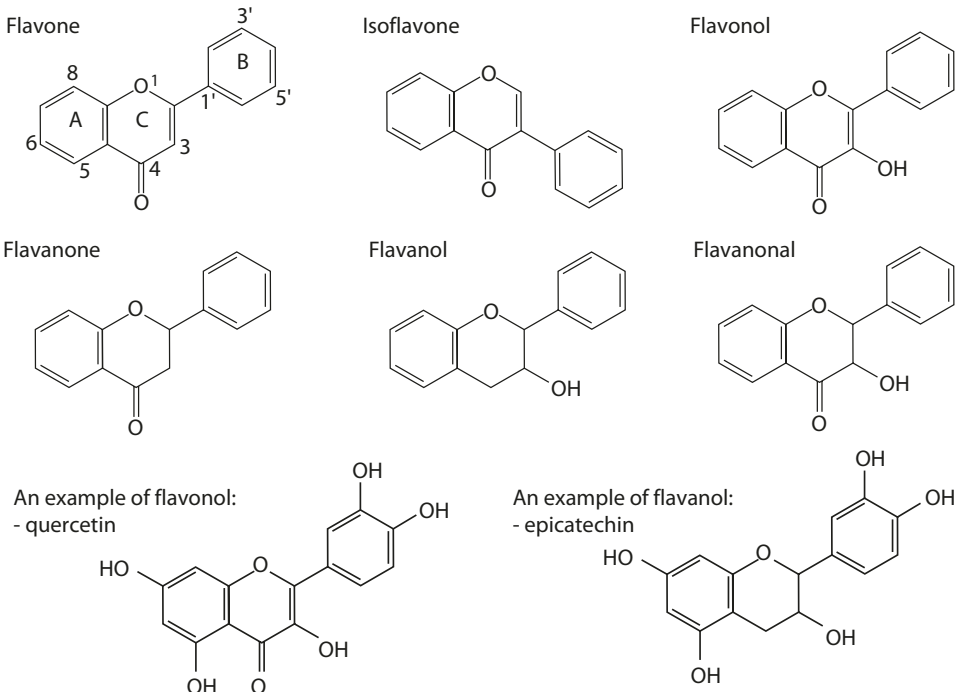
Flavonoids are a major family of polyphenolic secondary metabolites synthesized by plants, consisting of more than 8,000 known structures. Chemically, flavonoids consist of a 15-carbon skeleton with a core structure of 2-phenylbenzopyranone, in which the two benzene rings (A and B) are linked via a heterocyclic pyran cyclized with oxygen (C).

The variations in the bond structures and substitutions of the rings further divide this large family of compounds into subgroups: flavonols, flavones, isoflavones, flavanone, flavanones, and flavanols. These subgroups differ in the degree of unsaturation and the level of oxidation of the C ring. Within the individual subgroup, differentiation depends on the number and nature of the substituent groups in the A and B rings (■ Fig. A4.1).

In some classifications, anthocyanidins and chalcones are included as flavonoids. Refer to ► Chaps. 4 and 7 for their structures and reactions.

Flavonoids exist both as free aglycones and as glycosidic conjugates (with the glycone- sugar moiety) in fresh plant tissues. Flavonoids are usually found as *O*-glycosides and, less frequently, *C*-glycosides. The 3- and 7-hydroxyl groups are the favored glycosylation site. In *O*-glycosylation, the sugar moiety forms an acid-label hemiacetal bond. In *C*-glycosylation, the sugar is linked directly to the benzene ring forming an acid-resistant C–C bond. Glycosylation renders the flavonoid compound more water soluble, more polar, and less reactive. The glycone moiety may consist of mono-, di-, and higher saccharides (such as glucose, galactose, rhamnose,

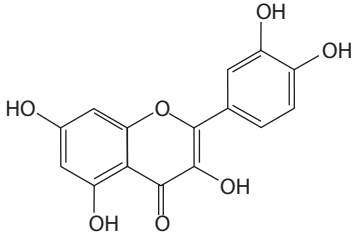
The Basic Structures of Flavonoids



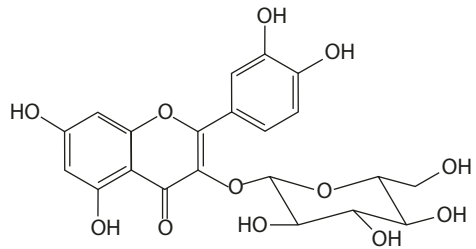
■ Fig. A4.1 Backbone structures of flavonoid subclasses

Flavonol

(onion, kale, broccoli, apple, tea)

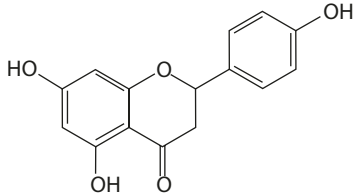


Quercetin



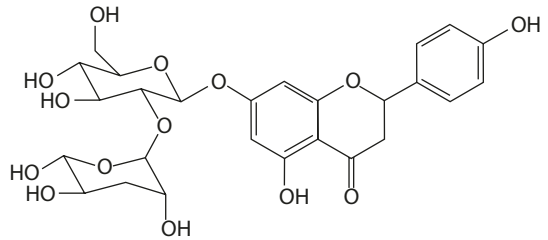
Quercetin 3-β-D-glucoside

Flavanone
(Citrus fruit)



Naringenin

(2-O-α-L-rhamnosyl-
α-D-glucoside)



Naringin

■ Fig. A4.2 Examples of flavonol and flavanone aglycones with their respective glycosides

gentiobiose, rutinose, neohesperidose). Di-O-glycosides are also found. Flavonoids are sometimes acylated by aromatic and aliphatic acids, such as malonic, malic, and coumaric.

Examples of flavonols and flavanones aglycones with their respective glycosides are illustrated below (■ Fig. A4.2). Also refer to ► Chap. 6 for catechins (which are flavanols) and derivatives.

Index

A

- Absorption spectrum
 – chlorophyll 213
 – conjugation 173
 – myoglobin 208–209
 – substituent effect 175
 – transition energy 171–172
 Acesulfame K 316–317
 Acetylation 41
 Acetylcholine 342
 Actin
 – G-and F-actins 85
 – phallotoxins action on 340
 – protein structure 84–85
 Action pattern
 – amylases 242–244
 – endo-polygalacturonases 248, 250
 Acylenzyme intermediate
 – lipase 253–254
 – papain 224
 Acyl transfer reaction 255
 Acylium ion 224, 226
 Additives 362–379
 – antimicrobial short-chain acid derivatives 371–372
 – citric acid 368–370
 – phosphates 362–367
 – phosphoric acid 371
 – sulfite 352–379
 – vitamin D 415
 Adenosine triphosphate (ATP)
 – energy conversion in muscle 85–87
 – rigor mortis 86–88
 Adipic acid anhydride 147
 Adsorption
 – emulsifier functions 45–46
 – proteins 65–66
 Aflatoxins 345–347
 Agaritine 341
 Aggregation
 – β -lactoglobulin 96
 – milk micelles 95
 – protein gel 67–68
 Aglycoside sweeteners 320–321
 Alanine 60
 Alcohol(s)
 – ester derivatives of 39–40
 – wheat protein classification 97–99
 Alcohol fractionation 40
 Alcoholate 142
 Aldose-ketose rearrangement 127
 Alginate 149–151
 – applications of 150
 – chemical structure of 155
 – gelling 149–150
 Alkali
 – monosaccharides and 127–130
 – sugar/metal ion 141–142
 – vitamin B₁ and 388–389
 – vitamin B₂ and 394
 Alkali degradation 68–70
 – β -elimination 69
 – hydrolysis 68
 – racemization 70
 Alkyldiazonium ion 357
 Allicin 287–288
 Allin 287
 Allinase 287
 Alloxazine 395
 (+)-S-Allyl-L-cysteine sulfoxide 287–288
 Allyl-2-propenethiosulfinate 287–288
 Allylic radical 15
 Allylsine 115
 Allura red AC 193
 Alpha-amylase. *See* Amylases
 Alumina hydrate [Al(OH)₃] 194
 Amadori rearrangement 133
 Amatoxins 340
 Amines 343–345
 Amino acids. *See also* Protein structure
 – collagen 113
 – heterocyclic amines 349–351
 – sweeteners 313–316
 – toxicants 338–340
 – water and 59–60
 α -Amino adipic acid- δ -semialdehyde 116
 1-Amino-1-deoxy-2- α -D-fructopyranose (Amadori product) 133
 2-Amino-2-deoxy- α -D-glucopyranose 138
 1-Amino-1-deoxy-2-ketose 136
 1-Amino-3-oxalylamino propionic acid 339
 Aminosulfonates 316–317
 Amygdalin 319
 Amylases 240–246
 – action pattern 243–244
 – characteristics of 240–241
 – corn sweeteners 322–323
 – industrial uses 246
 – multimolecular process 245
 – reaction mechanism 240–242
 – subsites 243–245
 Amylopectin 144, 145. *See also* Starch
 Amylose 144, 145. *See also* Starch
 Anhydro sugars 126, 130
 Annatto 182–183
 Anthocyanins 183–189
 – condensation 188
 – oxidation 189
 – pH effect on color 184–185
 – self-association and copigmentation 186–187
 – sulfur dioxide decoloration 98
 – thermal degradation 186
 Anthracene 174
 Antimicrobial action 374
 Antimicrobial short-chain acid derivatives 371–372
 Antioxidants 47–51
 – flavonoids 50
 – reaction mechanism 48–49
 – polyphenolics 47–48
 β -Apo-8'-carotenal 177, 384
 Aqueous lamella 67
 Arabinoxylan 159–160
 Ascorbic acid (vitamin C)
 – biochemical mechanism 409–410
 – biological functions 410–411
 – browning 373–374, 414
 – loss of activity 412–413
 – polyphenol oxidase 236
 – uses 414–415
 Ascorbigen 334
 Asparagusic acid 300
 ϵ -N-(β -Aspartyl)-lysine 71
 Aspartame 313–315
 Autoxidation
 – described 6–9
 – oxymyoglobin 206–208
 – stereochemistry of hydroperoxides 9–10
 Azetidino-2-carboxylic acid 339

B

- Bayer Villinger oxidation 189
 Beer flavor 283–284
 Benzene 63
 Benzoic acid type rearrangement 128
 Benzenoid 302
 Benzo[a]anthracene 348
 Benzoate 372

- Benzo[*a*]pyrene 348
 Benzo[*b*]fluoranthene 348
 Benzoin-type condensation 388
 Benzoyloxyphenylacetate 189
 Beta-amylase 240–241. *See also*
 Amylases
 Beta-carotene. *See* Carotene
 Beta-casein 92
 Betacyanin 189–190
 Beta-elimination 69
 Beta-meander 57–58
 Betamic acid 189–190
 Betanain 189–190
 Beta-oxidation 275
 Beta-plated sheet 56
 Betaxanthins 189
 Beverage caffeine 335–338
 Beverage flavors 280–285
 – beer 283–284
 – coffee 285–287
 – tea 280–283
 Bicarbonates 366–367
 Biotin 406–408
 Bis(methylthio)methane 300
 Bisulfite
 – additive 372–379
 – anthocyanin 186
 – flavin 394
 – Maillard reaction 132–135
 – thiamin and 390–391
 Bitter taste 266
 Bixin 177
 Bleaching 232
 Botulinum neurotoxin 341–343
 – mechanism of toxicity 342
 – structure 341–342
 Bread
 – flour into dough transformation
 104–105
 – lipoxigenase bleaching 232
 – staling of 245
 Brilliant blue FCF 193
 Bromelain 246–247
 1,3-Butadiene 173
 Butylated hydroxyanisole (BHA) 47–48
 Butylated hydroxytoluene (BHT) 47–48
- C**
- Caffeic acid 187, 286
 Caffeine 286–287, 335–338
 3-Caffeoylquinic acid 286
 Calcium, alginate 149–150
 Canthaxanthin 176–177
 Capsaicin 292
 Capsaicinoids 292
 Caramel 191–192
 Carbinol base 184–185
 Carbohydrates 125–166
 – acid action on monosaccharides
 130–131
 – alginate 149–150
 – alkali action on monosaccharides
 127–129
 – carrageenan 163–166
 – cellulose 153–155
 – β -glucan 156–158
 – glycosidic linkage 125–126
 – guar gum 162–163
 – hemicellulose 159–160
 – hydrocolloid 143
 – nonenzymatic browning (Maillard
 reaction) 132–134
 – pectin 151–152
 – starch 143–148
 – sugar/metal complexes 141–142
 – xanthum gum 161–162
 Carbonium ion 125–126
 Carbonyl compounds, protein reaction
 76
 Carboxymethyl cellulose 155
 Carcinogenic polycyclic aromatic
 hydrocarbons 348–352
 Carotene
 – isomerization 178–179
 – photosensitized oxidation 12
 – quenching 386–387
 – reaction with sulfite 376
 – singlet oxygen quenching 386–387
 – structure 383
 – vitamin A 383–387
 Carotenoids 176–182
 – autoxidation 179
 – carotenoproteins 181–182
 – color additive 180–181
 – epoxides 179
 – isomerization 178
 – photochemical reactions 180
 – tea oxidation 280–281
 – thermal degradation 179–180
 Carotenoproteins 181–182
 Carrageenan 163–166
 – chemical structure of 163–164
 – gelling 165
 – locust bean gum synergism 166
 – protein interactions 165–166
 Caseins
 – α -Casein, β -Casein, κ -Casein 92
 – interaction with carrageenan 166
 – interaction with β -lactoglobulin
 96–97
 – micelle models 93–95
 – nanocluster 93–94
 – proteolysis 95
 Catechin
 – condensation 188
 – tea flavor 281
 Catecholase. *See* Polyphenol oxidase
 Catechol oxidase. *See* Polyphenol
 oxidase
 Cellulose 153–156
 – chemical structure of 155
 – gelling 153–156
 Certified color additives 192–193
 α -Chaconine 330–331
 Chalcone
 – anthocyanidin 185
 – naringin 297
 – sweetener 317
 Character-impact compounds 271
 Chelated iron
 – ADP 10
 – perferryl iron 10
 Chemical oxidation 77–78
 Chlorin 212
 Chlorogenic acid 286
 Chlorophyll 212–216
 – derivatives of 214–215
 – dimers and oligomers 213–214
 – magnesium-ligand coordination 213
 – oxidation and reduction 216
 Chlorophyllide production 215
 Cholecalciferol (vitamin D) 415
 Chorismic acid 274
 Chroman ring 419
 Chrysene 348
 Chymosin 95
 Cinnamaldehyde 294
trans-Cinnamic acid 294
 Cinnamon flavor 294
Cis-trans isomerization 30–31
 Citral 296
 Citric acid 368–371
 Citrous red No. 2 193
 Coagulation (milk) 95
 Coalescence 36
 Cocoa powder 42
 Colipase 252–253
 Collagen 113–118
 – amino acid composition 119
 – cross-linking 115
 – gelatin and 117
 – triple helix structure 113
 Collagenase 227
 Colloidal calcium phosphate 93
 Colorants 171–216
 – annatto 182
 – anthocyanins 181–189
 – betanain 189–190
 – caramel 191–192
 – carotenoids 176–181

Index

- chlorophyll 212–216
- conjugation 173–174
- coordination chemistry 194–196
- dyes and lakes 192–193
- light absorption 171–172
- metalloporphyrin 197–199
- myoglobin 200–213
 - substituent effects, 175
- Complexation
 - lipid-starch 46–47
 - sugar with metal 141–142
- Condensation
 - amylases 243, 244
 - anthocyanins 188
- Conformation of proteins 60–65
- β -Conglycinin 108. *See also* Soybean proteins
- Conjugated diene 7–8, 18
- Conjugated tricarbonyl system 410
- Conjugation 173–174
- Coordination chemistry 194–196
- Cooxidation 232
- Copigmentation 186–187
- Copper 233–236
- Copper-pheophytin 215
- Corn sweeteners 322–323
- Counterion atmosphere 36–37
- Coulomb's law 63
- Creaming 35
- Cross-linking
 - collagen 115
 - pentosan 159–160
 - photolysis 75–76
 - protein-lipid 78–79
 - radiolysis 71–73
 - starch 147
- Crossover connection 56–57
- Crystal habit of fat 27–28
- Crystal structure 27–28
- Cured meat. *See also* Meat; Meat protein
 - nitrosamines in 354–355
 - nitrosylmyoglobin 210–211
- Cyanidin 183
- Cyanocobalamin 404
- Cyanogenic glycosides 329–330
- Cyanohydrin 330
- Cyclamate 316–317
- Cyclic adenosine 3',3'-monophosphate phosphodiesterase 337
- Cyclic dimer 17–18
- Cyclic esters: hop flavor 284
- Cyclodopa-5-O-glycoside 190
- Cysteine 72, 73, 75

D

γ -Decalactone 297–298

- Dehydroalanine 69–70
- Dehydroascorbic acid 409
- 7-Dehydrocholesterol 415
- Dehydro-L-ascorbic acid 409, 410
- Dehydrolysinonorleucine 116
- Delphinidin 183
- Delphinidin-3-[4-(*p*-coumaroyl)-L-rhamnosyl[(1,6)glucoside]-5-glucoside 183–184
- Denaturation 61
- 5'-Deoxyadenosylcobalamin 404
- 3-Deoxyglycosulose
 - alkali degradation 128
 - ascorbic degradation 110
 - flavor formation 272–275
 - Maillard reaction 133
 - reaction with sulfite 373
- Deoxymyoglobin 200, 202, 208, 210. *See also* Myoglobin
- Desmin 81
- Deuteroflavin 395
- Dialdehyde phenolate ion 347
- N,N'*-Dialkyldihydropyrazine 138–139
- Dialkylpyrazinium compound 138–139
- Diallyl disulfide 289–290
- Diallyl thiosulfonate 289–290
- α,γ -Diaminobutyric acid 339
- Diazonium ion 341
- 3,4-Dideoxy-glycosulose-3-ene
 - Maillard reaction 133
 - reaction with sulfite 373
- 3,4-Dideoxy-4-sulfo-D-glycosulose 139
- Dienoic dimer 17–18
- Dielectric constant 63
- Dietary fats and oils. *See* Lipids
- Dihydrocapsaicin 292
- Dihydrochalcone 317–319
- 7,8-Dihydro-7,8-epoxybenzo[*a*]pyrene 349
- 8,9-Dihydro-8-(N^7 -guanyl)-9-hydroxy-aflatoxin B₁, (AFB₁- N^7 -GUA) 346
- Dihydrothiachrome 389
- 5,6-Dihydrouracil-6-sulfonate 374
- Diglycerinate 32–33
- Dimers 213
- Dimethylanthranilate 295
- 7,7'-Dimethyl-6,8-dioxabicyclo [3.2.1] octane 284
- 2,5-Dimethyl-4-hydroxy-3(3*H*)-furanone 284
- 2,6-Dimethylnaphthalene 179–180
- Dinitroferrohemeochrome 210
- Dioxetane reaction 387
- Dioxindole-3-alanine 79
- Dipeptides 313–316
- Diperoxide 14
- Diphenol 333–334

- Disproportionation, emulsion 35
- Disulfide bonds
 - dough 104–105
 - protein gel 68
 - protein structure 58–59
- Dithiacyclopentene 301
- Dithiazine 279
- DNA
 - peptide toxicants 340–341
 - protein and 74
- Dopamine 344
- Dopamine hydroxylase 411
- Double displacement reaction 242
- Dough
 - ascorbic acid 414
 - dough reaction rate 367
 - flour transformation I 104–106
 - pentosan 159
- Dyes 192–194

E

- Egg box model 150–151
- Electric double layer 44–45
- Electronic structure, metalloporphyrin 197–198
- Electrostatic interaction
 - dipole-dipole 60
 - in emulsion 36–37
 - ion-dipole 60
- Emulsification (proteins) 65–66
- Emulsifier functions
 - adsorption at interface 45
 - complexation with starch 46
 - electric double layer 44
 - fat crystallization control 47
 - liquid-crystalline interface 46
 - protein interactions 47
- Emulsifiers 37–42
 - ester derivatives of alcohols 39
 - hydrophilic/lipophilic balance 42
 - lecithin 40–41
 - mesomorphic behavior 42–44
 - monoglyceride derivatives 38
 - monoglycerides 37–38
- Emulsions
 - breakdown 25
 - electrostatic repulsion 36
 - formation of 34
 - meat 90–91
 - phosphate 367
 - surface tension/area 34
 - van der Waals attraction 36
- 1,2-Enaminol 133
- Endocytosis 342
- Endo-polygalacturonase 246, 248
- Enediol 127–128, 131, 412–413

- "ene" reaction 11–12, 387
 Energy conversion 85–87
 Enolization
 – acid 130–131
 – aldose-ketose rearrangement 127–134
 – Maillard reaction 133
 – vitamin C 412–413
 Enzymes 221–259
 – amylases 240–246
 – flavors and 232
 – glucose oxidase 237–240
 – lipolytic enzymes 251–256
 – lipoxygenase 227–233
 – listing of 221–223
 – papain 223–227
 – pectinolytic enzymes 246–251
 – polyphenol oxidases 233–236
 – vitamin B₂ and 392
 – vitamin B₆ and 397
 – vitamin B₁₂ and 405
 – xylose (glucose) isomerase 256–258
 Epicatechin 280
 Epicatechin gallate 280
 Epichlorohydrin 147
 Epigallocatechin gallate 280
 Epoxide hydrase 349
 Epoxides 179
 Epoxy-cation intermediate 231–232
 5,6-Epoxy- β -ionene 282
 Ergocalciferol (vitamin D)
 – biological functions 416–417
 – chemical structures 415–416
 – irradiation 417–418
 – thermal reaction 418
 Erythrosine 193
 Ester derivative of alcohols 39
 Ethanol 40
 Ethoxylated monoglyceride 38
 2-Ethyl-3,6-dimethylpyrazine 299
 2-Ethyl-3-methoxypyrazine 299
 Ethyl-2-methylbutyrate 298
 Ethyl-*trans*-2-*cis*-4-decadienoate 204
 Eugenol 294
 Exciplex 423
 Exo-polygalacturonase 246, 248
- Ferrohemochrome 209
 Ferrimyoglobin 208
 Ferulic acid 286
 Fe²⁺-O₂ complex 204
 Fiber, dietary 158–161
 Ficin 280, 281
 Flavanol 280, 281
 Flavor(s)
 – beverages 280–286
 – character-impact compounds 271
 – citric acid additives 368–371
 – fruits 294–297
 – meat flavor 302–305
 – microencapsulation of 305
 – odor 263–270
 – origin of 272–279
 – oxidation, tea flavanoids 281
 – spice 287–294
 – taste sensation 265
 – vegetables 298–301
 Flavor potentiators (sweeteners) 268
 Flavylium cation 184, 187
 Flocculation 36
 Flour 104–146. *See also* Wheat proteins
 Foaming 65–67
 Folic acid (vitamin B₉)
 – biological functions 401
 – degradation 401–404
 – structure 399–400
 Food additives. *See* Additives
 Formylkynurenine 80
 Free radicals
 – lipid 6–7
 – sulfite 376–377
 – vitamin E 421–422
 α -D-Fructopyranosylamine 138
 Fructosyl oxacarbenium cations 192
 Fruit(s)
 – dihydrochalcone 317–319
 – pectic enzymes 250
 Fruit flavors 294–297
 Furan derivatives 130–131, 302
 Furanocoumarin 345
 5,8-Furanoxide 179
 Furfural 131–132
 2-Furylmethanethiol 285
- G**
- Galactan, 159
 Galactomannan 163
 Galactose-4-sulfate-3,6-anhydro-galactose 164
 Galactose-2-sulfate-galactose-2,6-disulfate 164
 Galactose-4-sulfate-3,6-anhydro-galactose-2-sulfate 164
 Galocatechin 280
 Garlic flavor 287–290
 Gelatin 117–118
 Gelatinization (starch) 146–147
 Gelation
 – meat protein 91
 – polysaccharides 149, 152, 153, 162, 165
 Gelling
 – alginate 149–150
 – carrageenan 165
 – cellulose 153
 – guar gum 163
 – pectin 152–153
 – pentosans 160
 – protein 67–68
 – xanthan gum 162
 Geraniol 282–283
 Ginger flavor 293
 Gingerol 293
 Gliadins, α -, β -, γ -, ω - 97–98
 Globin 205
 β -Glucan 156–159
 – flow behavior 157
 – soluble fibers 158–159
 – structure 156–157
 Glucoamylase 322–323. *See also* Amylase
 Glucobrassicin 299
 Glucomanan 162–163
 Glucose isomerase. *See* Xylose isomerase
 Glucose oxidase 237–240
 – characteristics of 228–238
 – flavin 392
 – industrial uses of 240
 – reaction mechanism 239–240
 – two-electron transfer 239–240
 β -Glucosidase 330
 Glucinoates 298, 332–335
 Glu-P-1 350, 351
 Glutamate, taste enhancer 267–269
 γ -L-Glutamyl-S-allyl-L-cystine sulfoxide 289
 γ -Glutamylaminopropionitrile 339
 ϵ -N-(γ -Glutamyl)-lysine 71
 γ -Glutamyltransferase 341
 Gluten 102–104. *See also* Wheat protein
 Glutenins 99–101
 – chain extender and terminator 101
 – HMW-GS 99–101
 – LMW-GS 101
 Glycerol monostearate 46
 Glycinin 107. *See also* Soybean proteins
 Glycoaldehyde alkylimine 138
 Glycoalkaloids 330–331

Index

Glycophore 310–312
 Glycosidic linkage 125–126
 Glycosulos-3-ene 133, 276
 Glycosylamine formation 132
 Glycyrrhizin 319–320
 Greek key pattern 57
 Grignard reaction 180
 Guansine 5'-monophosphate 268
 Guar gum 162–163
 Guluronic acid 149

H

Hairpin connection 56, 57
 Heat. *See also* entries under Thermal
 – betanain 190
 – caramel 191
 – gelatin 117
 – gel formation 67
 – isopeptide formation 70–71
 – meat emulsion 90
 – milk protein 96
 – protein structure 56–59
 – starch 146
 – wheat protein 105
 Heme iron 202–203
 Hemicellulose 159–161
 – dietary fiber 160–161
 Hemochromes 209
 2-Heptenal 15
 Heterocyclic amines 349–352
 Hexanal 15
 Hexaquoiron counterion 370
 Heyns rearrangement 138
 High fructose oligosaccharides 192
 Histamine 344
 Histamine-*N*-methyltransferase 345
 Histidine
 – back-bonding and 204
 – photolysis 75
 Homoarginine 339
 Homocapsaicin 292
 Humulene epoxide 283
 Humulol 283
 Humulone (α -acid) 283
 Hydrated electron, with amino acids
 71–72
 Hydrocolloids 143
 Hydrogenation 29–32
 – *cis-trans* isomerization 30–31
 – mechanism 30
 – trans fatty acids 33–34
 – selectivity 31–32
 Hydrogen bonding
 – alcoholate 142
 – described 58
 – pectin 152

– protein and water 59–60
 – tripartite model 310–312
 Hydrogen peroxide
 – anthocyanins 189
 – myoglobin 207–208
 – protein oxidation 71–78
 Hydrolysis
 – glycoside 125–127
 – lecithin 40–42
 – protein 66
 Hydroperoxide
 – autooxidation 6–9
 – heme 11
 – lipoxygenase 231–232
 – photosensitized oxidation 11–12
 – protein reactions with 78–79
 – secondary products 13–16
 – stereochemistry 9–10
 – with metal ions 10–11
 – with sulfite 377
 Hydroperoxide cyclic peroxides 14–15
 Hydroperoxide isomerase 231
 Hydroperoxide lyase 231
 13-Hydroperoxy-9-*cis*,11-*trans*-
 octadecadienoic acid 8
 12-*Ls*-Hydroperoxy-9-*cis*,11-*trans*-
 octadecadienoic acid 229
 Hydrophobic interaction
 – casein submicelles 93–95
 – described 58
 – pectin 152
 – thermodynamics 60
 Hydropropylmethyl cellulose 154
 Hydroxyallylsine 115
 Hydroxycyclohexadienyl radical 14
 11-Hydroxy-12:13-epoxy-9-*cis*-
 octadecenoic acid 229
 Hydroxylation 235
 Hydroxyl radical
 – lipid oxidation 10
 – with amino acids 72–73
 Hydroxylysine 115
 Hydroxymethyl furfural 133–134
 4-Hydroxymethyl-phenylhydrazine 341
 Hydroxynitrile lyase 330
 α -Hydroxy-*N*-nitroso compound 355
 Hydroxyproline 114
 Hydroxypropyl phosphate 147
 5-Hydroxytryptamine 344
 Hypoglycine 340

I

Imidazolium-ion pair 226
 Indicaxanthin 190
 Indole glucosinolate 334
 Inosine 5'-monophosphate 268

Interesterification 32–33
 Ionic strength 68
 Ionization 225
 Ionone 282
 Iron
 – chelated 10–11
 – lipoxygenase 230
 – myoglobin 202–204
 Iron-dioxygen complex 202–203
 Isoalloxazine 395
 3-Isobutylidene phthalide 301
 3-Isobutyl-2-methoxypyrazine 291
 Isomerization
 – carotenoids 178–179
 – hydrogenation 30–31
 Isopeptides 70–71
 Isoprene pathway 275
 Isothiocyanate 298, 334–335
 2-Isovalidene phthalide 301

K

Kappa-casein
 – described 92
 – kappa-carrageenan and 166
 Ketide unit 274
 Ketimine 6
 α -Keto fatty acid 232
 Kynurenine 80

L

Lactitol 321–322
 β -Lactoglobulin
 – characteristics 96–97
 – interactions with κ -casein 97
 Lactone 302
 Lakes 192–193
 Lamella
 – between oil droplets 35–36
 – mesophase 42–44
 – protein film 66–67
 Lanthionine 69–70
 Leavening 367
 Lecithin 40–42. *See also* Phospholipids
 Lemenx effect 311
 Lenthionine 300
 Leucine 60
 Leucodeuteroflavin 395
 Levulinic acid 132
 Ligand
 – exogenic 235
 – ionic 202
 – neutral 202
 – orbital 195
 – polyatomic 195
 – transition 195–197

- Light absorption 171–172
 δ -Limonene 295
 Limonin 297
 Limonoate A-ring lactone 297
 Linalool 282–283
 Linalool oxides 282–283
 Linoleate
 – lipid oxidation 6–9, 28, 29
 – lipoygenase 229
 Linolenate 8, 30
 Lipase 253–254
 – acyl transfer reaction 255
 – colipase 252
 – mechanism of catalysis 253–254
 – pancreatic 251–252
 – specificity 254
 Lipid oxidation 6–15
 – autoxidation 6–7
 – metal ion role in 10–11
 – myoglobin discoloration 211
 – photosensitized oxidation 11–13
 – primary products in 7–9
 – secondary products in 13–15
 – stereochemistry of autoxidation 9–10
 Lipids 3–50
 – antioxidants 6–7
 – emulsifiers 37–41
 – emulsifiers in stabilization 44–47
 – emulsions 34–37
 – fatty acids 3–5
 – hydrogenation 29–32
 – interesterification 32–33
 – liquid-crystalline mesophase 42–44, 46
 – oxidation 6–15 (see also Lipid oxidation)
 – oxidative thermal reactions 16–17
 – plasticity of fat 28–29
 – radiolysis 22–24
 – thermal reactions 17–20
 – triacylglycerols 3–5
 – triglyceride polymorphism 24–27
 Lipolytic enzymes 252–256
 – acyl transfer reaction 256
 – colipase role 254
 – mechanism of catalysis 254
 – pancreatic lipase 253
 – specificity 255
 Lipoygenase 227–233
 – aerobic reaction mechanism 230
 – anaerobic reaction mechanism 231
 – cooxidation 233
 – flavors and 275–276
 – hydroperoxides 232
 – iron in 232
 – regiospecificity/stereospecificity 229
 – soybean lipoygenase 1 228
 Liquid-crystalline mesophase 42–44, 46
 Locust bean gum
 – carrageenan synergism 166
 – xanthan and 162
 Lossen rearrangement 298, 334
 Lumisterol 417–418
 Lupulone (β acid) 283
 Lycopene 177
 Lysinoalanine 69
- ## M
- Macropeptide 95
 Magnasweet. See Glycyrrhizin
 Magnesium 213
 Maillard reaction. See also Nonenzymatic browning
 – carbohydrates 132–135
 – flavor 140–141
 – glucose oxidase and 239
 – sulfite additives 373
 Malonaldehyde 15
 Malvidin 183
 Malvidin-3,5-diglucoside 185, 187
 Mannan 163
 Mannuronic acid 149
 Margarine 42
 Meat
 – ascorbic acid 414
 – cured meats 210–211
 – enzyme treatment 247
 – papain 227
 Meat flavor
 – chemistry of 302–305
 – simulated 305
 Meat proteins. See also Protein(s)
 – emulsion formation 90
 – energy conversion 85–87
 – gelation 91
 – muscle macroscopic structure 80–81
 – muscle proteins 81–85
 – postmortum tenderness 89–91
 – rigor mortis 86–87
 – water holding capacity 266, 366–367
 MeIQ 350–351
 MeIQ_x 350–351
 Melanin 236
 Melanoidin formation 140
 1-*p*-Menthene-8-thiol 295
 Menthofuran 294
 Menthol 294
 3-Mercapto-3-methylpentan-2-one 305
 Mesophase. See Liquid-crystalline mesophase
 Metabolic pathways 272–275
 Metal ions
 – liquid oxidation 10–11
 – sugars and 141
 – vitamin C 414
 Metalloporphyrin, electronic structure 197–200
 Metaphosphates 362
 Methacrylic acid 289
 Methional 299
 Methionine 76
 2-Methy-4-amino-5-hydroxymethyl pyrimidine 10
 2-Methyl-2-butene-1-thiol 284
 2-Methylbutyl acetate 298
 Methylcellulose 153–154
 Methyl 1,2-dithiolane-1-carboxylate 301
 γ -Methylene glutamic acid 339
 bis-(2-Methyl-3-furyl)disulfide 305
 4-Methyl-5(2-hydroxyethyl)thiazole 305
 2-Methyl-3-mercapto-4,5-dihydrofuran 391
 Methyl octanoate 15
 Methyl 10-oxo-8-decenoate 15
 Methyl 9-oxononanoate 15
 1-Methyl-1,2,3,4-tetrahydro- β -carboline-3-carboxylic acid 355
 Methylxanthines 335–338
 Mevalonic acid 275
 Milk and milk proteins 91–97
 – α -caseins 92
 – β -caseins 92
 – κ -casein 92, 97
 – casein micelle 93–95
 – coagulation 95–96
 – heat stability 96–97
 – β -lactoglobulin 96–97
 – vitamin D fortification 415
 Miraculin 323–324
 M-line 81
 Monellin 323–324
 15,15'-Mono-*cis*- β -carotene 178
 Monoenoic dimer 17–18
 Monoglyceride derivatives 38–39
 Monoglycerides 37–38
 Monophenol 233, 235
 Monosaccharides
 – acid action on 130–131
 – alkali action on 127–129
 – carbohydrates 125–126
 Monosodium glutamate 268
 Monostearin-amylose helical complex 46–47

Index

- Monoterpenoids 293
 Muscle. *See also* Meat proteins
 – contraction 85–87
 – emulsion 90
 – energy conversion in 85–87
 – gelation 91
 – macroscopic structure of 80–81
 – postmortem tenderness 89–90
 – proteins of 80–85
 – rigor mortis 86–87
 – the ultimate pH 88
 – water-holding capacity 88–90
 Mycotoxin 345–348
 Myoglobin 200–211
 – absorption spectrum 208–210
 – discoloration 305
 – ferrimyoglobin reduction 208
 – globin's role in 205
 – heme iron 202–204
 – hemochromes 209
 – hydrogen peroxide in autoxidation 207
 – lipid oxidation and 305
 – myomesin 81
 – molecular structure 200–201
 – nitrosylmyoglobin 210–211
 – oxymyoglobin autoxidation 206–207
 Myosin
 – described 82–84
 – emulsion 90
 – gelation 91
 – muscle contraction 85–86
 Myrosinase 333
- N**
 Naringin 297, 317–318
 Natural toxicants 329–357
 – amines 343–345
 – amino acids 338–339
 – cyanogenic glycosides 329–330
 – glucosinolates 332–334
 – glycoalkaloids 330–331
 – heterocyclic amines 349–351
 – methylxanthines 335–337
 – mycotoxins 345–347
 – nitrosamines 352–357
 – peptides 340–341
 – polycyclic aromatic hydrocarbons 348–349
 – proteins 341–343
 Nebulin 81
 Neohesperidin 317–318
 Neohesperidoside 297
 Neotame 316
 Neurotoxins, botulinum 341–343
- Neutralizing value 367
 Niacin 408–409
 Nicotinic acid 408
 Nitric oxide 210
 Nitrate 210
 Nitrite 210
 S-Nitrocysteine 353
 p-Nitrophenol 353–354
 Nitrosamines 352–357
 Nitrosammonium ion 353
 N-Nitrosodiethylamine 354
 N-Nitrosodimethylamine (NDMA) 354
 Nitrosonium ion 352
 N-Nitrosopiperidine 354
 N-Nitrosopyrrolidine (NPYR) 354
 Nitrosylmyoglobin 210–211
 Nitrous oxide 210
 cis-3-Nonenal 232
 Nonenzymatic browning. *See also* Maillard reaction
 – chemistry of reactions 135–139
 – described 132–135
 – factors affecting 134–135
 – melanoidins 140
 – secondary reactions 139–141
 – Strecker degradation 140–141
 – sulfite additives 139
 Norbixin 182–183
 Nonprotein amino acids 338
 Nordihydrocapsaicin 292
 Nucleotides 268
 NutraSweet. *See* Aspartame
- O**
 Octahedral coordination 194–196
 1-Octen-3-ol 300
 1-Octen-3-one 300
 3-Octene-2-one 15
 Odor 226–228. *See also* Flavors
 Odorant receptor, mechanism 271–272
 Oil (fruit flavors) 294
 Oil. *See* Lipids
 Oleate 7–9, 28, 31, 32
 Olfaction, stereochemical theory 269–270
 Olfactory receptor sites 271
 Oligomers 213
 Onion flavor 287–289
 Organic solvents, proteins 63
 Ornithinoalanine 70
 Orthophosphates 362
 2-Oxalylamino-3-aminopropionic acid 8
 Oxalylidiaminopropionic acids 335
 Oxazoles 276
 Oxazolidine-2-thione 334–335
- Oxazoline 277
 Oxazolinide ion 277
 Oxidation. *See also* Lipid oxidation
 – anthocyanins 189
 – chlorophylls 216
 – diphenol 235–236
 – monophenol 235
 – protein 77–78
 Oxidative thermal reactions 16–17
 Oxodioenoic acid 240
 10-Oxo-13-hydroxy-11-trans-octadecenoic acid 232
 9-Oxononanoic acid 232
 Oxyferryl complex 207
 Oxymyoglobin 200, 205–208
- P**
 Palmitic acid 26
 Pancreatic lipase 253
 Papain 223–227
 – active site 224–225
 – ionization 225
 – meat tenderness 226–227
 – reaction mechanism 226
 Para-κ-casein 95
 Paraben 372
 Pectate lyases 250–251
 Pectic enzymes 246–251
 – industrial uses 250
 – pectate lyases 249
 – pectinesterase 246
 – polygalacturonases 248
 Pectin 151–153
 – chemical structure 151
 – classification 151–152
 – gelling 152
 Pectinesterase 246
 Pelargonidin 183, 186
 1,4-Pentadiene system 8, 227–228
 Pentane 159–160
 1,2,3,5,6-Pentathiepane 300
 2-Pentenyfuran 301
 Pentosans 159–160
 2-Pentylfuran 301
 Peonidin 183
 Pepper flavor 290–292
 Peppermint 293
 Peptides 340–341
 Perferryl ion 10
 Peroxydienone 48
 Peroxy epoxide mechanism 387
 Peroxy radical 6, 7, 9, 16, 48
 pH
 – amylases 240
 – antocyanins 184–185
 – gel formation 67

- meat protein 88
 - phosphates 365–367
 - protein conformation 63
 - soybean lipoxygenase 1 227
 - vitamin B₁ and 388–389
 - Phallotoxins 340–341
 - Phenolase. *See* Polyphenol oxidases
 - Phenoxy radical 48–49
 - Phenylalanine
 - amino acids 60
 - photolysis 75
 - 4-“Phenyl” anthocyanin 188
 - 2-Phenyl-benzopyrylium 183
 - Pheophorbide 215
 - Pheophytin 215
 - Phe-P-1 350–351
 - Phosphates 362–367
 - Phosphatidylcholine 40–41
 - Phosphatidylethanolamine 40–41
 - Phosphatidylinositol 40–41
 - O-Phosphobiotin 407
 - Phospholipids 40–41
 - Phosphoric acid 371
 - Phosphorus oxychloride 147
 - Photochemical reactions. *See*
 - Photolysis; Photosensitized reaction;
 - Radiolysis
 - Photolysis
 - nitrosamine 356–357
 - protein 75–76
 - riboflavin 395
 - thiamin 391
 - vitamin B₁₂ 405–406
 - Photosensitized oxidation
 - beta-carotene 180
 - carotenoids 180
 - “ene” reaction 11–12
 - protein 76–77
 - riboflavin 396–397
 - Phthalides 301
 - β-Pinene 295
 - Pipecolic acid 339
 - Piperine 290–291
 - pK_a amino acids 62
 - Plasticity (fats) 28–29
 - Poisoning. *See* Natural toxicants
 - Polycyclic aromatic hydrocarbons
 - 348–349
 - Polygalacturonases 248–249
 - endo-polygalacturonases 237, 248
 - exo-polygalacturonases 248–249
 - Polyglycerol 40
 - Polyhydric alcohol sweeteners 321–322
 - Polyketide pathway 274
 - Polymerorphism of triglycerides. *See*
 - Triglyceride polymerorphism
 - Polypeptide chain 56
 - Polyphenolase. *See* Polyphenol oxidases
 - Polyphenol oxidase 233–236
 - characteristics 233
 - reaction mechanism 234
 - secondary reaction products 234
 - Polypyrrole compounds 290
 - Polysorbate 44, 46
 - Polysulfide 289
 - Polysulfide heterocyclic compounds
 - 279
 - Porphin (free base) 200, 202
 - Porphyrin-Fe²⁺-O₂-Fe²⁺-porphyrin 205
 - Porphyrin
 - free base 197, 202
 - metal 198, 202
 - Postmortem tenderness 89
 - syn-Propanethiol S-oxide 288
 - 2-Propenesulfenic acid 287–288
 - 1-Propenyl propyl disulfide 289–290
 - trans-(+)-S-(1-Propenyl)-L-cysteine
 - sulfoxide 287–288
 - Propionate 372
 - Propylene glycol monostearate 39
 - 2-(propyldithiol)-3,4-dimethylthio-
 - phene 289–290
 - Propyl gallate 48
 - Propyl propanethiosulfonate 289–290
 - Protein(s) 56–118
 - carrageenan interaction 165
 - chemical reactions 68–80
 - emulsification and foaming 65–66
 - emulsifier interaction with 47
 - gel formation 67–68
 - organized systems 81–118
 - structure of 56–58
 - sweeteners 323–324
 - toxicants 341–343
 - Protein chemical reactions 68–80
 - alkali degradation 68–70
 - carbonyl compounds 78
 - chemical oxidation 77–78
 - heat-induced isopeptide 70–71
 - lipid oxidation products 78–79
 - photolysis 75–76
 - photosensitized oxidation 76–77
 - radiolysis 71–74
 - Protein structure
 - conformational change 56–58
 - water role in 61–65
 - Protein systems
 - collagen 113–108
 - meat proteins 80–91
 - milk proteins 91–97
 - soybean proteins 106–113
 - wheat proteins 97–106
 - Proteolysis 95
 - Protocatechuic acid 185
 - Protocollagen proline hydroxylase
 - 411
 - Protoporphyrin 202
 - Pseudobase
 - anthocyanin 184–185
 - thiamin 379
 - Pseudoplastic flow 162
 - Pyrazine 276–277, 291
 - β-Pyrazol-1-ylalane 339
 - Pyridine 286, 302
 - Pyridoxol (vitamin B₆) 397–399
 - Pyrimidines 374–375
 - Pyrochlorin 212
 - Pyrones 278
 - Pyrophosphates 362
 - Pyroporphin 212
 - Pyrrrole 140
 - Pyrrrolidines 277
 - Pyrrolines 277
- ## Q
- Quenching
 - β-carotene 180, 386
 - tocopherol 423
 - Quinoidal base 184, 185
 - Quinone methine 421
- ## R
- Racemization, amino acids 70
 - Radiolysis
 - lipids 22–23
 - proteins 71–74
 - vitamin D 417–418
 - Reduction 134, 138
 - Reductone 278
 - 11-*cis*-Retinal 384–385
 - Retinol (vitamin A) 383
 - Retrogradation 146
 - Retunidin 183
 - Reverse turns 57
 - Rhodanase 330
 - Rhodopsin 384–385
 - Riboflavin (vitamin B₂) 391–396
 - Rigor mortis 86–87
 - Ripening (fruits) 250
 - Rootkatone 295
 - Rutinose 318
- ## S
- Saccharin 316–317
 - Saccharinic acid 128
 - Salt effects

Index

- protein-“salting-in” and “salting-out” 63–65
 - Salt-soluble myofibrillar proteins 90
 - Salty taste 265
 - Scission products 13
 - Seaweed 163
 - Selectivity 31
 - Self-association 186–187
 - Semiquinone radical 393
 - Sesquiterpene 293
 - Sesquiterpenoid 284
 - Shagao 293
 - Shikimic pathway 273–274
 - Shortening effect 106
 - Sinalbin 299
 - Singlet oxygen 11–13
 - Sinigrin 299
 - Site-fitting theory 269–270
 - Sodium stearoyl-2-lacrylate 39
 - Solanidine 331
 - α -Solanine 331
 - Soluble *N*-ethylmaleimide-sensitive factor attachment protein receptor (SNARE) 342
 - Sorbate 372
 - Sorbitan monostearate 39
 - Sour taste 265
 - Soybean lipoxygenase 228
 - Soybean proteins 106–113
 - β -conglycinin 108
 - glycinin 107
 - heat treatment 111
 - pH and salt effects 109–111
 - tofu making 112
 - Spice flavor 287–294
 - black pepper 290–291
 - cinnamon 294
 - garlic/onion 287–289
 - ginger 293
 - hot pepper 292
 - peppermint 293
 - Staling of bread 46–47
 - Starch 143–149
 - chemical modification 147–148
 - chemical structure of 143–145
 - complexation with 46–47
 - digestibility 148–149
 - gelatinization 146–147
 - retrogradation 146–147
 - Stearoyl-2-lactylate 39
 - Stereochemistry, autoxidation 9–10
 - Steroids 320–321
 - Steviol 320–321
 - Stevioside 320–321
 - Strecker degradation
 - ascorbic acid 413
 - Maillard reaction 140–141
 - tea oxidation 281
 - Substituent effect 175–176
 - Succinylated monoglyceride 38
 - Sucrose 311
 - Sugar alcohol sweeteners 321–322
 - Sulfhydryl-disulfide exchange
 - in dough 104
 - gel 68
 - β -lactoglobulin 90–97
 - protein function 58
 - Sulfite
 - food additives 372–379
 - Maillard reaction 139
 - vitamin B₂ and 394–395
 - Sulfite oxidase 379
 - Sulfur dioxide 186
 - Superoxide anion 10
 - Surface tension/area 34
 - Sweeteners 310–324
 - amino acids/dipeptides 313–316
 - aminosulfonates 316–317
 - corn sweeteners 322–323
 - dihydrochalcone 317–318
 - glycyrrhizin 319
 - molecular theory 310
 - neotame 316
 - proteins 323–324
 - stevioside 320–321
 - sugar alcohol 321
 - sweet taste receptors 312–313
 - tripartite theory 310–312
 - Sweet taste 265–266
- T**
- Tartrazine 183
 - Tachysterol 418
 - Taste sensation 265–266
 - Tea flavor 280–281
 - Termolecular-shift binding 243–244
 - γ -Terpinene 295
 - Tertiary butylhydroquinone 48
 - 2,2,7,7-Tetramethyl-1,6-dioxaspiro[4,4]none-3,8-diene 284
 - 2,3,5,6-Tetramethyl-4-methoxyphenol 422
 - Thaumatococin 323–324
 - Theaflavin 280–281
 - Thearubigins 280
 - Theobromine 336
 - Theophylline 336
 - Thermal degradation 179–180
 - Thermal reactions. *See also* Heat
 - lipids 17–19
 - oxidative 20–22
 - vitamin D 418
 - Thiamine (vitamin B₁) 387–391
 - Thiapane 302
 - Thiazole 278–279, 302
 - Thiazoline 278–279, 302
 - Thiochrome 389–390
 - Thiocyanate 298, 334
 - Thio-disulfide intermediate. *See* Sulfhydryl-disulfide
 - β -Thioglucose 332
 - Thioglucoside glucosylhydrolase 333–334
 - Thiophene 289, 302
 - Thiosulfonate 289
 - Thixotropic flow 149–150
 - Thymol 295
 - Titin 81
 - α -Tocopherol quinone 421
 - Tocopherols, trocotrienol 419–420
 - chemical oxidation 420–421
 - free radical reaction 421
 - quenching singlet oxygen 423
 - thermal decomposition 420
 - Tropocollagen 113
 - Toxicants. *See* Natural toxicants
 - Transglycosylation 243–244
 - Triacylglycerol
 - compositions 5
 - nomenclature 3–5
 - Triglyceride polymorphism (lipids) 24–27
 - crystal habit of fat 27–28
 - crystal structure 27
 - Trigonal pyramidal intermediate 235
 - Trimethylamine (TMA) 304
 - Trimethylamine-*N*-oxide (TMAO) 304, 345
 - 1,3,7-Trimethyluric acid 337
 - Tripartite model 310–311
 - Triple helix 113
 - Trithiane 279
 - 1,2,3-Trithiane-5-carboxylic acid 301
 - Trithiolane 279, 300
 - Tropomyosin
 - energy conversion 82, 84–85
 - muscle protein 82
 - Troponin
 - energy conversion 84–85
 - muscle protein 82
 - postmortem tenderness 89–90
 - Trp-P-1 350, 351
 - Trypsin 227
 - Tyramine 344
 - Tyrosinase. *See* Polyphenol oxidase
 - Tyrosine 75–76
 - Two-electron transfer 239
- U**
- Umami

- enhancers 268
 - receptor 267
 - taste sensation 265–266
- Uncertified color additives 192
 Uridine-4-sulfonate 377

V

- Valencene 295
 Valine 60
 Van der Waals forces
- emulsions 36
 - liquid-crystalline mesophase 42
- Vanillyl alkylamine 292
 Vegetable flavor 298–301
 Vinyl- β -ionol 181
 5-Vinylloxazolidine-2-thione 334
 Vitamins 383–423
- A (retinol) 383–387
 - B₁ (thiamin) 387–391
 - B₂ (riboflavin) 391–397
 - B₆ (pyridoxol) 397–399
 - B₉ (folic acid) 399–404
 - B₁₂ 404–406
 - biotin 406–408

- C (ascorbic acid) 409–414
- D (ergocalciferol, cholecalciferol) 415–418
- E (tocopherol, tocotrienol) 419–423
- niacin 408–409

W

- Water
- dielectric constant 63
 - liquid-crystalline mesophase 42–44
 - phosphate 366
 - protein structure and 63
 - water-holding capacity 88–89
- Water holding capacity 366–367
- bicarbonates 366–367
 - phosphates 366
- Wheat proteins 97–106
- flour into dough transformation 104–106
 - gliadins 97–98
 - glutenin polymer models 102–104
 - glutenins 99–100
 - “loop and train” model 103
- Wittig reaction 180–181

X

- Xanthan gum 161–162
 Xanthophylls 176–178
 Xylan 159
 Xylitol 321
 Xylose isomerase 256–258
- metal ions 257–258
 - reaction mechanism 258–259
 - structure 256–257

Y

- Ylid 388

Z

- Z-disk 81
 Zeaxanthin 177
 Zingerone 293
 Zingiberene 293